



UNIVERSITAT DE
BARCELONA

Total Synthesis of Phlegmarine Alkaloids

Caroline Bosch

ADVERTIMENT. La consulta d'aquesta tesi queda condicionada a l'acceptació de les següents condicions d'ús: La difusió d'aquesta tesi per mitjà del servei TDX (www.tdx.cat) i a través del Dipòsit Digital de la UB (diposit.ub.edu) ha estat autoritzada pels titulars dels drets de propietat intel·lectual únicament per a usos privats emmarcats en activitats d'investigació i docència. No s'autoritza la seva reproducció amb finalitats de lucre ni la seva difusió i posada a disposició des d'un lloc aliè al servei TDX ni al Dipòsit Digital de la UB. No s'autoritza la presentació del seu contingut en una finestra o marc aliè a TDX o al Dipòsit Digital de la UB (framing). Aquesta reserva de drets afecta tant al resum de presentació de la tesi com als seus continguts. En la utilització o cita de parts de la tesi és obligat indicar el nom de la persona autora.

ADVERTENCIA. La consulta de esta tesis queda condicionada a la aceptación de las siguientes condiciones de uso: La difusión de esta tesis por medio del servicio TDR (www.tdx.cat) y a través del Repositorio Digital de la UB (diposit.ub.edu) ha sido autorizada por los titulares de los derechos de propiedad intelectual únicamente para usos privados enmarcados en actividades de investigación y docencia. No se autoriza su reproducción con finalidades de lucro ni su difusión y puesta a disposición desde un sitio ajeno al servicio TDR o al Repositorio Digital de la UB. No se autoriza la presentación de su contenido en una ventana o marco ajeno a TDR o al Repositorio Digital de la UB (framing). Esta reserva de derechos afecta tanto al resumen de presentación de la tesis como a sus contenidos. En la utilización o cita de partes de la tesis es obligado indicar el nombre de la persona autora.

WARNING. On having consulted this thesis you're accepting the following use conditions: Spreading this thesis by the TDX (www.tdx.cat) service and by the UB Digital Repository (diposit.ub.edu) has been authorized by the titular of the intellectual property rights only for private uses placed in investigation and teaching activities. Reproduction with lucrative aims is not authorized nor its spreading and availability from a site foreign to the TDX service or to the UB Digital Repository. Introducing its content in a window or frame foreign to the TDX service or to the UB Digital Repository is not authorized (framing). Those rights affect to the presentation summary of the thesis as well as to its contents. In the using or citation of parts of the thesis it's obliged to indicate the name of the author.



UNIVERSITAT DE
BARCELONA

UNIVERSITAT DE BARCELONA

FACULTAT DE FARMÀCIA I CIÈNCIES DE L'ALIMENTACIÓ

DEPARTAMENT DE FARMACOLOGIA, TOXICOLOGIA I QUÍMICA TERAPÈUTICA

LABORATORI DE QUÍMICA ORGÀNICA

TOTAL SYNTHESIS OF PHLEGMARINE ALKALOIDS

CAROLINE BOSCH
2016



UNIVERSITAT DE
BARCELONA

UNIVERSITAT DE BARCELONA

FACULTAT DE FARMÀCIA I CIÈNCIES DE L'ALIMENTACIÓ

DEPARTAMENT DE FARMACOLOGIA, TOXICOLOGIA I QUÍMICA TERAPÈUTICA

PROGRAMA DE DOCTORAT: QUÍMICA ORGÀNICA EXPERIMENTAL I INDUSTRIAL

TOTAL SYNTHESIS OF PHLEGMARINE ALKALOIDS

Memòria presentada per Caroline Bosch per optar al títol de doctor
per la Universitat de Barcelona

Dirigida per:

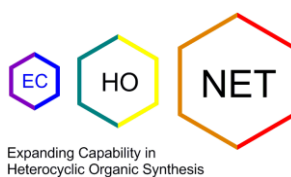
Dr. Ben Bradshaw

Dr. Josep Bonjoch

Caroline Bosch

Barcelona,
Octubre 2016

Financial support for this research was provided by the FP7 Marie Curie Actions of the European Commission via the ITN ECHONET Network (MCITN-2012-316379) and partially by the project CTQ2013-41338-P from the ministry of Economy and Competitiveness of Spain (MINECO).



En primer lugar, Josep, gracias por la dirección de este trabajo. Me has ayudado a entender tantas cosas, que sea del punto de vista de la química, como del mundo en general y por los buenos momentos de estos tres años.

Ben thanks for the supervision of this work, for the time you devoted to me and for everything I learned from you.

Gracias también a todos los amigos de Barcelona por todos los buenos momentos. Grazie Celeste, Elena, Francesco. Obrigado Alex. Merci Guillaume. Gracias Marie, Claudio, Juan, Aina. Gràcies Ferran, Sergi. Gracias también Mafalda, Carlos, Pau, Bruno, Nataly, Myriam, Lorenzo, Marina y a los que me olvide. Gracias a todos !

I also want to thank all the students from the Marie Curie program, ECHONET. Tim, Béla, Sylvestre, Martina, Malcolm, Jokin, Silvia, Ivan, Alejandra and Júlia !! Thanks for all the great times we had the past 3 years...

Thanks to all Rutjes group in Nijmegen for welcoming me for the few months spent there, and thanks Floris and Dani for your support and help. Thanks also to Pieter, Bas and Future Chemistry for the help during my stay in the Netherlands.

Merci Guilhem pour ces trois années, pour avoir toujours été là et avoir rendu le travail au quotidien beaucoup plus supportable ! Pour tout, merci !

Tout spécialement, merci à toi Nicolas pour m'avoir aidé tout au long de ce doctorat. Pour m'avoir supporté dans les moments difficiles, tout simplement pour avoir été là. Je n'en serai pas là sans ton aide. Je t'aime, merci...

Et finalement et surtout merci à ma famille : Papa, Maman, Jérémie, Christine... Merci pour votre soutien, votre support votre aide dans des débuts difficiles et une fin sur les rotules... Je vous aime. Merci pour tout, je vous suis très reconnaissante.

Prologue

The manuscript of this Doctoral Thesis has been divided into six main parts: a general introduction into phlegmarine alkaloids followed by five research chapters.

The general introduction provides an overview on the phlegmarine alkaloids, the total syntheses previously reported as well as the group precedents in the field of total synthesis of phlegmarine alkaloids.

The second chapter titled 'Asymmetric Synthesis of Octahydroindoles via a Domino Robinson Annulation/5-*Endo* Intramolecular aza-Michael Reaction' describes a straightforward two-step asymmetric synthesis of octahydroindoles. This allowed the construction of complex octahydroindoles with up to 4 stereocenters, excellent enantioselectivities (up to 95% ee) and complete diastereoselective control in a single pot operation. Those results have been published in *J. Org. Chem.* **2016**, (Featured Article) DOI: 10.1021/acs.joc.6b01568 (ASAP 08/09/2016). This project was performed in collaboration with Dr. Claudio Parra.

The third chapter titled 'Fischer Indole Reaction in Batch and Flow Employing a Sulfonic Acid Resin: Synthesis of Pyrido[2,3-*a*]carbazoles' describes an Amberlite IR 120 H-promoted one-pot Fischer indolization from a *cis*-decahydroquinoline using a range of phenylhydrazines. This methodology provides access to compounds with the unprecedented pyrido[2,3-*a*]carbazole scaffold. The process may be conducted either in batch mode or in a continuous manner in a flow reactor. This methodology allowed the synthesis of a small library of compounds sent for biological testing. These results have been published in *J. Flow Chem.* **2016**, DOI: 10.1556/1846.2016.00016. This project was performed in collaboration with the flow chemistry company Future Chemistry as well as Pr. Floris Rutjes Nijmegen, the Netherlands.

The fourth chapter titled 'Total Synthesis of *cis*-Phlegmarines via Stereodivergent Reduction: (+)-Serratezomine E and Putative Structure of (-)-Huperzine N' describes a unified strategy for the synthesis of the *cis*-phlegmarine group of alkaloids. This strategy was possible through contrasteric hydrogenation methods. This work led to the first synthesis of serratezomine E as well as the putative structure of huperzine N. Calculations were performed by Pr. Enrique Gómez-Bengoia and Dr. Béla Fiser, San Sebastian, Spain to determine the mechanism. Structures for huperzines M and N were reassigned. A part of these results has been published in *Org. Lett.*, **2015**, *17*, 5084-5087.

The fifth chapter titled 'Access to *trans*-Phlegmarines of Type D: Synthesis of (±)-Serralongamine A and the Revised Structure of Huperzine N' describes the proposed structure reassignment for the *Lycopodium* alkaloid huperzine N which is confirmed by synthesis. This route allowed first total synthesis of the alkaloid serralongamine A, and two additional steps led to the revised structure of huperzine N. Those results have been published in *J. Org. Chem.* **2016**, *81*, 2629-2634. This project was performed in collaboration with Dr. Gisela Saborit.

The sixth chapter titled 'Decahydroquinoline Ring NMR Patterns for the Stereochemical Elucidation of Phlegmarine Alkaloids: Synthesis of (-)-Serralongamine A and the Revised Structures of (-)-Huperzine K and Huperzine M' describes the structural reassignment of the *Lycopodium* alkaloids huperzine K, huperzine M and Lycoposerramine Y which were then confirmed by synthesis. In this paper we detail our efforts to develop general rules to deduce in an easy manner the stereochemistry of any phlegmarine-type alkaloids. A manuscript is in preparation for the publication of these results.

Table of Contents

List of Abbreviations and Acronyms	ix
1 Introduction and objectives	1
1.1. Introduction	3
1.2. Objectives	26
2. Asymmetric Synthesis of Octahydroindoles via a Domino Robinson Annulation/ <i>5-Endo</i> Intramolecular Aza-Michael Reaction	29
3. Fischer Indole Reaction in Batch and Flow Employing a Sulfonic Acid Resin; Synthesis of Pyrido[2,3- <i>a</i>]carbazoles	45
4. Total Synthesis of <i>cis</i> -Phlegmarines via Stereodivergent Reduction: (+)-Serratezomine E and Putative Structure of (-)-Huperzine N	57
5. Access to <i>trans</i> -Phlegmarines of Type D: Synthesis of (±)-Serralongamine A and the Revised Structure of Huperzine N	83
6. Decahydroquinoline Ring NMR Patterns for the Stereochemical Elucidation of Phlegmarine Alkaloids: Synthesis of (-)-Serralongamine A and the Revised Structures of (-)-Huperzine K and Huperzine M	95
7. Conclusions	113
8. Publications and experimental	121
* <i>J. Org. Chem.</i> 2016 , doi 10.1021/acs.joc.6b01568 and SI (2)	
* <i>J. Flow Chem.</i> doi 10.1556/1846.2016.00016 and SI (3)	
* <i>Org. Lett.</i> 2015 , <i>17</i> , 5084-5087 and SI (4) and addendum SI (4')	
* <i>J. Org. Chem.</i> 2016 , <i>81</i> , 2629-2634 and SI (5)	
* Experimental of chapter 6 unpublished results	

List of Abbreviations and Acronyms

In this manuscript, the abbreviations and acronyms most commonly used in organic chemistry have been used following the recommendations from “Guidelines for Authors” of *Journal of Organic Chemistry*

α_D	specific optical rotatory power at $\lambda = 589$ nm
acac	acetylacetonate
aq.	aqueous
atm	atmosphere
<i>ax</i>	axial
9-BBN	9-borabicyclo[3.3.1]nonane
BEMP	2- <i>tert</i> -butylimino-2-diethylamino-1,3-dimethylperhydro-1,3,2-diazaphosphorine
Boc	<i>tert</i> -butoxycarbonyl
Boc ₂ O	di- <i>tert</i> -butyl carbonate
bp	boiling point
BPR	back pressure regulator
br	broad
<i>c</i>	concentration
¹³ C NMR	carbon-13 nuclear magnetic resonance
calcd	calculated
Cbz	benzyloxycarbonyl
CDI	1,1'-carbonyldiimidazole
Celite [®]	filtration agent
CHD	cyclohexadiene
COSY	correlation spectroscopy
compd	compound
<i>d</i>	day(s), doublet (spectra)
δ	chemical shift
DBU	1,8-diazabicycloundec-7-ene

DCE	dichloroethane
dd	doublet of doublets
de	diastereomeric excess
DEAD	diethyl azodicarboxylate
DFT	density functional theory
DHQ	decahydroquinoline
dm	doublet of multiplets
DMF	<i>N,N</i> -dimethylformamide
DMSO	dimethyl sulfoxide
dpm	2,2,6,6-tetramethyl-3,5-heptanedionato
DPPA	diphenyl phosphoryl azide
dppf	1,1'-bis(diphenylphosphino)ferrocene
dr	diastereomeric ratio
dt	doublet of triplets
DTAD	di- <i>tert</i> -butylazodicarboxylate
ee	enantiomeric excess
<i>epi</i>	epimer
equiv.	equivalent
<i>eq</i>	equatorial
ETFE	ethylene tetrafluoroethylene
GC	gas chromatography
[H]	reduction
HAT	hydrogen atom transfer
HMPA	hexamethylphosphoramide
¹ H NMR	proton nuclear magnetic resonance
HPLC	high performance liquid chromatography
HRMS	high resolution mass spectrum
HSQC	heteronuclear single quantum correlation spectroscopy
HWE	Horner-Wadsworth-Emmons
<i>J</i>	coupling constant
LiHMDS	lithium bis(trimethylsilyl)amide

Lit.	literature
M	molar
m	multiplet
M ⁺	molecular ion
<i>m/z</i>	mass to charge ratio
<i>m</i> -CPBA	meta-chloroperoxybenzoic acid
mol	mol(es)
mp	melting point
MS	mass spectrometry / molecular sieves
Ms	mesyl (methylsulfonyl)
<i>n.a.</i>	not available
<i>n.d.</i>	not determined
<i>n.o.</i>	not observed
NOESY	nuclear Overhauser effect spectroscopy
Ns	nosyl (4-nitrobenzenesulfonyl)
[O]	oxidation
ox	oxalate
p	page
ppm	parts per million
PS-BEMP	polymer supported 2- <i>tert</i> -butylimino-2-diethylamino-1,3-dimethylperhydro-1,3,2-diazaphosphorine
quant.	quantitative
R	generalized alkyl group or substituent
<i>R_f</i>	retention factor
<i>rac</i>	racemic
ref.	reference
rfx	reflux
ROESY	rotating frame nuclear Overhauser effect spectroscopy
rt	room temperature
s	singlet
sat.	saturated

sol.	solution
t	triplet
TASF	tris(dimethylamino)sulfonium difluorotrimethylsilicate
TBAH	tetrabutylammonium hydroxide solution
TBDPS	<i>tert</i> -butyl(chloro)diphenylsilane
TBHP	<i>tert</i> -butyl hydroperoxyde
td	triplet of doublets
(-)-TCC	(-)- <i>trans</i> -2-(α -cumyl)cyclohexanol
Teoc	trimethylsilyl-ethoxycarbonyloxy
Tf	triflate
TFA	trifluoroacetic acid
TFE	trifluoroethanol
THF	tetrahydrofuran
TIPS	triisopropylsilyl
TLC	thin layer chromatography
Ts	tosyl (<i>p</i> -toluenesulfonyl)
TS	transition state
UHP	urea hydrogen peroxide
wt	weight

1. INTRODUCTION AND OBJECTIVES

1.1 Introduction

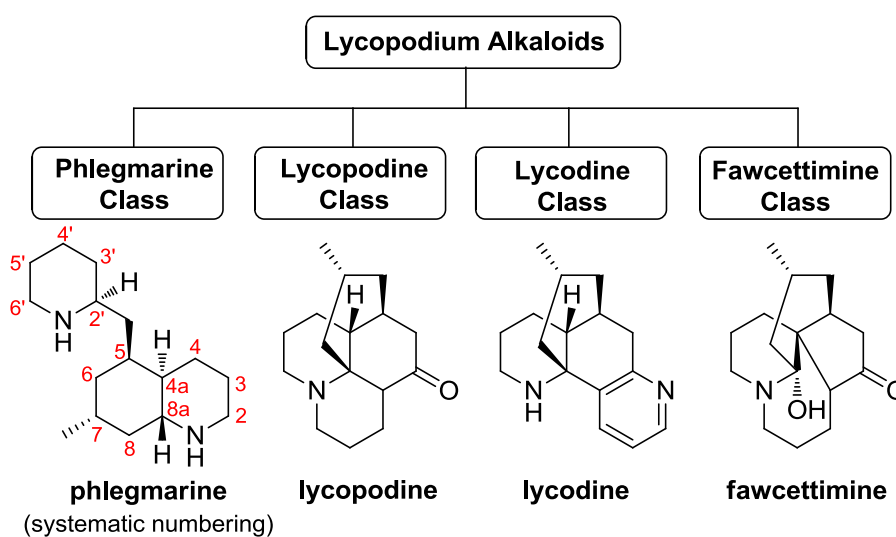


Figure 1.1 The four classes of lycopodium alkaloids

The lycopodium alkaloids,¹ isolated from the lycopodium genus of club mosses belonging to the family of *Lycopodiaceae*, represent a diverse group of structures with around 300 known members to date. These alkaloids can be divided into four distinct classes or subfamilies as illustrated in Figure 1.1.²

The phlegmarine-type lycopodium alkaloids which are the main focus of this thesis were first discovered by Braekman and co-workers in 1978³ and possess a C₁₆N₂-skeleton that consists of a piperidine ring and a decahydroquinoline ring connected through a methylene unit. Braekman also proposed that these compounds are likely the biogenetic precursors of the other main classes of lycopodium alkaloids thus indicating the central underlying importance of the phlegmarine class. Although lack of material from natural sources has prevented a full and extensive evaluation of the biological activities of these compounds, from the limited data available they show promise for the treatment of cancer and severe neurodegenerative diseases such as Alzheimer's¹

¹ Ma, X.; Gang, D. R. *Nat. Prod. Rep.* **2004**, *21*, 752-772.

² Ayer, W. A.; Trifonov, L. S. *Alkaloids (Academic Press)*, **1994**, *45*, 233-266.

³ Nyembo, L.; Goffin, A.; Hootel , C.; Braekman, J.C. *Can. J. Chem.* **1978**, *56*, 851-865.

- **Classification of the phlegmarine alkaloids**

The 5,7-disubstituted decahydroquinoline ring of the phlegmarine alkaloids exists in a variety of stereochemical arrangements according to the stereochemical relationship pattern between the C-7 methyl group, the (2-piperidyl)methyl side chain at C-5, and the type of ring fusion. To facilitate the identification we have grouped the four possible permutations based on the relation of the ring fusion hydrogens (*cis* or *trans*) to the C-7 methyl with letters A to D. Additionally, the orientation of the (2-piperidyl)methyl side chain at C-5 is denoted as α or β (Figure 1.2).⁴ The carbon atom linked to the methyl group is always R^5 and the stereochemistry in the piperidine ring appendage appears always to have the S configuration thus limiting the 32 possible stereochemical arrangements to just 8.

Type A compounds are those which contain the C-7 (methyl substituent) and C-4a and C-8a ring fusions hydrogens all arranged in a *cis* orientation. Compounds of this group are lycoposerramine Z⁶ and serratezomine E.⁷ **Type B** compounds are characterized by having the ring fusion hydrogens in *cis*, but *trans* respect the C-7 methyl group. This group includes cermizine A,⁸ which features an ethanoic acid appendage at C-2 of the decahydroquinoline ring, cermizine B,⁸ huperzine M, and huperzine N.⁹ **Type C** compounds are the most numerous group, in

⁴ It should be noted that at the start of this thesis the compounds in figure 1.2 were the known structures - the revised and corrected structures based on the work carried out in this thesis are depicted on page 119.

⁵ When the absolute configuration is unknown, some phlegmarine alkaloid isolation papers depict the enantiomer of the corresponding structure shown in Figure 1.2. The only related structure thus far known to have an S configuration at C-7 is spiroLucidine.

⁶ Katakawa, K.; Kitajima, M.; Yamaguchi, K.; Takayama, H. *Heterocycles* **2006**, *69*, 223-229.

⁷ Kubota, T.; Yahata, H.; Yamamoto, S.; Hayashi, S.; Shibata, T.; Kobayashi, J. *Bioorg. Med. Chem. Lett.* **2009**, *19*, 3577-3580.

⁸ Morita, H.; Hirasawa, Y.; Shinzato, T.; Kobayashi, J. *Tetrahedron* **2004**, *60*, 7015-7023.

⁹ Gao, W. Y.; Li, Y. M.; Jiang, S. H.; Zhu, D. Y. *Helv. Chim. Acta* **2008**, *91*, 1031-1035.

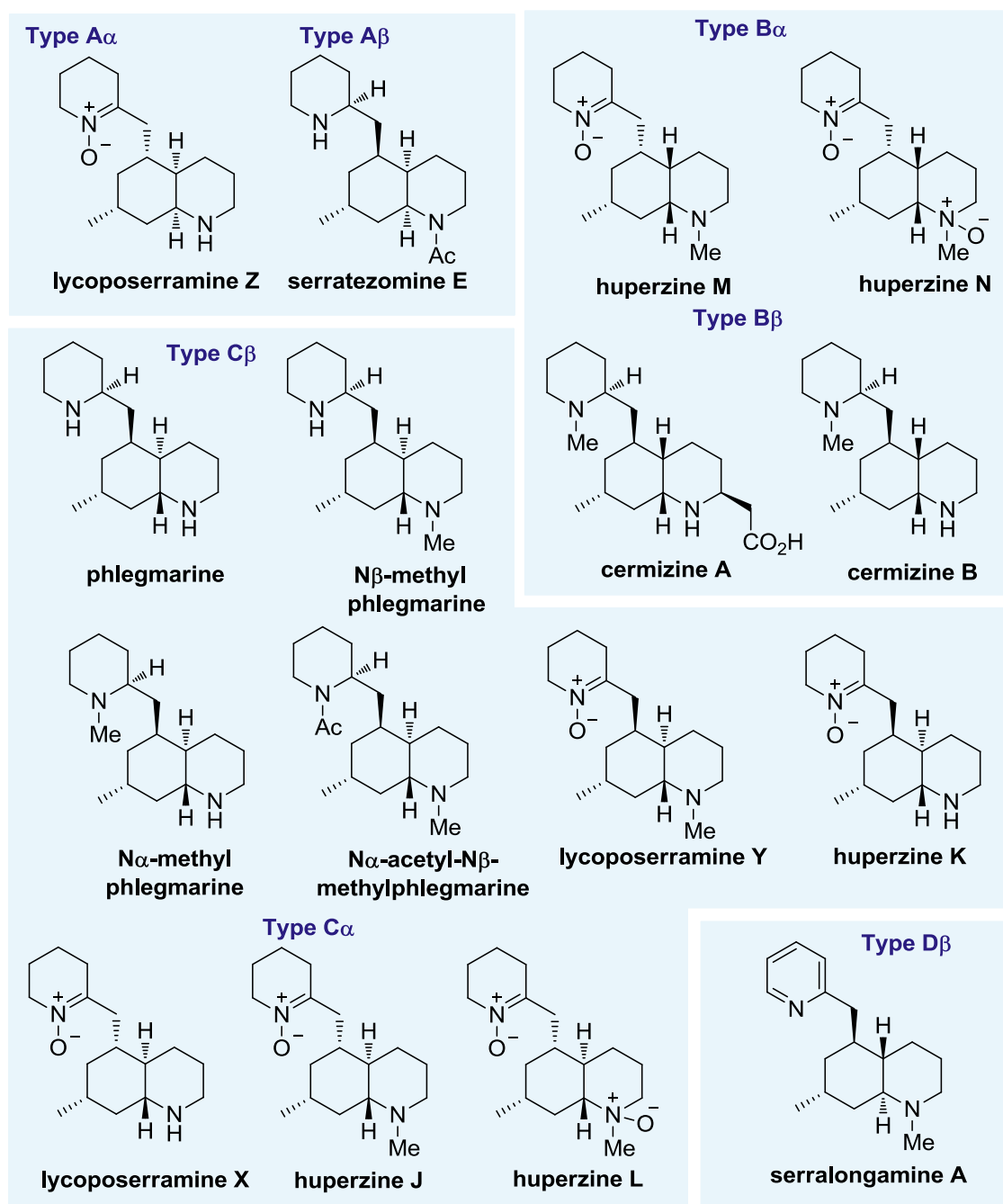


Figure 1.2 Phlegmarine alkaloids grouped by core structural type

which the ring fusion hydrogens and the C-7 methyl are all arranged *trans* to each other. This group includes phlegmarine³ and a number of *N*-methylated and acetylated derivatives as well as lycoposerramine Y⁶ and huperzine K,¹⁰ which posses a nitronne unit. Lycoposerramine X,⁶ huperzine J,¹⁰ and L¹⁰ also feature a nitronne unit but are epimeric at C-5

¹⁰Gao, W. Y.; Li, Y. M.; Jiang, S. H.; Zhu, D. Y. *Planta Med.* **2000**, *66*, 664-667.

with a 5α disposition. **Type D** stereochemistry has the ring fusion hydrogens arranged *trans* and the C-8a hydrogen *cis* to the C-7 methyl. Until relatively recently with the isolation of serralongamine A,¹¹ this stereochemical pattern was unknown.

- **Miscellaneous group lycopodium alkaloids**

From each of the core phlegmarine structures further complexity and diversity appear *via* three main modifications: oxidations, ring fragmentations and ring cross linkage.¹² Those compounds are grouped in the miscellaneous class (Figure 1.3). Most notably, in the vast majority of cases they are derived from bioprecursors presenting a *trans* relationship between the C-5 substituent and the C-8a hydrogen. The **type A β** skeleton is present in the compounds luciduline,¹³ hyperminone A,¹⁴ $\Delta^{13,N}$,N α -methylphlegmarine-N β -oxide,¹⁵ nankakurine B,¹⁶ lyconadin C, A, and B¹⁷ and dihydrolycolucine.¹⁸ The **type B α** phlegmarine is less prevalent featuring in the dimeric compound spirolicidine¹⁹ which also features a type A nucleus. Compounds derived from the **type C α** phlegmarine alkaloids include lycobelline A²⁰ via fragmentation of the

¹¹ Jiang, W. P.; Ishiuchi, K.; Wu, J. B.; Kitanaka, S. *Heterocycles* **2014**, *89*, 747-752.

¹² In a number of cases where the core stereochemistry is lost via an oxidation or fragmentation the resulting compound may arise from more than one possible precursor.

¹³ Ayer, W. A.; Masaki, N.; Nkunica, D. S. *Can. J. Chem.* **1968**, *46*, 3631-3642.

¹⁴ Hirasawa, Y.; Kato, Y.; Wong, C. P. Uchiyawa, N.; Goda, Y.; Hadi, H. A.; Morita, H. *Tetrahedron Lett.* **2013**, *54*, 1593-1595.

¹⁵ Wang, Z.; Wu, J.; Zhao, N.; Yang, Y.; Chen, Y. *Nat. Prod. Res.* **2015**, *30*, 241-245.

¹⁶ Hirasawa, Y.; Morita, H.; Kobayashi, J. *Org. Lett.* **2004**, *6*, 3389-3391.

¹⁷ Kobayashi, J.; Hirasawa, Y.; Yoshida, N.; Morita, H. *J. Org. Chem.* **2001**, *66*, 5901-5904.

¹⁸ Ayer, W. A.; Browne, L. M.; Nakahara, Y.; Tori, M.; Delbaere, L. T. *Can. J. Chem.* **1979**, *57*, 1105-1107.

¹⁹ Ayer, W. A.; Ball, L. F.; Browne, L. M.; Tori, M.; Delbaere, L. T. J.; Silverberg, A. *Can. J. Chem.* **1984**, *62*, 298-302.

²⁰ Hirasawa, Y.; Matsuya, R.; Shaari, K.; Lajis, N.-H.; Uchiyama, N.; Goda, Y.; Morita, H. *Tetrahedron Lett.* **2012**, *53*, 3971-3973.

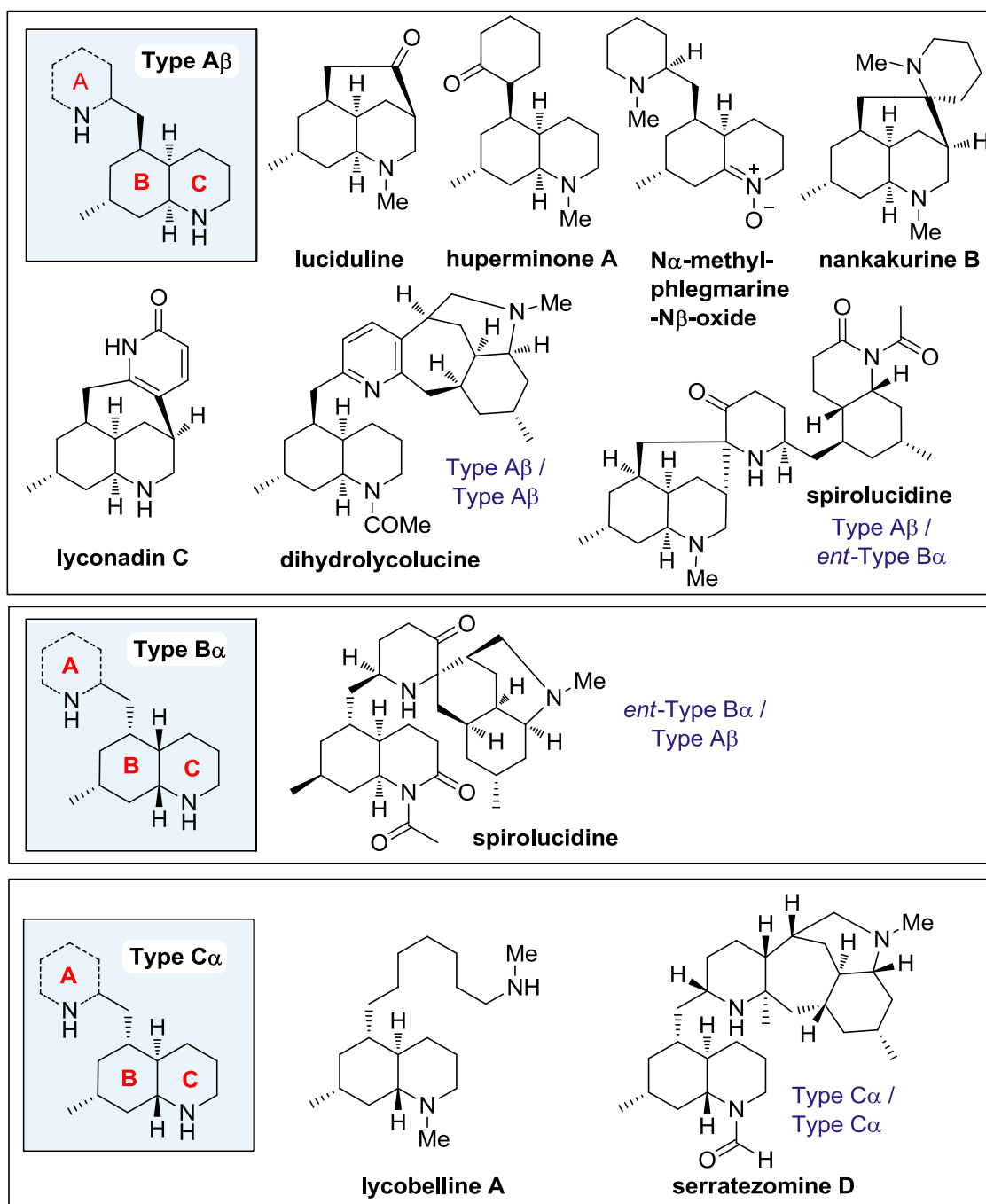
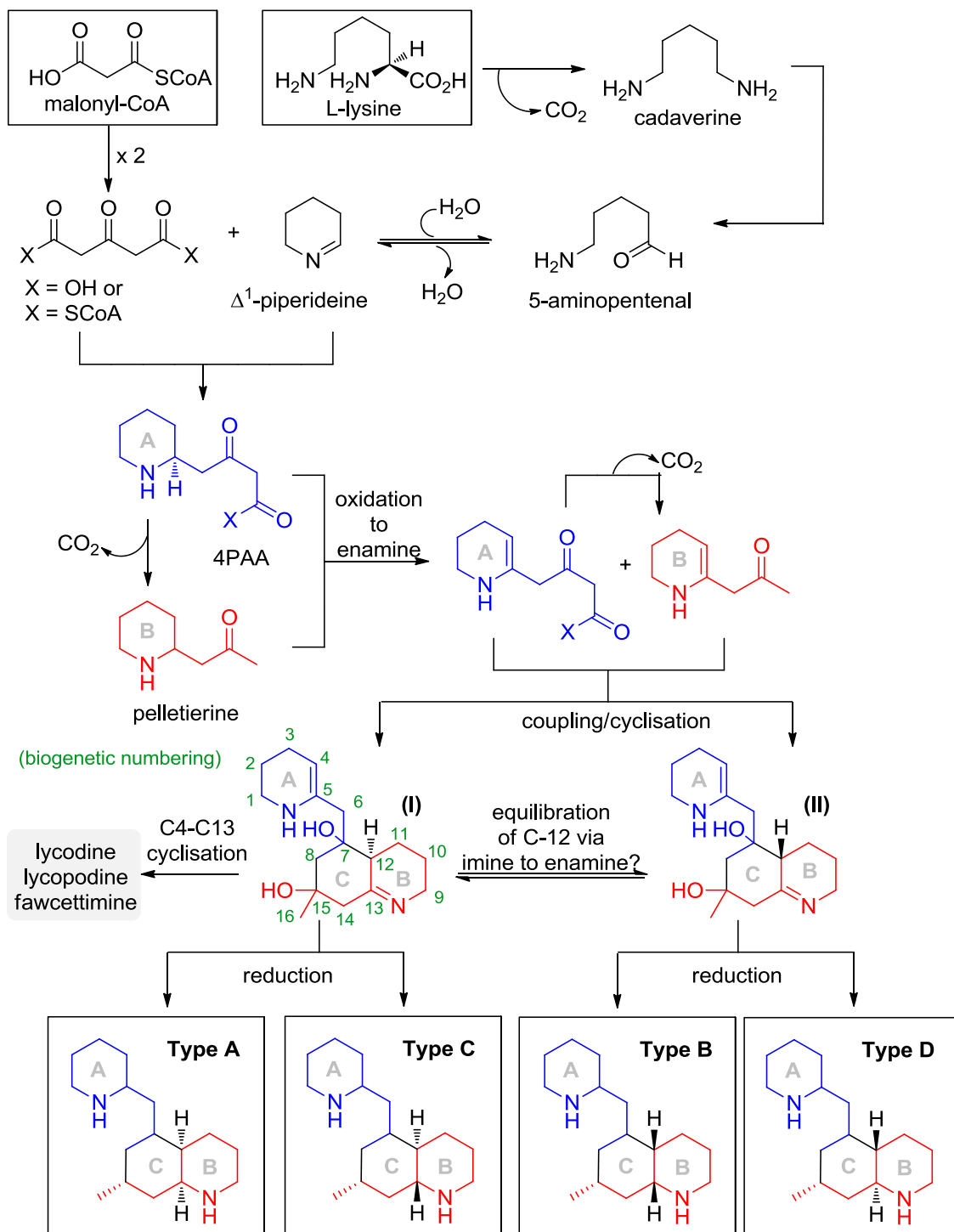


Figure 1.3 Miscellaneous and Lycopodium alkaloids related with phlegmarines piperidine ring and serratezomine D a dimeric compound, which contains two type C nuclei embedded within its structure. So far no derivatives containing a **type D β** nucleus are known.

- **Biosynthesis of the phlegmarine alkaloids**

An overview of the biosynthesis of the different phlegmarine nuclei is outlined in Scheme 1.1.¹ In this part biogenetic numbering is used (see Scheme 1.1).²¹ The pathway starts with the decarboxylation of lysine to form cadaverine which is then transformed to Δ^1 -piperideine. At the same time, two molecules of malonyl-CoA are condensed to form acetonedicarboxylic acid, which upon coupling with Δ^1 -piperideine leads to 4-(2-piperidyl) acetoacetate (4PAA). Subsequent decarboxylation forms pelletierine. At this point 4PAA and pelletierine are oxidized to their corresponding enamines prior to their joining via a decarboxylative aldol coupling. This is followed by a second aldol type coupling via the enamine to give **I** with the stereochemistry at C-12 required for type A and C compounds. It is possible at this point that **II** is also formed with the stereochemistry for type B and D compounds. Alternatively, the stereochemistry at C-12 of **II** might also arise from equilibration of **I** via imine to enamine equilibration. Finally, reduction at C-7, C-15, C-13 and C-5 from the corresponding precursor **I** or **II** gives the various decahydroquinoline ring stereochemistries observed. It should be noted that if instead of undergoing reduction, the enamine of the A ring of intermediate **I** is coupled intramolecularly to the C-13 position imine one can obtain access to the other three main lycopodium parent compounds.

²¹ Throughout this thesis two numbering system can be found: the systematic numbering is used for all synthetic aspects, whereas biogenetic numbering will be used for isolated natural products.



Scheme 1.1 Proposed biosynthesis of the phlegmarine alkaloids

- Previous syntheses of phlegmarine type alkaloids

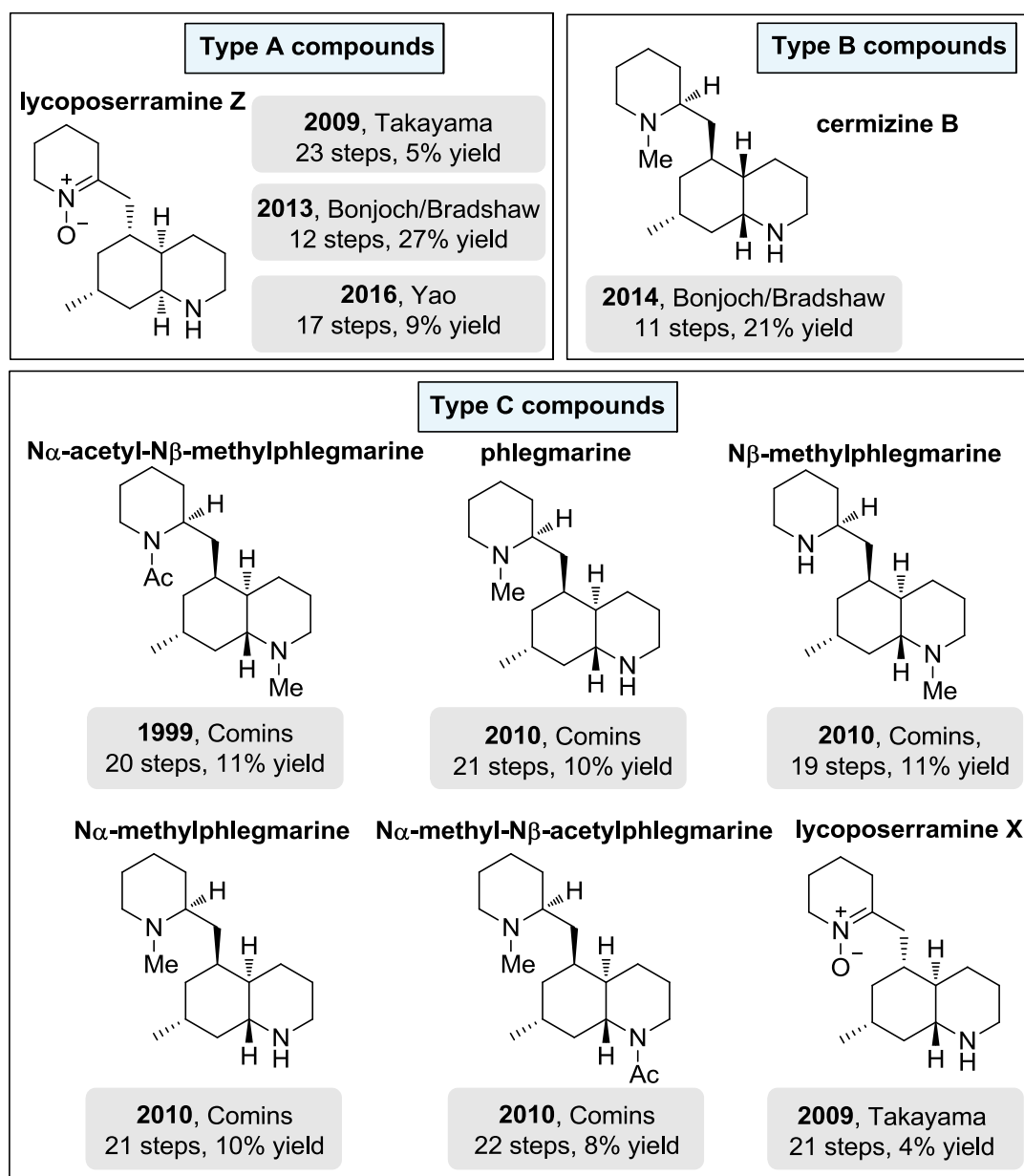
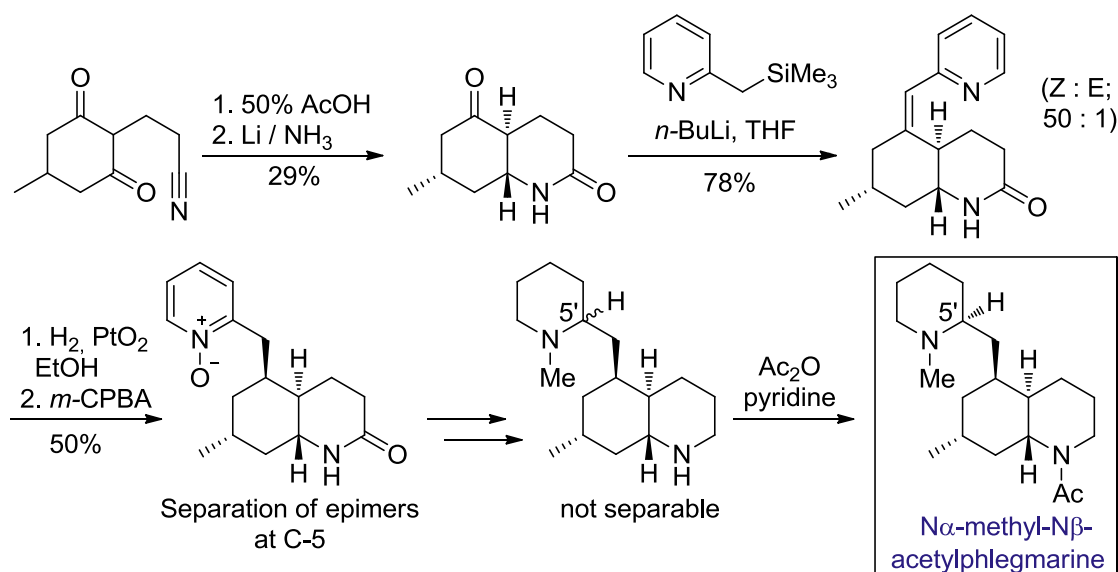


Figure 1.4 Previous syntheses of phlegmarine alkaloids

While there are numerous approaches towards the total synthesis of all the classes of lycopodium alkaloids,²² the phlegmarine subclass has received less attention until relatively recently. In this section an overview of all the prior syntheses of the phlegmarine alkaloids are presented in chronological order (Figure 1.4).

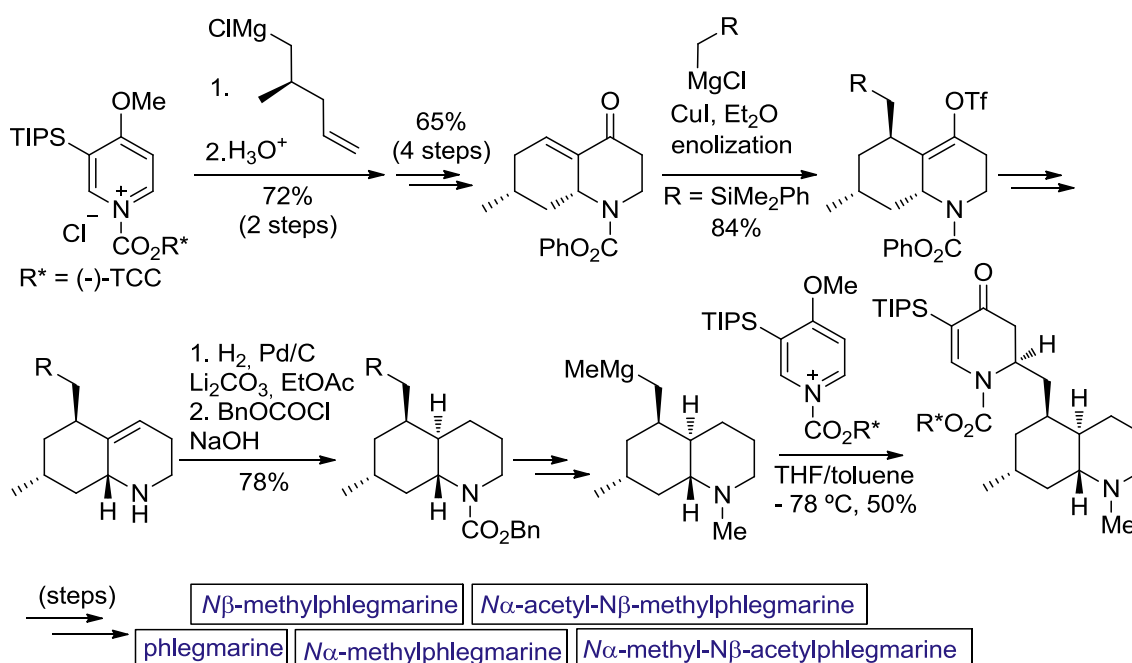
²² For an extensive review focusing on the total synthesis of the lycopodium alkaloids see: Siengalewicz, P.; Mulzer, J.; Rinner, U. *The Alkaloids*, **2013**, 72, 1-151.

Total synthesis of $N\alpha$ -methyl- $N\beta$ -acetylphlegmarine (Maclean)²³**Scheme 1.2** Total synthesis of $N\alpha$ -methyl- $N\beta$ -acetylphlegmarine (Maclean)

Starting from 2-(2-cyanoethyl)-5-methyl-1,3-cyclohexanedione the *trans* decahydroquinoline core was prepared in two steps.²⁴ Peterson olefination furnished a mixture of *Z/E* vinyl pyridines, which upon reduction with Pt gave two epimers that were separable in their *N*-oxide form. Transformation into the methyl pyridine and hydrogenation over Pt gave a mixture of diastereomeric piperidines at C-5', which could only be separated after *N*-acylation. The lack of material did not allow a determination of the stereochemistry at C-5' position. However, the synthesis of MacLean established the relative stereochemistry at four of the five stereogenic centers and showed that the stereochemistry pattern in phlegmarine is the same configuration found in lycopodium and most other lycopodium alkaloids (Scheme 1.2).

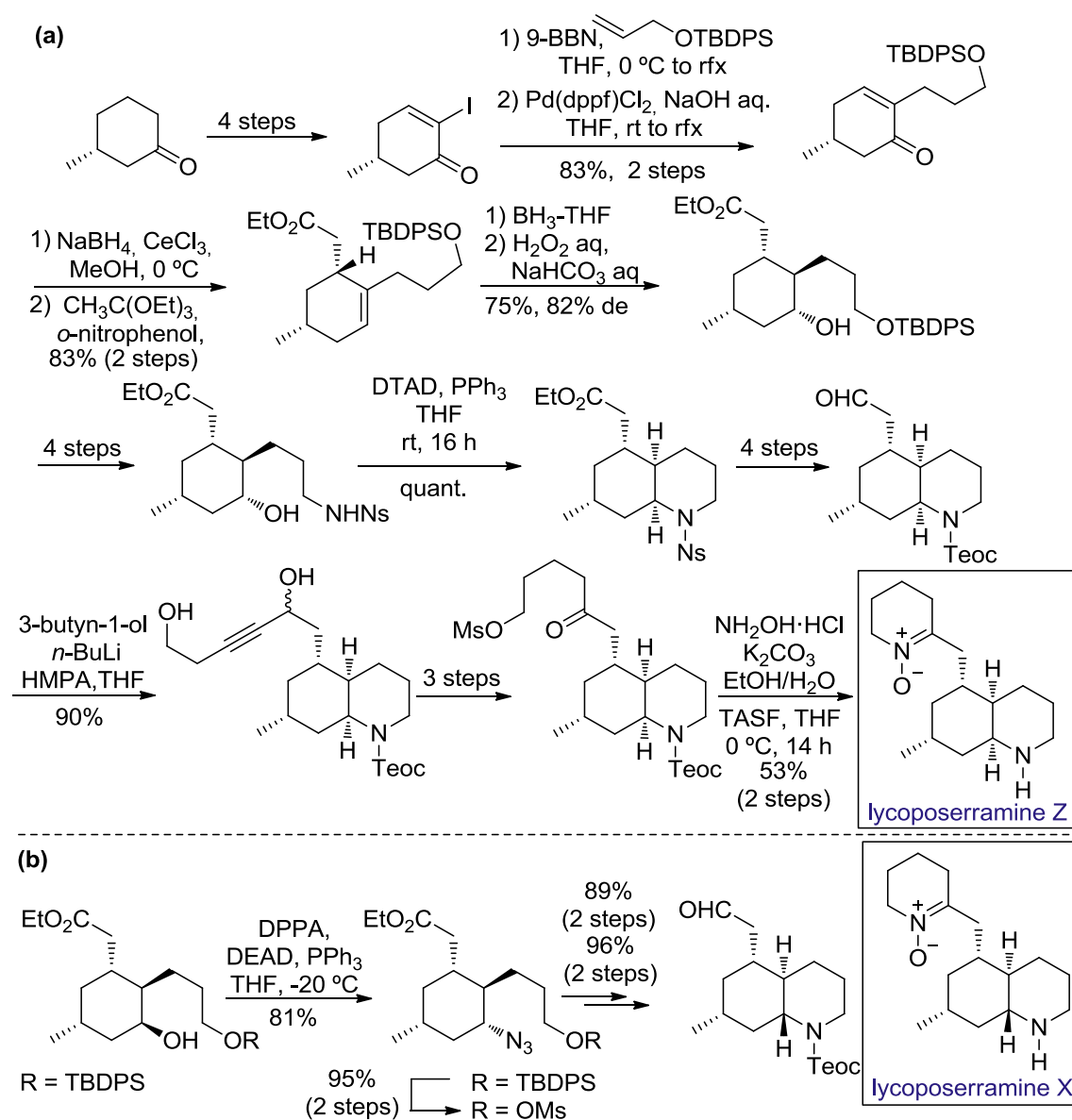
²³ (a) Szychowski, J.; Maclean, D. B. *Can. J. Chem.* **1979**, *57*, 1631-1637.
(b) Leniewski, A.; Szychowski, J.; Maclean, D. B. *Can. J. Chem.* **1981**, *59*, 2479-2490.

²⁴ When MacLean began the synthesis of phlegmarine he proposed that it contained an all *cis* decahydroquinoline system (type A). However, after arriving to a compound with this stereochemistry he realized that its NMR data did not match with that reported by Braekman and proposed that phlegmarine contains a *trans* decahydroquinoline core.

Total synthesis of type C β phlegmarine compounds (Comins)²⁵**Scheme 1.3** Total synthesis of type C β phlegmarine compounds (Comins)

In the first enantioselective synthesis of a naturally occurring phlegmarine, Comins established the configuration at C-8a using his acylpyridium salt methodology with (-)-TCC as the chiral auxiliary. Addition of the Grignard reagent of (*R*)-5-chloro-4-methylpentene followed by a conjugate addition of a silyl containing Grignard reagent took place with complete stereoselectivity, giving the correct stereochemistry at C-5. Hydrogenation of an endocyclic olefin provided the C-4a stereogenic center. Then, a second addition of the chiral auxiliary allowed the introduction of the piperidine ring with the correct stereochemistry at C-5'. From here reductions and various functional group manipulations allowed the synthesis of all the **type C β** phlegmarine compounds (Scheme 1.3).

²⁵ (a) Comins, D. L.; Libby, A. H.; Al-awar, R. S.; Foti, C. J. *J. Org. Chem.* **1999**, *64*, 2184-2185. (b) Wolfe, B. H.; Libby, A. H.; Al-awar, R. S.; Foti, C. J.; Comins, D. L. *J. Org. Chem.* **2010**, *75*, 8564-8570.

Total synthesis of lycoposerramine X and Z (Takayama)²⁶

Scheme 1.4 Takayama's total synthesis of (a) lycoposerramine Z and (b) lycoposerramine X

Starting from commercially available (*R*)-3-methylcyclohexanone installation of the side chain was achieved via a Pd-catalyzed Suzuki-Miyaura reaction followed by reduction and a Johnson-Claisen rearrangement.²⁷ An intramolecular Mitsunobu reaction gave the *cis*-

²⁶ Tanaka, T.; Kogure, N.; Kitajima, M.; Takayama, H. *J. Org. Chem.* **2009**, *74*, 8675-8680.

²⁷ The same approach was used in their previous approach to lycoposerramines V and W see: Shigeyama, T.; Katakawa, K.; Kogure, N.; Kitajima, M.; Takayama, H. *Org. Lett.* **2007**, *9*, 4069-4072

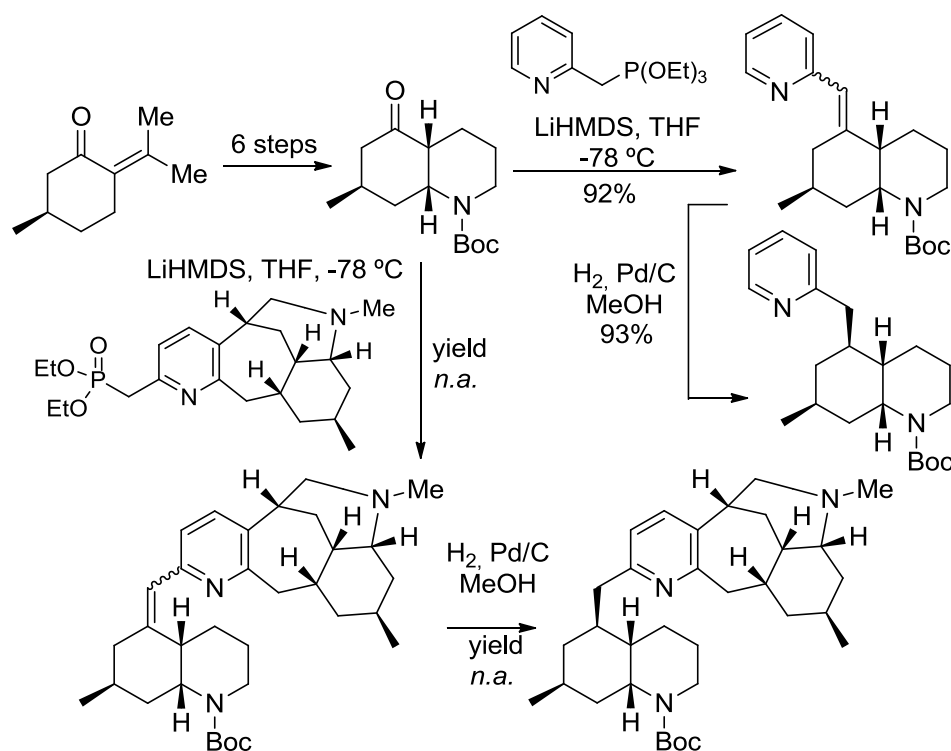
decahydroquinoline skeleton. After protecting group interchange, reduction and oxidation steps, the aldehyde was obtained, which was treated with an alkynyl anion to append the carbon chain necessary for the construction of the required nitron ring. Conversion to a ketomesylate and condensation with $\text{NH}_2\text{OH}\cdot\text{HCl}$ affords the cyclic nitron. Removal of the carbamate on the nitrogen resulted in the first synthesis of lycoposerramine Z, (Scheme 1.4a). A modification of the construction order allowed the route to access the *trans* decahydroquinoline nucleus which was converted to lycoposerramine X (Scheme 1.4b).

Towards the total synthesis of dihydrolycolucine (Sarpong)²⁸

The Sarpong group designed an approach to the highly complex dimeric compound dihydrolycolucine based on their synthesis of lyconadin A.²⁹ Appendage of a phosphonate unit to an advanced intermediate en route to lyconadin A and coupling to an enantiopure 5-oxodecahydroquinoline fragment gave a vinylpyridine intermediate. To test the coupling reaction and reduction they chose the phlegmarine compound serratezomine E as a model target which comprises of the same relative stereochemistry of the southern part of dihydrolycolucine. Thus the type A building block assembled using a modified approach developed by Maclean was subjected to a Horner-Wadsworth-Emmons reaction with a pyridine methyl phosphonate unit followed by hydrogenation. Whilst the reduction was diastereoselective it unfortunately gave the opposite stereochemistry to that required (notably, this is the same relative stereochemistry of lycoposerramine Z). Using the analogous sequence of coupling they elaborated tetracyclic phosphonate and hydrogenation towards dihydrolycolucine was carried out with the

²⁸ Sarpong, unpublished results: Sarah Elizabeth House, Ph. D. **2010**, University of California, Berkeley.

²⁹ Whilst this compound bears many similarities to the phlegmarine alkaloids the presence of the 7-membered ring led to a completely different disconnection approach: see: Bisai, A.; West, S. P.; Sarpong, R. *J. Am. Chem. Soc.* **2008**, *130*, 7222-7223.



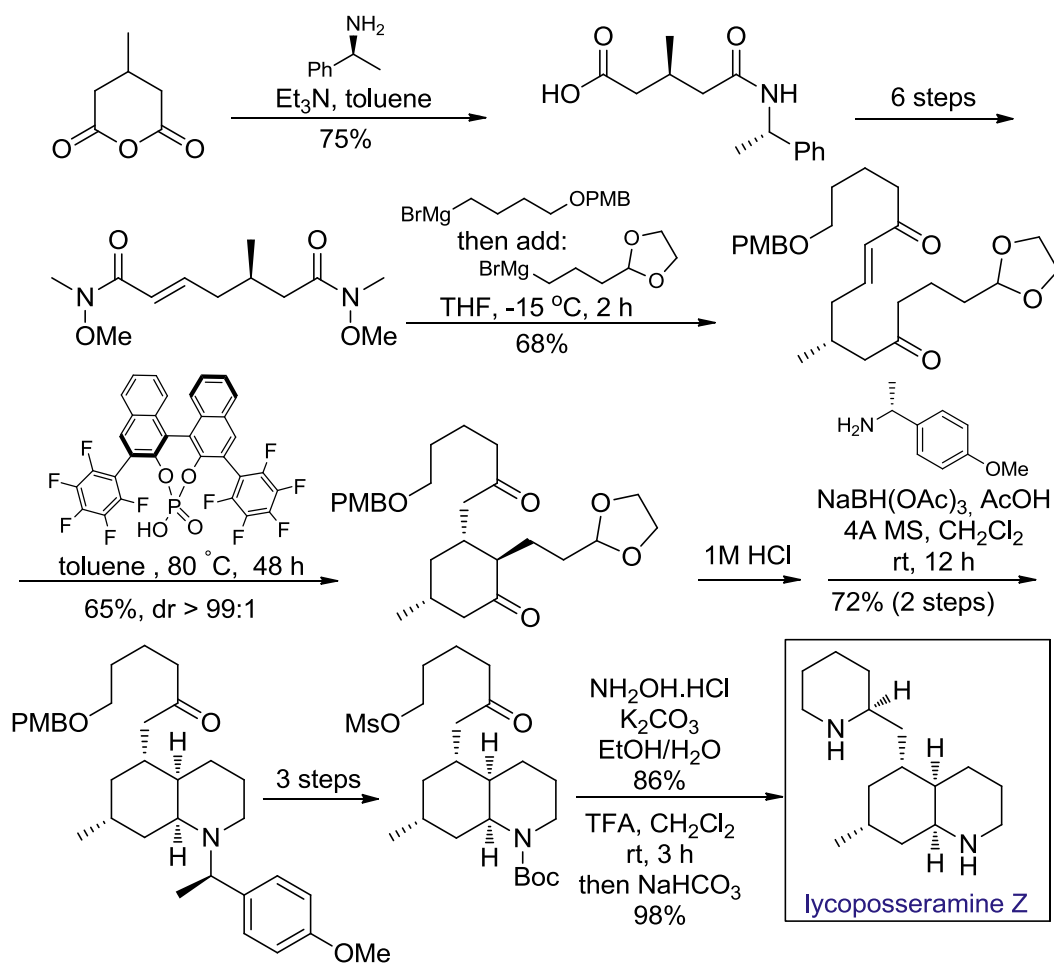
Scheme 1.5 Sarpong's approximation to serratezomine E and dihydrolycolucine

same unwanted facial selectivity. No yields are given presumably due lack of material which didn't allow them to quantify these transformations and ultimately led them to abandon the synthesis. It should be noted however that both the directness and modularity of this approach is interesting and a strategy that could overturn this observed facial selectivity could be used as the key step in the synthesis of not only dihydrolycolucine but also the other simple and complex miscellaneous group lycopodium alkaloids.

Total synthesis of lycoposerramine Z (Yao)³⁰

Desymmetrization of commercially available 3-methylglutaric anhydride with (*S*)-methylbenzylamine was used to introduce the chirality. Subsequent functional group manipulations then gave *bis*-Weinreb

³⁰ Zhang, L. D.; Zhong, L. R.; Xi, J.; Yang, X. L.; Yao, Z.Y. *J. Org. Chem.* **2016**, *81*, 1899-1904.



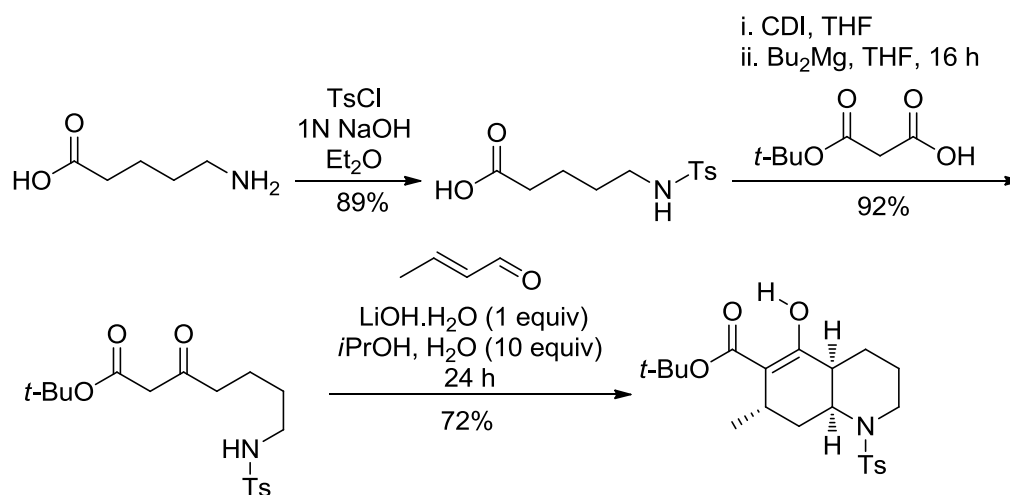
Scheme 1.6 Total synthesis of lycoposerramine Z by Yao

amide.³¹ Chemoselective Grignard addition onto the α, β unsaturated Weinreb amide addition over its aliphatic partner gave the corresponding diketo compound. Use of a chiral Brønsted acid catalyst gave the desired cyclohexenone in excellent 99% dr. Removal of the *O, O*-ketal with aq. HCl, followed by reductive amination with commercially available (*S*)-1-(4-methoxyphenyl)-ethylamine, provided the decahydroquinoline as a single diastereomer. Hydrogenation and Boc protection gave the *N*-Boc protected primary alcohol. Mesylation followed by treatment with $\text{NH}_2\text{OH}\cdot\text{HCl}$ and K_2CO_3 provided the cyclic nitrone. Finally, removal of the *N*-Boc protecting group with TFA gave lycoposerramine Z.

³¹ Yao employed this same intermediate in his prior synthesis of lycoposerramine V. See: Zhang, L.; Zhou, T. T.; Qi, S. X.; Xi, J.; Yang, X. L.; Yao, Z. Y. *Chem. Asian. J.* **2014**, *9*, 2740-2744.

- Previous Work by Our Research Group

Synthesis of 5-oxodecahydroquinoline



Scheme 1.7 Synthesis of type A decahydroquinoline

Using a tandem reaction sequence from a simple acyclic β -ketoester bearing a tosyl protected nitrogen tether our research group has developed a highly efficient route to 5-oxodecahydroquinolines (of type A structure).³² Treatment of the β -ketoester with crotonaldehyde in the presence of $\text{LiOH}\cdot\text{H}_2\text{O}$ and water in *i*PrOH initiated a tandem Robinson-annulation aza-Michael cyclization to give the decahydroquinoline ring (Scheme 1.7).

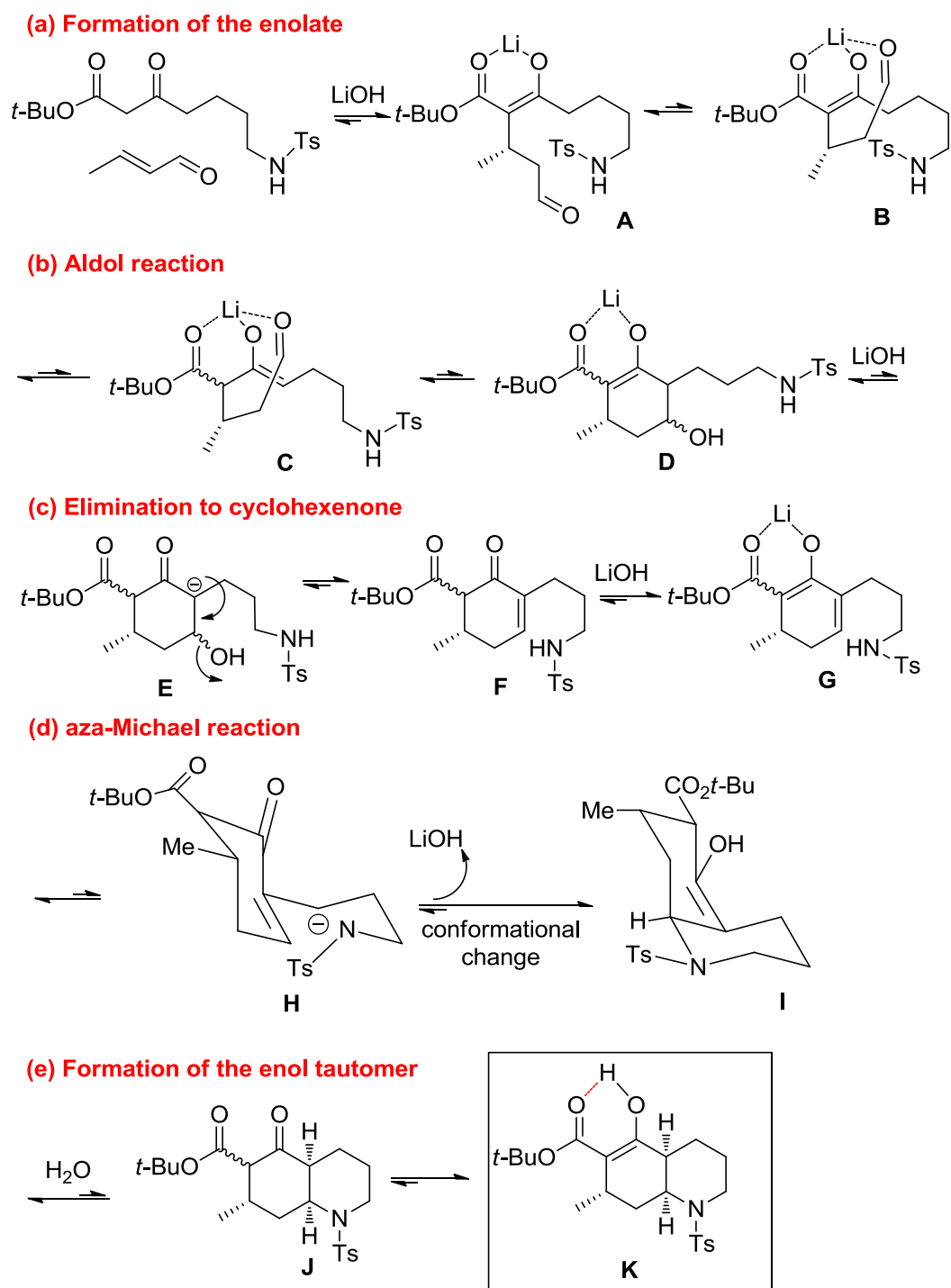
Only one single diastereoisomer was formed. This result was corroborated by calculation of the energies of the 4 possible diastereoisomers. Notably, the cyclic β -keto ester formed has the methyl group at C-7 axially located but was found to be thermodynamically more stable than the absent epimer with the methyl substituent equatorially located. This is believed to be due to steric crowding that would result from the bulky *tert*-butoxycarbonyl group if it was located on the same plane as the equatorial methyl substituent at C-7.

³² Bradshaw, B.; Luque-Corredera, C.; Bonjoch, J. *Org. Lett.* **2013**, *15*, 326-329.

Proposed Mechanism of the Tandem Reaction³³

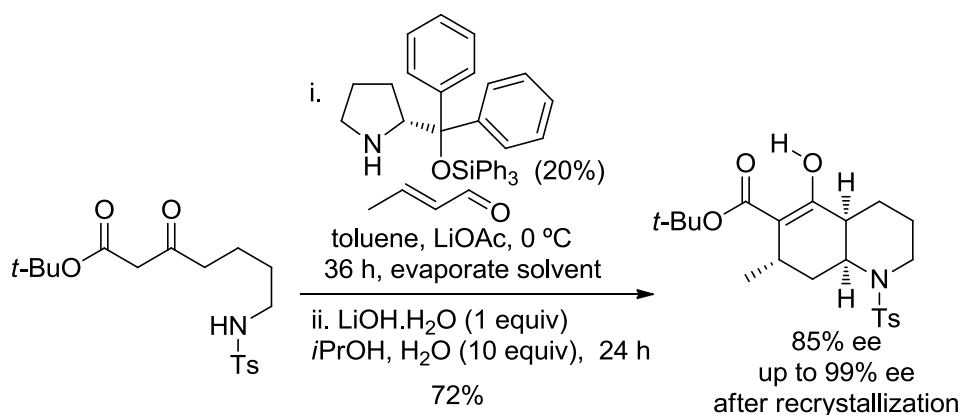
Based on the experimental results, a plausible mechanism for the reaction was proposed which was then refined and corroborated by DFT modelling studies (Scheme 1.8). The mechanism can be split into roughly 5 parts: **Formation of the correct enolate:** Michael reaction between the β -keto ester and crotonaldehyde gave the coupled product, which deprotonates further to give the more stable lithium enolate species **A** and effectively preventing the Robinson annulation from progressing (Scheme 1.8a). However, it was thought that the carbonyl group on the side chain forms a tricoordinated species **B** whose energy difference between the analogous tricoordinated species **C** is reduced lowering the energy enough of species **C** to form to allow sequence to continue. **Aldol reaction:** Once formed, the required regiospecific enolate undergoes an aldol reaction. However, proton transfer to the alkoxide from the keto ester reforms the more stable enolate **D**, which effectively halts the reaction once again (Scheme 1.8b). **Elimination to Cyclohexenone:** Despite the stability of **D** a small quantity of the less stable enolate **E** is present at equilibrium and undergoes dehydration to give enone **F**. Deprotonation of the keto ester once again prevents the reaction from progressing by forming the more stable enolate **G** (Scheme 1.8c). **Aza-Michael reaction and protonation:** A small amount of enone **H** present at equilibrium undergoes an aza-Michael with attack from the top face to give an intermediate, which immediately undergoes protonation and a ring flip to form **I** setting the methyl group in the axial position. The presence of water provides a ready source of protons to trap intermediate **I** before the retro aza-Michael product can revert back to the ring-opened form **H**. Finally, hydrogen bond formation between the enol form and the ester group locks the molecule and drives the reaction to completion and

³³ Bradshaw, B.; Luque-Corredera, C.; Saborit, G.; Cativiela, C.; Dorel, R.; Bo, C.; Bonjoch, J. *Chem. Eur. J.* **2013**, *19*, 13881-13892.



Scheme 1.8 Overview of the *bis*-cyclization process mechanism leading to 5-oxodecahydroquinolines (based on experimental DFT modelling studies)

ensuring the stability of **K**. Whilst the vast majority of steps are unfavourable the last step in which the enol of **K** is formed drives the various equilibria over to the right to allow the reaction to reach completion.

Organocatalyzed synthesis of decahydroquinolines**Scheme 1.9** Organocatalyzed synthesis of type A decahydroquinoline

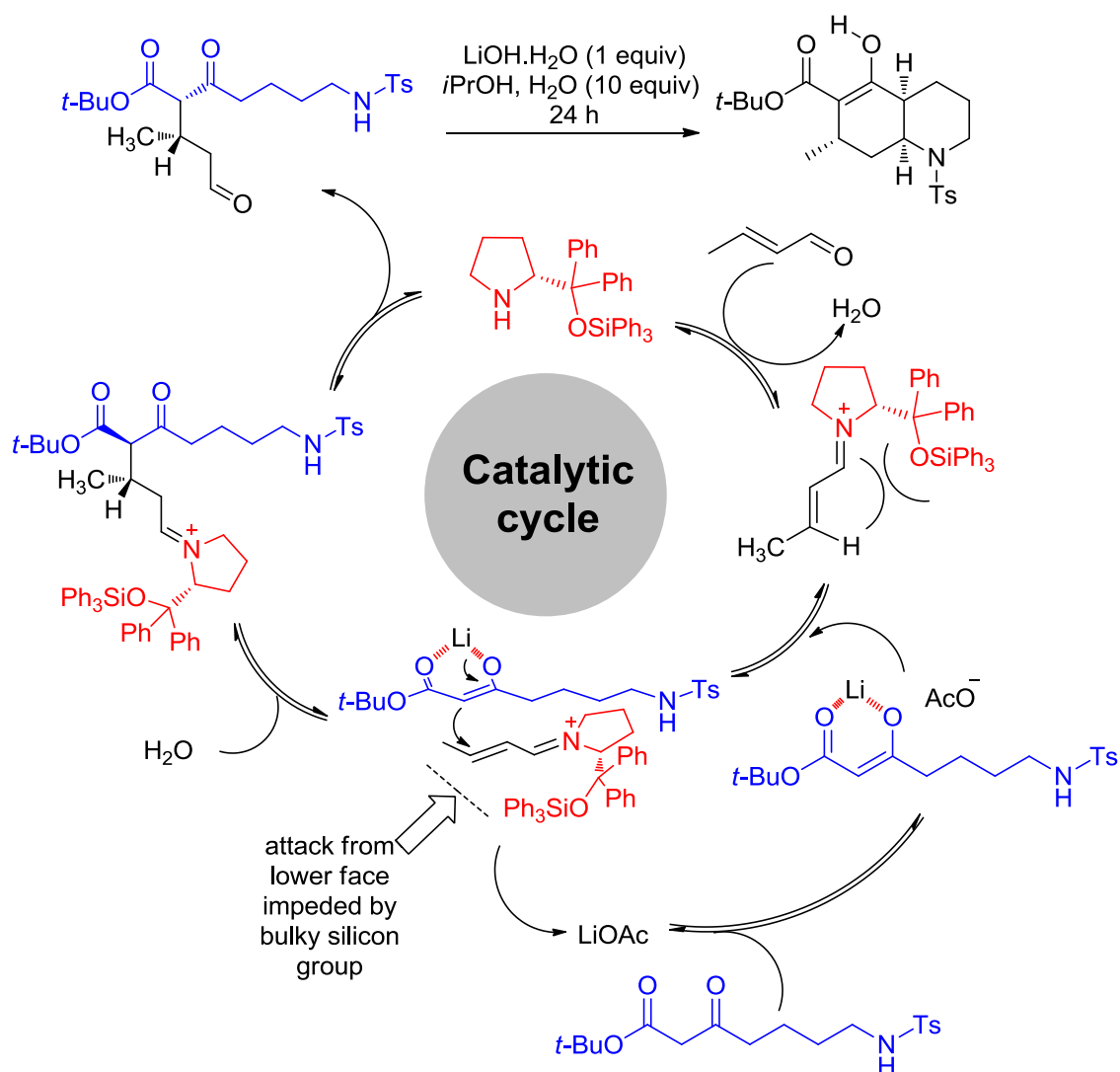
An asymmetric version was then developed by using the Hayashi-Palomo catalyst,³⁴ to render the initial Michael addition enantioselective allowing for the formation of the bicyclic product in 85% ee and >99% ee after recrystallization (Scheme 1.9).

Mechanism of the organocatalytic step

The mechanism for the organocatalytic part of the reaction is outlined in Scheme 1.10. The catalyst couples with crotonaldehyde to give an imine intermediate with the methyl orientated away from the bulky O-silyl substituent. The function of LiOAc presumably helps to activate the β -keto ester and make it more nucleophilic by helping to form the enolate.³⁵ Additionally, it may interact with the coupled product to form the tricoordinated species proposed in the previous section. This would remove the free aldehyde from the equilibrium, freeing the organocatalyst to re-enter the catalytic cycle.

³⁴ Palomo, C.; Landa, A.; Mielgo, A.; Oiarbide, M.; Puente, A.; Vera, S. *Angew. Chem. Int. Ed.* **2007**, *46*, 8431-8435.

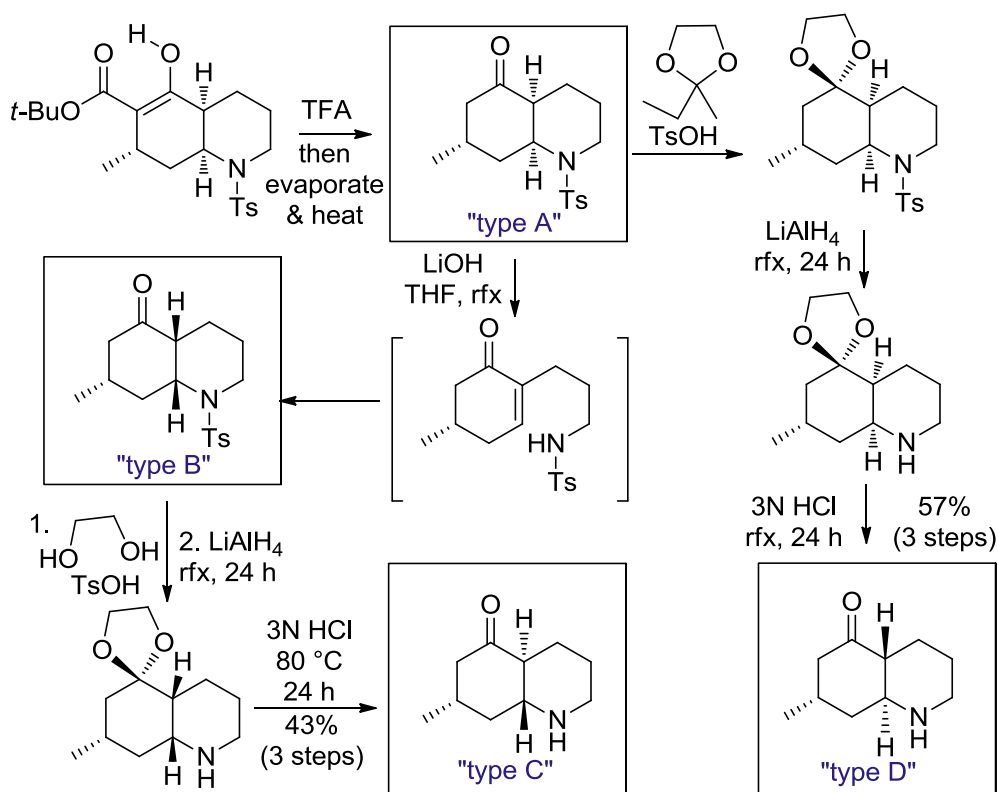
³⁵ In the absence of the additive less coupling was observed. For an interesting study on the effect of LiOAc in organocatalyzed Michael reactions, see: Duce, S.; Mateo, A.; Alonso, I.; García Ruano, J. L.; Cid, M. B. *Chem. Commun.* **2012**, *48*, 5184-5186.



Scheme 1.10 Mechanism for the organocatalytic step

It is not clear if the free NH-Ts on the side chain plays a key role in the reaction e.g. via H-bonding with another part of the molecule. It is likely that it must play more than just a passive role in the reaction mechanism due to the significant differences observed compared to those observed by Jørgensen using simple β -keto esters.³⁶

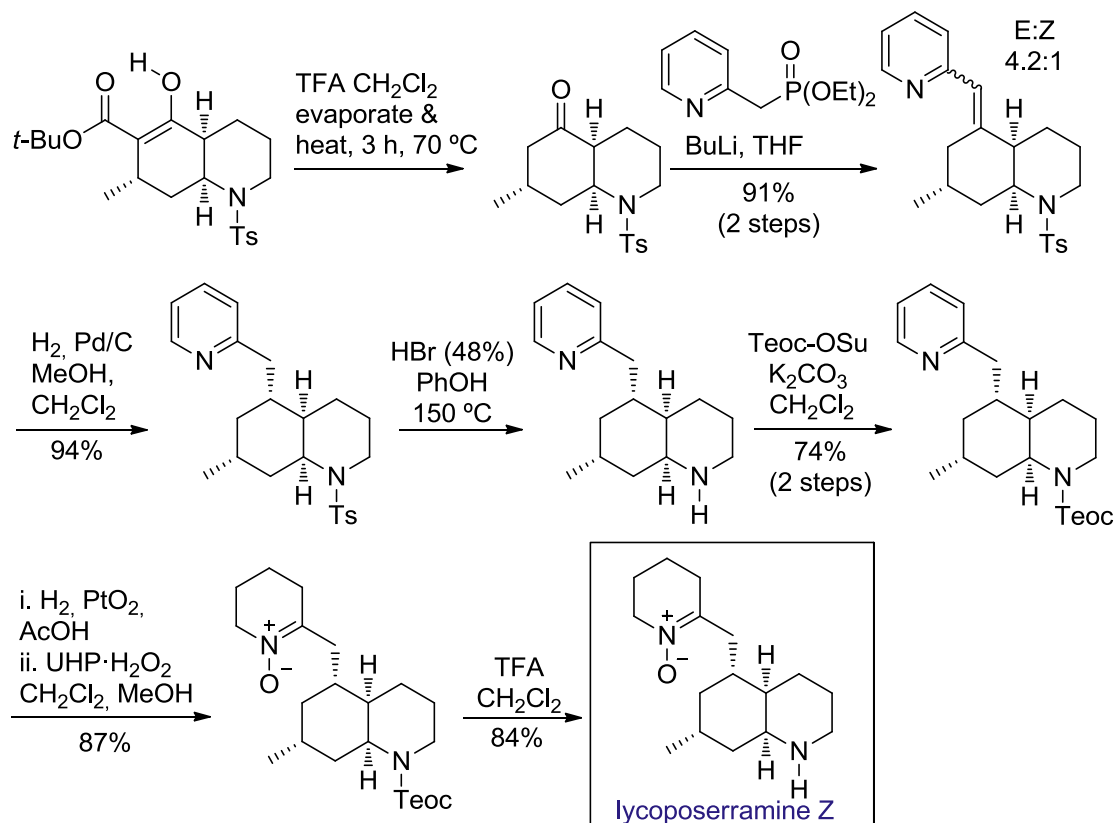
³⁶ Jensen, K. L.; Dickmeiss, G.; Jiang, H.; Albrecht, L.; Jørgensen, K. A. *Acc. Chem. Res.* **2012**, *45*, 248-264.

Access to 5-oxodecahydroquinolines of type B, C and D³³**Scheme 1.11** Access to 5-oxodecahydroquinolines of type B, C and D

After obtaining the type A stereochemistry it was subsequently shown that the other three relative stereochemistries of 7-methyl-5-oxodecahydroquinolines (“types B-D”) could also be obtained from this same intermediate through a series of configurationally controlled equilibration processes (see Scheme 1.11). When the ester was removed a retro aza-Michael reaction followed by re-closure of the ring, the type B stereochemistry was observed and found to be the most thermodynamically stable compound by calculation. After formation of the acetal of the type B compound and removing the nitrogen-substituent group, isomerization at C-4a via enolization and reprotonation from the opposite face gave the desired *trans* stereochemistry. An analogous process from the type A substrate allowed access to type D compounds.

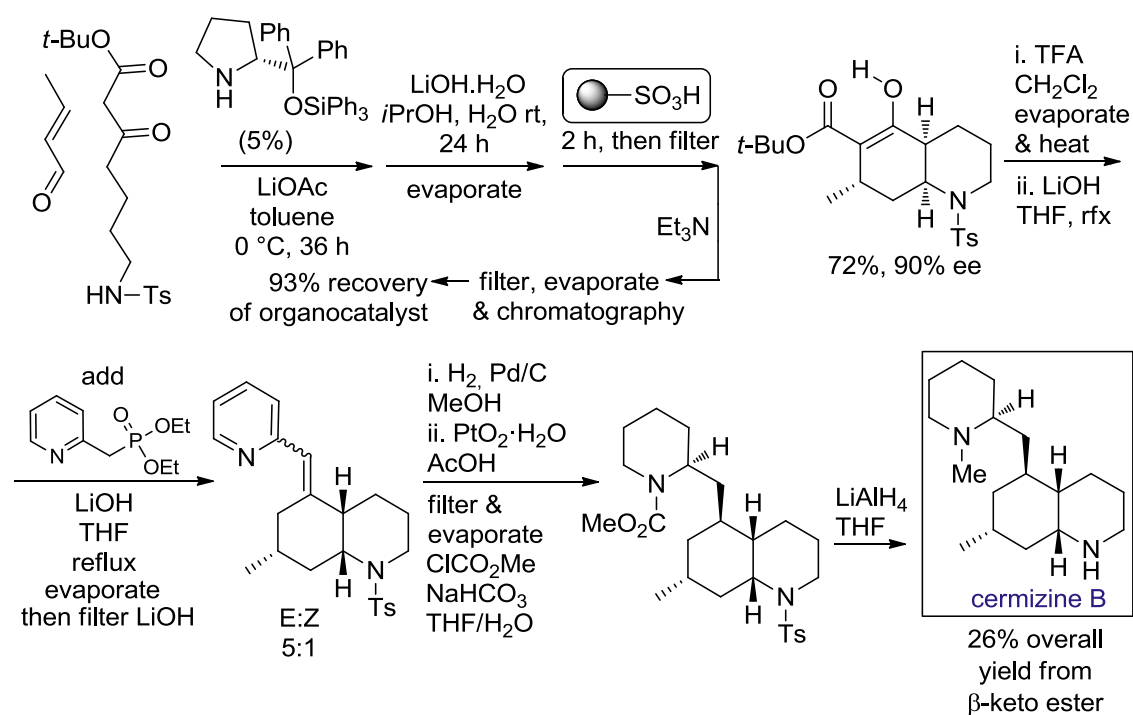
- Use of Decahydroquinoline building block in total synthesis

Total synthesis of lycoposerramine Z³²



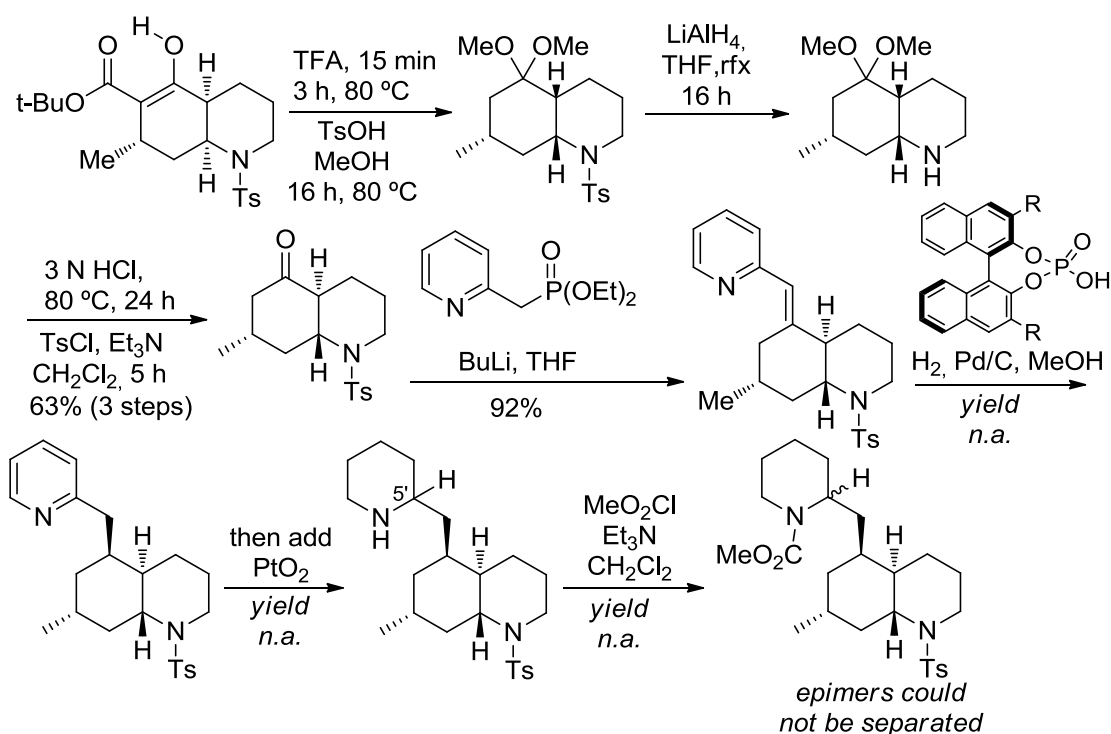
Scheme 1.12 Total synthesis of lycoposerramine Z

The building block containing the all *cis* type A stereochemistry ideally positioned it for a synthesis of the phlegmarine alkaloid lycoposerramine Z (Scheme 1.12). After decarboxylation, the decahydroquinoline building block underwent a Horner-Wadsworth-Emmons with a pyridine phosphonate to install all the remaining carbon atoms. Hydrogenation of the resulting vinyl pyridine took place selectively from the top face to install all the required stereogenic centres. Since the conditions required to remove the tosyl group were not compatible with the sensitive nitron moiety, it was exchanged for the more easily removable Teoc group (used by Takayama in his synthesis of the same compound). Hydrogenation of the pyridine, oxidation with urea peroxide and finally treatment with TFA gave lycoposerramine Z.

Total synthesis of cermizine B³⁷**Scheme 1.13** Total synthesis of cermizine B

Total synthesis of cermizine B³⁷ was achieved using similar method (Scheme 1.13). After formation of the decahydroquinoline nucleus the reaction mixture was treated with an acidic resin to scavenge the basic residues and to capture and recover the organocatalyst. Treatment with TFA removed the ester whilst refluxing with LiOH allowed partial equilibration to the type B stereochemistry, which could be driven to completion by selective trapping of the type B intermediate with a pyridine phosphonate. Finally, hydrogenation of the vinyl pyridine with Pd/C followed by addition of PtO_2 gave the piperidine, which was converted to the methyl carbamate allowing the undesired epimer to be removed by chromatography. Finally, reduction with LiAlH_4 removed the tosyl group and converted the carbamate to a methyl affording the desired product. Notably most steps did not require work-up or chromatography and could be carried out in the same flask and on a gram scale.

³⁷ Bradshaw, B.; Luque-Corredera, C.; Bonjoch, J. *Chem. Commun.* **2014**, 50, 7099-7102.

Attempted synthesis of phlegmarine (2016)³⁸**Scheme 1.14** Attempted synthesis of phlegmarine (2016).

Based on the method outlined in Scheme 1.11 the type C nucleus was obtained. Coupling was initially attempted with a chiral piperidine phosphonate but unfortunately this led only to ring opening of the decahydroquinoline ring.³⁹ However the pyridine phosphonate readily coupled in excellent 92% yield. Reduction only mildly selective for the desired epimer could be improved to 4:1 by addition of a chiral phosphoric acid. Reduction with PtO_2 in AcOH reduced the pyridine to a piperidine ring. This reduction could also be done in the presence of the same chiral phosphoric acid used above however no selectivity for the piperidine C-5' position was observed. Unfortunately the epimers could not be separated even by the formation of the methyl carbamate. Lack of material⁴⁰ at this point did not allow the completion of the synthesis.

³⁸ Gisela Saborit, Universitat de Barcelona, thesis, unpublished results.

³⁹ Notably the enantiomer of the chiral piperidine readily coupled indicating that the desired stereochemistry was mismatched.

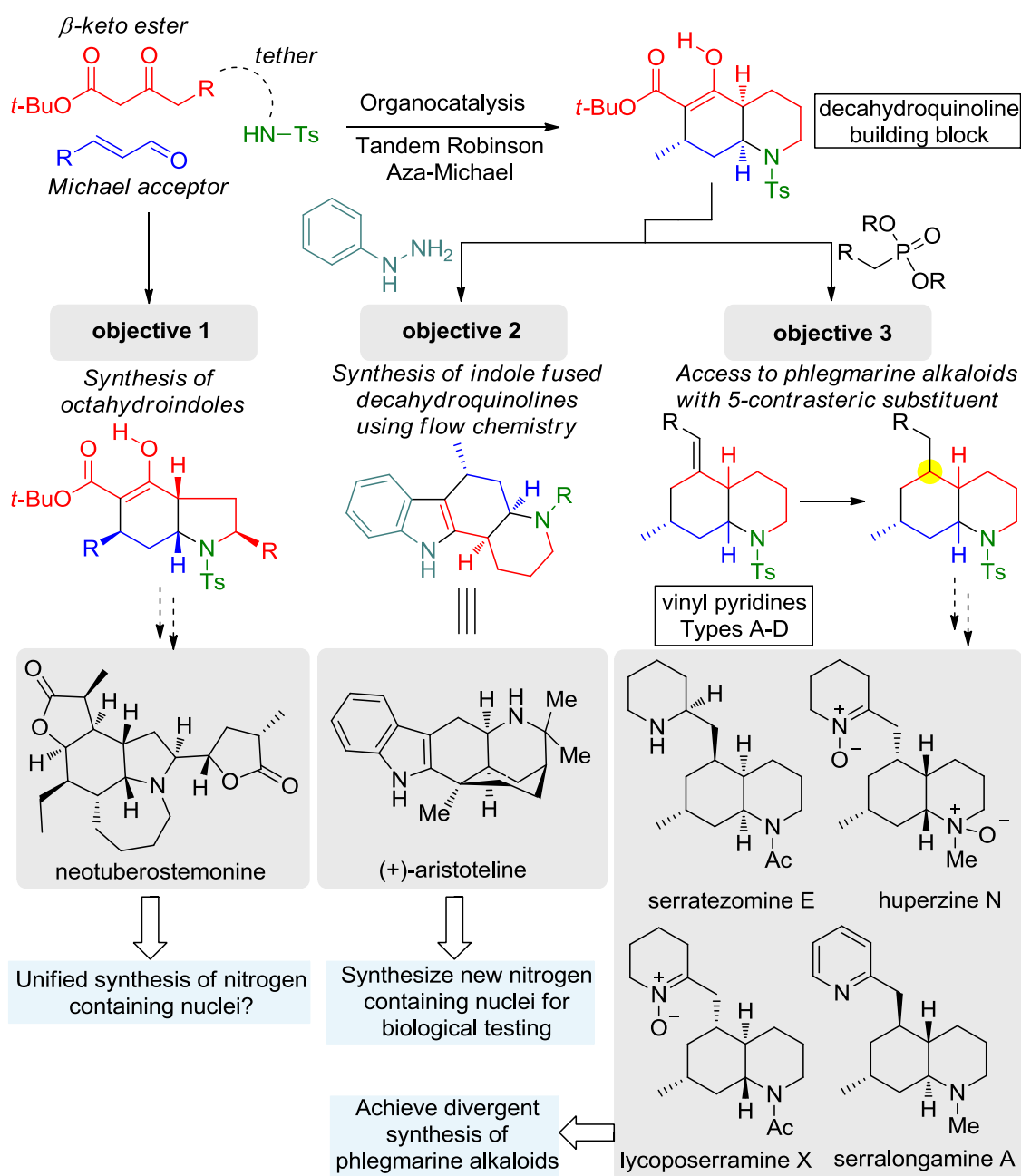
⁴⁰ Last steps were performed on small scale: yields are not available.

1.2 Objectives

Objective 1: The organocatalyzed construction of highly functionalized polycyclic nuclei in a one-pot operation from simple acyclic precursors has the potential to greatly shorten a synthetic sequence targeting complex natural products. The developed organocatalytic strategy toward decahydroquinolines (Scheme 1.9) was instrumental in enabling highly efficient syntheses of the phlegmarine alkaloids lycoposerramine Z (Scheme 1.12) and cermizine B (Scheme 1.13). Looking to expand the potential of this methodology, it soon became apparent that the principles behind the reaction sequence, namely a β -keto ester, a tethered sulfonamide and an enal engaging in a tandem Robinson aza-Michael reaction (Scheme 1.15) could be more general in scope, providing access to a range of different important nitrogen bicyclic nuclei in enantiopure form. Indeed, this proved to be the case, and allowed our research group to achieve the first efficient synthetic entry to the morphan nucleus using organocatalysis from simple acyclic precursors.⁴¹ Here, we propose to examine the scope of this strategy to include the octahydroindole unit, another privileged scaffold found in an extensive and diverse range of compounds such as neotuberostemonine.

Objective 2: Heterocyclic scaffolds bearing a tetrahydrocarbazole structural subunit and an additional nitrogen-containing ring are found both in natural products (alkaloids) and pharmacologically active compounds developed in medicinal chemistry research. More particularly, a series of tetracyclic indoles have been reported as androgen receptor ligands, among which an unprecedented pyrido[2,3-*a*]carbazole scaffold was evaluated. Considering the pharmacological interest in pyridocarbazole compounds and the availability of *cis*-5-oxodecahydroquinolines we decided to study the Fischer indole reaction

⁴¹ Bradshaw, B.; Parra, C.; Bonjoch, J. *Org. Lett.* **2013**, *15*, 2458-2461.



Scheme 1.15 Overview of objectives

on the latter compounds. Besides studying conventional efficient batchwise approaches, we were also interested in comparing those with continuous flow procedures employing immobilized catalysts.

Objective 3: So far the two strategies developed by our group to synthesize the phlegmarine alkaloids have been dependent on using sterics to control the diastereoselectivity in the hydrogenation step of the vinyl pyridine unit. In both cases the resultant products of the reduction

present a *cis* relationship between the C-5 substituent and the C-8a hydrogen. As discussed previously a large number of lycopodium natural products present a *trans* relationship between the C-5 substituent and the C-8a hydrogen. Thus, development of a contrasteric reduction process would open access to this large pool of natural products. Our proposal is to develop such a process and use it to allow us to achieve a unified synthesis of representative examples of all of the phlegmarine alkaloids in a divergent synthetic process.

Regarding the philosophy behind this work, two sentences of K. C. Nicolaou from a classical paper published some years ago are pertinent.⁴²

“The total synthesis of natural products has served as the flagship of chemical synthesis and the principal driving force for discovering new chemical reactivity, evaluating physical organic theories, testing the power of existing synthetic methods, and enabling biology and medicine”

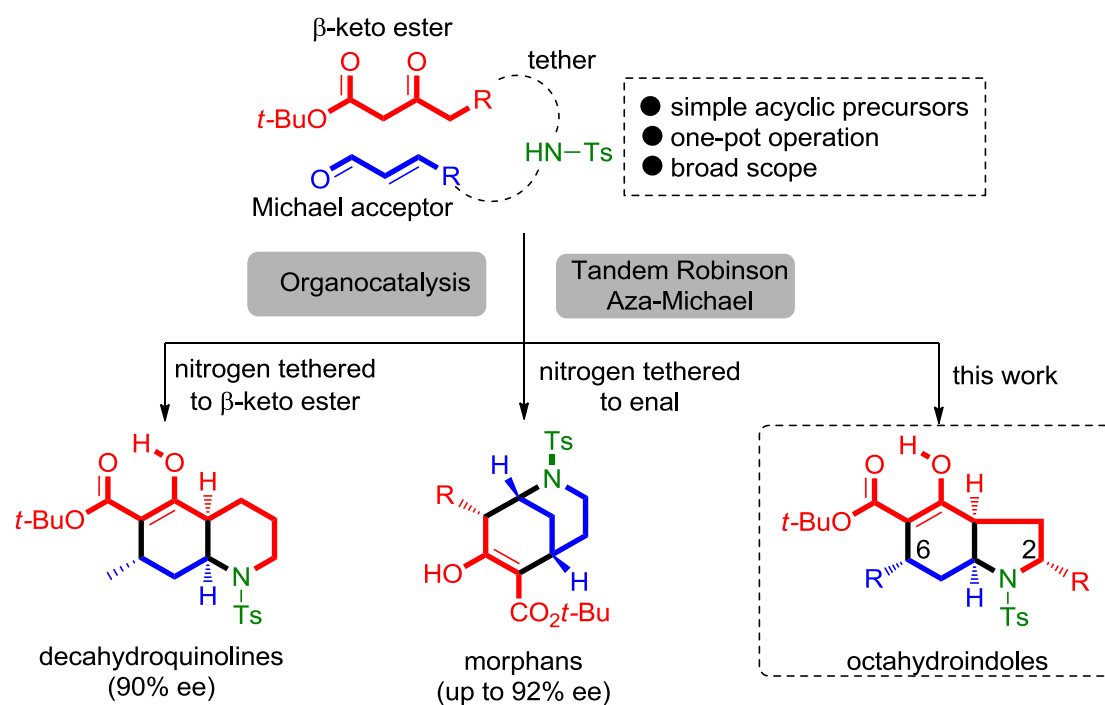
Among others, a reason for practicing natural product synthesis is

“To exploit the opportunity that a challenging molecular architecture presents for the discovery and invention of new synthetic strategies and methods to be used in a wide range of applications”

⁴² Nicolaou, K. C.; Snyder, S. A. *Proc. Natl. Acad. Sci. USA* **2004**, *101*, 11929-11936.

**2. Asymmetric Synthesis of Octahydroindoles via a
Domino Robinson Annulation/5-*Endo* Intramolecular
Aza-Michael Reaction**

J. Org. Chem. **2016**, DOI: 10.1021/acs.joc.6b01568



Scheme 2.1 Unified Synthesis of Nitrogen Containing Nuclei

The organocatalyzed construction of highly functionalized polycyclic nuclei in a one-pot operation from simple acyclic precursors has the potential to greatly shorten a synthetic sequence targeting complex natural products.⁴³ Previously, we have developed an organocatalytic strategy toward decahydroquinolines, which allowed the efficient synthesis of natural products such as lycoposerramine Z³² and cermizine B.³⁷ In both cases, the tandem reaction was instrumental in enabling highly efficient syntheses of these natural products. Looking to expand the potential of this methodology, it soon became apparent that the principles³³ behind the reaction sequence, namely a β -keto ester, a tethered sulfonamide and an enal engaging in a tandem Robinson aza-Michael reaction, could be more general in scope, providing access to a range of different important nitrogen bicyclic nuclei in enantiopure form.

⁴³ For reviews of organocatalysis in the synthesis of natural products, see: (a) Marqués-López, E.; Herrera, R. P.; Christmann, M. *Nat. Prod. Rep.* **2010**, *27*, 1138-1167. (b) Abbasov, M. E.; Romo, D. *Nat. Prod. Rep.* **2014**, *31*, 1318-1327. (c) Sun, B. F. *Tetrahedron Lett.* **2015**, *56*, 2133-2140. (d) Ishikawa, H.; Shiomi, S. *Org. Biomol. Chem.* **2016**, *14*, 409-424.

Indeed, this proved to be the case, and allowed us to achieve the first efficient synthetic entry to the morphan nucleus using organocatalysis from simple acyclic precursors.⁴¹

In this chapter of the thesis we detail our efforts to expand the scope of this strategy to the octahydroindole unit,⁴⁴ another privileged scaffold found in an extensive and diverse range of compounds. These include natural products such as aeruginosin 298-A,⁴⁵ neotuberostemonine,⁴⁶ lycorine,⁴⁷ pharmaceutical products such as perindopril,⁴⁸ and a number of proline analog organocatalysts.⁴⁹

While a number of methods have been developed to synthesize octahydroindoles in enantiopure form, using the chiral pool approach⁵⁰ or asymmetric metal-catalyzed reactions,⁵¹ there are few previous approaches using aminocatalysis.⁵²

⁴⁴ We have recently become aware of a new approach to hydroindoles through organocatalysis from acyclic precursors (Prof. F. P. Cossío, XXVI Reunión Bienal GEQOR, Punta Umbría, Spain, June 2016, personal communication).

⁴⁵ For total syntheses, see: (a) Valls, N.; Lopez-Canet, M.; Vallribera, M.; Bonjoch, J. *J. Am. Chem. Soc.* **2000**, *122*, 11248–11249. (b) Dailler, D.; Danoun, G.; Baudoin, O. *Angew. Chem. Int. Ed.* **2015**, *54*, 4919–4922 and references therein.

⁴⁶ Frankowski, K. J.; Golden, J. E.; Zeng, Y.; Lei, Y.; Aubé, J. *J. Am. Chem. Soc.* **2008**, *130*, 6018–6024.

⁴⁷ For total synthesis, see: Ghavre, M.; Froese, J.; Pour, M.; Hudlicky, T. *Angew. Chem. Int. Ed.* **2016**, *55*, 5642–5691 and references therein.

⁴⁸ Hurst, M.; Jarvis, B. *Drugs* **2001**, *61*, 867–896.

⁴⁹ (a) Sayago, F. J.; Laborda, P.; Calaza, M. I.; Jiménez, A. I.; Cativiela, C. *Eur. J. Org. Chem.* **2011**, *11*, 2011–2028. (b) Arceo, E.; Jurberg, I. D.; Alvarez-Fernández, A.; Melchiorre, P. *Nat. Chem.* **2013**, *5*, 750–756.

⁵⁰ (a) Wipf, P.; Kim, Y.; Goldstein, D. M. *J. Am. Chem. Soc.* **1995**, *117*, 11106–11112. (b) Bonjoch, J.; Catena, J.; Isábal, E.; López-Canet, M.; Valls, N. *Tetrahedron: Asymmetry* **1996**, *7*, 1899–1902. (c) Trembay, M.; Hanessian, S. *Org. Lett.* **2004**, *6*, 4683–4686. (d) Ruff, B. M.; Zhong, S.; Nieger, M.; Sickert, M.; Schneider, C.; Bräse, S. *Eur. J. Org. Chem.* **2011**, *11*, 6558–6566. (e) Hanessian, S.; Dorich, S.; Menz, H. *Org. Lett.* **2013**, *15*, 4134–4137.

⁵¹ (a) Schindler, C. S.; Diethelm, S.; Carreira, E. M. *Angew. Chem. Int. Ed.* **2009**, *48*, 6296–6299. (b) Trost, B. M.; Kaneko, T.; Andersen, N. G.; Tappertzhofen, C.; Fahr, B. *J. Am. Chem. Soc.* **2012**, *134*, 18944–18947. (c) Sun, Z.; Zhou, M.; Li, X.; Meng, X.; Peng, F.; Zhang, H.; Shao, Z. *Chem. Eur. J.* **2014**, *20*, 6112–6119. (d) Dailler, D.; Danoun, G.; Baudoin, O. *Angew. Chem. Int. Ed.* **2015**, *54*, 4919–4922.

⁵² Using aminocatalysis: (a) Pantaine, L.; Coeffard, V.; Moreau, X.; Greck, C. *Org. Lett.* **2015**, *17*, 3674–3677. Using a chiral Brønsted acid catalyst: (b) Ruff, B. M.; Zhong, S.; Nieger, M.; Sickert, M.; Schneider, C.; Bräse, S. *Eur. J. Org. Chem.* **2011**, *11*, 6558–6566. (c) Han, Y.; Zheng, B.; Peng, Y. *Adv. Synth. Catal.* **2015**, *357*, 1136–1142.

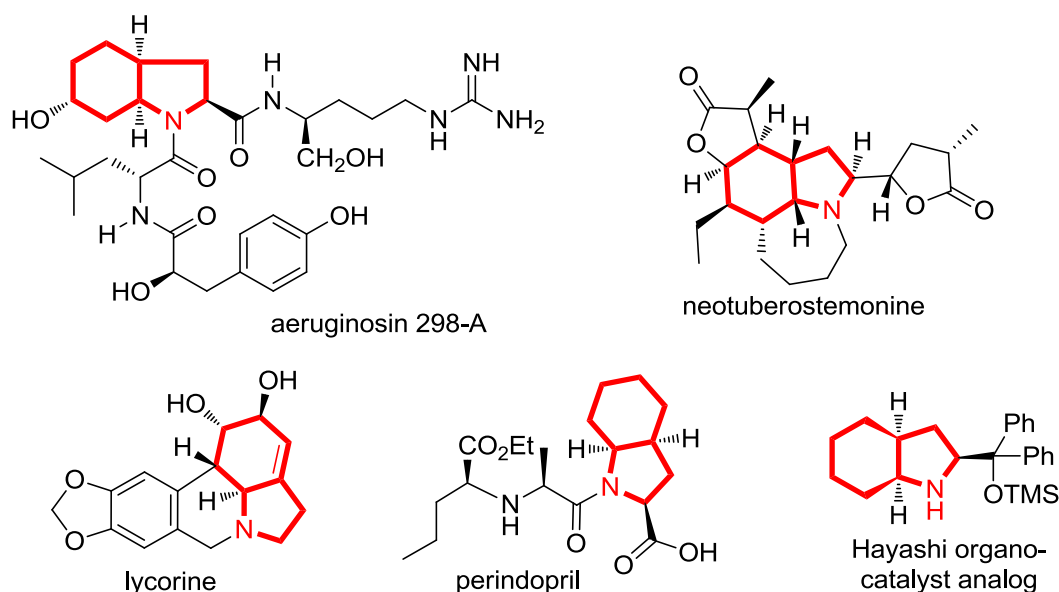
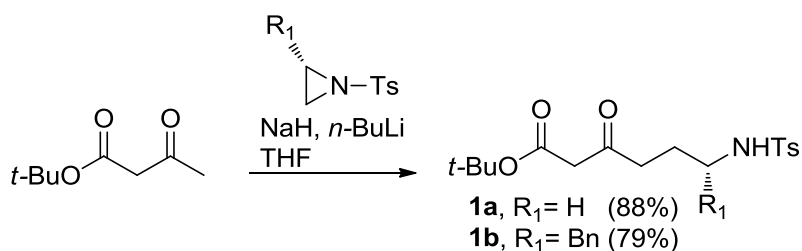


Figure 2.1 Octahydroindoles in natural and synthetic compounds

Detailed herein is the development of an organocatalysis-mediated synthesis of octahydroindoles from a non-cyclic precursor. Moreover, the domino process (Robinson annulation followed by an intramolecular aza-Michael reaction) was also studied using an enantiomerically pure starting material to check its influence on the stereochemical outcome.

Preparation of the required starting material was achieved in a one-step manner by ring opening of the commercially available tosyl aziridines via the dianion of *t*-butyl acetoacetate⁵³

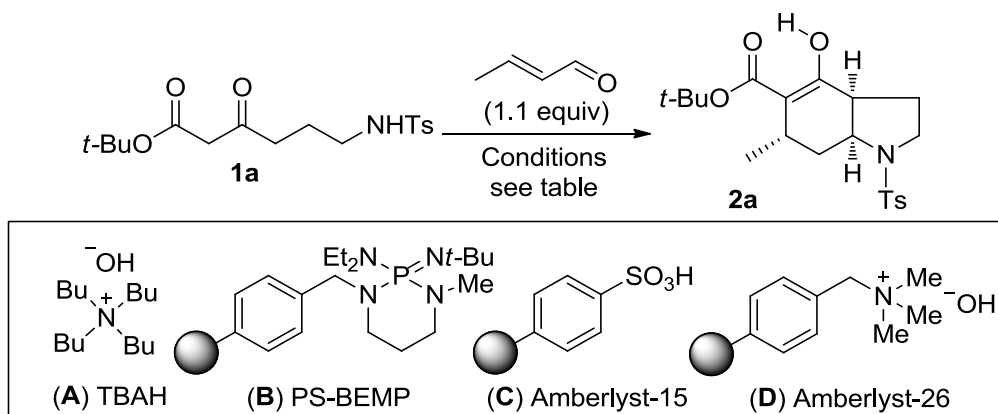


Scheme 2.2 Synthesis of starting materials

⁵³ For reaction of *N*-tosylaziridines with dianions derived from β -keto esters, see: Lygo, B. *Synlett* **1993**, 764–766.

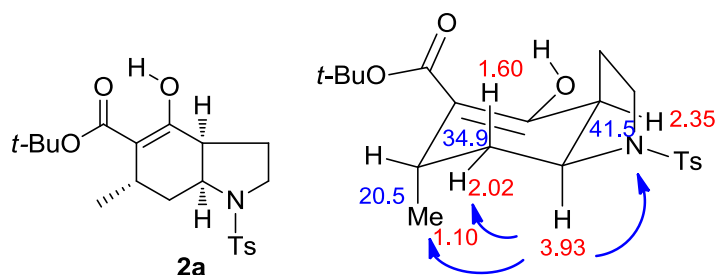
With the starting material **1a** in hand, the non-asymmetric version of the tandem cyclization reaction was initially investigated. Different bases were evaluated to perform the reaction (see Table 2.1). Satisfactorily, using the optimal conditions (crotonaldehyde LiOH·H₂O, *i*PrOH, H₂O) developed for the decahydroquinoline series³² gave the desired analogous octahydroindole product **2a**, which maintained the all-*cis* stereochemistry. The moderate 44% yield led us to evaluate other conditions using different bases and solvent system. The best results were obtained using PS-BEMP alone in *i*PrOH which gave **2a** in a 68% yield (entry 8) with 72 h reaction time but other bases could also promote this reaction giving around 40-60% yield.

The relative stereochemistry of *rac*-**2a** was elucidated by 2D NMR spectra (COSY, HSQC, and NOESY). Octahydroindole **2a** shows a preferred conformation in which the C7-C7a bond of the carbocyclic ring adopts an axial disposition with respect to the nitrogen-containing ring to avoid the allylic strain with the sulfonamide group. The key evidence for the structure depicted in Figure 2.2 was found in the ¹H NMR coupling pattern for H-7_{ax}, which appears as a triplet of doublets ($J = 12.8, 5.2$ Hz). This coupling pattern is only compatible with an axially disposed location of the methyl group at C-6. Moreover, the axial proton H-7_a is strongly coupled with only one adjacent axial proton. Hence, its resonance signal appears deceptively as a doublet ($J = 12.8$ Hz) of other doublets ($J = 8.0, 4.8$ Hz). This structural elucidation is fully confirmed by the NOE contacts observed for H-7_a.

Table 2.1 Screening of tandem cyclization conditions leading to octahydroindole

entry	base (equiv)	solvent	time (h)	yield ^a (%)
1	LiOH·H ₂ O (1) ^b	<i>i</i> PrOH	24	44
2	<i>t</i> -BuOK (0.3)	<i>t</i> -BuOH	24	15 ^c
3	A ^d (0.3), KOH(aq.)	Et ₂ O / THF	72	57
4	B ^e (0.1), C (2)	CH ₂ Cl ₂	72	--
5	B (1), C (2)	<i>i</i> PrOH	24	56 ^f
6	B (1), C (2)	<i>t</i> -BuOH	24	45
7	B (1)	<i>i</i> PrOH	24	42
8	B (1)	<i>i</i> PrOH	72	68
9	B (0.1)	<i>i</i> PrOH	72	54
10	D (1)	<i>i</i> PrOH	24	43

^a Yield refers to the products isolated by flash chromatography. ^b 10 equiv of H₂O added. ^c Significant amounts of the non-cyclized cyclohexenone were also obtained (~40%). ^d TBAH refers to 40% *n*Bu₄NOH in H₂O. ^e PS-BEMP refers to polymer-supported 2-*tert*-butylimino-2-diethylamino-1,3-dimethylperhydro-1,3,2-diazaphosphorine. ^f Isolated as a mixture of esters by a solvent transesterification process.

**Figure 2.2** NMR structure elucidation

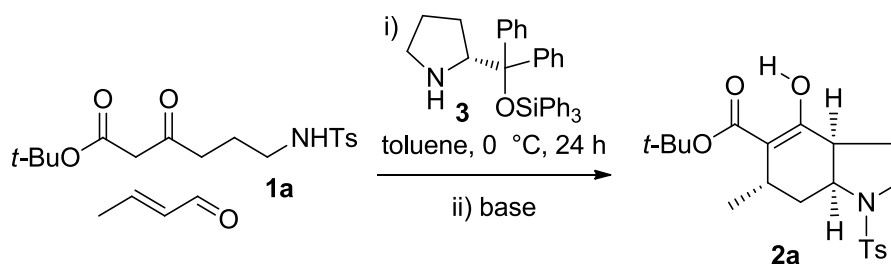
This process constitutes a rare example of an intramolecular aza-Michael reaction through a *5-endo-trig* cyclization,⁵⁴ the latter process being disfavored according to Baldwin's rules.⁵⁵

In order to render the initial Michael addition step in the tandem Robinson/aza-Michael reaction enantioselective, we applied the conditions developed in the decahydroquinoline series³² (using the Hayashi-Palomo catalyst **3**,³⁴ LiOAc as an additive, and toluene as a solvent) to see if the octahydroindole series followed the same reactivity pattern. A brief solvent screen for the organocatalytic step proved this to be the case, so toluene was again selected as the solvent of choice based on enantiomeric excess (ee) and yield. The use of different cyclization conditions for the tandem reaction was evaluated (see Table 2.2). With no clear winner for the base for the cyclization step, we decided to test all the conditions that had given good results.

We were surprised to observe that the choice of base was indeed crucial for obtaining good enantioselectivities. Compared to LiOH, the use of *t*-BuOK resulted in a quite considerable reduction of the ee to 73% (entry 2), while the use of KOH with TBAH under biphasic conditions gave an improved 94% (entry 3). The treatment with PS-BEMP (1 equiv) performed almost equally well, giving 90% ee (entry 4). Using catalytic PS-BEMP conditions, the ee dropped slightly to 87% and the yield was significantly reduced (entry 5). The use of the Amberlyst-26 resin resulted in a moderate 84% ee and also a moderate yield. While the KOH, TBAH conditions (entry 3) were the best in terms of enantioselectivity, we chose PS-BEMP (entry 4) as the optimum conditions based on the following

⁵⁴ For a general overview of the organocatalytic intramolecular aza-Michael reaction, see: Sánchez-Roselló, M.; Aceña, J. L.; Simón-Fuentes, A.; del Pozo, C. *Chem. Soc. Rev.* **2014**, *43*, 7430-7453.

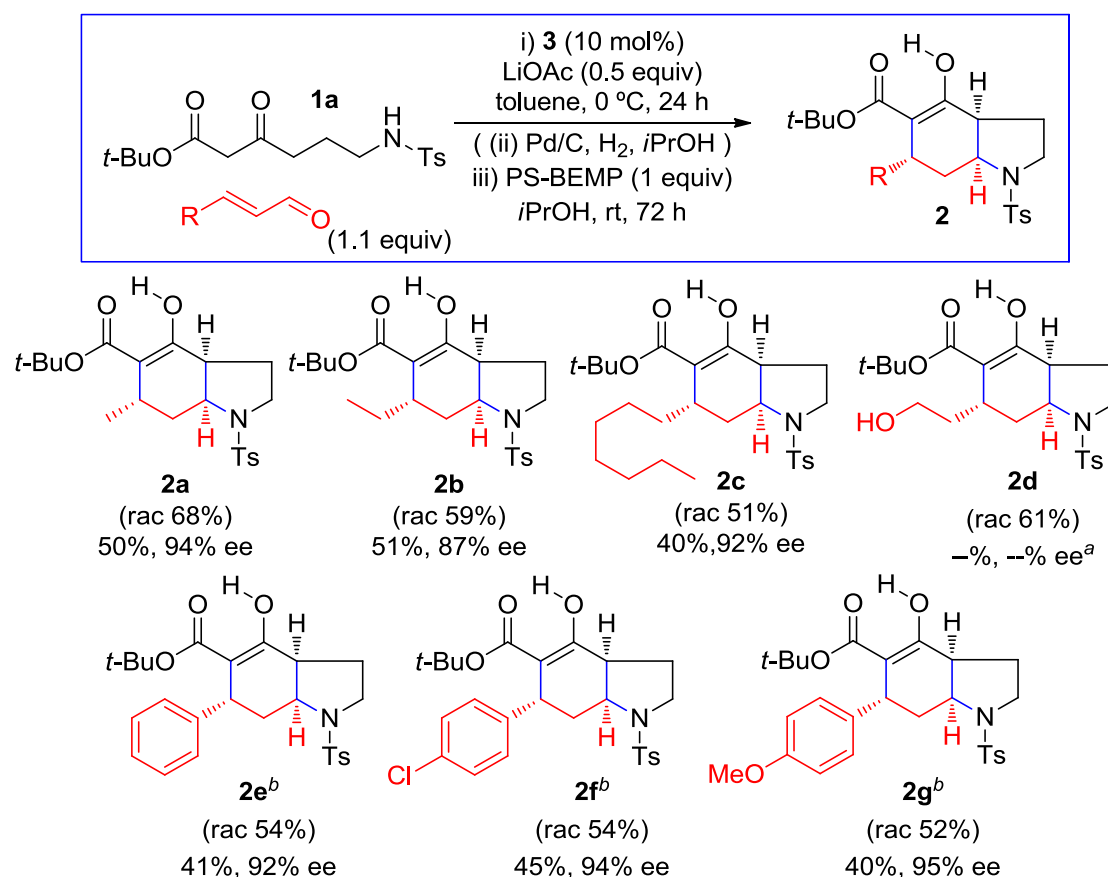
⁵⁵ Johnston, C. P.; Kothari, A.; Sergeieva, T.; Okovytyy, S. I.; Jackson, K. E.; Paton, R. S.; Smith, M. D. *Nat. Chem.* **2015**, *7*, 171-177.

Table 2.2 Organocatalyzed Michael reaction/aldol/intramolecular aza-Michael process

entry ^a	base used for cyclization (equiv)	yield ^b (%)	ee ^c (%)
1	LiOH.H ₂ O (1)	55	87
2	<i>t</i> -BuOK (0.3)	61	73
3	KOH(aq.), TBAH(0.3)	51	94
4	PS-BEMP(1)	50	90
5	PS-BEMP(0.1)	29	87
6	Amberlyst-26(1)	44	84

^a Reactions were carried out with 1.1 equiv of crotonaldehyde and 0.5 equiv of LiOAc, as an additive, and the reaction time for the first step (i) was 24 h. The second step (ii) was carried out with the base indicated in *i*PrOH for 72 h. ^b Yield refers to the products isolated by flash chromatography. ^c Determined by HPLC analysis.

criteria: (i) the reaction setup and work-up was significantly easier, requiring simple addition and filtration, and (ii) we observed that KOH, TBAH was less effective when the enal substituent was not a methyl group. The absolute configuration proposed for octahydroindole (+)-**2a** is based on the accepted mechanism of organocatalyzed Michael addition of β -keto esters upon enals,³⁶ as well as the absolute stereochemistry reported in the related process leading to enantiopure decahydroquinolines.³⁷



Each compound was prepared initially in racemic form. ^a Organocatalytic conditions did not lead to any significant quantity of coupled product. ^b Excess unreacted non-volatile enal was converted by hydrogenation to the corresponding aldehyde

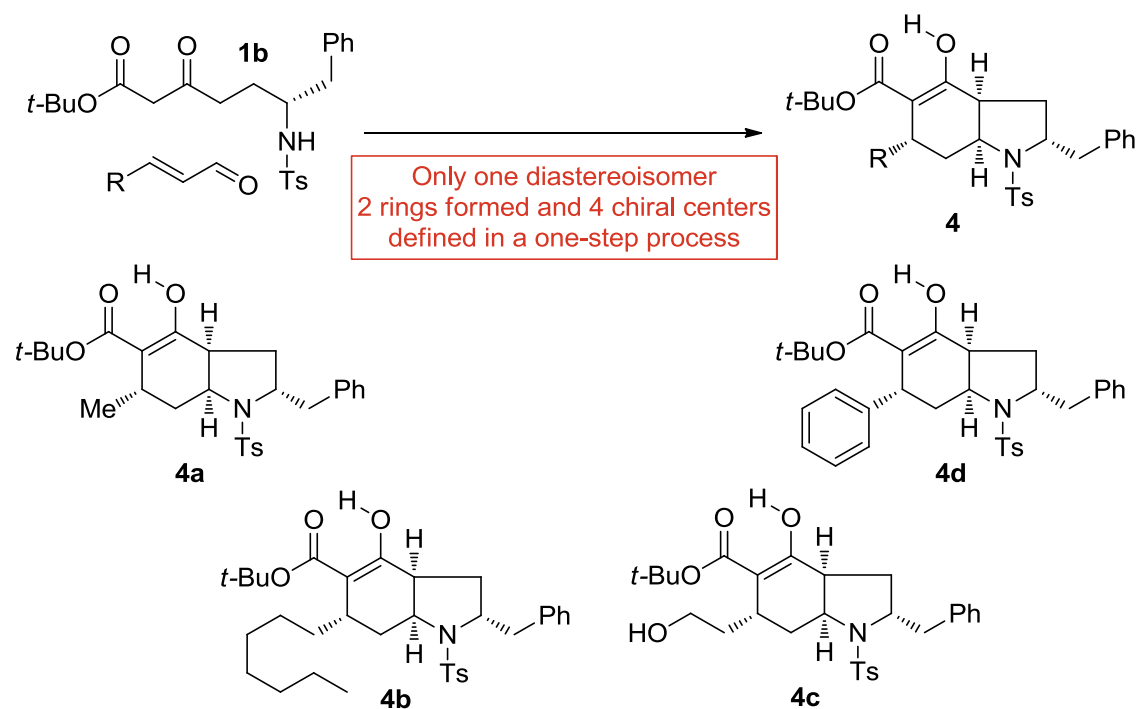
Scheme 2.3 Scope of the Organocatalyzed Octahydroindole synthesis

To test the scope of the reaction, a range of enals were examined. It should be noted that in cases where the enal was not volatile, it was necessary to reduce any excess material by hydrogenation before adding the base to initiate the tandem cyclization reaction. Aliphatic enals gave the corresponding octahydroindoles **2b** and **2c** with good enantioselectivities (87% and 92% ee, respectively). The enal bearing a free hydroxyl group efficiently gave **2d** under racemic conditions but did not evolve under organocatalysis due to the formation of a stable heminal species. The reaction also generally performed well when using enals with an aromatic substituent, giving **2e** (phenyl group), **2f** (*p*-chlorophenyl) or **2g** (*p*-methoxyphenyl), the latter bearing an electron-donating substituent, and all with excellent enantioselectivities.

Since many octahydroindole products bear a substituent at the 2-position, we were interested in examining the effect of placing a corresponding substituent in the β -keto ester starting material α to the nitrogen (see Table 2.3). We began by taking α -substituted β -keto ester **1b** and reacting it under the racemic conditions (PS-BEMP, *i*PrOH). Notably, the isolation of compound **4a** indicated that the incorporation of a stereogenic center at the α -position of the nitrogen atom (*i.e.* a benzyl group) caused an effective remote 1,6-asymmetric induction.⁵⁶ The stereostructure of **4a** was assigned on the basis that the set of signals in its NMR spectra (¹H and ¹³C) showed a close correlation with those observed in **2a**. Thus, considering that the pattern of chemical shifts and coupling constants for H-3a, H-6, H-7, and H-7a in **4a** was the same as in **2a**, a stereostructure analogous to that depicted in Figure 2.2, but having the benzyl substituent at C-2 was assigned to **4a** with the all-*cis* configuration. This was also confirmed with bidimensional NMR analysis. To see if the above asymmetric induction was an effect unique to PS-BEMP, the previously evaluated bases were analysed and the product found in each case was **4a** (see Table 2.3). The effect of using the organocatalyst **3** in the initial Michael step was then examined. While the matched organocatalyst *ent*-**3** gave a similar result regarding the all-*cis* stereochemistry, *ent*-**3** failed to provide the opposite stereochemistry at C-6.

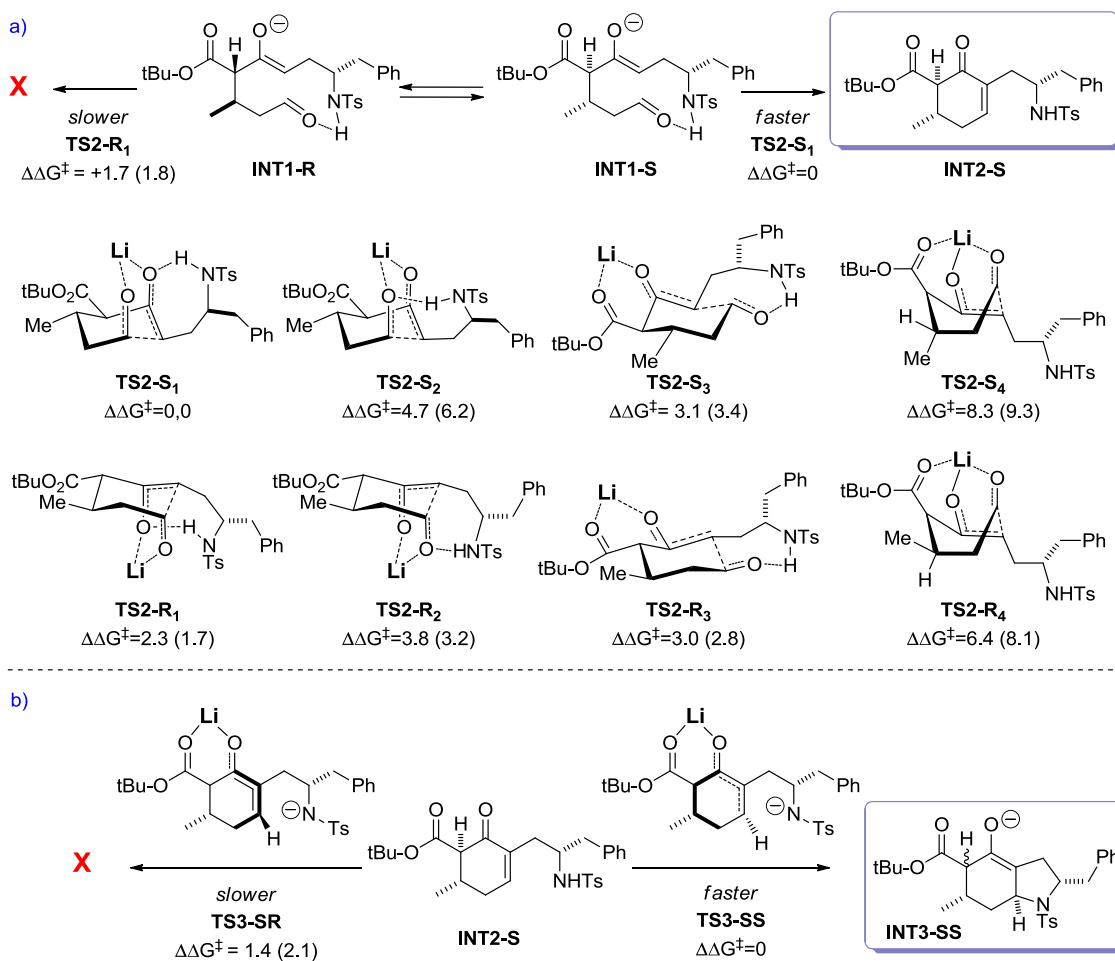
To explore the scope of the reaction, some different unsaturated aldehydes were used in the coupling reaction. As can be seen in Table 2.3, the reaction worked with a variety of substrates, leading to the octahydroindoles **4a-4d** in a non-optimized moderate yield.

⁵⁶ For diastereoselective construction of remote stereocenters, see: (a) Hayashi, R.; Walton, M. C.; Hsung, R. P.; Schwab, J. H.; Yu, X. *Org. Lett.* **2010**, *12*, 5768-5771. (b) Aron, Z. D.; Ito, T.; May, T. L.; Overman, L. E.; Wang, J. *J. Org. Chem.* **2013**, *78*, 9929-9948. (c) Kwon, K. H.; Serrano, C. M.; Koch, M.; Barrows, L. R.; Looper, R. E. *Org. Lett.* **2014**, *16*, 6048-6051. (d) Kobayakawa, T.; Narumi, T.; Tamamura, H. *Org. Lett.* **2015**, *17*, 2302-2305.

Table 2.3 Synthesis of 2,4,5,6-Tetrasubstituted Octahydroindoles via 1,6-Remote Induction

entry ^a	R	compound	conditions	yield (%)
1	Me	4a	PS-BEMP	44
2	Me	4a	LiOH.H ₂ O	60
3	Me	4a	Amberlyst A-26	29
5	Me	4a	BEMP	24
6	Me	4a	3^b then PS-BEMP	27
7	Me	4a	<i>ent-3^b</i> then PS-BEMP	-- ^c
8	Me	4a	PS-BEMP (0.3)	45
9	Me	4a	PS-BEMP (0.3) ^d	36
10	hept	4b	PS-BEMP	28
11	(CH ₂) ₂ OH	4c	PS-BEMP	30
12	Ph	4d	PS-BEMP	43

^a Unless otherwise stated, reactions were carried out with 1 equiv of Base in *i*PrOH for 72 h. ^b Conditions for the organocatalytic step were carried out as in Table 2.2. ^c Mixture of various unidentified compounds was obtained with only traces of **4a**. ^d 10 equiv of H₂O were added.

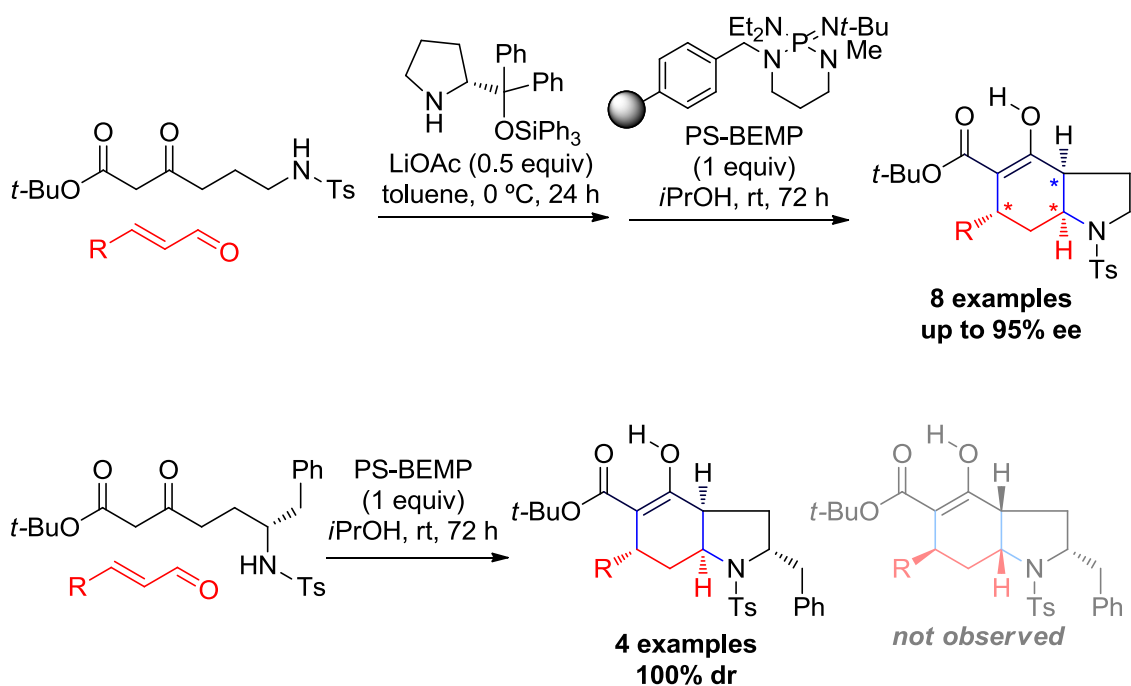


Scheme 2.4 DFT calculations

DFT calculations were performed in order to shed light on the unexpected complete diastereoselectivity exerted by the benzyl substituent on the bicycle formation. At first sight, any of the C-C or C-N bond-forming processes is a potential candidate to be the stereodetermining transformation. We thus considered all possibilities, starting with the initial Michael addition of the dicarbonylic compound to crotonaldehyde (**TS1**, see supporting information) to form **INT1-R** and **INT1-S** (Scheme 2.4), which, as expected, turned out to be non-selective. The absence of interaction between the forming C-C bond and the stereogenic center α to the nitrogen atom might be behind the observed lack of stereo-control. The fact that **TS1** is non-selective undoubtedly means that **INT1-R** and **INT1-S** must be in equilibrium (Curtin-Hammett conditions) prior to the stereo-determining step, which we hypothesized to

be **TS2** (Scheme 2.4a). A number of **TS2** structures were located, showing different Li cation and H-bond (TsNH) activation modes of the ring formation process. Gratifyingly, the transition state lowest in energy (**TS2-S₁**) corresponds to the formation of the **S** epimer, which is the one experimentally observed. In this structure (**TS2-S₁**), the lithium atom is bonded to the two reacting oxygen units (enolate and aldehyde), and the NH of the tosyl group is hydrogen bonding the enolate-oxygen. Any other Li/NH bond combination (**TS2-S₂** to **TS2-S₄**, Scheme 2.4a) is not so favorable in terms of energy. Similar activation modes can be found in the transition states leading to the **R** epimer, **TS2-R₁** being the lowest one, but their energies are at least 1.7-2.0 kcal/mol larger than those of the **S** isomer, in agreement with the experimental selectivity data. We hypothesized that the reason for the energy difference between **TS2-S₁** and **TS2-R₁** might be the tight character of these *tricyclic* structures, where the steric interaction of the benzyl group with the rest of the molecule gains significance.

We also studied the diastereoselectivity of the second ring formation by attack of the nitrogen atom to **INT2-S**. The most favorable transition states located were **TS3-SR** and **TS3-SS** (Scheme 2.4b), and the comparison of their relative Gibbs Free energies is again in agreement with the experimental results, predicting the formation of the **SS** adduct. In both diastereoisomers, the lithium cation is bonded to the oxygens of the dicarbonylic system, activating the enone (**INT2-S**) toward the nucleophilic attack of the tosylamine.



Scheme 2.5 Conclusions

In summary, an effective enantioselective organocatalytic route to polyfunctionalized octahydroindoles was developed using a one-pot sequence, further expanding the potential scope of the organocatalyzed Robinson/aza-Michael reaction for the rapid construction of important natural product nuclei. Moreover, a diastereoselective route starting from commercially available enantiopure aziridine was developed, in which a 1,6-remote control induction was observed in a process leading to enantiopure 2,4,5,6-tetrasubstituted hydroindoles.

**3. Fischer Indole Reaction in Batch and Flow
Employing a Sulfonic Acid Resin: Synthesis of
Pyrido[2,3-a]carbazoles**

J. Flow Chem. **2016**, DOI: 10.1556/1846.2016.00016

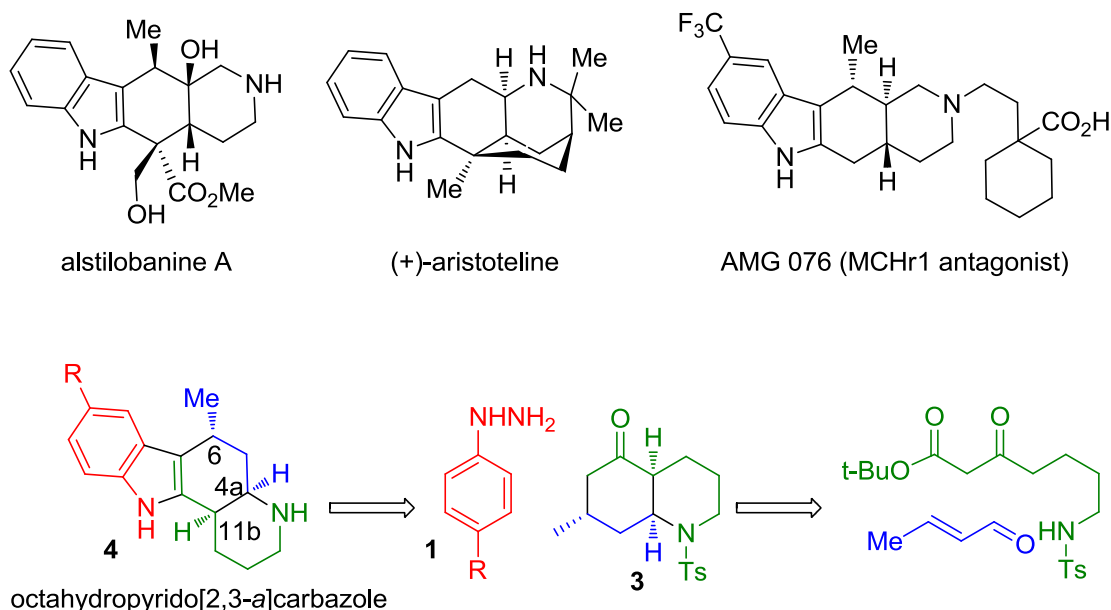


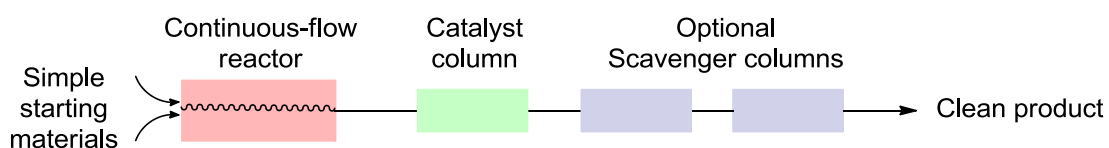
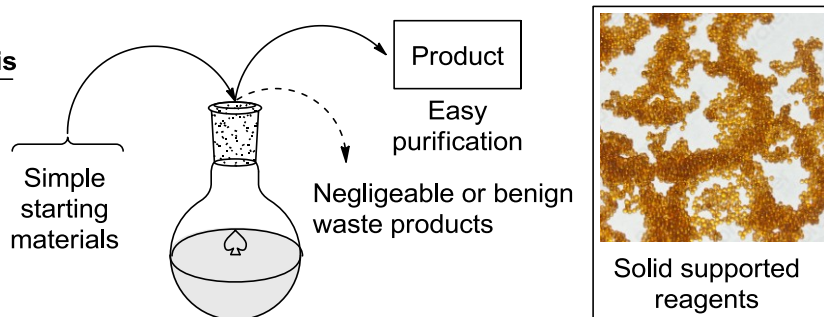
Figure 3.1 Heterocyclic Carbazole Structures

Heterocyclic scaffolds bearing a tetrahydrocarbazole structural subunit and an additional nitrogen-containing ring are found both in natural products (alkaloids) and pharmacologically active compounds developed in medicinal chemistry research⁵⁷ (Figure 3.1). More particularly, a series of tetracyclic indoles have been reported as androgen receptor ligands,⁵⁸ among which an unprecedented pyrido[2,3-a]carbazole scaffold was evaluated. Considering this pharmacological interest in pyridocarbazole compounds⁵⁹ and the easy availability of *cis*-5-oxodecahydroquinolines,³² through the tandem Michael addition / aldol condensation / aza-Michael reaction process developed previously in the research group (see chapter 1), we decided to study the Fischer indole reaction on the latter compounds.

⁵⁷ Zhao, F.; Li, N.; Zhu, Y. F.; Han, Z. Y. *Org. Lett.* **2016**, *18*, 1506-1509 and references therein.

⁵⁸ Zhang, X.; Li, X.; Allan, G. F.; Musto, A.; Lundeen, S. G.; Sui, A. *Bioorg. Med. Chem. Lett.* **2006**, *16*, 3233-3237.

⁵⁹ (a) Pagano, N.; Wong, E. Y.; Breiding, T.; Liu, H.; Wilbuer, A.; Bregman, H.; Shen, Q.; Diamond, S. L.; Meggers, E. *J. Org. Chem.* **2009**, *76*, 8997-9009. (b) Schmidt, A. W.; Reddy, K. R.; Knölker, H. J. *Chem. Rev.* **2012**, *112*, 3193-3328. (c) Mihalic, J. T.; Fan, P.; Chen, X.; Chen, X.; Fu, Y.; Motani, A.; Liang, L.; Lindstrom, M.; Tang, L.; Chen, J. L.; Jaen, J.; Dai, K.; Li, L. *Bioorg. Med. Chem. Lett.* **2012**, *22*, 3781-3785.

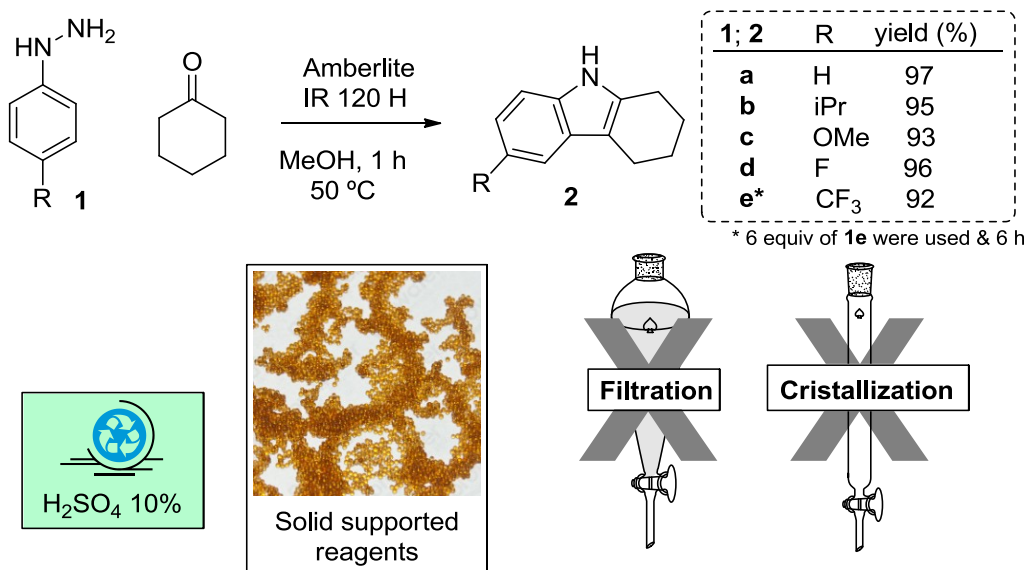
Continuous flow synthesis**Batch "ideal" synthesis****Figure 3.2** Flow versus Batch

Conducting the Fischer indole synthesis using continuous flow systems has caught the attention of several research groups in recent years.⁶⁰ The reaction rate of the Fischer indole synthesis can be significantly increased when run at higher temperatures and pressures or employing microwave irradiation, which renders this reaction highly suitable for new continuous flow techniques. Moreover, a heterogeneous approach using a solid acid could avoid the potentially problematic clogging of microreactor devices due to the facile precipitation or crystallization of the indole, and eventually allow for a one-pot process.⁶¹

Besides studying flow approaches, we were also interested in comparing those with more conventional procedures employing immobilized catalysts to perform the reaction in one-pot efficient processes and get closer to the batch "ideal" synthesis stated by Wender as the one "in which the target molecule is prepared from readily available starting materials in one simple, safe, environmentally acceptable, and

⁶⁰ (a) Wahab, B.; Ellames, G.; Passey, S.; Watts, P. *Tetrahedron* **2010**, *66*, 3861-3865. (b) Pagano, N.; Heil, M. L.; Cosford, N. D. P. *Synthesis* **2012**, *44*, 2537-2546. (c) Gutmann, B.; Gottsponer, M.; Elsner, P.; Cantillo, D.; Roberge, D. M.; Kappe, C. O. *Org. Process Res. Dev.* **2013**, *17*, 294-302. (d) Ranasinghe, N.; Jones, G. B. *Current Green Chem.* **2015**, *2*, 66-76.

⁶¹ For pioneering work in this field, see: Prochazka, M. P.; Carlson, R. *Acta Chem. Scand.* **1990**, *44*, 614-616.



Scheme 3.1 Model substrate – cyclohexanone experiments in Batch

resource-effective operation that proceeds quickly and in quantitative yield”.⁶²

Various catalytic methods have been reported for the Fischer indole synthesis,⁶³ including the polymeric sulfonic acid resin Amberlite IR 120 H,⁶⁴ which despite its frequent use in ion exchange applications has not been extensively used for this particular purpose.⁶⁵

The availability of the reagent, combined with its high ability to catalyze the Fischer indole synthesis, prompted us to choose it for this study. Also the use of a solid supported acidic resin might facilitate every manipulation avoiding the need for work-up of the reaction medium, simple filtration of the resin beads. Finally the indole / carbazole tendency to precipitate and crystallize easily could allow us to avoid any purification by column chromatography and permit a simple purification by precipitation – crystallization of the desired heterocycle.

⁶² Wender, P.A. & Miller, B. L. in “Organic Synthesis: Theory and Applications”, T. Hudlicky, Ed., Greenwich: *JAI Press*, **1993**, 2, 27-66.

⁶³ For recent studies on the Fischer indole synthesis, see: (a) Gore, S.; Baskaran, S.; König, B. *Org. Lett.* **2012**, 14, 4568-4571. (b) Inman, M.; Moody, C. J. *Chem. Sci.*, **2013**, 4, 29-41. (c) Smith, J. M.; Moreno, J.; Boal, B. W.; Garg, N. K. *J. Org. Chem.* **2015**, 80, 8954-8967.

⁶⁴ Yamada, S.; Chibata, I.; Tsurui, R. *Chem. Pharm. Bull.* **1953**, 1, 14-16.

⁶⁵ Chandrasekhar, S.; Mukherjee, S. *Synth. Commun.* **2015**, 45, 1018-1022.

As a preliminary task, we decided to examine the behaviour of cyclohexanone as model compound in batch and flow reaction conditions. We were pleased to observe that the use of Amberlite IR 120 H resin in a batch process readily and efficiently catalyzed the Fischer indole reaction of hydrazine **1a** with cyclohexanone under mild conditions. It is interesting to note that the resin can be regenerated without any loss of activity by simple stirring in a 10% H₂SO₄ solution for 15–30 min. These conditions were successfully applied to various substituted phenylhydrazines (Scheme 3.1), in all cases providing excellent isolated yields of products whose data correspond to the literature descriptions.

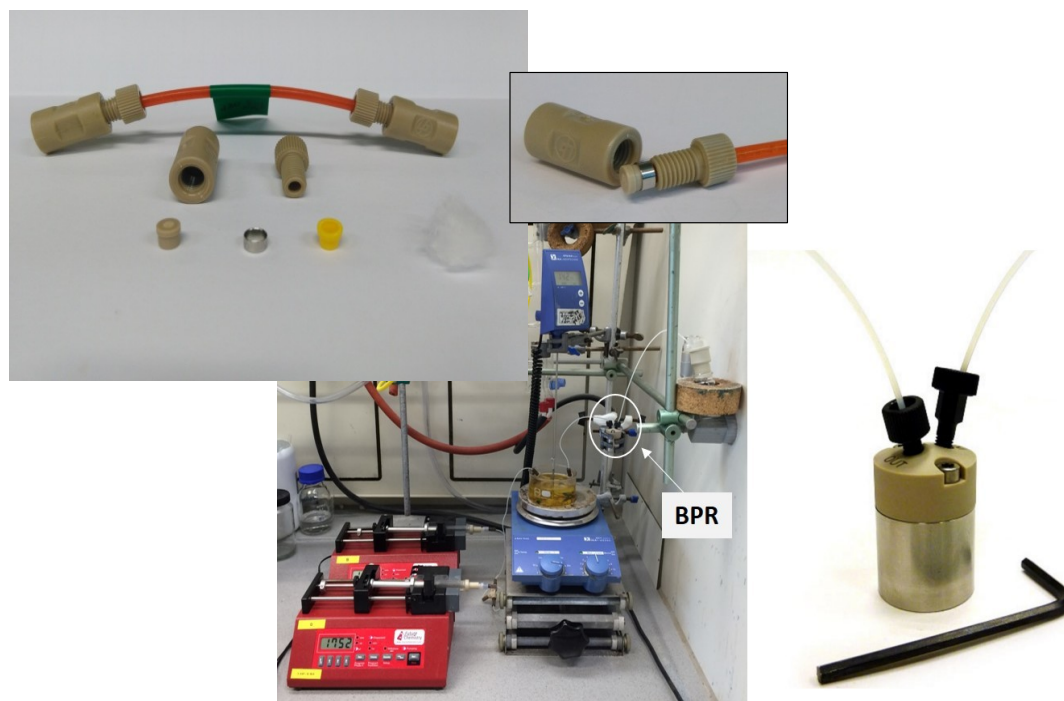
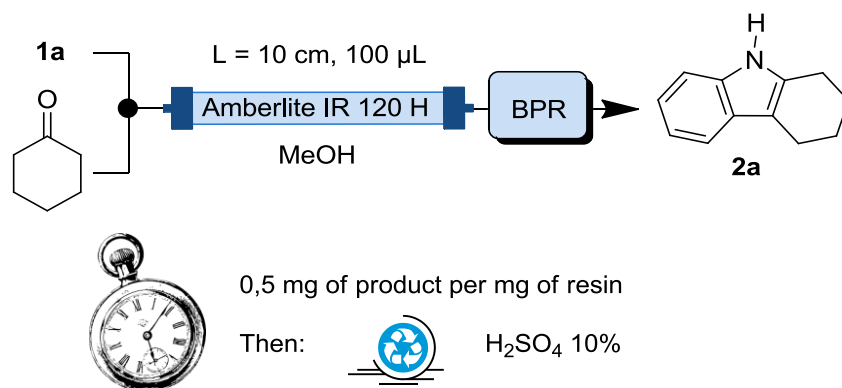


Figure 3.3 Flow set-up

Encouraged by the results obtained in batch, we attempted to conduct the process under continuous flow conditions. For this purpose, a 10 cm long ETFE tubing (1/8" outer diameter, 1/16" inner diameter) packed with Amberlite IR 120 H (100 mg) and sealed with cotton wool was used as the reactor cartridge (100 μ L inner volume). The flow system consisted of two syringe pumps, a T-mixer unit for homogenization of the reaction mixture, and a back pressure regulator (BPR), while the cartridge was submerged in an oil bath for heating.

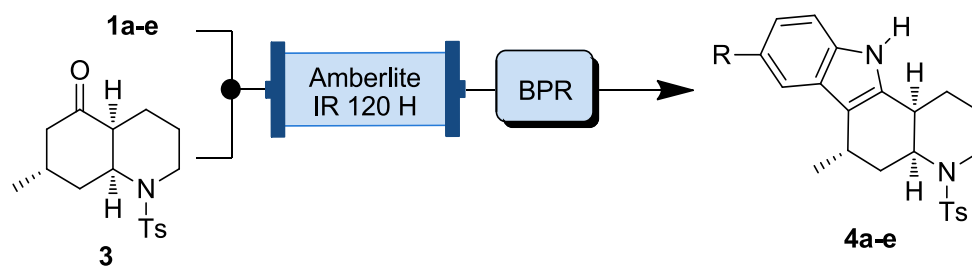
Table 3.1 Model substrate in Flow

entry	residence time (min)	temperature (°C)	conversion (%) <i>calculated by ¹H NMR</i>
1	5	50	62
2	10	50	100
3	2.5	90	57
4	5	90	100

Optimization of the residence time was performed using feed solutions of phenylhydrazine **1a** (0.5 M) and cyclohexanone (0.5 M) both dissolved in MeOH. Entries 2 and 4 illustrate that it was possible to shorten the reaction time to 10 min at 50 °C and even to 5 min at 90 °C for 0.5 M solutions of the reagents. The straightforward regeneration of the catalyst proved rather useful in the flow process. It was possible to produce with a small cartridge of 100 μ L inner volume and 100 mg of resin up to 50 mg of pure product before observing any decrease in conversion. Then, as soon as a loss of efficiency was observed, a simple rinse of the resin with a 10% H₂SO₄ solution for 15-30 min allowed full activity to be regained. With these results in hand we moved to the application of those conditions on the 5-oxodecahydroquinoline substrate (**3**).

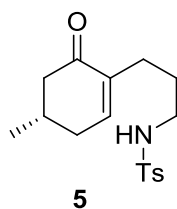
Our first attempt to use this flow system with compound **3** and hydrazine **1a** gave, besides the anticipated product **4a**, the side product **5** arising from a retro-aza-Michael reaction causing opening of the decahydroquinoline ring (Table 3.2, entry 1). This retro-aza-Michael reaction was attributed to ammonia being formed as a side product of the Fischer indole reaction. This could be circumvented by using acetic acid as a co-solvent to immediately quench the ammonia in solution and hence prevent this ring-opening and formation of enone **5** (entry 2). A control experiment was performed by heating compounds **3** and **1a** in MeOH/AcOH for 20 min and 1 h at 70 °C. In both cases, only hydrazone intermediates were observed, showing the importance of the Amberlite resin in the one-pot process. A short increase in reaction time allowed a clean and full conversion into the tetracyclic compound in 76% isolated yield under flow conditions (entry 3).

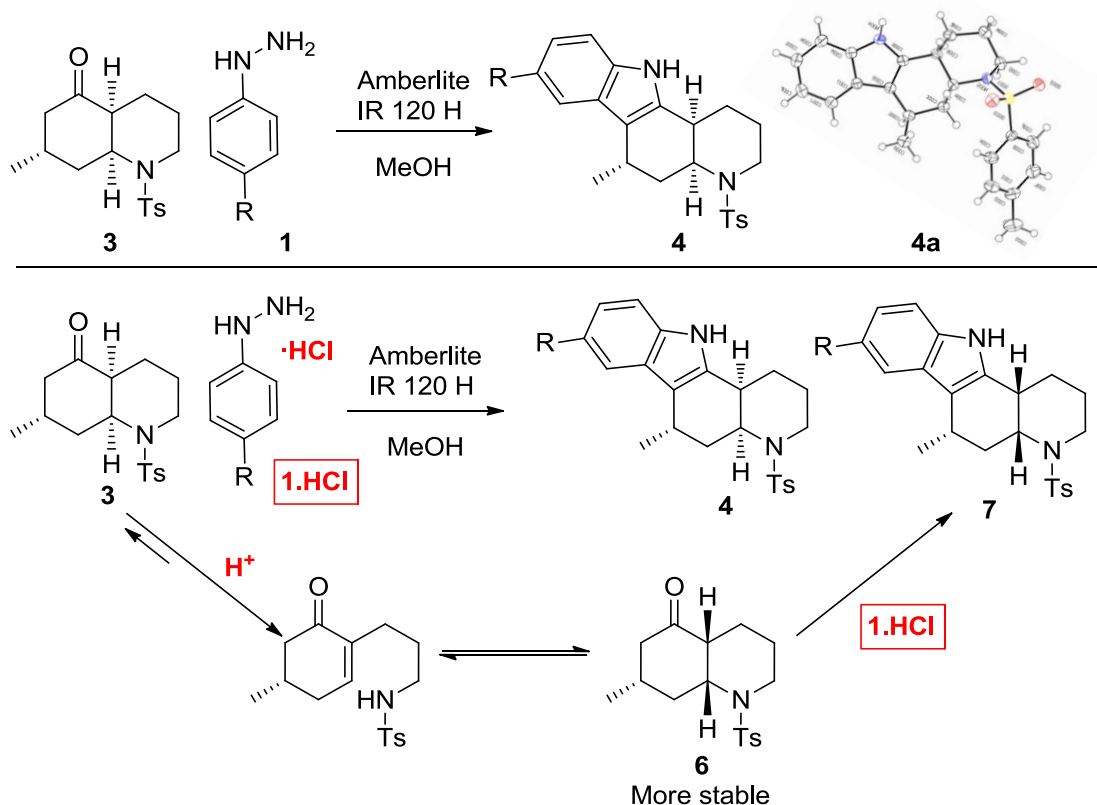
When the process was applied to *p*-substituted phenylhydrazines, some solubility problems were experienced, but these were solved by the dilution of feed solutions to 0.05 M and the use of adapted ternary solvent systems. This flow methodology thus allowed us to gain access to the different products **4a-e** in moderate to good yields (entries 3-7).

Table 3.2 Screening of Flow Conditions

entry ^a	1^b	solvent	residence time (min)	conv ^c (%)
1	1a	MeOH	10	44 ^d
2	1a	MeOH/AcOH	10	90
3	1a	MeOH/AcOH (1:1)	20	100 ^e
4	1b.HCl	MeOH/AcOH/DCE (9:7:4)	30	100 ^f
5	1c.HCl	MeOH/AcOH/DCE (7:2:1)	60	55
6	1d.HCl	MeOH/AcOH/DCE (14:5:1)	60	42
7	1e	MeOH/AcOH/DCE (5:4:1)	60	22

^a For detailed reaction conditions, see supporting information. Reactor cartridge: Entries 1-3: 10 cm long, packed with 100 mg Amberlite IR 120 H (100 μ L inner volume). Entries 4-7: 1.0 m long, packed with 1000 mg Amberlite IR 120 H (1000 μ L inner volume). ^b For **1** and **4**: a, R = H; b, R = *i*Pr; c, R = OMe; d, R = F; e, R = CF₃. ^c Determined from crude ¹H NMR spectra (unless otherwise stated, remaining product corresponds to a mix of starting material **3** and its corresponding hydrazone). ^d Formation of side product **5** (14%), see Scheme 1. ^e 76% isolated yield. ^f 75% isolated yield.



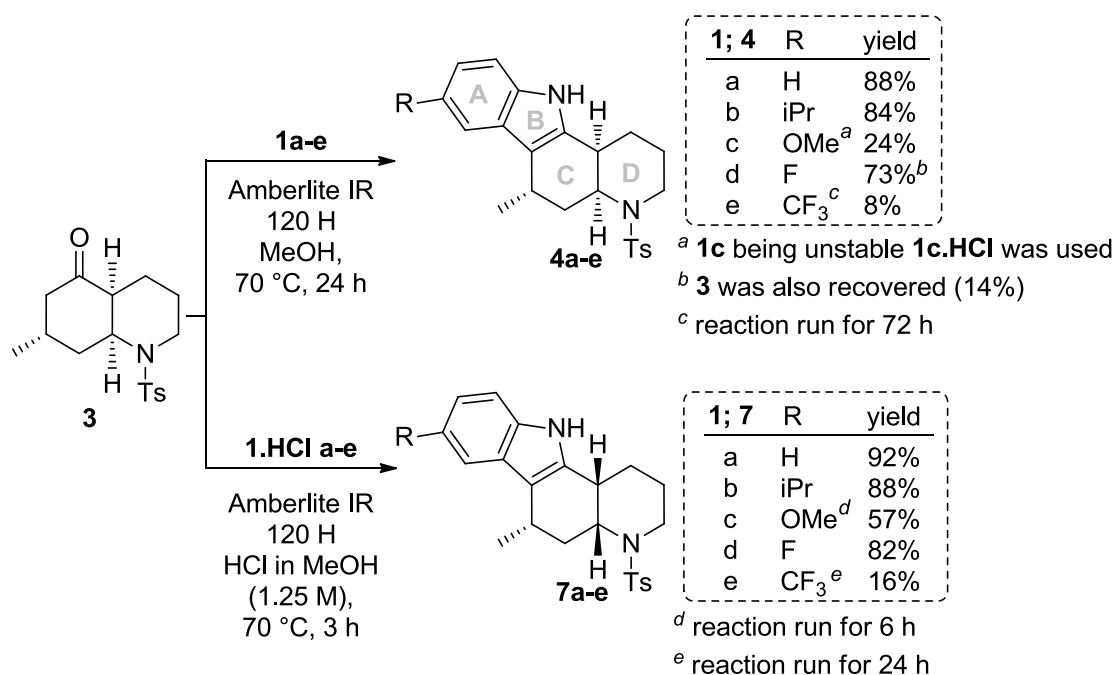


Scheme 3.2 Adaptation of Synthesis in Batch

We decided to explore the Fischer indole synthesis from ketone **3** under more classic reaction conditions, without performing the phenylhydrazone, *i.e.* carrying out the reaction in a one-pot/two-step procedure.⁶⁶ Application of batch reaction conditions, previously reported in Scheme 3.1, to compound **3** proved successful, although with a drastic increase in reaction time (24 h) and amount of phenylhydrazine (10 equiv) required. A premix of the Amberlite acidic resin with the free hydrazine base prior to the addition of the decahydroquinoline **3** and refluxing for 24 h gave selective access to products **4a-e** the stereochemistry being confirmed by X-ray analysis.

⁶⁶ For one-pot/one-step microwave-assisted Fischer indole synthesis from ketones, see: Creencia, E. C.; Tsukamoto, M.; Horaguchi, T. *J. Heterocycl. Chem.* **2011**, *48*, 1095-1102.

On the other hand, we soon realized that the use of hydrochloride salts of the hydrazines (as used in flow conditions) gave a mixture of diastereoisomers **4** and **7** (see Scheme 3.2). This is due to a retro-aza-Michael process occurring in high acidic conditions.⁶⁷ Thus, in order to promote a faster isomerization of the initial ketone **3** to **6**, which should be the precursor of **7**, more acidic reaction conditions were used. In fact, upon submitting **3** to an equilibration process to produce **6** followed by a Fischer indolization reaction, only compounds of type **7** were isolated (see Scheme 3.3).



Scheme 3.3 Scope of the reaction

In summary, in batch the stereochemical outcome for the Fischer indolization from the protected β -amino ketone **3** is different when using phenylhydrazine or its hydrochloride salt (either alone or using HCl-MeOH as additive). In the latter case, prior to the indole ring formation,⁶⁸ an initial isomerization of **3** via a retro Aza-Michael ring opening followed by a

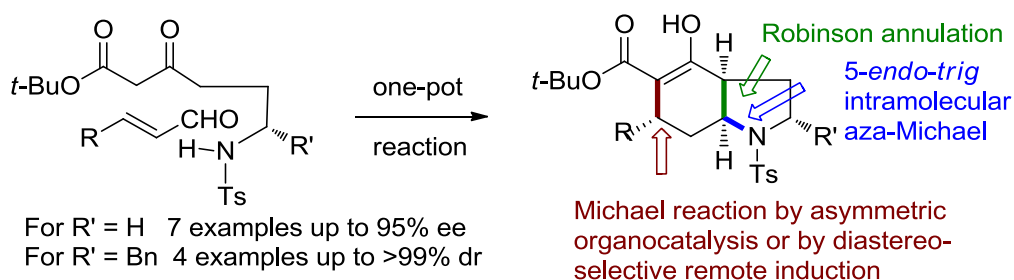
⁶⁷ Probably coming from the HCl counter ion present in solution.

⁶⁸ Treatment of pyridocarbazole **4a** under acid conditions (HCl-MeOH 1.25 M, 10 equiv, MeOH/DCE/AcOH 6:3:6, 70 °C, 24 h) did not produce any level of isomerization to the isomer **7a**.

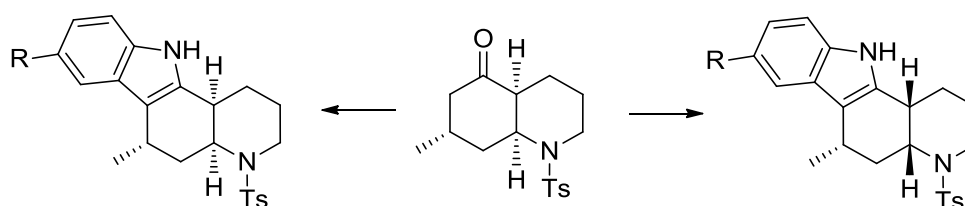
**4. Total Synthesis of *cis*-Phlegmarines via
stereodivergent reduction:
(+)-Serratezomine E and Putative Structure of
(-)-Huperzine N**

Org. Lett **2015**, *17*, 5084-5087

a) Chapter 2



b) Chapter 3



Scheme 4.1 Recapitulation of Chapters 2 and 3

We have shown in the first part of this Ph. D. manuscript how the asymmetric organocatalyzed intermolecular Michael/intramolecular aldol/intramolecular aza-Michael reaction introduced by our research group to achieve decahydroquinolines³² could be extended to the non-analogs of octahydroindole type (Chapter 2). In a second part, we have used the 5-oxodecahydroquinoline, the building-block for previous synthesis of *cis*-phlegmarines (lycoposerramine Z³² and cermizine B³⁷), for the synthesis of a small library of pyridocarbazoles, taking advantage of the easy isomerization of 5-oxodecahydroquinolines and applying the Fischer indole reaction either in flow as in batch chemistry. In this program we were able to prepare 10 different compounds which were sent for biological testing (Chapter 3).

The second part of the manuscript of this Doctoral Thesis is focused in the synthesis of phlegmarine alkaloids for which there are no precedents of synthesis.

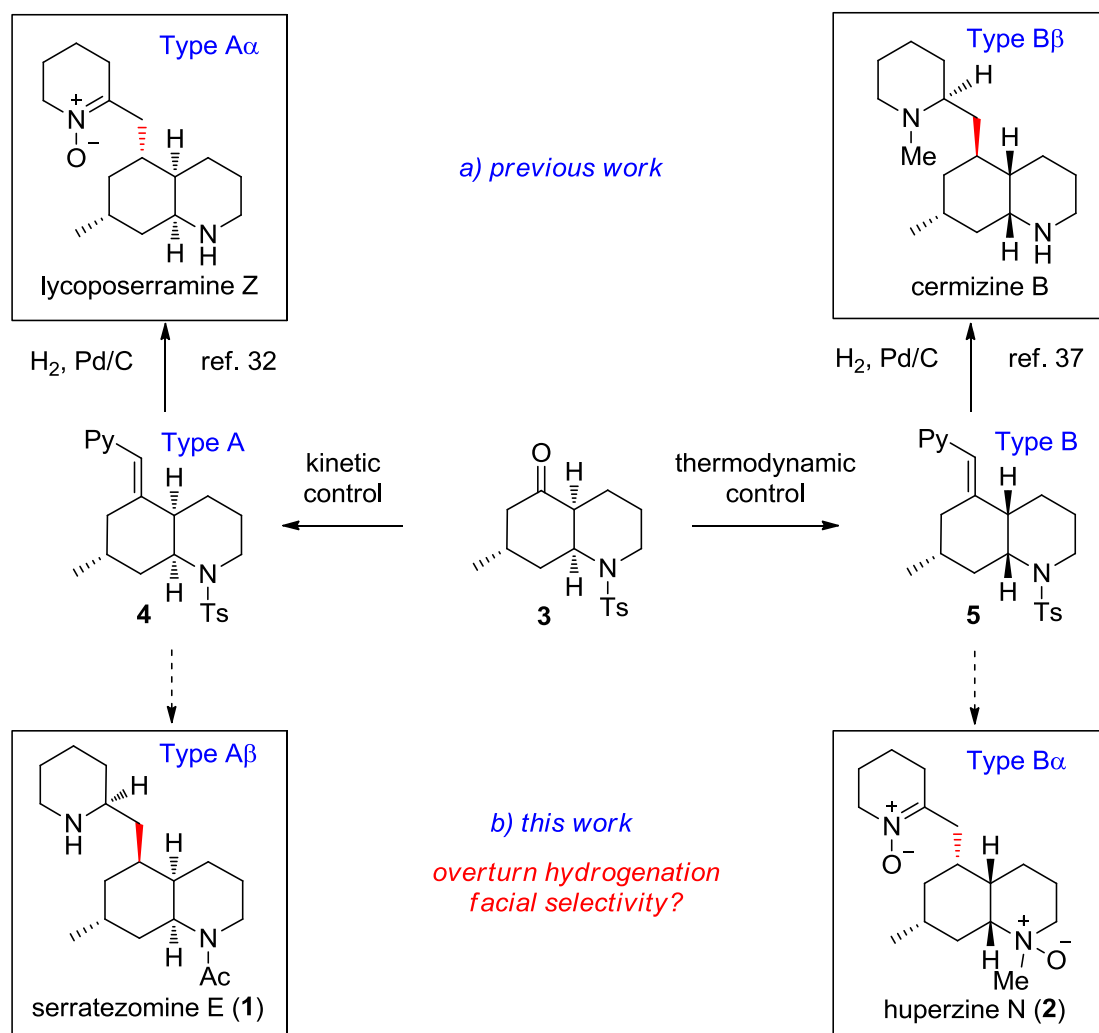
The work introduced in this chapter targets the synthesis of serratezomine E⁷ and huperzine N.⁹ Both compounds present a *cis*-decahydroquinoline nucleus with a different stereochemical pattern at C-5 with respect to the *cis*-phlegmarines previously synthesized in the research group.

A cornerstone of the project is to achieve these targets from the same building block (*i.e.* the 5-oxodecahydroquinoline) previously used for the synthesis of lycoposerramine Z³² and cermizine B³⁷ in order to achieve a unified synthesis of this group of compounds.

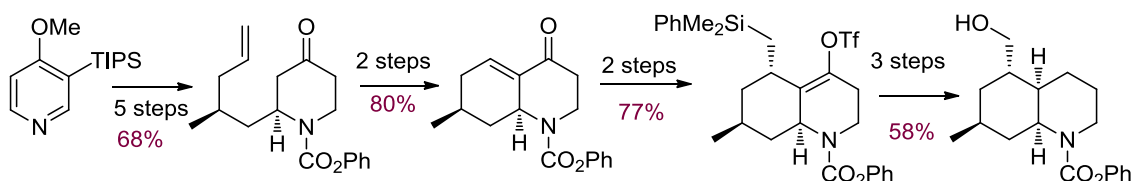
As presented in the introduction, in our research group we have developed an organocatalyzed tandem cyclization to access the 5-oxodecahydroquinoline bearing three stereogenic centers in a one-pot manner. Difference in stability along with retro-aza-Michael process occurring or not during the following coupling step generated the first point of diversification, providing type A or B vinylpyridines depending on the conditions employed.^{32, 37}

Hydrogenation of the formed alkene led to a second point of diversification, which from type A vinylpyridine almost exclusively gave the stereochemistry required for the synthesis of lycoposerramine Z.³² Similarly, hydrogenation of type B vinylpyridine, under the same conditions, allowed the synthesis of cermizine B.³⁷

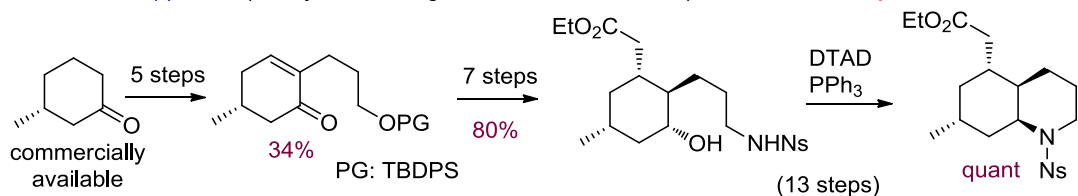
Access to C-5 epimeric phlegmarine alkaloids, such as serratezomine E and huperzine N would require the facial selectivity of this hydrogenation step to be completely overturned. We herein report our efforts to achieve this objective and develop a stereodivergent hydrogenation procedure.



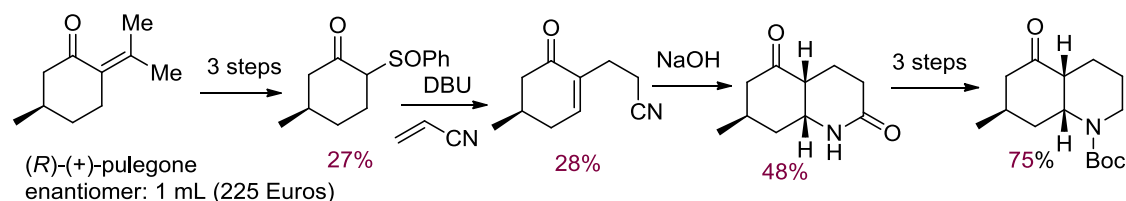
Chiral Auxiliary Approach (Comins, *Tetrahedron Lett.* **2012**, 53, 1347) **24% overall yield**



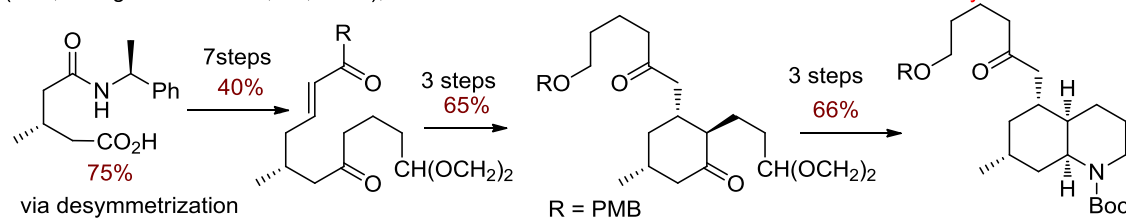
Chiral Pool Approach (Takayama, *J. Org. Chem.* **2009**, 74, 8675) **27% overall yield**



Chiral Pool Approach (Sarpong, unpublished results: S: H. House Ph D **2010**) **3% overall yield**



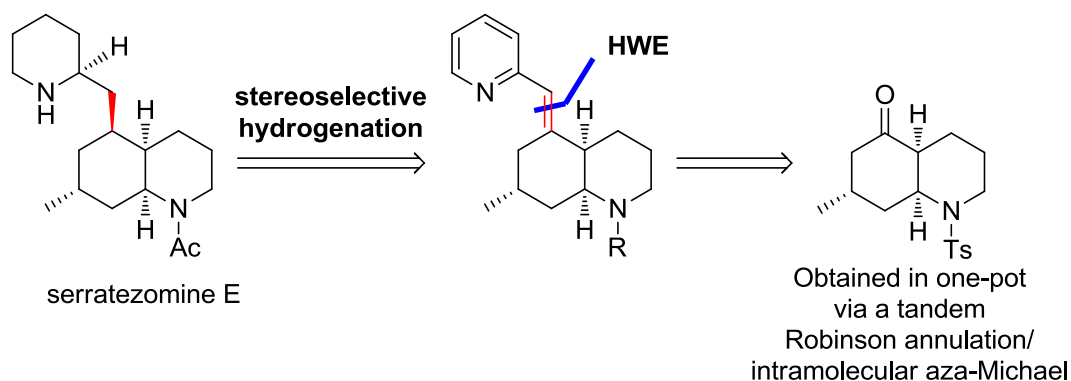
Chiral Auxiliary Approach and Chiral Phosphoric Acid Catalyzed Intramolec Michael
(Yao, *J. Org. Chem.* **2016**, 81, 1899);



Scheme 4.3 Synthesis of *cis*-decahydroquinolines in phlegmarine field

A brief summary of *cis*-decahydroquinoline previous synthesis in the phlegmarine alkaloids field is presented in Scheme 4.3. These syntheses usually involve the use of chiral auxiliary approach,⁶⁹ chiral pool approach^{26,28} or chiral auxiliary approach and chiral phosphoric acid catalyzed intramolecular Michael reaction.³⁰

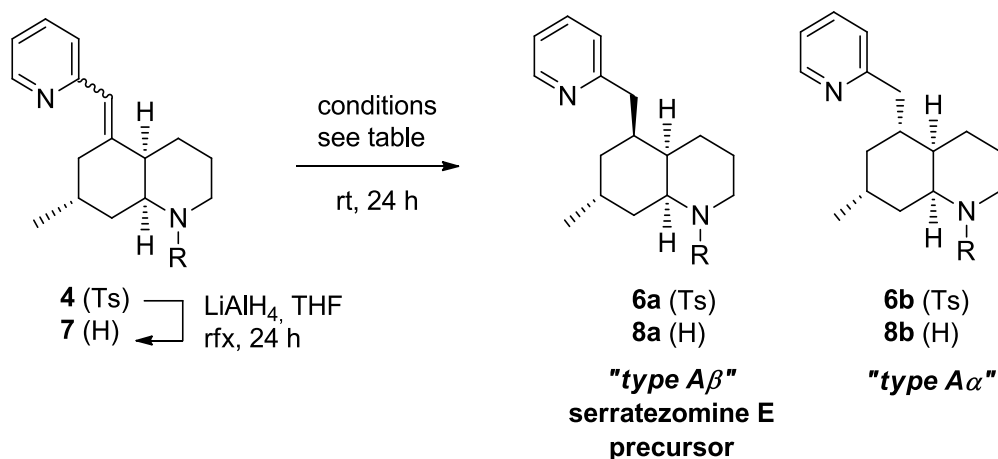
⁶⁹ Sahn, J. J.; Bharathi, P.; Comins, D. L. *Tetrahedron Lett.* **2012**, 53, 1347-1350.



Scheme 4.4 Retrosynthesis of serratezomine E

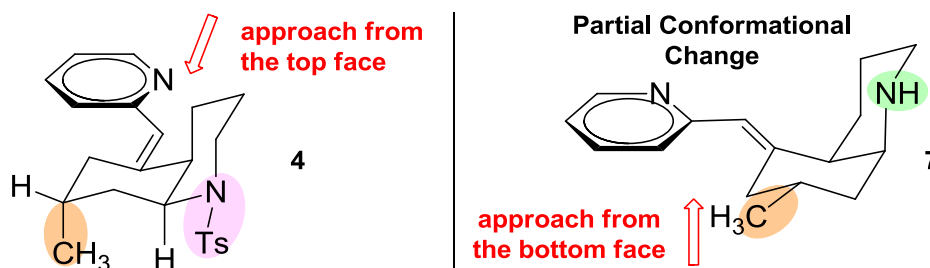
Using the methodology developed in our research group^{32,37} the key point of our approach would be the stereoselective hydrogenation of the vinylpyridine intermediate. The latter compound can be obtained through a Horner-Wadsworth-Emmons coupling with kinetic stereocontrol of the pyridine unit on the ketone intermediate.

This ketone intermediate can be easily obtained through the one pot organocatalyzed cyclization from simple acyclic precursors.

Table 4.1 Hydrogenation with heterogeneous catalysts

entry	R	catalyst ^a	solvent	dr ^b a:b
1	Ts	Pd-C	MeOH	3:97
2	Ts	Pd/C	CH ₂ Cl ₂	10:90
3	Ts	Pd-C + LiOH	MeOH	1:99
4	Ts	Ra-Ni	MeOH	14:86 ^c
5	H	Pd/C	MeOH	36:64
6	H	Pd/C + LiOH	MeOH	22:78
7	H	Pd/C + AcOH	MeOH	35:65

^a Catalyst loading 20% w/w ^b Determined by analysis of crude ¹H NMR.
^c 75% conversion.



Hydrogenation of double bonds is commonly done using heterogeneous catalyst such as palladium on carbon in the presence of hydrogen. The control of the stereochemistry obtained is, in this case, almost exclusively governed by the steric constraints of the molecule. The selectivity of the hydrogenation of vinylpyridine **4** using either Pd-C or Raney nickel is believed to be governed by an axially positioned methyl group, which combined with the tosyl protecting group blocks the approach from the lower face of the molecule, leading to the

decahydroquinoline **6b** (Table 4.1, entries 1-4). *A priori*, compound **7** appeared to be a convenient precursor of **8a**, since its different conformation could allow a kinetic hydrogenation from the less sterically demanding bottom face and lead to the decahydroquinoline having the required stereochemistry for the serratezomine E synthesis (*i.e.* **8a**).

However, hydrogenation of the secondary amine **7** (entries 5-7) did not give the expected reversal of selectivity. An explanation is that the haptophilicity⁷⁰ of the secondary amino function binds it to the catalyst surface and thus directs the delivery of the hydrogen from the top face of **7** to give **8b** as the major epimer.

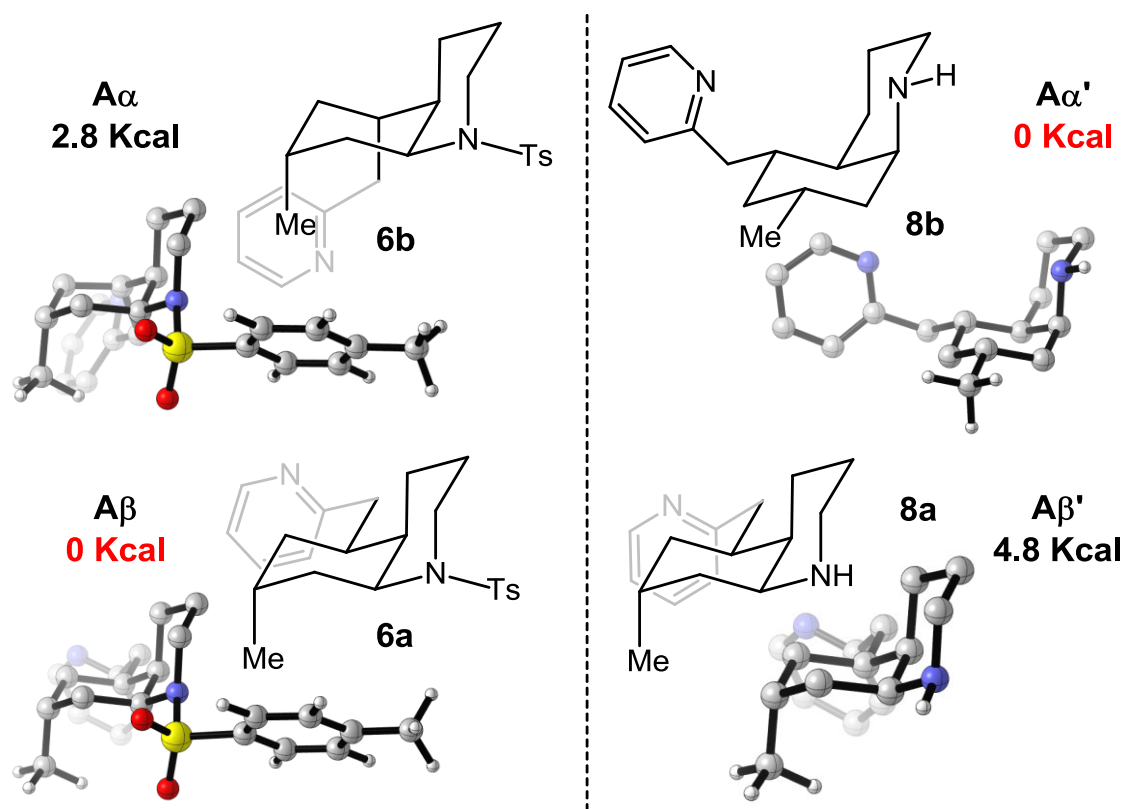
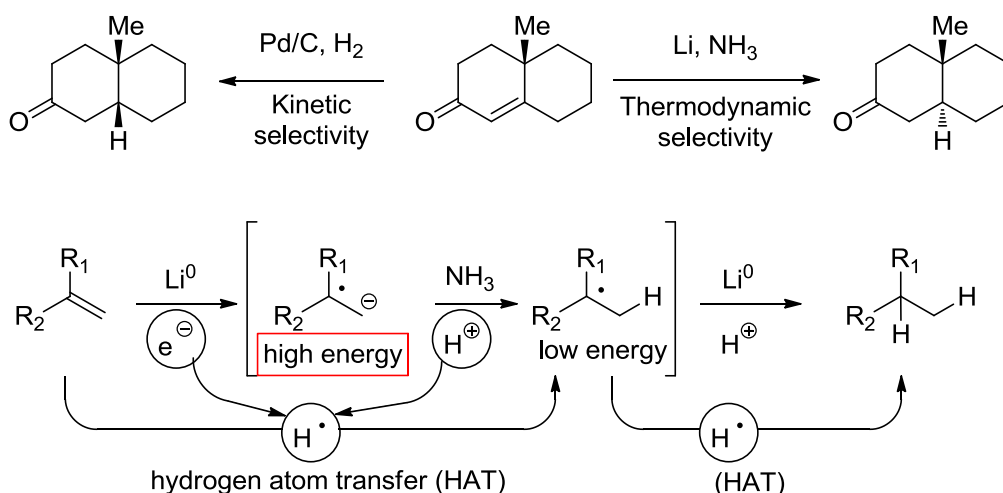


Figure 4.1 Relative stability of hydrogenation products

Considering that the desired compound A β (N-Ts, *i.e.* **6a**) is thermodynamically more stable (2.8 Kcal) than epimer A α (*i.e.* **6b**) obtained in the hydrogenation process using Pd as a catalyst, we thought we could carry out the hydrogenation of vinylpyridine **4** using novel

⁷⁰ Thompson, H. W.; Rashid, S. Y. *J. Org. Chem.* **2002**, *67*, 2813-2825.

procedures for reduction of alkenes. When a thermodynamic stereocontrol is required, the standard procedure is the use of dissolving metal reductions,⁷¹ despite its poor chemoselectivity. Indeed most other functional groups are reduced preferentially to alkenes with dissolving metal conditions making this process not compatible with complex structures.

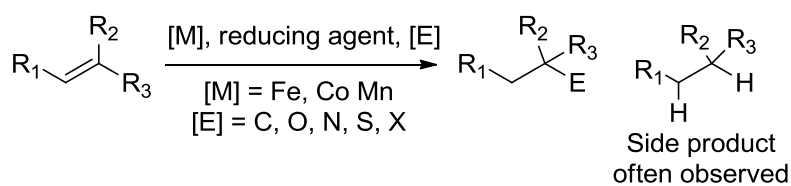


Scheme 4.5 Hydrogenation with thermodynamic stereocontrol

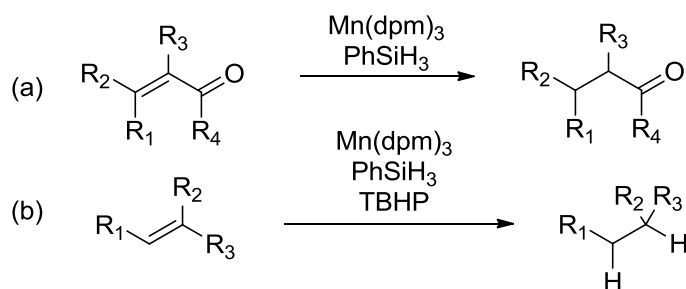
Since radical methods operate under thermodynamic conditions, it can give access to compounds that were previously unattainable through standard hydrogenation procedures when steric constraint of the molecule favors the formation of the kinetic isomer. Hydrogenation atom transfer (HAT) can be found as a good compromise to obtain thermodynamic hydrogenation on elaborated substrates (Scheme 4.5). Indeed this procedure allows to prevent formation of the high energy radical anion intermediate responsible for the poor chemoselectivity

⁷¹ (a) Jonhson, W. S. ; Bannister, B. ; Bloom, B. M.; Kemp, A. D.; Pappo, R.; Rogier, E. R.; Szmuszkovicz, J. *J. Am. Chem. Soc.* **1953**, *75*, 2275-2276. (b) Stork, G.; Darling, S. D. *J. Am. Chem. Soc.* **1960**, *82*, 1512-15313. (c) Whitesides, G. M.; Ehmann, W. J. *J. Org. Chem.* **1970**, *35*, 3565-3567.

Olefin functionalization (Baran, Carreira, Mukaiyama, and others)



Olefin hydrogenation (a) Magnus 2000 and b) Shenvi 2014)



Scheme 4.6 Hydrogenation with thermodynamic stereocontrol

observed in dissolving metal conditions. Recently a range of radical reduction⁷² and olefin coupling⁷³ conditions following this concept have been developed (Scheme 4.6).

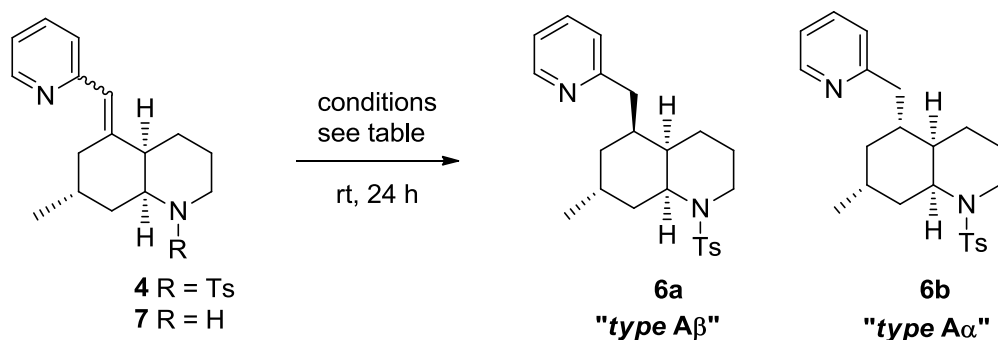
⁷² (a) Iwasaki, K.; Wan, K. K.; Oppedisano, A.; Crossley, S. W. M.; Shenvi, R. A. *J. Am. Chem. Soc.* **2014**, *136*, 1300-1303. (b) Magnus, P.; Waring, M. J.; Scott, D. A. *Tetrahedron Lett.* **2000**, *41*, 9731-9733.

⁷³ (a) Mukaiyama, T.; Yamada, T. *Bull. Chem. Soc. Jpn.* **1995**, *68*, 17-35. (b) Waser, J.; Gaspar, B.; Nambu, H.; Carreira, E. M. *J. Am. Chem. Soc.* **2006**, *128*, 11693-11712. (c) Magnus, P.; Payne, A. H.; Waring, M. J.; Scott, D. A.; Lynch, V. *Tetrahedron Lett.* **2000**, *41*, 9725-9730. (d) Gaspar, B.; Carreira, E. M. *J. Am. Chem. Soc.* **2009**, *131*, 13214-13215. (e) Leggans, E. K.; Barker, T. J.; Duncan, K. K.; Boger, D. L. *Org. Lett.* **2012**, *14*, 2010-2013. (f) King, S. M.; Ma, X.; Herzon, S. B. *J. Am. Chem. Soc.* **2014**, *136*, 6884-6887. (g) Lo, J. C.; Yabe, Y.; Baran, P. S. *J. Am. Chem. Soc.* **2014**, *136*, 1304-1307. (h) Lo, J. C.; Gui, J.; Yabe, Y.; Pan, C.-M.; Baran, P. S. *Nature* **2014**, *516*, 343-348.

With this background, we decided to evaluate the reductive radical conditions to attempt the hydrogenation of **4** to **6a**. We began using the hydrogen atom transfer (HAT) radical conditions reported by Shenvi^{72a} (Mn(dpm)₃ and PhSiH₃ in the presence of *t*-BuOOH). Although the desired epimer **6a** was obtained as the main compound in a 73:27 ratio (Table 4.2, entry 1), the products were accompanied by significant amounts of byproducts, which were difficult to separate from the main products.⁷⁴ When the same conditions were applied to the N-H compound **7**, there was no reaction and the starting material was completely recovered. Similar radical methods based on other protocols,^{73e-g} either directly or modified, were also evaluated, but with no significant improvements. On trying the reductive coupling conditions by Baran,^{73g} but omitting the acceptor compound (entry 2), we were pleased to observe significantly reduced byproduct formation but the reaction ran only to 50% completion (with recovery of unreacted starting material). Attempts to modify the conditions by adding more equivalent of reagents were unsuccessful. Screening of other catalysts that have been employed for various olefin couplings gave only traces of the product (entries 3, 4). Other complexes and conditions were screened, but same ratio along with additional byproducts formation resulted in overall lower conversions.⁷⁵

⁷⁴ While it was not possible to fully determine the structure of the by-products, we speculatively assigned them as migrated double bond products and miscellaneous oxygenated compounds.

⁷⁵ For comprehensive experimental studies of radical reduction of vinylpyridine **3** (catalysts, additives, solvent, and optimization process for entry 9, see Tables in Supporting Information 4'). Detailed herein attempts to perform the reaction with catalytic amount of catalyst (10 mol%) and with an excess of catalyst, without any improvement.

Table 4.2 Screening of Radical Reduction⁷⁵

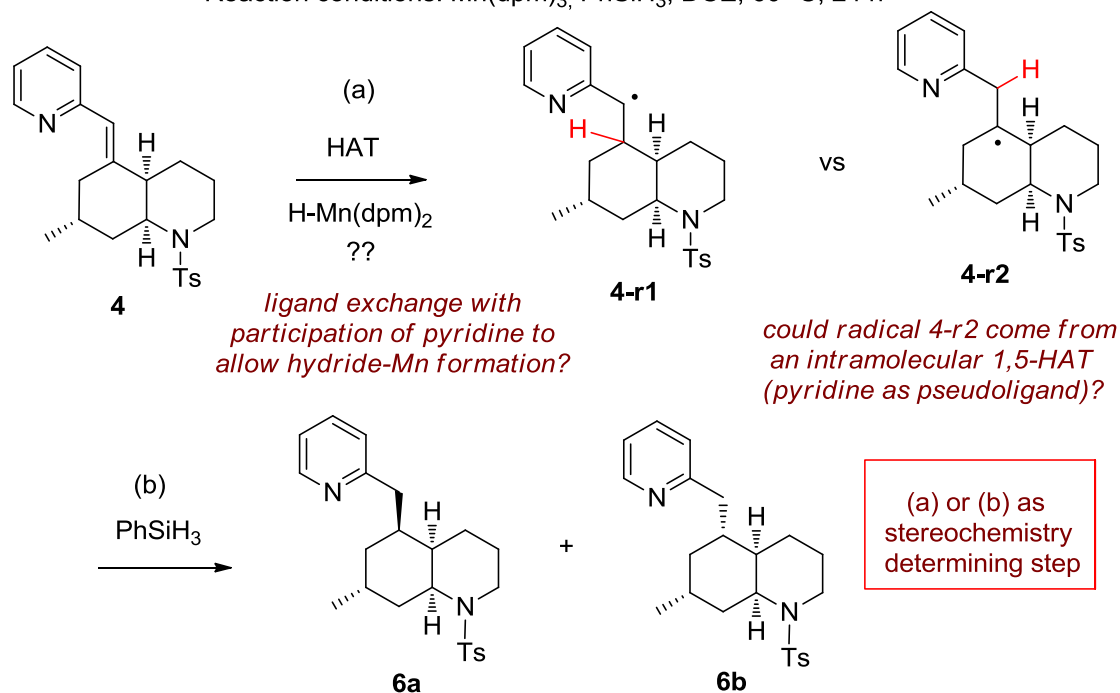
entry ^a	method ^b	conv ^c (%)	dr ^c a:b
1	Mn(dpm) ₃ , ^d PhSiH ₃ , TBHP, <i>i</i> PrOH	63 ^e	73:27
2	Fe(acac) ₃ , ^f PhSiH ₃ , EtOH	49	67:33
3	Fe ₂ (ox) ₃ ·H ₂ O, ^g NaBH ₄ , H ₂ O, EtOH	10	75:25
4 ^h	Co(acac) ₂ , ^f Et ₃ SiH, TBHP, <i>n</i> -PrOH	7	<i>n.d.</i>
5	Mn(dpm) ₃ , ^f PhSiH ₃ , EtOH	97	63:37
6 ⁱ	Mn(dpm) ₃ , ^f PhSiH ₃ , DCE	100	69:31

^a Reactions were performed on a mixture of *E:Z* isomers (4:1). ^b For detailed reaction conditions see Supporting Information. ^c Determined by analysis of crude ¹H NMR, conversion to the epimeric mixture of reduced product. ^d 10 mol% of catalyst used. ^e Byproducts observed lowering the conversion. ^f 1 equiv of catalyst used. ^g 2 equiv of catalyst used. ^h 1,4-cyclohexadiene used as additive. ⁱ Isolated yield of the epimer mix of product reduced = 86%

Using a modification of the original conditions with Mn(dpm)₃ in stoichiometric quantities in EtOH as the solvent, but without *t*-BuOOH, gave for the first time a complete and clean conversion to the desired compound **6a** (entry 5). Extensive screening to improve the results allowed us to optimize the conditions for our type of substrate, affording the desired product with a full conversion, total absence of byproducts, 86% isolated yield and a dr = 69:31 (entry 6). Thus, during this study, we found that the reaction worked best in non-protic solvent (DCE or MeCN). This finding is not in agreement with the supposed mechanism where a protic solvent (*i.e.* alcohol) supposedly plays a crucial role.

How does the radical reduction of vinylpyridine **4** occur?

Reaction conditions: $\text{Mn}(\text{dpm})_3$, PhSiH_3 , DCE, 60 °C, 24 h



Scheme 4.7 Mechanism insight

It should be noted that a mechanism still needs to be proposed to explain the use of the reaction conditions described here. Although the mechanism of this reaction remains unclear, as a tentative starting point, a simple proposal is depicted in Scheme 4.7.

The points to be clarified in the near future are:

- i) Regioselectivity in the initial HAT: we need to evaluate the stability of a tertiary radical (at C-5) compared with a benzylic radical (adjacent to pyridine ring).
- ii) How is the first hydrogen atom transferred? It was observed that the treatment of a dark olive-green solution of $\text{Mn}(\text{dpm})_3$ in DCE with stoichiometric amounts of PhSiH_3 produced no change, but after the addition of isopropyl alcohol, the solution rapidly turned pale yellow to give $\text{HMn}(\text{dpm})_2$.⁷⁶ The latter is considered to be the species that

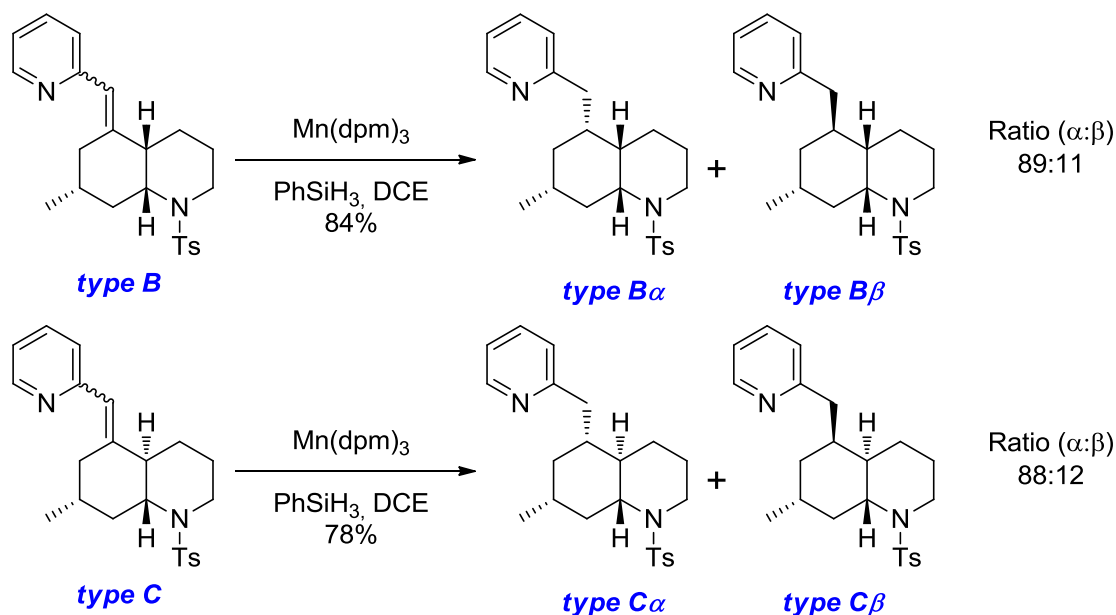
⁷⁶ This intermediate was not isolated but was described as the active species in the reference publication (Ref. 72b)

transfers the hydrogen atom, but in our case we were working in an aprotic medium.

A possible explanation could be that the pyridine gets involved in a coordination with the manganese.⁷⁷ This would allow the formation of the hydride manganese species (by a hydride transfer from the PhSiH₃), which can evolve through an intramolecular hydrogen atom transfer, probably a 1,5-HAT.

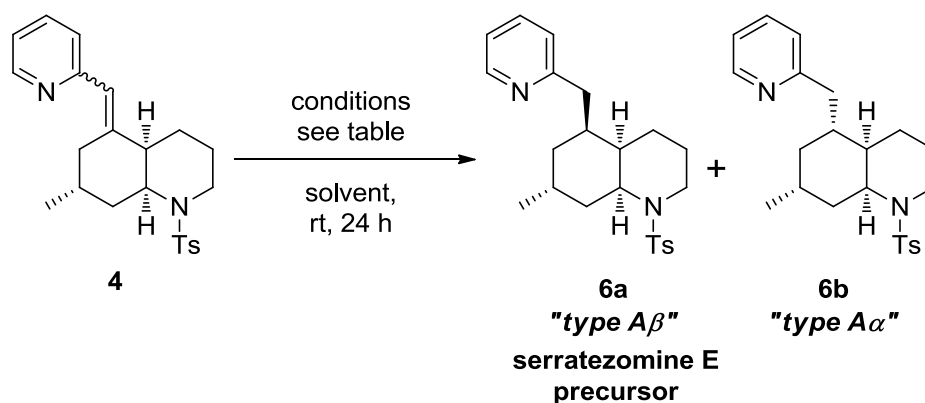
iii) Working in a stoichiometric manner, the radical formed could be reduced by the PhSiH₃. A study using a deuterated silane could provide valuable data.

Finally, although not part of the core of this research project, it is noteworthy that the optimized radical reaction conditions introduced here, using Mn(dpm)₃ (Table 4.2, entry 6) were also successfully applied to vinylpyridines of Type B and C, leading to a 89:11 and 88:12 α/β diastereomeric ratio, respectively. The study and scope of this reaction awaits exploration by its application to phlegmarine alkaloid synthesis.



Scheme 4.8 Optimized conditions applied to type B and C

⁷⁷ Attempts to reduce the benzene analog of **4** lacking the pyridine nitrogen, only traces of product was obtained and was accompanied with unreacted starting material and unidentified byproducts in an unseparable mixture.

Table 4.3 Hydrogenation under homogeneous catalysts

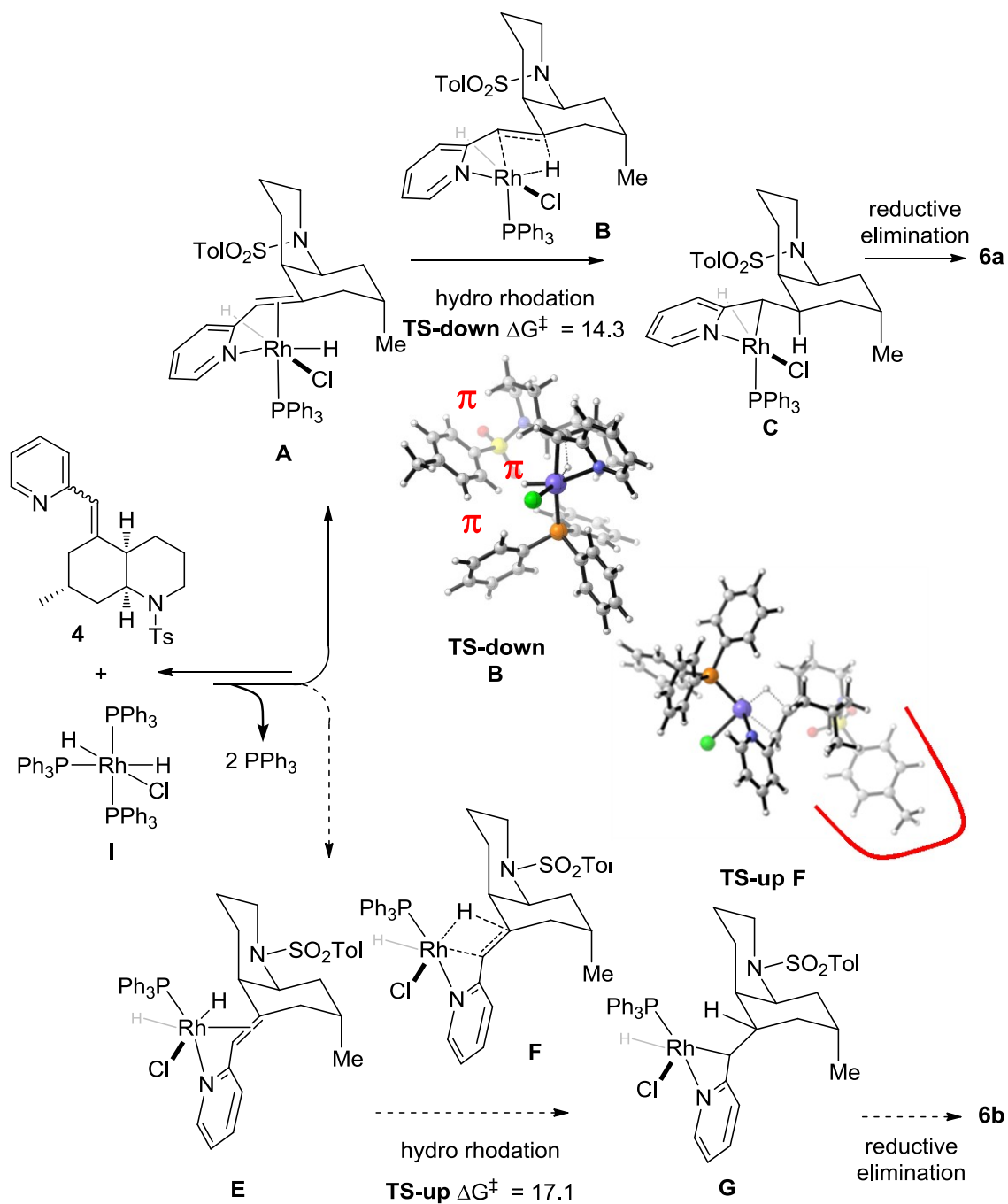
entry	catalyst	loading	solvent	isolated yield ^a (%)	dr ^b a:b
1	Pd/C	20% w/w	MeOH	98	3:97
2	Crabtree	15 mol%	CH ₂ Cl ₂	96	68:32
3	Crabtree	15 mol%	MeOH	95	86:14
4	RhCl(PPh ₃) ₃	15 mol%	CH ₂ Cl ₂	97	91:9
5	RhCl(PPh ₃) ₃	15 mol%	MeOH	96	95:5
6 ^c	RhCl(PPh ₃) ₃	15 mol%	MeOH	96	95:5
7 ^d	RhCl(PPh ₃) ₃	15 mol%	MeOH	96	95:5
8	RhCl(PPh ₃) ₃	5 mol%	MeOH	97	96:4
9	RhCl(PPh ₃) ₃	2 mol%	MeOH	98	96:4

^a Isolated yield of the epimer mix of product reduced. ^b Determined by ¹H NMR analysis.

^c Using Z isomer only. ^d Using E isomer only.

Crabtree's reagent: [Ir(PCy₃)₃(cod)(py)]PF₆

In parallel we also explored more conventional hydrogenation methods. Our idea being that even if the alkene functionality presents a high steric constraint we thought that the presence of the pyridine ring system could help to coordinate metal catalyst in the case of standard homogenous catalysis with Crabtree's or Wilkinson's catalyst. This reaction proved really powerful enabling us to achieve almost complete diastereoselectivity (96:4) in a clean quantitative manner using only 2 mol% of catalyst (entry 9). We were pleased to observe equal result performing the reaction on each isolated E or Z isomers



Scheme 4.9 DFT calculations

of vinylpyridine **4** (entries 6 and 7) proving that this reaction is not sensitive to the *Z/E* ratio. It should also be noted that the free N-H compound **7** did not react with either catalyst.

Given the sterically impeded nature of the β,β -disubstituted vinyl pyridine and large size of Wilkinson's catalyst, we presumed the reaction

proceeded via a coordination of the catalyst.⁷⁸ Indeed, when the benzene analog of **4** (not shown) lacking the pyridine nitrogen was used, no reduction was observed.

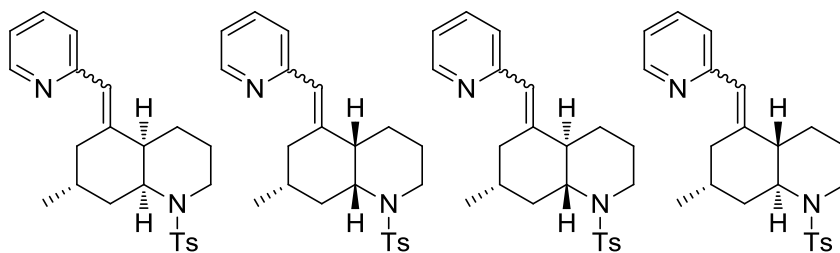
To understand the reaction and account for the excellent stereocontrol observed, calculations were performed and the proposed reaction mechanism is outlined in Scheme 4.9. The hydrogenated Wilkinson's catalyst (**I**) forms an initial complex **A** by coordination to the double bond and the pyridine nitrogen atom of the substrate, releasing two molecules of phosphine in the process, which can occur through both faces of the double bond. In complex **A**, the Rh atom is coordinated to the pyridine ring and the double bond with short interatomic Rh-N (2.4 Å), and Rh-alkene (2.3 Å) distances, inducing a slight deconjugation of the double bond and the pyridine ring, which is partially responsible for its 10 kcal/mol higher energy than the initial hydrogenated Wilkinson catalyst. Thus, the initial equilibrium between the starting materials and **A** is shifted towards the former (Scheme 4.9). However, the very low activation energy required for the hydro-rhodation (**TS-down** is only 4 kcal/mol above **A**) makes the whole process feasible, triggering an easy formation of **C**, and the consumption of the starting material. After the insertion of hydrogen into **C**, the reaction proceeds through reductive elimination, liberating the final product **6a**. As mentioned, the hydro-rhodation step can occur on either face of the double bond, through two diastereoisomeric transition states, **TS-down** and **TS-up** (**E** → **G**). The computed activation energies predict that **TS-down** is favored by 2.8 kcal/mol over **TS-up**, justifying the experimental formation of the major diastereoisomer **6a**. The main difference between the two diastereoisomeric transition states consists in the different orientation of the *N*-tosyl moiety

⁷⁸ For directed-hydrogenations leading to products with contrasteric selectivity, see: Friedfeld M. R., Margulieux, G. W.; Schaefer B. A.; Chirik, P. J. *J. Am. Chem. Soc.* **2014**, *136*, 13178-13181.

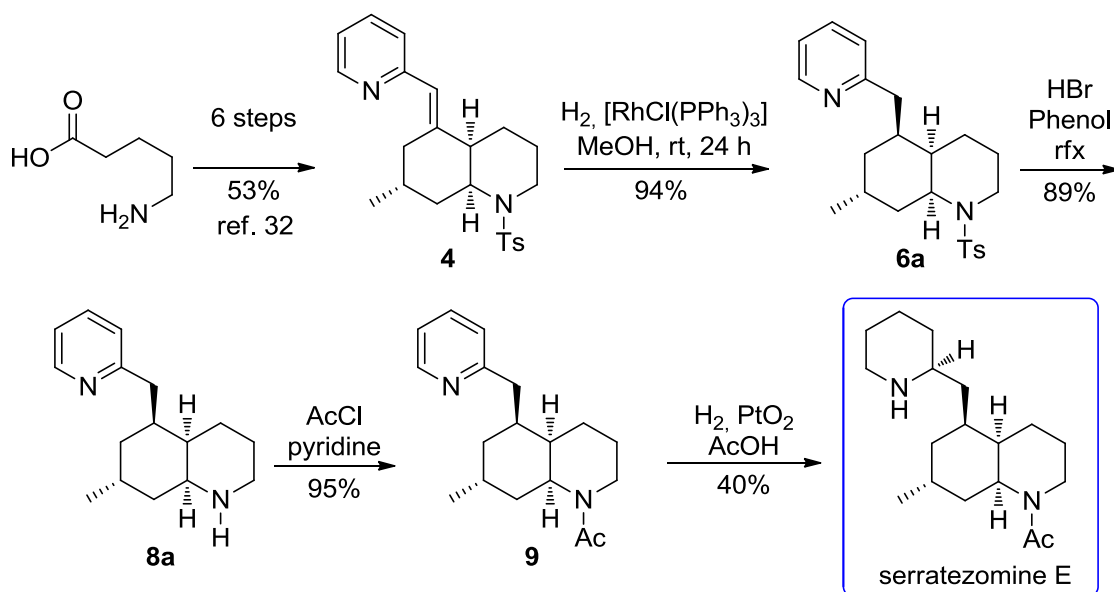
of the substrate. In **B**, the phenyl ring of the tosyl group forms at least three strong π -stacking interactions, with one of the rings of the PPh_3 group, and with two different H atoms of the bicyclic skeleton. During the transition state, the Rh-alkene bond is even tighter than in **A** (2.1 Å), inducing a weakening of the Rh-N coordination (2.5 Å).

We were pleased to observe that this pattern of hydrogenation can be also observed in the other types (B, C, and D) of decahydroquinolines obtained using previously described methodology^{32,33} useful for phlegmarine alkaloids synthesis (see Table 4.4).

Table 4.4 Comparison of hydrogenation methods on each type



ratio (α : β)	type A	type B	type C	type D
H_2 , Pd/C	97 : 3	9 : 91	40 : 60	66 : 33
PhSiH_3 , $\text{Mn}(\text{dpm})_3$	31 : 69	89 : 11	88 : 12	<i>n.d.</i>
H_2 , $[\text{RhCl}(\text{PPh}_3)_3]$	4 : 96	90 : 10	>99 : 1	1 : >99



Scheme 4.10 Total synthesis of serratezomine E

With the optimum reduction method in hand, transformation of **4** (prepared in six steps from the commercially available 5-aminopentanoic acid, see Scheme 1.7 and 1.12) led to a concise synthesis of serratezomine E (**1**, Scheme 4.10). Hydrogenation with Wilkinson's catalyst, and removal of the tosyl group of **6a** led to the secondary amine **8a** in a pure form, introduction of the required acetyl group gave **9**. Subsequent reduction of the pyridine provided serratezomine E (**1**) as a white solid,⁷⁹ whose structure was unequivocally confirmed by X-ray analysis (Figure 4.2), having the absolute configuration (*S*) at the C-2 piperidine ring and (*R*) at the C-7 decahydroquinoline ring, characteristic of phlegmarine alkaloids.

⁷⁹ The remaining mass comprised the epimer in the form of an oil, which enabled its simple separation from the desired product, despite the two compounds having identical R_f values.

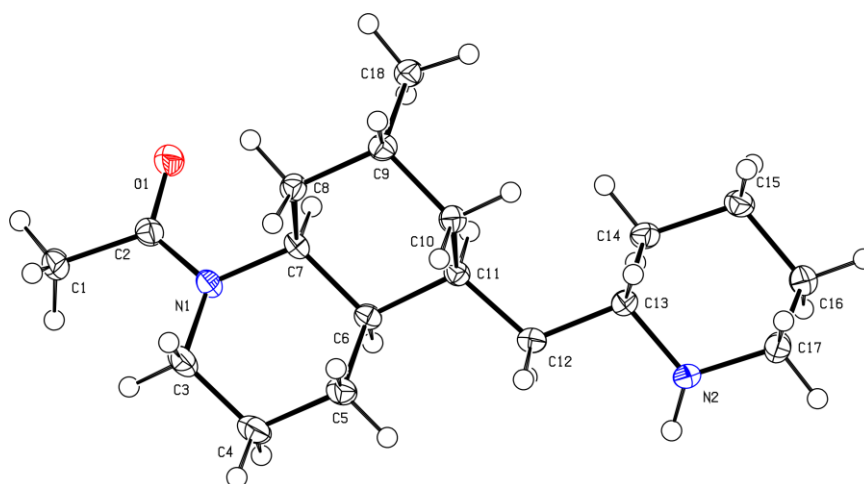


Figure 4.2 X-ray of serratezomine E

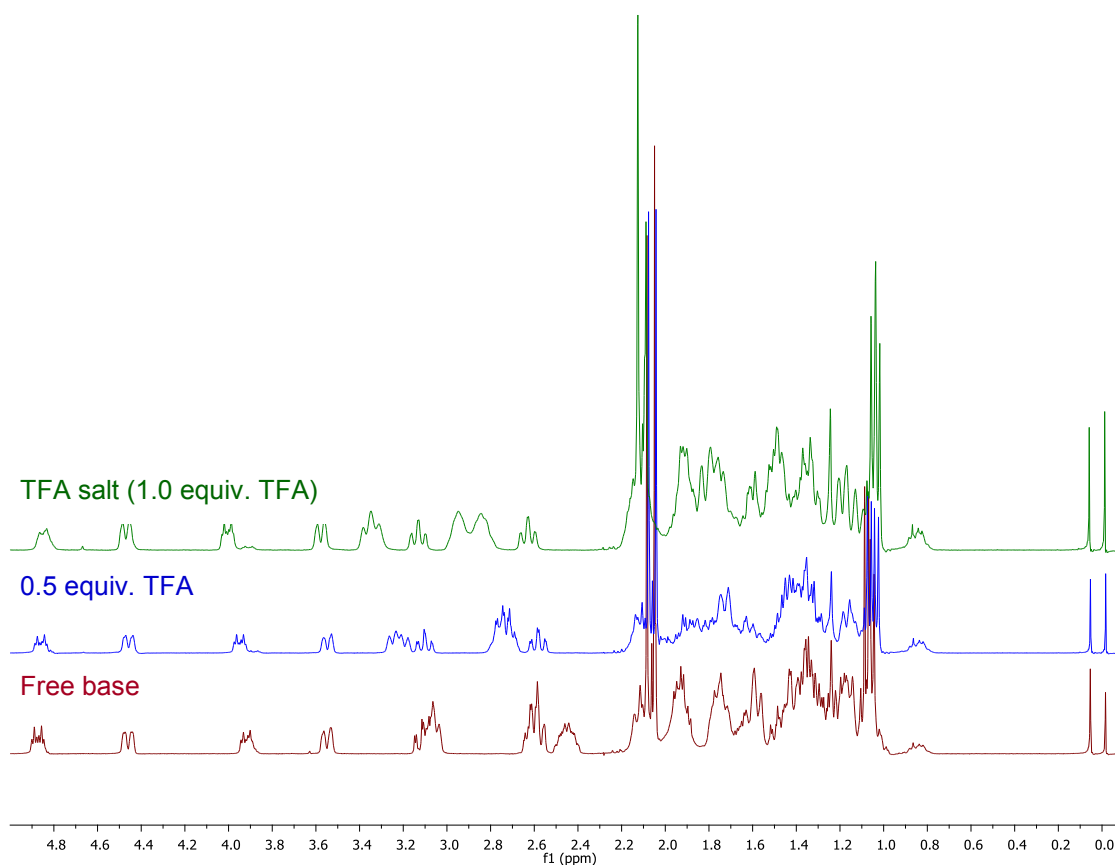


Figure 4.3 ¹H NMR spectra of synthetic serratezomine E (1) in CDCl₃ before and after addition of trifluoroacetic acid. For comparison of NMR data for natural serratezomine E (partially protonated) and compound **1**, see Supporting Information.

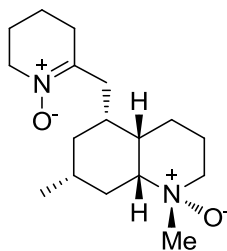
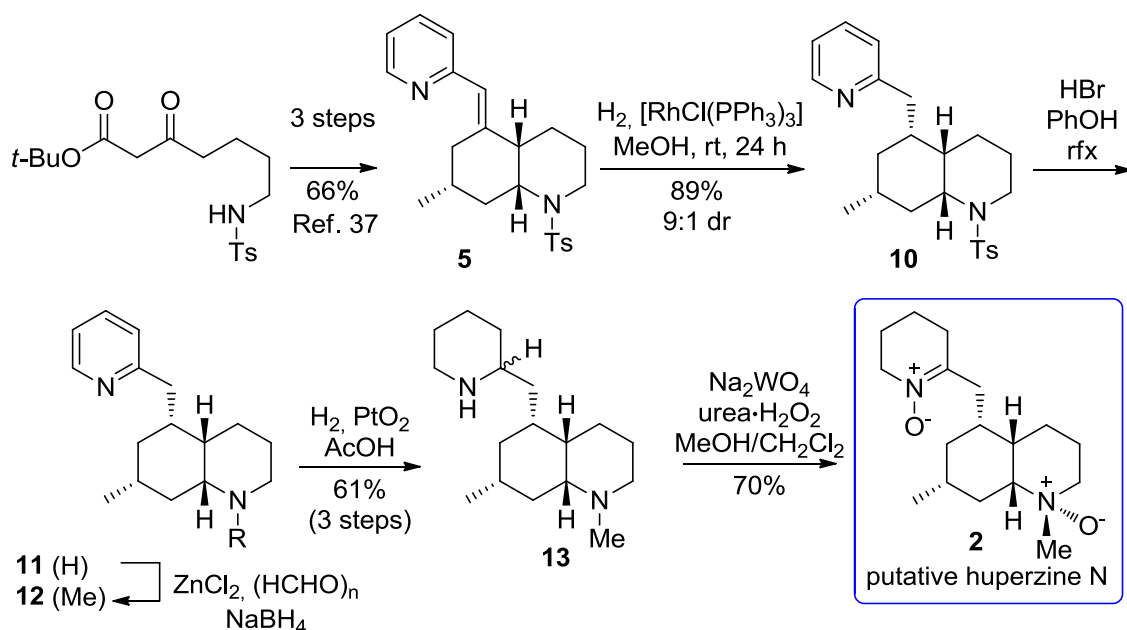


Figure 4.4 Huperzine N

Having already achieved total synthesis of lycoposerramine Z,³² cermizine B³⁷ and now total synthesis of serratezomine E, the next target to achieve a unified synthesis of all the *cis*-phlegmarine alkaloids was huperzine N.⁹

The unusual nitronium moiety, which also appears in other phlegmarine alkaloids (e.g. lycoposerramine Z), is postulated to act as a radical trap halting destructive cascades initiated by free radicals and, hence, shows potential application in neurodegenerative diseases.⁸⁰

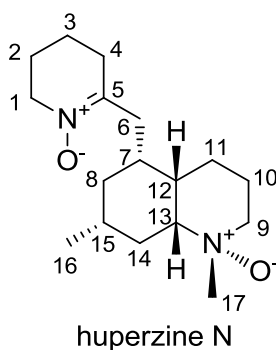
⁸⁰ Sun, Y.; Yu, P.; Zhang, G.; Wang, L.; Zhong, H.; Zhai, Z.; Wang, L.; Wang, Y. *J. Neurosci. Res.* **2012**, *90*, 1662-1669.



Scheme 4.11 Total synthesis of putative huperzine N

The total synthesis of huperzine N was achieved using an analogous procedure used for the synthesis of serratezomine E, but starting from the vinylpyridine substituted *cis*-decahydroquinoline **5** of type B instead of the type A analog (Scheme 4.11).

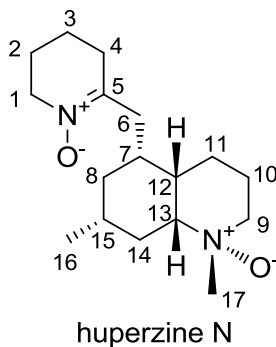
Hydrogenation of **5** with Wilkinson's catalyst gave the desired epimer **10** in a 9:1 ratio. Removal of the tosyl group, formation of the *N*-methyl via reductive amination with ZnCl_2 and reduction of the pyridine gave **11** in good overall yield. Finally, oxidation with Na_2WO_4 / $\text{urea}\cdot\text{H}_2\text{O}_2$ gave the reported structure of huperzine N, although the NMR spectra of **2** did not match those described (see Tables 4.5 and 4.6).

Table 4.5 Comparison of ^1H NMR data for (-)-huperzine N and **2** in CDCl_3 

^1H	synthetic ¹ 2	huperzine N ²
1	3.80 (t, 6.0)	3.75 (t, 6.0)
2	1.92 (m)	1.84-1.92 (m)
3	1.75 (m)	1.64-1.69 (m)
4	2.40 (dd, 6.0, 6.0)	2.34 (t, 6.0)
5		
6	2.73 (dd, 13.5, 8.0)	2.96 (dd, 12, 3)
	2.46 (dd, 13.5, 6.5)	1.91 (d, 12)
7	1.96 (m)	2.10-2.17 (m)
8	1.39 (m)	1.34 (ddd, 12, 8, 4)
	1.05 (ddd, 13.0, 13.0, 13.0)	1.29 (br d, 12)
9	3.16 (m)	3.35 (br d, 12)
	3.05 (br dd, 11.2, 3.5)	3.14 (ddd, 12, 11, 3)
10	2.41 (m)	1.34-43 (m)
	1.62 (m)	1.57 (br d, 14)
11	1.68 (m)	2.01-2.06 (m)
	1.37 (m)	1.08-1.13 (m)
12	2.94(ddd, 12.4, 3.8, 3.8, 3.8)	1.78-1.83 (m)
13	3.17 (m)	2.89 (ddd, 11, 10, 3)
14	1.81 (m)	2.06-2.17 (m)
	1.30 (m)	1.67-1.72 (m)
15	1.53 (m)	2.16-2.25 (m)
16	0.99 (d, 6.5)	0.93 (d, 7)
17	3.11 (s)	3.04 (s)

¹ Recorded at 400 MHz. Assignments were aided by COSY and HSQC spectra.

² Recorded at 400 MHz (*Helv. Chim. Acta*, **2008**, *91*, 1031-1035).

Table 4.6 Comparison of ^{13}C NMR data for (-)-huperzine N and **2** in CDCl_3 

^{13}C	synthetic ¹ 2	huperzine N ²
1	58.4	58.2
2	23.1	23.1
3	18.8	18.8
4	28.9	30.0
5	147.4	148.0
6	34.4	36.4
7	36.8	32.3
8	34.8	36.6
9	61.0	69.0
10	20.2	20.1
11	16.2	27.0
12	33.4	40.8
13	76.8	73.4
14	31.8	30.0
15	31.8	26.8
16	22.2	19.0
17	58.2	57.6

¹ Recorded at 100 MHz. Assignments were aided by COSY and HSQC spectra.

² Recorded at 100 MHz (*Helv. Chim. Acta*, **2008**, *91*, 1031-1035).

Instead, the NMR data of the natural huperzine N would be explained by the structure depicted in Figure 4.5. This proposal was validated after the total synthesis of a compound with the reassigned structure (see Chapter 5).

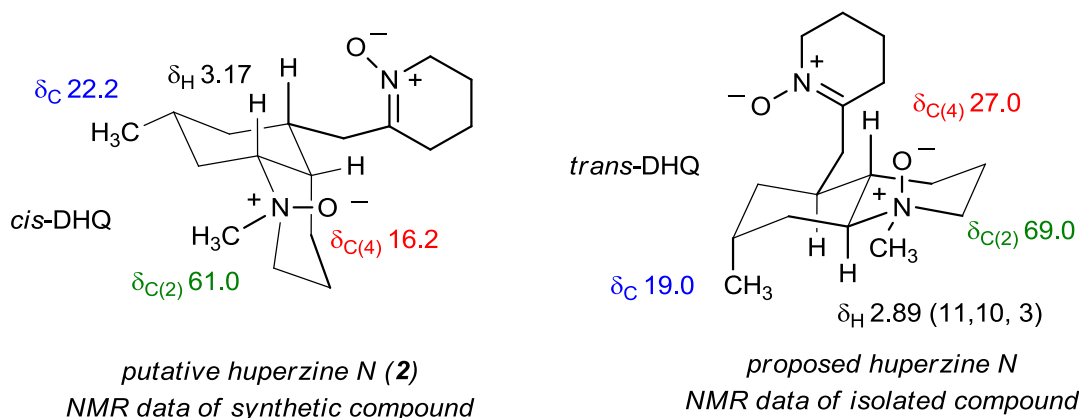


Figure 4.5 Proposed reassignment of huperzine N by NMR data

In summary, a divergent hydrogenation protocol was developed, providing access to a range of phlegmarine compounds unattainable by standard hydrogenation of common vinyl pyridine intermediates. Via rhodium complexation with the pyridine nitrogen and selective facial delivery, it was possible to invert the course of hydrogenation from 97:3 to 4:96 dr. This method was successfully applied for the first total synthesis of serratezomine E as well as huperzine N. The latter turned out to be a putative structure, and the natural one was structurally reassigned. The application of this strategy to *trans*-phlegmarine alkaloids was the next step of our work.

**5. Access to *trans*-Phlegmarines of Type D:
Synthesis of (±)-Serralongamine A and the Revised
Structure of Huperzine N**

J. Org. Chem. **2016**, *81*, 2629-2634.

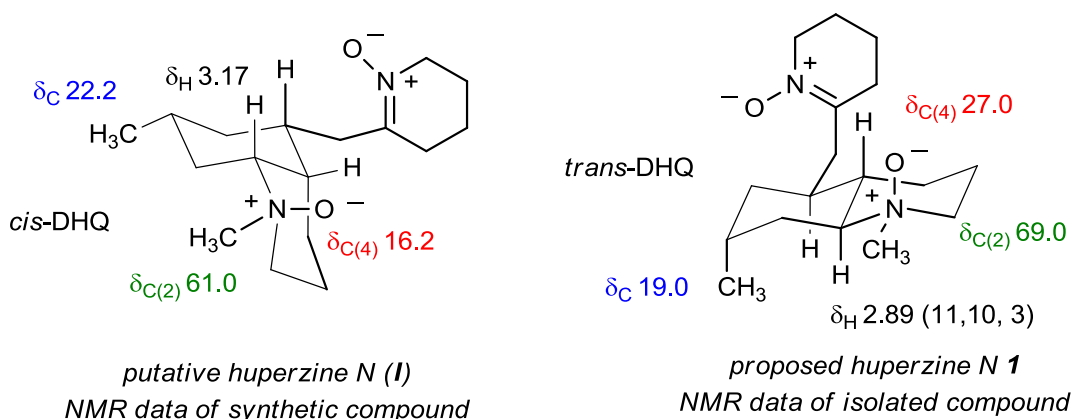
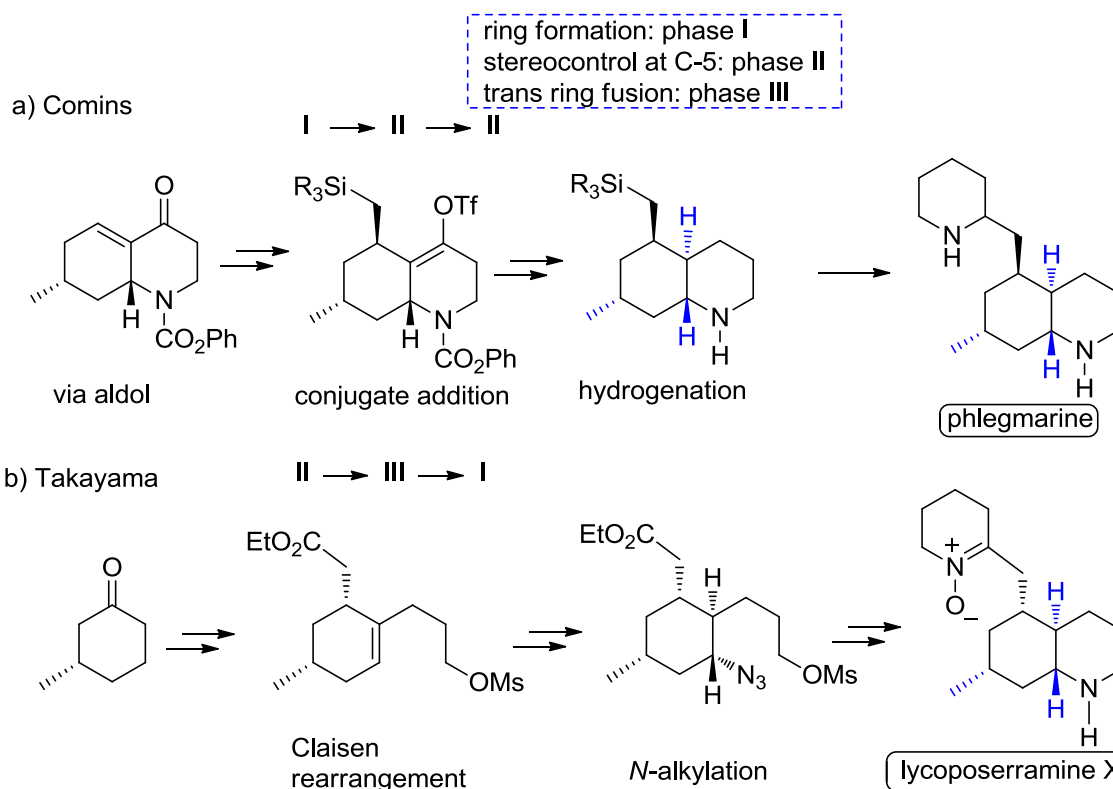


Figure 5.1 Objective

The second goal related to the synthesis of phlegmarines was to open the access to *trans*-phlegmarine alkaloids using the same building block used for the synthesis of *cis*-phlegmarines, *i.e.* the 5-oxodecahydroquinoline.

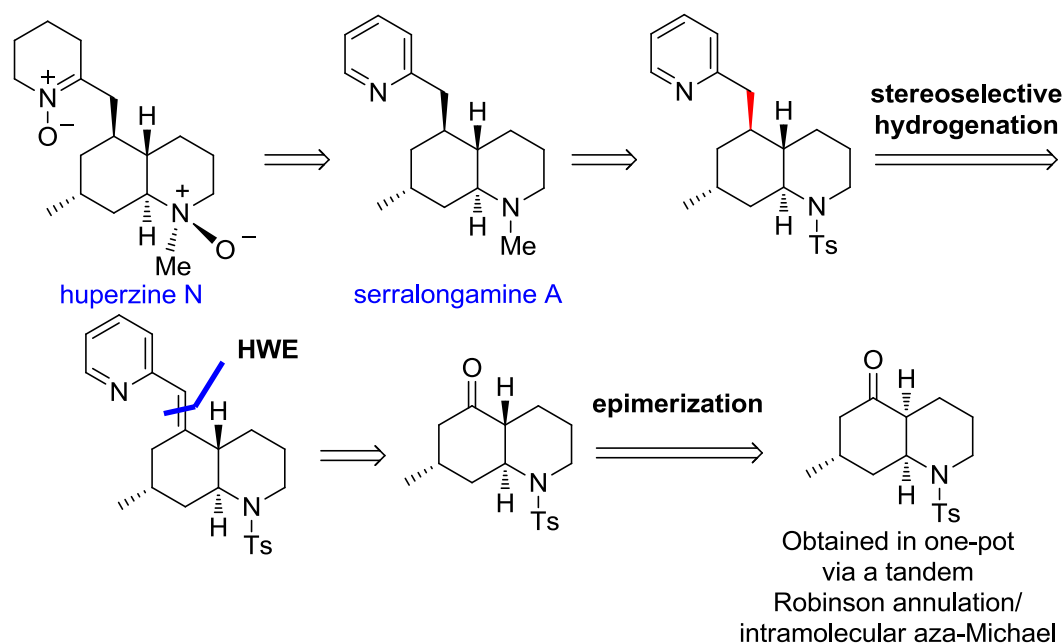
Indeed the structure reassignment proposed for huperzine N (**1**) (in Chapter 4) corresponds to a *trans*-dehydroquinoline scaffold of type D as presented in Figure 5.1.

As discussed previously, the application of our stereodivergent hydrogenation process to the *trans*-decahydroquinoline series could allow us to complete the total synthesis of any phlegmarine alkaloids



Scheme 5.1 Precedents: Series *trans* type C

Previous *trans*-phlegmarine syntheses have targeted alkaloids with the type C stereoparent. The synthesis of phlegmarine itself was completed by Comins,²⁵ who also reported the synthesis of three related alkaloids bearing different substituents at the two nitrogen atoms, while Takayama²⁶ achieved lycoposerramine X. The key challenges in the synthesis of these alkaloids are the generation of the *trans*-decahydroquinoline core and the stereocontrol in the genesis of the stereocenter at C-5 where the pyridylmethyl backbone is attached. The two different approaches to construct the *trans*-decahydroquinoline ring with the required stereochemistry in the four stereogenic centers are summarized in Scheme 5.1. Comins, applying his methodology based on pyridinium salts, prepared a polysubstituted piperidine that furnished the bicyclic ring by an aldol reaction. Stereoselective conjugated addition followed by a hydrogenation process allowed a stereochemical control at

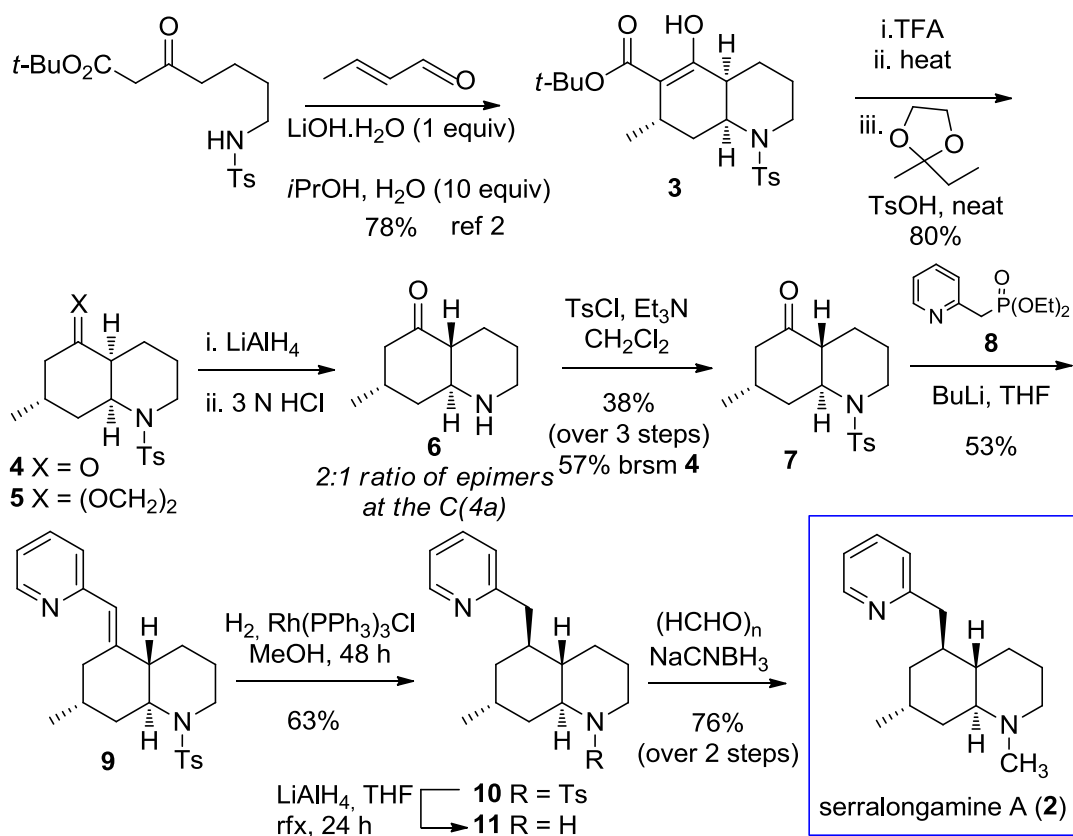


Scheme 5.2 Retrosynthetic analysis series *trans*-decahydroquinoline type D

C-5 and in the ring fusion, respectively. In contrast, the Takayama approach involved the elaboration of a polyfunctionalized cyclohexane compound in which the four stereogenic centers were established before cyclization leading to the decahydroquinoline ring.

Our approach differs from the aforementioned both in its synthetic strategy and the targeted compounds, presenting a type D decahydroquinoline core.⁸¹ The synthetic plan involved the same building-block used in our previous synthesis of *cis*-phlegmarines which after epimerization of the C-4a stereogenic center affords the *trans*-decahydroquinoline ring of type D. This procedure allows access to phlegmarine alkaloids with a new stereochemical pattern. Control of the stereochemistry at C-5 through a substrate-directable hydrogenation process would be crucial in this synthetic proposal (Scheme 5.2).

⁸¹ For a synthetic approach to 5-oxo-*trans*-decahydroquinoline used in the synthesis of the lycopodium alkaloid lycoperine, see: Nakamura, Y.; Burke, A. M.; Kotani, S.; Zilber, J. W.; Rychnovsky, S. D. *Org. Lett.* **2010**, *12*, 72-75.



Scheme 5.3 First total synthesis of serralongamine

Commencing the synthesis from the easily available ketone **4**,³² our original protocol³³ allowed the ring fusion to be changed from *cis* to *trans*, via the conversion of acetal **5** to the corresponding secondary amine and acid-induced epimerization at C-4a. Tosylation of the resulting 2:1 mixture of ketones **6** and its C4a-epimer furnished the required decahydroquinoline **7** with a *trans* ring fusion⁸² as a single isomer after chromatographic separation (see Scheme 5.3). This ketone reacted with a solution of the lithium anion of phosphonate **8**⁸³ to give vinylpyridine derivative **9** in 53% yield, diastereoselectively providing the *E* isomer.⁸⁴

⁸² The coupling constants of H-4a (11.4, 11.4, 11.4, 3.2 Hz) and H-8a (11.4, 11.4, 4.0 Hz) allow the *trans*-ring fusion in **7** to be clearly established.

⁸³ Gan, X.; Binyamin, I.; Rapko, B. M.; Fox, J.; Duesler, E. N.; Paine, R. T. *Inorg. Chem.* **2004**, *43*, 2443-2448.

⁸⁴ The downfield shift of the H-6eq (δ 3.07) and the upfield shift at C-6 (δ 35.2) agree with a steric crowding of the pyridyl ring upon H-6eq associated with the *E* configuration of the exocyclic double bond. For comparison of NMR data in a related system, see ref 32.

Hydrogenation of vinylpyridine **9** using Wilkinson's catalyst allowed the hydrogen to be delivered exclusively from the bottom face. Thus, a pyridine-directed hydrogenation provided access to the valuable intermediate **10** with a contra-steric selectivity (Figure 5.2).

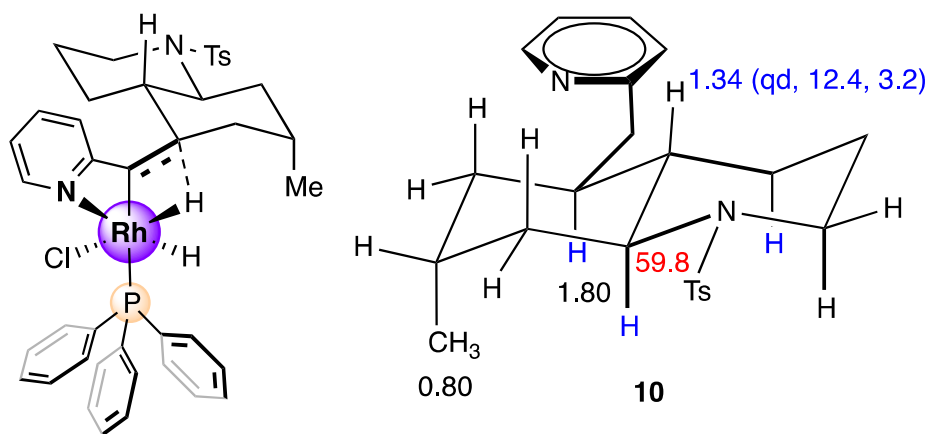


Figure 5.2 Transition state leading to **10** and its representative NMR data

The stereoselectively formed decahydroquinoline **10** showed the same relative configuration in its four stereogenic centers as the target **1** and serralongamine A (**2**). The configuration at C-5 was ascertained considering the multiplicity of the signal corresponding to H-4a, which implies a *trans* relationship between H-4a and H-5, both in an axial disposition. Moreover, the chemical shift for C-8a (δ 59.8) did not differ from that observed in the precursors **7** (δ 60.3) and **9** (δ 60.6), indicating that the pyridylmethyl side chain is not axially located (Figure 5.2).⁸⁵

Removal of the tosyl group in **10** using LiAlH₄ followed by reductive *N*-methylation of **11** gave serralongamine A (**2**) in 76% yield for the two steps, which constitutes the first synthetic entry to a phlegmarine alkaloid embodying its decahydroquinoline stereoparent. The *trans*-decahydroquinoline serralongamine A differs from phlegmarine itself in the stereochemical relationship between the configuration at C-7 and the *trans* ring fusion carbons, C-4a and C-8a (see chapter 1, p 5, Figure 1.2).

⁸⁵ For the influence of the steric compression effect on NMR chemical shifts, see: (a) Katakawa, K.; Kitajima, M.; Yamaguchi, K.; Takayama, H. *Heterocycles* **2006**, 69, 223-229. (b) Kolocouris, A. *Tetrahedron Lett.* **2007**, 48, 2117-2122.

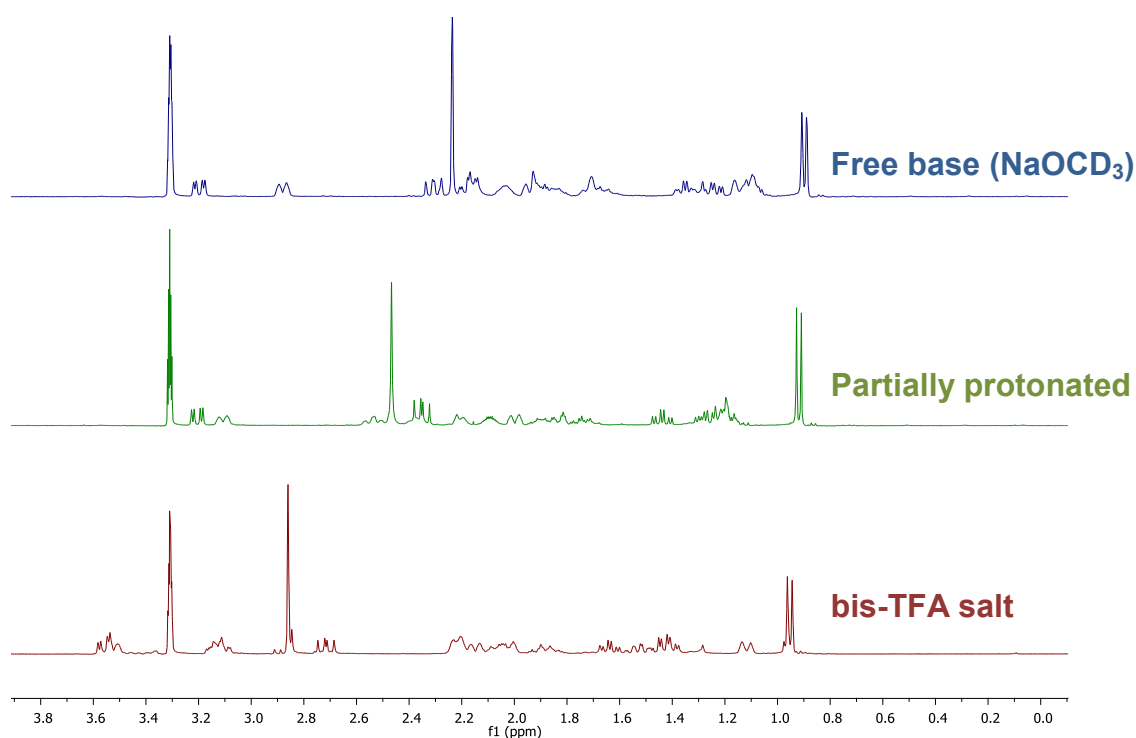
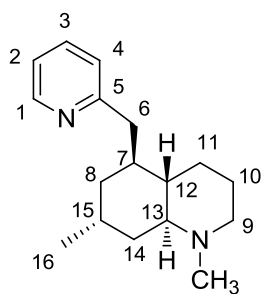


Figure 5.3 ^1H NMR spectra of synthetic serralongamine A (**2**) in $\text{CD}_3\text{OD}/\text{NaOCD}_3$ before and after addition of trifluoroacetic acid

It is noteworthy that the NMR data of our synthetic **2** were clearly different from those reported for the isolated serralongamine A in CD_3OD . Since basic nitrogen atoms readily protonate, we were able to reproducibly obtain ^1H and ^{13}C NMR spectra of the free base forms of serralongamine A in CD_3OD containing NaOCD_3 .⁸⁶ We surmised that the natural isolate corresponded to its ditrifluoroacetate salt. Thus, the NMR spectra of synthetic serralongamine A was examined by titrating a sample of the free base with TFA. For a comparison of NMR data for natural and synthetic serralongamine A (**2**) as the double TFA salt, see Table 5.1. As reproduced in Figure 5.3, NMR spectra identical to those reported for the natural product were obtained.

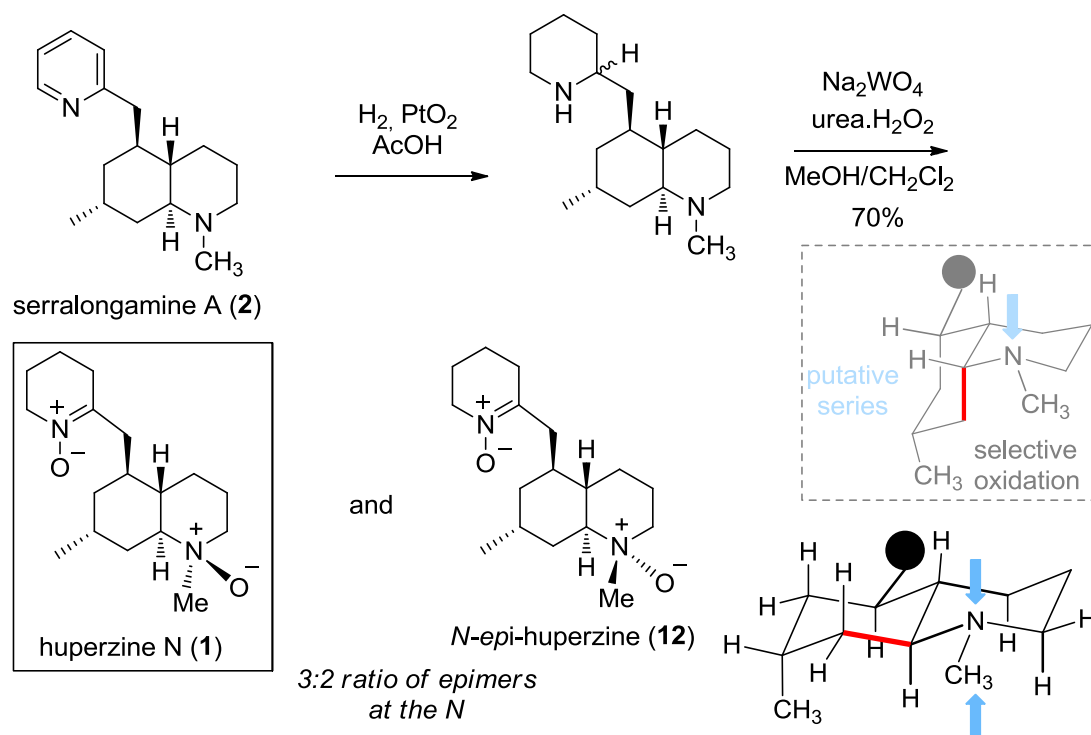
⁸⁶ For a similar NMR protocol to measure the free base and its TFA salt spectra in alkaloid synthesis, see: (a) Altman, R. A.; Nilsson, B. L.; Overman, L. E.; Read de Alaniz, J.; Rohde, J. M.; Taupin, V. *J. Org. Chem.* **2010**, *75*, 7519-7534. (b) Lee, A. S.; Liao, B. B.; Shair, M. D. *J. Am. Chem. Soc.* **2014**, *136*, 13442-13452.

Table 5.1 ^{13}C NMR data for serralongamine A in CD_3OD serralongamine A (**2**)

δ ^{13}C	synthetic free base (2) ¹	2 bis-TFA salt ¹	isolated serralongamine A ²
1	149.5	142.8	143.8
2	125.7	126.3	125.9
3	138.4	147.8	146.6
4	122.7	129.4	128.8
5	162.6	157.7	158.1
6	42.6	37.9	38.5
7	37.8	37.5	37.5
8	38.0	36.8	36.8
9	58.5	57.4	57.4
10	26.1	24.0	24.1
11	29.6	27.1	27.2
12	47.8	46.3	46.4
13	64.8	66.0	66.0
14	36.6	33.8	33.9
15	28.5	28.1	28.1
16	19.5	18.3	18.3
17	43.1	41.4	41.4

¹ ^{13}C NMR recorded at 100 MHz. Assignments were aided by COSY and HSQC spectra.

² Jiang, W. P.; Ishiuchi, K.; Wu, J. B.; Kitanaka, S. *Heterocycles*, **2014**, *89*, 747-752.



Scheme 5.4 First total synthesis of revised structure of huperzine N

Having achieved **2**, we were two steps from completing the new structure proposed for huperzine N (**1**). Toward this end, reduction of the pyridine ring gave the corresponding piperidine, which after oxidation with $\text{Na}_2\text{WO}_4/\text{urea}\cdot\text{H}_2\text{O}_2$ (UHP)⁸⁷ led to **1** by formation of both the amine *N*-oxide and nitron functionalities, which were further confirmed by ^{15}N chemical shift NMR data. The spectroscopic data of the synthetic sample were identical in all respects to those reported for the natural product,⁹ although a side product purified together with huperzine N was also formed. Two-dimensional NMR spectroscopy of the mixture identified the minor product as the *N*-oxide epimer of huperzine N. Although the oxidation of cyclic tertiary amines normally takes place axially,⁸⁸ the presence of an equatorial substituent increases the equatorial oxidation,⁸⁹

⁸⁷ Ohtake, H.; Imada, Y.; Murahashi, S. *Bull. Chem. Soc. Jpn.* **1999**, *72*, 2737-2754.

⁸⁸ Shvo, Y.; Kaufman, E. D. *J. Org. Chem.* **1981**, *46*, 2148-2152.

⁸⁹ Kawazoe, Y.; Tsuda, M. *Chem. Pharm. Bull.* **1967**, *15*, 1405-1410.

as occurred in our substrate (C8-C8a bond). Thus, the reaction did not work diastereoselectively and epimeric *N*-oxide **12** was also formed.

The stereostructure and the complete ^1H , ^{13}C , and ^{15}N chemical shifts assignment of both epimers **1** and **12** (Figure 5.5) and also their protonated forms⁹⁰ (see the Supporting Information for details) were performed from the analysis of COSY, ROESY,⁹¹ HSQC, HMBC, and TOCSY correlation spectra of the mixture.

The configuration of the new stereogenic center at the nitrogen atom in huperzine N was corroborated as *R*, on the basis of ^1H and ^{13}C chemical shift NMR analysis of **1** and its *N*-epimer **12**. Thus, a clear upfield shift for C-3, C-4a and C-8 was observed, due to the 1,3-*cis* relationship between the N→O bond and the axial C-H bond of these carbon atoms (see Figure 5.5), compared with either the free amine base nucleus (e.g. in **2**) or the *N*-epimeric *N*-oxide with the oxygen atom in an equatorial disposition (i.e. **12**).⁹² The NMR data of synthetic huperzine N matched those described for the natural product, thus establishing its configuration as 1*R*,4*aS*,5*S*,7*R*,8*aS*. Although we have reported the racemic form, the phlegmarine alkaloids have always shown an *R* absolute configuration in the carbon bonded to the methyl group in the

⁹⁰ In **1** and **12**, the protonation of the *N*-oxide function leads to a deshielding of the α -hydrogens (see supporting information). It should be noted that the protons in a 1,3-diaxial relationship with the *N*-oxide function are not affected or even slightly shielded upon protonation (e.g., H-10, H-12, and H-14 in huperzine N). For NMR studies in this field, see: Lebrun, B.; Braekman, J. C.; Daloz, D. *Magn. Reson. Chem.* **1999**, *37*, 60-64.

⁹¹ When huperzine N was originally isolated (ref 9), NOE correlations were established between the putative H-12 proton and signals at N-Me and H-13. However, according to our ROESY NMR spectrum of **1**, which allowed the revised *trans* configuration to be established, these cross-peaks were due to H-14eq. This error is attributed to the ^1H chemical shift degeneracy between H-12 and H-14eq in **1**. This observation is fully confirmed by the NOE contacts observed in the related epimer (**12**) (see Figure 5.4) and protonated *N*-oxide (see supporting information Figure S2) derivatives, as well as of the characteristic multiplet *J* pattern of H-12 and H-13.

⁹² For NMR studies in *N*-oxide piperidine compounds, see: (a) Potmischil, F.; Cimpeanu, V.; Herzog, H.; Buddrus, J.; Duddeck, H. *Magn. Reson. Chem.* **2003**, *41*, 554-556. (b) Budesinsky, M.; Vanek, V.; Dracinsky, M.; Pohl, R.; Postova-Slavetinska, L.; Sychrovsky, V.; Picha, J.; Cisarova, I. *Tetrahedron* **2014**, *70*, 3871-3886.

decahydroquinoline ring. Thus, the relative configuration allowed the absolute configuration to be proposed

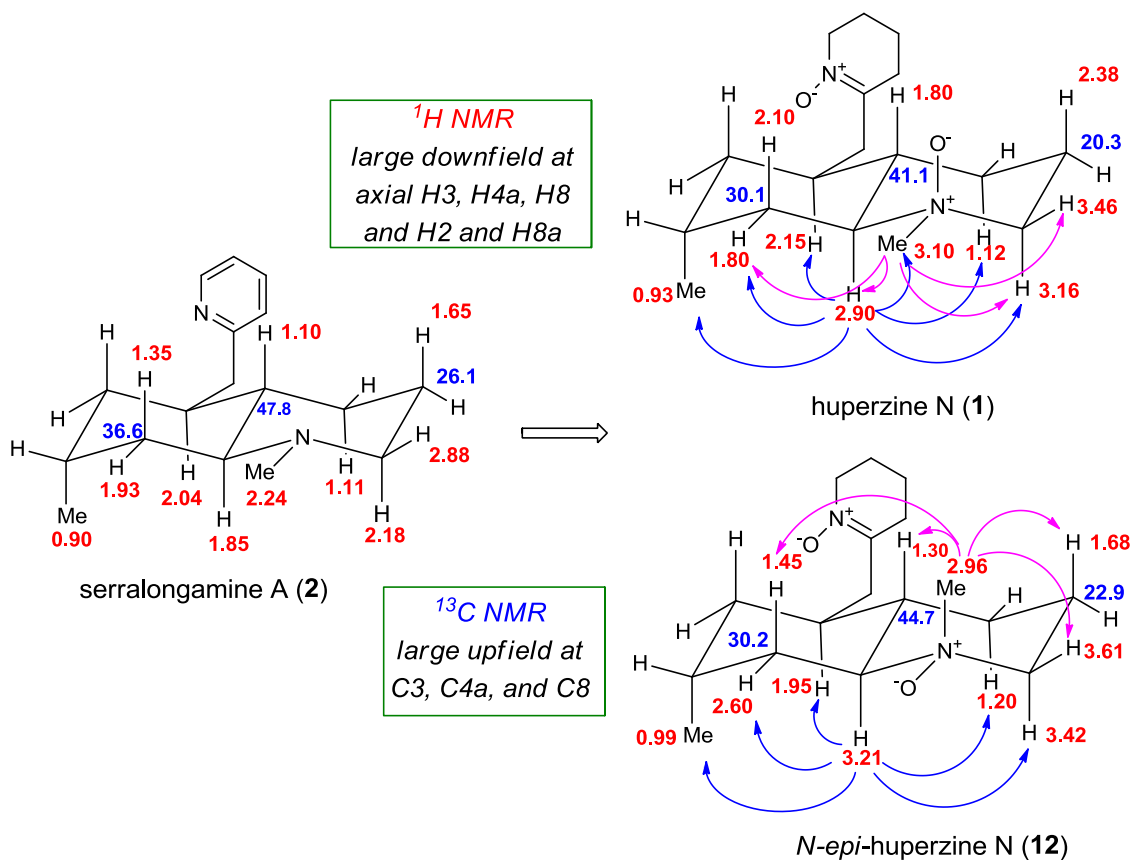


Figure 5.5 NMR of serralongamine A, Huperzine N and its epimer

In summary, in this work on the phlegmarine subset of *Lycopodium* alkaloids, the first total synthesis of serralongamine A and the revised structure of huperzine N have been accomplished. The absolute configuration of huperzine N was established and the NMR data of the serralongamine A in its free base form are reported for the first time.

**6. Decahydroquinoline Ring NMR Patterns for the
Stereochemical Elucidation of Phlegmarine
Alkaloids: Synthesis of (-)-Serralongamine A and the
Revised Structures of (-)-Huperzine K and
(-)-Huperzine M**

Manuscript in preparation

Considering the erroneous structure assigned to huperzine N, we decided to examine in more details the NMR data of all phlegmarines to find if there are other missassigned alkaloids in the literature. All NMR data available for phlegmarines are listed in Tables 6.1 and 6.2, according to the structural types used in this chapter.

As presented in the introduction the C7-Me always presents the same configuration for biogenetic reasons. Thus all phlegmarine alkaloids can be divided into four groups according the relationship of the hydrogens of the decahydroquinolines ring fusion with the methyl group, two *cis*-fused (types A and B) and the other two *trans* (types C and D). In each type two subunits can be found depending on the configuration at C-5. Thus, a letter (α or β) is added: when the two substituents of the carbocyclic ring (at C-5 and C-7) are *cis* (α) and when they are *trans* (β). Figure 6.1 summarizes this type of notation, which helps to clarify the stereochemical patterns of the NMR data to facilitate the prediction of the configuration of any phlegmarine alkaloid.

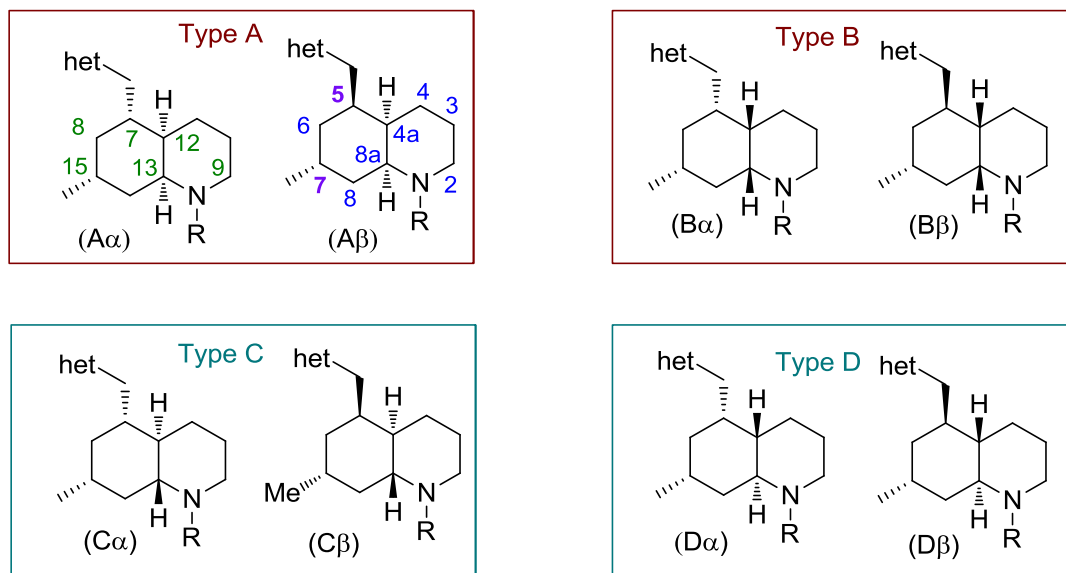


Figure 6.1 Stereoparents for decahydroquinoline rings in phlegmarine alkaloids

6.1 Decahydroquinoline Ring NMR Patterns for the Stereochemical Elucidation of Phlegmarine Alkaloids

Due to the stereochemical diversity of phlegmarine alkaloids, structure elucidation of those kind of compounds mainly focus in a first part in the stereochemical pattern present in the decahydroquinoline core structure and in a second part in the relative position of the substituents on this ring.

In order to shed light on the structural elucidation of those compound the basis point was first to look at the unsubstituted decahydroquinoline ring system. As presented in Figure 6.2 the *cis*-decahydroquinoline found in some phlegmarine alkaloids (Type A and B) can be conformationally mobile. At low temperature two conformers presenting different ^{13}C NMR data have been characterized.⁹³ What we observe is that for the *N-endo* compounds C4a-C5 and N-C8a bonds induce upfield shifts through diaxial interactions respectively at C-3 and C-5, C-7. For the *N-exo* compounds C8-C8a and C4-C4a respectively induce upfield shifts at C-2, C-4 and C-6, C-8 positions (see Figure 6.2).

In natural and synthetic compounds, both conformations of the *cis* can be found depending on the substitution pattern on the decahydroquinoline ring system, this conformation being fixed for a defined compound.

On the other hand, the *trans*-decahydroquinoline (found in Type C and D) present a rigid conformation with only one conformer possible, whose characteristic NMR signal present notably a clear difference from *cis*-systems at the ring junction carbons.

⁹³ Spande, T. F.; Jain, P.; Garraffo, H. M.; Pannell, L. K.; Yeh, H. J. C.; Daly, J. W.; Fukumoto, S.; Imamura, K.; Tokuyama, T.; Torres, J. A.; Snelling, R. R.; Jones, T. H. *J. Nat. Prod.* **1999**, *62*, 5-21.

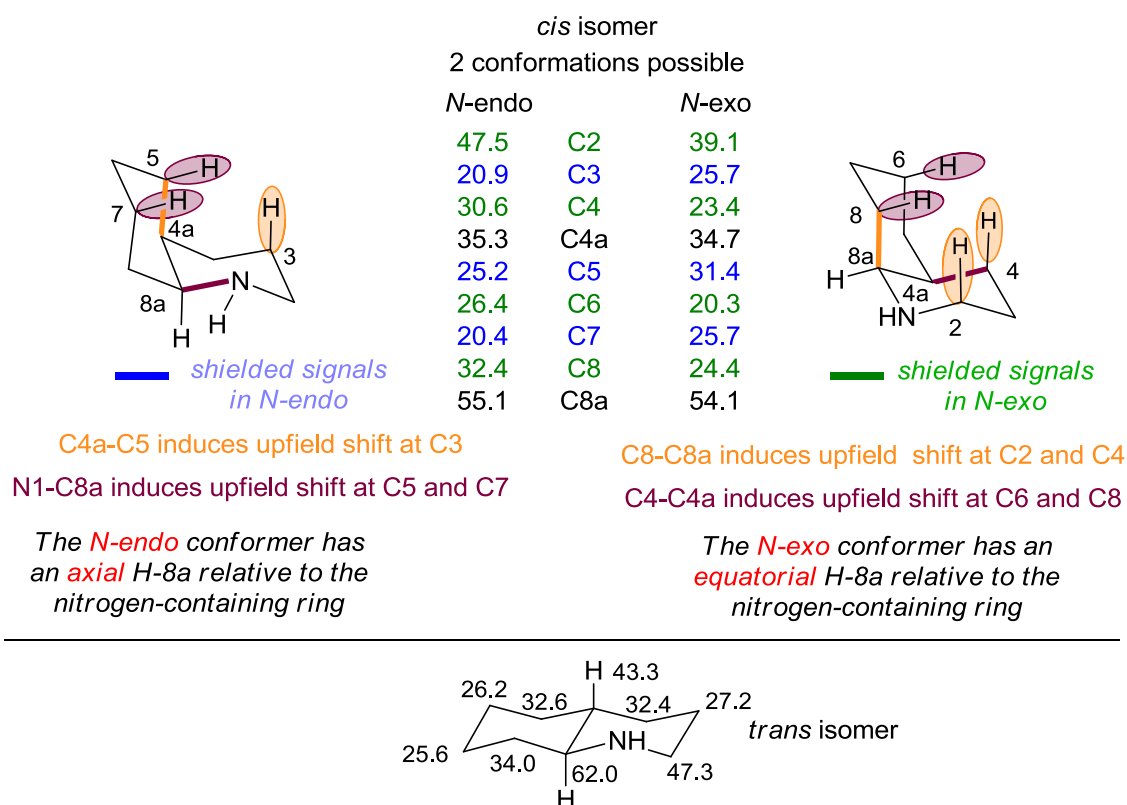


Figure 6.2 Different conformations in the decahydroquinoline system

All NMR spectroscopic data available for the isolated phlegmarine alkaloids have been analyzed and are reported in the next pages. Taking as the base structures supported by X-ray and/or total synthesis in the phlegmarine field, we propose a NMR pattern of the decahydroquinoline core to elucidate the stereostructure of phlegmarine alkaloids. On the basis of the available data information, the structure of some alkaloids should be revised. The corresponding reassigned stereostructures will be verified by total synthesis (see *section 6.2*).

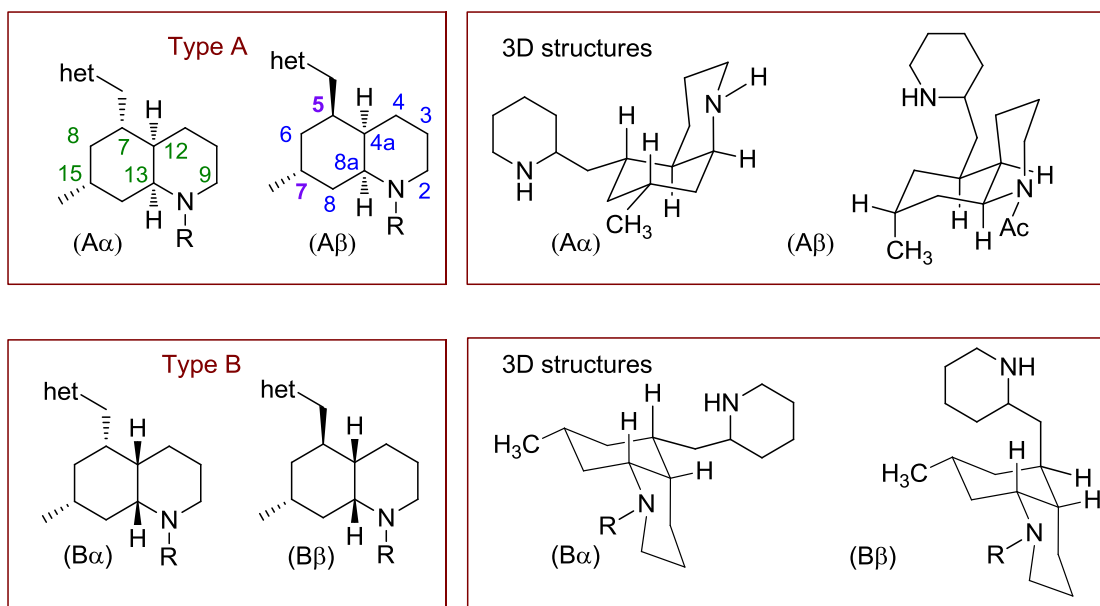
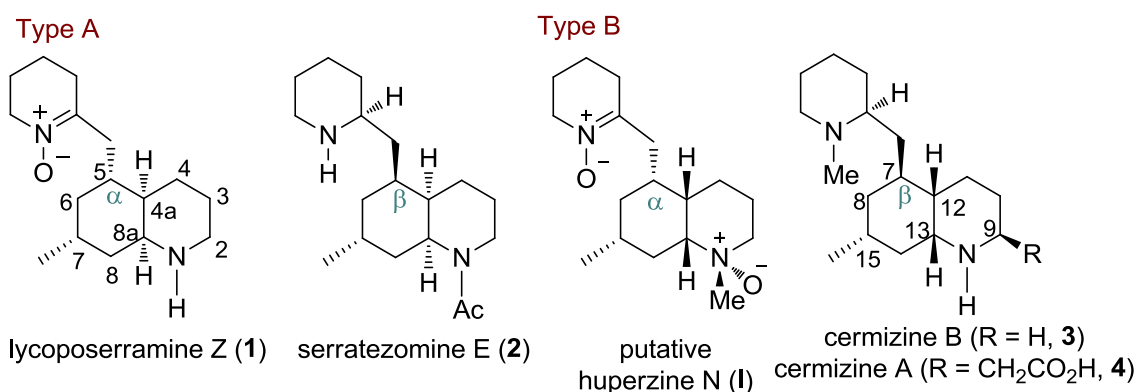


Figure 6.3 Stereoparents for *cis*-phlegmarines (Type A and Type B)
Biogenetic (left) and systematic (right) numbering are indicated in Type A drawing

In Figure 6.3 are represented the preferred conformation of the *cis*-phlegmarine alkaloids. Some synthetic compounds, intermediate in total syntheses, show a different conformation induced by a different *N*-substituent type in the decahydroquinoline ring.

In Table 6.1 are summarized the decahydroquinoline core NMR data assignment for each *cis*-phlegmarine natural product. It should be noted that when a total synthesis has already been achieved, the data of the synthetic compound are reported. On the other hand, when no total synthesis of the natural product was reported, the NMR data of the isolated product is given (same method was used for Table 6.2).

We can observe that each stereoisomer present defined signals that allows to differentiate it from the other compounds. For example, for type A α lycoposerramine Z an upfield shield at C-3 and C-5 signals is induced by the *N-endo* specific conformation only observed in this natural product. For type A β serratezomine E, the presence of rotamers complicates the data but strong upfield shift at C-2, C-4 and C-8 is characteristic of this subtype of compounds.

Table 6.1 ^{13}C NMR data of *cis*-phlegmarines

compd	1 ⁹⁴	2 ⁹⁵	I ⁹⁶	3 ⁹⁷	4 ⁹⁸	biogenetic numbering
type	A α	A β	B α	B β	B β	
C-2	47.1	41.8/36.4	61.0	40.4	49.6	9
C-3	20.0	26.0/25.0	20.2	27.0	39.6	10
C-4	26.2	17.5/17.5	16.2	26.2	25.2	11
C-4a	40.4	38.5/39.7	33.4	41.6	39.7	12
C-5	29.8	29.5	36.8	38.4	37.6	7
C-6	41.0	32.8/32.5	34.8	33.7	33.2	8
C-7	26.5	27.3/27.7	31.8	28.0	27.6	15
Me	22.5	22.1/21.3	22.2	22.9	22.6	16
C-8	40.4	27.6/29.6	31.8	34.2	32.9	14
C-8a	56.6	46.3/52.1	76.8	52.0	52.8	13

For type B α compound, only present in a synthetic structure, the *N*-oxide add complexity to the NMR pattern but strong upfield shift at C-4 and downfield shift at C-5 can be found as characteristic values. Finally for type B β compounds we observe a downfield shift at C-3 and C-5 compared to the others compounds.

⁹⁴ (a) Isolation: Katakawa, K.; Kitajima, M.; Yamaguchi, K.; Takayama, H. *Heterocycles* **2006**, *69*, 223-229. (b) Synthesis: Bradshaw, B.; Luque-Corredera, C.; Bonjoch, J. *Org. Lett.* **2013**, *15*, 326-329.

⁹⁵ (a) Isolation: Kubota, T.; Yahata, H.; Yamamoto, S.; Hayashi, S.; Shibata, T.; Kobayashi, J. *Bioorg. Med. Chem. Lett.* **2009**, *19*, 3577-3580. (b) Synthesis: Bosch, C.; Fiser, B.; Gómez-Bengoia, E.; Bradshaw, B.; Bonjoch, J. *Org. Lett.* **2015**, *17*, 5084-5087.

⁹⁶ Synthesis: see ref 95b.

⁹⁷ (a) Isolation: Morita, H.; Hirasawa, Y.; Shinzato, T.; Kobayashi, J. *Tetrahedron* **2004**, *60*, 7015-7023. (b) Synthesis: Bradshaw, B.; Luque-Corredera, C.; Bonjoch, J. *Chem. Commun.* **2014**, *50*, 7099-7102.

⁹⁸ Isolation: see ref 97a.

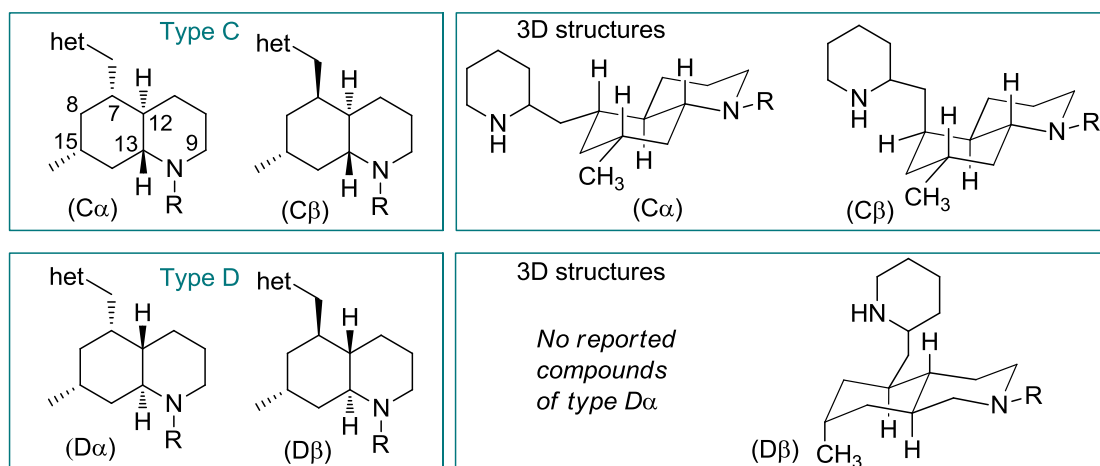


Figure 6.4 Stereoparents for *trans*-phlegmarines (Type C and Type D)

After the total synthesis of huperzine N (see chapter 5) it was evident that huperzine M (**12**), isolated and reported in the same paper as huperzine N,⁹⁹ should have a *trans*-configuration in the decahydroquinoline ring fusion, considering the close correlation with its *N*-oxide analog (huperzine N, **13**) and the reassigned structure for it.

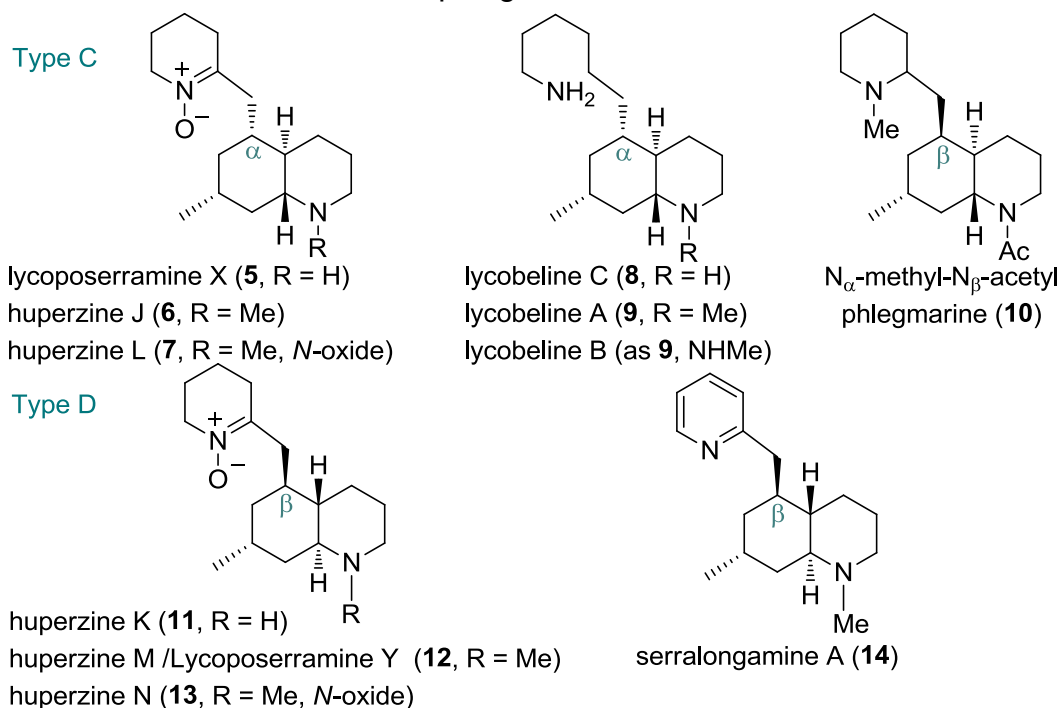
Moreover, it was clear that lycoposerramine Y¹⁰⁰ was also missassigned, since its NMR data were identical to those reported for huperzine M (**12**). We also disclose that the structure of huperzine K (**11**), a secondary amine, whose stereochemistry was first unknown in the isolation paper,¹⁰¹ and then assigned as the same stereochemistry as lycoposerramine Y (its *N*-methyl analog, **12**) due to the strong similarities in the NMR pattern of both isolated molecules,¹⁰⁰ and the observed correlation between *N*-methyl oxide, *N*-methyl and *N*-H,¹⁰² is also missassigned. According to ¹³C NMR data, those compounds should belong to type D class of phlegmarine alkaloids, as depicted in Table 6.2.

⁹⁹ Gao, W. Y.; Li, Y. M.; Jiang, S. H.; Zhu, D. Y. *Helv. Chim. Acta*, **2008**, *91*, 1031-1035.

¹⁰⁰ Katakawa, K.; Kitajima, M.; Yamaguchi, K.; Takayama, H. *Heterocycles*, **2006**, *69*, 223-229.

¹⁰¹ Gao, W. Y.; Li, Y. M.; Jiang, S. H.; Zhu, D. Y. *Planta Med.* **2000**, *66*, 664-667.

¹⁰² A clear upfield shift for C-3, C-4a and C-8 is observed in **13**, due to the 1,3-*cis* relationship between the *N*→O bond and the axial C-H bond of these carbon atoms, compared with the free amine base nucleus (e.g. in **11**) or the *N*-Me compound (i.e. **12**) (see ref. 92, Chapter 5)

Table 6.2 ^{13}C NMR data of *trans*-phlegmarines

compd	5 ¹⁰³	6 ¹⁰⁴	7 ¹⁰⁴	8 ¹⁰⁵	9 ¹⁰⁵	10 ¹⁰⁶	11 ¹⁰⁷	12 ¹⁰⁸	13 ¹⁰⁸	14 ¹⁰⁹
type	C α	C α	C α	C α	C α	C β	D β	D β	D β	D β
C-2	47.2	57.5	68.7	47.3	58.5	37.9	46.4	57.5	69.0	58.5
C-3	27.1	25.3	20.0	27.1	26.1	23.1	26.5	25.1	20.1	26.1
C-4	29.3	28.4	27.0	29.4	29.5	25.9	28.1	28.3	27.0	29.6
C-4a	47.9	46.1	40.0	46.7	45.8	41.5	48.0	46.7	40.8	47.8
C-5	39.2	37.6	36.9	41.9	42.1	35.4	32.7	32.8	32.3	37.8
C-6	42.4	40.6	35.6	41.8	41.4	38.7	38.6	35.4	36.6	38.0
C-7	32.0	30.5	30.1	32.2	32.1	26.8	27.2	27.1	26.8	28.5
Me	22.7	22.6	22.4	22.9	23.2	22.5	18.9	19.3	19.0	19.5
C-8	41.9	38.7	32.6	42.7	39.7	39.7	38.8	37.5	30.0	36.6
C-8a	61.6	68.0	77.0	62.1	69.9	54.7	55.7	63.3	73.4	64.8

¹⁰³ (a) Isolation: Takayama and co-workers *Heterocycles* **2006**, 69, 223-229. (Carinatumin C *Bioorg. Med. Chem.* **2007**, 15, 1703-1707 present the same structure, partially protonated average difference in NMR signals 0.3 ppm). (b) Synthesis: Takayama and co-workers *J. Org. Chem.* **2009**, 74, 8675-8680.

¹⁰⁴ (a) Isolation: Zhu and co-workers, *Planta Med.* **2000**, 66, 664-667.

¹⁰⁵ (a) Isolation: Morita and co-workers *Tetrahedron Lett.* **2012**, 53, 3971-3973.

¹⁰⁶ (a) Isolation: Braekman and co-workers *Can. J. Chem.* **1978**, 56, 851-856. (b) Synthesis: MacLean and co-workers *Can. J. Chem.* **1981**, 59, 2695-2702 and Comins, and co-workers *J. Org. Chem.* **2010**, 75, 8564-8570. In the latter publication phlegmarine was synthesized along with all the type C β phlegmarines (for ^{13}C NMR structure attribution of each compound see Figure 6.8).

¹⁰⁷ (a) Isolation: see ref 104a and ref 103a.

¹⁰⁸ (a) Isolation: Huperzine M and N: Zhu and co-workers *Helv. Chim. Acta* **2008**, 91, 1031-1035 and lycoposerramine Y: see ref 103a reassigned as the same compound.

¹⁰⁹ (a) Isolation: Kitanaka and co-workers *Heterocycles* **2014**, 89, 747-752. (b) Synthesis: Bonjoch and co-workers *J. Org. Chem.* **2016**, 81, 2629-2634.

The NMR characteristic data for each representative stereoparent of decahydroquinoline framework (NH series) are presented in Figure 6.5, Figure 6.6 and Table 6.3. For more consistency, and to avoid any influence of the nature of the C-5 substituent and N-functionalisation, NMR data of the precursors bearing pyridine substituent at C-5 and without substituent on the N atom are represented.

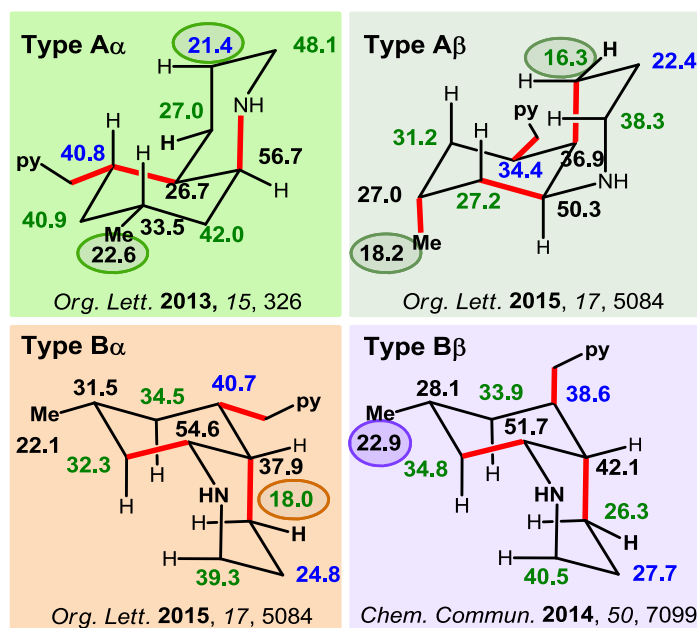


Figure 6.5 Characteristic NMR data of *cis*-phlegmarine alkaloids precursors

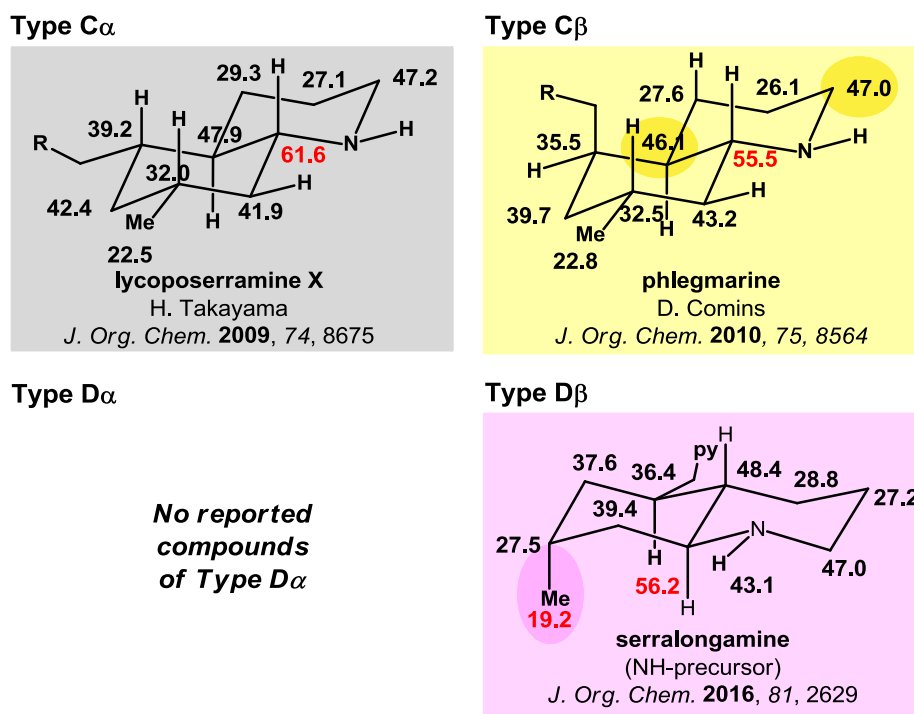


Figure 6.6 Characteristic NMR data of *trans*-phlegmarine alkaloids precursors

Table 6.3 Characteristic NMR data of all phlegmarine alkaloids

	A α	A β	B α	B β	C α	C β	D β
C-2	48.1	38.3	39.3	40.5	47.2	47.0	47.0
C-3	21.4	22.4	24.8	27.7	27.1	26.1	27.2
C-4	27.0	16.3	18.0	26.3	29.3	27.6	28.8
C-4a	26.7*	36.9	37.9	42.1	47.9	46.1	48.4
C-5	40.8	34.4	40.7	38.6	39.2	35.5	36.4
C-6	40.9	31.20	34.5	33.9	42.4	39.7	37.6
C-7	33.5*	27.0	31.5	28.1	32.0	32.5	27.5
C-8	42.0	27.2	32.3	34.8	41.9	43.2	39.4
C-8a	56.7	50.3	54.6	51.7	61.6	55.5	56.2
Me	22.6	18.2	22.1	22.9	22.5	22.8	19.2

How to predict the stereoparent for a new compound?

2 signals $\delta < 20$ ppm \rightarrow Type A β	1 signal (=Me) $\delta < 20 \rightarrow$ Type D β
1 signal (\neq Me) $\delta < 20 \rightarrow$ Type B α	1 signal (C-8a) $\delta > 60 \rightarrow$ Type C α
2 signals δ 20-23 ppm \rightarrow Type A α	1 signal δ 20-23 ppm \rightarrow Type C β
1 signal δ 20-23 ppm \rightarrow Type B β	
\neq Type B β & C β : C-2 and C-4a are shielded (\sim 40-42 ppm) in B β	

Figure 6.7 Basic Rules

By looking carefully at those data we realized that it is possible to deduce basic rules to determine the stereochemistry of a defined compound, as depicted in Figure 6.7. Of course, when applied to natural products, additional parameters (electronic and steric effects) depending on the nitrogen atom substituent should be considered.¹¹⁰

¹¹⁰ For classical ¹³C NMR studies of piperidines and decahydroquinolines (NH, N-alk, R₃N⁺H, N-COR), see: (a) Eliel, E. L.; Vierhapper, W. *J. Org. Chem.* **1976**, *41*, 199-209. (b) Vierhapper, F. W.; Eliel, E. L. *J. Org. Chem.* **1979**, *44*, 1081-1087. (c) Eliel, E. L.;

It is also noteworthy that ^1H NMR spectra of these alkaloids are, of course, important for their structure elucidation. Indeed, if an upfielded quartet signal (δ 0.7-1.0) appears, it is the diagnostic for an axial H-6. This proton has a geminal (H-6) and two *trans* relationships (H-5 and H-7). This is only possible in alkaloids of type $\text{A}\alpha$, $\text{B}\alpha$ and $\text{C}\alpha$.

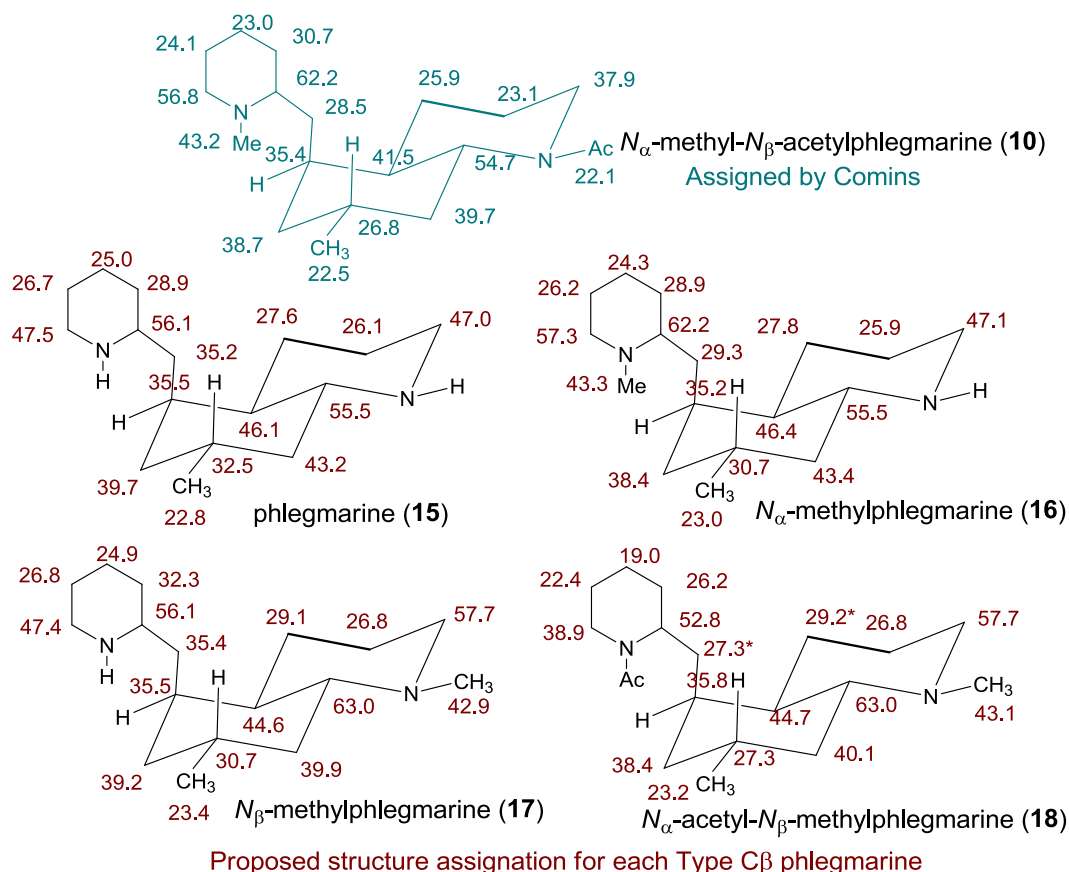


Figure 6.8 ^{13}C NMR of phlegmarine **10** and related alkaloids (**15-18**)

On the basis of the correlation of secondary and tertiary amines data with the *N*-acetyl derivatives reported in the literature, a proposal for the assignment of the ^{13}C NMR data of phlegmarines **15-18** has been carried out. This assignment was performed using the data assigned by Comins for **10** and the ^{13}C NMR non-assigned data reported by Comins in the total synthesis of phlegmarine alkaloids **15-18** (all of them of Type $\text{C}\beta$) as presented in Figure 6.8.

Kandasamy, D.; Yen, C.-Y.; Hargrave, K. D. *J. Am. Chem. Soc.* **1980**, *102*, 3698-3707.
(d) Potmischil, F.; Herzog, H.; Buddrus, J. *Monatsh. Chem.* **1999**, *130*, 691-702.

Putative structures proposed in the isolation paper

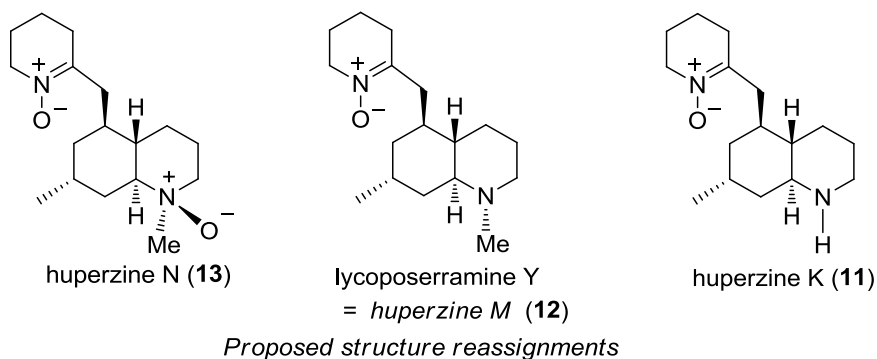
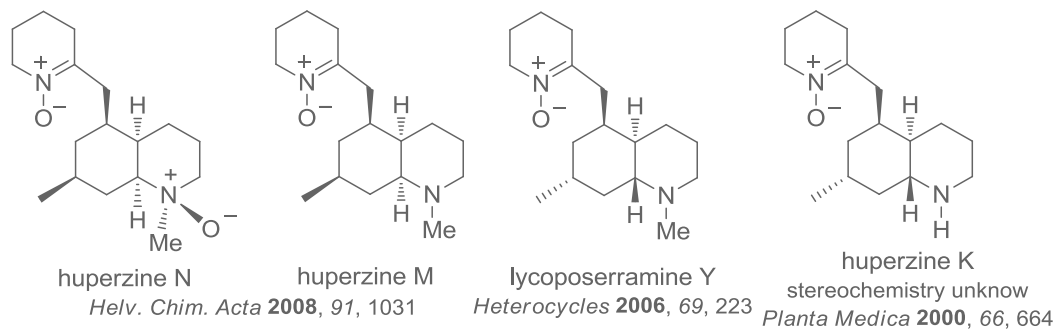


Figure 6.9 Missassigned phlegmarine alkaloids: putative and corrected structures

Structure reassignments have been proposed for the phlegmarine alkaloids depicted above. These agree with all the combined data and rules presented here. In order to prove and check the structure reassignments (Figure 6.9), we decided to perform the enantioselective total synthesis of huperzine K (**11**) and huperzine M (**12**). The synthesis of huperzine N (**13**) has been reported in Chapter 5.

6.2 Total Synthesis of Revised Structures of (-)-Huperzine K and (-)-Huperzine M

Similarly as in chapter 5, the enantiopure β -ketoester **(+)-19** was decarboxylated by treatment with trifluoroacetic acid affording ketone **(+)-20** which was then protected as the acetal **(+)-21**. Further deprotection of the tosyl protecting group followed by acidic promoted epimerization of position C-4a allowed to obtain the 2:1 epimeric mixture **(+)-23**. Tosylation of this ketone intermediate allowed to obtain **(+)-24** as a single isomer after chromatographic separation. Horner-Wadsworth-Emmons coupling of the phosphonate unit⁸³ afforded the key intermediate **(+)-25**. This compound submitted to the optimized conditions using Wilkinson's catalyst afforded compound **(+)-26** with complete diastereoselectivity.

Further deprotection of the tosyl protecting group and reductive *N*-methylation afforded the enantiopure serralongamine A **(-)-14** whose optical data corresponds to the isolated natural $\alpha_D^{25} = -17.9$ (c 0.07, CHCl₃) (Lit.¹¹¹ $\alpha_D^{20} = -16.8$ (c 0.06, CHCl₃)).

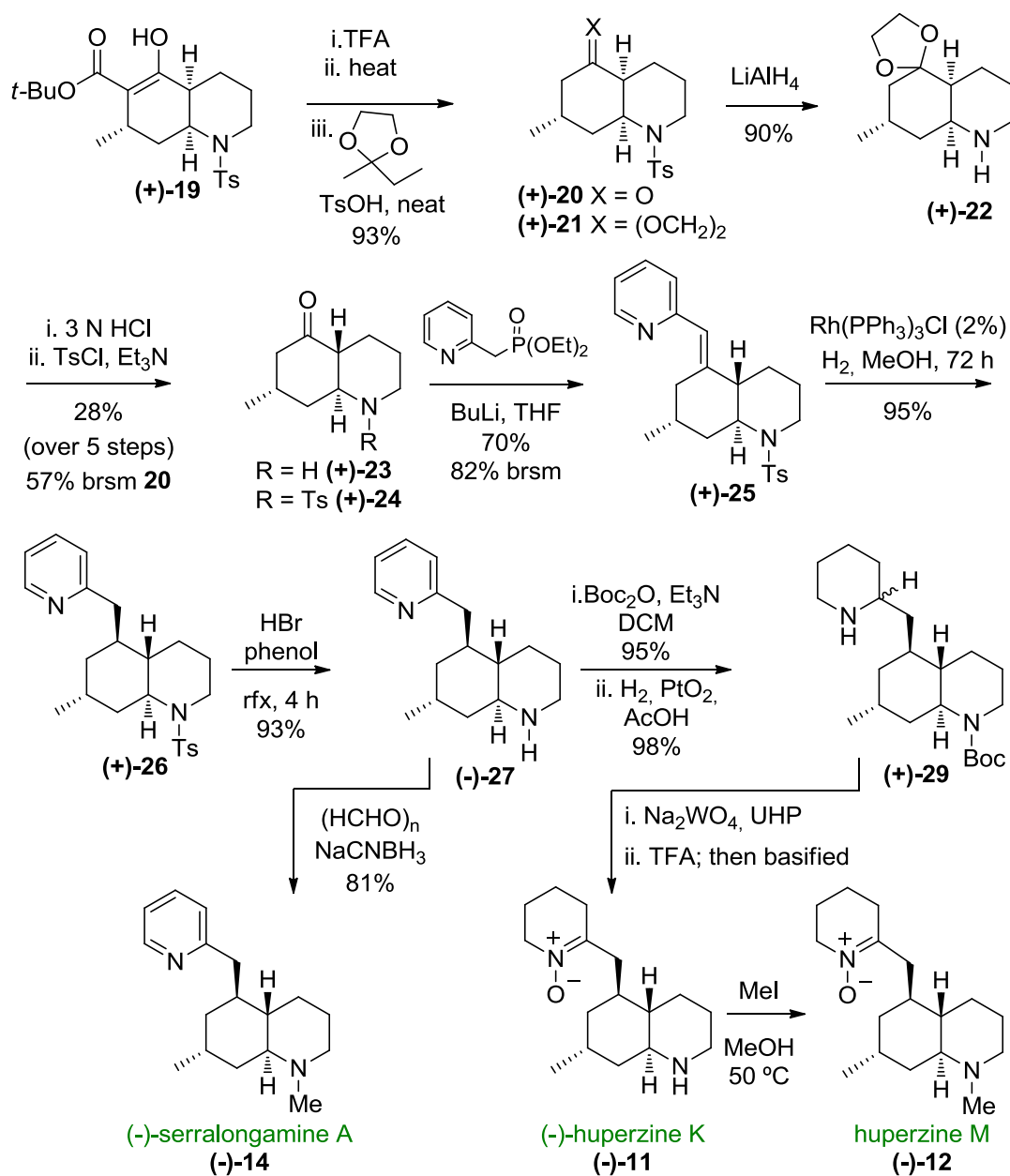
In a second part Boc protection of the secondary amine moiety of intermediate **(+)-27** and reduction of the pyridine ring compound affords compound **(+)-29**. Treatment with Na₂WO₄ / urea·H₂O₂ to form the nitron followed by trifluoroacetic acid mediated deprotection of the Boc group led to the first total synthesis of (-)-huperzine K **(-)-11**.

Unoptimized conditions to perform the *N*-methylation using methyl iodide as the methylating agent afforded huperzine M **(-)-12** (~50% conversion in an unseparable mix from huperzine K).¹¹²

It is noteworthy to mention that ¹H NMR data for huperzine K is not available,¹⁰¹ since in the original paper the data introduced corresponds

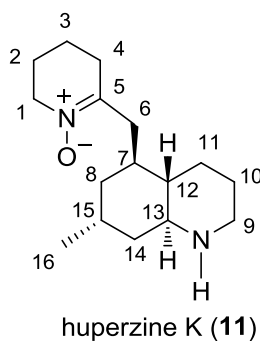
¹¹¹ Jiang, W. P.; Ishiuchi, K.; Wu, J. B.; Kitanaka, S. *Heterocycles* **2014**, *89*, 747-752

¹¹² Product was contaminated by diethyl phthalate. This product will soon be synthesized again with the leftover precursors available.



Scheme 6.1 First total synthesis of revised structure of huperzine K and huperzine M

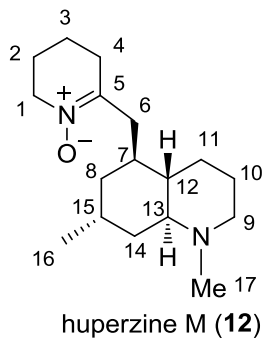
to the *N*-methyl compound and in the next paper in which a putative structure is proposed the ¹H NMR data¹⁰⁰ does not appear.

Table 6.4 ^{13}C NMR data for huperzine K in CDCl_3 

bio #	synthetic (-)- 11 ¹ partially protonated	synthetic (-)- 11 ¹ free base	isolated huperzine K ²
1	58.2	58.2	58.3
2	22.6	23.1	23.2
3	18.6	18.8	18.9
4	30.6	30.0	30.1
5	<i>n. o.</i>	148.4	148.2
6	35.0	35.2	35.2
7	32.3	32.6	32.6
8	35.0	37.5	37.8
9	44.4	45.7	46.0
10	23.0	25.3	25.6
11	26.4	27.6	27.8
12	44.5	47.0	47.2
13	56.1	55.9	56.0
14	37.0	37.7	37.8
15	26.8	27.1	27.2
16	18.1	18.8	18.9

¹ ^{13}C NMR recorded at 100 MHz. Assignments were aided by COSY and HSQC spectra.

² Katakawa, K.; Kitajima, M.; Yamaguchi, K.; Takayama, H. *Heterocycles*, **2006**, *69*, 223-229.

Table 6.5 ^{13}C NMR data for huperzine M in CDCl_3 

bio #	synthetic (-)- 12 ¹	huperzine M ²	lycoposerramine Y ³
1	58.2	58.1	58.3
2	23.1	23.1	23.3
3	18.7	18.8	19.0
4	30.2	29.9	29.9
5	148.6	148.6	148.5
6	35.7	35.6	35.8
7	32.7	32.8	33.0
8	35.3	35.4	37.7
9	57.2	57.5	57.7
10	24.6	25.1	25.4
11	28.0	28.3	28.5
12	46.2	46.7	47.0
13	63.6	63.3	63.4
14	37.3	37.5	35.7
15	27.1	27.1	27.3
16	19.2	19.3	19.5
17	42.1	42.5	42.8

¹ ^{13}C NMR recorded at 100 MHz. Assignments were aided by COSY and HSQC spectra.

² Gao, W. Y.; Li, Y. M.; Jiang, S. H.; Zhu, D. Y. *Helv. Chim. Acta*, **2008**, *91*, 1031-1035.

³ Katakawa, K.; Kitajima, M.; Yamaguchi, K.; Takayama, H. *Heterocycles*, **2006**, *69*, 223-229.

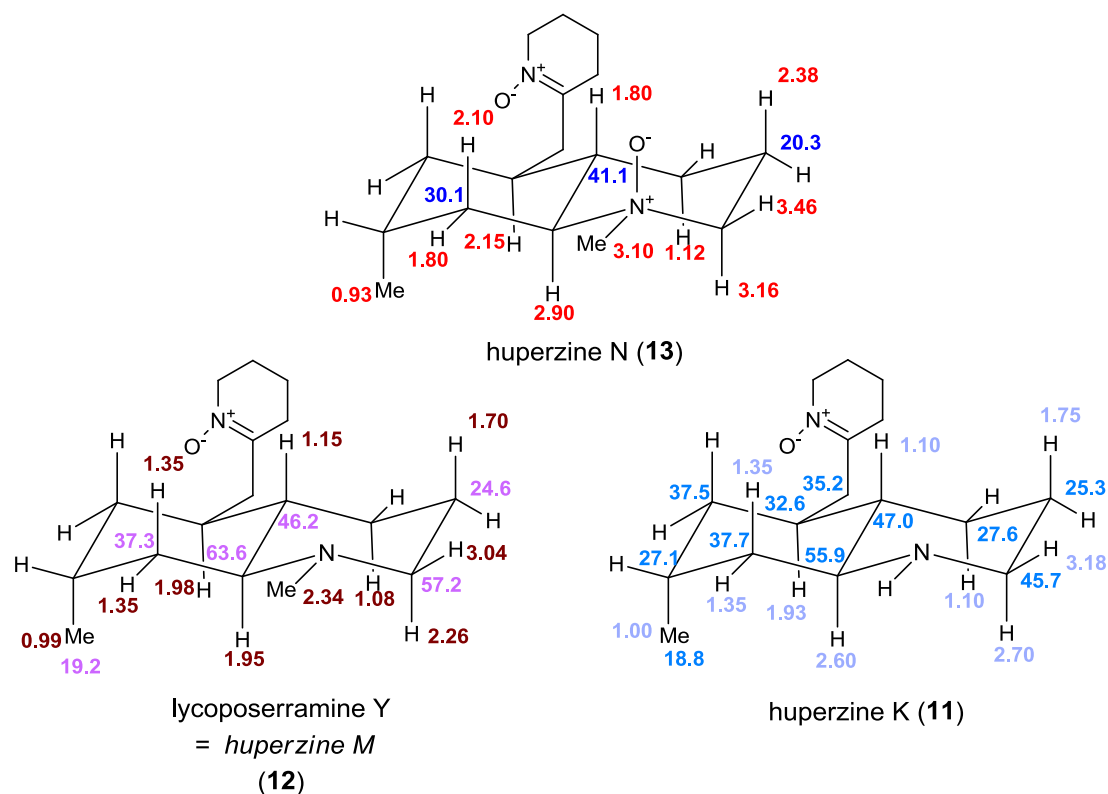


Figure 6.10 NMR based reassignment of huperzine K, huperzine M and lycoposerramine Y

In summary, in this work, the exhaustive study of NMR data of each phlegmarine alkaloid led us to the establishment of general rules to determine easily the stereochemistry of any new phlegmarine type compound. This work led to structure reassignment of several described phlegmarines alkaloids.

These reassignments were then confirmed by total synthesis using the unified methodology developed during this Ph. D. (see chapter 4). First total synthesis of (-)-serralongamine A ((-)-14), (-)-huperzine K ((-)-11) and huperzine M (11) was achieved and proved in agreement with the structural reassignment proposed.

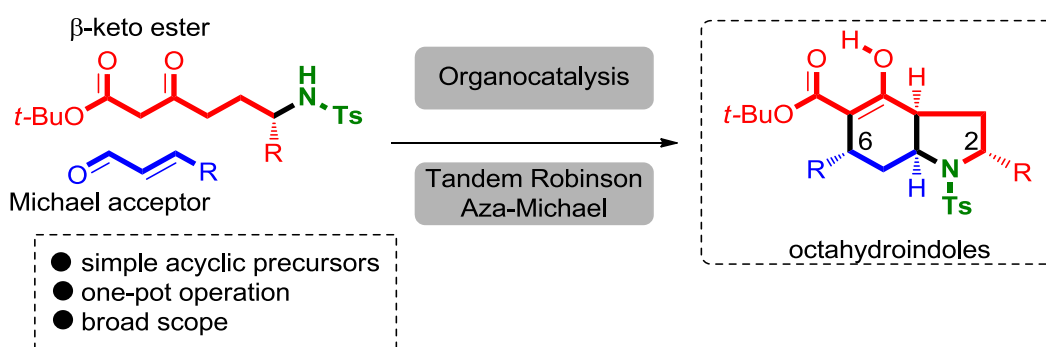
7. CONCLUSIONS

As we have seen, this doctoral thesis consists in two distinct parts. The first part focus in the study of methodology development in order to bring modularity and diversification to compounds studied within the research group. It consists in one part in the development of an easy procedure to access enantiopure substituted octahydroindoles relevant for natural products synthesis, but also in the diversification of a common building block used for the total synthesis of phlegmarine alkaloids allowing access to unprecedented heterocyclic tetrahydrocarbazoles compounds. In the second part, a more synthetic focus resulted first in the development of a methodology to allow access to any phlegmarine alkaloids from a simple common precursor *i.e.* using a unified methodology. This allowed us to perform the first total synthesis of various phlegmarine alkaloids and also shed light on missassigned structures for which reassignment was proposed and subsequently confirmed by total synthesis using our unified synthesis methodology.

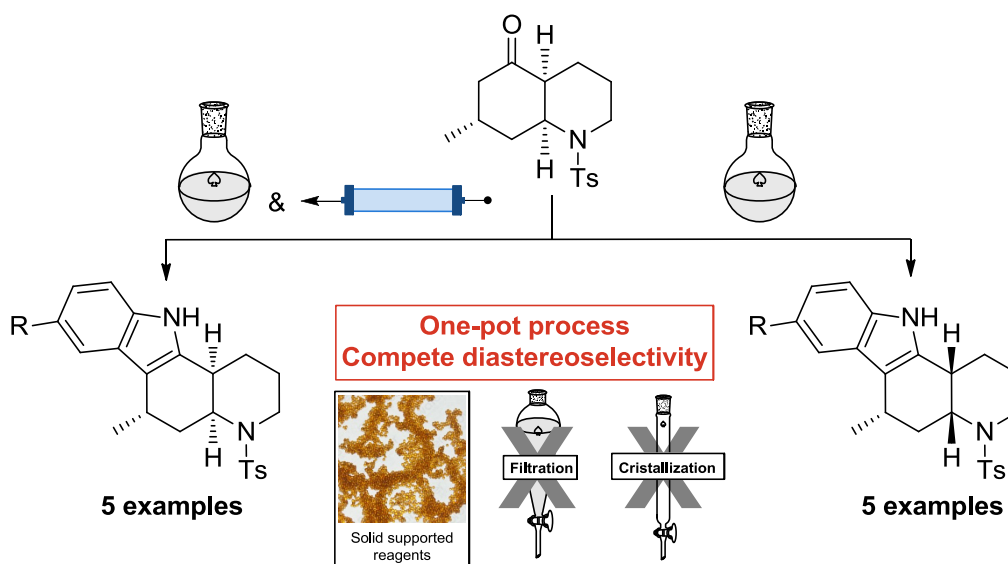
Regarding the methodological studies and based on the previously established targets we can conclude that:

- We were able to develop an efficient organocatalytic route to polyfunctionalized octahydroindoles using a one-pot / two steps sequence and solid supported reagents facilitating any manipulation. This allowed the construction of complex octahydroindoles with up to 4 stereocenters excellent enantioselectivities and complete diastereoselective control in a one-pot operation opening the way for the rapid construction of important natural product nuclei. Further application of this methodology and its use

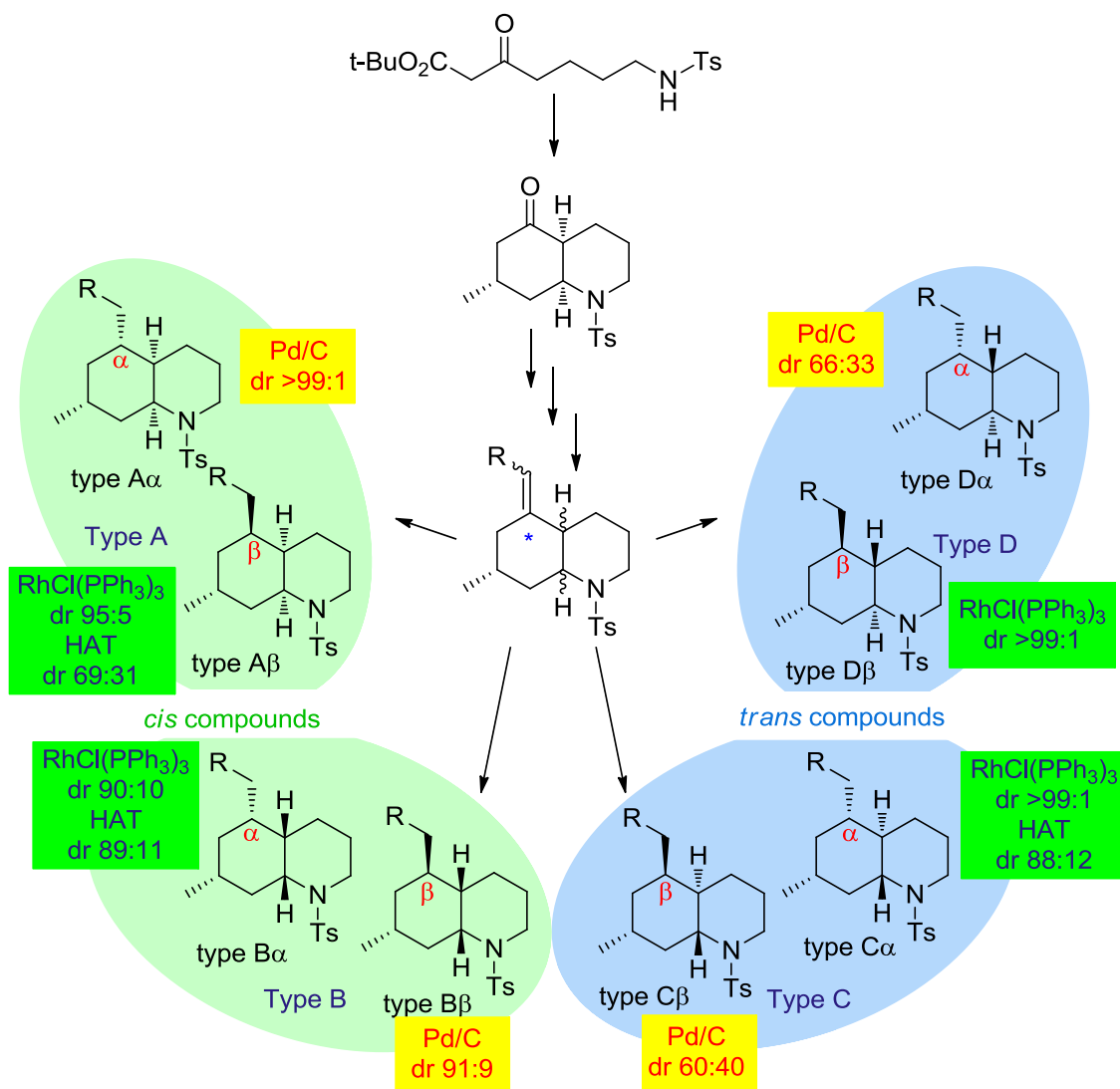
in total synthesis is currently in progress in our laboratory.



It was possible to get easy and stereoselective access to an unprecedented pyrido[2,3,*a*]carbazole scaffold presenting potential biological activity. Two different efficient batch procedures were developed allowing to access selectively the different stereoisomers in a one-pot process using supported reagents and no column chromatography needed. An alternate flow methodology was also developed in which no isomerization was observed. This work allowed us to build a small library of compounds which were then submitted for biological testing.

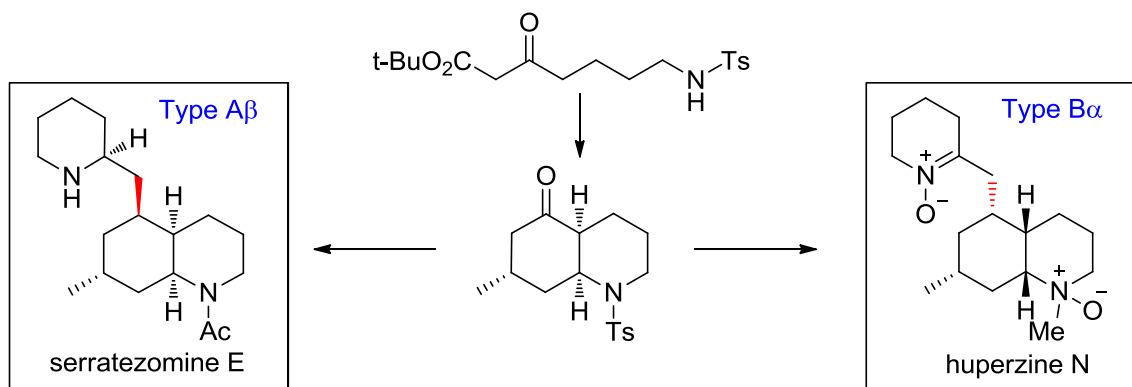


- Two stereodivergent hydrogenation protocols were developed providing access to a wide range of phlegmarine alkaloids unattainable by standard hydrogenation. This methodology allowed us to complete a unified methodology for the synthesis of phlegmarine alkaloids.

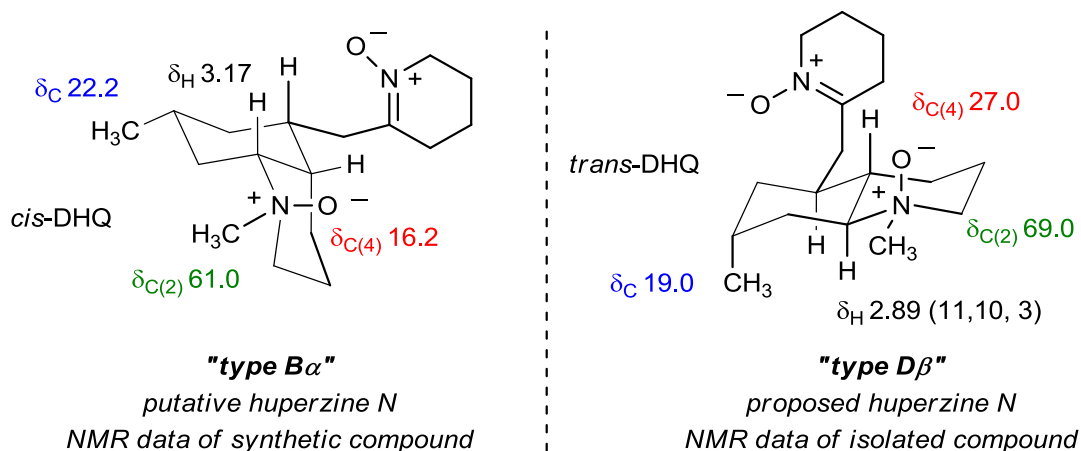


Regarding the direct application of the unified methodology to the total synthesis of natural products we can conclude that:

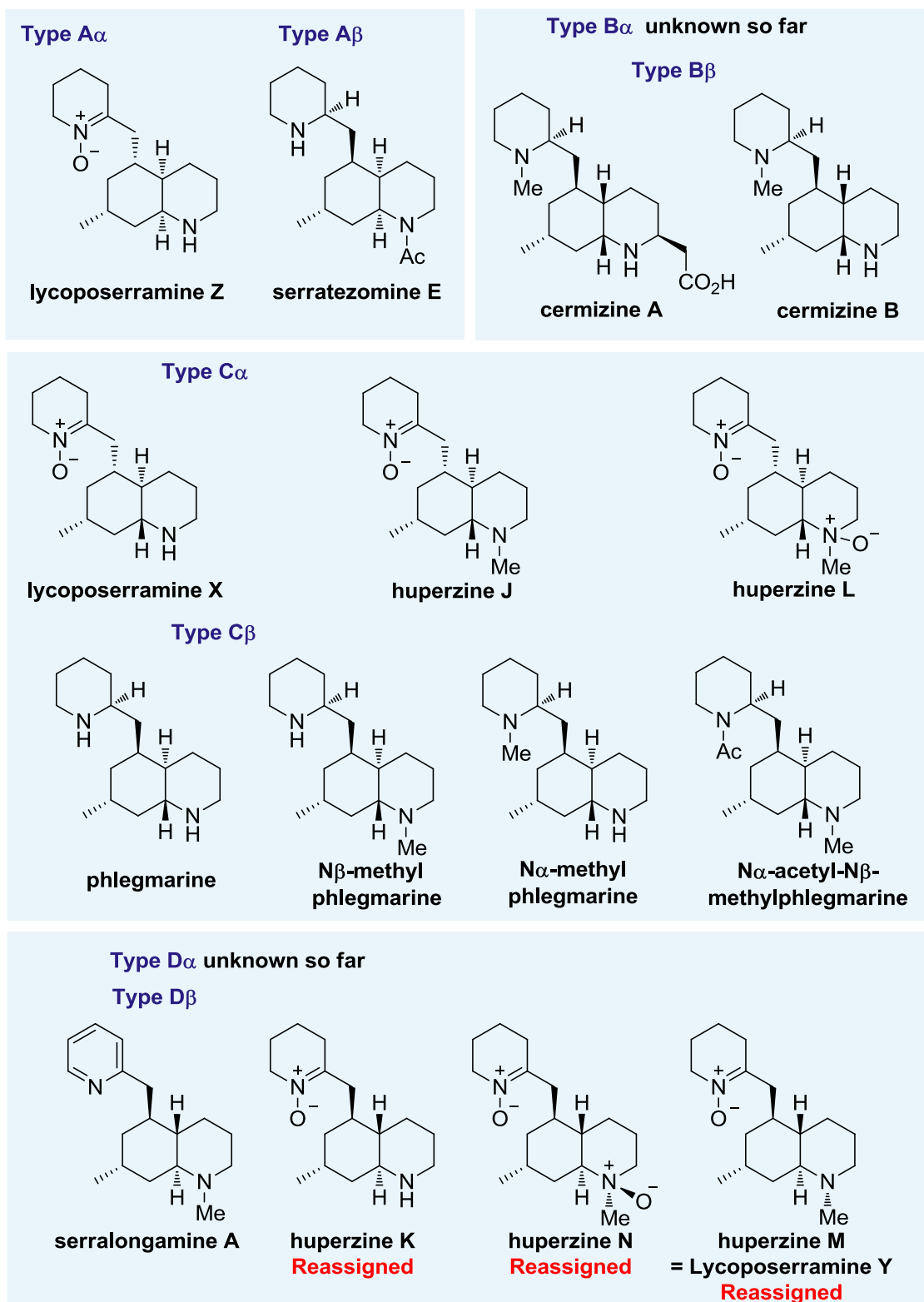
- This new methodology was successfully applied for the first total synthesis of (+)-serratezomine E as well as (-)-huperzine N:



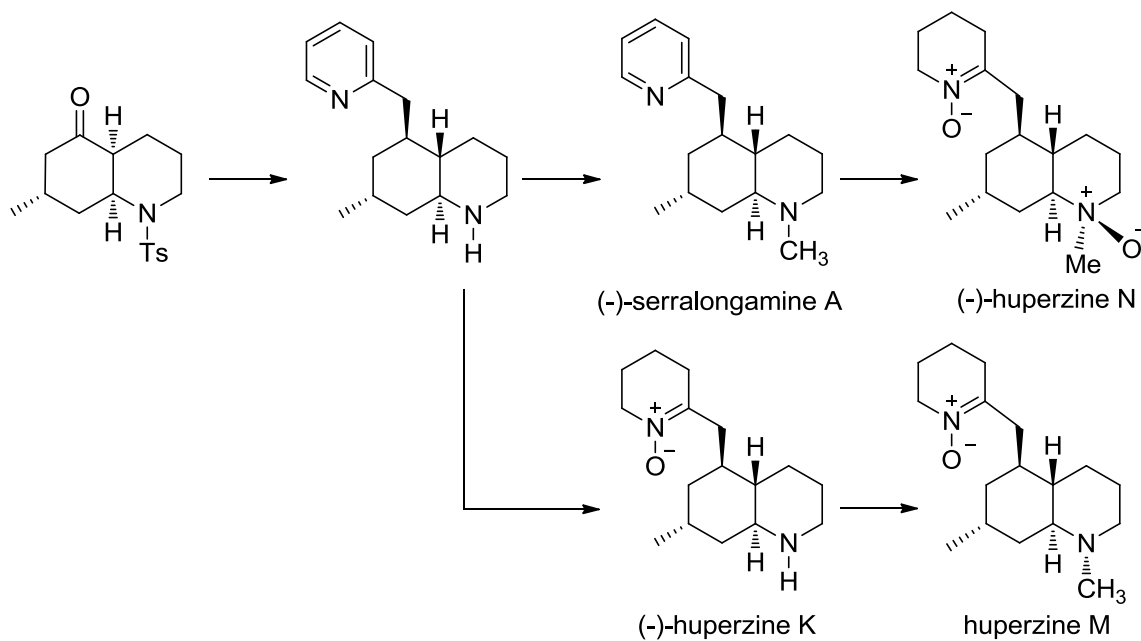
- The structure of huperzine N turned out to be a putative structure and a structure reassignment was proposed based on NMR analysis:



- This structure reassignment led us to investigate all the described phlegmarine alkaloids and shed light on missassignments for various phlegmarine alkaloids giving birth to a new Table for all the existing phlegmarine alkaloids:



- All structure reassignments were subsequently confirmed by total synthesis using the unified methodology developed, leading to first total synthesis of all those compounds:



- All of the NMR data obtained during this project led us to the establishment of general rules to easily determine the stereochemistry of any plegmarine type alkaloids.

8. Publications and Experimental

Asymmetric Synthesis of Octahydroindoles via a Domino Robinson Annulation/5-Endo Intramolecular Aza-Michael Reaction

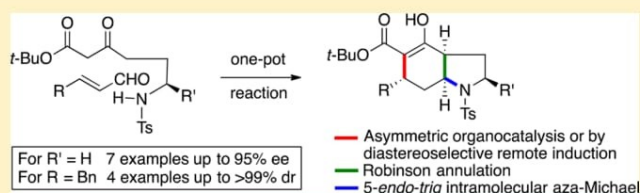
Claudio Parra,[†] Caroline Bosch,[†] Enrique Gómez-Bengo,[‡] Josep Bonjoch,^{*,†} and Ben Bradshaw^{*,†,§}

[†]Laboratori de Química Orgànica, Facultat de Farmàcia, IBUB, Universitat de Barcelona, Av Joan XXIII s/n, 08028 Barcelona, Spain

[‡]Departamento de Química Orgánica I, Universidad del País Vasco, Manuel Lardizábal 3, 20018 San Sebastián, Spain

S Supporting Information

ABSTRACT: A straightforward, two-step asymmetric synthesis of octahydroindoles has been developed on the basis of two complementary strategies: (i) an organocatalyzed Michael reaction followed by a tandem Robinson–aza-Michael double cyclization catalyzed by PS-BEMP, and (ii) a diastereoselective cyclization, which formally constitutes a remote 1,6 asymmetric induction mediated by PS-BEMP. This allowed the construction of complex octahydroindoles with up to four stereocenters, excellent enantioselectivities (up to 95% ee), and complete diastereoselective control in a single-pot operation. DFT calculations were performed to understand the origin of this effect.



INTRODUCTION

The organocatalyzed construction of highly functionalized polycyclic nuclei in a one-pot operation from simple acyclic precursors has the potential to greatly shorten a synthetic sequence targeting complex natural products.¹ Previously, we have developed an organocatalytic strategy toward decahydroquinolines that allowed the synthesis of an advanced common building block for a number of lycopodium alkaloids, such as lycoposerramine Z² and cermizine B.³ In both cases, the tandem reaction was instrumental in enabling highly efficient syntheses of these natural products. Looking to expand the potential of this methodology, it soon became apparent that the principles⁴ behind the reaction sequence, namely a β -keto ester, a tethered sulfonamide, and an enal engaging in a tandem Robinson aza-Michael reaction (see Figure 1), could be more general in scope, providing access to a range of different important nitrogen bicyclic nuclei in enantiopure form. Indeed, this proved to be the case and allowed us to achieve the first efficient synthetic entry to the morphan nucleus using organocatalysis from simple acyclic precursors.⁵ Here, we expand the scope of this strategy to include the octahydroindole unit,⁶ another privileged scaffold found in an extensive and diverse range of compounds (Figure 2). These include natural products such as aeruginosin 298-A,⁷ lycorine,⁸ daphniyunnine D,⁹ neotuberostemonine,¹⁰ pharmaceutical products such as perindopril,¹¹ and a number of proline analogue organocatalysts.¹²

While a number of methods have been developed to synthesize octahydroindoles in enantiopure form, using the chiral pool approach¹³ or asymmetric metal-catalyzed reactions,¹⁴ there are few previous approaches using amino-catalysis.¹⁵

Detailed herein is the development of an organocatalysis-mediated synthesis of octahydroindoles from a noncyclic

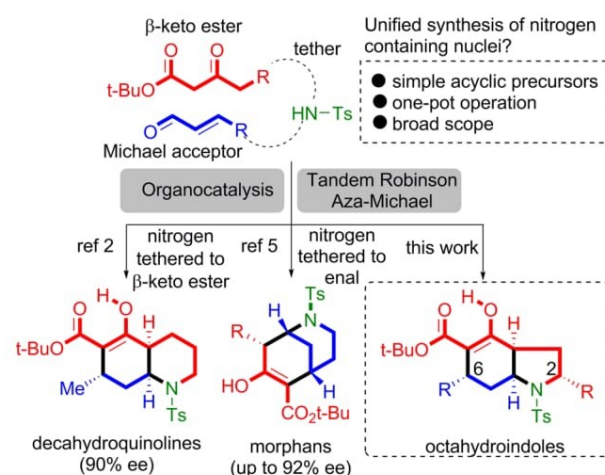


Figure 1. Unified strategy to important nitrogen-containing nuclei using an organocatalysis-initiated tandem Robinson aza-Michael reaction.

precursor. Notably, the process constitutes a rare example of an intramolecular aza-Michael reaction through a 5-endo-trig cyclization,¹⁶ the latter process being disfavored according to Baldwin's rules.¹⁷

RESULTS AND DISCUSSION

Preparation of the required starting material was achieved in a one-step manner by ring opening of the commercially available tosyl aziridines via the dianion of *tert*-butyl acetoacetate¹⁸ (eq

Special Issue: Heterocycles

Received: June 30, 2016

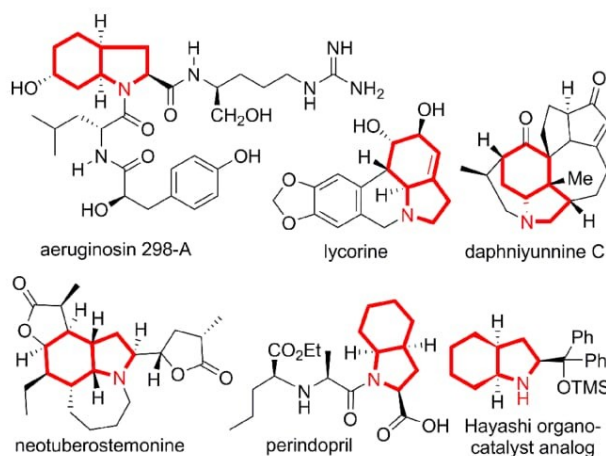
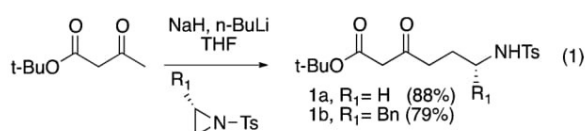


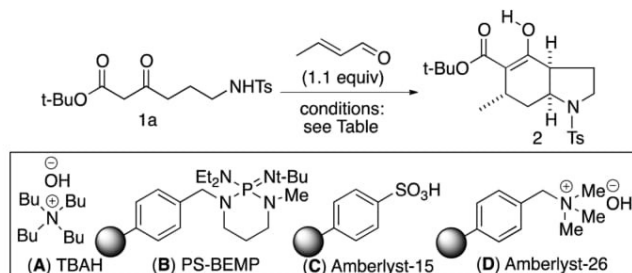
Figure 2. Diverse nitrogen-containing heterocycles with an embedded octahydroindole ring.

1). With the starting material **1a** in hand, the nonasymmetric version of the tandem cyclization reaction was initially



investigated. The key results are outlined in Table 1. Satisfactorily, using the optimal conditions (crotonaldehyde $\text{LiOH}\cdot\text{H}_2\text{O}$, *i*-PrOH, H_2O) developed for the decahydroquinoline series gave the desired analogous octahydroindole product

Table 1. Screening of Tandem Cyclization Conditions Leading to Octahydroindole **2a**



entry	base (equiv)	solvent	time (h)	yield ^a (%)
1	$\text{LiOH}\cdot\text{H}_2\text{O}$ (1) ^b	<i>i</i> -PrOH	24	44
2	<i>t</i> -BuOK (0.3)	<i>t</i> -BuOH	24	15 ^c
3	A ^d (0.3), KOH (aq)	$\text{Et}_2\text{O}/\text{THF}$	72	57
4	B ^e (0.1), C (2)	CH_2Cl_2	72	
5	B (1), C (2)	<i>i</i> -PrOH	24	56 ^f
6	B (1), C (2)	<i>t</i> -BuOH	24	45
7	B (1)	<i>i</i> -PrOH	24	42
8	B (1)	<i>i</i> -PrOH	72	68
9	B (0.1)	<i>i</i> -PrOH	72	54
10	D (1)	<i>i</i> -PrOH	24	43

^aYield refers to the products isolated by flash chromatography. ^b10 equiv of H_2O added. ^cSignificant amounts of the noncyclized cyclohexenone were also obtained (~40%). ^dTBAH refers to 40% *n*-Bu₄NOH in H_2O . ^ePS-BEMP refers to polymer-supported 2-(*tert*-butylimino)-2-(diethylamino)-1,3-dimethylperhydro-1,3,2-diazaphosphorine. ^fIsolated as a mixture of esters by a solvent transesterification process.

2a, which maintained the *all-cis* stereochemistry (Table 1, entry 1). The moderate yield led us to evaluate other conditions⁴ such as *t*-BuOK in *t*-BuOH¹⁹ (entry 2), which gave just 15% of **2a**, with the rest (40%) recovered as the uncyclized cyclohexenone. The use of *n*-Bu₄NOH/KOH²⁰ gave similar results, but it was found that if the reaction was lengthened to 72 h the desired product could be obtained in moderately good yield (entry 3). We also evaluated the use of PS-BEMP with Amberlyst-15 (**B** and **C**, Table 1) under the concept of site-isolated reactivity using the conditions reported by Dixon.²¹ However, only traces of the Michael product were observed (entry 4). Increasing the amount of PS-BEMP to 1 equiv gave a good yield, but significant quantities of the transesterification products were also isolated, presumably catalyzed by the acid resin (entry 5). Switching the solvent to *t*-BuOH gave a slightly less efficient conversion, but with no transesterification side products (entry 6). However, using PS-BEMP alone in *i*-PrOH gratifyingly gave **2a** in moderate yield (entry 7), while extending the reaction to 72 h gave the best yield so far of 68% (entry 8). Reducing the amount of PS-BEMP to catalytic quantities was feasible, albeit at a cost of slightly reducing the yield (entry 9). We also evaluated the more economical Amberlyst-26 resin, but this did not perform so well, with the yield dropping to 43% (entry 10).²²

The relative stereochemistry of *rac*-**2**, which is the same for all compounds synthesized in this series (see below), was elucidated by 2D NMR spectra (COSY, HSQC, NOESY). Octahydroindole **2a** shows a preferred conformation in which the C7–C7a bond of the carbocyclic ring adopts an axial disposition with respect to the nitrogen-containing ring to avoid the allylic strain with the sulfonamide group. The key

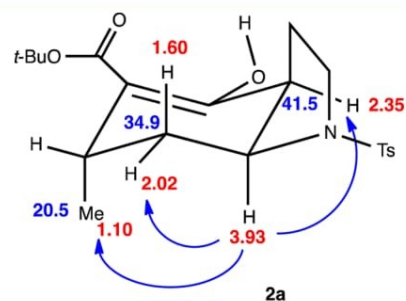


Figure 3. Characteristic NMR data and selected NOEs of hydroindole **2a**.

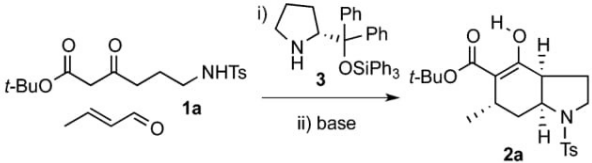
evidence for the structure depicted in Figure 3 was found in the ¹H NMR coupling pattern for H-7ax, which appears as a triplet of doublets ($J = 12.8, 5.2$ Hz). This coupling pattern is only compatible with an axially disposed location of the methyl group at C-6. Moreover, the axial proton H-7a is strongly coupled with only one adjacent axial proton. Hence, its resonance signal appears deceptively as a doublet ($J = 12.8$ Hz) of other doublets ($J = 8.0, 4.8$ Hz). This structural elucidation is fully confirmed by the NOE contacts observed for H-7a (Figure 3).

In order to render the initial Michael addition step in the tandem Robinson/aza-Michael reaction enantioselective, we applied the conditions developed in the decahydroquinoline series² (using the Hayashi–Palomo catalyst **3**,²³ LiOAc as an additive, and toluene as a solvent) to see if the octahydroindole series followed the same reactivity pattern. A brief solvent

screen for the organocatalytic step proved this to be the case, so toluene was again selected as the solvent of choice based on ee and yield. With the organocatalytic step sufficiently optimized, the use of different cyclization conditions for the tandem reaction were then evaluated. With no clear winner for the base for the cyclization step, we decided to test all the conditions that had given good results (see Table 1).

The use of LiOH gave 82% ee (Table 2, entry 1), which was increased to 87% by lowering the reaction temperature (entry

Table 2. Organocatalyzed Michael Reaction/Aldol/Intramolecular Aza-Michael Process Leading to Octahydroindole 2a



entry	solvent	temp (°C)	cyclization conditions ^a	yield ^b (%)	ee (%)
1	toluene	rt	LiOH·H ₂ O (T1 ^c : entry 1)	51	82
2	free	rt	T1: entry 1	7	14
3	MeOH	rt	T1: entry 1	40	77
4	CH ₂ Cl ₂	rt	T1: entry 1	27	85
5	toluene	0	LiOH·H ₂ O, (T1: entry 1)	55	87
6	toluene	0	<i>t</i> -BuOK (T1: entry 2)	61	73
7	toluene	0	KOH, A, (T1: entry 3)	51	94
8	toluene	0	B (T1: entry 8)	50	90
9	toluene	0	B (T1: entry 9)	29	87
10	toluene	0	D (T1: entry 10)	44	84

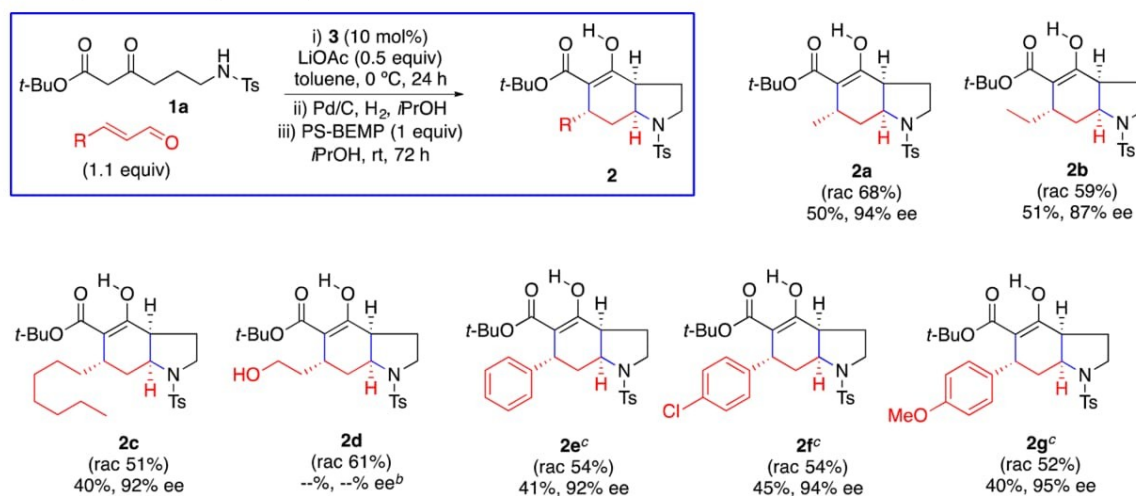
^aReactions were carried out with 1.1 equiv of crotonaldehyde and 0.5 equiv of LiOAc, as an additive, and the reaction time for the first step (i) was 24 h. The second step (ii) was carried out with the base indicated in *i*-PrOH for 72 h. ^bYield refers to the products isolated by flash chromatography. ^cT1 refers to reaction conditions in Table 1.

5). We were surprised to observe that the choice of base was indeed crucial for obtaining good enantioselectivities. Compared to LiOH, the use of *t*-BuOK resulted in a quite considerable reduction of the ee to 73% (entry 6), while the use of KOH with TBAH under biphasic conditions gave an improved ee of 94% (entry 7). The treatment with PS-BEMP (1 equiv) performed almost equally well, giving 90% ee (entry 8). Using catalytic PS-BEMP conditions, the ee dropped slightly to 87%, and the yield was significantly reduced (entry 9). The use of the Amberlyst A26 resin resulted in a moderate 84% ee and also a moderate yield. While the KOH, TBAH conditions (entry 7) were the best in terms of enantioselectivity, we chose PS-BEMP (entry 8) as the optimum conditions based on the following criteria: (i) the reaction setup and work was significantly easier, requiring simple addition and filtration, and (ii) we observed that KOH, TBAH was less effective when the enal substituent was not a methyl group. The absolute configuration proposed for octahydroindole (+)-2a is based on the accepted mechanism of organocatalyzed Michael addition of β -keto esters upon enals²⁴ as well as the absolute stereochemistry reported in the related process leading to enantiopure decahydroquinolines.³

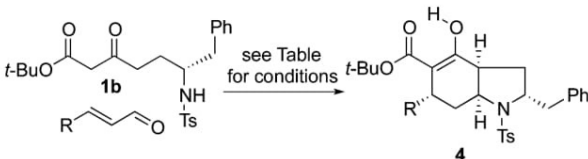
To test the scope of the reaction, a range of enals were examined (Scheme 1). It should be noted that in cases where the enal was not volatile, it was necessary to reduce any excess material by hydrogenation before adding the base to initiate the tandem cyclization reaction. Aliphatic enals gave the corresponding octahydroindoles **2b** and **2c** with good enantioselectivities (87% and 92% ee, respectively). The enal bearing a free hydroxyl group efficiently gave **2d** under racemic conditions but did not evolve under organocatalysis due to the formation of a stable heminal species. The reaction also generally performed well when enals with a β -aromatic substituent were used, giving **2e** (phenyl group), **2f** (*p*-chlorophenyl) or **2g** (*p*-methoxyphenyl), the latter bearing an electron-donating substituent, and all with excellent enantioselectivities.

Since many octahydroindole products bear a substituent at the 2-position, we were interested in examining the effect of

Scheme 1. Scope of the Organocatalyzed Reaction^a



^aEach compound was prepared initially in racemic form using only the conditions of part iii of the transformation of **1a** to **2b–g**. ^bOrganocatalytic conditions did not lead to any significant quantity of coupled product. ^cExcess unreacted nonvolatile enal was converted by hydrogenation to the corresponding aldehyde (see procedure C in the Experimental Section).

Table 3. Scope of the Domino Process from Enantiopure Acyclic β -Keto Ester 1b


entry ^a	R	compd	conditions	yield (%)
1	Me	4a	PS-BEMP	44
2	Me	4a	LiOH.H ₂ O	60
3	Me	4a	Amberlyst A-26	29
5	Me	4a	BEMP	24
6	Me	4a	3 ^b then PS-BEMP	27
7	Me	4a	ent-3 ^b then PS-BEMP	^c
8	Me	4a	PS-BEMP (0.3)	45
9	Me	4a	PS-BEMP (0.3) ^d	36
10	hept	4b	PS-BEMP	28
11	(CH ₂) ₂ OH	4c	PS-BEMP	30
12	Ph	4d	PS-BEMP ^e	43

^aUnless otherwise stated, reactions were carried out with 1 equiv of base in *i*-PrOH for 72 h. ^bConditions for the organocatalytic step were carried out as in Table 2, entry 8. ^cA mixture of various unidentified compounds was obtained with only traces of 4a. ^d10 equiv of H₂O was added. ^eThe use of LiOH·H₂O gave significantly lower yields when R was > Me.

placing a corresponding substituent in the β -keto ester starting material α to the nitrogen (Table 3). We began by taking α -substituted β -keto ester 1b and reacting it under the racemic conditions (PS-BEMP, *i*-PrOH). Notably, the isolation of compound 4a indicated that the incorporation of a stereogenic center at the α -position of the nitrogen atom (i.e., a benzyl group) caused an effective remote 1,6-asymmetric induction.²⁵ The stereostructure of 4a was assigned on the basis that the set of signals in its NMR spectra (¹H and ¹³C) showed a close correlation with those observed in 2. Thus, considering that the pattern of chemical shifts and coupling constants for H-3a, H-6, H-7, and H-7a in 4a was the same as in 2a, a stereostructure analogous to that depicted in Figure 1 but having the benzyl substituent at C-2 was assigned to 4a with the *all-cis* configuration.

To see if the above asymmetric induction was an effect unique to PS-BEMP, the previously evaluated bases were analyzed, and the product found in each case was 4a (Table 3). The effect of using the organocatalyst 3 in the initial Michael step was then examined. While the matched organocatalyst (–)-3 gave a similar result regarding the *all-cis* stereochemistry, ent-3 failed to provide the opposite stereochemistry at C-6.

To explore the scope of the reaction, some different unsaturated aldehydes were used in the coupling reaction. As can be seen in Table 3, the reaction worked with a variety of substrates, leading to the octahydroindoles 4b–d in a nonoptimized moderate yield.

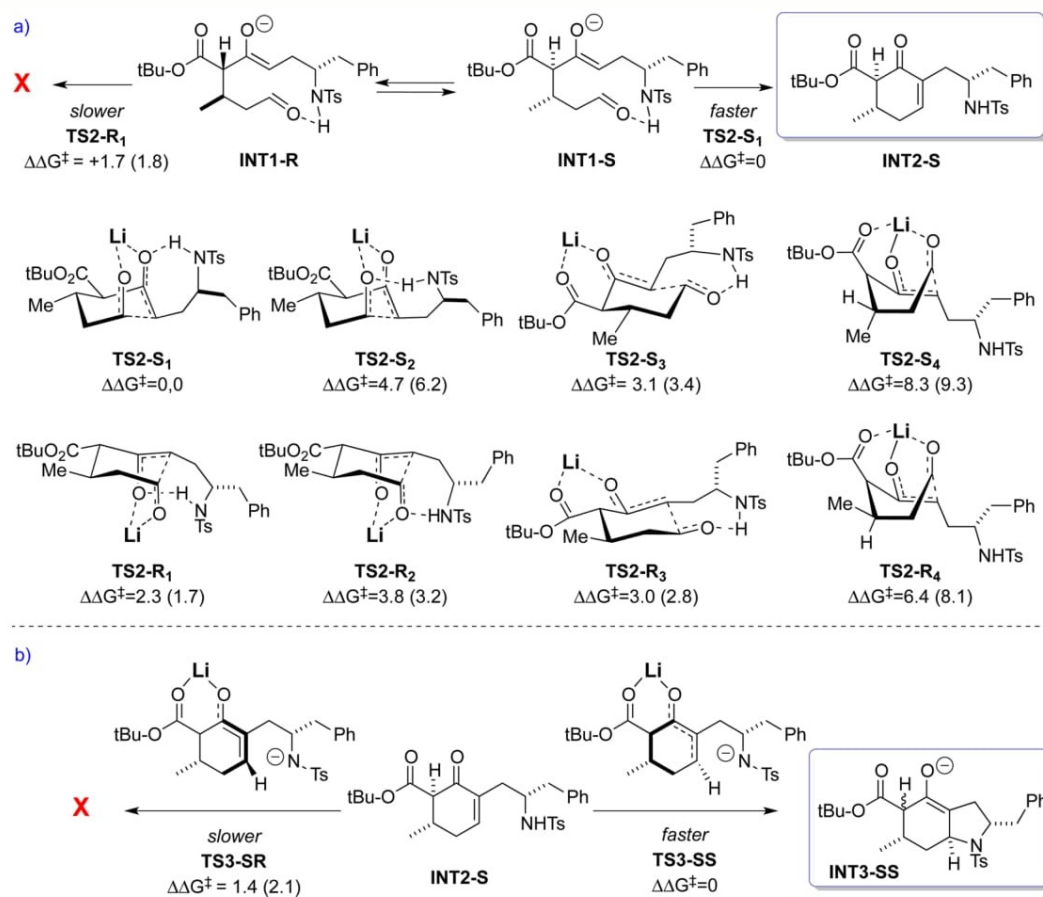


Figure 4. Proposed mechanism for the diastereoselective synthesis of enantiopure octahydroindoles 4: (a) Robinson annulation; (b) intramolecular aza-Michael. Relative activation Gibbs Free energies computed at M062x/6-311+G** (CPM = water) level of theory. Value in parentheses corresponds to wB97xD/6-311+G** (water) single points.

Next, we conducted DFT calculations²⁶ in order to shed light on the unexpected complete diastereoselectivity exerted by the benzyl substituent on the bicycle formation. At first sight, any of the C–C or C–N bond-forming processes is a potential candidate to be the stereodetermining transformation. We thus considered all possibilities, starting with the initial Michael addition of the dicarbonylic compound to crotonaldehyde (**TS1**, see the SI), to form **INT1-R** and **INT1-S** (Figure 4), which, as expected, turned out to be nonselective. The absence of interaction between the forming C–C bond and the stereogenic center α to the nitrogen atom might be behind the observed lack of stereocontrol. The fact that **TS1** is nonselective undoubtedly means that **INT1-R** and **INT1-S** must be in equilibrium (Curtin–Hammett conditions) prior to the stereodetermining step, which we hypothesized to be **TS2** (Figure 4a). A number of **TS2** structures were located, showing different Li cation and H-bond (TsNH) activation modes of the ring formation process. Gratifyingly, the transition state lowest in energy (**TS2-S₁**) corresponds to the formation of the *S* epimer, which is the one experimentally observed. In this structure (**TS2-S₁**), the lithium atom is bonded to the two reacting oxygen units (enolate and aldehyde) and the NH of the tosyl group is hydrogen bonding the enolate oxygen. Any other Li/NH bond combination (**TS2-S₂** to **TS2-S₄**, Figure 4a) is not so favorable in terms of energy. Similar activation modes can be found in the transition states leading to the *R* epimer, **TS2-R₁** being the lowest one, but their energies are at least 1.7–2.0 kcal/mol larger than those of the *S* isomer, in agreement with the experimental selectivity data. We hypothesized that the reason for the energy difference between **TS2-S₁** and **TS2-R₁** might be the tight character of these tricyclic structures, where the steric interaction of the benzyl group with the rest of the molecule gains significance.

We also studied the diastereoselectivity of the second ring formation by attack of the nitrogen atom to **INT2-S**. The most favorable transition states located were **TS3-SR** and **TS3-SS** (Figure 4b), and the comparison of their relative Gibbs free energies is again in agreement with the experimental results, predicting the formation of the *SS* adduct. In both diastereoisomers, the lithium cation is bonded to the oxygens of the dicarbonylic system, activating the enone (**INT2-S**) toward the nucleophilic attack of the tosylamine.

In conclusion, an effective, enantioselective, organocatalytic route to polyfunctionalized octahydroindoles was developed using a one-pot sequence, further expanding the potential scope of the organocatalyzed Robinson/aza-Michael reaction for the rapid construction of important natural product nuclei. The further application of this methodology to synthesize other azabicyclic scaffolds and its use in total synthesis is currently in progress in our laboratory. Moreover, a diastereoselective route starting from commercially available enantiopure aziridine was developed, in which a 1,6-remote control induction was observed in a process leading to enantiopure 2,4,5,6-tetrasubstituted hydroindoles.

EXPERIMENTAL SECTION

General Methods. All reactions were carried out under an argon atmosphere with dry, freshly distilled solvents under anhydrous conditions. Analytical thin-layer chromatography was performed on SiO₂ (silica gel 60 F₂₅₄), and the spots were located with 1% aqueous KMnO₄. Chromatography refers to flash chromatography and was carried out on SiO₂ (silica gel 60 ACC, 35–75 μ m, 230–240 mesh). Drying of organic extracts during workup of reactions was performed

over anhydrous Na₂SO₄. Chemical shifts of ¹H and ¹³C NMR spectra are reported in ppm downfield (δ) from Me₄Si. All NMR data assignments are supported by gCOSY and gHSQC experiments. The triphenylsilyl catalyst **3** was prepared by a literature procedure.²³

tert-Butyl 6-(4-Methylphenylsulfonamido)-3-oxohexanoate (1a).¹⁶ THF (40 mL) was added to NaH (60% in mineral oil) (0.37 g, 9.22 mol), and the resulting suspension was cooled 0 °C. *tert*-Butyl acetoacetate (0.73 g, 4.61 mmol) was added dropwise, and the colorless solution was stirred at 0 °C for 10 min. Then *n*-butyllithium (1.9 mL, 2.6 M in hexanes, 4.94 mmol) was added dropwise, and the resulting orange solution was stirred at 0 °C for an additional 10 min. *N*-Tosylaziridine (1.00 g, 5.07 mmol) in THF (5 mL) was added (the color of the dianion faded on addition of the aziridine), and the reaction mixture was stirred at room temperature for 15 min. The mixture was quenched with aqueous NH₄Cl (2 mL) plus 5 mL of water (5 mL) and diluted with Et₂O (15 mL). The organic phase was washed with water, dried, and concentrated. Purification by chromatography (hexane to hexane/EtOAc 1:1) gave β -keto ester **1a** (1.44 g, 88%) as a light colored oil: ¹H NMR (CDCl₃, 400 MHz) δ 1.44 (s, 9H, CH₃), 1.75 (qd, *J* = 6.4, 0.8 Hz, 2H, CH₂), 2.40 (s, 3H, CH₃), 2.54 (td, *J* = 6.8, 1.2 Hz, 2H, CH₂), 2.92 (qd, *J* = 6.8, 1.2 Hz, 2H, CH₂), 3.31 (s, 2H, CH₂), 4.76 (br, 1H, NH), 7.28 (d, 2H, *m*-ArH), 7.71 (d, 2H, *o*-ArH); ¹³C NMR (100 MHz, CDCl₃) δ 21.4 (ArCH₃), 23.1 (C-5), 27.8 (CH₃), 39.4 (C-4), 42.2 (C-6), 50.4 (C-2), 82.1 (C), 127.1 (*o*-Ar), 129.7 (*m*-Ar), 136.9 (*p*-Ar), 143.3 (*ipso*-Ar), 166.6 (C-3), 202.9 (CO); HRMS (ESI-TOF) *m/z* [*M* + NH₄]⁺ calcd for C₁₇H₂₉N₂O₅S 373.1792, found 373.1798.

tert-Butyl (S)-6-((4-Methylphenyl)sulfonamido)-3-oxo-7-phenylheptanoate (1b). THF (10 mL) was added to NaH (60% mineral oil, 113 mg, 2.84 mmol), and the resulting suspension was cooled to 0 °C. *tert*-Butyl acetoacetate (144 mg, 0.949 mmol) was added dropwise, and the colorless solution was stirred at 0 °C for 10 min. Then *n*-butyllithium (385 μ L of 2.6 M in hexanes, 1.00 mmol) was added dropwise, and the orange solution was stirred at 0 °C for an additional 10 min. (*S*)-(+)-2-Benzyl-1-(*p*-tolylsulfonyl)aziridine (1.04 mmol, 300 mg) in THF (1 mL) was added (the color of the dianion faded immediately on addition of the aziridine), and the reaction mixture was stirred at room temperature for 15 min. The mixture was quenched with aqueous NH₄Cl (1 mL) plus water (3 mL) and diluted with Et₂O (7 mL). The organic phase was washed with water, dried, and concentrated. Purification by chromatography (hexane to hexane/EtOAc 1:1) gave β -keto ester **1b** (334 mg, 79%) as a yellow oil: ¹H NMR (CDCl₃, 400 MHz) δ 1.46 (s, 9H, CH₃), 1.51–1.61 (m, 1H, H-5), 1.78–1.86 (m, 1H, H-5), 2.41 (s, 3H, CH₃), 2.52–2.65 (m, 4H, 2CH₂), 3.29 (dd, *J* = 3.2 Hz, 2H, CH₂), 3.40–3.49 (m, 1H, H-6), 4.63 (br, 1H, NH), 6.94 (dd, *J* = 7.6, 2.8 Hz, 2H, Ph), 7.17–7.20 (m, 3H, Ph), 7.24 (d, *J* = 8.4 Hz, 2H, *m*-ArH), 7.64 (d, *J* = 8.4 Hz, 2H, *o*-ArH); ¹³C NMR (100 MHz, CDCl₃) δ 21.5 (ArCH₃), 27.9 (C-5), 28.0 (CH₃), 38.9 (C-4), 41.8 (CH₂), 50.5 (C-2), 54.3 (C-6), 81.9 (C), 126.7 (*p*-Ph), 126.9 (*o*-Ph), 128.5 (*o*-Ar), 129.3 (*m*-Ph), 129.7 (*m*-Ar), 136.6 (*p*-Ar), 137.7(*p*-Ph), 143.3 (*ipso*-Ar), 166.6 (C-3), 203.3 (CO); HRMS (ESI-TOF) *m/z* [*M* + NH₄]⁺ calcd for C₂₄H₃₅N₂O₅S 463.2261, found 463.2254.

Representative Experimental Procedures for the Intermolecular Michael/Aldol Cyclization/Intramolecular Aza-Michael Reaction. **General Procedure A.** PS-BEMP (1.0 equiv) was added to a solution of the β -keto ester (1.0 equiv) and Michael acceptor (1.1 equiv) in *i*-PrOH (4 mL/mmol), and the resulting mixture was stirred at room temperature for 72 h. Filtration, evaporation of the solvent, and chromatography gave the corresponding octahydroindole product.

General Procedure B. To β -keto ester (1.0 equiv) and Michael acceptor (1.1 equiv) in toluene at 0 °C was added LiOAc (0.5 equiv) followed by pyrrolidine **3** (0.1 equiv), and the resulting mixture was stirred at 0 °C for 24 h. The solvent was removed in vacuo and the residue dissolved in *i*-PrOH (4 mL/mmol). PS-BEMP (1.0 equiv) was added, and the resulting mixture was stirred at room temperature for 72 h. Filtration, concentration, and chromatography gave the corresponding enantioenriched octahydroindole product.

General Procedure C. To β -keto ester (1.0 equiv) and Michael acceptor (1.1 equiv) in toluene at 0 °C was added LiOAc (0.5 equiv)

followed by catalyst **3** (0.1 equiv), and the resulting mixture was stirred at 0 °C for 24 h. The solvent was removed and the residue dissolved in *i*-PrOH (4 mL/mmol). Pd/C (20% w/w) was added, and the flask was fitted with a hydrogen balloon and hydrogenated until no enal was observed. The mixture was filtered through Celite, and the solvent was evaporated in vacuo. PS-BEMP (1.0 equiv) was then added, and the resulting mixture was stirred at room temperature for 72 h. Filtration of the resin and chromatography gave the corresponding enantioenriched octahydroindole product.

(3aR,6R,7aR)-tert-Butyl 4-Hydroxy-6-methyl-1-(4-methylphenylsulfonyl)-2,3,3a,6,7,7a-hexahydro-1H-indole-5-carboxylate (rac-2a). Prepared according to general procedure A using crotonaldehyde (26 μL, 0.309 mmol), β-keto ester **1a** (100 mg, 0.281 mmol), PS-BEMP (130 mg, 0.286 mmol), and *i*-PrOH (1 mL). Purification by chromatography (hexane to hexane/EtOAc 3:1) gave octahydroindole **rac-2a** (78 mg, 68%) as a white solid: mp 131–132 °C; ¹H NMR (CDCl₃, 400 MHz) δ 1.10 (s, 3H, CH₃), 1.50 (s, 9H, CH₃), 1.60 (td, *J* = 12.8, 5.2 Hz, 1H, H-7ax), 1.90 (qd, *J* = 12.0, 8.0 Hz, 1H, H-3β), 2.02 (ddd, *J* = 13.0, 5.0, 2.4 Hz, 1H, H-7eq), 2.26 (dt, *J* = 12.0, 6.0 Hz, 1H, H-3α), 2.35 (ddd, *J* = 12.0, 8.0, 7.2 Hz, 1H, H-3a), 2.44 (s, 3H, ArCH₃), 2.72 (qdd, *J* = 7.2, 2.8, 2.0 Hz, 1H, H-6eq), 3.06 (ddd, *J* = 12.0, 8.0, 6.0 Hz, 1H, H-2α), 3.58 (t, *J* = 8.0 Hz, 1H, H-2β), 3.93 (ddd, *J* = 12.8, 8.0, 4.8 Hz, 1H, H-7a), 7.35 (d, 2H, *m*-ArH), 7.75 (d, 2H, *o*-ArH); ¹³C NMR (100 MHz, CDCl₃) δ 20.5 (CH₃), 21.5 (ArCH₃), 27.5 (C-6), 28.2 (CH₃), 29.3 (C-3), 34.9 (C-7), 41.5 (C-3a), 47.9 (C-2), 55.0 (C-7a), 81.5 (C), 104.2 (C-5), 127.4 (*o*-Ar), 129.8 (*m*-Ar), 134.4 (*p*-Ar), 143.5 (*ipso*-Ar), 169.0 (C-4), 171.9 (CO); HRMS (ESI-TOF) *m/z* [M + H]⁺ calcd for C₂₁H₃₀NO₅S 408.1839, found 408.1848.

(3aR,6R,7aR)-tert-Butyl 4-Hydroxy-6-methyl-1-(4-methylphenylsulfonyl)-2,3,3a,6,7,7a-hexahydro-1H-indole-5-carboxylate (2a). Prepared according to general procedure B using β-keto ester **1a** (100 mg, 0.281 mmol), crotonaldehyde (22 mg, 0.309 mmol), catalyst **3** (14 mg, 0.028 mmol), LiOAc (9 mg, 0.141 mmol), and toluene (1.0 mL) at 0 °C for 24 h followed by cyclization with PS-BEMP (128 mg, 0.281 mmol) and *i*-PrOH (1 mL). Chromatography (hexane to hexane/EtOAc 1:1) gave octahydroindole **2a** (57 mg, 50%) as a white solid: [α]_D²⁵ +110.9 (c 1, CHCl₃). For analysis data, see the procedure for **rac-2a**.

(3aS,6R,7aR)-tert-Butyl 4-Hydroxy-6-ethyl-1-(4-methylphenylsulfonyl)-2,3,3a,6,7,7a-hexahydro-1H-indole-5-carboxylate (2b). Prepared according to general procedure B using *trans*-pentanal (34 mg, 0.402 mmol), β-keto ester **1a** (130 mg, 0.366 mmol), organocatalyst **3** (19 mg, 0.037 mmol), and LiOAc (12 mg, 0.183 mmol) in toluene (1.4 mL) at 0 °C for 24 h followed by cyclization with PS-BEMP (166 mg, 0.366 mmol) and *i*-PrOH (1 mL). Chromatography (hexane to hexane/EtOAc 3:1) gave octahydroindole **2b** (78 mg, 51%) as a yellow oil: ¹H NMR (CDCl₃, 400 MHz) δ 0.98 (t, *J* = 7.4 Hz, 3H, CH₃), 1.19–1.28 (m, 1H, H₆-CH₂), 1.38–1.44 (m, 1H, H-7), 1.49 (s, 9H, CH₃), 1.50–1.57 (m, 1H, H₆-CH₂), 1.89 (ddd, *J* = 19.6, 11.6, 7.6 Hz, 1H, H-3β), 2.20 (ddd, *J* = 4.7, 2.4 Hz, 1H, H-7eq), 2.21–2.29 (m, 1H, H-3α), 2.32–2.40 (m, 1H, H-6), 2.43 (s, 3H, ArCH₃), 2.41–2.48 (m, 1H, H-3a), 3.05 (ddd, *J* = 11.6, 9.6, 6.4 Hz, 1H, H-2α), 3.58 (ddd, *J* = 9.1, 7.8, 1.0 Hz, 1H, H-2β), 3.86 (ddd, *J* = 12.8, 8.2, 4.8 Hz, 1H, H-7a), 7.32 (d, *J* = 7.9 Hz, 2H, *m*-ArH), 7.72 (d, *J* = 8.3 Hz, 2H, *o*-ArH); ¹³C NMR (100 MHz, CDCl₃) δ 12.8 (CH₃), 21.6 (ArCH₃), 27.4 (CH₂), 28.3 (CH₃), 29.5 (C-3), 30.8 (C-7), 34.3 (C-6), 41.5 (C-3a), 48.0 (C-2), 55.1 (C-7a), 81.6 (C), 104.0 (C-5), 127.5 (*o*-Ar), 129.9 (*m*-Ar), 134.4 (*p*-Ar), 143.6 (*ipso*-Ar), 169.4 (C-4), 172.1 (CO); HRMS (ESI-TOF) *m/z* [M + H]⁺ calcd for C₂₂H₃₂NO₅S 422.2005, found 422.1996.

(3aS,6S,7aS)-tert-Butyl 6-Heptyl-4-hydroxy-1-(4-methylphenylsulfonyl)-2,3,3a,6,7,7a-hexahydro-1H-indole-5-carboxylate (2c). Prepared according to general procedure C using β-keto ester **1a** (100 mg, 0.281 mmol), *trans*-2-decenal (57 μL, 0.309 mmol), catalyst **3** (15 mg, 0.028 mmol), and LiOAc (9 mg, 0.140 mmol) in toluene (1 mL). Chromatography (hexane to hexane/EtOAc 1:1) gave octahydroindole **2c** (55 mg, 40%) as a white solid: mp 118–121 °C; ¹H NMR (400 MHz, CDCl₃) δ 0.91 (t, *J* = 6.8 Hz, 3H, CH₃), 1.15–1.40 (m, 12H, H-alkyl), 1.41–1.50 (m, 1H, H-7), 1.50 (s, 9H,

CH₃), 1.88 (dddd, *J* = 12.0, 12.0, 12.0, 8.0 Hz, 1H, H-3) 2.19 (ddd, *J* = 13.2, 4.4, 2.4 Hz, 1H, H-7), 2.27 (ddd, *J* = 12.4, 6.4, 6.4 Hz, 1H, H-3), 2.37 (dt, *J* = 12.0, 7.6 Hz, 1H, H-3a), 2.44 (s, 3H, ArCH₃), 2.49–2.57 (m, 1H, H-6), 3.06 (ddd, *J* = 11.2, 9.6, 6.4 Hz, 1H, H-2), 3.58 (dd, *J* = 8.8, 8.8 Hz, 1H, H-2), 3.86 (ddd, *J* = 12.8, 8.4, 4.8 Hz, 1H, H-7a), 7.32 (d, *J* = 8.0 Hz, 2H, *m*-ArH), 7.71 (d, *J* = 8.4 Hz, 2H, *o*-ArH), 12.4 (s, 1H, enal); ¹³C NMR (100 MHz, CDCl₃) δ 14.1 (CH₃ side chain), 21.5 (ArCH₃), 22.7 (CH₂-alkyl), 27.8 (CH₂-alkyl), 28.2 (CH₃ *t*-Bu), 29.26 (CH₂-alkyl), 29.33 (CH₂-alkyl), 29.6 (C-3), 30.9 (C-7), 31.9 (CH₂-alkyl), 32.3 (C-6), 34.2 (CH₂-alkyl), 41.4 (C-3a), 47.9 (C-2), 54.9 (C-7a), 81.5 (C *t*-Bu), 104.0 (C-5), 127.4 (*o*-Ar), 129.7 (*m*-Ar), 134.3 (*p*-Ar), 143.5 (*ipso*-Ar), 169.2 (C-4), 172.0 (CO); HRMS (ESI-TOF) *m/z* [M + H]⁺ calcd for C₂₇H₄₂NO₅S 492.2778, found 492.2779.

(3aS,6R,7aS)-tert-Butyl 4-Hydroxy-6-(2-hydroxyethyl)-1-(4-methylphenylsulfonyl)-2,3,3a,6,7,7a-hexahydro-1H-indole-5-carboxylate (rac-2d). Prepared according to general procedure A using (*E*)-5-hydroxypent-2-enal²⁷ (17 mg, 0.171 mmol), β-keto ester **1a** (55 mg, 0.155 mmol), PS-BEMP (70 mg, 0.155 mmol), and *i*-PrOH (0.6 mL). Chromatography (hexane to hexane/EtOAc 1:1) gave octahydroindole **rac-2d** (42 mg, 61%) as a yellow oil: ¹H NMR (400 MHz, CDCl₃) δ 1.52 (s, 9H, CH₃), 1.53–1.62 (m, 2H, H-7 and H-1'), 1.71–1.79 (m, 1H, H-1') 1.90 (ddd, *J* = 12.0, 4.0 Hz, 1H, H-3), 2.19 (ddd, *J* = 4.8, 2.4 Hz, 1H, H-7eq), 2.25–2.32 (m, 1H, H-3α), 2.37–2.42 (m, 1H, H-3a), 2.44 (s, 3H, ArCH₃), 2.69–2.75 (m, 1H, H-6), 3.04 (ddd, *J* = 11.2, 9.6, 6.4 Hz, 1H, H-2α), 3.58 (ddd, *J* = 9.2, 7.6, 0.8 Hz, 1H, H-2β), 3.67–3.78 (m, 2H, H-2'), 3.93 (ddd, *J* = 13.2, 8.4, 4.8 Hz, 1H, H-7a), 7.32 (d, *J* = 7.9 Hz, 2H, *m*-ArH), 7.72 (d, *J* = 8.3 Hz, 2H, *o*-ArH); ¹³C NMR (100 MHz, CDCl₃) δ 21.7 (ArCH₃), 28.4 (CH₃), 29.4 (C-3), 29.5 (C-6), 32.2 (C-7), 37.6 (C-1'), 41.6 (C-3a), 48.0 (C-2), 55.1 (C-7a), 61.4 (C-2'), 82.3 (C), 103.3 (C-5), 127.6 (*o*-Ar), 129.9 (*m*-Ar), 134.3 (*p*-Ar), 143.8 (*ipso*-Ar), 170.1 (C-4), 171.9 (CO); HRMS (ESI-TOF) *m/z* [M + H]⁺ calcd for C₂₂H₃₂NO₆S 438.1949, found 438.1945.

(3aR,6R,7aR)-tert-Butyl 4-Hydroxy-1-(4-methylphenylsulfonyl)-6-phenyl-2,3,3a,6,7,7a-hexahydro-1H-indole-5-carboxylate (2e). Prepared according to general procedure C using cinnamaldehyde (23 mg, 0.176 mmol), β-keto ester **1a** (57 mg, 0.160 mmol), organocatalyst **3** (8 mg, 0.016 mmol), and LiOAc (5 mg, 0.080 mmol) in toluene (0.5 mL). Chromatography (hexane to hexane/EtOAc 1:1) gave octahydroindole **2e** (36 mg, 41%) as a white solid: mp 168–170 °C; ¹H NMR (400 MHz, CDCl₃) δ 1.23 (s, 9H, CH₃), 1.89–1.97 (m, 1H, H-7ax), 1.90–1.98 (m, 1H, H-3β), 2.17–2.20 (m, 1H, H-7eq), 2.90–2.26 (m, 1H, H-3α), 2.41–2.51 (m, 1H, H-3a), 2.41 (s, 3H, ArCH₃), 3.08 (td, *J* = 10.1, 6.6 Hz, 1H, H-2α), 3.54–3.58 (m, 1H, H-7a), 3.58 (ddd, *J* = 12.0, 9.6, 7.6, 2.0 Hz, 1H, H-2β), 3.90 (t, *J* = 8.8 Hz, 1H, H-6eq), 7.07 (d, *J* = 7.2 Hz, 2H, *m*-Ph), 7.22 (d, *J* = 8.0 Hz, 2H, *o*-Ph), 7.28 (d, *J* = 8.0 Hz, 2H, *m*-ArH), 7.60 (d, *J* = 8.4 Hz, 2H, *o*-ArH); ¹³C NMR (100 MHz, CDCl₃) δ 21.5 (ArCH₃), 27.8 (CH₃), 28.8 (C-3), 35.7 (C-7), 38.5 (C-6), 41.8 (C-3a), 48.2 (C-2), 54.7 (C-7a), 81.6 (C), 101.7 (C-5), 126.0 (*o*-Ph), 127.2 (*m*-Ph), 127.4 (*o*-Ar), 128.1 (*p*-Ph), 129.6 (*m*-Ar), 133.7 (*p*-Ar), 143.4 (*ipso*-Ar), 144.1 (*ipso*-Ph), 170.7 (C-4), 171.7 (CO); HRMS (ESI-TOF) *m/z* [M + H]⁺ calcd for C₂₆H₃₂NO₅S 470.2001, found 470.1996.

(3aS,6R,7aS)-tert-Butyl 6-(4-Chlorophenyl)-4-hydroxy-1-(4-methylphenylsulfonyl)-2,3,3a,6,7,7a-hexahydro-1H-indole-5-carboxylate (2f). Prepared according to general procedure C using 4-chlorocinnamaldehyde (33 mg, 0.198 mmol), β-keto ester **1a** (64 mg, 0.180 mmol), organocatalyst **3** (9 mg, 0.018 mmol), and LiOAc (6 mg, 0.090 mmol) in toluene (0.7 mL). Chromatography (hexane to hexane/EtOAc 1:1) gave octahydroindole **2f** (39 mg, 43%) as a white solid: mp 185–187 °C; ¹H NMR (400 MHz, CDCl₃) δ 1.24 (s, 9H, CH₃), 1.89–2.00 (m, 2H, H-7ax, H-3β), 2.14 (dt, *J* = 7.6, 3.6 Hz, 1H, H-7eq), 2.22 (dtd, *J* = 13.6, 8.8, 6.8 Hz, H-3α), 2.42 (s, 3H, ArCH₃), 2.44–2.52 (m, 1H, H-3a), 3.08 (dt, *J* = 10.0, 6.4 Hz, 1H, H-2α), 3.47–3.53 (m, 1H, H-6), 3.88 (t, *J* = 4.8 Hz, 1H, H-2β), 7.03 (d, *J* = 8.4 Hz, 2H, *o*-Ar), 7.25 (d, *J* = 8.8 Hz, 2H, *m*-Ar), 7.27 (d, *J* = 6.4 Hz, 2H, *o*-Ph), 7.48 (d, *J* = 8.0 Hz, 2H, *m*-Ph); ¹³C NMR (100 MHz, CDCl₃) δ 21.6 (ArCH₃), 28.0 (CH₃), 28.9 (C-3), 35.9 (C-7), 38.2 (C-6), 41.9 (C-3a), 48.3 (C-2), 54.7 (C-7a), 82.0 (C), 101.4 (C-5), 127.6 (*o*-Ar),

128.4 (*o*-Ph), 128.7 (*m*-Ph), 129.8 (*m*-Ar), 131.9 (*p*-Ph), 133.8 (*p*-Ar), 143.0 (*ipso*-Ar), 143.8 (*ipso*-Ph), 170.9 (C-4), 171.6 (CO); HRMS (ESI-TOF) m/z [M + H]⁺ calcd for C₂₆H₃₁ClNO₅S 504.1606, found 504.1609.

(3*aR*,6*R*,7*aR*)-*tert*-Butyl 4-Hydroxy-6-(methoxyphenyl)-1-(4-methylphenylsulfonyl)-2,3,3*a*,6,7,7*a*-hexahydro-1*H*-indole-5-carboxylate (**2g**). Prepared according to general procedure C using *trans*-4-methoxycinnamaldehyde (29 mg, 0.179 mmol), β -keto ester **1a** (58 mg, 0.163 mmol), catalyst **3** (8 mg, 0.016 mmol), and LiOAc (5 mg, 0.082 mmol) in toluene (0.5 mL). Chromatography (hexane to hexane/EtOAc 1:1) gave octahydroindole **2g** (32 mg, 40%) as a white solid: mp 152–154 °C; ¹H NMR (400 MHz, CDCl₃) δ 1.25 (s, 9H, CH₃), 1.87 (td, J = 12.8, 7.6 Hz, 1H, H-7 α), 1.90–2.00 (m, 1H, H-3 β), 2.16 (dt, J = 8.0, 4.0 Hz, 1H, H-7eq), 2.23 (ddd, J = 14.0, 8.4, 6.8 Hz, H-3 α), 2.41 (s, 3H, ArCH₃), 2.42–2.49 (m, 1H, H-3a), 3.07 (dt, J = 10.0, 6.4 Hz, 1H, H-2 α), 3.56–3.62 (m, 2H, H-6 and H-2 β), 3.83 (s, 3H, CH₃), 3.86 (dd, J = 5.2, 2.8 Hz, 1H, H-7a), 6.83 (d, J = 8.8 Hz, 2H, *o*-Ph), 6.99 (d, J = 8.8 Hz, 2H, *o*-Ar), 7.23 (d, J = 8.0 Hz, 2H, *m*-Ar), 7.48 (d, J = 8.4 Hz, 2H, *m*-Ph); ¹³C NMR (100 MHz, CDCl₃) δ 21.5 (ArCH₃), 27.9 (CH₃), 28.9 (C-3), 35.9 (C-7), 37.7 (C-6), 41.7 (C-3a), 48.2 (C-2), 54.7 (C-7a), 55.3 (OCH₃), 81.6 (C), 101.8 (C-5), 113.5 (*o*-Ph), 127.4 (*o*-Ar), 128.1 (*m*-Ph), 129.6 (*m*-Ar), 133.7 (*p*-Ar), 136.2 (*p*-Ph), 143.4 (*ipso*-Ar), 157.8 (*ipso*-Ph), 170.3 (C-4), 171.7 (CO); HRMS (ESI-TOF) m/z [M + H]⁺ calcd for C₂₇H₃₄NO₆S 500.2103, found 500.2101.

(2*R*,3*aS*,6*S*,7*aS*)-*tert*-Butyl 2-Benzyl-4-hydroxy-6-methyl-1-(4-methylphenylsulfonyl)-2,3,3*a*,6,7,7*a*-hexahydro-1*H*-indole-5-carboxylate (**4a**). Prepared according to general procedure A using β -keto ester **1b** (190 mg, 0.426 mmol), crotonaldehyde (36 mg, 0.511 mmol), PS-BEMP (194 mg, 0.426 mmol), and *i*-PrOH (2 mL). Chromatography (hexane to hexane/EtOAc 1:1) gave octahydroindole **4a** (105 mg, 44%) as a colorless oil: [α]_D –6.7 (c 1, CHCl₃); ¹H NMR (400 MHz, CDCl₃) δ 1.07 (d, J = 7.2 Hz, 3H, CH₃), 1.24–1.27 (m, 1H, H-7 α), 1.47 (s, 9H, CH₃), 1.62–1.72 (m, 1H, H-3), 1.77 (ddd, J = 13.2, 4.8, 2.0 Hz, 1H, H-7eq), 1.98–2.04 (m, 1H, H-3a), 2.12–2.18 (m, 1H, H-3), 2.44 (s, 3H, ArCH₃), 2.61 (qdd, J = 7.2, 5.6, 2.4 Hz, 1H, H-6), 2.94 (dd, J = 13.2, 8.8 Hz, 1H, CH₂Ph), 3.40 (dd, J = 13.2, 3.2 Hz, 1H, CH₂Ph), 3.67–3.74 (m, 1H, H-2), 3.98 (ddd, J = 12.5, 7.8, 4.8 Hz, 1H, H-7a), 7.21–7.35 (m, 7H, ArH), 7.78 (d, J = 8.3 Hz, 2H, *o*-ArH); ¹³C NMR (100 MHz, CDCl₃) δ 20.7 (CH₃), 21.7 (ArCH₃), 27.5 (C-6), 28.4 (CH₃), 34.8 (C-7), 35.8 (C-3), 40.3 (C-3a), 43.1 (CH₂-Ph), 56.9 (C-7a), 62.2 (C-2), 81.7 (C), 104.0 (C-5), 126.7 (*o*-Ph), 127.6 (*o*-Ar), 128.4 (*m*-Ph), 130.0 (*m*-Ar), 130.1 (*p*-Ph), 134.6 (*p*-Ar), 137.7 (Ph), 143.9 (*ipso*-Ar), 169.3 (C-4), 172.1 (CO); HRMS (ESI-TOF) m/z [M + H]⁺ calcd for C₂₈H₃₆NO₅S 498.2309, found 498.2293.

(2*R*,3*aS*,6*S*,7*aS*)-*tert*-Butyl 2-Benzyl-6-heptyl-4-hydroxy-1-(4-methylphenylsulfonyl)-2,3,3*a*,6,7,7*a*-hexahydro-1*H*-indole-5-carboxylate (**4b**). Prepared according to general procedure A using β -keto ester **1b** (100 mg, 0.224 mmol), *trans*-2-decenal (46 μ L, 0.246 mmol), PS-BEMP (102 mg, 0.225 mmol), and *i*-PrOH (1 mL). Chromatography (hexane to hexane/EtOAc 1:1) gave octahydroindole **4b** (36 mg, 28%) as a colorless oil: [α]_D –12.7 (c 1, CHCl₃); ¹H NMR (400 MHz, CDCl₃) δ 0.83–0.92 (m, 3H, CH₃ alkyl), 1.10–1.18 (m, 1H, H-7), 1.18–1.38 (m, 12H, CH₂ alkyl), 1.47 (s, 9H, CH₃), 1.67 (ddd, J = 12.4, 12.4, 10.4 Hz, 1H, H-3), 1.93 (ddd, J = 13.2, 4.8, 2.4 Hz, 1H, H-7), 2.04 (ddd, J = 12.4, 7.6, 7.2 Hz, 1H, H-3a), 2.16 (ddd, J = 12.4, 7.2, 6.8 Hz, 1H, H-3), 2.38–2.46 (m, 1H, H-6), 2.44 (s, 3H, ArCH₃), 2.93 (dd, J = 13.2, 9.2 Hz, 1H, CH₂Ph), 3.42 (dd, J = 13.2, 3.2 Hz, 1H, CH₂Ph), 3.65–3.75 (m, 1H, H-2), 3.91 (ddd, J = 12.8, 8.0, 4.8 Hz, 1H, H-7a), 7.20–7.36 (m, 7H, ArH), 7.76 (d, J = 8.4 Hz, 2H, *m*-Ar); ¹³C NMR (100 MHz, CDCl₃) δ 14.1 (CH₃ alkyl), 21.5 (ArCH₃), 22.7 (CH₂ alkyl), 27.8 (CH₂ alkyl), 28.2 (CH₃ *t*-Bu), 29.3 (CH₂ alkyl), 29.6 (CH₂ alkyl), 30.7 (C-7), 31.9 (CH₂ alkyl), 32.2 (C-6), 34.2 (CH₂ alkyl), 35.8 (C-3), 40.0 (C-3a), 42.9 (CH₂Ph), 56.8 (C-7a), 62.0 (C-2), 81.5 (C *t*-Bu), 103.5 (C-5), 126.5, 127.5, 128.3, 129.8, 129.9, 134.5, 137.6, 143.7, 169.4 (C-4), 172.0 (CO); HRMS (ESI-TOF) m/z [M + H]⁺ calcd for C₃₄H₄₈NO₅S 582.3253, found 582.3262.

(2*R*,3*aS*,6*R*,7*aS*)-*tert*-Butyl 2-Benzyl-4-hydroxy-6-(2-hydroxyethyl)-1-(4-methylphenylsulfonyl)-2,3,3*a*,6,7,7*a*-hexahydro-1*H*-indole-5-carboxylate (**4c**). Prepared according to general procedure A using β -keto ester **1b** (56 mg, 0.126 mmol), (*E*)-5-hydroxypent-2-enal (14 mg, 0.138 mmol), PS-BEMP (57 mg, 0.126 mmol), and *i*-PrOH (0.5 mL). Purification by chromatography (hexane to hexane/EtOAc 1:1) gave octahydroindole **4c** (20 mg, 30%) as a colorless oil: [α]_D –17.1 (c 1, CHCl₃); ¹H NMR (400 MHz, CDCl₃) δ 1.14–1.21 (m, 1H, H-1'), 1.48–1.56 (m, 1H, H-3), 1.49 (s, 9H, CH₃), 1.64–1.74 (m, 1H, H-3), 1.91–1.95 (dm, 1H, H-1'), 2.04–2.10 (m, 1H, H-3a), 2.14–2.20 (m, 1H, H-7), 2.44 (s, 3H, ArCH₃), 2.60–2.62 (m, 1H, H-6), 2.95 (dd, J = 13.6, 8.8 Hz, 1H, CH₂Ph), 3.40 (dd, J = 13.6, 3.2 Hz, 1H, CH₂Ph), 3.61–3.75 (m, 3H, H-2, H-2'), 3.97 (ddd, J = 12.4, 7.2, 4.4 Hz, 1H, H-7a), 7.21–7.35 (m, 5H, ArH), 7.35 (d, J = 8.0 Hz, 2H, *o*-Ar), 7.77 (d, J = 8.0 Hz, 2H, *m*-Ar); ¹³C NMR (100 MHz, CDCl₃) δ 21.7 (ArCH₃), 28.4 (CH₃), 29.3 (C-6), 31.9 (C-1'), 35.9 (C-7), 37.6 (C-3), 40.1 (C-3a), 42.8 (CH₂-Ph), 57.0 (C-7a), 61.4 (C-2'), 62.2 (C-2), 82.3 (C), 102.9 (C-5), 126.7, 127.6, 128.4, 130.1, 130.2, 134.4, 137.6, 144.0, 170.1 (C-4), 171.9 (CO); HRMS (ESI-TOF) m/z [M + H]⁺ calcd for C₂₉H₃₈NO₆S 528.2434, found 528.2414.

(2*R*,3*aS*,6*R*,7*aS*)-*tert*-Butyl 2-Benzyl-4-hydroxy-1-(4-methylphenylsulfonyl)-6-phenyl-2,3,3*a*,6,7,7*a*-hexahydro-1*H*-indole-5-carboxylate (**4d**). Prepared according to general procedure A using β -keto ester **1b** (49 mg, 0.110 mmol), cinnamaldehyde (16 mg, 0.121 mmol), PS-BEMP (50 mg, 0.110 mmol), and *i*-PrOH (0.4 mL). Chromatography (hexane to hexane/EtOAc 1:1) gave octahydroindole **4d** (26 mg, 43%) as a white solid: mp 145–147 °C; [α]_D –46.8 (c 1, CHCl₃); ¹H NMR (400 MHz, CDCl₃) δ 1.19 (s, 9H, CH₃), 1.49–1.55 (m, 1H, H-3), 1.71–1.81 (m, 1H, H-7) 1.88 (dt, J = 13.2, 7.2, 3.2 Hz, 1H, H-3), 2.11–2.20 (m, 2H, H-7, H-3a), 2.42 (s, 3H, ArCH₃), 2.96 (dd, J = 13.2, 8.8 Hz, 1H, CH₂Ph), 3.38 (dd, J = 13.2, 2.8 Hz, 1H, CH₂Ph), 3.63 (ddd, J = 12.0, 7.6, 4.4 Hz, 1H, H-7a), 3.72–3.84 (m, 2H, H-2, H-6), 7.01 (d, J = 7.6 Hz, 2H, *o*-Ar), 7.21–7.35 (m, 10H, ArH), 7.49 (d, J = 8.0 Hz, 2H, *m*-Ar); ¹³C NMR (100 MHz, CDCl₃) δ 21.7 (ArCH₃), 28.0 (CH₃), 34.9 (C-7), 35.5 (C-3), 38.8 (C-6), 40.4 (C-3a), 42.9 (CH₂-Ph), 56.4 (C-7a), 62.5 (C-2), 81.7 (C), 101.2 (C-5), 126.2, 126.7, 127.3, 127.6, 128.2, 128.3, 128.6, 128.8, 129.8, 130.0, 130.2, 134.0, 137.7, 143.8, 144.2, 170.9 (C-4), 171.8 (CO); HRMS (ESI-TOF) m/z [M + H]⁺ calcd for C₃₃H₃₈NO₅S 560.2469, found 560.2465.

■ ASSOCIATED CONTENT

Supporting Information

The Supporting Information is available free of charge on the ACS Publications website at DOI: 10.1021/acs.joc.6b01568.

Analytical data and copies of HPLC and ¹H and ¹³C NMR spectra of the new compounds; Cartesian coordinates and energies for all species considered in Figure 4 (PDF)

■ AUTHOR INFORMATION

Corresponding Authors

*E-mail: josep.bonjoch@ub.edu.

*E-mail: benbradshaw@ub.edu.

Author Contributions

[§]ISHC member.

Notes

The authors declare no competing financial interest.

■ ACKNOWLEDGMENTS

Financial support for this research was provided by the Projects CTQ2013-41338-P and CTQ2013-47925_C2 from MINECO (the Ministry of Economy and Competitiveness of Spain) and the FP7 Marie Curie Actions of the European Commission via the ITN ECHONET Network (MCITN-2012-316379). C.P. is a recipient of a predoctoral fellowship (CONICYT, Chile). We

also thank IZO-SGI SGIker of UPV/EHU for their technical and human support.

REFERENCES

- (1) For reviews of organocatalysis in the synthesis of natural products, see: (a) Marqués-López, E.; Herrera, R. P.; Christmann, M. *Nat. Prod. Rep.* **2010**, *27*, 1138–1167. (b) Abbasov, M. E.; Romo, D. *Nat. Prod. Rep.* **2014**, *31*, 1318–1327. (c) Sun, B.-F. *Tetrahedron Lett.* **2015**, *56*, 2133–2140. (d) Ishikawa, H.; Shiomi, S. *Org. Biomol. Chem.* **2016**, *14*, 409–424.
- (2) Bradshaw, B.; Luque-Corredera, C.; Bonjoch, J. *Org. Lett.* **2013**, *15*, 326–329.
- (3) Bradshaw, B.; Luque-Corredera, C.; Bonjoch, J. *Chem. Commun.* **2014**, *50*, 7099–7102.
- (4) For a mechanistic study of the reaction, see: Bradshaw, B.; Luque-Corredera, C.; Saborit, G.; Cativiela, C.; Dorel, R.; Bo, C.; Bonjoch, J. *Chem. - Eur. J.* **2013**, *19*, 13881–13892.
- (5) Bradshaw, B.; Parra, C.; Bonjoch, J. *Org. Lett.* **2013**, *15*, 2458–2461.
- (6) We have recently become aware of a new approach to hydroindoles through organocatalysis from acyclic precursors. Cossío, F. P. (XXVI Reunión Bienal GEQOR, Punta Umbria, Spain) Personal communication, June 2016.
- (7) For total syntheses, see: (a) Valls, N.; Lopez-Canet, M.; Vallribera, M.; Bonjoch, J. *J. Am. Chem. Soc.* **2000**, *122*, 11248–11249. (b) Dailier, D.; Danoun, G.; Baudoin, O. *Angew. Chem., Int. Ed.* **2015**, *54*, 4919–4922 and references cited therein.
- (8) For total synthesis, see: Ghavre, M.; Froese, J.; Pour, M.; Hudlicky, T. *Angew. Chem., Int. Ed.* **2016**, *55*, 5642–5691 and references cited therein.
- (9) For its isolation, see: Zhang, H.; Yang, S.-P.; Fan, C.-Q.; Ding, J.; Yue, J.-M. *J. Nat. Prod.* **2006**, *69*, 553–557.
- (10) Frankowski, K. J.; Golden, J. E.; Zeng, Y.; Lei, Y.; Aubé, J. *J. Am. Chem. Soc.* **2008**, *130*, 6018–6024.
- (11) Hurst, M.; Jarvis, B. *Drugs* **2001**, *61*, 867–896.
- (12) (a) Sayago, F. J.; Laborda, P.; Calaza, M. I.; Jiménez, A. I.; Cativiela, C. *Eur. J. Org. Chem.* **2011**, *2011*, 2011–2028. (b) Arceo, E.; Jurberg, I. D.; Alvarez-Fernández, A.; Melchiorre, P. *Nat. Chem.* **2013**, *5*, 750–756.
- (13) (a) Wipf, P.; Kim, Y.; Goldstein, D. M. *J. Am. Chem. Soc.* **1995**, *117*, 11106–11112. (b) Bonjoch, J.; Catena, J.; Isábal, E.; López-Canet, M.; Valls, N. *Tetrahedron: Asymmetry* **1996**, *7*, 1899–1902. (c) Hanessian, S.; Tremblay, M. *Org. Lett.* **2004**, *6*, 4683–4686. (d) Ruff, B. M.; Zhong, S.; Nieger, M.; Sickert, M.; Schneider, C.; Bräse, S. *Eur. J. Org. Chem.* **2011**, *2011*, 6558–6566. (e) Hanessian, S.; Dorich, S.; Menz, H. *Org. Lett.* **2013**, *15*, 4134–4137.
- (14) (a) Schindler, C. S.; Diethelm, S.; Carreira, E. M. *Angew. Chem., Int. Ed.* **2009**, *48*, 6296–6299. (b) Trost, B. M.; Kaneko, T.; Andersen, N. G.; Tappertzhofen, C.; Fahr, B. *J. Am. Chem. Soc.* **2012**, *134*, 18944–18947. (c) Sun, Z.; Zhou, M.; Li, X.; Meng, X.; Peng, F.; Zhang, H.; Shao, Z. *Chem. - Eur. J.* **2014**, *20*, 6112–6119. (d) Dailier, D.; Danoun, G.; Baudoin, O. *Angew. Chem., Int. Ed.* **2015**, *54*, 4919–4922.
- (15) Using aminocatalysis: (a) Pantaine, L.; Coeffard, V.; Moreau, X.; Greck, C. *Org. Lett.* **2015**, *17*, 3674–3677. Using a chiral Brønsted acid catalyst: (b) Ruff, B. M.; Zhong, S.; Nieger, M.; Sickert, M.; Schneider, C.; Bräse, S. *Eur. J. Org. Chem.* **2011**, *2011*, 6558–6566. (c) Han, Y.; Zheng, B.; Peng, Y. *Adv. Synth. Catal.* **2015**, *357*, 1136–1142.
- (16) For a general overview of the organocatalytic intramolecular aza-Michael reaction, see: Sánchez-Roselló, M.; Aceña, J. L.; Simón-Fuentes, A.; del Pozo, C. *Chem. Soc. Rev.* **2014**, *43*, 7430–7453.
- (17) Johnston, C. P.; Kothari, A.; Sergeieva, T.; Okovytyy, S. I.; Jackson, K. E.; Paton, R. S.; Smith, M. D. *Nat. Chem.* **2015**, *7*, 171–177.
- (18) For reaction of *N*-tosylaziridines with dianions derived from β -keto esters, see: Lygo, B. *Synlett* **1993**, *1993*, 764–766.
- (19) Chong, B.; Ji, Y.; Oh, S.; Yang, J.; Baik, W.; Koo, S. *J. Org. Chem.* **1997**, *62*, 9323–9325.
- (20) Hagiwara, H.; Okabe, T.; Ono, H.; Kamat, V. P.; Hoshi, T.; Suzuki, T.; Ando, M. *J. Chem. Soc. Perkin Trans. 1* **2002**, 895–900.
- (21) Pilling, A. W.; Boehmer, J.; Dixon, D. *J. Angew. Chem., Int. Ed.* **2007**, *46*, 5428–5430.
- (22) Other conditions evaluated without improvement include the use of BEMP without solid support, the addition of water (10 equiv) to PS-BEMP (1 equiv), and variations in the quantities and reaction times employed with Amberlyst-26.
- (23) Palomo, C.; Landa, A.; Mielgo, A.; Oiarbide, M.; Puente, A.; Vera, S. *Angew. Chem., Int. Ed.* **2007**, *46*, 8431–8435.
- (24) Jensen, K. L.; Dickmeiss, G.; Jiang, H.; Albrecht, L.; Jørgensen, K. A. *Acc. Chem. Res.* **2012**, *45*, 248–264.
- (25) For diastereoselective construction of remote stereocenters, see: (a) Hayashi, R.; Walton, M. C.; Hsung, R. P.; Schwab, J. H.; Yu, X. *Org. Lett.* **2010**, *12*, 5768–5771. (b) Aron, Z. D.; Ito, T.; May, T. L.; Overman, L. E.; Wang, J. *J. Org. Chem.* **2013**, *78*, 9929–9948. (c) Kwon, K.-H.; Serrano, C. M.; Koch, M.; Barrows, L. R.; Looper, R. E. *Org. Lett.* **2014**, *16*, 6048–6051. (d) Kobayakawa, T.; Narumi, T.; Tamamura, H. *Org. Lett.* **2015**, *17*, 2302–2305.
- (26) For further details, see the Supporting Information.
- (27) Zhang, W.; Bah, J.; Wohlfarth, A.; Franzén, J. *Chem. - Eur. J.* **2011**, *17*, 13814–13824.

Asymmetric Synthesis of Octahydroindoles via a Domino Robinson Annulation/5-*Endo* Intramolecular Aza-Michael Reaction

Claudio Parra^a, Caroline Bosch^a, Enrique Gómez-Bengo^b, Josep Bonjoch^{a*} and Ben Bradshaw^{a*}

^a*Laboratori de Química Orgànica, Facultat de Farmàcia, IBUB, Universitat de Barcelona, Av. Joan XXIII s/n, 08028-Barcelona, Spain*

^b*Departamento de Química Orgánica I, Universidad del País Vasco, Manuel Lardizabal 3, 20018-San Sebastian, Spain*

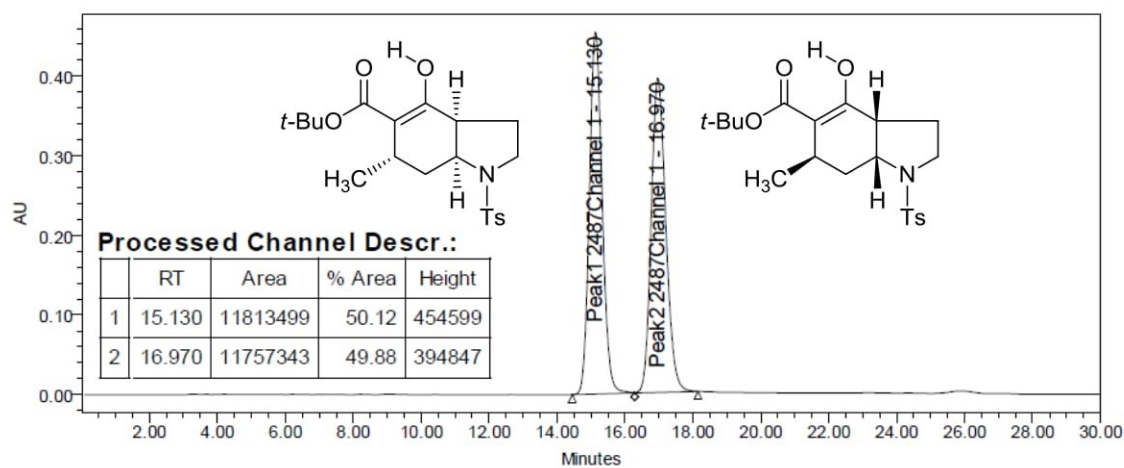
josep.bonjoch@ub.edu; benbradshaw@ub.edu

Supporting Information

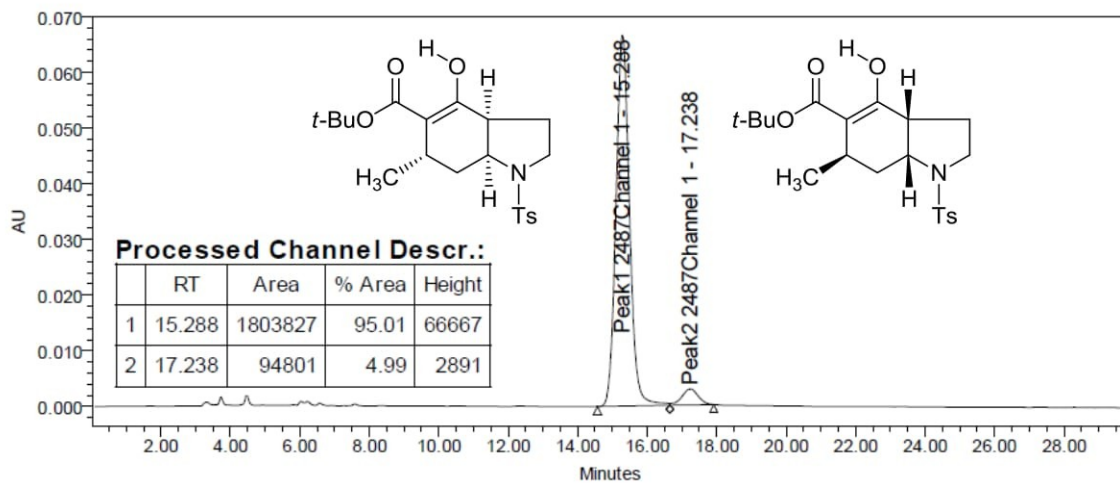
Table of Contents

Copies of HPLC analysis	S2-S7
Copies of ¹ H- and ¹³ C-NMR spectra	S8-S33
Computational studies supporting information	S34-S54

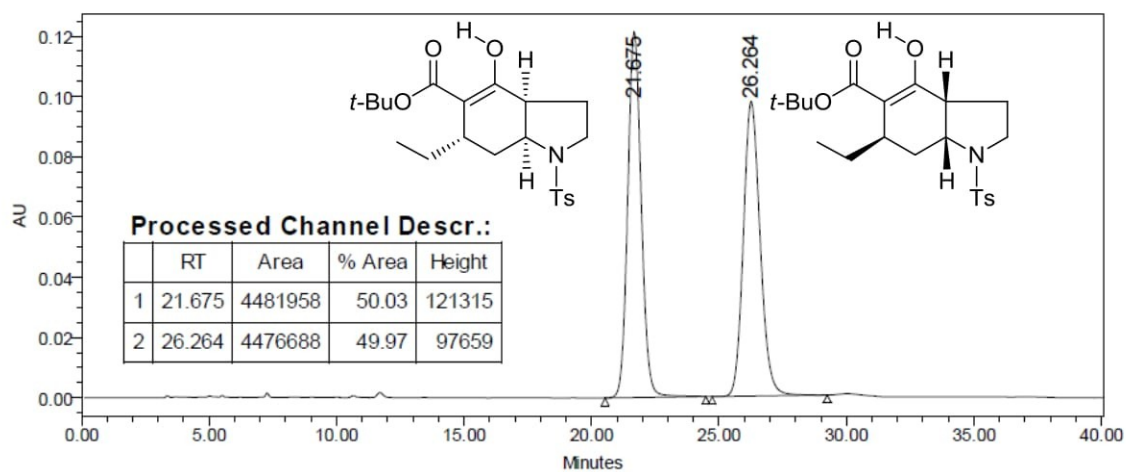
HPLC of racemic **2a** (isocratic Hexane/*i*PrOH 8/2):



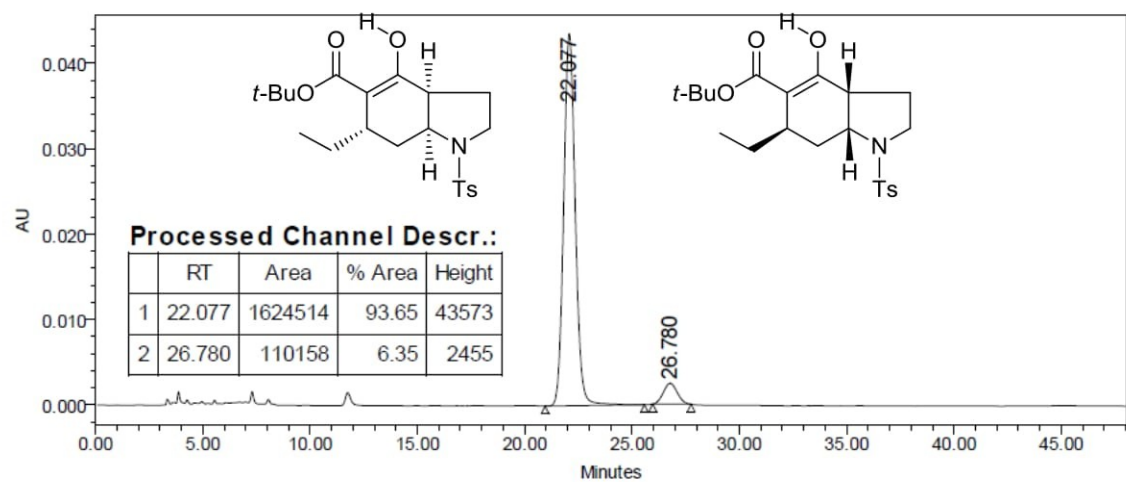
HPLC of organocatalyzed **2a** (isocratic Hexane/*i*PrOH 8/2):



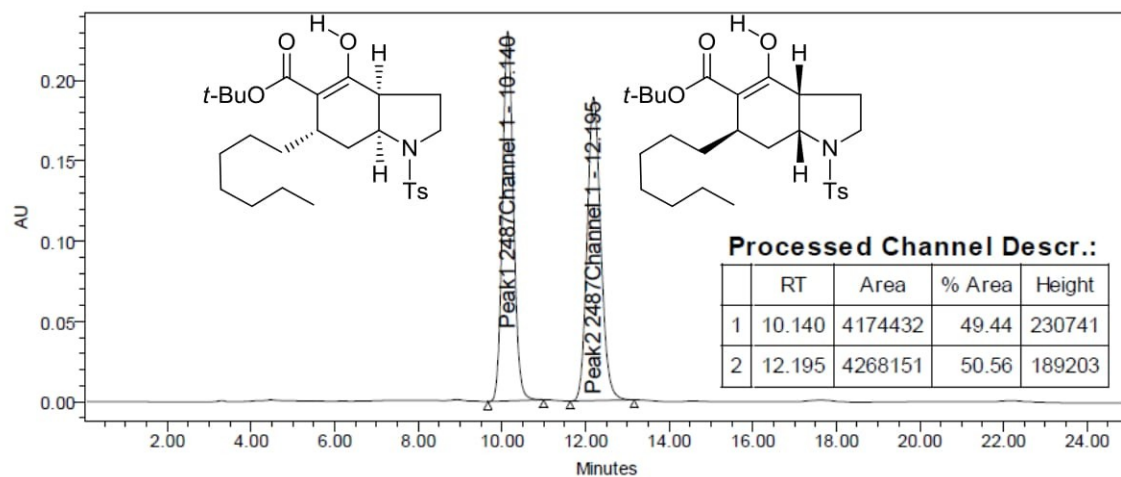
HPLC of racemic **2b** (isocratic Hexane/*i*PrOH 9/1):



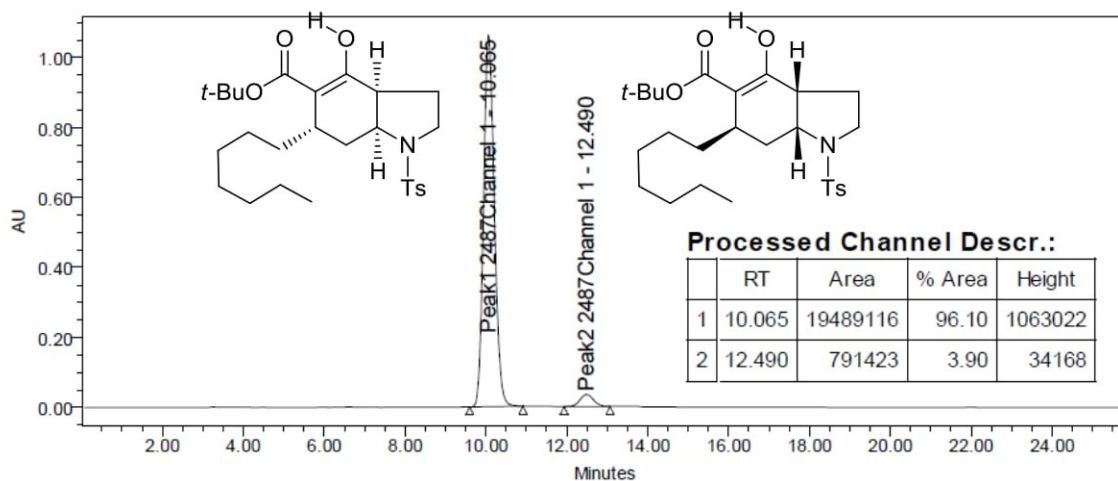
HPLC of organocatalyzed **2b** (isocratic Hexane/*i*PrOH 9/1):



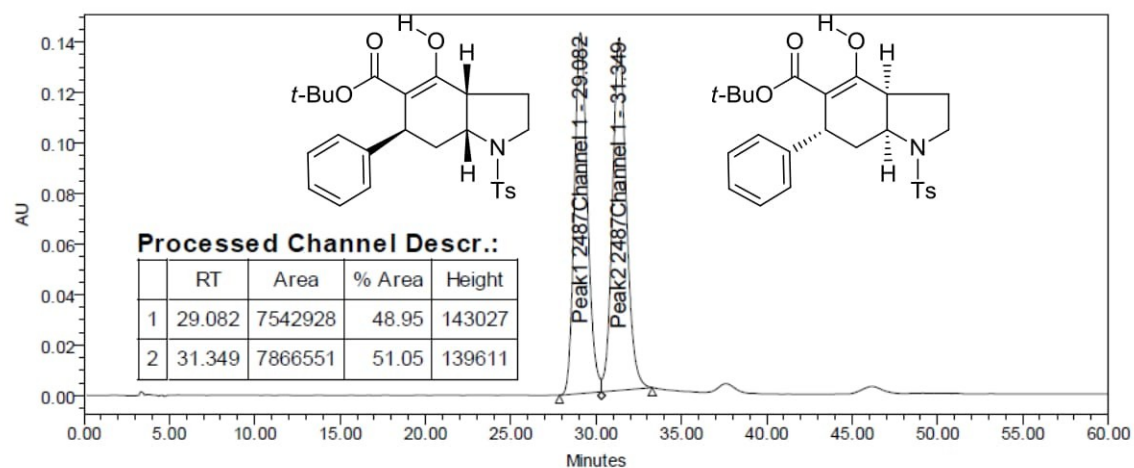
HPLC of racemic **2c** (isocratic Hexane/*i*PrOH 8/2):



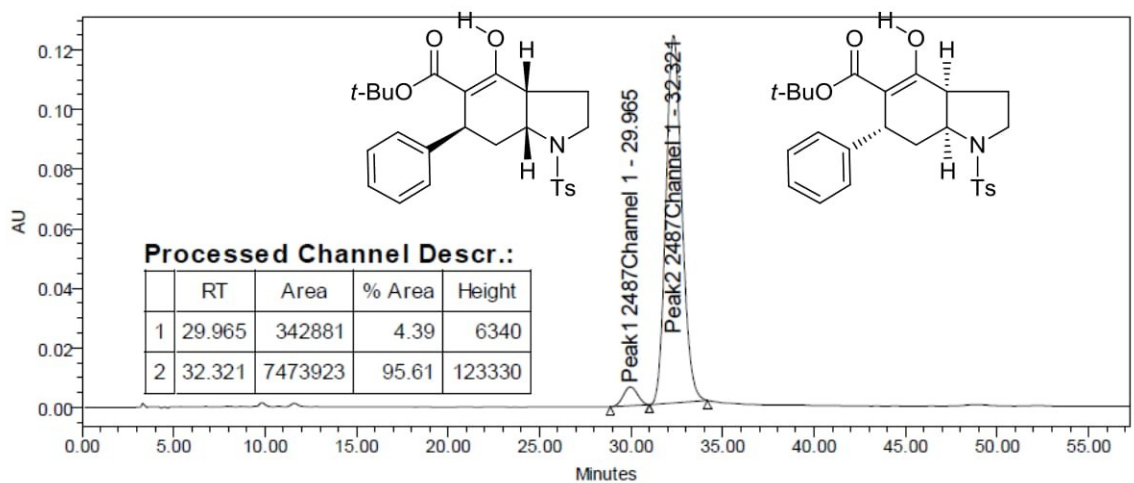
HPLC of organocatalyzed **2c** (isocratic Hexane/*i*PrOH 8/2):



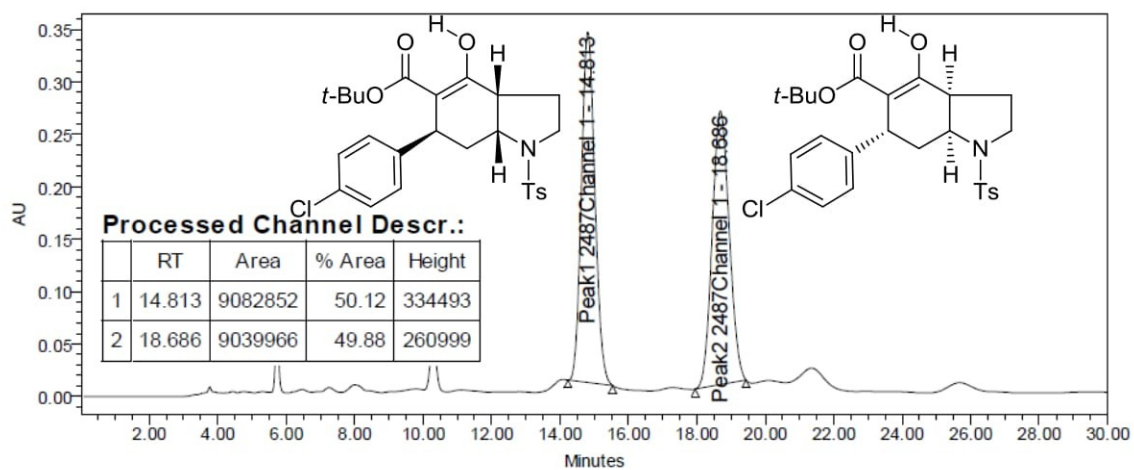
HPLC of racemic **2e** (isocratic Hexane/*i*PrOH 9/1):



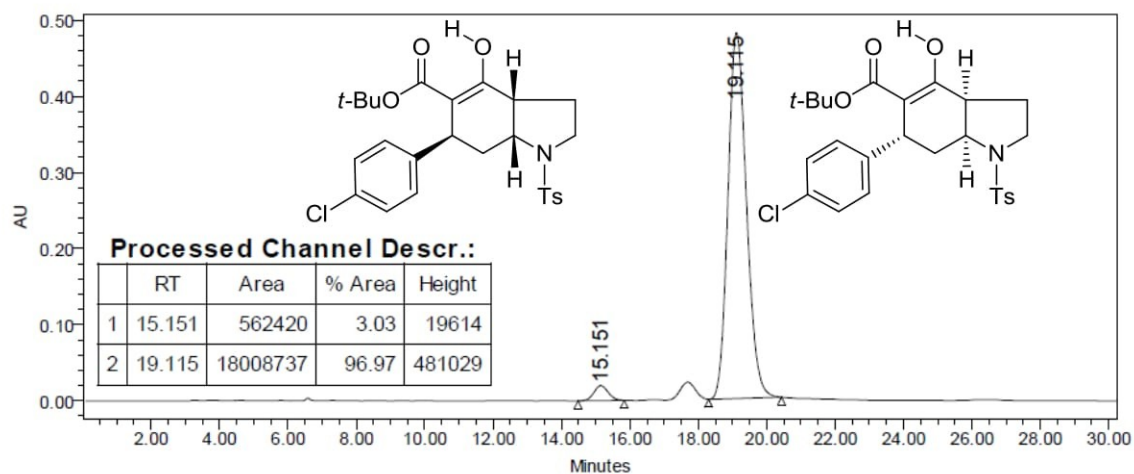
HPLC of organocatalyzed **2e** (isocratic Hexane/*i*PrOH 9/1):



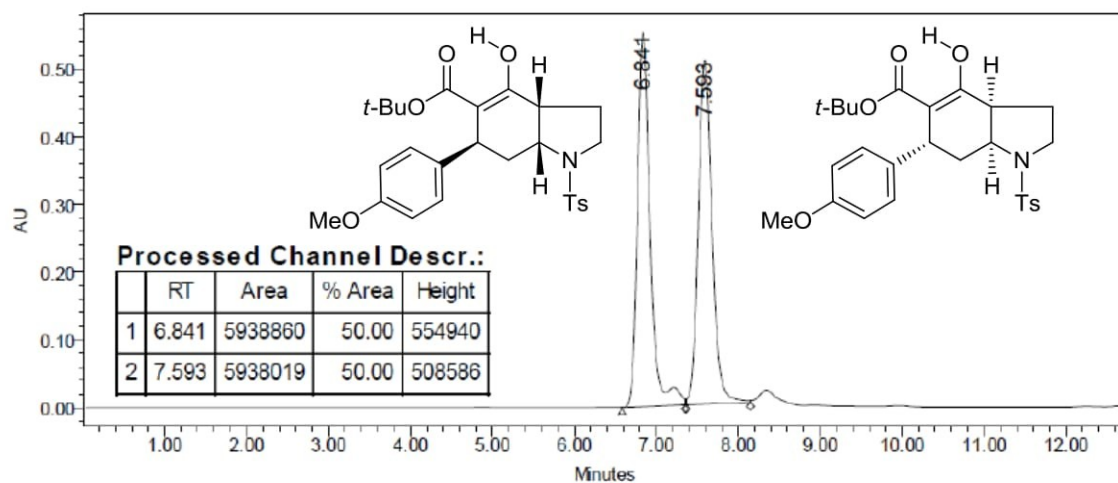
HPLC of racemic **2f** (isocratic Hexane/*i*PrOH 8/2):



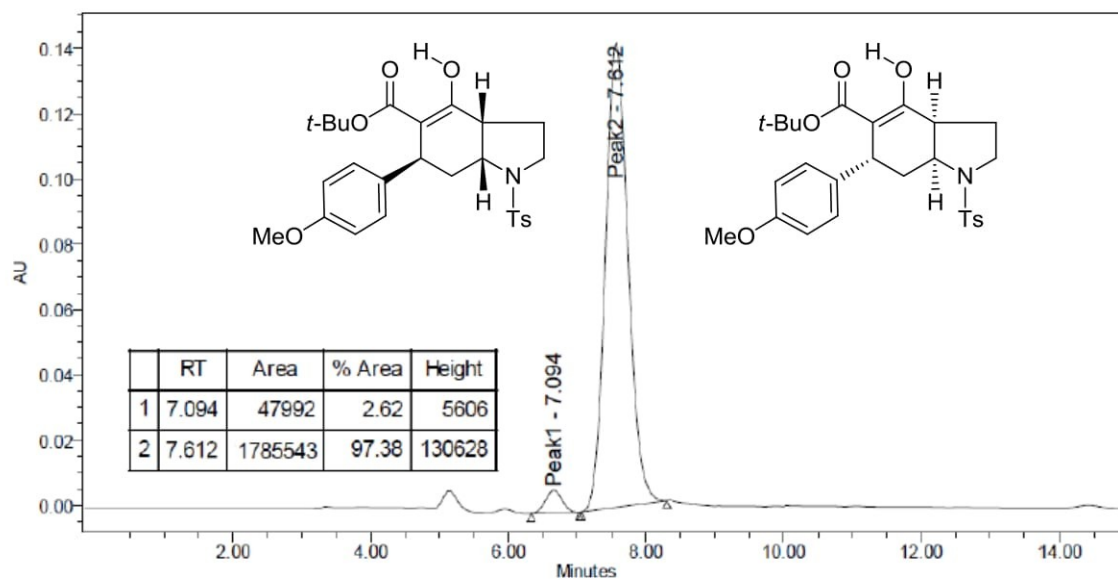
HPLC of organocatalyzed **2f** (isocratic Hexane/*i*PrOH 8/2):



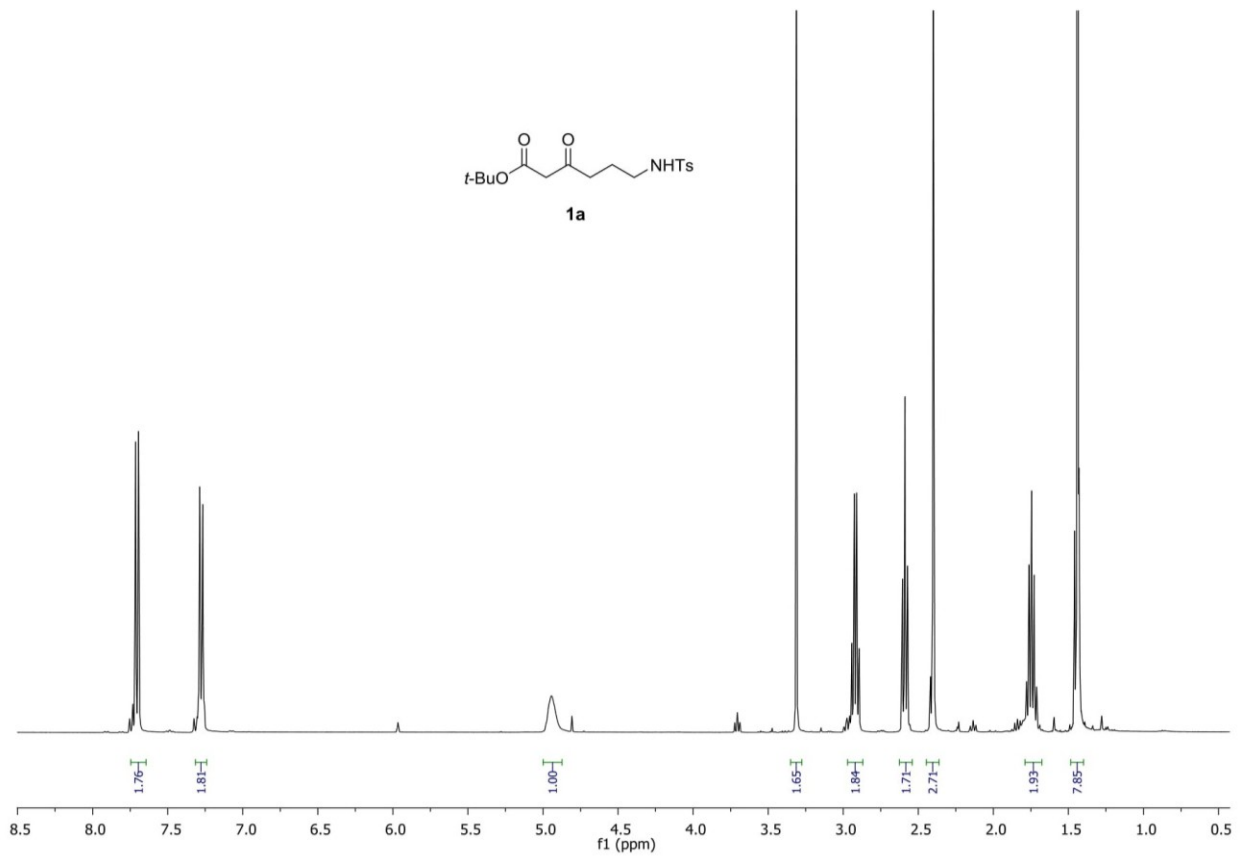
HPLC of racemic **2g** (isocratic Hexane/*i*PrOH 7/3):



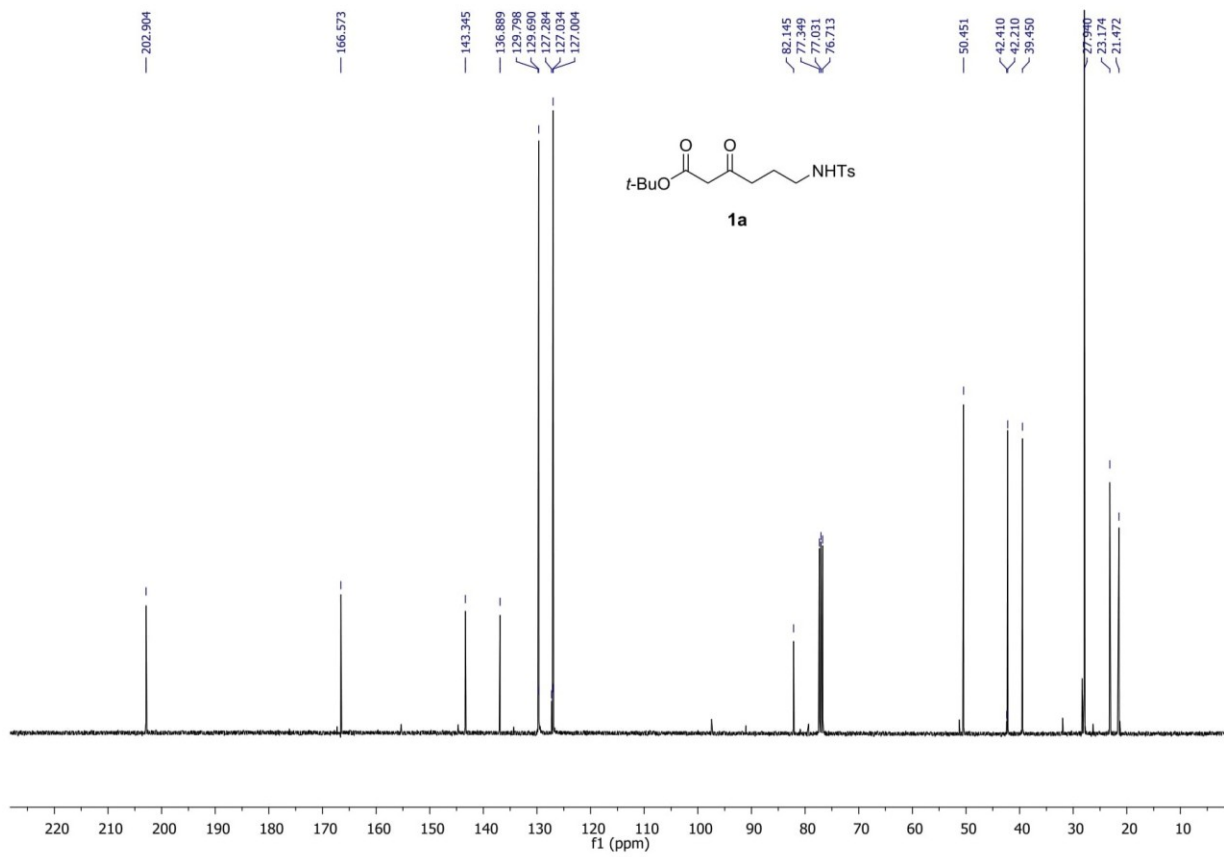
HPLC of organocatalyzed **2g** (isocratic Hexane/*i*PrOH 7/3):

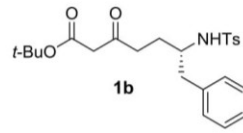


85

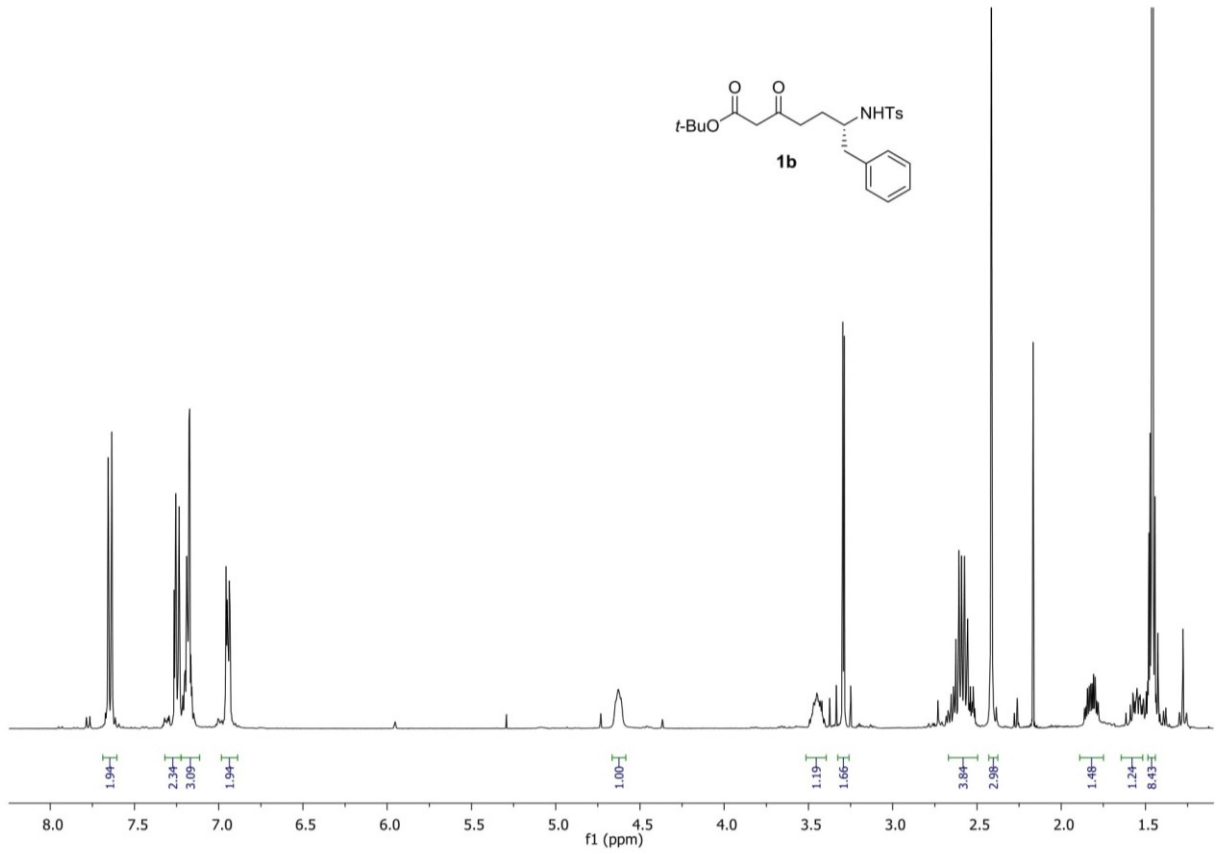


65

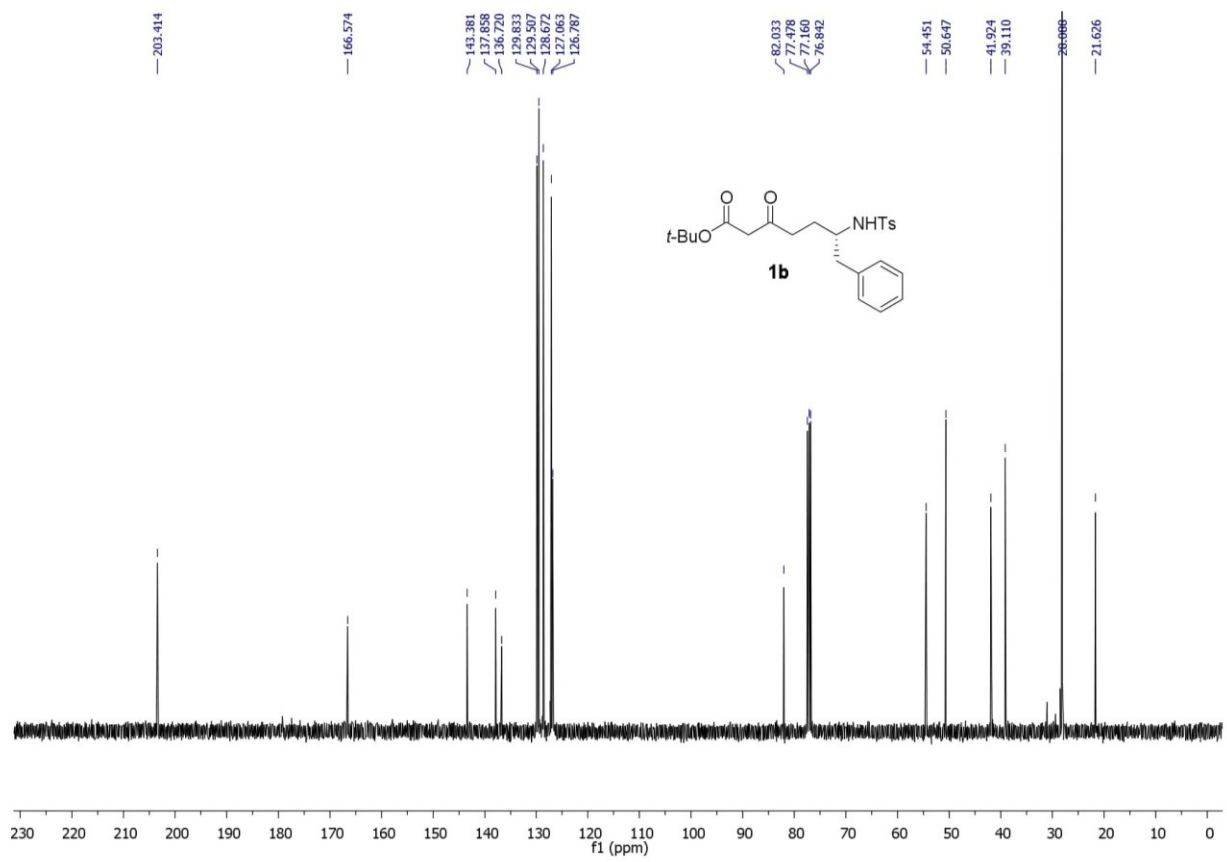




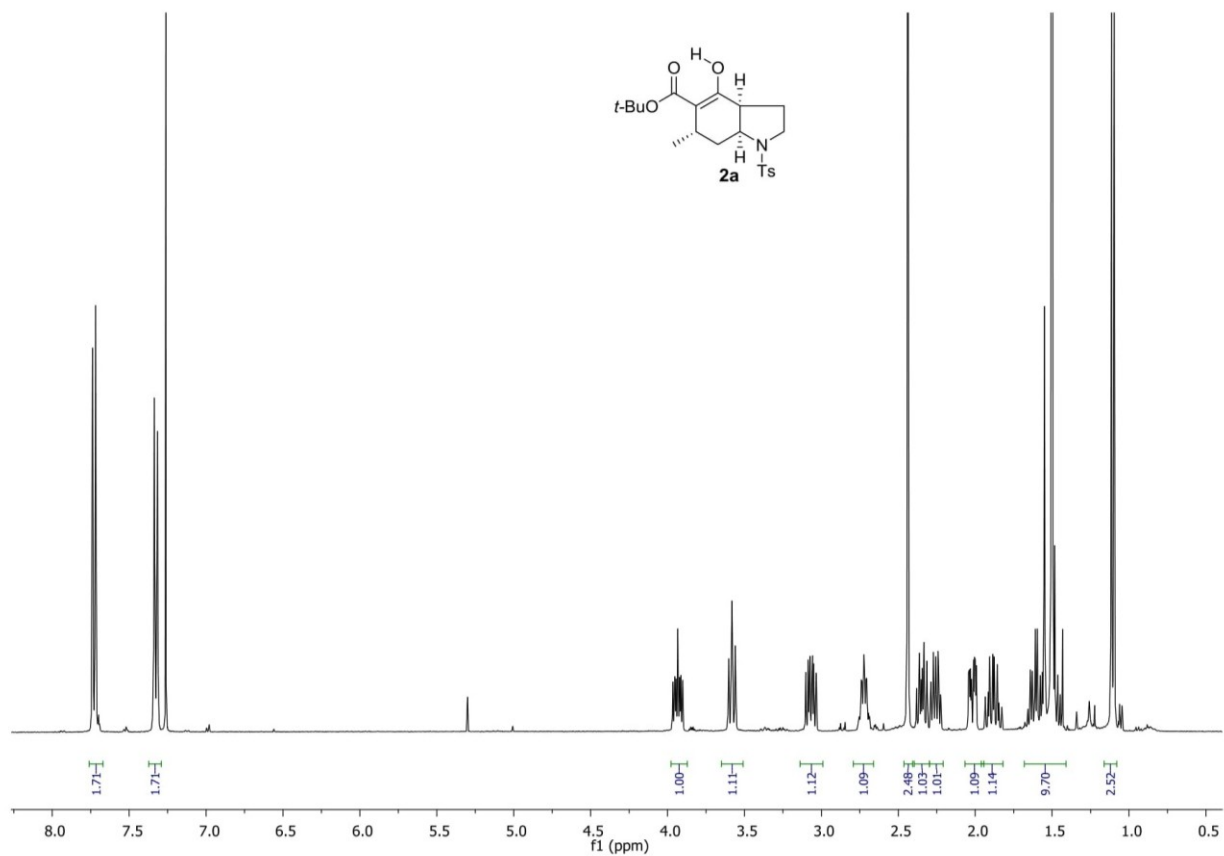
015



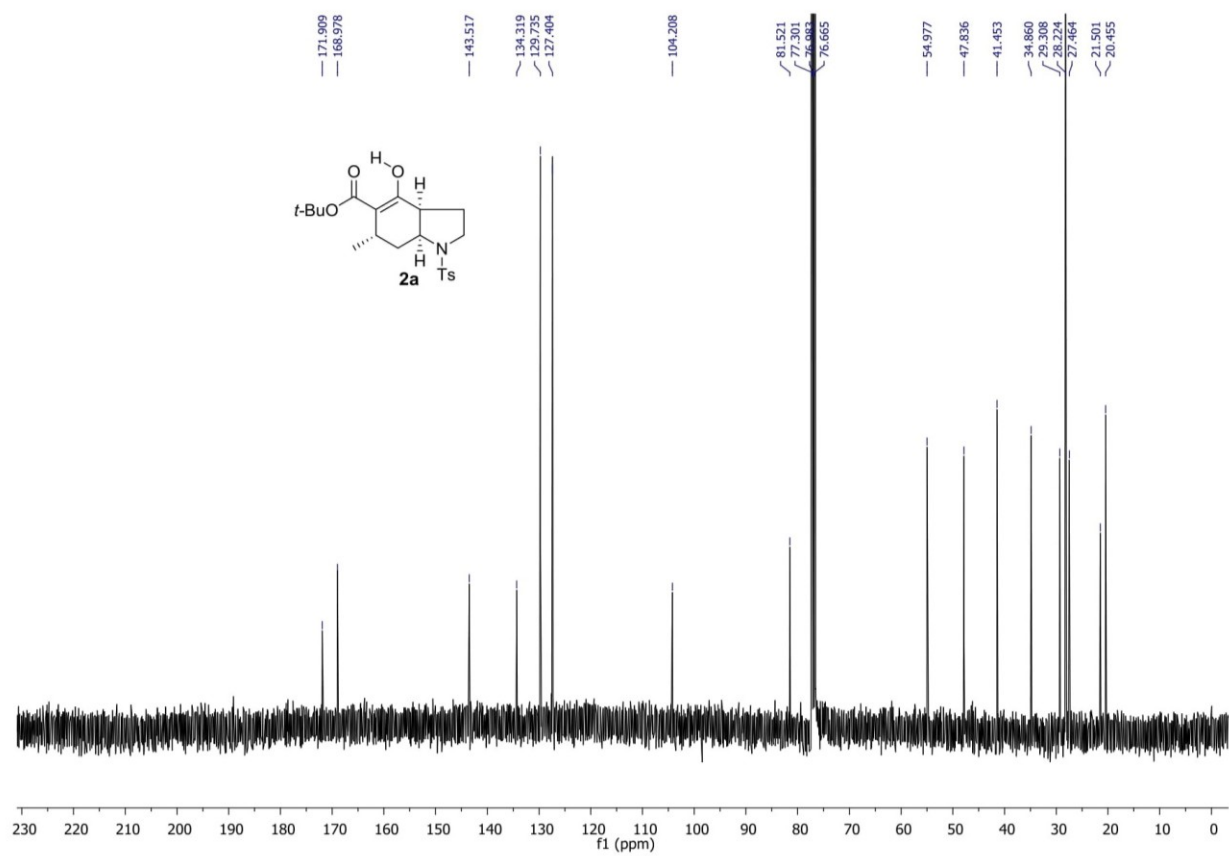
511



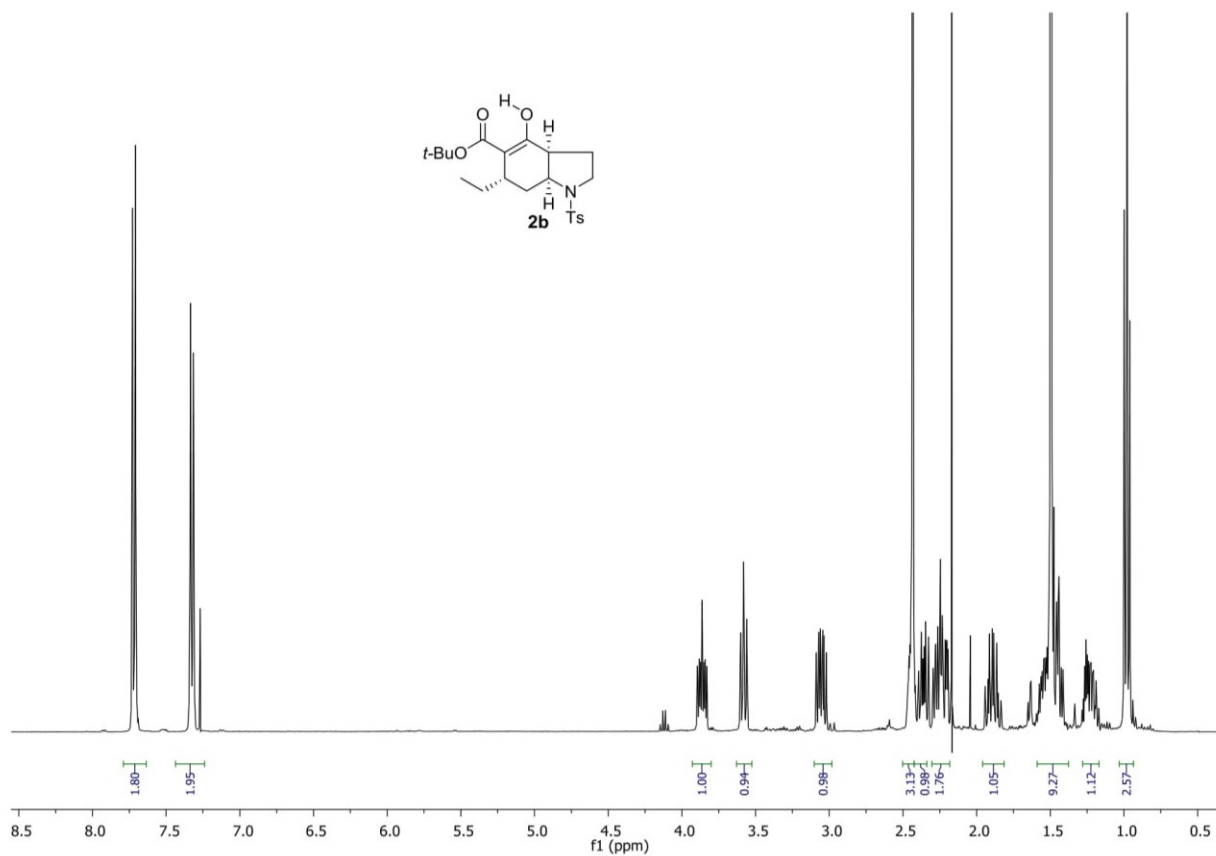
S12



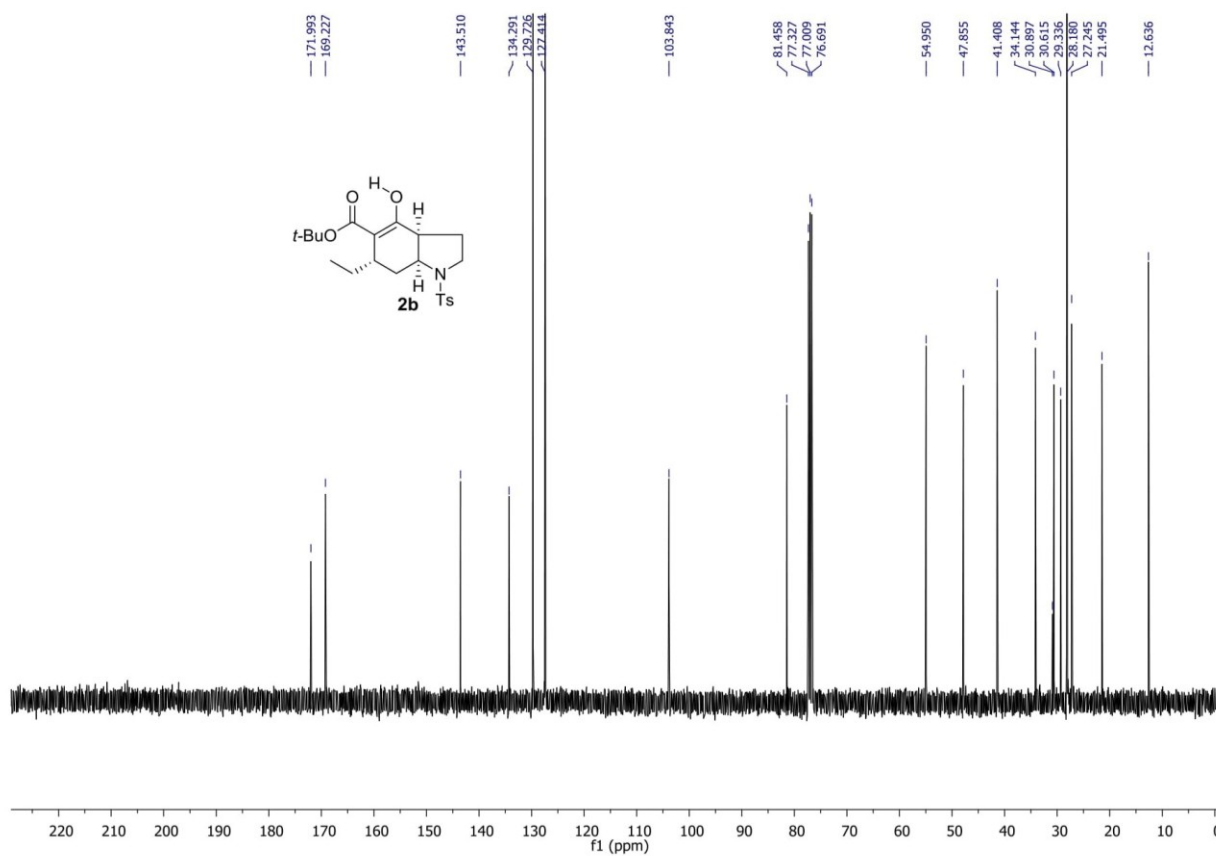
S13



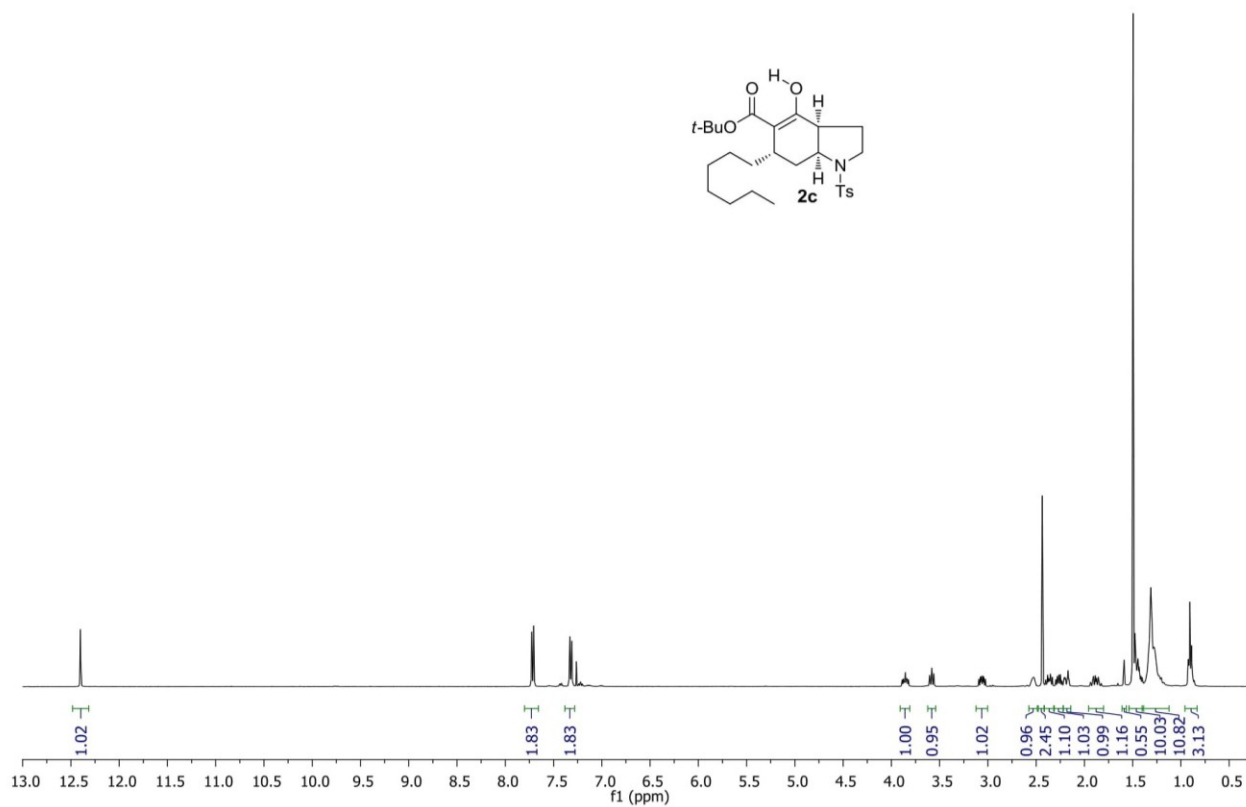
S14



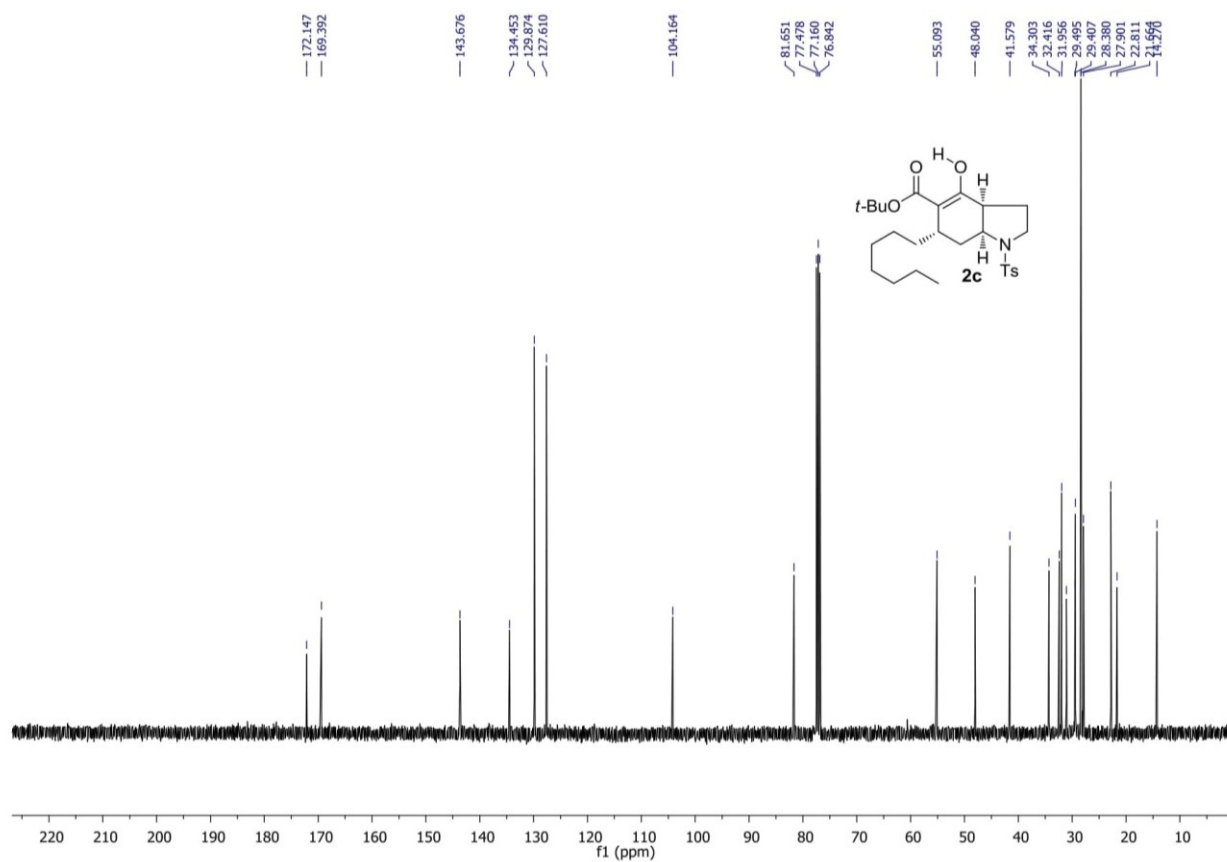
S15



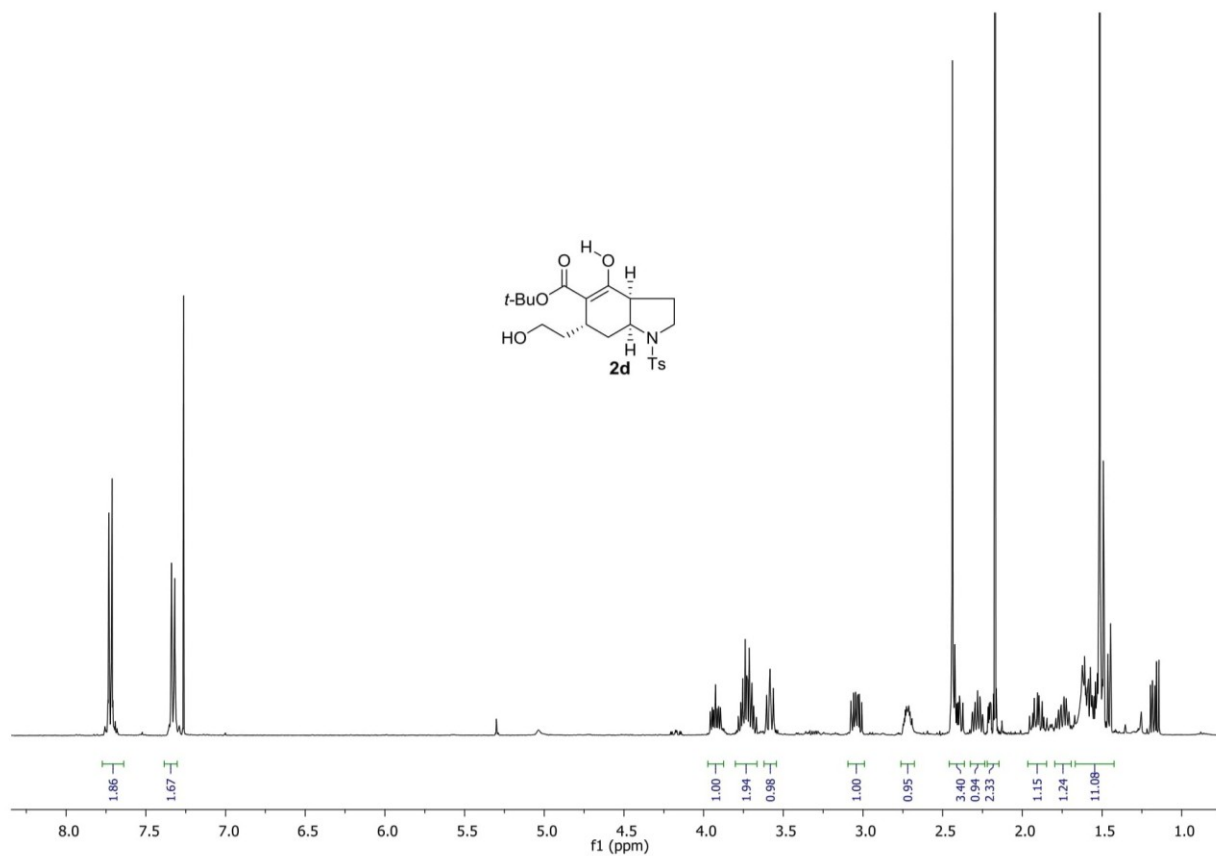
S16



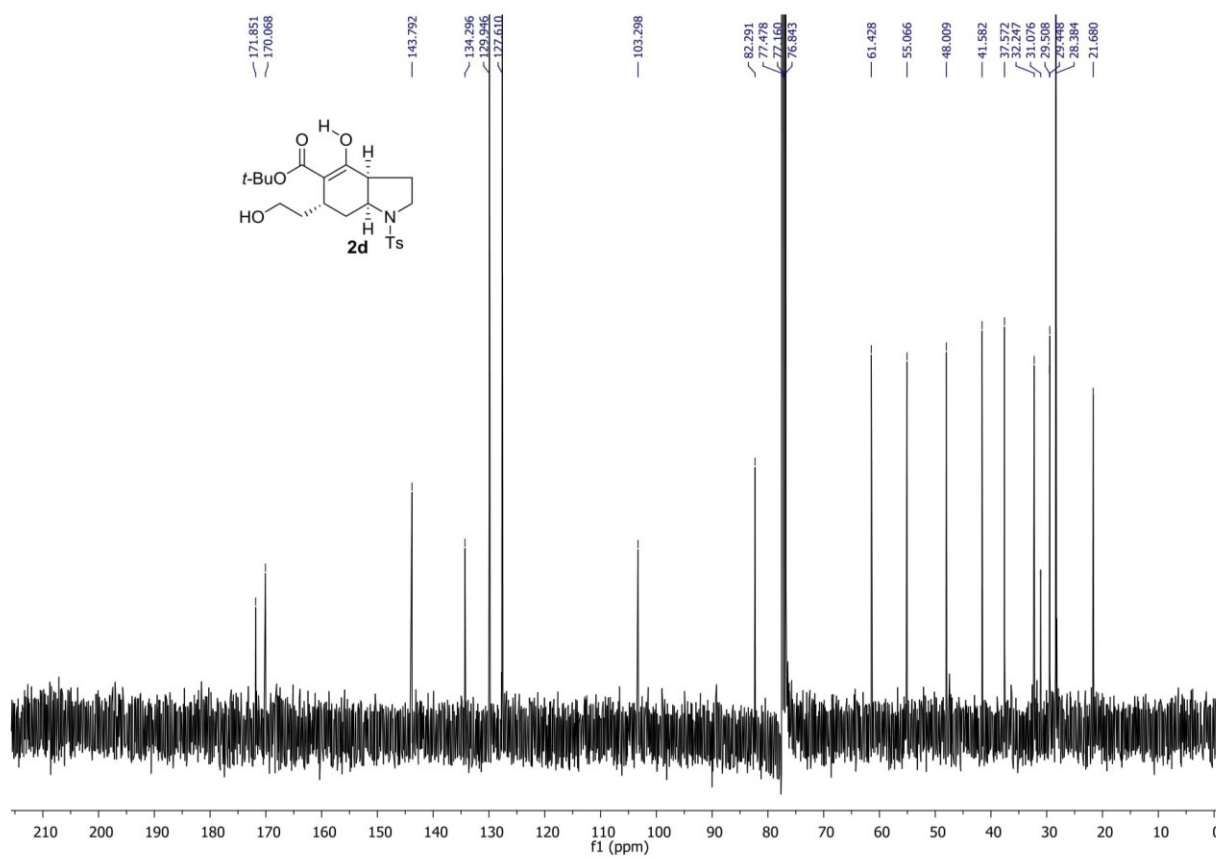
S17



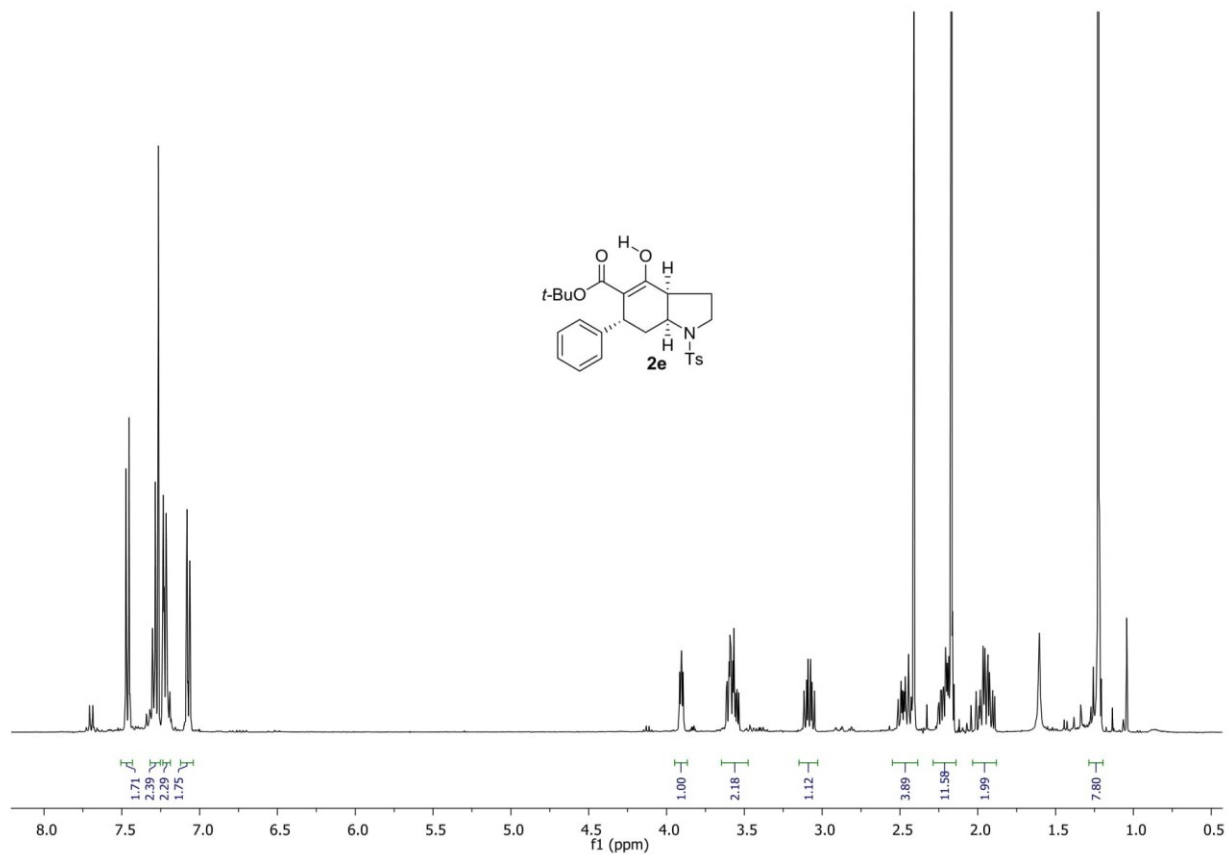
S18



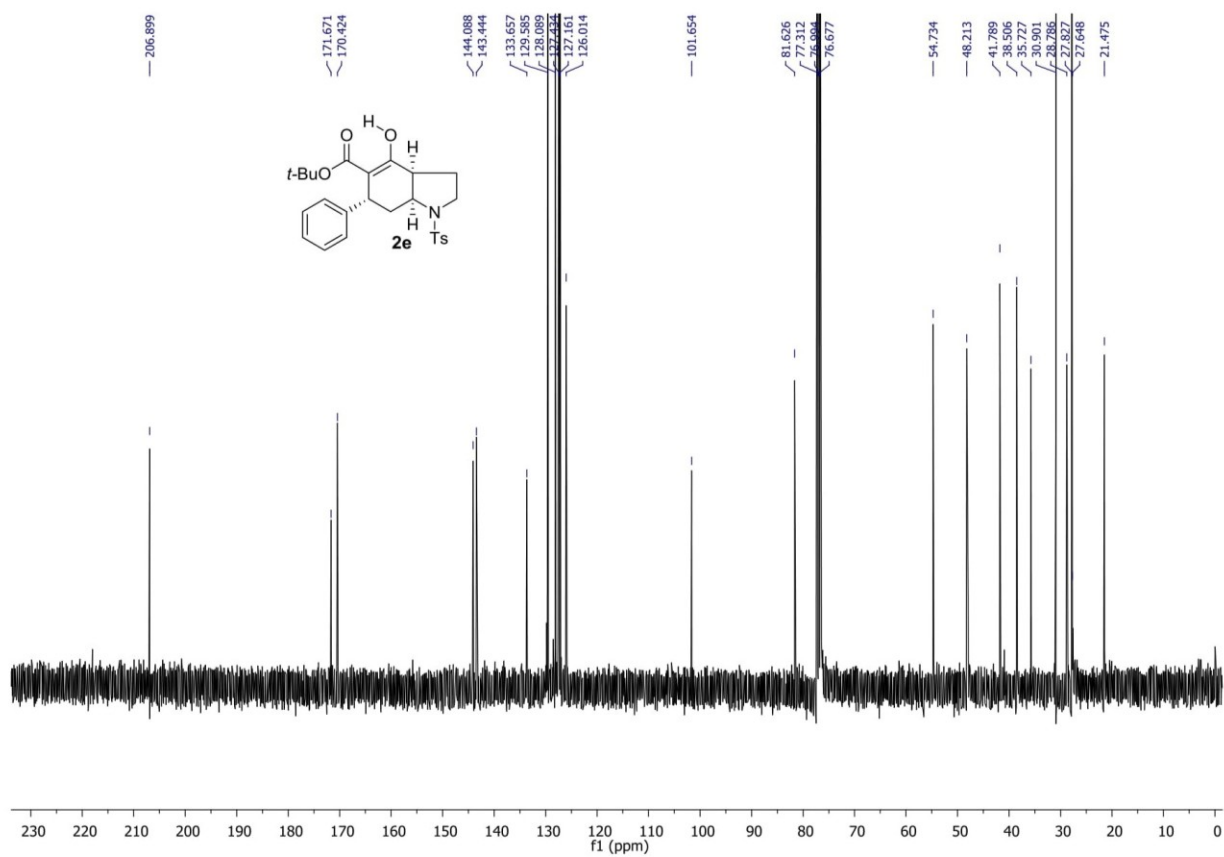
S19



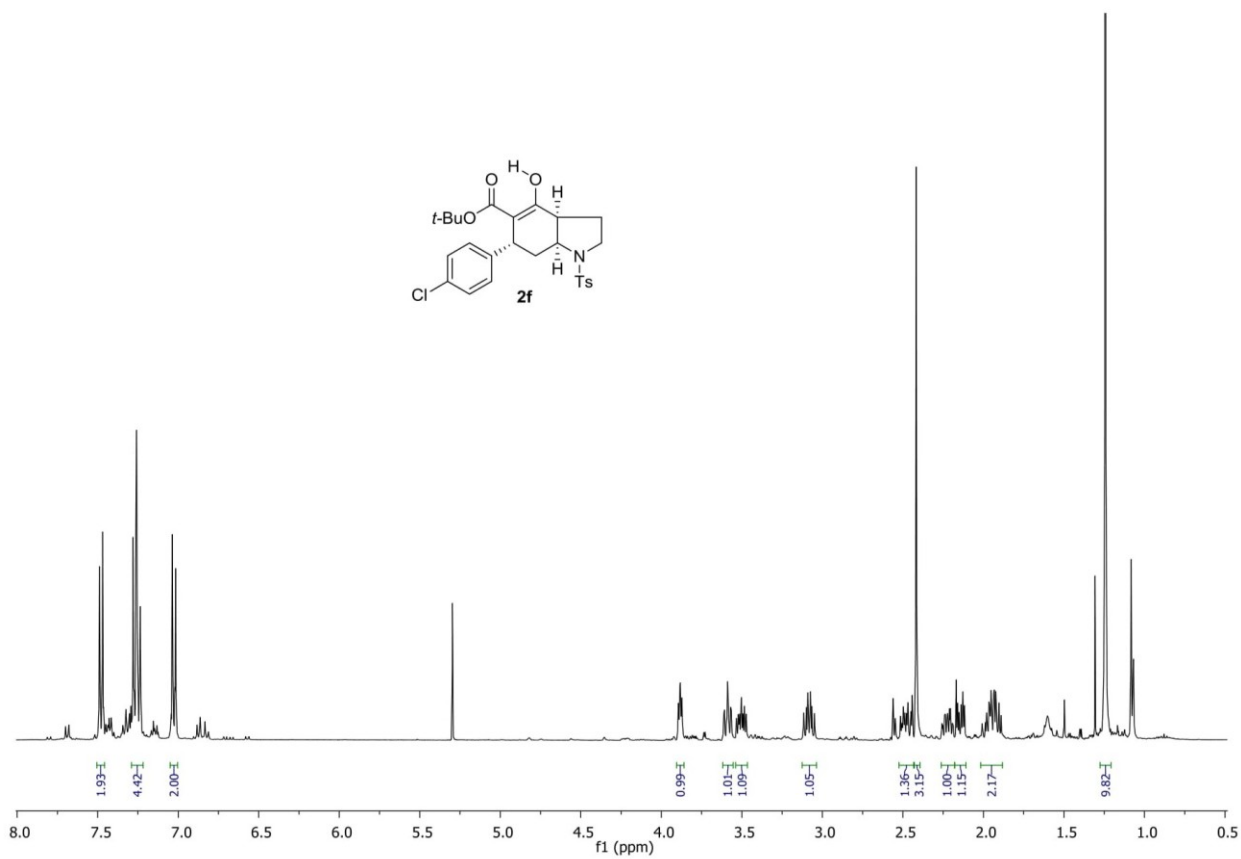
S20



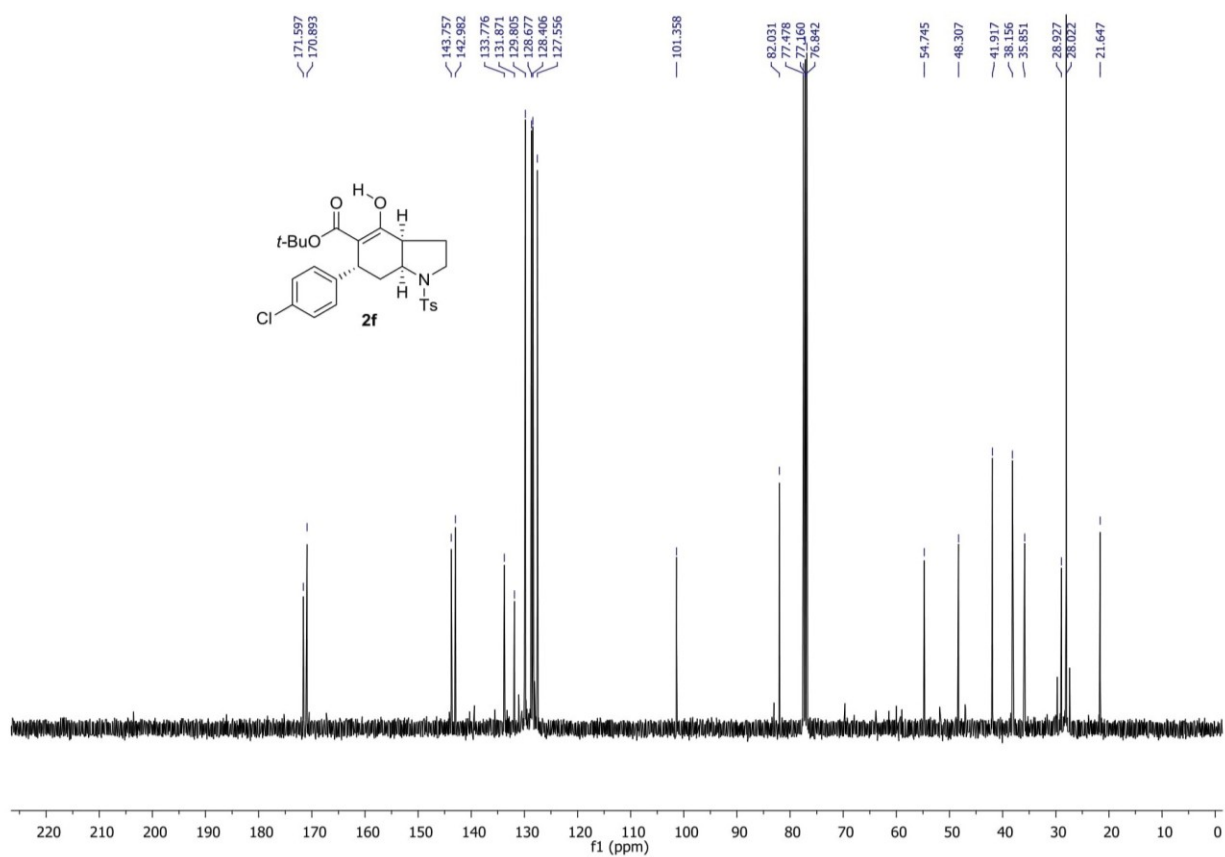
S21



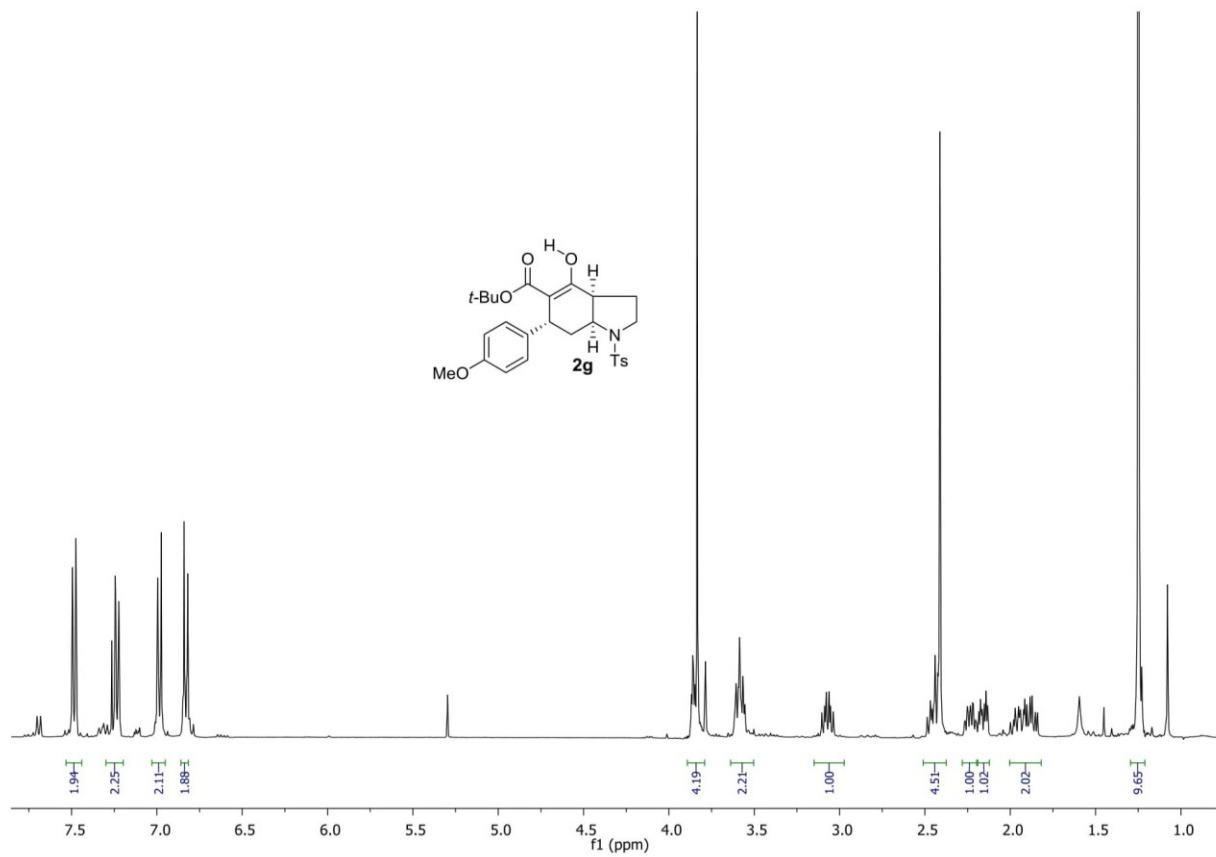
S22



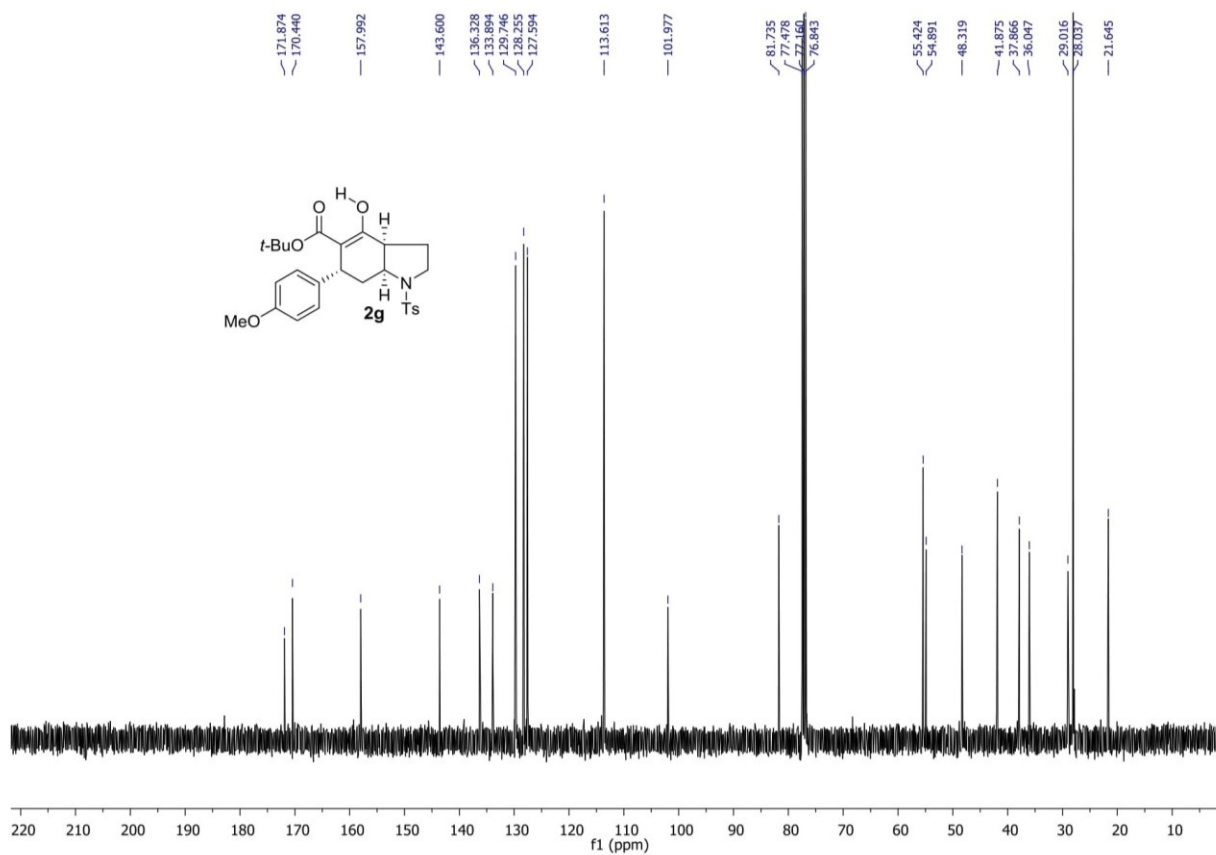
S23



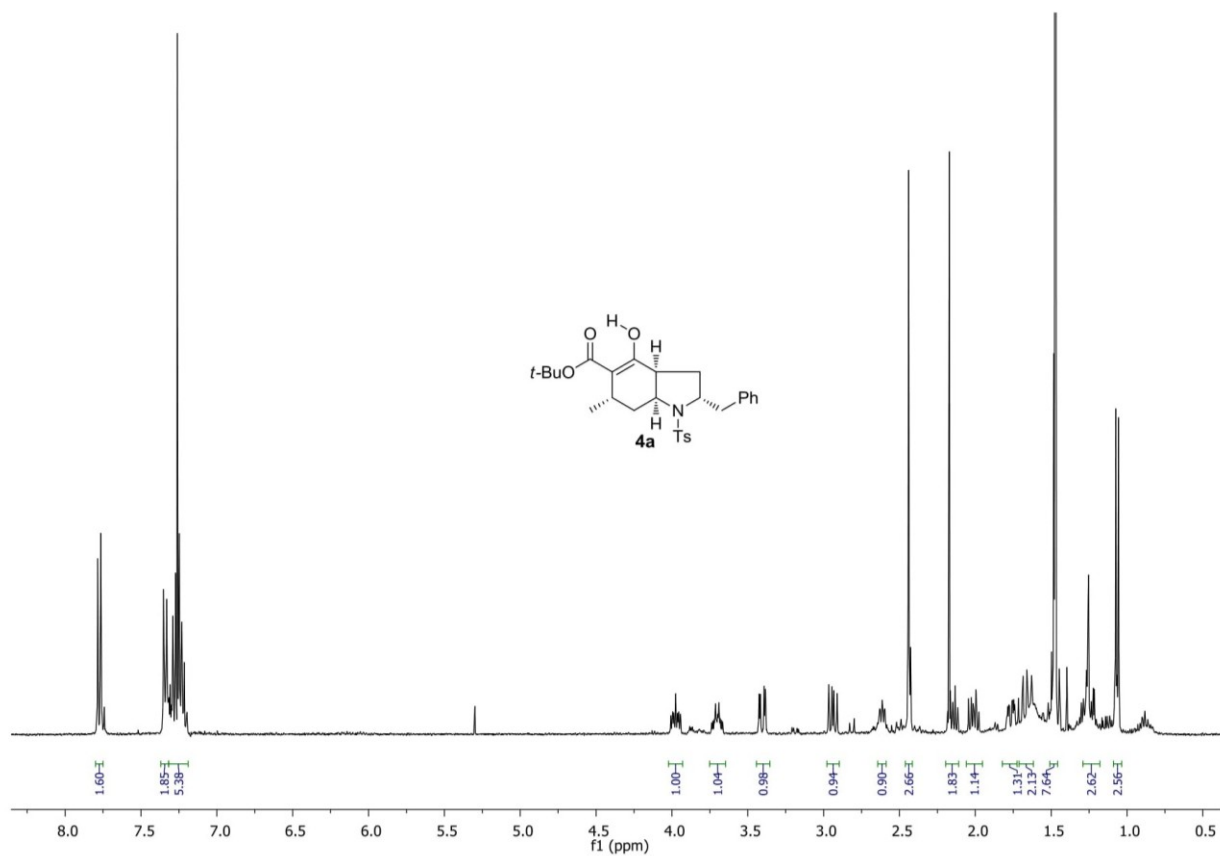
S24



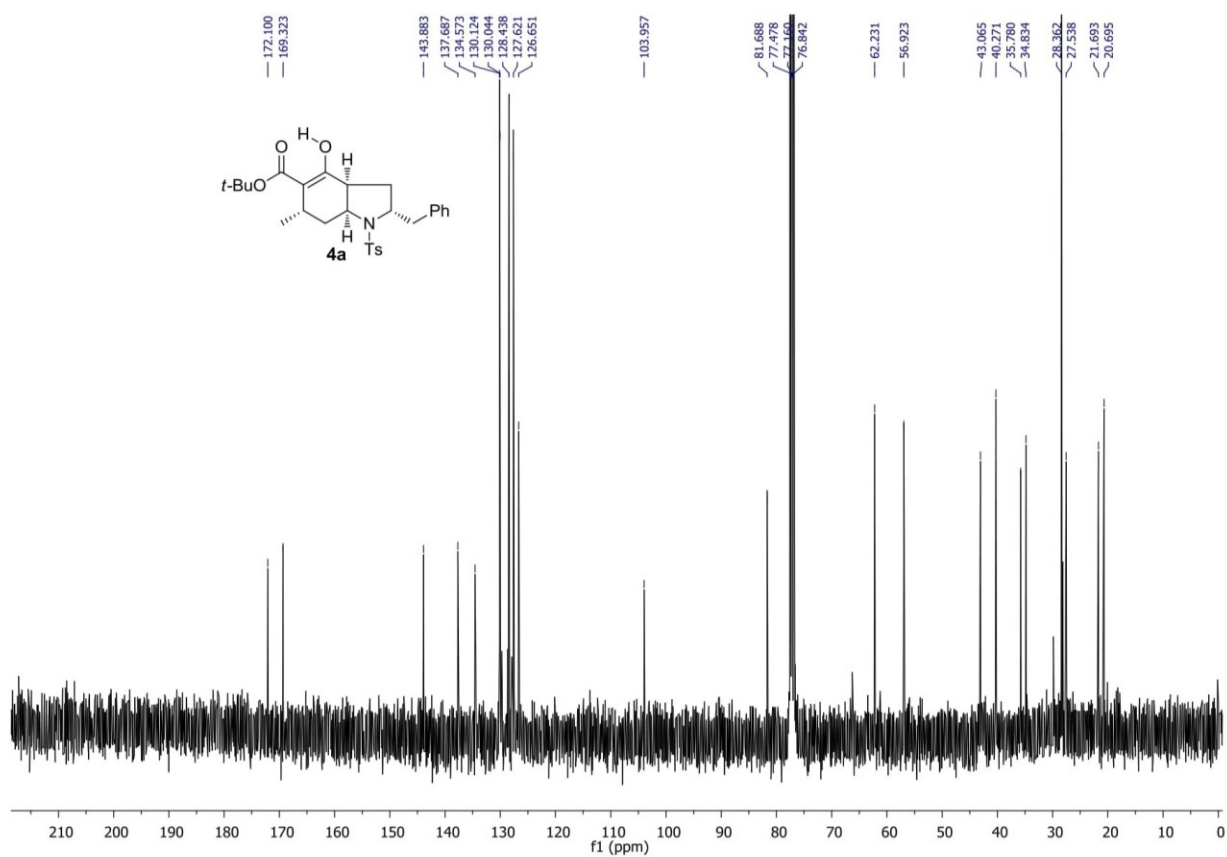
S25



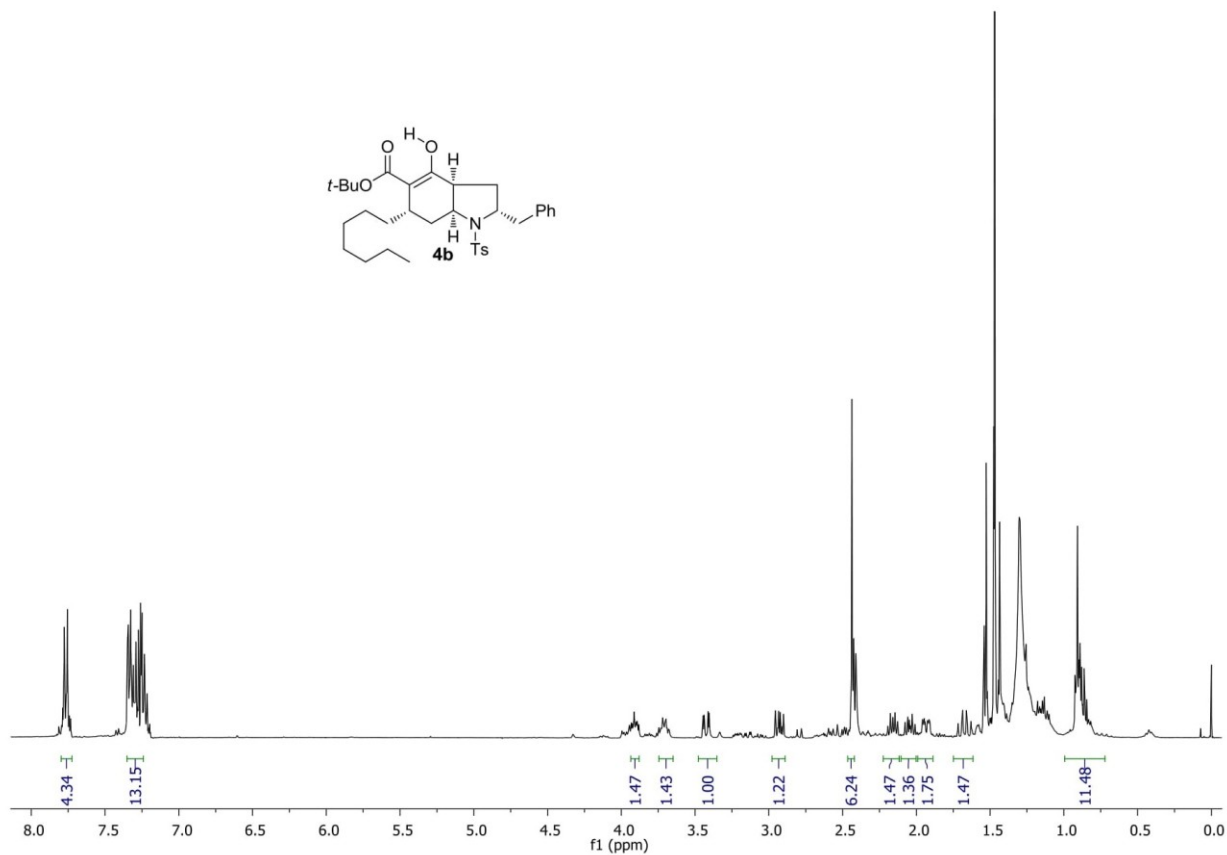
S26



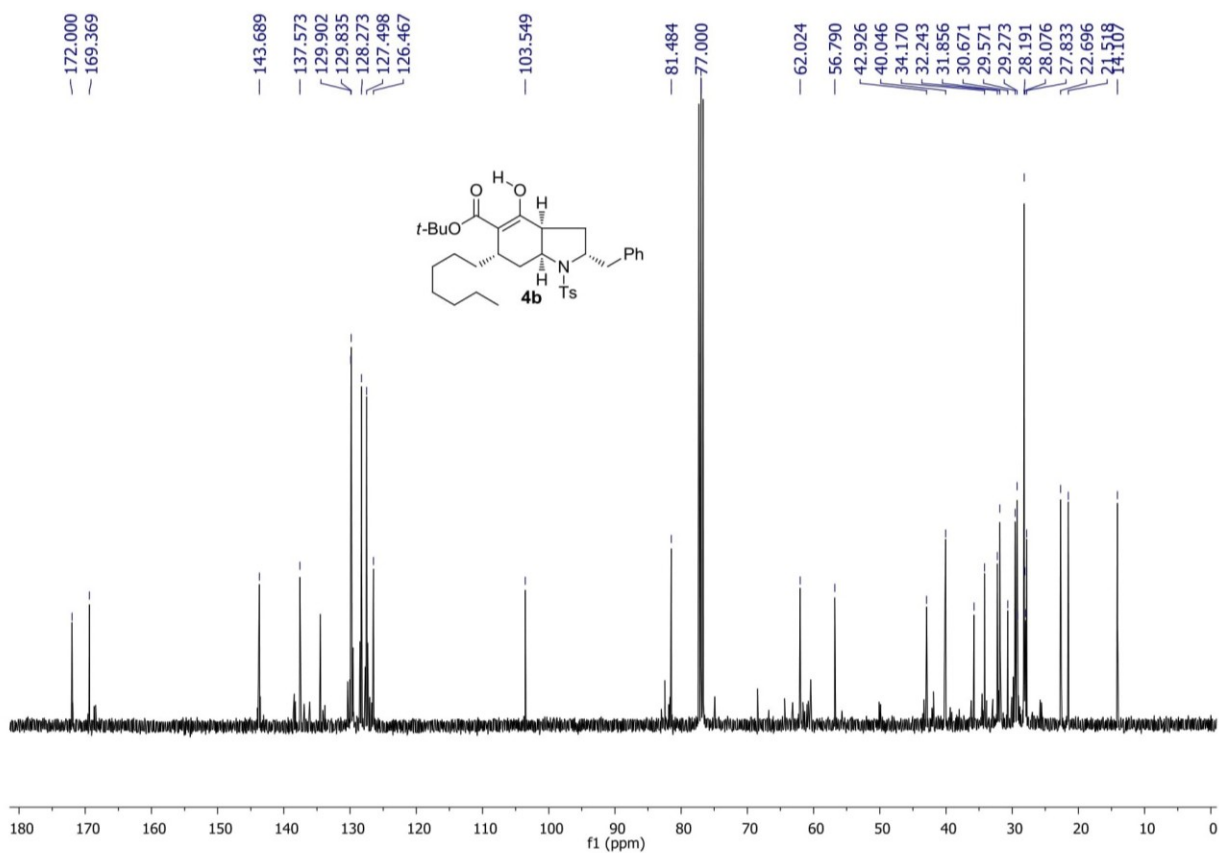
S27



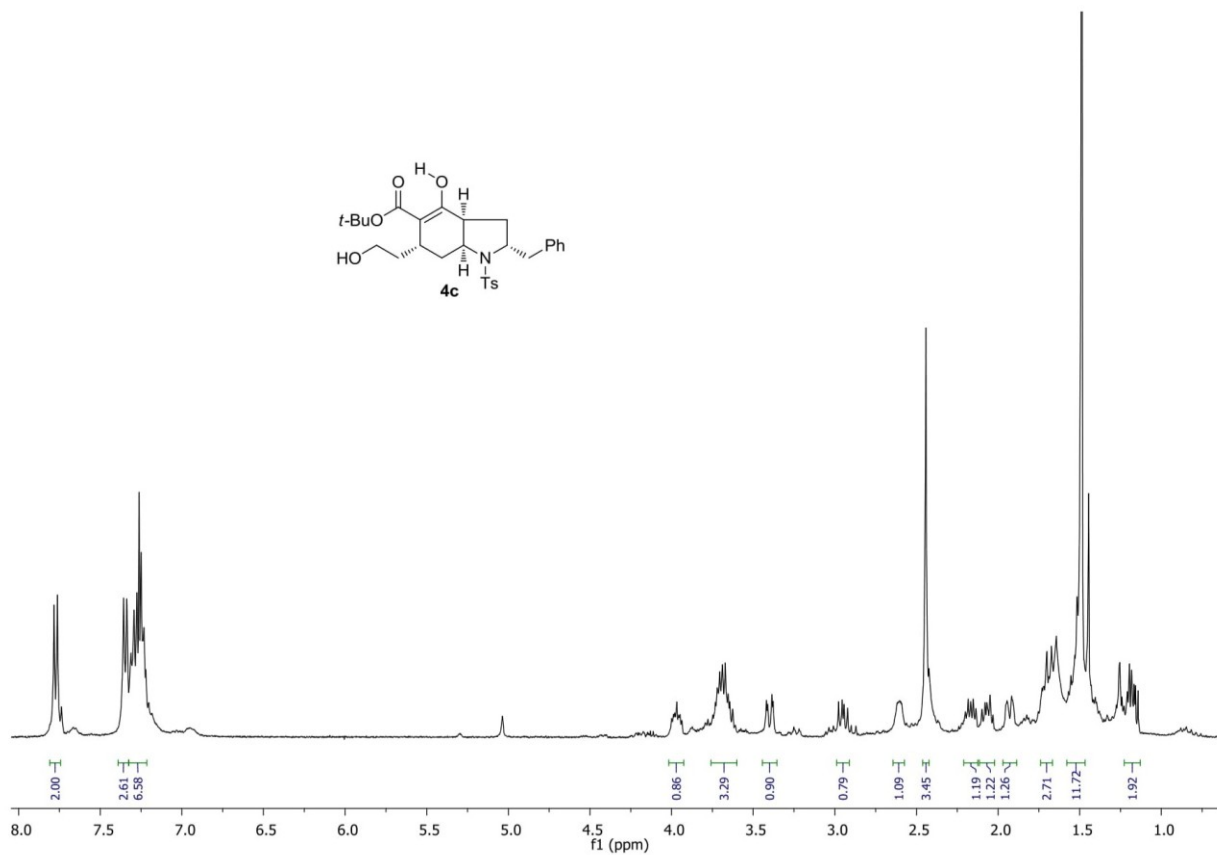
828



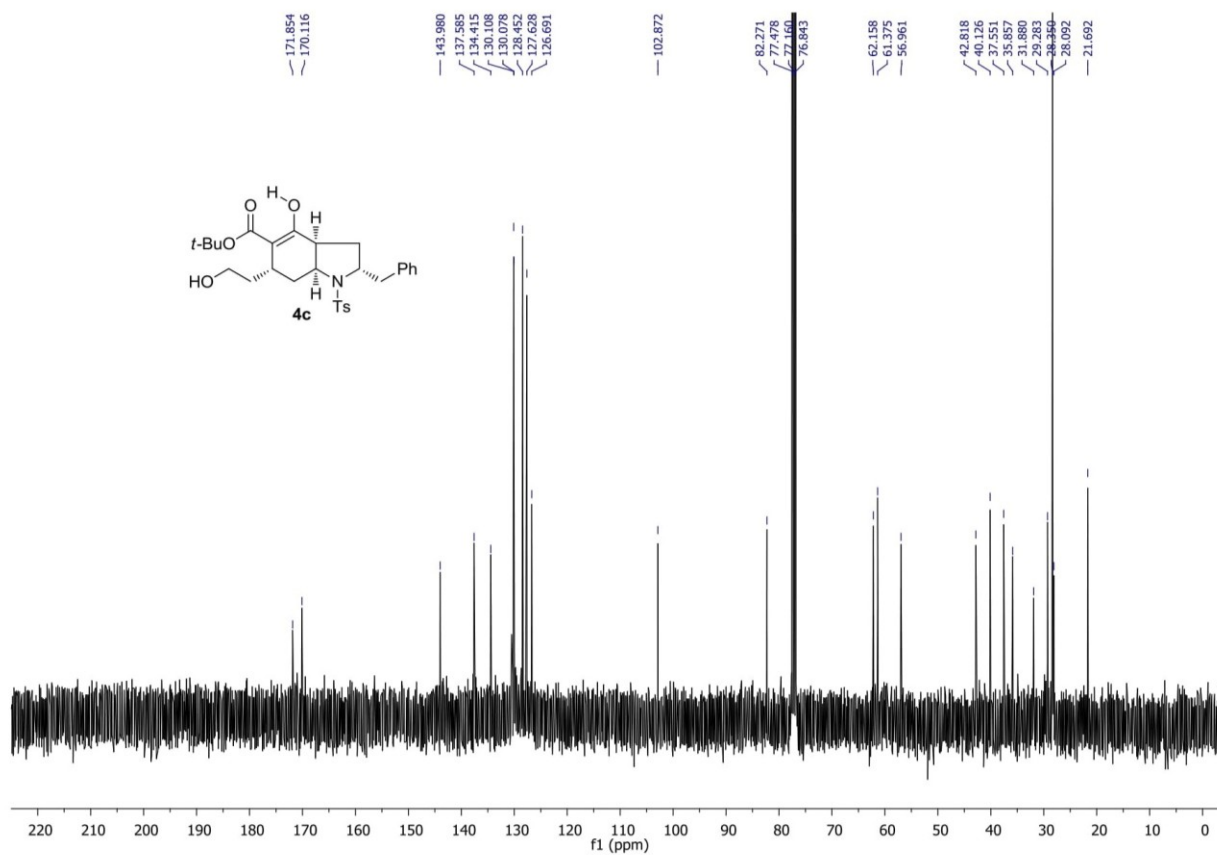
829



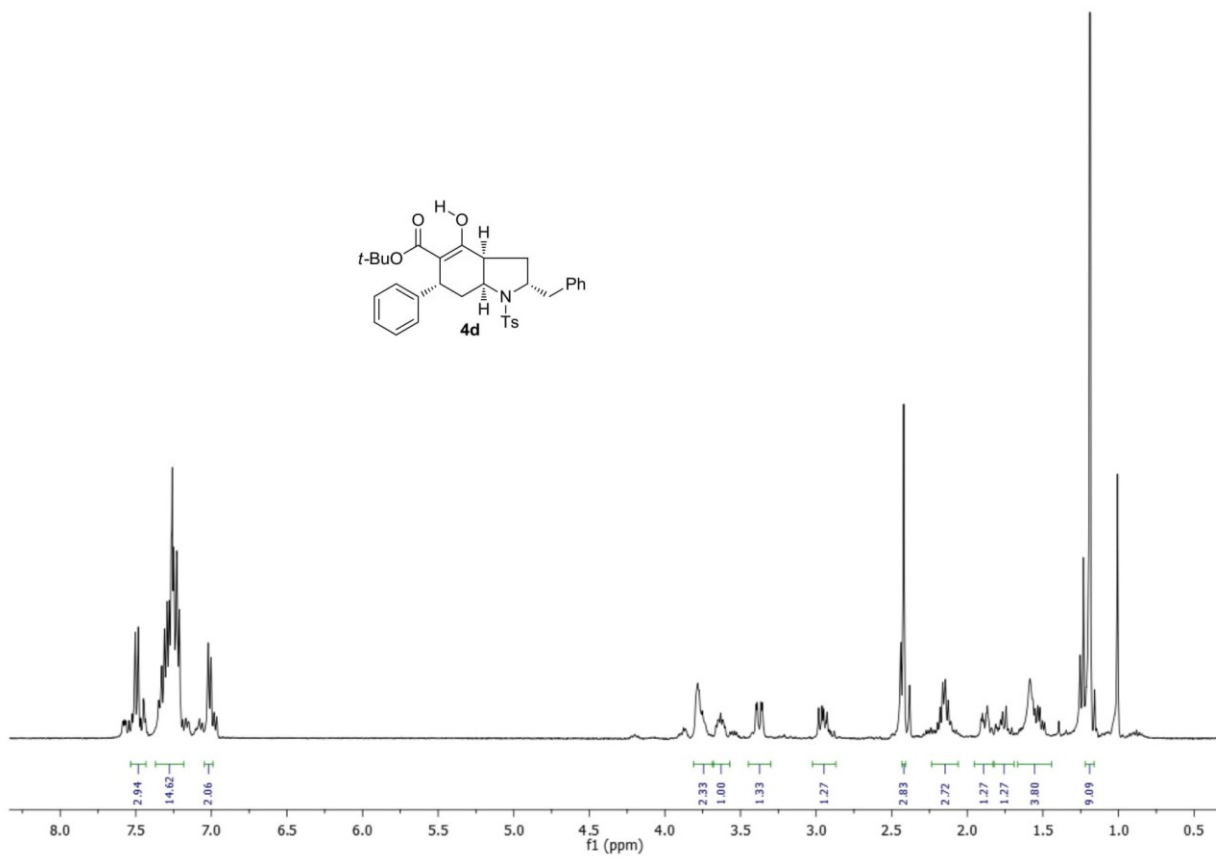
S30



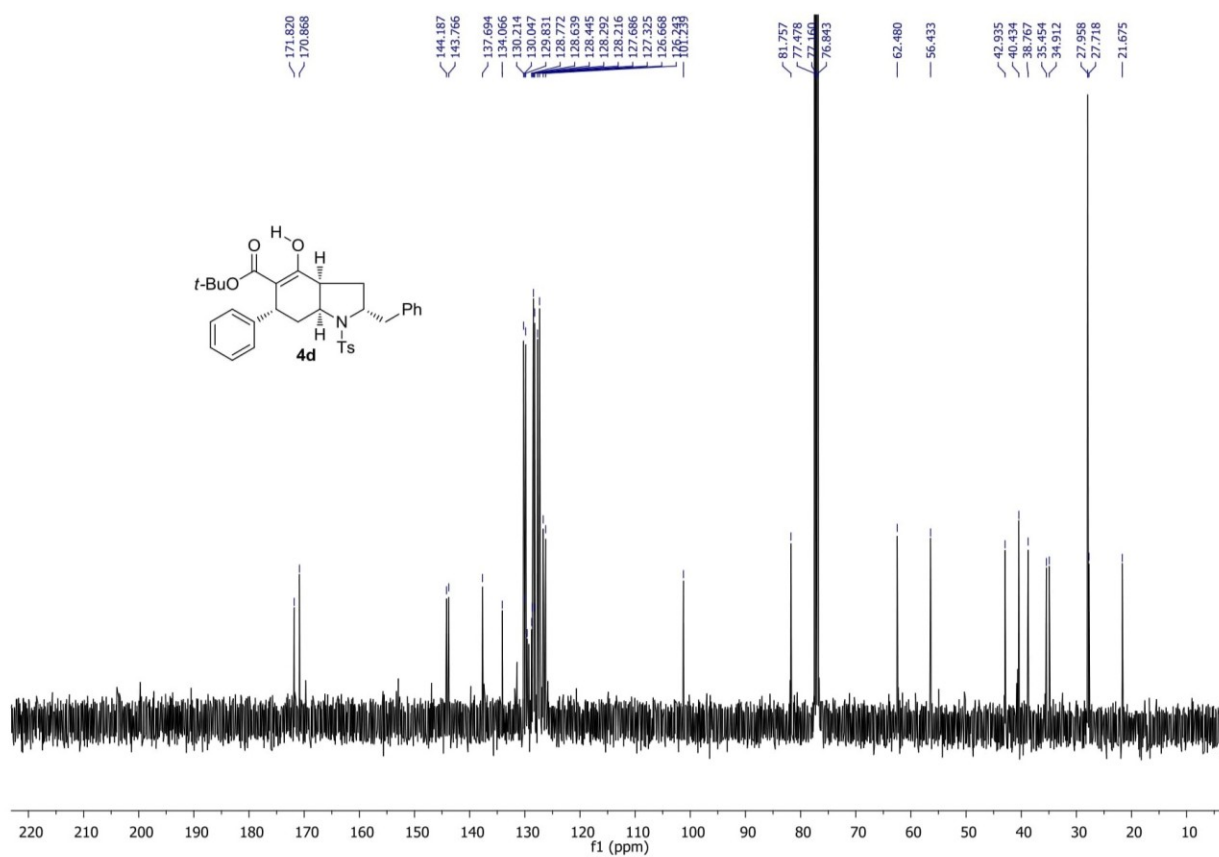
S31



S32



S33



Fischer Indole Reaction in Batch and Flow Employing a Sulfonic Acid Resin: Synthesis of Pyrido[2,3-*a*]carbazoles

Caroline Bosch¹, Pablo López-Lledó¹, Josep Bonjoch¹, Ben Bradshaw^{1*}, Pieter J. Nieuwland², Daniel Blanco-Ania³ and Floris P. J. T. Rutjes^{3*}

¹Laboratori de Química Orgànica, Facultat de Farmàcia, IBUB, Universitat de Barcelona, Av. Joan XXIII s/n, 08028-Barcelona, Spain

²FutureChemistry Holding BV, Toernooiveld 100, 6525 EC Nijmegen, The Netherlands

³Institute for Molecules and Materials, Radboud University, Heyendaalseweg 135, 6525 AJ Nijmegen, The Netherlands

Received: 29 April 2016; accepted: 31 May 2016

An Amberlite IR 120 H-promoted one-pot Fischer indolization from a *cis*-decahydroquinoline using a range of phenylhydrazines led to compounds with the pyrido[2,3-*a*]carbazole scaffold. The process may be conducted either in batch mode or in a continuous manner in a flow reactor. The stereochemical course of the Fischer indole reaction changed in going from using free phenylhydrazine to the corresponding hydrochloride in batch conditions, whereas, with the short reaction times in continuous flow, no changes due to isomerization processes were observed.

Keywords: Fischer indole synthesis, one-pot synthesis, continuous-flow synthesis, sulfonic acid resin, immobilized reagents, pyrido[2,3-*a*]carbazoles

Heterocyclic scaffolds bearing a tetrahydrocarbazole structural subunit and an additional nitrogen-containing ring are found in both natural products (alkaloids) and pharmacologically active compounds developed in medicinal chemistry research [1] (Figure 1). More particularly, a series of tetracyclic indoles has been reported as androgen receptor ligands [2], among which an unprecedented pyrido[2,3-*a*]carbazole scaffold was evaluated.

Considering this pharmacological interest in pyridocarbazole compounds [3] and the availability of *cis*-5-oxodecahydroquinolines [4], we decided to study the Fischer indole reaction on the latter compounds. Besides studying conventional batch-wise approaches, we were also interested in comparing those with continuous-flow procedures employing immobilized catalysts.

Conducting the Fischer indole synthesis using continuous-flow systems has caught the attention of several research groups in recent years [5]. The reaction rate of the Fischer indole synthesis can be significantly increased when run at higher temperatures and pressures or employing microwave irradiation, which renders this reaction highly suitable for new continuous-flow techniques. Moreover, a heterogeneous approach using a solid acid could avoid the potentially problematic clogging of micro-reactor devices due to the facile precipitation or crystallization of the indole and, eventually, allow for a one-pot process [6]. We thus decided to explore the solid acid-catalyzed Fischer indole synthesis using 5-oxo-*cis*-decahydroquinolines as the substrates.

Various catalytic methods have been reported for the Fischer indole synthesis [7], including the polymeric sulfonic acid resin Amberlite IR 120 H [8], which, despite its frequent use in ion exchange applications, has not been extensively used for this particular purpose [9]. The availability of the reagent, combined with its high ability to catalyze the Fischer indole synthesis, prompted us to choose it for this study. As a preliminary task, we decided to examine the behavior of cyclohexanone as model compound in batch and flow reaction conditions. As shown in Table 1, the use of Amberlite IR 120 H resin in a batch process readily and efficiently catalyzed the Fischer indole reaction of hydrazine **1a** with cyclohexanone under mild conditions (entry 1). It is interesting to note that the resin could be regenerated

without any loss of activity by simply stirring in a 10 % H₂SO₄ solution for 15–30 min (entry 2). These conditions were successfully applied to various substituted phenylhydrazines (entries 3–6), in all cases providing excellent isolated yields of products whose data correspond to the literature descriptions.

Encouraged by these results, we attempted to conduct the process under continuous-flow conditions. For this purpose, a 10-cm-long ETFE tubing (1/8" outer diameter, 1/16" inner diameter) packed with Amberlite IR 120 H (100 mg) and sealed with cotton wool was used as the reactor cartridge (100 μ L inner volume). The flow system consisted of two syringe pumps, a T-mixer unit for homogenization of the reaction mixture and a back pressure regulator (BPR), while the cartridge was submerged in an oil bath for heating.

Optimization of the residence time was performed (Table 2) using feed solutions of phenylhydrazine **1a** (0.5 M) and cyclohexanone (0.5 M) both dissolved in MeOH. Entries 2 and 4 illustrate that it was possible to shorten the reaction time to 10 min at 50 °C and even to 5 min at 90 °C for 0.5 M solutions of the reagents.

The straightforward regeneration of the catalyst proved rather useful in the flow process. It was possible to produce with a small cartridge of 100 μ L inner volume and 100 mg of resin up to 50 mg of pure product before observing any decrease in conversion. Then, as soon as a loss of efficiency was observed, a simple rinse of the resin with a 10 % H₂SO₄ solution for 15–30 min allowed full activity to be regained.

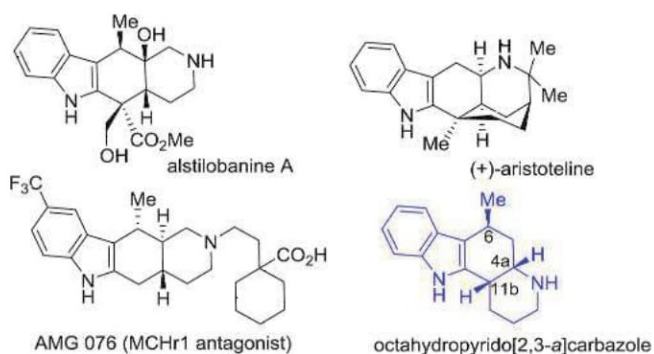
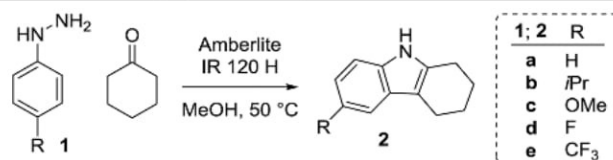


Figure 1. Pyridocarbazoles

* Authors for correspondence: josep.bonjoch@ub.edu (J. Bonjoch); F.Rutjes@science.ru.nl (P.J.T. Rutjes)

Table 1. Fischer indole synthesis of cyclohexanone with arylhydrazine using Amberlite IR 120 H (batch conditions)^a

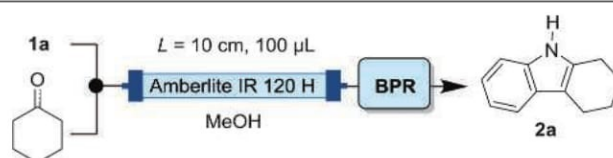
Entry ^a	R	Time (h)	Yield (%) ^b
1	H	1	97
2 ^c	H	1	96
3	<i>i</i> Pr	1.5	95
4	OMe	2	93
5	F	2	96
6	CF ₃ ^d	3	92

^a General procedure: arylhydrazine (1.1 equiv.) and sulfonic acid resin (5 equiv., w/w) were mixed in MeOH, followed by the addition of ketone (1.0 equiv.) and stir mixing at 50 °C for the indicated time.

^b Yields refer to isolated pure products.

^c The regenerated catalyst was used.

^d 6 Equiv. of hydrazine was used.

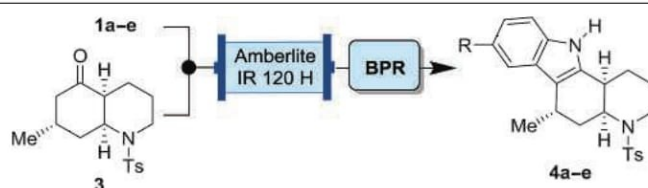
Table 2. Optimization of residence time in flow

Entry	Residence time (min)	Temperature (°C)	Conversion (%) ^a
1	5	50	62
2	10	50	100
3	2.5	90	57
4	5	90	100

^a Calculated by ¹H NMR.

Our first attempt to use this flow system with compound **3** and hydrazine **1a** gave, besides the anticipated product **4a**, the side product **5** arising from a retro-aza-Michael reaction, causing opening of the decahydroquinoline ring (Table 3, entry 1). This retro-aza-Michael reaction was attributed to ammonia

being formed as a side product of the Fischer indole reaction. This could be circumvented by using acetic acid as a cosolvent to immediately quench the ammonia in solution and, hence, prevent this ring-opening and formation of enone **5** (entry 2). A control experiment was performed by heating compounds **3** and

Table 3. Screening of flow conditions^a

Entry ^a	I ^b	Solvent	Residence time (min)	Conv.(%) ^c
1	1a	MeOH	10	44 ^d
2	1a	MeOH–AcOH	10	90
3	1a	MeOH–AcOH (1:1)	20	100 ^e
4	1b·HCl	MeOH–AcOH–DCE (9:7:4)	30	100 ^f
5	1c·HCl	MeOH–AcOH–DCE (7:2:1)	60	55
6	1d·HCl	MeOH–AcOH–DCE (14:5:1)	60	42
7	1e	MeOH–AcOH–DCE (5:4:1)	60	22

^a For detailed reaction conditions, see Supporting Information. Reactor cartridge: Entries 1–3: 10-cm long, packed with 100 mg Amberlite IR 120 H (100 µL inner volume). Entries 4–7: 1.0-m long, packed with 1000 mg Amberlite IR 120 H (1000 µL inner volume).

^b For **1** and **4**: a, R=H; b, R=*i*Pr; c, R=OMe; d, R=F; e, R=CF₃.

^c Determined from crude ¹H NMR spectra (unless otherwise stated, remaining product corresponds to a mix of starting material **3** and its corresponding hydrazine).

^d Formation of side product **5** (14%), see Scheme 1.

^e 76% Isolated yield.

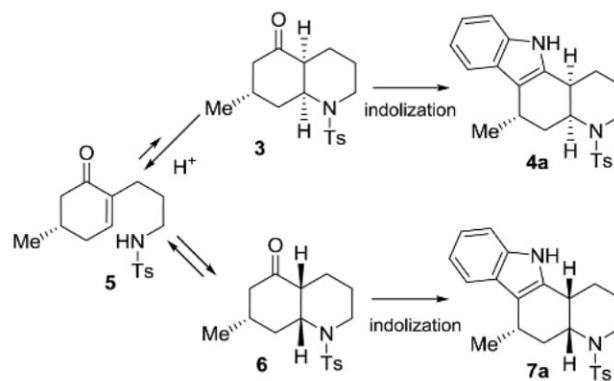
^f 75% Isolated yield.

1a in MeOH–AcOH for 20 min and 1 h at 70 °C. In both cases, only hydrazone intermediates were observed, showing the importance of the amberlite resin in the one-pot process. A short increase in reaction time allowed a clean and full conversion into the tetracyclic compound in 76% isolated yield under flow conditions (entry 3).

When the process was applied to *p*-substituted phenylhydrazines, some solubility problems were experienced, but these were solved by the dilution of feed solutions to 0.05 M and the use of adapted ternary solvent systems. This flow methodology, thus, allowed us to gain access to the different products **4a–e** in moderate to good yields (entries 4–7).

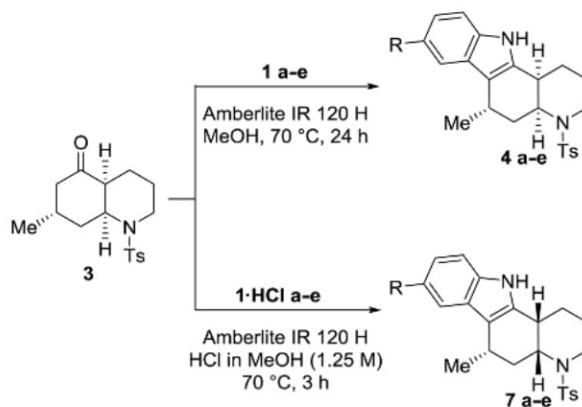
At that time, we decided to explore the Fischer indole synthesis from ketone **3** under more classic reaction conditions, but without performing the phenylhydrazone, i.e., carrying out the reaction in a one-pot/two-step procedure [10]. Application of batch reaction conditions, previously reported in Table 1, to compound **3** proved successful, although with a drastic increase in reaction time (24 h) and amount of phenylhydrazine (10 equiv.) required (Table 4, entry 1). A premix of the Amberlite acidic resin with the free hydrazone base prior to the addition of the decahydroquinoline **3** and refluxing for 24 h gave selective access to products **4a–e** (Scheme 1, entries 1–5 in Table 4). In cases of R = OMe, the free hydrazone base appeared too unstable (entry 3) [11], and in cases of R = CF₃, the reactions were too slow (entry 5) to obtain high yields.

Scheme 1. Batch Fischer indole synthesis from ketone **3**



On the other hand, when applying the above flow conditions reported in Table 3 to batch synthesis, we soon realized that the use of hydrochloride salts of the hydrazines gave a mixture of diastereoisomers **4** and **7** (see Table 4, entries 6–8). In order to promote a faster isomerization of the initial ketone **3** to **6**, which should be the precursor of **7**, more acidic reaction conditions were used. In fact, upon submitting **3** to an equilibration process to produce **6** followed by a Fischer indolization reaction, only compounds of type **7** were isolated. Thus, mixing of the hydrazone

AQ4 **Table 4.** Fischer indole synthesis of decahydroquinoline **3** in batch mode



Entry ^a	R	Method	Product	Yield ^b (%)
1	H	A	4a	88
2	<i>i</i> Pr	A	4b	84
3	OMe	A	4c	24 ^c
4	F	A	4d	73 ^d
5	CF ₃	A ^e	4e	8 ^f
6	H	B	4a+7a	21:79 ^g
7	<i>i</i> Pr	B	4b+7b	26:74 ^g
8	F	B	4d+7d	28:72 ^g
9	H	C	7a	92
10	H	C ^h	7a	66 (conversion)
11	<i>i</i> Pr	C	7b	88
12	OMe	C	7c	57
13	F	C	7d	82
14	CF ₃	C ⁱ	7e	16

AQ5 ^a General procedure: method A, entries 1–5: **1** (10 equiv.) and sulfonic acid resin (10 equiv., w/w) were mixed in MeOH; then, **3** (1 equiv.) was added and the mixture was stirred at 70 °C for 24 h; method B, entries 6–8: **1·HCl** (10 equiv.) and sulfonic acid resin (10 equiv., w/w) were mixed in MeOH; then, **3** (1 equiv.) was added and the mixture was stirred at 70 °C for 24 h; method C, entries 9–13: **1·HCl** (2.5 equiv.) and sulfonic acid resin (10 equiv., w/w) were mixed in HCl in MeOH (1.25 M); then, **3** (1 equiv.) was added and the mixture was stirred at 70 °C for 3 h.

^b Yields refer to isolated pure products.

^c Due to **1c** being unstable, the reaction was performed with **1c·HCl** affording a mixture **4c/7c** 1/1 (yield to **4c**: 24%).

^d Ketone **3** was also recovered (14%).

^e Reaction was run for 72 h.

^f A mixture **4e/7e** 1/1 (yield to **4e**: 8%) was obtained.

^g Ratio determined from the ¹H NMR of the reaction mixture after complete disappearance of starting material **3**.

^h The reaction was run without sulfonic acid resin, as a control experiment.

ⁱ The reaction was run for 24 h.

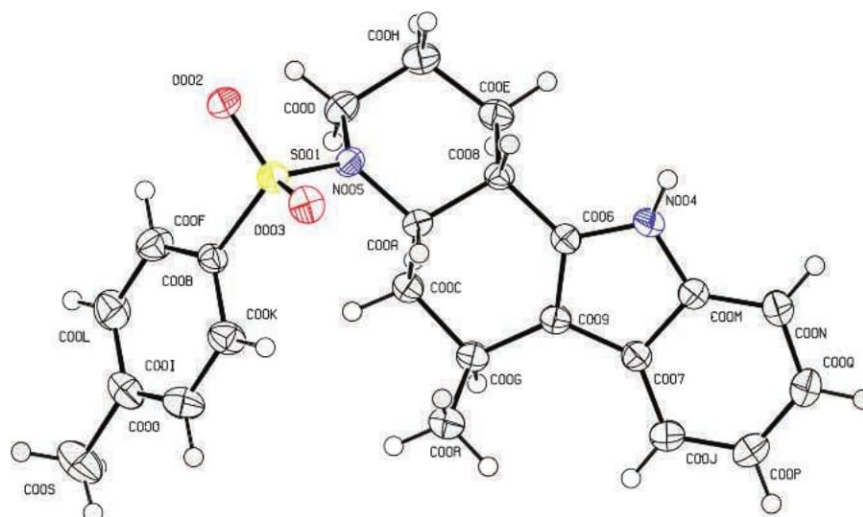


Figure 2. X-ray for compound 4a

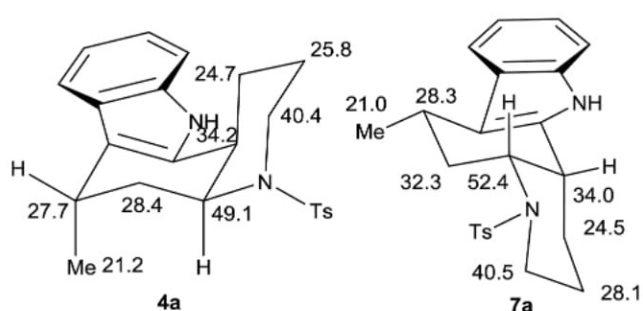


Figure 3. Conformations of pyridocarbazoles of types 4 and 7

hydrochloride salt, acidic amberlite, and decahydroquinoline **3** in a 1.25-M methanolic HCl solution prior to reflux for 3 h allowed a full retro-aza-Michael/aza-Michael cyclization towards the formation of compounds **7a–e** (entries 9–14).

The stereochemistry of pyridocarbazole **4a** was confirmed by X-ray crystallography (Figure 2), and the nuclear magnetic resonance (NMR) data allowed to establish a pattern of chemical shifts (^1H and ^{13}C) that were similar for the signals of the CD rings of compounds **4b–e**. For the isomeric pyridocarbazoles **7**, the major differences were observed for C(4a) and C(5) since, in this series, the methyl group at C(6) is located in an equatorial position (Figure 3 and NMR data in Tables S1 and S2 in Supporting Information).

In summary, in batch, the stereochemical outcome for the Fischer indolization from the protected β -amino ketone **3** is different when using phenylhydrazine or its hydrochloride salt (either alone or using HCl–MeOH as additive). In the latter case, prior to the indole ring formation [12], an initial isomerization of **3** via a retro-aza-Michael ring-opening followed by a recyclization to the more stable ketone **6** occurs, as we have previously observed in other transformations from ketone **3** [13]. In contrast, if the process is very fast, as occurs in the continuous-flow procedure, using either phenylhydrazine or its hydrochloride salt, the epimerization process is not observed.

Acknowledgment. Financial support for this research was provided by the projects CTQ2013-41338-P from the Ministry of Economy and Competitiveness of Spain and the FP7 Marie Curie Actions of the European Commission via the ITN ECHO-NET Network (MCITN-2012-316379).

Supporting Information

Electronic Supplementary Material (ESM) with experimental procedures, characterization data for all new compounds, and X-ray data for **4a** (CIF) is available in the online version at doi: 10.1556/1846.2016.00016.

References

- Zhao, F.; Li, N.; Zhu, Y.-F.; Han, Z.-Y. *Org. Lett.* **2016**, *18*, 1506–1509 and references therein.
- Zhang, X.; Li, X.; Allan, G. F.; Musto, A.; Lundeen, S. G.; Sui, A., *Bioorg. Med. Chem. Lett.* **2006**, *16*, 3233–3237.
- (a) Pagano, N.; Wong, E. Y.; Breiding, T.; Liu, H.; Wilbuer, A.; Bregman, H.; Shen, Q.; Diamond, S. L.; Meggers, E. *J. Org. Chem.* **2009**, *74*, 8997–9009; (b) Schmidt, A. W.; Reddy, K. R.; Knölker, H.-J. *Chem. Rev.* **2012**, *112*, 3193–3328; (c) Mihalic, J. T.; Fan, P.; Chen, X.; Chen, X.; Fu, Y.; Motani, A.; Liang, L.; Lindstrom, M.; Tang, L.; Chen, J.-L.; Jaen, J.; Dai, K.; Li, L. *Bioorg. Med. Chem. Lett.* **2012**, *22*, 3781–3785.
- Bradshaw, B.; Luque-Corredera, C.; Saborit, G.; Cativiela, C.; Dorel, R.; Bo, C.; Bonjoch, J. *Chem. Eur. J.* **2013**, *19*, 13881–13892.
- (a) Wahab, B.; Ellames, G.; Passey, S.; Watts, P. *Tetrahedron* **2010**, *66*, 3861–3865; (b) Pagano, N.; Heil, M. L.; Cosford, N. D. P. *Synthesis* **2012**, *44*, 2537–2546; (c) Gutmann, B.; Gottsponer, M.; Elsner, P.; Cantillo, D.; Roberge, D. M.; Kappe, C. O. *Org. Process Res. Dev.* **2013**, *17*, 294–302; (d) Ranasinghe, N.; Jones, G. B. *Current Green Chem.* **2015**, *2*, 66–76.
- For pioneering work in this field, see: Prochazka, M. P.; Carlson, R. *Acta Chem. Scand.* **1990**, *44*, 614–616.
- For recent studies on the Fischer indole synthesis, see: (a) Gore, S.; Baskaran, S.; König, B. *Org. Lett.* **2012**, *14*, 4568–4571; (b) Inman M.; Moody C. J. *Chem. Sci.* **2013**, *4*, 29–41; (c) Smith, J. M.; Moreno, J.; Boal, B. W.; Garg, N. K. *J. Org. Chem.* **2015**, *80*, 8954–8967.
- Yamada, S.; Chibata, I.; Tsurui, R. *Chem. Pharm. Bull.* **1953**, *1*, 14–16.
- Chandrasekhar, S.; Mukherjee, S. *Synth. Commun.* **2015**, *45*, 1018–1022.
- For one-pot/one-step microwave-assisted Fischer indole synthesis from ketones, see: Creencia, E. C.; Tsukamoto, M.; Horaguchi, T. *J. Heterocyclic Chem.* **2011**, *48*, 1095–1102.
- For the peculiarity of methoxy-substituted phenylhydrazones in Fischer indole synthesis, see: Murakami, Y. *Proc. Jpn. Acad., Ser. B.* **2012**, *88*, 1–17.
- Treatment of pyridocarbazole **4a** under acid conditions (HCl in MeOH 1.25 M, 10 equiv., MeOH–DCE–AcOH 6:3:6, 70 °C, 24 h) did not produce any level of isomerization to the isomer **7a**.
- Bradshaw, B.; Luque-Corredera, C.; Bonjoch, J. *Chem. Commun.* **2014**, *50*, 7099–7102.

Fischer Indole Reaction in Batch and Flow Employing a Sulfonic Acid Resin: Synthesis of Pyrido[2,3-*a*]carbazoles

Caroline Bosch,[†] Pablo López-Lledó,[†] Josep Bonjoch^{*,†}, Ben Bradshaw,[†] Pieter J. Nieuwland[‡], Daniel Blanco-Ania[§], and Floris P. J. T. Rutjes^{*,§}

[†] Laboratori de Química Orgànica, Facultat de Farmàcia, IBUB, Universitat de Barcelona, Av. Joan XXIII s/n, 08028-Barcelona, Spain

[‡] FutureChemistry Holding BV, Toernooiveld 100, 6525 EC Nijmegen, The Netherlands

[§] Institute for Molecules and Materials, Radboud University, Heyendaalseweg 135, 6525 AJ Nijmegen, The Netherlands

e-mail address: josep.bonjoch@ub.edu; F.Rutjes@science.ru.nl

Contents

General information	S2
Experimental procedures	S3
NMR tables of all compounds	S14
¹ H, ¹³ C-NMR spectra	S18
X-ray data for (4a)	S38

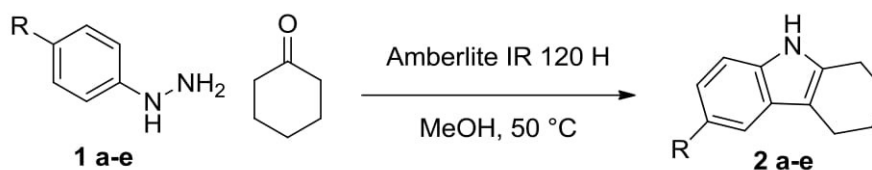
GENERAL INFORMATION

All reactions were carried out under an argon atmosphere in dry solvents under anhydrous conditions. Drying of organic extracts during workup of reactions was performed over anhydrous Na_2SO_4 except where otherwise stated. Evaporation of solvents was accomplished with a rotatory evaporator. Analytical thin layer chromatography was performed on SiO_2 (Merck silica gel 60 F₂₅₄) or on glass-backed plates pre-coated with silica and the spots were located with aqueous KMnO_4 or *p*-anisaldehyde. Chromatography refers to flash chromatography and was carried out on SiO_2 (silica gel 60 ACC, 35-75 μm , 230-240 mesh ASTM). NMR spectra were recorded in CDCl_3 on a Varian Mercury 400 MHz or Varian VNMRS 400 MHz. Chemical shifts of ^1H and ^{13}C NMR spectra are reported in ppm downfield (δ) from Me_4Si . All NMR data assignments are supported by COSY and HSQC experiments.

Melting points were performed on recrystallized solids and are uncorrected.

EXPERIMENTAL PROCEDURES

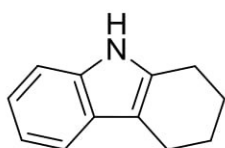
Batch Reactions



General procedure A:

To a stirring solution of cyclohexanone (1 equiv) and solid acid catalyst Amberlite IR 120 H[®] (5 equiv w/w) in MeOH (0.1-0.5 M) at 50 °C, was added phenylhydrazine **1** or phenylhydrazine hydrochloric salt **1·HCl** (1.1 equiv). The mixture was left stirring at 50 °C for the indicated time. After cooling, the reaction mixture was filtered and the resin was washed with CH₂Cl₂ and MeOH and the crude product was purified by crystallization from MeOH/H₂O to afford the pure carbazole.

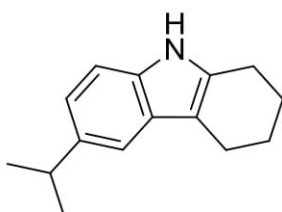
2,3,4,9-Tetrahydro-1H-carbazole (2a)



Following the general procedure using cyclohexanone (260 μ L, 2.5 mmol) and phenylhydrazine **1a** (270 μ L, 2.75 mmol) for 1 h, **2a** was isolated as a pale yellowish solid (415 mg, 97%) whose data proved consistent with the literature.¹

Mp: 115-119 °C (lit.^{1a} 119-120 °C); ¹H NMR (CDCl₃, 400 MHz): δ 1.85-1.98 (m, 4H), 2.70-2.76 (m, 4H), 7.06-7.16 (m, 2H), 7.28 (br d, J = 7.5 Hz, 1H), 7.48 (br d, J = 7.5 Hz, 1H) 7.63 (br s, 1H); ¹³C NMR (CDCl₃, 100 MHz): δ 21.1, 23.36, 23.40, 23.44, 110.3, 110.4, 117.9, 119.2, 121.1, 128.0, 134.2, 135.8

6-Isopropyl-2,3,4,9-tetrahydro-1H-carbazole (2b)



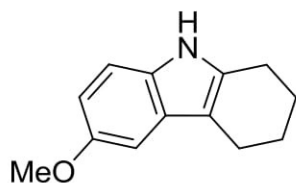
Following the general procedure using cyclohexanone (230 μ L, 2.2 mmol) and *p*-isopropylphenylhydrazine hydrochloride salt **1b·HCl** (467 mg, 2.4 mmol) for 1.5 h, **2b** was isolated as a pale yellowish solid (445 mg, 95%) whose data proved consistent with the literature.²

Mp: 67-69 °C (lit.² 68-70 °C); ¹H NMR (CDCl₃, 400 MHz): δ 1.34 (d, J = 7.0 Hz, 6 H), 1.87-1.98 (m, 4H), 2.69-2.77 (m, 4H), 3.04 (hep, J = 7.0 Hz, 1H), 7.04 (dd, J = 8.5, 2.0 Hz, 1H), 7.20 (d, J = 8.5 Hz, 1H), 7.34 (d, J = 2.0 Hz, 1H), 7.53 (br s, 1H); ¹³C NMR (CDCl₃, 100 MHz): δ 21.1, 23.39, 23.40, 23.5, 24.9, 34.4, 110.0, 110.2, 114.8, 120.1, 128.0, 134.3, 134.4, 140.0

¹ a) Welch W. M., *Synthesis*, **1977**, 9, 645-646 b) Sun K., Liu S., Bec P. M., and Driver T. G., *Ang. Chem. Int. Ed.* **2011**, 50, 1702-1706

² Yeung C. S., Ziegler R. E., Porco J. A., Jr. and Jacobsen E. N., *J. Am. Chem. Soc.*, **2014**, 136, 13614-13617

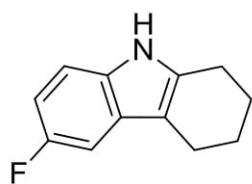
6-Methoxy-2,3,4,9-tetrahydro-1H-carbazole (2c)



Following the general procedure using cyclohexanone (230 μ L, 2.2 mmol) and *p*-methoxyphenylhydrazine hydrochloride salt **1c·HCl** (442 mg, 2.5 mmol) for 2 h, **2c** was isolated as a pale pink solid (389 mg, 93%) whose data proved consistent with the literature.^{3a}

Mp: 89-90 °C (lit. 91-92 °C); ¹H NMR (CDCl₃, 400 MHz): δ 1.83-1.95 (m, 4H), 2.65-2.75 (m, 4H), 3.87 (s, 3H), 6.78 (dd, *J* = 8.5, 2.5 Hz, 1H), 6.94 (d, *J* = 2.5 Hz, 1H), 7.16 (d, *J* = 8.5 Hz, 1H), 7.56 (br s, 1H); ¹³C NMR (CDCl₃, 100 MHz): δ 21.1, 23.3, 23.4, 23.5, 56.1, 100.4, 110.1, 110.6, 111.1, 128.3, 130.9, 135.2, 154.0

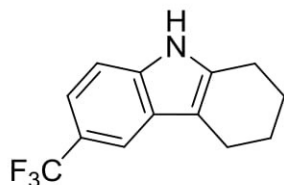
6-Fluoro-2,3,4,9-tetrahydro-1H-carbazole (2d)



Following the general procedure using cyclohexanone (230 μ L, 2.2 mmol) and *p*-fluorophenylhydrazine hydrochloride salt **1d·HCl** (408 mg, 2.5 mmol) for 2 h, **2d** was isolated as a pale yellowish solid (389 mg, 93%) whose data proved consistent with the literature.³

Mp: 103-104 °C (lit.³ 106-108 °C); ¹H NMR (CDCl₃, 400 MHz): δ 1.83-1.96 (m, 4H), 2.64-2.74 (m, 4H), 6.85 (td, *J* = 9.5, 2.5 Hz, 1H), 7.10 (dd, *J* = 9.5, 2.5 Hz, 1H), 7.17 (dd, *J* = 9.0, 4.5 Hz, 1H), 7.65 (br s, 1H); ¹³C NMR (CDCl₃, 100 MHz): δ 21.0, 23.2, 23.3, 23.4, 103.0 (d, *J* = 23.5 Hz), 108.9 (d, *J* = 26.0 Hz), 110.6, 110.8 (d, *J* = 9.5 Hz), 128.3, 132.2, 136.3, 157.9 (d, *J* = 232 Hz)

6-Trifluoromethyl-2,3,4,9-tetrahydro-1H-carbazole (2e)

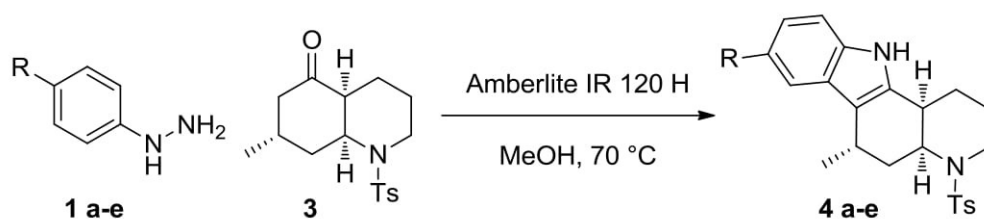


Following the general procedure using cyclohexanone (104 μ L, 1 mmol), *p*-trifluoromethylphenylhydrazine **1e** (1.05 g, 6.0 mmol) and Amberlite IR 120 H (2.7g) for 3 h, filtration on silica with 10% EtOAc /hexane prior to crystallization affords **2e** as brown yellow solid (220 mg, 92%) whose data proved consistent with the literature.⁴

¹H NMR (CDCl₃, 400 MHz): δ 1.85-1.98 (m, 4H), 2.70-2.77 (m, 4H), 7.30-7.38 (m, 2H), 7.75 (s, 1H), 7.83 (br s, 1H); ¹³C NMR (CDCl₃, 100 MHz): δ 20.8, 23.1, 23.2, 23.3, 110.5, 111.2, 115.5 (q, *J* = 4.2 Hz), 117.9 (q, *J* = 3.6 Hz), 121.6 (q, *J* = 31.4 Hz), 125.7 (q, *J* = 269.6 Hz), 127.4, 136.1, 137.1

³ a) Chen J. and Hu Y., *Synth. Comm.* **2006**, *36*, 1485 b) Sun K., Liu S., Bec P. M., and Driver T. G., *Ang. Chem. Int. Ed.* **2011**, *50*, 1702-1706

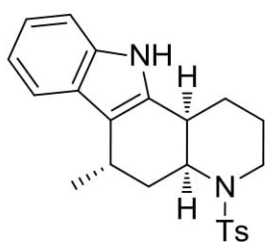
⁴ Desroses M., Wieckowski K., Stevens M. and Odell L. R., *Tet. Lett.* **2011**, *52*, 4417-4420



General procedure B:

A stirring solution of phenylhydrazine (10 equiv) and solid acid catalyst Amberlite IR 120 H[®] (10 equiv w/w with respect to **3**) in MeOH (0.05-0.1 M) was mixed for 5 min at 70 °C. To this mixture was added ketone **3** (1 equiv). The mixture was left stirring at 70 °C for 24 h. After cooling, the reaction mixture was filtered and the resin was washed with CH₂Cl₂ and MeOH and the crude product was purified by crystallization from cold MeOH or cold CH₂Cl₂ to afford the pure carbazole product.

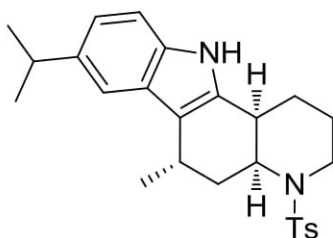
(4aRS,6RS,11bRS)-6-Methyl-4-(4-methylphenylsulfonyl)-2,3,4,4a,5,6,11,11b-octahydro-1H-pyrido[3,2-*a*]carbazole (4a)



Following the general procedure B using phenylhydrazine **1a** (915 μL , 9.33 mmol), 5-oxodecahydroquinoline **3** (300 mg, 0.93 mmol) and Amberlite IR 120 H[®] (3 g) for 20 h, **4a** was isolated as a pale yellow solid (320 mg, 88%) further crystallization from CHCl₃ and dichloroethane afforded pale yellow crystal.

Mp: 213-215 °C; ¹H NMR (COSY, CDCl₃, 400 MHz): δ 1.28-1.38 (m, 1H, H-5eq), 1.32 (d, $J = 7.2$ Hz, 3H, H-12), 1.53-1.61 (m, 2H, H-1 and H-2), 1.65-1.70 (m, 1H, H-2), 1.92-2.01 (m, 1H, H-1), 2.31 (ddd, $J = 12.8, 12.8, 6.0$ Hz, 1H, H-5ax), 2.45 (s, 3H, H-17), 2.88 (ddd, $J = 10.4, 5.2, 5.2$ Hz, 1H, H-11b), 2.97 (ddd, $J = 12.8, 12.8, 2.8$ Hz, 1H, H-3ax), 3.21 (br quint, $J = 7.0$ Hz, 1H, H-6), 3.95 (br d, $J = 13.2$ Hz, 1H, H-3eq), 4.56 (ddd, $J = 13.2, 5.2, 3.2$ Hz, 1H, H-4a), 7.05-7.15 (m, 2H, H-8 and H-9), 7.27 (d, $J = 8.0$ Hz, 1H, H-10), 7.31 (d, $J = 8.0$ Hz, 2H, H-15), 7.47 (d, $J = 7.6$ Hz, 1H, H-7), 7.66 (br s, 1H, H-11), 7.76 (d, $J = 8.4$ Hz, 2H, H-14); ¹³C NMR (100 MHz, HSQC, CDCl₃): δ 21.2 (C-12), 21.5 (C-17), 24.7 (C-2), 25.8 (C-6), 27.7 (C-1), 28.4 (C-5), 34.2 (C-11b), 40.5 (C-3), 49.1 (C-4a), 110.7 (C-10), 113.5 (C-6a), 118.3 (C-7), 119.3 (C-8), 121.5 (C-9), 126.5 (C-6b), 127.0 (C-14), 129.7 (C-15), 135.8 (C-10a), 136.2 (C-13), 138.5 (C-16), 143.1 (C-11a); HRMS: m/z calcd for C₂₃H₂₇N₂O₂S (M + H)⁺ 395.1788, found 395.1801

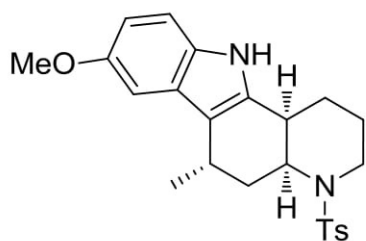
(4aRS,6RS,11bRS)-8-Isopropyl-6-methyl-4-(4-methylphenylsulfonyl)-2,3,4,4a,5,6,11,11b-octahydro-1H-pyrido[3,2-*a*]carbazole (4b)



Following the general procedure B using *p*-isopropylphenylhydrazine **1b** (467 mg, 3.11 mmol), 5-oxodecahydroquinoline **3** (100 mg, 0.31 mmol) and Amberlite IR 120 H[®] (1.00 g) for 20 h **4b** was isolated after trituration in cold MeOH and recrystallization in dichloroethane as a white solid (103 mg, 84%).

Mp:161-163 °C; ¹H NMR (COSY, CDCl₃, 400 MHz): δ 1.25-1.35 (m, 1H, H-5eq), 1.30 (br d, *J* = 6.8 Hz, 6H, 2 x CH₃ *i*Pr), 1.33 (d, *J* = 7.2 Hz, 3H, H-12), 1.52-1.59 (m, 2H, H-1 and H-2), 1.62-1.68 (m, 1H, H-2), 1.92-1.98 (m, 1H, H-1), 2.30 (ddd, *J* = 13.2, 13.2, 6.4 Hz, 1H, H-5ax), 2.45 (s, 3H, H-17), 2.85 (ddd, *J* = 11.6, 5.0, 5.0 Hz, 1H, H-11b), 2.91-3.05 (m, 2H, H-3ax & CH *i*Pr), 3.20 (br quint, *J* = 7.2 Hz, 1H, H-6), 3.94 (br d, *J* = 12.4 Hz, 1H, H-3eq), 4.56 (ddd, *J* = 13.2, 5.0, 3.2 Hz, 1H, H-4a), 7.02 (dd, *J* = 8.4, 2.0 Hz, 1H, H-9), 7.20 (br d, *J* = 8.4 Hz, 1H, H-10), 7.27-7.37 (m, 3H, H-7 & H-15), 7.56 (br s, 1H, H-11), 7.76 (d, *J* = 8.4 Hz, 2H, H-14); ¹³C NMR (100 MHz, HSQC, CDCl₃): δ 21.2 (C-12), 21.5 (C-17), 24.68 (C-2), 24.75 (CH₃ *i*Pr), 25.8 (C-6), 27.7 (C-1), 28.5 (C-5), 34.25 (CH *i*Pr), 34.28 (C-11b), 40.5 (C-3), 49.1 (C-4a), 110.5 (C-10), 113.3 (C-6a), 115.3 (C-7), 120.5 (C-9), 126.5 (C-6b), 127.0 (C-14), 129.7 (C-15), 134.8 (C-10a), 136.0 (C-8), 138.5 (C-13), 140.2 (C-16), 143.0 (C-11a); HRMS: *m/z* calcd for C₂₆H₃₃N₂O₂S (M + H)⁺ 437.2257, found 437.2256

(4a*RS*,6*RS*,11*BS*)-8-Methoxy-6-methyl-4-(4-methylphenylsulfonyl)-2,3,4,4a,5,6,11,11b-octahydro-1*H*-pyrido[3,2-*a*]carbazole (4c)

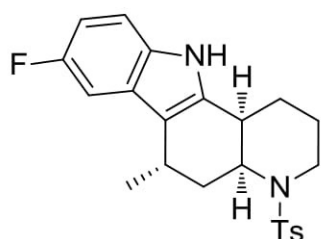


A stirring solution of *p*-methoxyphenylhydrazine hydrochloride **1c** (380 mg, 2.17 mmol), and solid acid catalyst Amberlite IR 120 H[®] (350 mg, 5 equiv w/w with respect to **3**) in MeOH (2.1 mL, 0.1M) was mix for 5 minutes at 70 °C. On this mixture was added the 5-oxodecahydroquinoline **3** (70 mg, 0.22 mmol). The mixture was left stirring at 70 °C for 24 h. After cooling, the reaction mixture was filtered and the resin

was washed with CH₂Cl₂ and MeOH and the crude product was purified by chromatography (10-25-50% EtOAc/hexane) to afford 69 mg of a mixture **4c/7c** in a ratio 33/67 (yield of **4c**: 24%). (NMR data of **4c** were determined by removing signals of **7c**).

¹H NMR (COSY, CDCl₃, 400 MHz): δ 1.28-1.35 (m, 1H, H-5eq), 1.31 (d, *J* = 7.2 Hz, 3H, H-12), 1.50-1.62 (m, 2H, H-1 and H-2), 1.62-1.70 (m, 1H, H-2), 1.92-2.00 (m, 1H, H-1), 2.31 (ddd, *J* = 12.8, 12.8, 6.0 Hz, 1H, H-5ax), 2.44 (s, 3H, H-17), 2.80-2.88 (m, 1H, H-11b), 2.92-3.02 (m, 1H, H-3ax), 3.12-3.20 (m, 1H, H-6), 3.83 (s, 3H, OMe), 3.95 (br d, *J* = 12.8 Hz, 1H, H-3eq), 4.55 (ddd, *J* = 13.2, 5.2, 2.8 Hz, 1H, H-4a), 6.78 (dd, *J* = 8.4, 2.4 Hz, 1H, H-9), 6.91 (d, *J* = 2.4 Hz, 1H, H-7), 7.16 (d, *J* = 8.4 Hz, 1H, H-10), 7.31 (d, *J* = 8.0 Hz, 2H, H-15), 7.53 (br s, 1H, H-11), 7.75 (d, *J* = 8.4 Hz, 2H, H-14); ¹³C NMR (100 MHz, HSQC, CDCl₃): δ 21.0 (C-12), 21.5 (C-17), 24.7 (C-2), 25.8 (C-6), 27.8 (C-1), 28.5 (C-5), 34.3 (C-11b), 40.5 (C-3), 49.1 (C-4a), 56.0 (OMe), 100.9 (C-7), 111.0 (C-9), 111.4 (C-10), 113.4 (C-6a), 126.9 (C-6b), 127.0 (C-14), 129.7 (C-15), 131.3 (C-10a), 136.8 (C-13), 138.5 (C-16), 143.0 (C-11a), 153.9 (C-8); HRMS: *m/z* calcd for C₂₄H₂₉N₂O₃S (M + H)⁺ 425.1893, found 425.1881

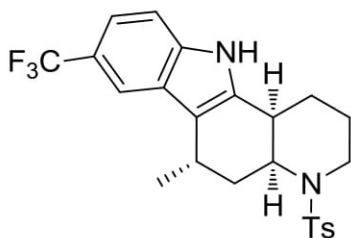
(4a*RS*,6*RS*,11*BS*)-8-Fluoro-6-methyl-4-(4-methylphenylsulfonyl)-2,3,4,4a,5,6,11,11b-octahydro-1*H*-pyrido[3,2-*a*]carbazole (4d)



Following the general procedure B using *p*-fluorophenylhydrazine **1d** (392 mg, 3.11 mmol), 5-oxodecahydroquinoline **3** (100 mg, 0.31 mmol) and Amberlite IR 120 H[®] (1.00 g) for 20 h, **4d** was isolated after trituration in cold MeOH and recrystallization in dichloroethane as a white solid (96 mg, 75%).

Mp: 242-244 °C; ^1H NMR (COSY, CDCl_3 , 400 MHz): δ 1.25-1.35 (m, 1H, H-5eq), 1.29 (d, $J = 6.8$ Hz, 3H, H-12), 1.52-1.63 (m, 2H, H-1 and H-2), 1.63-1.73 (m, 1H, H-2), 1.92-2.02 (m, 1H, H-1), 2.30 (ddd, $J = 12.8, 12.8, 6.2$ Hz, 1H, H-5ax), 2.45 (s, 3H, H-17), 2.87 (ddd, $J = 11.6, 5.0, 5.0$ Hz, 1H, H-11b), 2.96 (br t, $J = 12.8$ Hz, 2H, H-3ax), 3.14 (br quint, $J = 6.8$ Hz, 1H, H-6), 3.94 (br d, $J = 12.8$ Hz, 1H, H-3eq), 4.54 (ddd, $J = 13.2, 5.2, 3.2$ Hz, 1H, H-4a), 6.86 (ddd, $J = 8.8, 8.8, 2.4$ Hz, 1H, H-9), 7.09 (dd, $J = 9.0, 2.4$ Hz, 1H, H-7), 7.17 (dd, $J = 8.8, 4.4$ Hz, 1H, H-10), 7.31 (d, $J = 8.4$ Hz, 1H, H-15), 7.64 (br s, 1H, H-11), 7.75 (d, $J = 8.4$ Hz, 2H, H-14); ^{13}C NMR (100 MHz, HSQC, CDCl_3): δ 21.0 (C-12), 21.5 (C-17), 24.7 (C-2), 25.7 (C-6), 27.7 (C-1), 28.3 (C-5), 34.3 (C-11b), 40.4 (C-3), 49.0 (C-4a), 103.4 (d, $J = 23.3$ Hz, C-7), 109.5 (d, $J = 26.1$ Hz, C-9), 111.2 (d, $J = 9.6$ Hz, C-10), 113.8 (C-6a), 126.9 (C-6b), 127.0 (C-14), 129.7 (C-15), 132.7 (C-10a), 137.8 (C-13), 138.4 (C-16), 143.1 (C-11a), 157.7 (d, $J = 234.4$ Hz, C-8); HRMS: m/z calcd for $\text{C}_{23}\text{H}_{26}\text{FN}_2\text{O}_2\text{S}$ ($M + \text{H}$) $^+$ 413.1694, found 413.1684

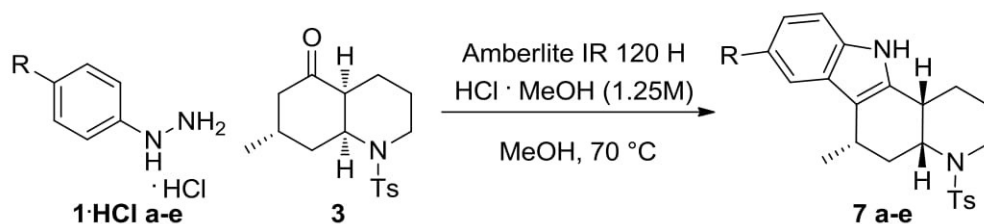
(4a*RS*,6*RS*,11*bRS*)-8-Trifluoromethyl-6-methyl-4-(4-methylphenylsulfonyl)-2,3,4,4a,5,6,11,11b-octahydro-1*H*-pyrido[3,2-*a*]carbazole (4e)



Following the general procedure B using *p*-trifluoromethylphenylhydrazine **1e** (548 mg, 3.11 mmol), 5-oxodecahydroquinoline **3** (100 mg, 0.31 mmol) and Amberlite IR 120 H $^{\circ}$ (1.00 g) for 72 h. Purification by chromatography (10-25-50% EtOAc/hexane) followed by trituration in cold MeOH allowed to obtain a mixture **4e/7e** in a ratio 75/25 (yield of **4e**: 8 mg, 5.5%). Another fraction was isolated 19 mg

containing 50% of **4e/7e** 1/2. The remaining part corresponding to hydrazone and 5-oxodecahydroquinoline **3** (yield of **4e** combined: 8%). (NMR data of **4e** were determined by removing signals of **7e**).

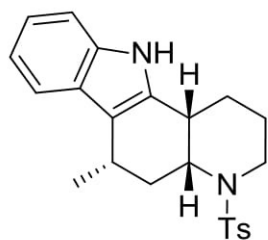
^1H NMR (COSY, CDCl_3 , 400 MHz): δ 1.28-1.35 (m, 1H, H-5eq), 1.32 (d, $J = 6.8$ Hz, 3H, H-12), 1.52-1.63 (m, 2H, H-1 & H-2), 1.66-1.73 (m, 1H, H-2), 1.95-2.05 (m, 1H, H-1), 2.31 (ddd, $J = 13.2, 13.2, 6.8$ Hz, 1H, H-5ax), 2.45 (s, 3H, H-17), 2.89-3.08 (m, 2H, H-3ax & H-11b), 3.22 (quint, $J = 6.8$ Hz, 1H, H-6), 3.95 (br d, $J = 12.4$ Hz, 1H, H-3eq), 4.57 (ddd, $J = 13.2, 5.2, 2.8$ Hz, 1H, H-4a), 7.28-7.38 (m, 4H, H-7, H-10 & H-15), 7.70-7.74 (m, 3H, H-9 & H-14), 7.89 (br s, 1H, H-11); ^{13}C NMR (100 MHz, HSQC, CDCl_3): δ 21.3 (C-12), 21.5 (C-17), 24.7 (C-2), 25.6 (C-6), 27.7 (C-1), 28.2 (C-5), 34.3 (C-11b), 40.4 (C-3), 48.9 (C-4a), 110.9 (C-7), 114.4 (C-6a), 115.9 (d, $J = 4.1$ Hz, C-9), 118.3 (d, $J = 3.4$ Hz, C-10), 121.8 (q, $J = 31.6$ Hz, C-8), 125.3 (q, $J = 269.6$ Hz, C-18), 125.9 (C-6b), 127.0 (C-14), 129.8 (C-15), 137.7 (C-13 & C-10a), 138.4 (C-16), 143.2 (C-11a); HRMS: m/z calcd for $\text{C}_{24}\text{H}_{26}\text{F}_3\text{N}_2\text{O}_2\text{S}$ ($M + \text{H}$) $^+$ 463.1662, found 463.1675



General procedure C:

A stirring solution of phenylhydrazine hydrochloride **1·HCl** (2.5 equiv), solid acid catalyst Amberlite IR 120 H[®] (10 equiv w/w with respect to **3**) and 5-oxodecahydroquinoline **3** (1 equiv) in HCl/MeOH (1.25 M, 30 equiv) was stirred at 70 °C for the indicated time. After cooling, the reaction mixture was filtered and the resin was washed with CH₂Cl₂ and MeOH. The excess hydrazine salt was removed by precipitation in cold dichloromethane and the crude product was purified by precipitation from cold MeOH to afford the pure carbazole product.

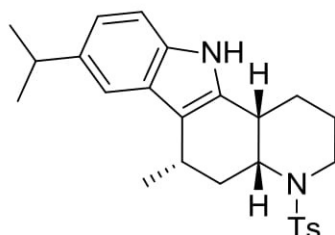
(4*aRS*,6*SR*,11*bRS*)-6-Methyl-4-(4-methylphenylsulfonyl)-2,3,4,4*a*,5,6,11,11*b*-octahydro-1*H*-pyrido[3,2-*a*]carbazole (**7a**)



Following the general procedure C using phenylhydrazine hydrochloride **1a·HCl** (61 mg, 0.42 mmol), 5-oxodecahydroquinoline **3** (54 mg, 0.17 mmol) and Amberlite IR 120 H[®] (500 mg) for 3 h, **7a** was isolated as a pale yellow solid (62 mg, 92%) further crystallization from CHCl₃ and DCE afforded pale yellow crystals.

Mp: 205-207 °C; ¹H NMR (COSY, CDCl₃, 400 MHz): δ 1.41 (d, *J* = 6.8 Hz, 3H, H-12), 1.45-1.52 (m, 1H, H-2), 1.60-1.72 (m, 2H, H-1 & H-2), 1.75-1.93 (m, 2H, H-5), 1.95-2.02 (m, 1H, H-1), 2.44 (s, 3H, H-17), 2.78 (ddd, *J* = 12.0, 4.8, 4.8 Hz, 1H, H-11*b*), 3.05 (ddd, *J* = 13.4, 13.4, 2.4 Hz, 1H, H-3*ax*), 3.10-3.24 (m, 1H, H-6), 3.92 (br d, *J* = 13.4 Hz, 1H, H-3*eq*), 4.36 (ddd, *J* = 12.8, 4.8, 3.6 Hz, 1H, H-4*a*), 7.05-7.15 (m, 2H, H-8 & H-9), 7.27 (d, *J* = 7.6 Hz, 1H, H-10), 7.30 (d, *J* = 8.4 Hz, 1H, H-15), 7.61 (d, *J* = 7.6 Hz, 1H, H-7), 7.68 (br s, 1H, H-11), 7.75 (d, *J* = 8.4 Hz, 2H, H-14); ¹³C NMR (100 MHz, HSQC, CDCl₃): δ 21.3 (C-12), 21.5 (C-17), 24.5 (C-2), 28.14 (C-1), 28.32 (C-6), 32.3 (C-5), 34.0 (C-11*b*), 40.5 (C-3), 52.4 (C-4*a*), 110.7 (C-10), 113.1 (C-6*a*), 119.3 (C-8), 119.9 (C-7), 121.3 (C-9), 126.6 (C-6*b*), 127.0 (C-14), 129.7 (C-15), 136.1 (C-10*a*), 136.3 (C-13), 138.5 (C-16), 143.1 (C-11*a*); HRMS: *m/z* calcd for C₂₃H₂₇N₂O₂S (M + H)⁺ 395.1788, found 395.1805

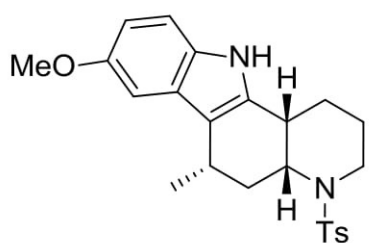
(4*aRS*,6*SR*,11*bRS*)-8-Isopropyl-6-methyl-4-(4-methylphenylsulfonyl)-2,3,4,4*a*,5,6,11,11*b*-octahydro-1*H*-pyrido[3,2-*a*]carbazole (**7b**)



Following the general procedure C using *p*-isopropylphenylhydrazine hydrochloride **1b·HCl** (145 mg, 0.78 mmol), 5-oxodecahydroquinoline **3** (100 mg, 0.31 mmol) and Amberlite IR 120 H[®] (1.00 g) for 3 h, **7b** was isolated after trituration in cold MeOH and recrystallization in DCE as a white solid (119 mg, 88%).

^1H NMR (COSY, CDCl_3 , 400 MHz): δ 1.29 (dd, $J = 7.5, 1.6$ Hz, 6H, 2 x CH_3 *i*Pr), 1.40 (d, $J = 6.8$ Hz, 3H, H-12), 1.43-1.53 (m, 1H, H-2), 1.53-1.68 (m, 2H, H-1 & H-2), 1.72-1.90 (m, 2H, H-5), 1.91-1.99 (m, 1H, H-1), 2.42 (s, 3H, H-17), 2.74 (ddd, $J = 12.0, 4.8, 4.8$ Hz, 1H, H-11b), 2.91-3.15 (m, 3H, CH *i*Pr, H-3ax & H-6), 3.89 (br d, $J = 13.6$ Hz, 1H, H-3eq), 4.32 (ddd, $J = 12.8, 4.8, 3.6$ Hz, 1H, H-4a), 7.01 (bd, $J = 8.4$ Hz 1H, H-9), 7.18 (d, $J = 8.4$ Hz, 1H, H-10), 7.28 (d, $J = 8.4$ Hz, 2H, H-15), 7.43 (bs, 1H, H-7), 7.66 (s, 1H, H-11), 7.73 (d, $J = 8.4$ Hz, 2H, H-14); ^{13}C NMR (100 MHz, HSQC, CDCl_3): δ 21.3 (C-12), 21.5 (C-17), 24.4 (C-2), 24.7 (CH_3 *i*Pr), 24.8 (CH_3 *i*Pr), 28.1 (C-1), 28.3 (C-6), 32.3 (C-5), 34.0 (C-11b), 34.3 (CH *i*Pr), 40.5 (C-3), 52.5 (C-4a), 110.5 (C-10), 112.7 (C-6a), 116.9 (C-7), 120.3 (C-9), 126.6 (C-6b), 126.8 (C-14), 129.7 (C-15), 134.9 (C-10a), 136.4 (C-8), 138.5 (C-13), 139.9 (16), 143.0 (C-11a); HRMS: m/z calcd for $\text{C}_{26}\text{H}_{33}\text{N}_2\text{O}_2\text{S}$ ($\text{M} + \text{H}$) $^+$ 437.2257, found 437.2256

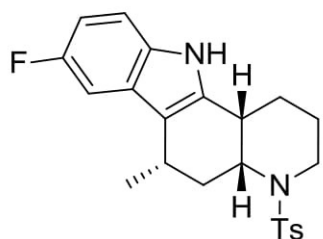
(4a*RS*,6*SR*,11*bRS*)-8-Methoxy-6-methyl-4-(4-methylphenylsulfonyl)-2,3,4,4a,5,6,11,11b-octahydro-1*H*-pyrido[3,2-*a*]carbazole (7c)



Following the general procedure C using *p*-methoxyphenylhydrazine hydrochloride **1c-HCl** (136 mg, 0.78 mmol), 5-oxodecahydroquinoline **3** (100 mg, 0.31 mmol) and Amberlite IR 120 H $^{\circ}$ (1.00 g) for 6 h, **7c** was isolated after purification by chromatography (10-25-50% EtOAc/hexane) followed by trituration in cold MeOH as a light pink solid (75 mg, 57%).

^1H NMR (COSY, CDCl_3 , 400 MHz): δ 1.40 (d, $J = 6.8$ Hz, 3H, H-12), 1.45-1.52 (m, 1H, H-2), 1.60-1.72 (m, 2H, H-1 & H-2), 1.75-1.95 (m, 2H, H-5), 1.95-2.02 (m, 1H, H-1), 2.44 (s, 3H, H-17), 2.74 (ddd, $J = 12.0, 5.0, 5.0$ Hz, 1H, H-11b), 3.05 (ddd, $J = 13.6, 13.6, 2.4$ Hz, 1H, H-3ax), 3.10-3.20 (m, 1H, H-6), 3.84 (s, 3H, CH_3O), 3.94 (br d, $J = 13.6$ Hz, 1H, H-3eq), 4.34 (ddd, $J = 12.8, 5.0, 3.6$ Hz, 1H, H-4a), 6.79 (dd, $J = 8.8, 2.4$ Hz, 1H, H-9), 7.07 (d, $J = 2.4$ Hz, 1H, H-7), 7.15 (d, $J = 8.8$ Hz, 1H, H-10), 7.29 (d, $J = 8.4$ Hz, 2H, H-15), 7.51 (br s, 1H, H-11), 7.74 (d, $J = 8.4$ Hz, 2H, H-14); ^{13}C NMR (100 MHz, HSQC, CDCl_3): δ 21.2 (C-12), 21.5 (C-17), 24.4 (C-2), 28.15 (C-1), 28.24 (C-6), 32.3 (C-5), 34.1 (C-11b), 40.5 (C-3), 52.4 (C-4a), 56.1 (CH_3O), 102.8 (C-7), 110.8 (C-9), 111.2 (C-10), 113.0 (C-6a), 126.96 (C-14), 127.01 (C-6b), 129.7 (C-15), 131.5 (C-10a), 137.1 (C-13), 138.6 (C-16), 143.0 (C-11a), 153.7 (C-8); HRMS: m/z calcd for $\text{C}_{24}\text{H}_{29}\text{N}_2\text{O}_3\text{S}$ ($\text{M} + \text{H}$) $^+$ 425.1893, found 425.1881

(4a*RS*,6*SR*,11*bRS*)-8-Fluoro-6-methyl-4-(4-methylphenylsulfonyl)-2,3,4,4a,5,6,11,11b-octahydro-1*H*-pyrido[3,2-*a*]carbazole (7d)

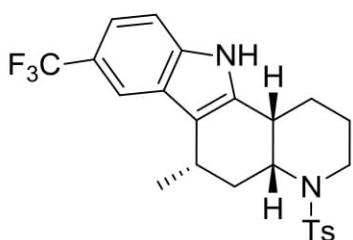


Following the general procedure C using *p*-fluorophenylhydrazine hydrochloride **1d-HCl** (127 mg, 0.78 mmol), 5-oxodecahydroquinoline **3** (100 mg, 0.31 mmol) and Amberlite IR 120 H $^{\circ}$ (1.00 g) for 3 h, **7d** was isolated after trituration in cold MeOH and recrystallization in DCE as a white solid (101 mg, 82%).

^1H NMR (COSY, CDCl_3 , 400 MHz): δ 1.37 (d, $J = 6.4$ Hz, 3H, H-12), 1.46-1.53 (m, 1H, H-2), 1.58-1.72 (m, 2H, H-1 & H-2), 1.73-1.92 (m, 2H, H-5), 1.94-2.03 (m, 1H, H-1), 2.44 (s, 3H, H-17), 2.78 (ddd, $J = 12.0, 5.0, 5.0$ Hz, 1H, H-11b), 3.04 (ddd, $J = 13.2, 13.2, 2.4$

Hz, 1H, H-3ax), 3.08-3.16 (m, 1H, H-6), 3.91 (ddd, $J = 13.2, 2.4, 2.4$ Hz, 1H, H-3eq), 4.34 (ddd, $J = 12.4, 5.0, 3.6$ Hz, 1H, H-4a), 6.86 (ddd, $J = 9.0, 9.0, 2.6$ Hz, 1H, H-9), 7.16 (dd, $J = 9.0, 4.4$ Hz, 1H, H-10), 7.24 (dd, $J = 9.6, 2.6$ Hz, 1H, H-7), 7.30 (br d, $J = 8.4$ Hz, 2H, H-15), 7.64 (s, 1H, H-11), 7.74 (br d, $J = 8.4$ Hz, 2H, H-14); ^{13}C NMR (100 MHz, HSQC, CDCl_3): δ 21.0 (C-12), 21.5 (C-17), 24.5 (C-2), 28.1 (C-1), 28.2 (C-6), 32.2 (C-5), 34.1 (C-11b), 40.5 (C-3), 52.3 (C-4a), 105.0 (d, $J = 23.9$ Hz, C-7), 109.4 (d, $J = 26.1$ Hz, C-9), 111.1 (d, $J = 9.9$ Hz, C-10), 113.4 (C-6a), 126.9 (C-6b), 127.0 (C-14), 129.7 (C-15), 132.8 (C-10a), 138.1 (C-13), 138.5 (C-16), 143.1 (C-11a), 157.5 (d, $J = 233.8$ Hz, C-8); HRMS: m/z calcd for $\text{C}_{23}\text{H}_{26}\text{FN}_2\text{O}_2\text{S}$ ($\text{M} + \text{H}$) $^+$ 413.1694, found 413.1695

(4a*RS*,6*SR*,11*bRS*)-8-Trifluoromethyl-6-methyl-4-(4-methylphenylsulfonyl)-2,3,4,4a,5,6,11,11b-octahydro-1*H*-pyrido[3,2-*a*]carbazole (7e**)**



Following the general procedure C using *p*-trifluoromethylphenylhydrazine hydrochloride **1e·HCl** (166 mg, 0.78 mmol), 5-oxodecahydroquinoline **3** (100 mg, 0.31 mmol) and Amberlite IR 120 H $^{\circ}$ (1.00 g) for 24 h, **7e** was isolated after purification by chromatography (10-25-50% EtOAc/hexane) followed by trituration in cold MeOH as a white solid (15 mg, 10.5%) and the recovered filtrate 50 mg containing 15% of the

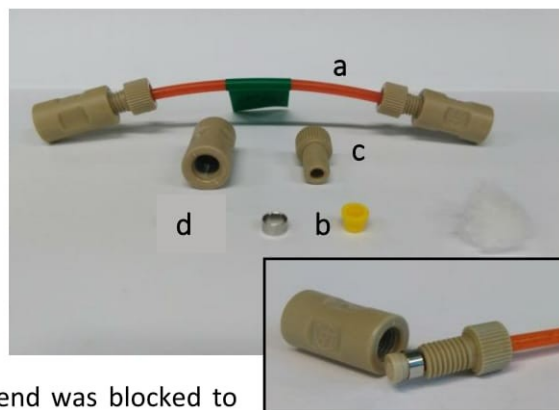
product (Yield of **7e** combined : 16%).

^1H NMR (COSY, CDCl_3 , 400 MHz): δ 1.40 (d, $J = 6.8$ Hz, 3H, H-12), 1.47-1.53 (m, 1H, H-2), 1.62-1.71 (m, 2H, H-1 & H-2), 1.72-1.92 (m, 2H, H-5), 1.97-2.07 (m, 1H, H-1), 2.44 (s, 3H, H-17), 2.84 (ddd, $J = 12.0, 4.8, 4.8$ Hz, 1H, H-11b), 3.03 (ddd, $J = 13.2, 13.2, 2.4$ Hz, 1H, H-3ax), 3.12 (br quint, $J = 6.8$ Hz, 1H, H-6), 3.90 (br d, $J = 13.2$ Hz, 1H, H-3eq), 4.36 (ddd, $J = 12.8, 4.8, 3.6$ Hz, 1H, H-4a), 7.28-7.38 (m, 4H, H-7, H-10 & H-15), 7.74 (d, $J = 8.4$ Hz, 2H, H-14), 7.86 (s, 1H, H-9), 7.96 (s, 1H, H-11); ^{13}C NMR (100 MHz, HSQC, CDCl_3): δ 21.2 (C-12), 21.5 (C-17), 24.5 (C-2), 28.06 (C-1), 28.13 (C-6), 31.9 (C-5), 34.1 (C-11b), 40.5 (C-3), 52.2 (C-4a), 110.8 (C-7), 114.0 (C-6a), 117.3 (d, $J = 4.2$ Hz, C-9), 118.1 (d, $J = 3.3$ Hz, C-10), 121.6 (q, $J = 31.6$ Hz, C-8), 125.4 (q, $J = 269.8$ Hz, C-18), 126.0 (C-6b), 126.9 (C-14), 129.8 (C-15), 137.8 (C-10a), 138.0 (C-13), 138.4 (C-16), 143.2 (C-11a); HRMS: m/z calcd for $\text{C}_{24}\text{H}_{26}\text{F}_3\text{N}_2\text{O}_2\text{S}$ ($\text{M} + \text{H}$) $^+$ 463.1662, found 463.1669

Synthesis of indoles in flow

Cartridge assembly:

Both ends of 10-cm Tefzel® (ETFE) tubing (1/8" OD, 1/16" ID, a) were blocked with cotton wool, fitted with assembled flat bottom super flangeless fittings + metal ferrules (1/8" OD, P-359, IDEX, b) and male nut parts (LT-215, IDEX, c). These connections were mounted onto flat unions (P-703-01, IDEX, d). For the filling of the cartridges, only one end was blocked at first, the cartridge was filled with the catalyst (~100 mg) employing vacuum suction and after, the other end was blocked to seal the cartridge.



Microreactor setup:

All gas-tight syringes (5 mL, B-247, FutureChemistry Holding BV) were mounted on syringe pumps (B-230, FutureChemistry Holding BV) and connected to Tefzel® tubing (1/16" OD, 1529, IDEX) via female Luer adapters (P-628, IDEX). Throughout the flow system, all the tubing (Tefzel® 1/16" OD, 1529, IDEX) was assembled with super flangeless nut connections (P-287, IDEX) and assembled ferrules (P-259, IDEX) in order to achieve leak-free fluid connections. Also, a 5 bar back pressure regulator (B-444, FutureChemistry Holding BV) guaranteed pressurization inside the system before eluting into a collection flask (see Figure 1).

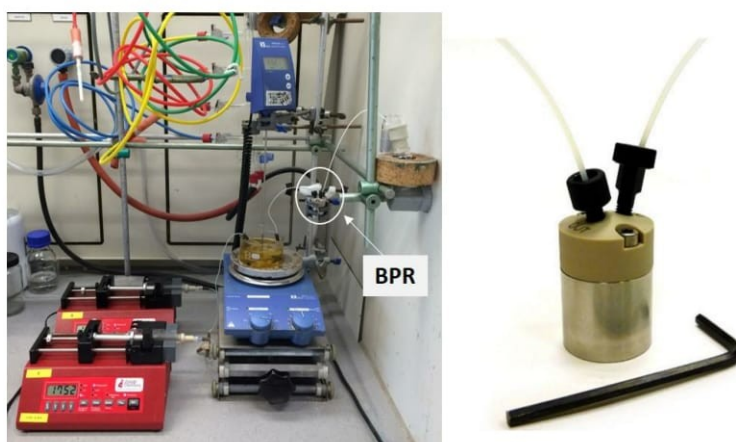


Figure 1. Flow set-up including back pressure regulator (detail, right).

Flow general procedure C:

Two feed solutions were employed: stream A containing the ketone in solution, and stream B containing the hydrazine in solution both driven by syringe pumps ($\phi_A = \phi_B$). These were mixed in a PEEK T-mixer connection (P-713, IDEX) before entering the microreactor (consisting of a ETFE cartridge packed with Amberlite® IR 120 H) at 70 °C for 10 to 60 minutes. By removing the solvent *in vacuo*, the desired indole products were obtained. In some cases, further purification was achieved by recrystallization CH_2Cl_2 or methanol.

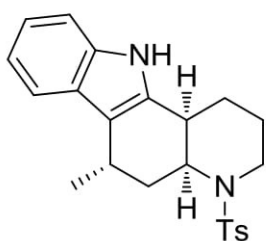
Full characterization of the indole products can be found within the general procedure for the preparation of the title compounds in batch.

Calculation for reactions performed under flow conditions:

For the reactions performed in flow, yields were calculated taking into account the total moles of product obtained ($n(\text{Collected Product})$), the flow rate (ϕ_{SM}) and the concentration ($[SM]$) of the starting material and the overall collection time ($t(\text{Collection})$), as shown in the equation below.

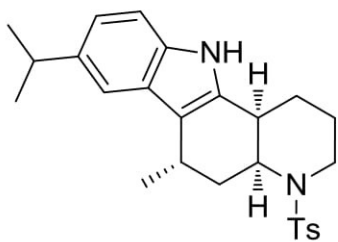
$$\eta_{Flow} (\%) = \frac{n(\text{Collected Product})}{[SM] \times \phi_{SM} \times t(\text{Collection})} \times 100$$

(4aRS,6RS,11bRS)-6-Methyl-4-(4-methylphenylsulfonyl)-2,3,4,4a,5,6,11,11b-octahydro-1H-pyrido[3,2-a]carbazole (4a)



Following the flow general procedure C using 5-oxodecahydroquinoline **3** (0.05 M in MeOH/AcOH/DCE 4/2/4) and phenylhydrazine **1a** (0.5 M in MeOH/AcOH 1/1) with reaction time = 20 min, total flow = 15.00 $\mu\text{L}\cdot\text{min}^{-1}$ and collecting for 2 h (2 mL of ketone), product **4a** was isolated as a pale yellow solid (31.2 mg, 76%).

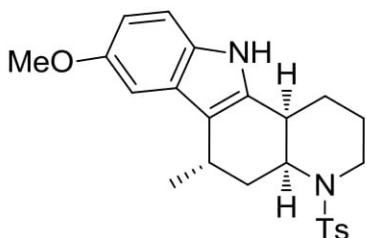
(4aRS,6RS,11bRS)-8-Isopropyl-6-methyl-4-(4-methylphenylsulfonyl)-2,3,4,4a,5,6,11,11b-octahydro-1H-pyrido[3,2-a]carbazole (4b)



Following the flow general procedure C using a 30 cm cartridge (inner volume 300 μL) 5-oxodecahydroquinoline **3** (0.05 M in MeOH/AcOH/DCE 4/2/4) and *p*-isopropylphenylhydrazine hydrochloride salt **1b-HCl** (0.5 M in MeOH/AcOH 1/1) with reaction time = 30 min, total flow = 10.00 $\mu\text{L}\cdot\text{min}^{-1}$ and collecting for 2 h (2 mL of ketone), the crude ^1H NMR spectrum showed full conversion to **4b** which was isolated as a pale yellow solid

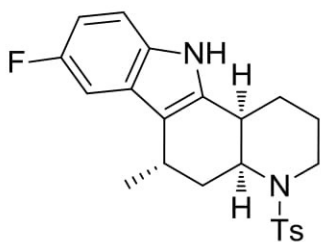
(32 mg, 75%).

(4aRS,6RS,11bRS)-8-Methoxy-6-methyl-4-(4-methylphenylsulfonyl)-2,3,4,4a,5,6,11,11b-octahydro-1H-pyrido[3,2-a]carbazole (4c)



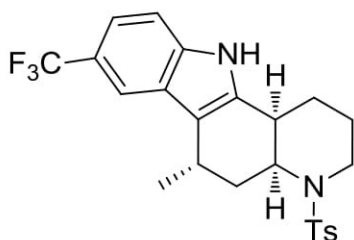
Following the flow general procedure C using a 1 m cartridge (inner volume 1 mL), 5-oxodecahydroquinoline **3** (0.02 M in MeOH/AcOH/DCE 4/4/2) and *p*-methoxyphenylhydrazine hydrochloride salt **1c-HCl** (0.2 M in MeOH) with reaction time = 60 min, total flow = 16.00 $\mu\text{L}\cdot\text{min}^{-1}$ and collecting for 2 h (2 mL of ketone), the crude ^1H NMR spectrum showed 55 % conversion to **4c** with the remaining part corresponding to a mix hydrazone/ 5-oxodecahydroquinoline.

(4a*RS*,6*RS*,11*BR*S)-8-Fluoro-6-methyl-4-(4-methylphenylsulfonyl)-2,3,4,4a,5,6,11,11b-octahydro-1*H*-pyrido[3,2-*a*]carbazole (4d)



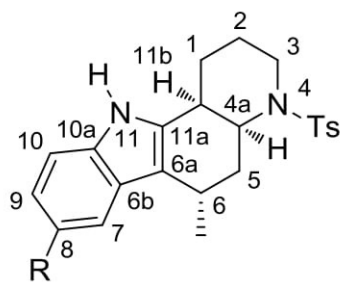
Following the flow general procedure C using a 1 m cartridge (inner volume 1 mL), 5-oxodecahydroquinoline **3** (0.01 M in MeOH/AcOH/DCE 4/5/1) and *p*-fluorophenylhydrazine hydrochloride salt **1d·HCl** (0.1 M in MeOH) with reaction time = 60 min, total flow = 16.00 $\mu\text{L}\cdot\text{min}^{-1}$ and collecting for 2 h (2 mL of ketone), the crude ^1H NMR spectrum showed 42% conversion to **4d** with the remaining part corresponding to a mix hydrazone/ 5-oxodecahydroquinoline.

(4a*RS*,6*RS*,11*BR*S)-8-Trifluoromethyl-6-methyl-4-(4-methylphenylsulfonyl)-2,3,4,4a,5,6,11,11b-octahydro-1*H*-pyrido[3,2-*a*]carbazole (4e)



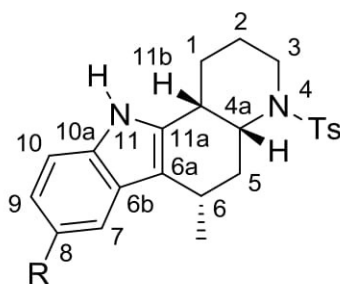
Following the flow general procedure C using a 1 m cartridge (inner volume 1 mL), 5-oxodecahydroquinoline **3** (0.04 M in AcOH/DCE 8/2) and *p*-trifluoromethylphenylhydrazine **1e** (0.4 M in MeOH) with reaction time = 60 min, total flow = 16.00 $\mu\text{L}\cdot\text{min}^{-1}$ and collecting for 2 h (2 mL of ketone), the crude ^1H NMR spectrum showed 22% conversion to **4e** with the remaining part corresponding to a mix hydrazone/ 5-oxodecahydroquinoline.

Table 1. ¹H NMR data of 6-Methyl-4-(4-methylphenylsulfonyl)-1*H*-2,3,4,4a,5,6,11,11*b*-octahydropyrido[3,2-*a*]carbazoles



Series 4

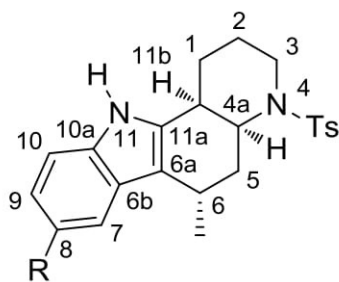
	4a H	4b <i>i</i> Pr	4c OMe	4d F	4e CF ₃
H-1	1.53-1.61 (m) 1.92-2.01 (m)	1.52-1.59 (m) 1.92-1.98 (m)	1.50-1.62 (m) 1.92-2.00 (m)	1.52-1.63 (m) 1.92-2.02 (m)	1.52-1.63 (m) 1.95-2.05 (m)
H-2	1.53-1.61 (m) 1.65-1.70 (m)	1.52-1.59 (m) 1.62-1.68 (m)	1.50-1.62 (m) 1.62-1.70 (m)	1.52-1.63 (m) 1.63-1.73 (m)	1.52-1.63 (m) 1.66-1.73 (m)
H-3	ax 2.97 (ddd, 12.8, 12.8, 2.8)	2.91-3.05 (m)	2.92-3.02 (m)	2.96 (br t, 12.8)	2.89-3.08 (m)
	eq 3.95 (br d, 13.2)	3.94 (br d, 12.4)	3.95 (br d, 12.8)	3.94 (br d, 12.8)	3.95 (br d, 12.4)
H-4a	4.56 (ddd, 13.2, 5.2, 3.2)	4.56 (ddd, 13.2, 5.0, 3.2)	4.55 (ddd, 13.2, 5.2, 2.8)	4.54 (ddd, 13.2, 5.2, 3.2)	4.57 (ddd, 13.2, 5.2, 2.8)
H-5	ax 2.31 (ddd, 12.8, 12.8, 6.0)	2.30 (ddd, 13.2, 13.2, 6.4)	2.31 (ddd, 12.8, 12.8, 6.0)	2.30 (ddd, 12.8, 12.8, 6.2)	2.31 (ddd, 13.2, 13.2, 6.8)
	eq 1.28-1.38 (m)	1.25-1.35 (m)	1.28-1.35 (m)	1.25-1.35 (m)	1.28-1.35 (m)
H-6	3.21 (quint, 7.0)	3.20 (quint, 7.2)	3.12-3.20 (m)	3.14 (quint, 6.8)	3.22 (quint, 6.8)
H-7	7.47	7.27-7.37	6.91	7.09	7.28-7.38
H-8	7.05-7.15	---	---	---	---
H-9	7.05-7.15	7.02	6.78	6.86	7.70-7.74
H-10	7.27	7.20	7.16	7.17	7.28-7.38
H-11	7.66	7.56	7.53	7.64	7.89
H-11b	2.88 (ddd, 11.4, 5.2, 5.2)	2.85 (ddd, 11.6, 5.0, 5.0)	2.80-2.88 (m)	2.87 (ddd, 11.6, 5.0, 5.0)	2.89-3.08 (m)
Me	1.32 (d, 7.2)	1.33	1.31	1.29	1.32
H-14	7.76	7.76	7.75	7.75	7.70-7.74
H-15	7.31	7.27-7.37	7.31	7.31	7.28-7.38
Me-Ts	2.45	2.45	2.44	2.45	2.45
Other		1.30 & 2.91- 3.05 (<i>i</i> Pr)	3.84 (OCH ₃)		



Series 7

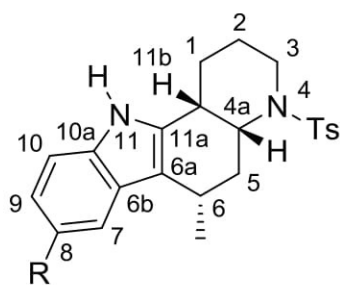
	7a H	7b <i>i</i> Pr	7c OMe	7d F	7e CF ₃
H-1	1.60-1.72 (m) 1.95-2.02 (m)	1.53-1.68 (m) 1.91-1.99 (m)	1.60-1.72 (m) 1.95-2.02 (m)	1.58-1.72 (m) 1.94-2.03 (m)	1.62-1.71 (m) 1.97-2.07 (m)
H-2	1.42-1.52 (m) 1.60-1.72 (m)	1.43-1.53 (m) 1.53-1.68 (m)	1.45-1.52 (m) 1.60-1.72 (m)	1.46-1.53 (m) 1.58-1.72 (m)	1.47-1.53 (m) 1.62-1.71 (m)
H-3	ax 3.05 (ddd, 13.4, 13.4, 2.4)	2.91-3.15 (m)	3.05 (ddd, 13.6, 13.6, 2.4)	3.04 (ddd, 13.2, 13.2, 2.4)	3.03 (ddd, 13.2, 13.2, 2.4)
	eq 3.92 (br d, 13.4)	3.89 (br d, 13.6)	3.94 (br d, 13.6)	3.91 (br d, 13.2)	3.90 (br d, 13.2)
H-4a	4.36 (ddd, 12.8, 4.8, 3.6)	4.32 (ddd, 12.8, 4.8, 3.6)	4.34 (ddd, 12.8, 5.0, 3.6)	4.34 (ddd, 12.4, 5.0, 3.6)	4.36 (ddd, 12.8, 4.8, 3.6)
H-5	1.75-1.93 (m)	1.72-1.90 (m)	1.75-1.95 (m)	1.73-1.92 (m)	1.72-1.92 (m)
H-6	3.10-3.24 (m)	2.91-3.15 (m)	3.10-3.20 (m)	3.08-3.16 (m)	3.12 (quint, 6.8)
H-7	7.61	7.43	7.07	7.24	7.28-7.38
H-8	7.05-7.15	---	---	---	---
H-9	7.05-7.15	7.01	6.79	6.86	7.86
H-10	7.27	7.18	7.15	7.16	7.28-7.38
H-11	7.68	7.66	7.51	7.64	7.96
H-11b	2.78 (ddd, 12.0, 4.8, 4.8)	2.74 (ddd, 12.0, 4.8, 4.8)	2.74 (ddd, 12.0, 5.0, 5.0)	2.78 (ddd, 12.0, 5.0, 5.0)	2.84 (ddd, 12.0, 4.8, 4.8)
Me	1.41 (d, 6.8)	1.40 (d, 6.8)	1.40 (d, 6.8)	1.37 (d, 6.4)	1.40 (d, 6.8)
H-14	7.75	7.73	7.74	7.74	7.74
H-15	7.30	7.28	7.29	7.30	7.28-7.38
Me-Ts	2.44	2.42	2.44	2.44	2.44
Other		1.29 & 2.91- 3.15 (<i>i</i> Pr)	3.84 (OCH ₃)		

Table 2. ^{13}C NMR data of 6-Methyl-4-(4-methylphenylsulfonyl)-1*H*-2,3,4,4a,5,6,11,11b-octahydropyrindo[3,2-*a*]carbazoles



Series 4

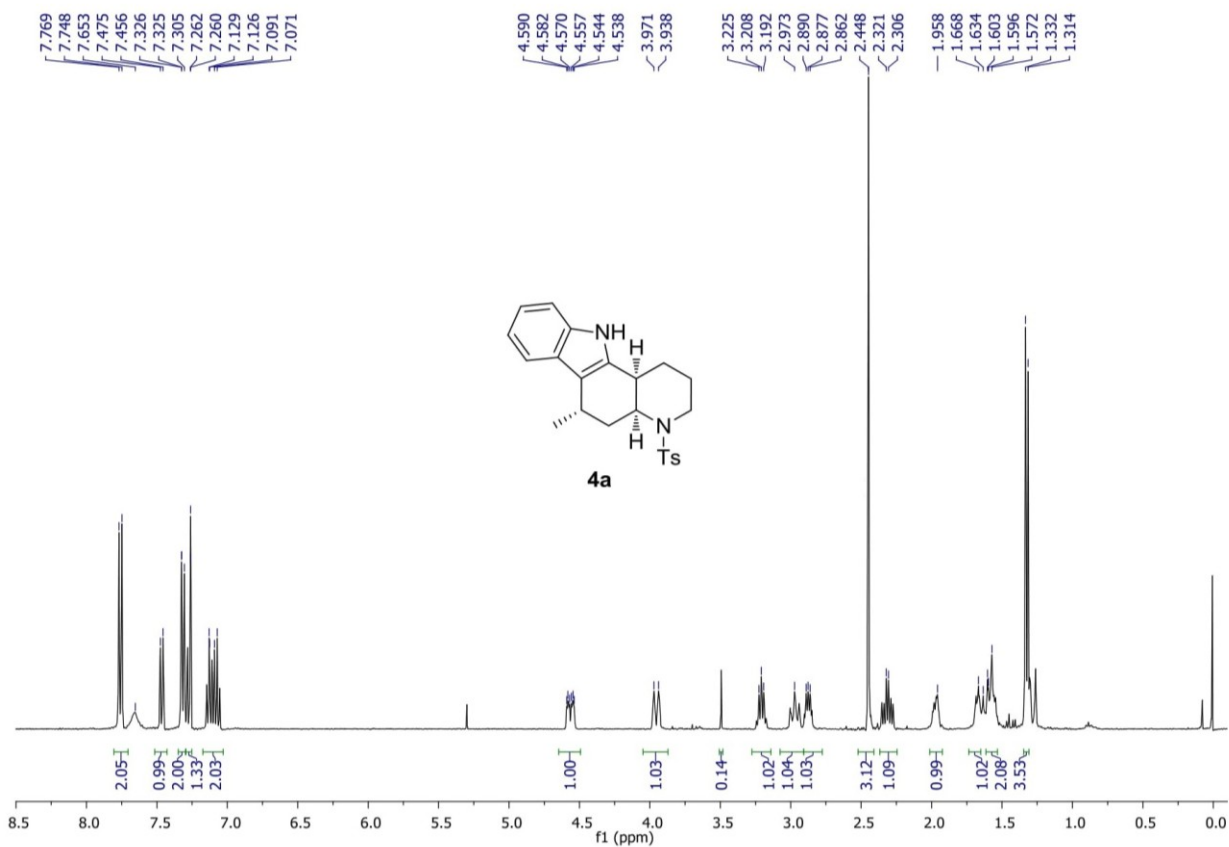
	4a H	4b <i>i</i> Pr	4c OMe	4d F	4e CF ₃
C-1	27.7	27.7	27.8	27.7	27.7
C-2	24.7	24.7	24.7	24.7	24.7
C-3	40.5	40.5	40.5	40.4	40.5
C-4a	49.1	49.1	49.1	49.0	48.9
C-5	28.4	28.5	28.5	28.3	28.2
C-6	25.8	25.8	25.8	25.7	25.6
C-6a	113.5	113.3	113.4	113.8	114.4
C-6b	126.5	126.5	126.9	126.9	125.9
C-7	118.3	115.3	100.9	103.4	110.9
C-8	119.3	136.0	153.9	157.7	121.6
C-9	121.5	120.5	111.0	109.5	115.9
C-10	110.7	110.5	111.4	111.2	118.3
C-10a	135.8	134.8	131.3	132.7	137.7
C-11a	143.1	143.0	143.0	143.1	143.2
C-11b	34.2	34.3	34.3	34.3	34.3
Me	21.2	21.2	21.0	21.0	21.3
Me-Ts	21.5	21.5	21.5	21.5	21.6
C-13	136.2	138.5	136.8	137.8	137.8
C-14	127.0	127.0	127.0	127.0	127.0
C-15	129.7	129.7	129.7	129.7	129.8
C-16	138.5	140.2	138.5	138.4	138.4
Other		24.8 & 34.3 (<i>i</i> Pr)	56.0 (OCH ₃)		125.3 (CF ₃)



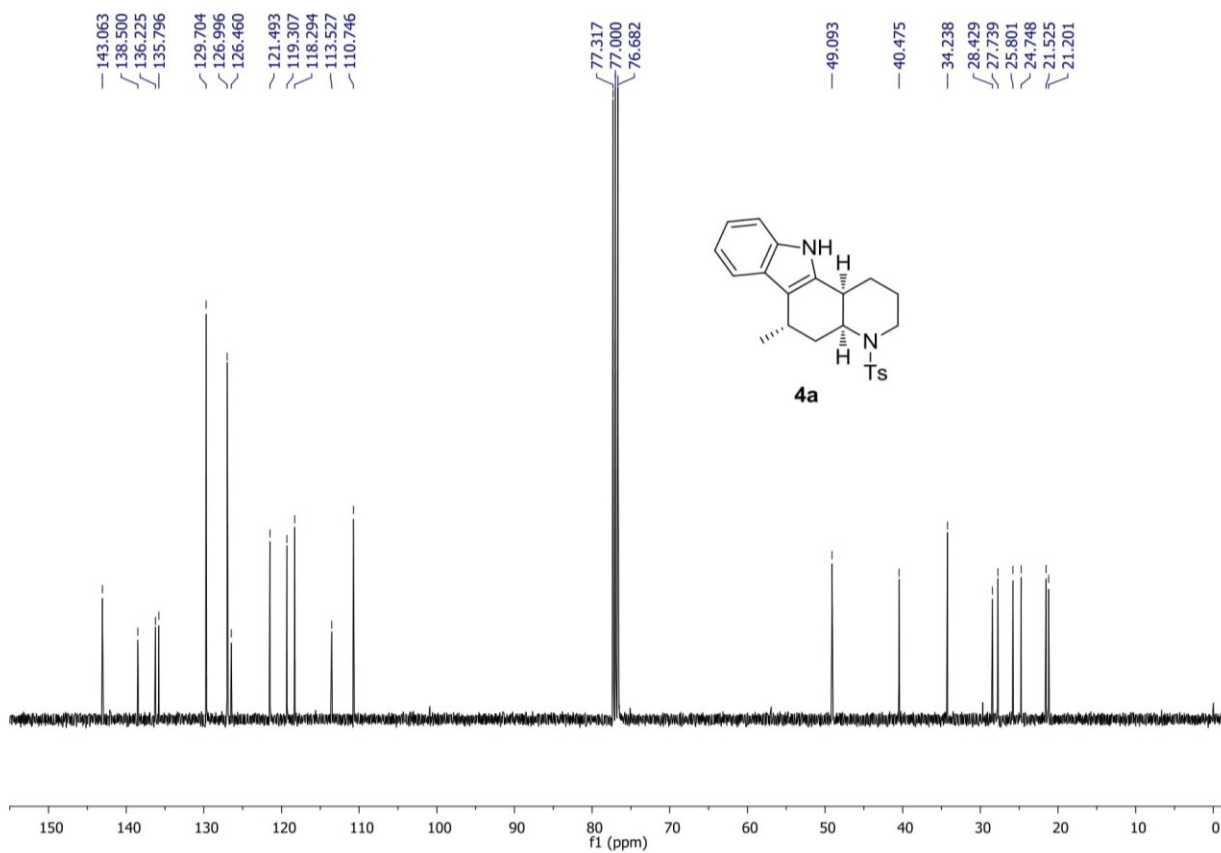
Series 7

	7a H	7b <i>i</i> Pr	7c OMe	7d F	7e CF ₃
C-1	28.1	28.1	28.2	28.1	28.1
C-2	24.5	24.4	24.4	24.5	24.5
C-3	40.5	40.5	40.5	40.5	40.5
C-4a	52.4	52.5	52.4	52.3	52.2
C-5	32.3	32.3	32.3	32.2	31.9
C-6	28.3	28.3	28.2	28.2	28.1
C-6a	113.1	112.7	113.0	113.4	114.0
C-6b	126.6	126.6	127.01	126.9	126.0
C-7	119.9	116.9	102.8	105.0	110.8
C-8	119.3	136.4	153.7	157.5	121.6
C-9	121.3	120.3	110.8	109.4	117.3
C-10	110.7	110.5	111.2	111.1	118.1
C-10a	136.1	134.9	131.5	132.8	137.8
C-11a	143.1	143.0	143.0	143.1	143.2
C-11b	34.0	34.0	34.1	34.1	34.1
Me	21.3	21.3	21.2	21.0	21.2
Me-Ts	21.5	21.5	21.5	21.5	21.5
C-13	136.3	138.5	137.1	138.1	138.0
C-14	127.0	126.8	126.96	127.0	126.9
C-15	129.7	129.7	129.7	129.7	129.8
C-16	138.5	139.9	138.6	138.5	138.4
Other		24.7 & 34.3 (<i>i</i> Pr)	56.1 (OCH ₃)		125.3 (CF ₃)

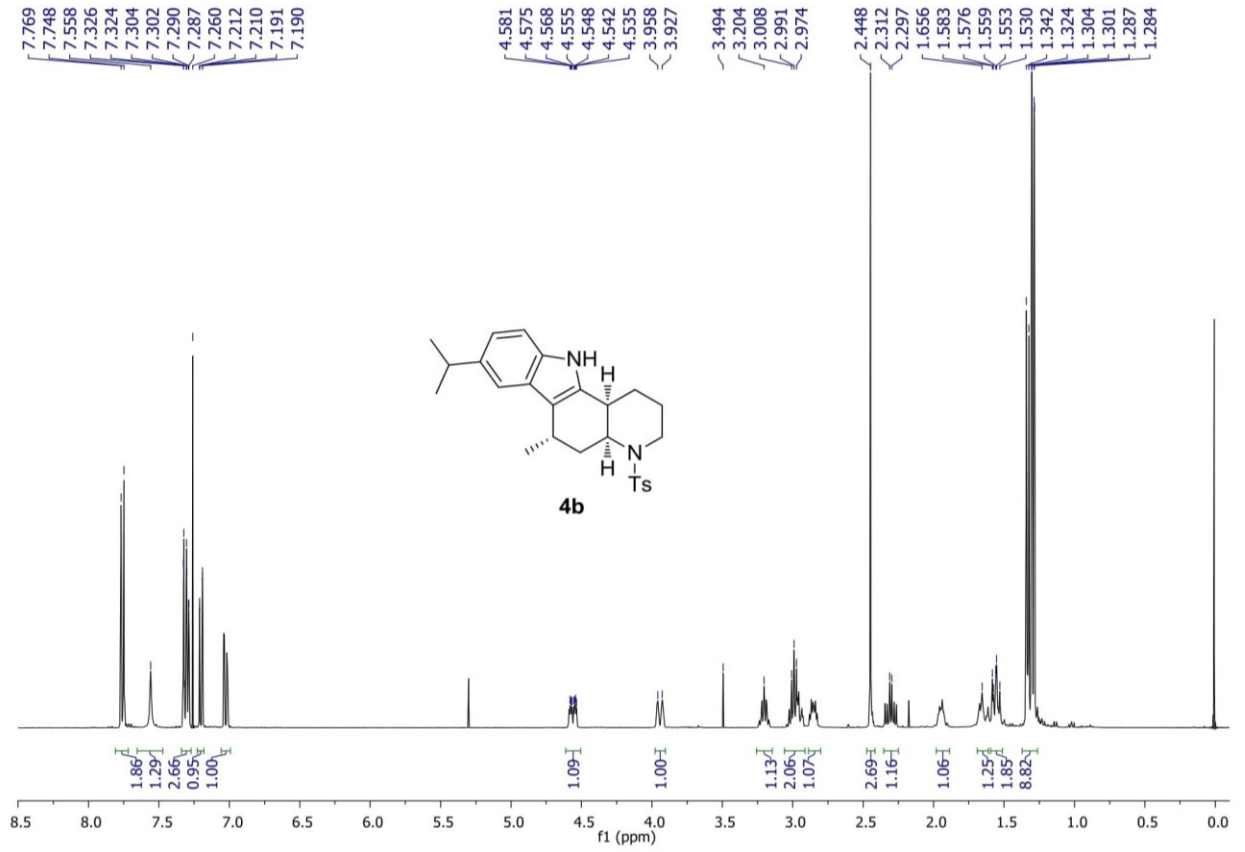
S18



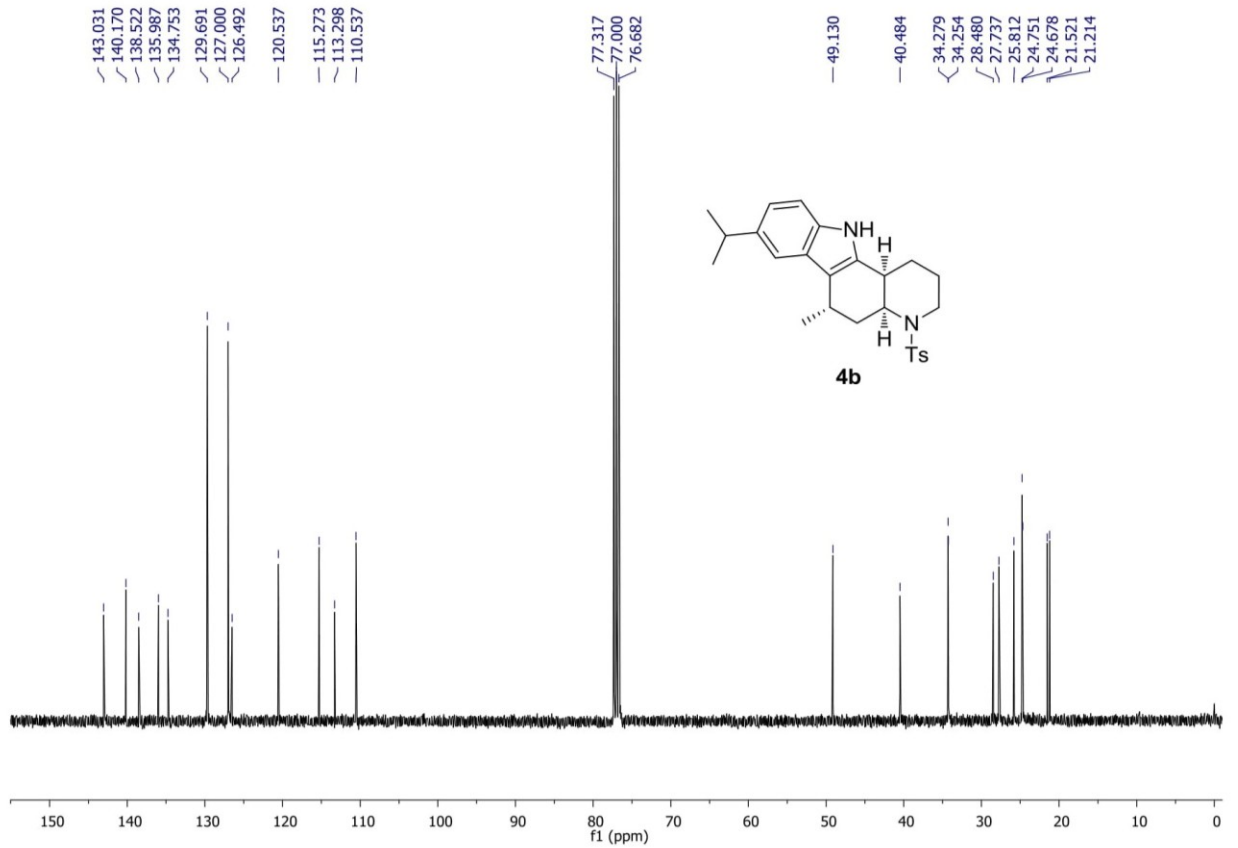
S19

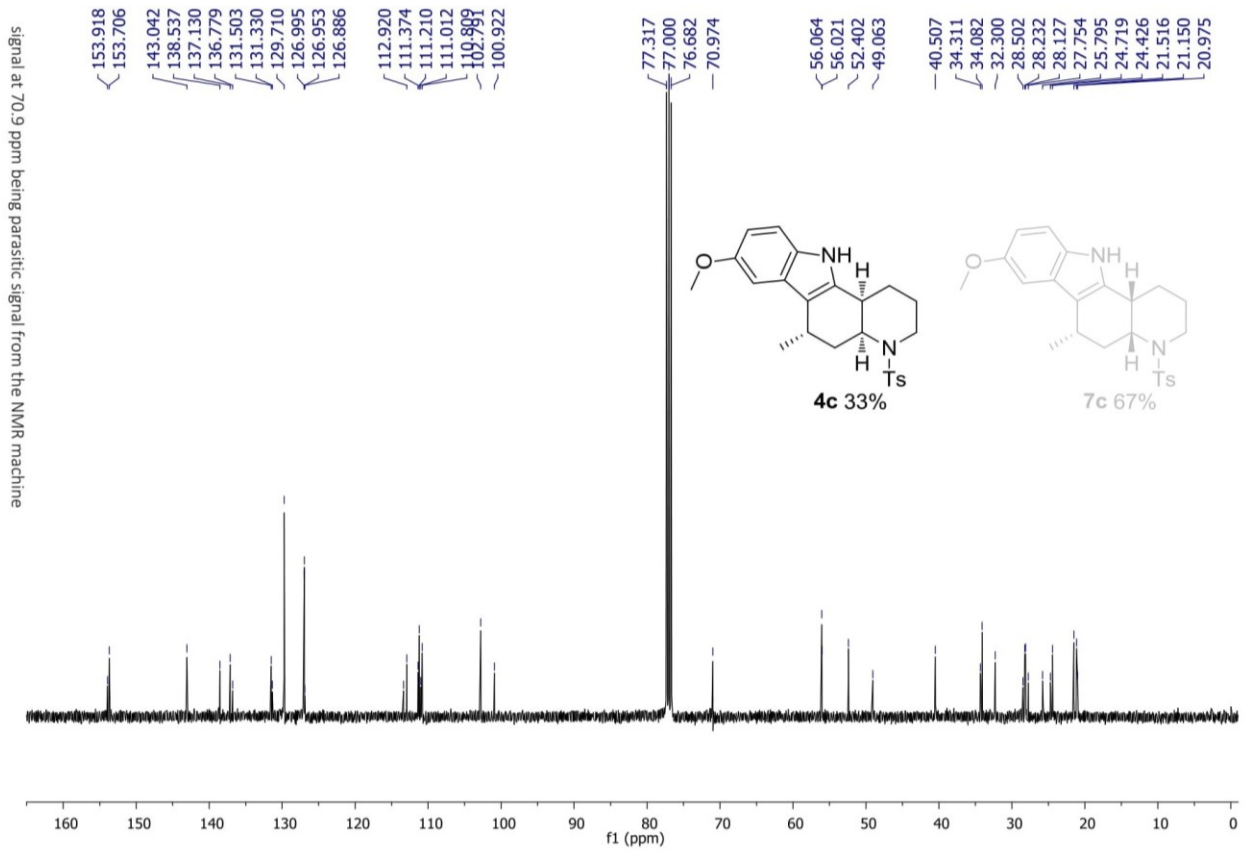
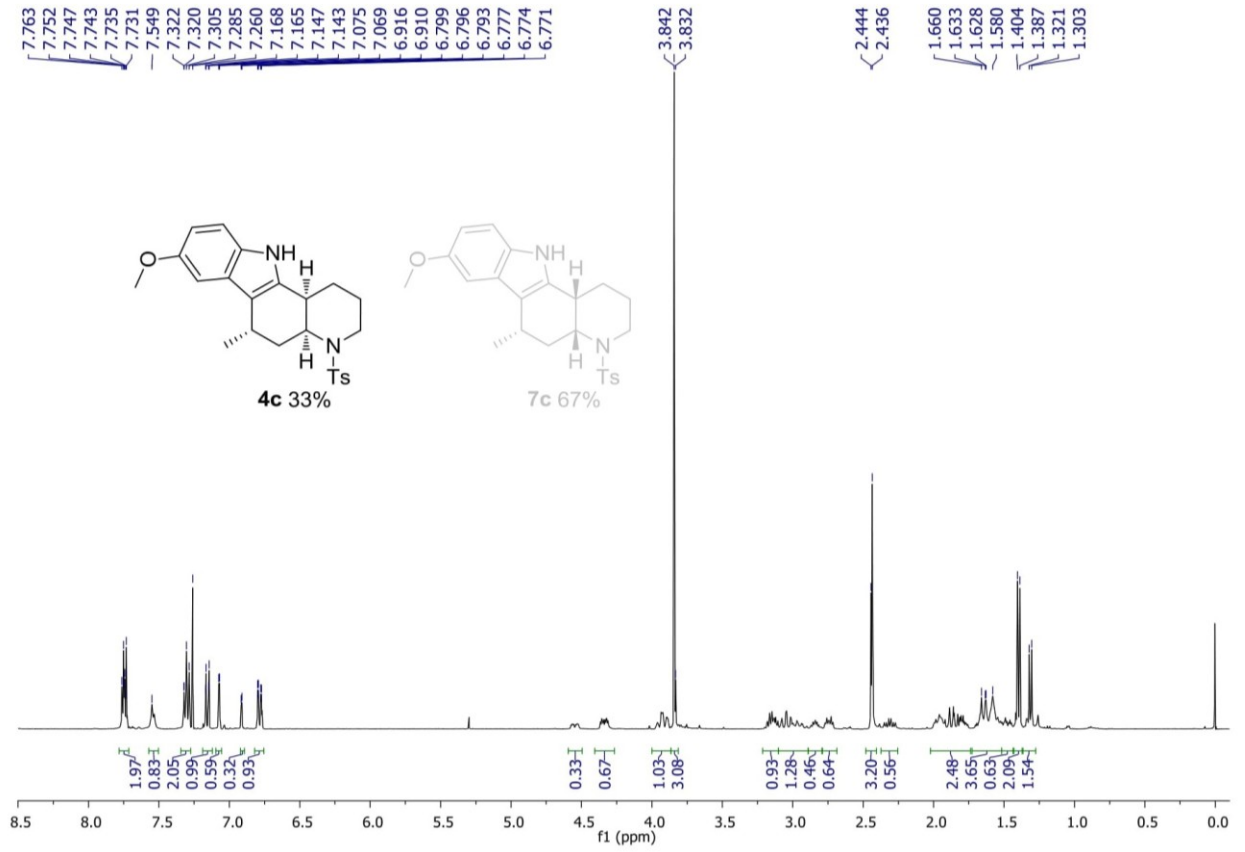


S20

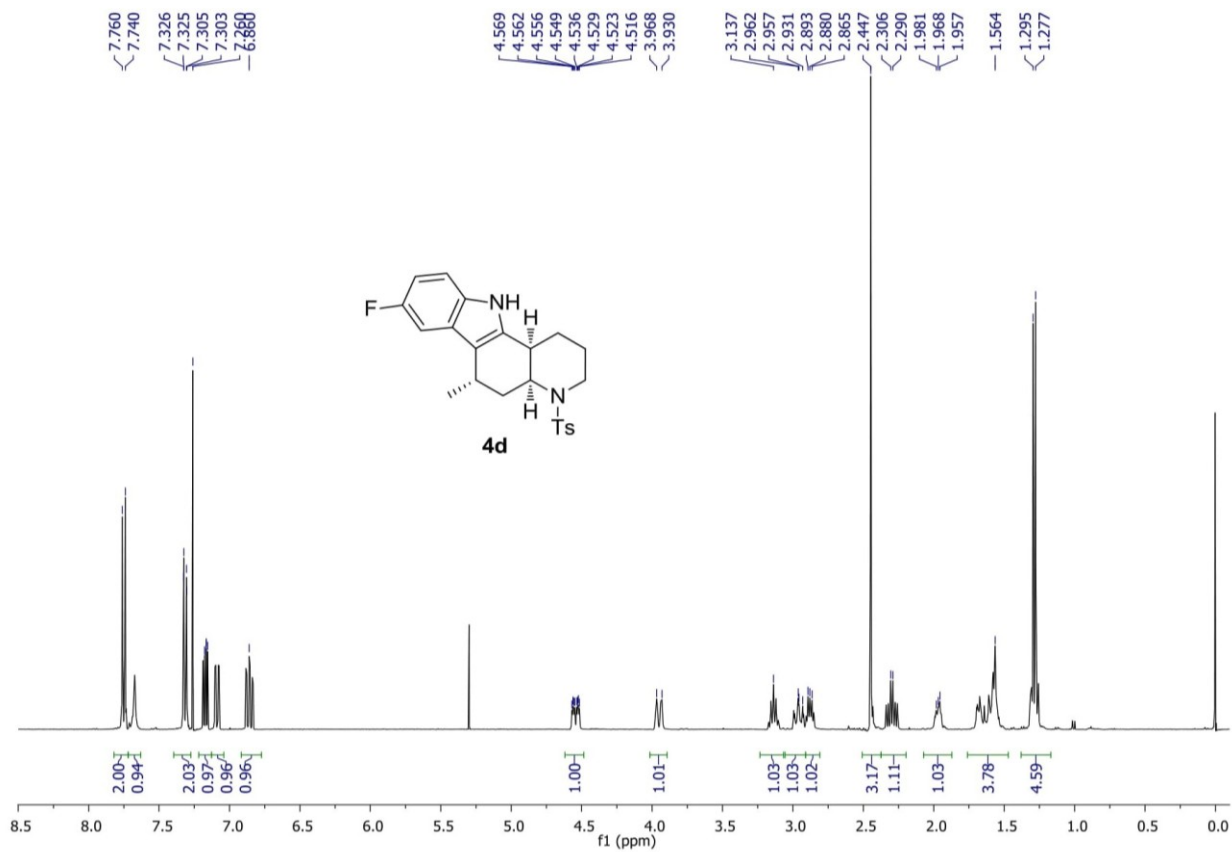


S21

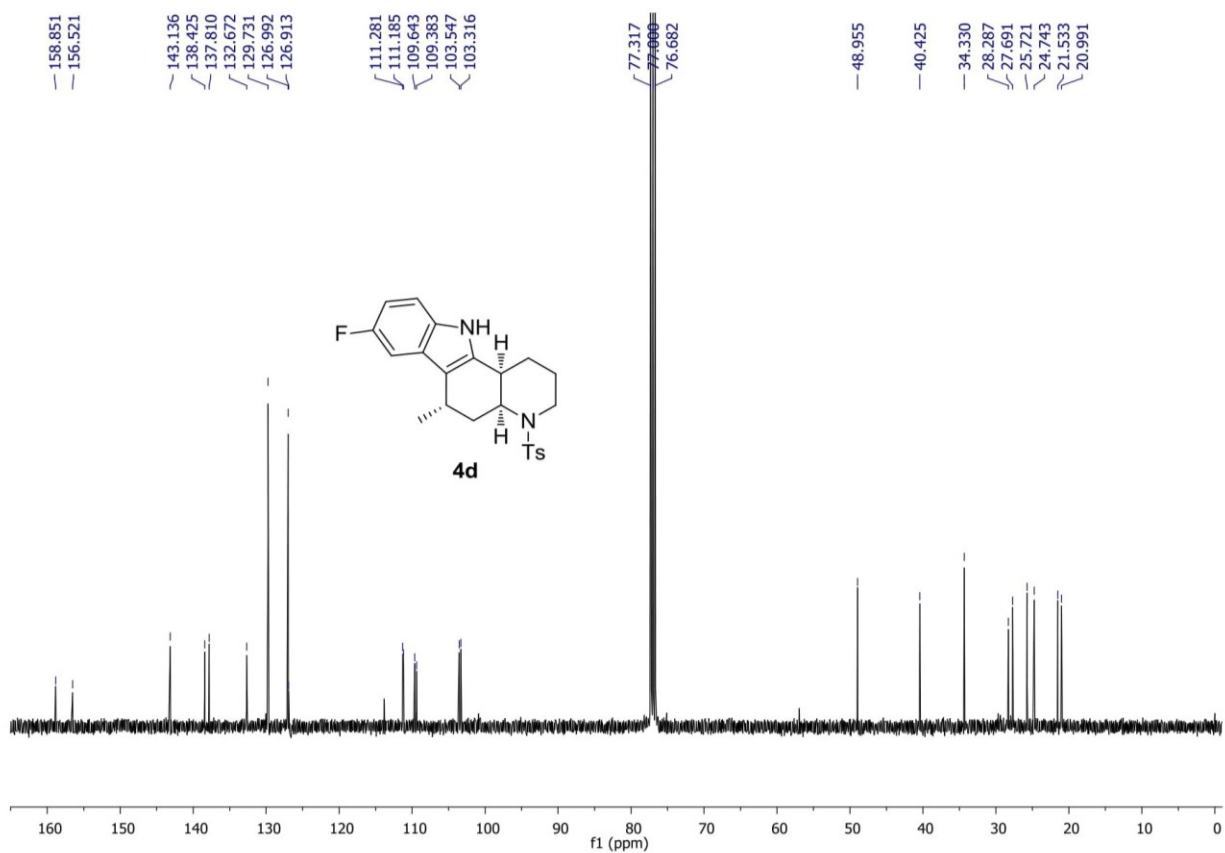


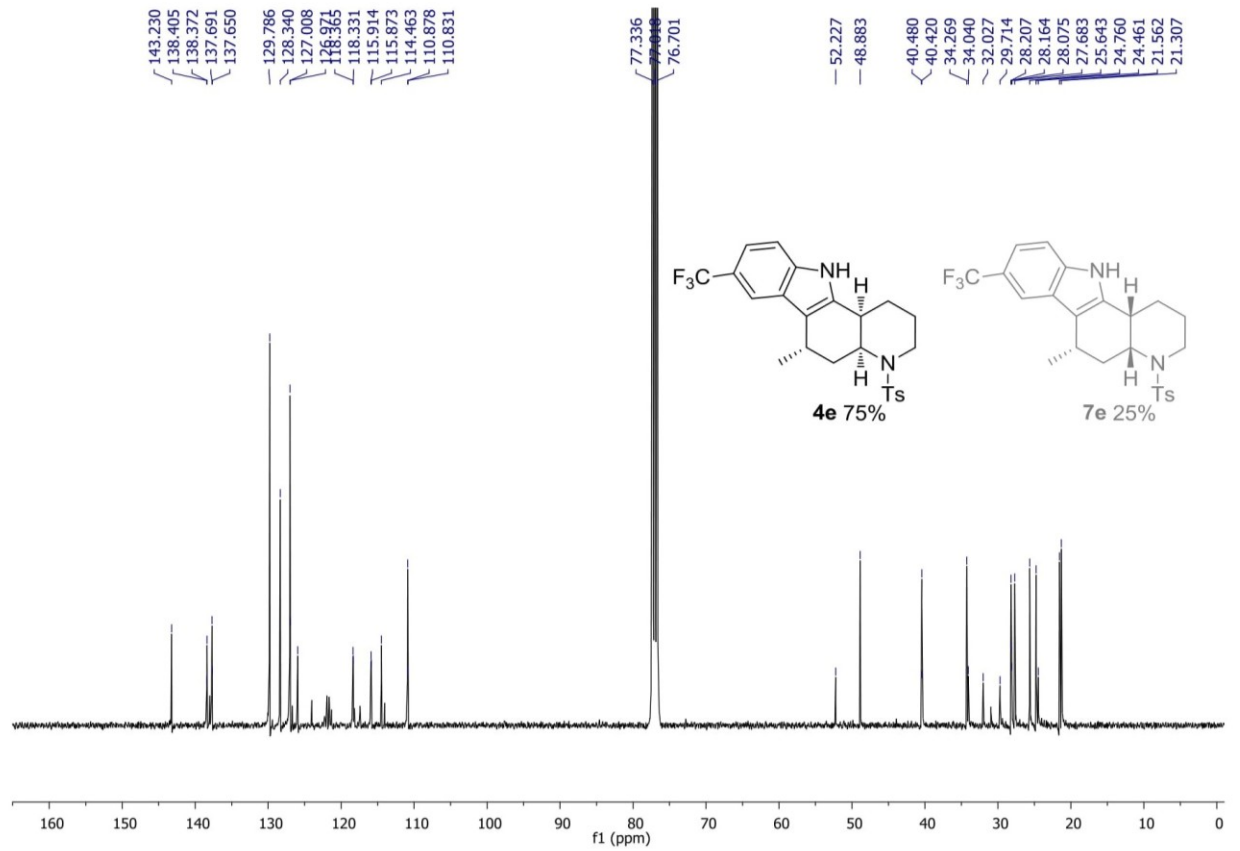
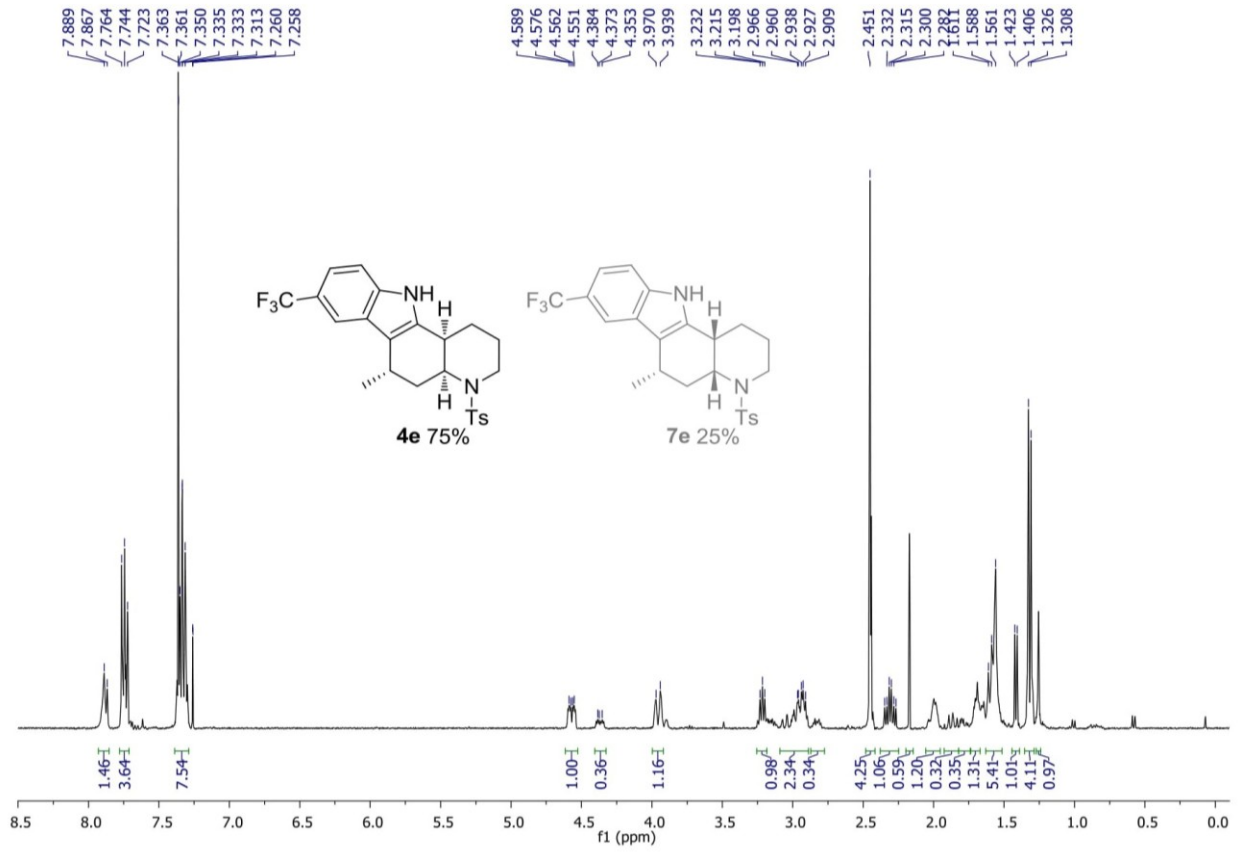


S24

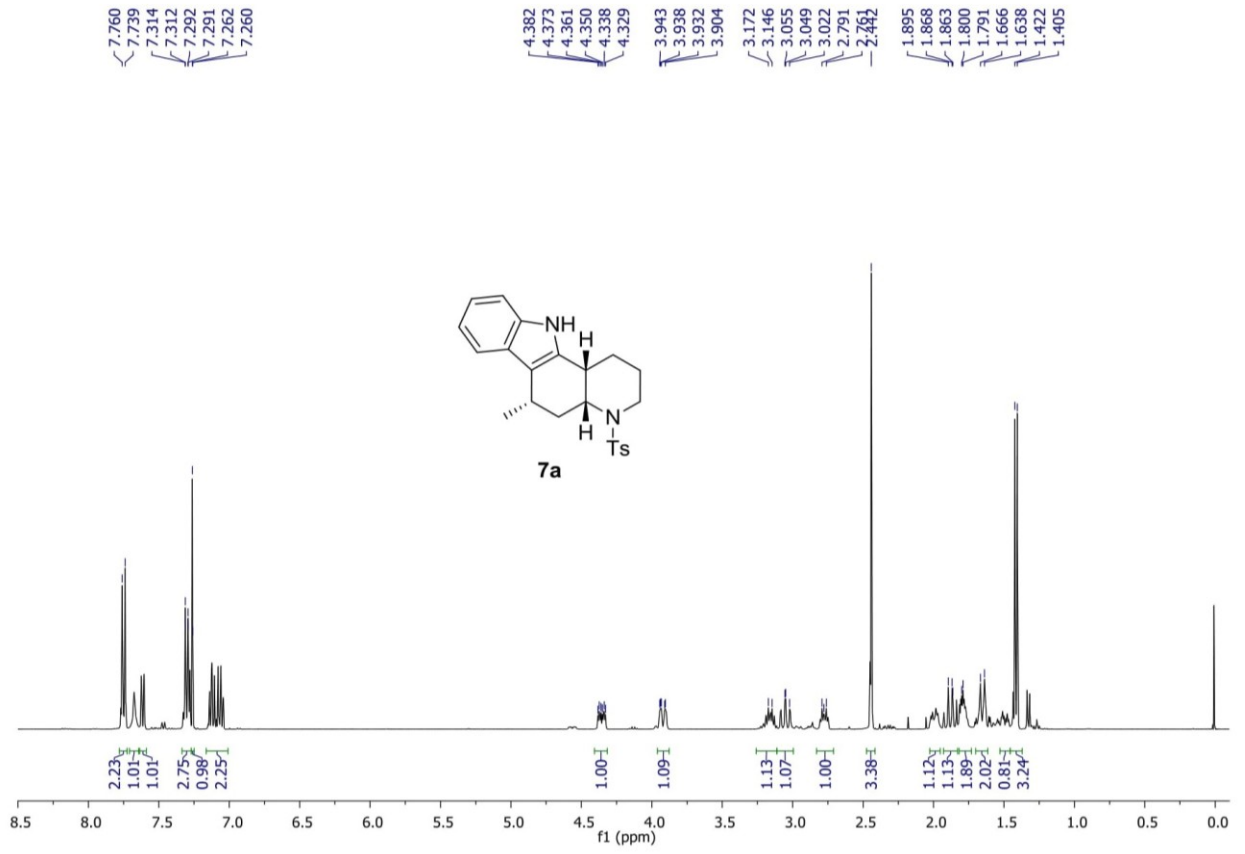


S25

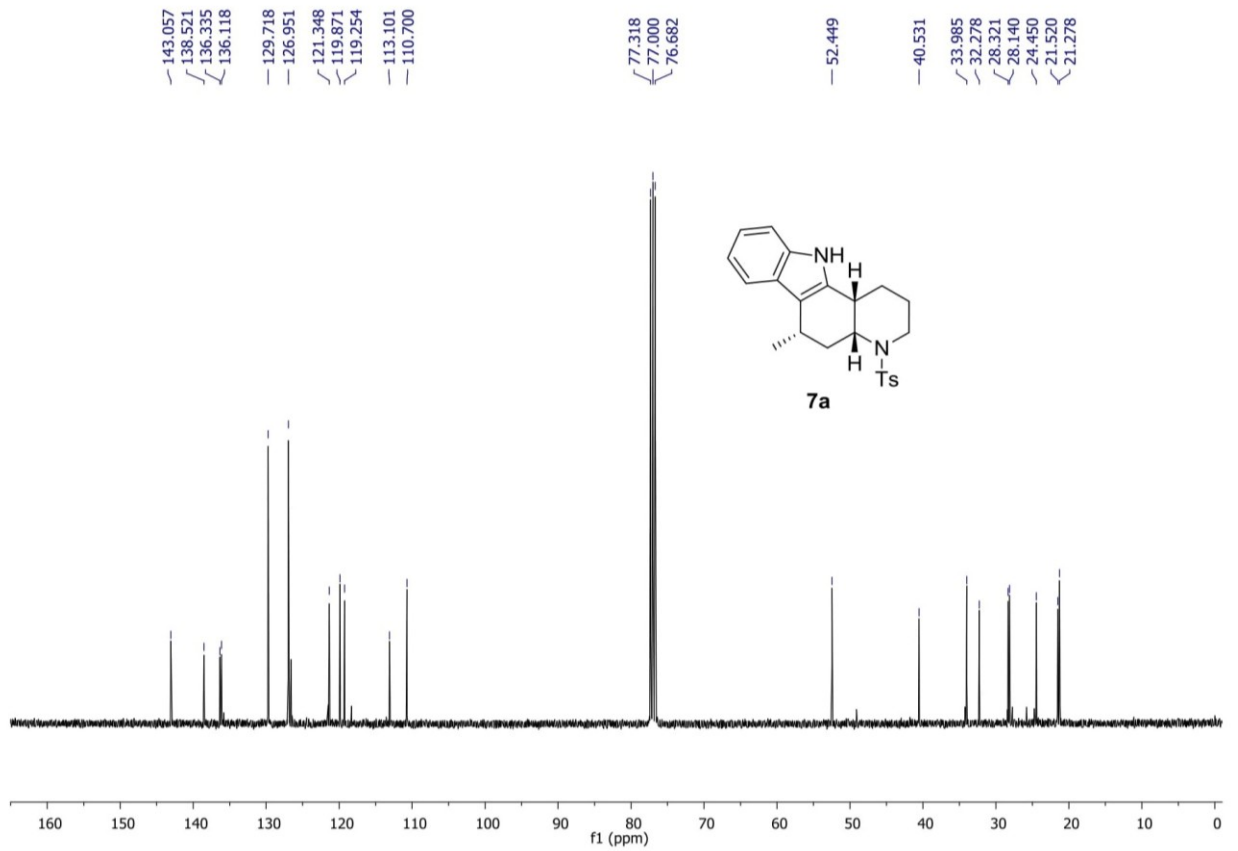


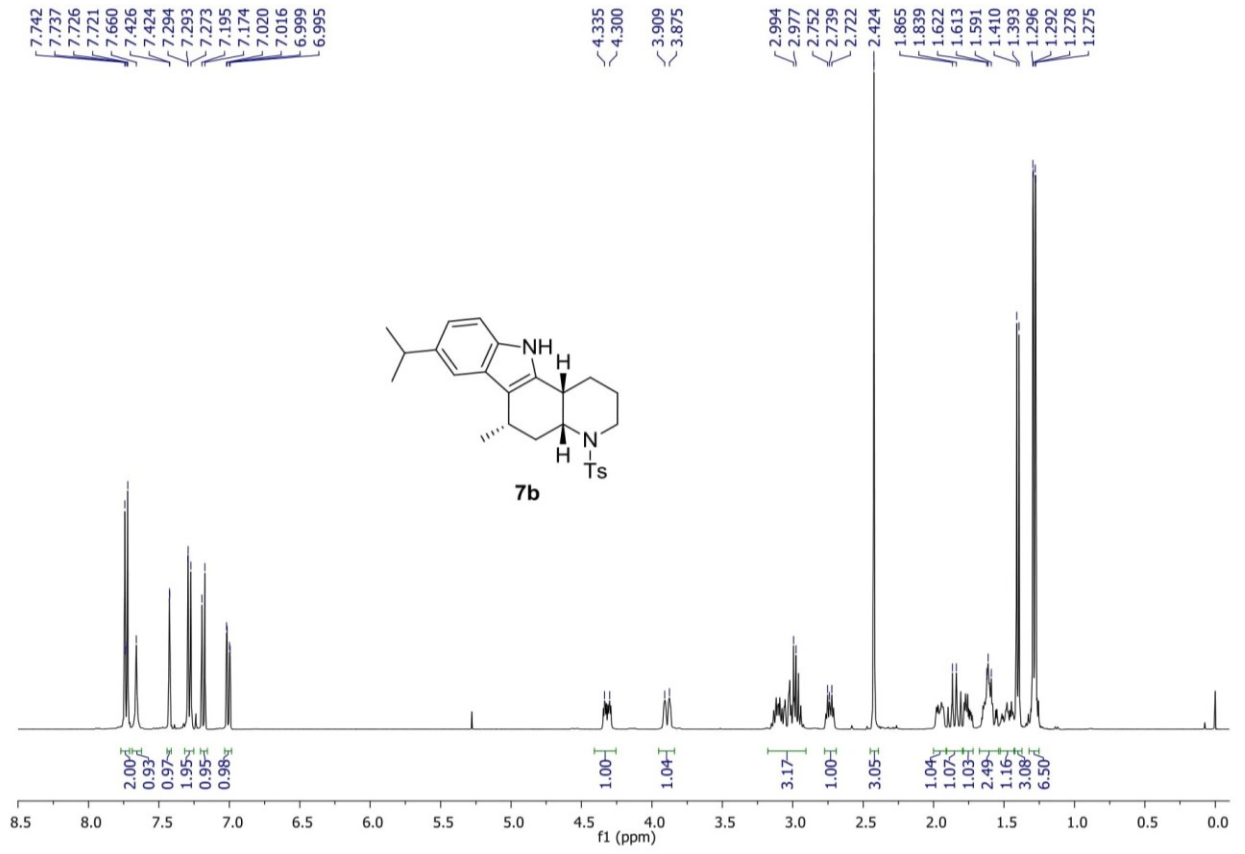


S28

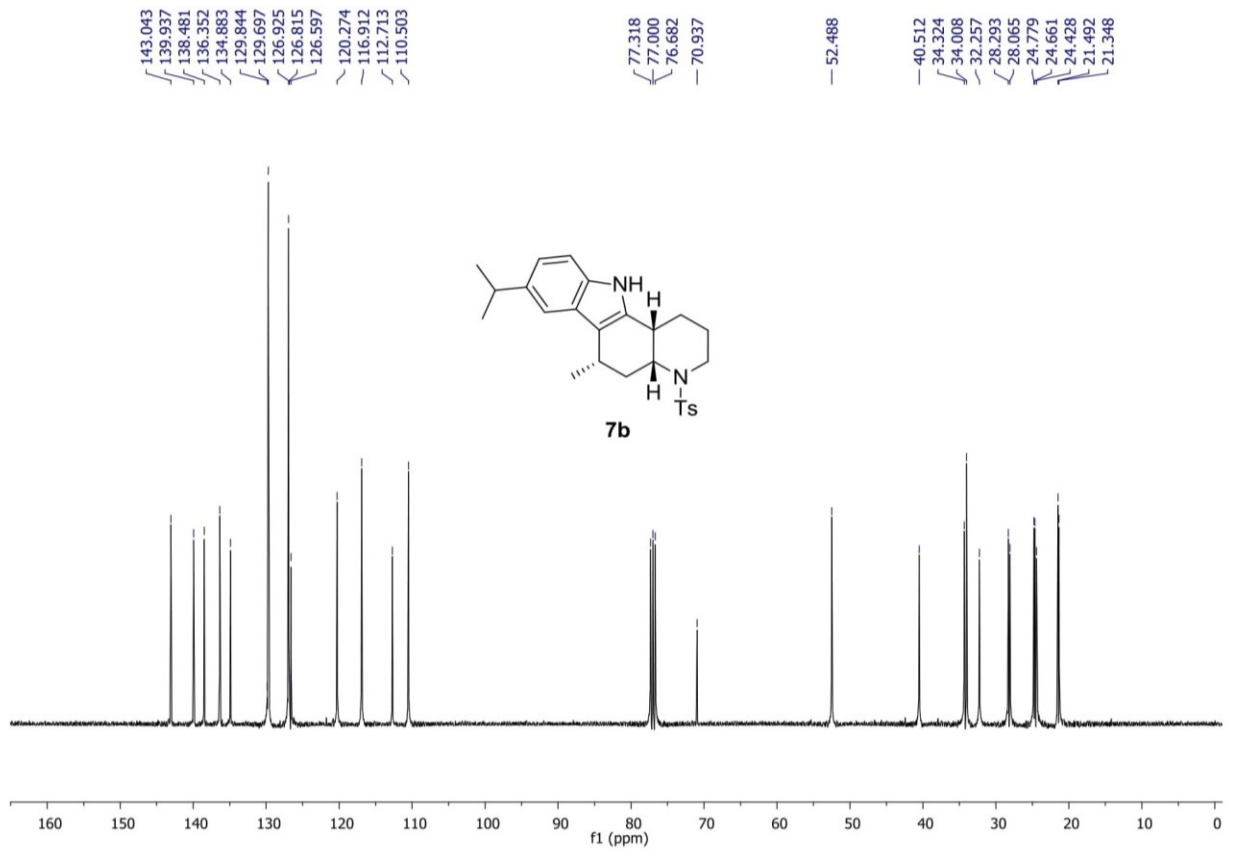


S29

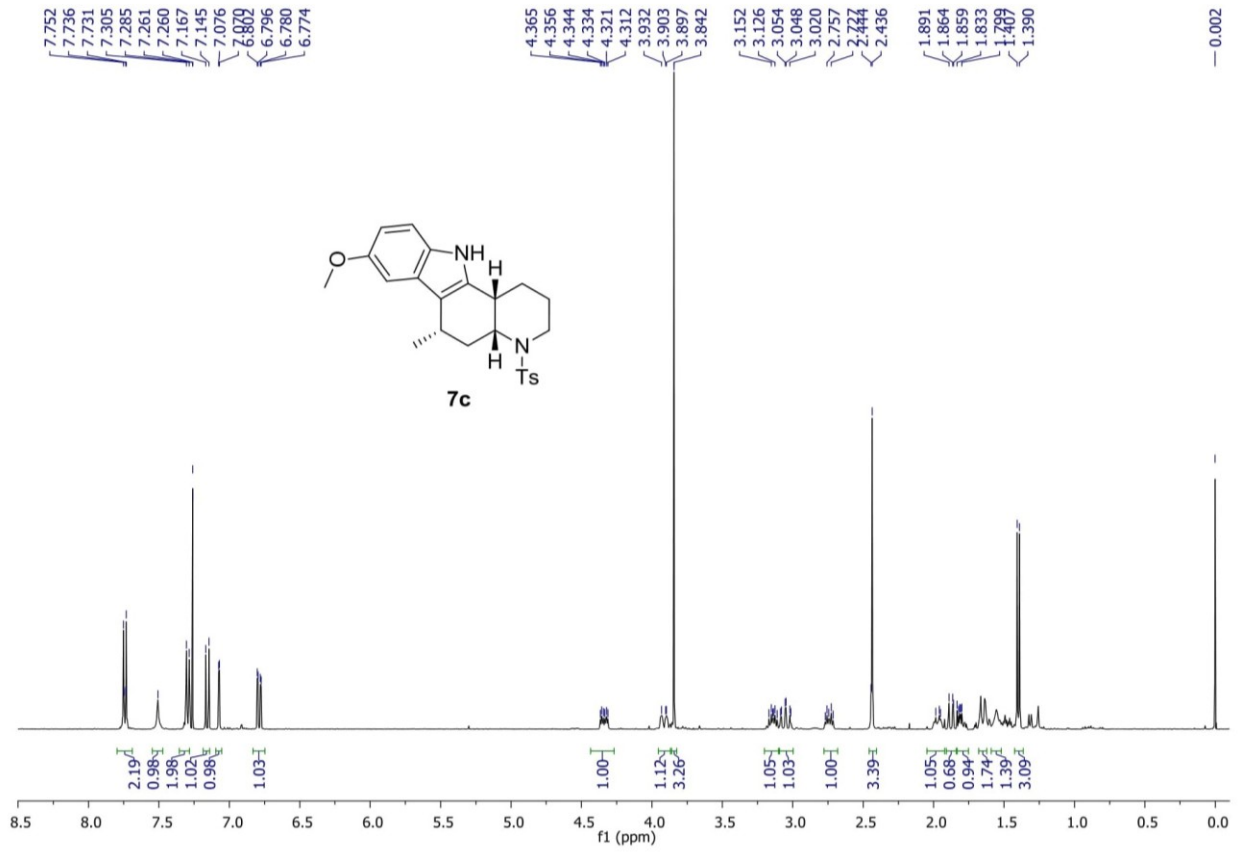




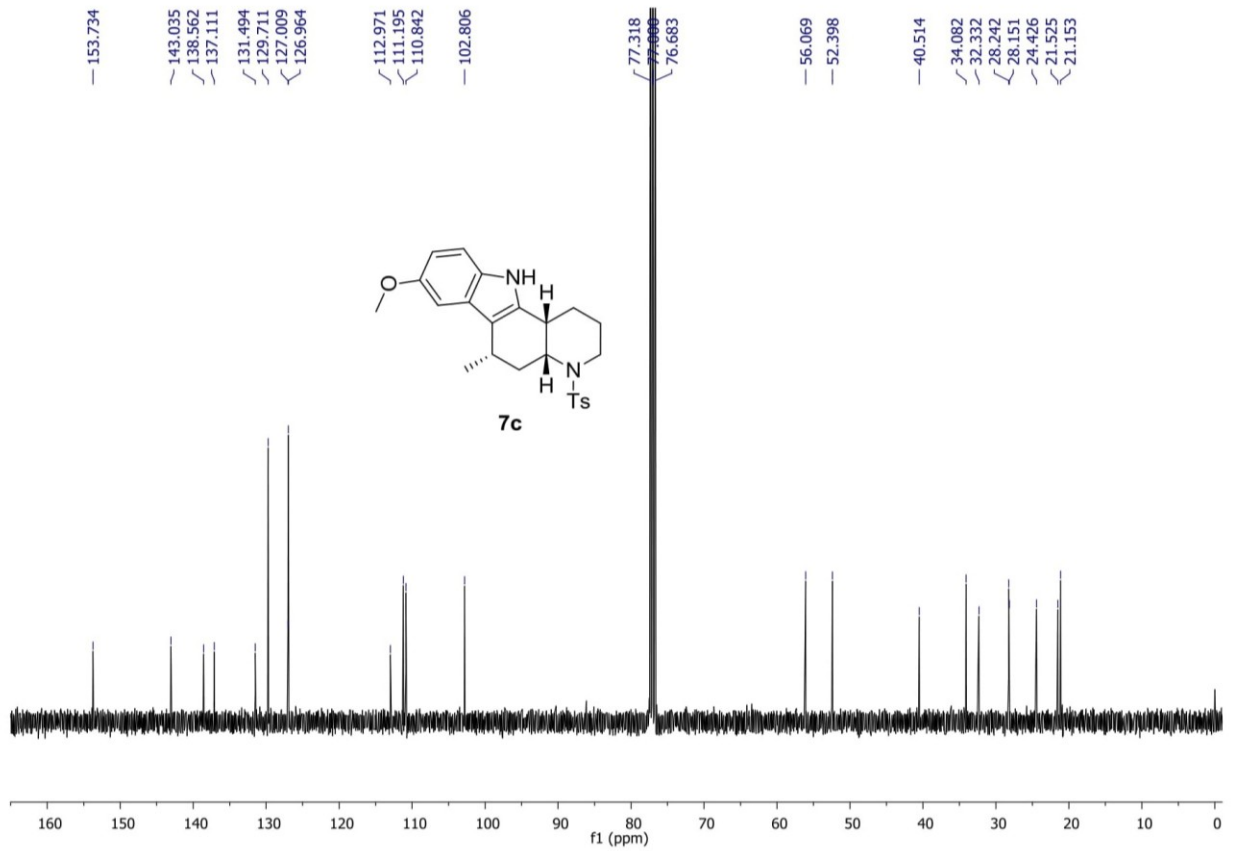
signal at 70.9 ppm being parasitic signal from the NMR machine

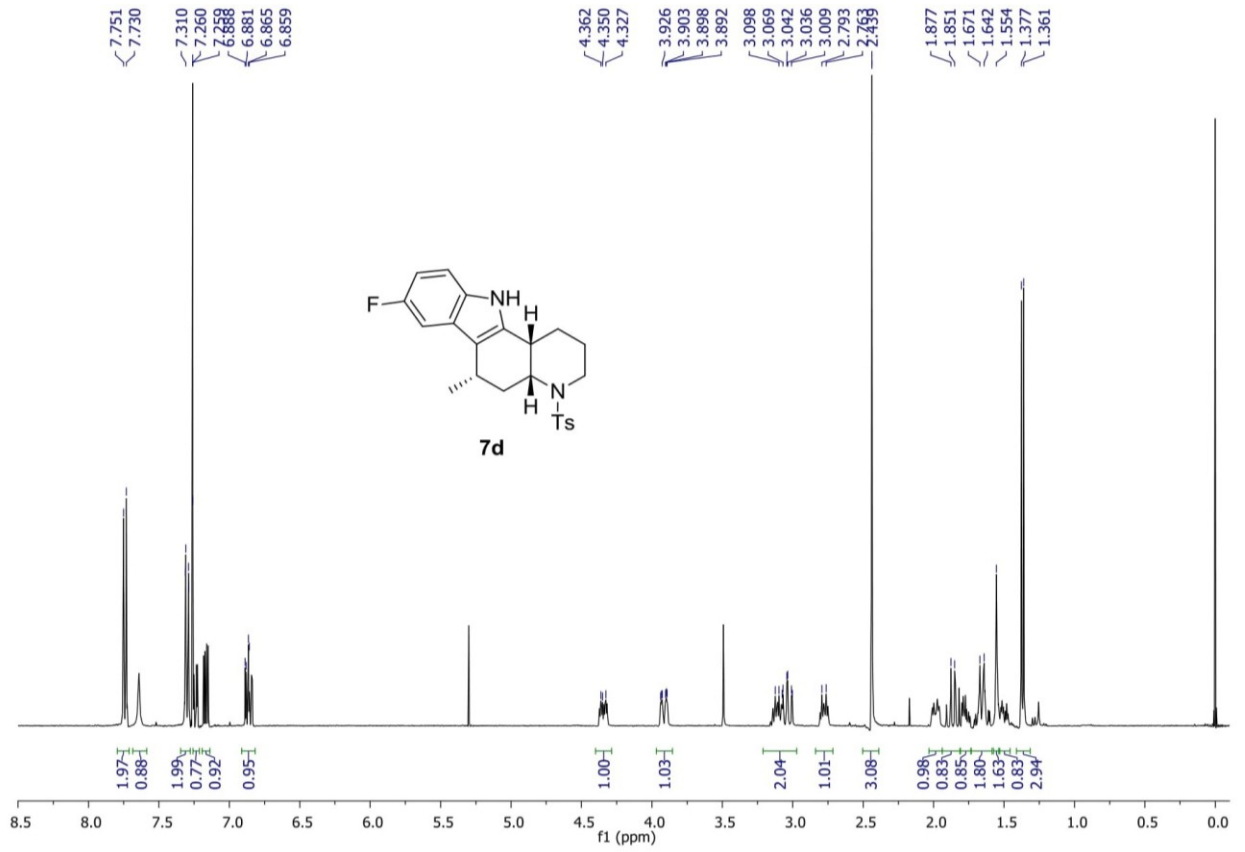


S32

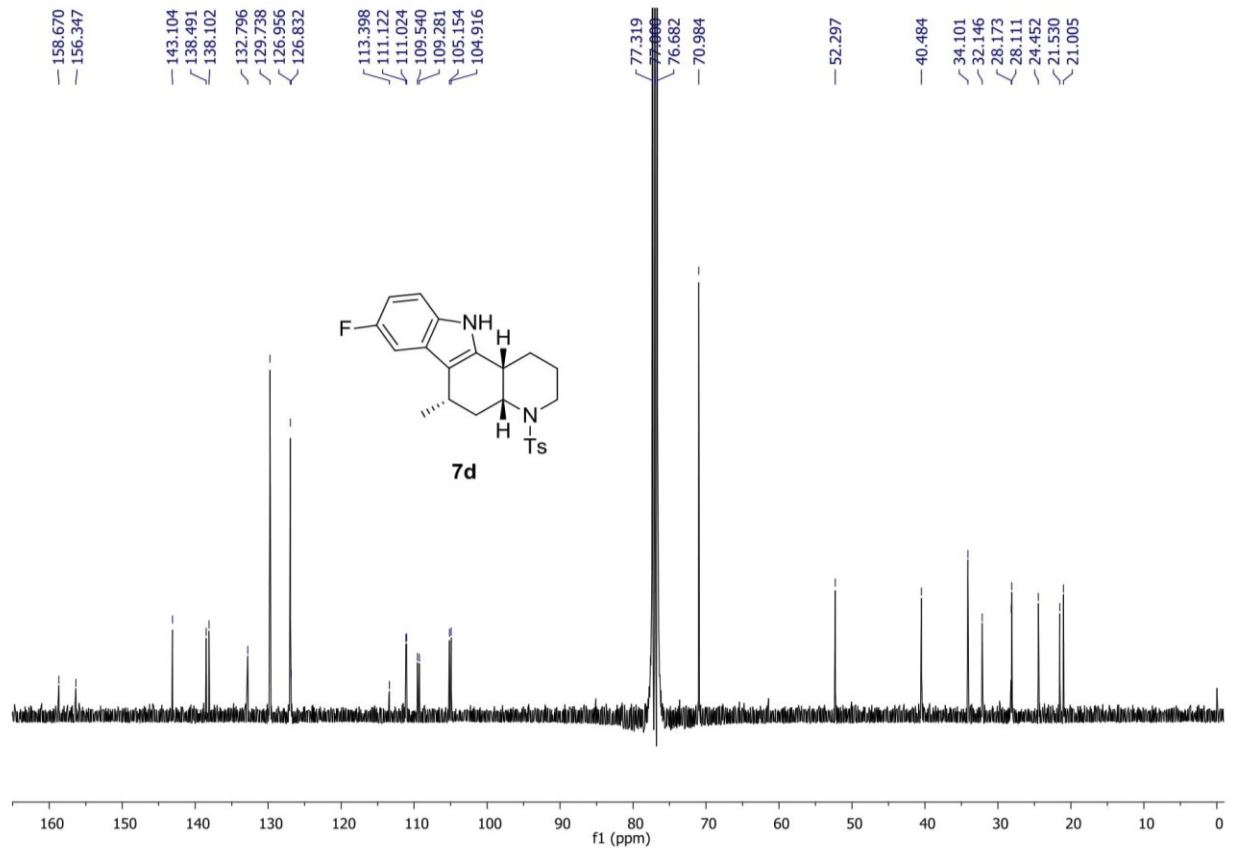


S33





signal at 70.9 ppm being parasitic signal from the NMR machine



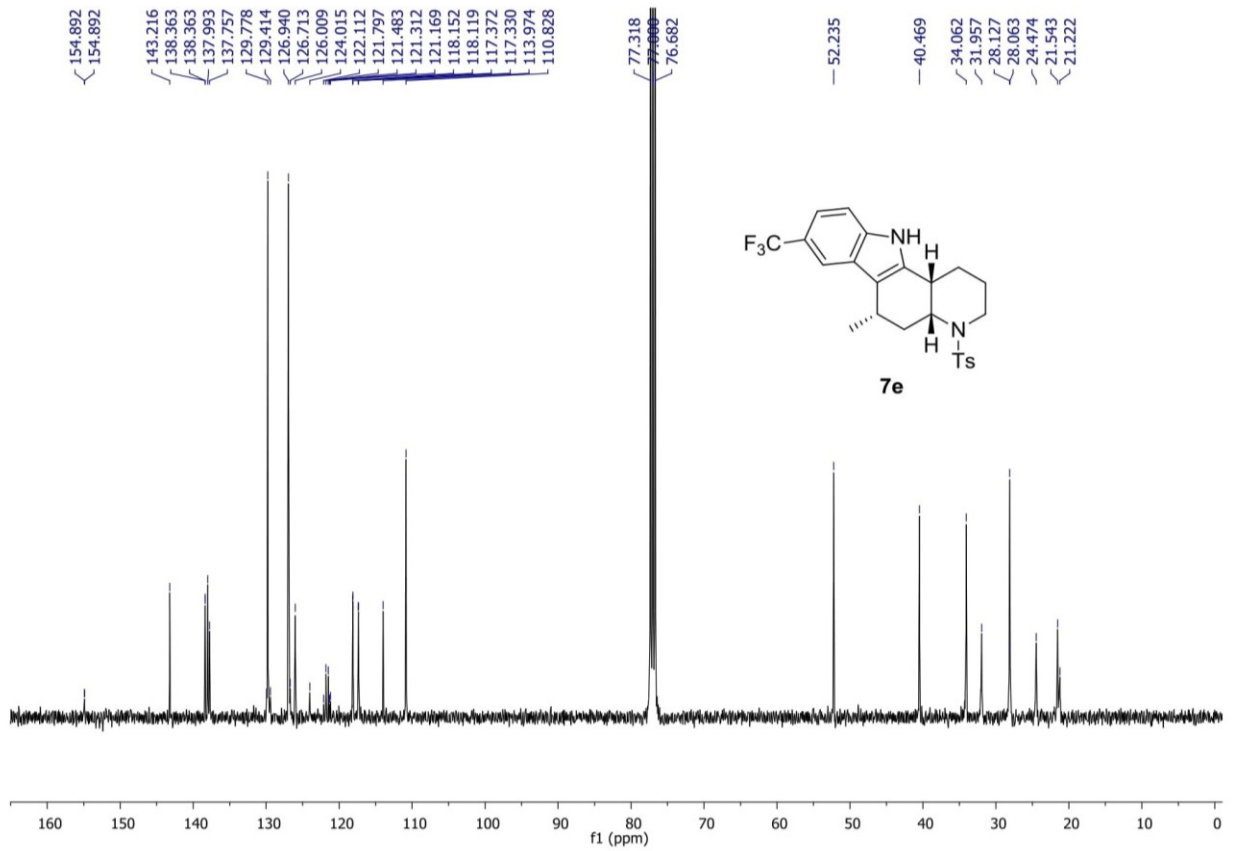
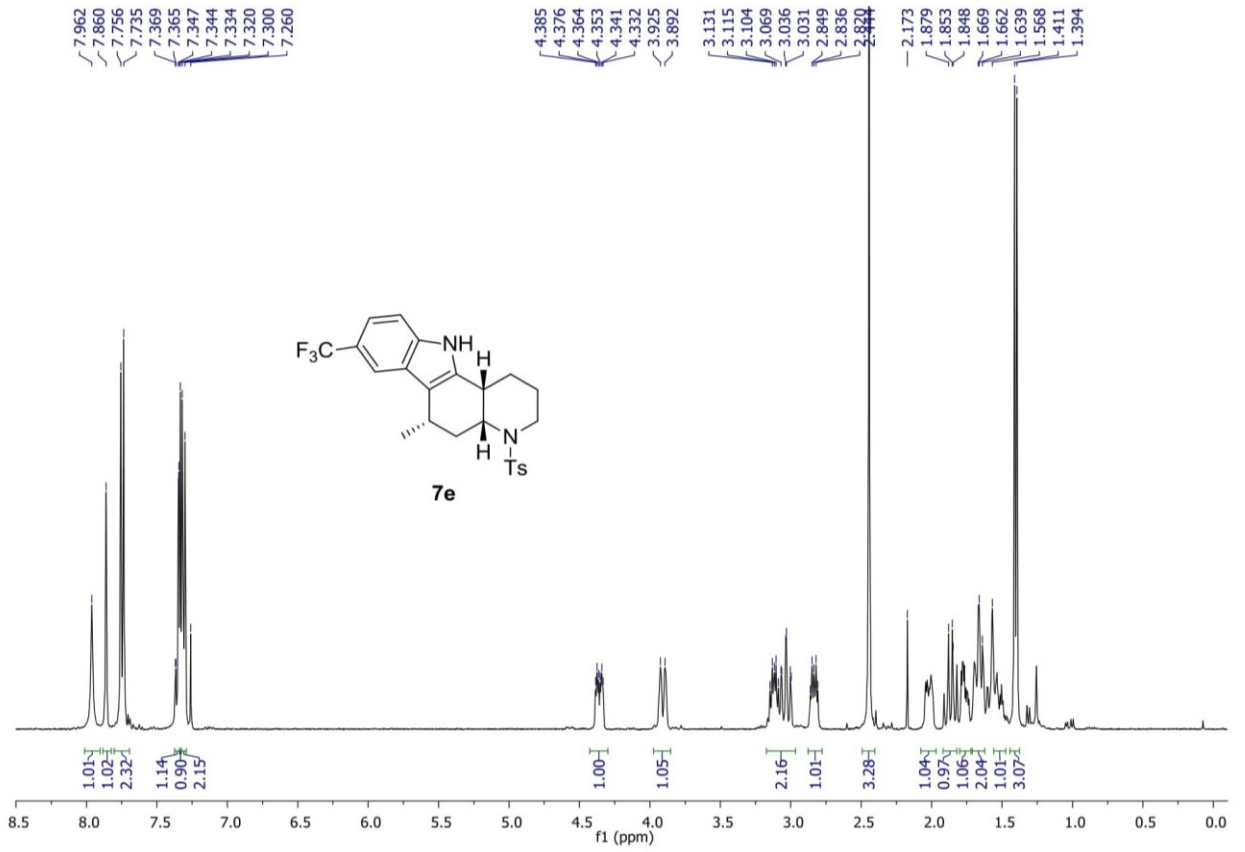


Table 4. Atomic coordinates ($\times 10^4$) and equivalent isotropic displacement parameters ($\text{\AA}^2 \times 10^3$) for p1585c. Parameters of the non-Hydrogen atoms for: p1585c P 21/c R = 0.05
 $U(\text{eq})$ is defined as one third of the trace of the orthogonalized U^{ij} tensor.

	x	y	z	U(eq)
S001	0.40290(3)	0.77954(6)	0.57944(3)	0.0259(1)
O002	0.48372(8)	0.86539(16)	0.59223(9)	0.0326(4)
O003	0.38857(9)	0.66776(15)	0.64496(8)	0.0318(4)
N004	0.33093(11)	0.24063(19)	0.33126(11)	0.0282(5)
N005	0.40455(10)	0.70656(17)	0.47755(10)	0.0250(5)
C006	0.31249(12)	0.3774(2)	0.36039(12)	0.0245(6)
C007	0.17961(12)	0.2719(2)	0.31596(12)	0.0265(6)
C008	0.38393(11)	0.4809(2)	0.39469(12)	0.0225(6)
C009	0.22112(12)	0.4012(2)	0.35133(12)	0.0261(6)
C00A	0.33633(11)	0.5964(2)	0.44869(12)	0.0240(6)
C00B	0.30839(12)	0.8933(2)	0.57866(12)	0.0245(6)
C00C	0.25294(12)	0.6550(2)	0.39099(13)	0.0283(6)
C00D	0.44791(13)	0.7774(2)	0.40104(13)	0.0297(6)
C00E	0.43421(12)	0.5454(2)	0.31441(12)	0.0289(6)
C00F	0.31183(14)	1.0302(2)	0.54148(13)	0.0339(7)
C00G	0.17858(12)	0.5410(2)	0.37577(14)	0.0309(6)
C00H	0.49788(12)	0.6652(2)	0.34870(13)	0.0308(6)
C00I	0.15359(14)	1.0631(3)	0.56712(13)	0.0348(7)
C00J	0.09007(13)	0.2272(2)	0.29436(13)	0.0339(7)
C00K	0.22838(13)	0.8419(2)	0.61037(13)	0.0332(7)
C00L	0.23504(15)	1.1133(2)	0.53682(14)	0.0388(7)
C00M	0.25027(13)	0.1735(2)	0.30409(13)	0.0279(6)
C00N	0.23431(14)	0.0357(2)	0.27137(14)	0.0372(7)
C00O	0.15184(14)	0.9269(3)	0.60395(13)	0.0370(7)
C00P	0.07417(14)	0.0894(3)	0.26361(15)	0.0405(7)
C00Q	0.14492(14)	-0.0050(3)	0.25177(14)	0.0419(8)
C00R	0.12054(14)	0.5294(3)	0.45857(16)	0.0467(8)
C00S	0.06945(15)	1.1552(3)	0.55820(16)	0.0512(9)

Approach to *cis*-Phlegmarine Alkaloids via Stereodivergent Reduction: Total Synthesis of (+)-Serratezomine E and Putative Structure of (–)-Huperzine N

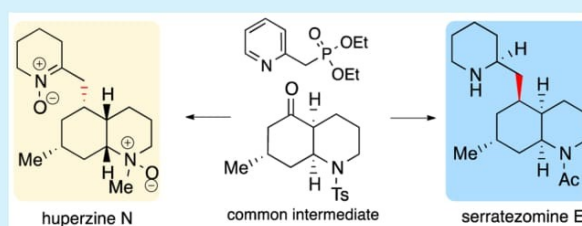
Caroline Bosch,[†] Béla Fiser,[‡] Enrique Gómez-Bengo,[‡] Ben Bradshaw,^{*,†} and Josep Bonjoch^{*,†}

[†]Laboratori de Química Orgànica, Facultat de Farmàcia, IBUB, Universitat de Barcelona, Av. Joan XXIII s/n, 08028 Barcelona, Spain

[‡]Departamento de Química Orgánica I, Universidad del País Vasco, Manuel Lardizábal 3, 20018 San Sebastián, Spain

S Supporting Information

ABSTRACT: A unified strategy for the synthesis of the *cis*-phlegmarine group of alkaloids is presented, leading to the first synthesis of serratezomine E (1) as well as the putative structure of huperzine N (2). A contrasteric hydrogenation method was developed based on the use of Wilkinson's catalyst, which allowed the facial selectivity of standard hydrogenation to be completely overturned. Calculations were performed to determine the mechanism, and structures for huperzines M and N are reassigned.

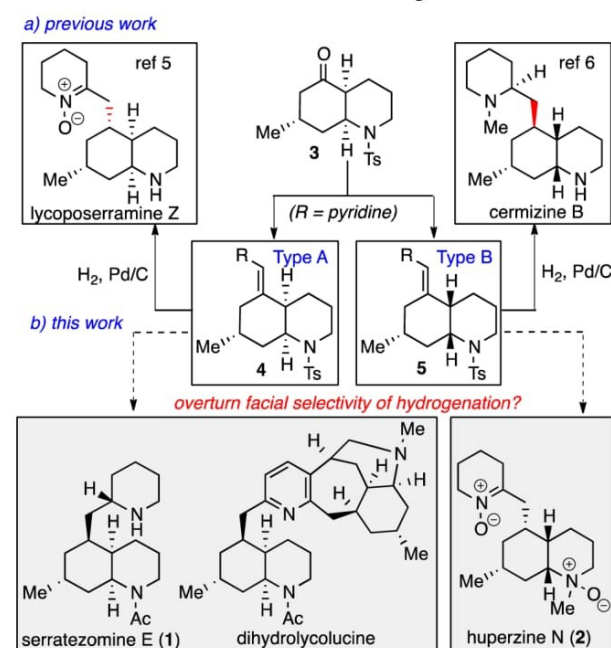


In the field of natural product synthesis there is a growing trend toward developing strategies that can prepare diverse molecular skeletons from a common intermediate.¹ Such “unified synthesis” approaches have an advantage in that they produce the maximum amount of molecular diversity in the most efficient manner possible, thereby facilitating structure–activity relationship studies. Our interest in this field stems from our research program to develop a unified synthesis of the *Lycopodium* alkaloids.² In particular, our efforts have focused on the phlegmarine alkaloid subset, since not only do their multiple stereochemical arrangements present synthetic challenges, but the core framework, embedded throughout the *Lycopodium* alkaloids, would constitute an ideal common scaffold in a unified synthesis of these compounds.^{3,4}

Previously, we have developed an organocatalyzed tandem cyclization to access 5-oxodecahydroquinoline 3 bearing three stereogenic centers in a one-pot manner. Subsequent coupling generated the first point of diversification, providing vinylpyridines 4 or 5 depending on the conditions employed. Hydrogenation of the formed alkene led to a second point of diversity, which from 4 almost exclusively gave the stereochemistry required for the synthesis of lycoposerramine Z.⁵ Similarly, hydrogenation of vinylpyridine 5, under the same conditions, allowed the synthesis of cermizine B⁶ (Scheme 1). Access to a wide range of C-5 epimeric *Lycopodium* alkaloids, such as those shown in Scheme 1,⁷ would require the facial selectivity of this hydrogenation step to be completely overturned.⁸ We herein report a highly efficient process to achieve this objective and its application to the first total synthesis of serratezomine E.^{7a} Using this strategy, we also accomplished the total synthesis of the putative structure of huperzine N^{7c} and its reassignment.

The selectivity of the hydrogenation of vinylpyridine 4 (Figure 1) using either Pd–C or Raney nickel is believed to be

Scheme 1. Stereochemistries of *cis*-Phlegmarine Alkaloids



governed by an axially positioned methyl group, which blocks the approach from the lower face of the molecule, leading to the kinetic decahydroquinoline 6b (Table 1, entries 1 and 2). A priori, compound 7 appeared to be a convenient precursor of 8a, since its different conformation (Figure 1) could allow a

Received: September 9, 2015

Published: September 25, 2015

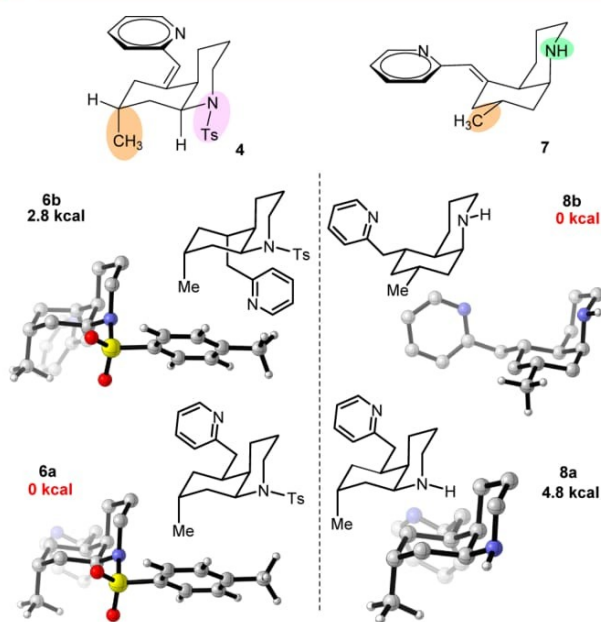
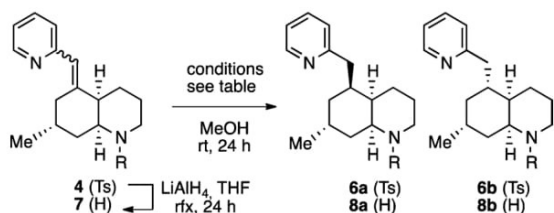


Figure 1. Structural conformations and relative stabilities of **6a/b** and **8a/b**, computed at B3LYP/6-311G** (LANL2DZ) level of theory.

Table 1. Screening of Conditions for the Reduction Reaction^a



entry	compd	method ^a	yield ^b (%)	dr ^c a:b
1	4	H ₂ , Pd–C	100	3:97
2	4	H ₂ , Ra–Ni	75	14:86
3	7	H ₂ , Pd–C	100	36:64
4	4	Mn(dpm) ₃ , PhSiH ₃ , TBHP	63	73:27
5	7	Mn(dpm) ₃ , PhSiH ₃ , TBHP	0	
6 ^d	4	Fe ₂ (ox) ₃ ·H ₂ O, NaBH ₄ , H ₂ O	10	75:25
7 ^e	4	Co(acac) ₃ , Et ₃ SiH, TBHP	7	nd
8 ^d	4	Fe(acac) ₃ , PhSiH ₃	49	67:33
9	4	H ₂ , [Ir(PCy ₃) ₃ (cod)(py)]PF ₆	100	68:32
10	4	H ₂ , [RhCl(PPh ₃) ₃]	100	96:4

^aFor detailed reactions conditions, see the Supporting Information. Reactions were performed on a mixture of *E/Z* isomers (4:1). ^bYield of hydrogenated compounds refers to the conversion determined from ¹H NMR spectra. ^cThe ratio was determined by ¹H NMR spectroscopy of the unpurified reaction mixture. ^dEtOH used as solvent. ^ePrOH used as solvent and 1,4-cyclohexadiene as additive.

kinetic hydrogenation from the bottom face and lead to the thermodynamically more stable epimer **8a**. However, hydrogenation of the secondary amine **7** (entry 3) did not give the expected reversal of selectivity. An explanation is that the haptophilicity⁹ of the secondary amino function binds it to the catalyst surface and thus directs the delivery of the hydrogen from the top face of **7** to give **8b** as the major epimer.

We then evaluated the reductive radical conditions recently reported by Shenvi,¹⁰ known to give more thermodynamically

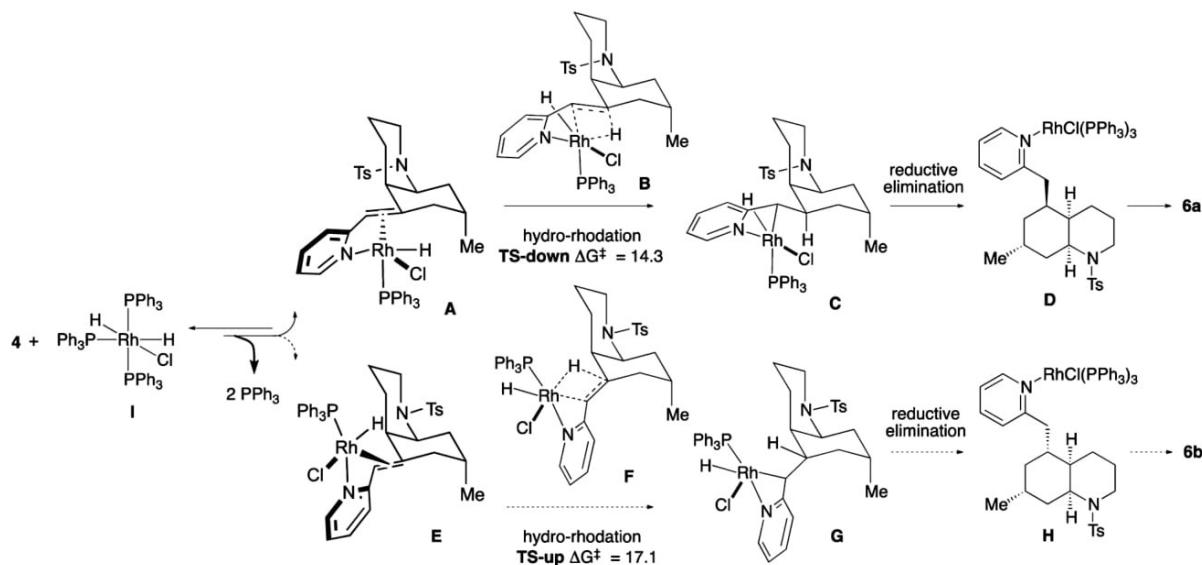
favored products. Calculations showed that the targeted **6a** was 2.8 kcal more stable than its epimer **6b** (Figure 1), and indeed, it was obtained as the main compound in a ratio of 73:27 (entry 4), although it was difficult to separate from significant amounts of byproducts (>30%).¹¹ When the same conditions were applied to the N–H compound **7**, there was no reaction and the starting material was completely recovered (entry 5). Similar radical-based methods based on other protocols,¹² either directly or modified, were also evaluated, but with no significant improvements (entries 6–8). We then assessed homogeneous hydrogenation catalysts and were pleased to observe that Crabtree's catalyst provided the same stereoselectivity as Mn(dpm)₃ but without any byproducts (entry 9). Finally, Wilkinson's catalyst proved more successful, enabling us to achieve almost complete diastereoselectivity (96:4) in a clean quantitative manner using only 2 mol % of catalyst (entry 10).¹³

Given the sterically impeded nature of the β,β disubstituted vinylpyridine and large size of Wilkinson's catalyst, we presumed the reaction proceeded via a coordination of the catalyst.¹⁴ Indeed, when the analogous benzene analogue of **4** (not shown) lacking the pyridine nitrogen was prepared, no reduction was observed.

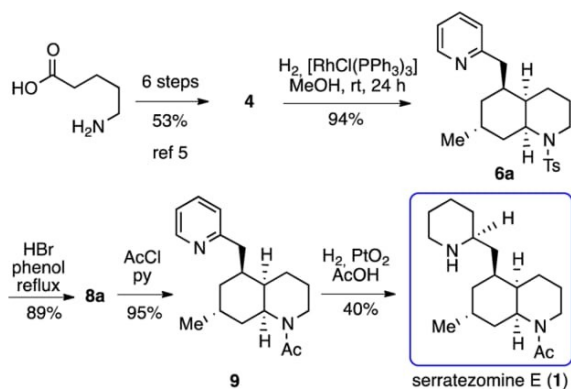
To understand the reaction and account for the excellent stereocontrol observed, calculations were performed, and the proposed reaction mechanism is outlined in Scheme 2. The hydrogenated Wilkinson's catalyst (**I**) forms an initial complex **A** by coordination of the double bond and the pyridine nitrogen atom of the substrate, releasing two molecules of phosphine in the process, which can occur through both faces of the double bond. In complex **A**, the Rh atom is coordinated to the pyridine ring and the double bond with short interatomic Rh–N (2.4 Å) and Rh–alkene (2.3 Å) distances, inducing a slight deconjugation of the double bond and the pyridine ring, which is partially responsible for its 10 kcal/mol higher energy than the initial hydrogenated Wilkinson catalyst. Thus, the initial equilibrium between the starting materials and **A** is shifted toward the former (Scheme 2). However, the very low activation energy required for the hydro-rhodation (**TS-down** is only 4 kcal/mol above **A**) makes the whole process feasible, triggering an easy formation of **C**, and the consumption of the starting material. After the insertion of hydrogen into **C**, the reaction proceeds through reductive elimination, liberating the final product **D**. As mentioned, the hydro-rhodation step can occur on either face of the double bond, through two diastereoisomeric transition states, **TS-down** and **TS-up** (**E** → **G**). The computed activation energies predict that **TS-down** is favored by 2.8 kcal/mol over **TS-up**, justifying the experimental formation of the major diastereoisomer **6a**. The main difference between the two diastereomeric transition states consists of the different orientation of the *N*-tosyl moiety of the substrate. In **B**, the phenyl ring of the tosyl group forms at least three strong π-stacking interactions, with one of the rings of the PPh₃ group, and with two different H atoms of the bicyclic skeleton (see Supporting Information). During the transition state, the Rh–alkene bond is even tighter than in **A** (2.1 Å), inducing a weakening of the Rh–N coordination (2.5 Å).

With the optimum reduction method in hand, transformation of **4** (prepared in six steps from the commercially available 5-aminopentanoic acid) led to a concise synthesis of serratezomine **E** (**1**, Scheme 3). Hydrogenation with Wilkinson's catalyst and removal of the tosyl group of **6a** led to the secondary amine **8a** in a pure form and the introduction

Scheme 2. Proposed Mechanism for the Rh-Catalyzed Hydrogenation of 4



Scheme 3. Synthesis of Serratezomine E (1)



of the required acetyl group gave **9**. Subsequent reduction of the pyridine provided serratezomine E (**1**) as a white solid,¹⁵ whose structure was unequivocally confirmed by X-ray analysis (Figure 2), having the absolute configuration (*S*) at the C2 piperidine ring and (*R*) at the C7 decahydroquinoline ring, characteristic of phlegmarine alkaloids.^{16,17}

An analogous procedure allowed for the synthesis of huperzine N (**2**, Scheme 4). Hydrogenation of **5** with

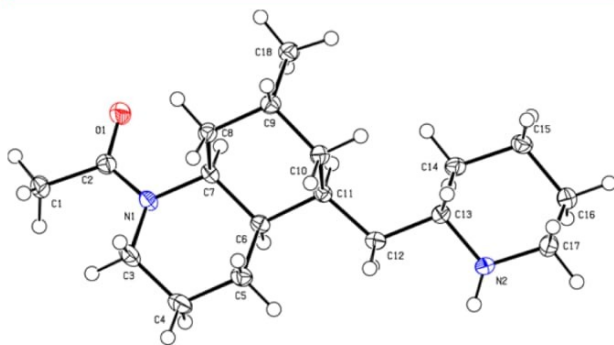
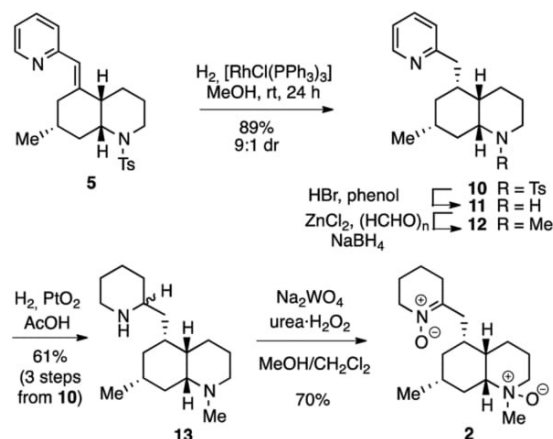


Figure 2. X-ray structure of (+)-serratezomine E (1).

Scheme 4. Synthesis of Putative Huperzine N (2)



Wilkinson's catalyst gave the desired epimer **10** in a 9:1 ratio. Removal of the tosyl group, formation of the *N*-methyl via reductive amination with ZnCl_2 ,¹⁸ and reduction of the pyridine gave **11** in good overall yield. Finally, oxidation with Na_2WO_4 /urea- H_2O_2 ⁵ gave the reported structure of huperzine N, although the NMR spectra of **2** did not match those described (see the Supporting Information). Instead, the ¹³C NMR data of natural huperzine N would be explained by structure **14** (Figure 3), whose NMR data are consistent with the *N*-oxide form of the previously isolated lycoposerramine Y.¹⁹ Indeed, the closely related alkaloid huperzine M (**15**)^{7c} should also be

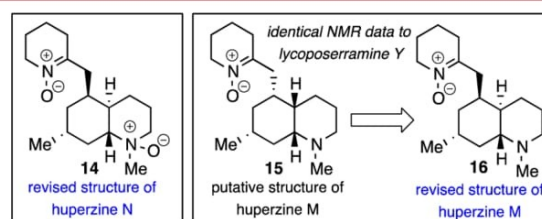


Figure 3. Revised structure for huperzines M and N.

reassigned, its NMR data being identical to those of lycoposerramine Y (**16**).

In summary, a divergent hydrogenation protocol was developed that provides access to a range of *Lycopodium* compounds unattainable by standard hydrogenation of common vinylpyridine intermediates. Via rhodium complexation with the pyridine nitrogen and selective facial delivery, it was possible to invert the course of hydrogenation from 97:3 to 4:96 dr. This method was successfully applied for the first total synthesis of serrazomine E as well as huperzine N. The latter turned out to be a putative structure, and the natural one was structurally reassigned. The application of this strategy to other *cis* and *trans* *Lycopodium* alkaloids is now in progress.

■ ASSOCIATED CONTENT

Supporting Information

The Supporting Information is available free of charge on the ACS Publications website at DOI: 10.1021/acs.orglett.5b02581.

Experimental procedures, spectroscopic and analytical data, and NMR spectra of new compounds; Cartesian coordinates and energies for all species considered in Scheme 2 (PDF)
X-ray data for **1** (CIF)

■ AUTHOR INFORMATION

Corresponding Authors

*E-mail: benbradshaw@ub.edu.

*E-mail: josep.bonjoch@ub.edu.

Notes

The authors declare no competing financial interest.

■ ACKNOWLEDGMENTS

Financial support for this research was provided by Project CTQ2013-41338-P and CTQ2013-47925-C2 from MINECO the Ministry of Economy and Competitiveness of Spain and the FP7 Marie Curie Actions of the European Commission via the ITN ECHONET Network (MCITN-2012–316379). We also thank SGLker (UPV/EHU) for providing computational resources.

■ REFERENCES

- (1) (a) Jones, S. B.; Simmons, B.; Mastracchio, A.; MacMillan, D. W. C. *Nature* **2011**, *475*, 183. (b) Anagnostaki, E. E.; Zografos, A. L. *Chem. Soc. Rev.* **2012**, *41*, 5613. (c) Mercado-Marin, E. V.; Sarpong, R. *Chem. Sci.* **2015**, *6*, 5048.
- (2) (a) Ma, X.; Gang, D. R. *Nat. Prod. Rep.* **2004**, *21*, 752. (b) Hirasawa, Y.; Kobayashi, J.; Morita, H. *Heterocycles* **2009**, *77*, 679. (c) Siengalewicz, P.; Mulzer, J.; Rinner, U. *Alkaloids* **2013**, *72*, 1.
- (3) For initial studies to access all stereoparents of the 7-methyl-5-oxodecahydroquinoline core of phlegmarine alkaloids, see: Bradshaw, B.; Luque-Corredera, C.; Saborit, G.; Cativiela, C.; Dorel, R.; Bo, C.; Bonjoch, J. *Chem. - Eur. J.* **2013**, *19*, 13881.
- (4) For total synthesis of *trans*-phlegmarine alkaloids, see: (a) Wolfe, B. H.; Libby, A. H.; Al-awar, R. S.; Foti, C. J.; Comins, D. L. *J. Org. Chem.* **2010**, *75*, 8564 and references cited therein. (b) Tanaka, T.; Kogure, N.; Kitajima, M.; Takayama, H. *J. Org. Chem.* **2009**, *74*, 8675.
- (5) Bradshaw, B.; Luque-Corredera, C.; Bonjoch, J. *Org. Lett.* **2013**, *15*, 326.
- (6) Bradshaw, B.; Luque-Corredera, C.; Bonjoch, J. *Chem. Commun.* **2014**, *50*, 7099.
- (7) (a) Serratezomine E: Kubota, T.; Yahata, H.; Yamamoto, S.; Hayashi, S.; Shibata, T.; Kobayashi, J. *Bioorg. Med. Chem. Lett.* **2009**,

- 19, 3577. (b) Dihydrolycolucine: Ayer, W. A.; Browne, L. M.; Nakahara, Y.; Tori, M.; Delbaere, L. T. *Can. J. Chem.* **1979**, *57*, 1105. (c) Huperzine N: Gao, W. Y.; Li, Y. M.; Jiang, S. H.; Zhu, D. Y. *Helv. Chim. Acta* **2008**, *91*, 1031.

(8) For an unsuccessful analogous reduction of the vinylpyridine unit in an approach to the alkaloid dihydrolycolucine, leading to the opposite stereochemistry to that required, see: House, S. E. Ph.D thesis, University of California, Berkeley, 2010.

(9) Thompson, H. W.; Rashid, S. Y. *J. Org. Chem.* **2002**, *67*, 2813.

(10) Iwasaki, K.; Wan, K. K.; Oppedisano, A.; Crossley, S. W. M.; Shenvi, R. A. *J. Am. Chem. Soc.* **2014**, *136*, 1300.

(11) While it was not possible to fully determine the structure of the byproducts, we speculatively assigned them as migrated double-bond products and miscellaneous oxygenated compounds.

(12) (a) Leggans, E. K.; Barker, T. J.; Duncan, K. K.; Boger, D. L. *Org. Lett.* **2012**, *14*, 1428. (b) King, S. M.; Ma, X.; Herzon, S. B. *J. Am. Chem. Soc.* **2014**, *136*, 6884. (c) Lo, J. C.; Yabe, Y.; Baran, P. S. *J. Am. Chem. Soc.* **2014**, *136*, 1304.

(13) The use of the *E* isomer alone gave the same result. It should also be noted that the free N–H compound **7** did not react with either catalyst.

(14) For directed hydrogenations leading to products with contrasteric selectivity, see: Friedfeld, M. R.; Margulieux, G. W.; Schaefer, B. A.; Chirik, P. J. *J. Am. Chem. Soc.* **2014**, *136*, 13178.

(15) The remaining mass comprised the epimer in the form of an oil, which enabled its simple separation from the desired product, despite the two compounds having identical R_f values.

(16) The NMR data for the piperidine ring atoms are slightly different from those reported for the natural product. However, partial protonation of our synthetic **1** afforded NMR data identical to those described for natural **1**. For a similar titration of a free base with TFA, see: Altman, R. A.; Nilsson, B. L.; Overman, L. E.; Read de Alaniz, J.; Rohde, J. M.; Taupin, V. *J. Org. Chem.* **2010**, *75*, 7519.

(17) Although **1** shows the same dextrorotatory character as natural serratezomine E, there are differences in the value of the specific rotation. For a strong change in specific rotation upon protonation in the alkaloid field, see: (a) Kuehne, P.; Linden, A.; Hesse, M. *Helv. Chim. Acta* **1996**, *79*, 1085. (b) Weiss, M. E.; Carreira, E. M. *Angew. Chem., Int. Ed.* **2011**, *50*, 11501.

(18) Bhattacharyya, S. *Synth. Commun.* **1995**, *25*, 2061.

(19) Katakawa, K.; Kitajima, M.; Yamaguchi, K.; Takayama, H. *Heterocycles* **2006**, *69*, 223.

An approach to *cis*-phlegmarine alkaloids via stereodivergent reduction: total synthesis of (+)-serratezomine **E** and putative structure of (-)-huperzine **N**

Caroline Bosch, Béla Fiser, Enrique Gómez-Bengoa, Ben Bradshaw and Josep Bonjoch

Laboratori de Química Orgànica, Facultat de Farmàcia, IBUB,
Universitat de Barcelona, Av. Joan XXIII s/n, 08028-Barcelona, Spain

Departamento de Química Orgánica I, Universidad del País Vasco,
Manuel Lardizabal 3, 20018-San Sebastian, Spain

josep.bonjoch@ub.edu; benbradshaw@ub.edu

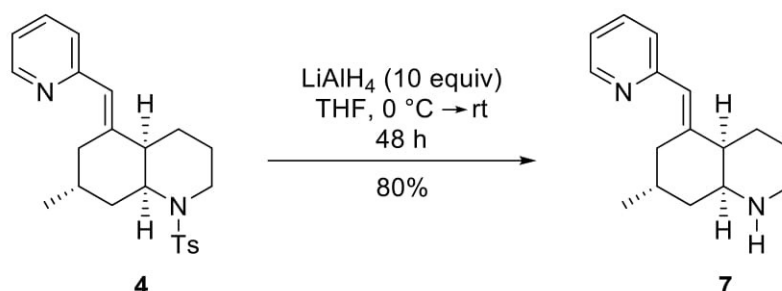
Contents

Experimental and NMR Data of compounds 1 , 2 , 6a-13 , including comparison of ¹ H- and ¹³ C NMR data for serratezomine E and 1 (tables S1 and S2); huperzine N and 2 (Tables S3 and S4), and huperzine M and lycopserramine Y (Tables S5 and S6)	S2
Copies of ¹ H- and ¹³ C-NMR spectra of compounds 1 , 2 , 6a-13	S20
X-Ray data for serratezomine E (1)	S42
Cartesian coordinates and potential energies of all species studied in Scheme 2	S54

Experimental Section

General: All reactions were carried out under an argon atmosphere with dry solvents under anhydrous conditions. Drying of organic extracts during workup of reactions was performed over anhydrous Na₂SO₄ except where otherwise stated. Evaporation of solvents was accomplished with a rotatory evaporator. Analytical thin-layer chromatography was performed on SiO₂ (Merck silica gel 60 F₂₅₄) or Al₂O₃ (Merck TLC aluminium oxide neutral 60 F₂₅₄), and the spots were located with aqueous KMnO₄, vanilline or iodoplatinate. Chromatography refers to flash chromatography and was carried out on SiO₂ (SDS silica gel 60 ACC, 35-75 μm, 230-240 mesh ASTM) or Al₂O₃ (Aluminium oxide neutral, 63 – 200 μm). NMR spectra were recorded in CDCl₃ on a Varian Mercury 400 MHz or Varian VNMRs 400 MHz. Chemical shifts of ¹H and ¹³C NMR spectra are reported in ppm downfield (δ) from Me₄Si. All NMR data assignments are supported by COSY and HSQC experiments. Compounds **3-5** were synthesized according to our previous published procedures.¹

(4a*R*,7*R*,8a*S*)-7-Methyl-5-(pyridin-2-ylmethylene)decahydroquinoline (**7**)



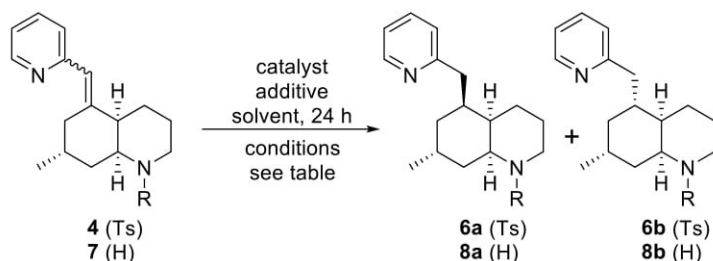
To a stirred solution of sulfonamide **4**² (500 mg, 1.26 mmol) in THF (108 mL) was added LiAlH₄ (493 mg, 12.9 mmol) at 0 °C. The resulting mixture was stirred at room temperature for 72 h. The reaction was quenched by the careful addition of water (0.5 mL), 15% aq. NaOH (0.5 mL) and a second portion of water (1.5 mL). The mixture was diluted with CH₂Cl₂ before it was filtered through a pad of celite, and washed through with CH₂Cl₂. The filtrate was concentrated *in vacuo* and the product was purified by chromatography (2.5→5% MeOH/CH₂Cl₂ followed by 1:2:0.1 MeOH/CH₂Cl₂/concd NH₄OH) to give **7** as a 1:5.9 mixture of *Z/E* isomers (244 mg, 80%) *R_f* 0.57 (1:2:0.1

¹ (a) B. Bradshaw, C. Luque-Corredera, J. Bonjoch, *Org. Lett.* **2013**, *15*, 326-329. (b) B. Bradshaw, C. Luque-Corredera, J. Bonjoch, *Chem. Commun.* **2014**, *50*, 7099-7102.

² Compound **4** is a 4.2:1 epimeric mixture of *E* and *Z* isomers, respectively

MeOH/CH₂Cl₂/concd NH₄OH); ¹H NMR *E*-isomer³ (400 MHz, COSY) δ 0.90 (d, *J* = 6.0 Hz, 3H, Me), 1.60 (m, 1H, H-4), 1.50 (m, 1H, H-8), 1.70 (m, 1H, H-3), 1.90 (m, 1H, H-4), 2.00 (m, 2H, H-6, H-8), 2.03 (m, 1H, H-7_{ax}), 2.23 (m, 1H, H-3), 2.58 (q, *J* = 4.0 Hz, 1H, H-4_a), 2.90 (td, 1H, *J* = 12.4, 3.4 Hz H-2_{ax}), 2.94 (m, 1H, H-6), 3.16 (dm, *J* = 12.4 Hz, 1H, H-2_{eq}), 3.55 (q, *J* = 4.0 Hz, 1H, H-8_a), 6.48 (s, 1H, C=CH), 7.08 (dd, *J* = 8.0, 4.8 Hz 1H, H-5 Py), 7.23 (d, *J* = 8.0 Hz, 1H, H-3 Py), 7.62 (td, *J* = 8.0, 1.2 Hz, 1H, H-4 Py), 8.57 (dd, *J* = 4.8, 1.2 Hz, 1H, H-6 Py); ¹³C NMR (400 MHz, HSQC) *E*-isomer δ 20.9 (CH₃), 21.6 (C-4), 25.3 (C-3), 28.0 (C-7), 38.3 (C-6), 38.6 (C-8), 42.1 (C-4_a), 44.5 (br, C-2), 55.4 (br, C-8_a), 120.9 (C-5 Py), 124.3 (C-3 Py), 125.4 (=CH), 135.9 (C-4 Py), 143.7 (C-6), 149.0 (C-6 Py), 157.0 (C-2 Py); HRMS calcd for C₁₆H₂₃N₂ (M+H)⁺ 243.1856, found 243.1855.

Table S1: Screening of conditions for reduction reaction

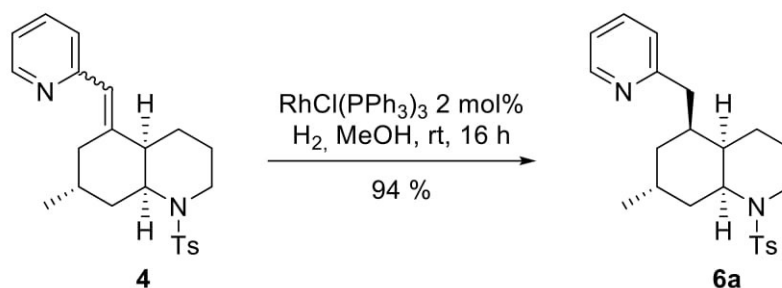


entry	R	catalyst	loading	solvent ^a	conv (%)	Ratio a:b
1	Ts	Pd/C	20% w/w	MeOH	100	3:97
2	Ts	Pd/C	20% w/w	CH ₂ Cl ₂	100	10:90
3	Ts	Ni raney	20% w/w	MeOH	75	14:86
4	Ts	Mn(dpm) ₃ , TBHP	10%/150%	<i>i</i> -PrOH	63	73:27
5	Ts	Fe ₂ (ox) ₃ ·6H ₂ O, NaBH ₄	200%/400%	EtOH/H ₂ O	0	--
6	Ts	Co(acac) ₂ , TBHP, 1,4-CHD	100%/100%/500%	<i>n</i> -PrOH	7	nd
7	H	Mn(dpm) ₃ , TBHP	10%/150%	<i>i</i> -PrOH	0	--
8	H	Pd/C	20% w/w	MeOH	100	36:64
9	H	Pd/C	20% w/w	MeOH, AcOH (10 eq.)	100	27:73
10	H	Pd/C	20% w/w	AcOH	100	35:65
11	Ts	Crabtree	15 mol%	CH ₂ Cl ₂	100	68:32
12	H	Crabtree	15 mol%	CH ₂ Cl ₂	0	-
13	Ts	Crabtree	15 mol%	MeOH	100	86:14
14	Ts	Wilkinson	15 mol%	CH ₂ Cl ₂	100	91:9
15	Ts	Wilkinson	15 mol%	MeOH	100	95:5
16	H	Wilkinson	15 mol%	MeOH	0	-
17 ^b	Ts	Wilkinson	15 mol%	MeOH	100	95:5
18 ^c	Ts	Wilkinson	15 mol%	MeOH	100	95:5
19	Ts	Wilkinson	5 mol%	MeOH	100	96:4
20	Ts	Wilkinson	2 mol%	MeOH	100	96:4

^a Solvent concentration: 0.04 M. ^b *E* isomer only. ^c *Z* isomer only.

³ Minor signals at 1.00 (δ, *J* = 6.8 Hz, 3H, Me), 6.29 (s, 1H, C=CH) were observed for *Z*-isomer.

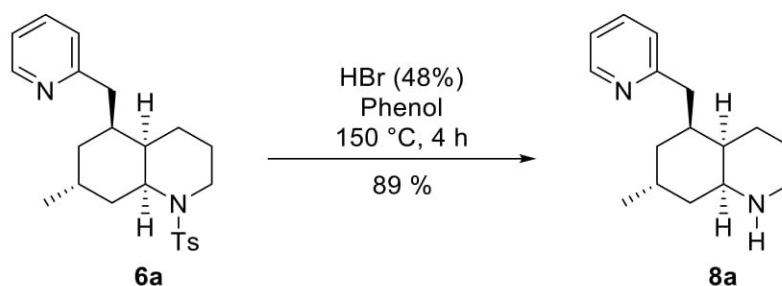
(4a*R*,5*S*,7*R*,8a*S*)-7-Methyl-1-(4-methylphenylsulfonyl)- 5-(pyridin-2-ylmethyl)decahydroquinoline (6a)



To a stirred solution of **4** (1.06 g, 2.67 mmol) in MeOH (100 mL) was added Wilkinson's catalyst $\text{RhCl}(\text{PPh}_3)_3$ (50 mg, 0.054 mmol, 2 mol%) at room temperature. The resulting mixture was rapidly evacuated and backfilled with hydrogen 3 times and then stirred under an atmosphere of H_2 for 16 h. Evaporation of the solvent and purification by chromatography (10→25→40% EtOAc in hexanes) gave **6a** (989 mg, 93%) as a white solid⁴: mp 115-116 °C; R_f 0.39 (50% EtOAc/hexanes); $[\alpha]_D^{25} +29.4$ (c 1, CHCl_3); $^1\text{H NMR}$ (400 MHz, COSY) δ 0.98 (d, $J = 7.3$ Hz, 3H, CH_3), 1.05-1.15 (m, 2H, H-6 and H-8), 1.19-1.30 (m, 1H, H-3), 1.30-1.46 (m, 1H, H-6), 1.46-1.59 (m, 2H, H-4), 1.59-1.67 (m, 2H, H-3 and H-4a), 1.93 (td, $J = 13.0, 5.3$ Hz, 1H, H-8), 1.99-2.07 (m, 1H, H-7), 2.28-2.38 (m, 1H, H-5), 2.40 (s, 3H, ArCH_3), 2.59 and 2.66 (2 dd, $J = 13.6, 7.6$ Hz, 1H each, CH_2Py), 2.93 (td, $J = 13.4, 2.8$ Hz, 1H, H-2ax), 3.70 (dd, $J = 13.4, 3.0$ Hz, 1H, H-2eq), 4.17 (td, $J = 13.0, 4.3$ Hz, 1H, H-8a), 7.07 (d, $J = 7.8$ Hz, 1H, H-3 Py), 7.12 (ddd, $J = 7.6, 4.8, 1.0$ Hz, 1H, H-5 Py), 7.22 (d, $J = 8.2$ Hz, 2H, m -Ts), 7.58 (td, $J = 7.6, 1.0$ Hz, 1H, H-4 Py), 7.65 (dt, $J = 8.2, 1.8$ Hz, 2H, o -Ts), 8.52 (d, $J = 4.8$ Hz, 1H, H-6 Py); $^{13}\text{C NMR}$ (400 MHz, HSQC) δ 17.1 (C-4), 18.5 (CH_3), 21.5 (ArCH_3), 24.9 (C-3), 27.5 (C-7), 28.2 (C-8), 31.6 (C-6), 35.3 (C-5), 38.7 (C-4a), 40.2 (C-2), 41.8 (CH_2Py), 51.2 (C-8a), 121.0 (C-5 Py), 123.2 (C-3 Py), 126.8 (o -Ts), 129.5 (m -Ts), 136.2 (C-4 Py), 138.7 ($ipso$ -Ts), 142.6 (p -Ts), 149.2 (C-6 Py), 160.5 (C-2 Py); HRMS calcd for $\text{C}_{23}\text{H}_{31}\text{N}_2\text{O}_2\text{S}$ ($\text{M}+\text{H}$)⁺ 399.2101, found 399.2110.

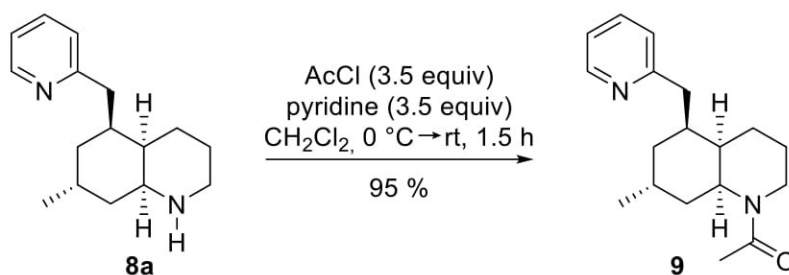
⁴ Presence of 5% of the 5*R* epimer (**6b**), whose data match the those reported in the literature: Bradshaw, B.; Luque-Corredera, C.; Bonjoch, *J. Org. Lett.* **2013**, *15*, 326–329.

(4a*R*,5*S*,7*R*,8a*S*)-7-Methyl-5-(pyridin-2-ylmethyl)decahydroquinoline (8a)



A solution of **6a** (855 mg, 2.15 mmol) and phenol (707 mg, 7.51 mmol) in HBr 48% (15 mL) was stirred at reflux for 3 h. The reaction was quenched by addition of H₂O (15 mL) and diluted with EtOAc (15 mL). The organic layer was separated, and the aqueous layer was basified with sat. aq. NaOH and extracted with CH₂Cl₂ (3 × 25 mL). The combined organic extracts were dried over MgSO₄, concentrated and the resulting crude material was purified by chromatography on alumina (0→2.5→5→10% MeOH/CH₂Cl₂) to give amine **8a** (464 mg, 89 %) as a white foam/oil: *R_f* 0.15 (10% MeOH/CH₂Cl₂); [α]_D +8.7 (*c* 1, CHCl₃); ¹H NMR (400 MHz, COSY) δ 0.98 (d, *J* = 7.2 Hz, 3H, CH₃), 1.18 (br d, *J* = 14.0 Hz, 1H, H-6eq), 1.44 (td, *J* = 14.0, 4.8 Hz, 1H, H-6ax), 1.52-1.72 (m, 2H, H-4), 1.78 (br d, *J* = 13.2 Hz, H-8eq), 1.81-1.91 (m, 2H, H-3), 2.03 (td, *J* = 13.2, 5.6 Hz, 1H, H-8ax), 2.12-2.24 (m, 2H, H-7 and H-4a), 2.28-2.38 (m, 1H, H-5), 2.61 (dd, *J* = 13.6, 8.8 Hz, 1H, CH₂Py), 2.74 (dd, *J* = 13.6, 6.4 Hz, 1H, CH₂Py), 2.93 (td, *J* = 12.2, 5.2 Hz, 1H, H-2ax), 3.17 (br d, *J* = 12.2 Hz, 1H, H-2eq), 3.68 (dt, *J* = 9.6, 4.4 Hz, 1H, H-8a), 7.09 (d, *J* = 7.6 Hz, 1H, H-3 Py), 7.11 (dd, *J* = 7.6, 4.8 Hz, 1H, H-5 Py), 7.58 (td, *J* = 7.6, 1.8 Hz, 1H, H-4 Py), 8.50 (d, *J* = 4.8 Hz, 1H, H-6 Py); ¹³C NMR (400 MHz, HSQC) δ 16.3 (C-4), 18.2 (CH₃), 22.4 (C-3), 27.0 (C-7), 27.2 (C-8), 31.2 (C-6), 34.4 (C-5), 36.9 (C-4a), 38.3 (C-2), 41.6 (CH₂Py), 50.3 (C-8a), 121.3 (C-5 Py), 123.1 (C-3 Py), 136.4 (C-4 Py), 149.3 (C-6 Py), 160.0 (C-2 Py); HRMS calcd for C₁₆H₂₅N₂ (M+H)⁺ 245.2012, found 245.2021.

(4a*R*,5*S*,7*R*,8a*S*)-1-Acetyl-7-methyl-5-(pyridin-2-ylmethyl)decahydroquinoline (9)



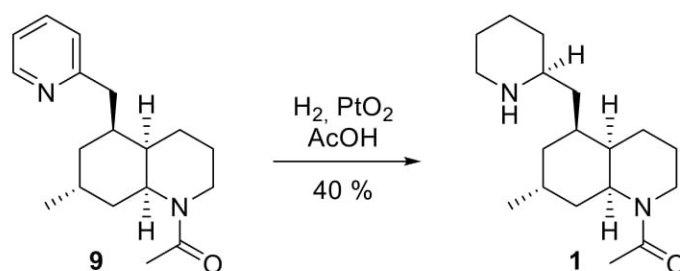
To a stirred solution of amine **8a** (350 mg, 1.43 mmol) and pyridine (405 μ L, 5.01 mmol) in CH₂Cl₂ (25 mL) at 0 °C was added dropwise acetyl chloride (360 μ L, 5.01 mmol), and the mixture was stirred at 0 °C for 30 min, and then at room temperature for 1 h. The reaction was quenched by addition of saturated NaHCO₃ (15 mL). The phases were separated and the aqueous layer was extracted with CH₂Cl₂ (4 x 20 mL). The combined organic extracts were dried, concentrated and purified by chromatography on silica (0→2.5→5→10% MeOH/CH₂Cl₂) providing **9** (389 mg, 95 %) as a 4:5 mixture of rotamers (colourless oil). *R_f* 0.46 (5% MeOH/CH₂Cl₂); [α]_D +44.0 (*c* 1, CHCl₃); HRMS calcd for C₁₈H₂₆N₂O (M+H)⁺ 287.2118, found 287.2126.

Rotamer *Z*: ¹H NMR (400 MHz, COSY) δ 1.06 (d, *J* = 7.2 Hz, 3H, CH₃), 1.13-1.21 (m, 2H, H-6 and H-8), 1.21-1.33 (m, 1H, H-3), 1.41-1.52 (m, 1H, H-6), 1.52-1.69 (m, 3H, H-4 and H-4a), 1.69-1.76 (m, 1H, H-3), 1.94 (ddd, *J* = 13.0, 13.0, 5.3 Hz, 1H, H-8ax), 2.01 (s, 3H, COCH₃), 2.06-2.20 (m, 1H, H-7), 2.28-2.44 (m, 1H, H-5), 2.62-2.75 (m, 2H, CH₂Py), 3.10 (td, *J* = 13.2, 3.2 Hz, 1H, H-2ax), 3.51 (ddd, *J* = 13.2, 2.4, 2.4 Hz, 1H, H-2eq), 4.86 (ddd, *J* = 13.2, 4.0, 4.0 Hz, 1H, H-8a), 7.04-7.14 (m, 2H, H-3 Py and H-5-py), 7.56 (ddd, *J* = 7.2, 1.2, 1.2 Hz, 1H, H-4 Py), 8.49 (bd, *J* = 4.0 Hz, 1H, H-6 Py); ¹³C NMR (400 MHz, HSQC) δ 17.5 (C-4), 18.7(CH₃), 22.1 (COCH₃), 25.9 (C-3), 27.7 (C-7), 28.4(C-8), 32.1 (C-6), 35.1 (C-5), 38.3 (C-4a), 41.7 (C-2), 42.0 (CH₂Py), 46.2 (C-8a), 121.0 (C-5 Py), 123.0 (C-3 Py), 136.1 (C-4 Py), 149.2 (C-6 Py), 160.8 (C-2 Py), 168.6 (CO).

Rotamer *E*: ¹H NMR (400 MHz, COSY) δ 1.01 (d, *J* = 7.2 Hz, 3H, CH₃), 1.13-1.21 (m, 2H, H-6 and H-8), 1.21-1.33 (m, 1H, H-3), 1.41-1.52 (m, 1H, H-6), 1.52-1.69 (m, 3H, H-4 and H-4a), 1.69-1.76 (m, 1H, H-3), 2.04 (s, 3H, COCH₃), 2.06-2.20 (m, 2H, H-7 and H-8), 2.28-2.44 (m, 1H, H-5), 2.60 (ddd, *J* = 14.0, 14.0, 3.6 Hz, 1H, H-2ax), 2.62-2.75 (m, 2H, CH₂Py), 3.92 (ddd, *J* = 12.4, 4.0, 4.0 Hz, 1H, H-8a), 4.44 (ddd, *J* = 13.2, 3.2, 3.2 Hz, 1H, H-2eq), 7.04-7.14 (m, 2H, H-3 Py and H-5 Py), 7.58 (ddd, *J* = 7.6, 1.6, 1.6 Hz, 1H, H-4 Py), 8.54 (bd, *J* = 4.0 Hz, 1H, H-6 Py); ¹³C NMR (400 MHz, HSQC) δ

17.7 (C-4), 18.4(CH₃), 21.3 (COCH₃), 24.9 (C-3), 27.3 (C-7), 29.8 (C-8), 31.5 (C-6), 35.2 (C-5), 36.3 (C-2), 39.8 (C-4a), 42.0 (CH₂Py), 52.0 (C-8a), 121.1 (C-5 Py), 123.4 (C- 3 Py), 136.2 (C-4 Py), 149.4 (C-6 Py), 160.5 (C-2 Py), 169.0 (CO).

(4a*R*,5*S*,7*R*,8a*S*)-1-Acetyl-7-Methyl-5-[(2*S*)-pyridin-2-ylmethyl]decahydroquinoline (1, serratezomine E)



To a stirred solution of **9** (207 mg, 0.72 mmol) in AcOH (6 mL) was added PtO₂ (20% w/w, 40 mg) at rt. The resulting mixture was evacuated and backfilled with hydrogen 3 times and then stirred under an atmosphere of H₂ for 16 h. The mixture was diluted with CH₂Cl₂ (10 mL) before it was filtered through a pad of celite and washed through with CH₂Cl₂. The filtered solution was washed with 1 N NaOH, dried and concentrated *in vacuo*. The resulting crude material was purified by crystallization from hexane to give **1** (84 mg, 40%) as a white solid and as a 4:5 mixture of *Z/E* rotamers. *R_f* 0.53 (90/10/1 CH₂Cl₂/MeOH/conc NH₄OH); [α]_D +9.0 (*c* 1, CHCl₃); ¹H NMR (400 MHz, COSY) δ 1.06 and 1.09 (2d, *J* = 7.2 Hz, 3H, CH₃), 1.10 (masked, 1H), 1.12 (m, 1H), 1.18 (m, 1H), 1.20 (m, 2H), 1.35 (m, 1H) 1.40 (m, 1H), 1.42 (m, 1H), 1.40-1.50 (m, 2H), 1.55-1.60 (m, 2H), 1.65 (m, H-4a, 0.5H, *Z*), 1.75 (m, 2H and H-4a, *E*), 1.94 (m, 2H), 2.06 and 2.10 (2s, 3H, COCH₃), 2.10-2.20 (m, 2H, H-7 and H-8), 2.45 (m, 1H, H-2'), 2.60 (m, 1H, H-6'), 2.63 (td, *J* = 12.2, 2.8 Hz, 0.5H, H-2ax, *E*), 3.05 (m, 1H, H-6'), 3.12 (td, *J* = 13.2, 4.0 Hz, 1H, H-2ax, *Z*), 3.55 (dm, *J* = 13.2 Hz, 1H, H-2eq, *Z*), 3.90 (dt, *J* = 12.2, 4.0, 0.5 H, H-8a, *E*), 4.45 (dm, *J* = 13.0 Hz, 0.5 H, H-2eq, *E*), 4.88 (ddd, *J* = 13.2, 4.4, 0.5 Hz, 1H, H-8a, *Z*); ¹³C NMR (400 MHz, HSQC) *Z* rotamer δ 17.5 (C-4), 18.7 (CH₃), 22.1 (COCH₃), 25.9 (C-3), 27.7 (C-7), 28.4 (C-8), 32.1 (C-6), 35.1 (C-5), 38.3 (C-4a), 41.8 (C-2), 42.0 (CH₂Py), 46.2 (C-8a), 121.0 (C-5 Py), 123.0 (C- 3 Py), 136.1 (C-4 Py), 149.2 (C-6 Py), 160.8 (C-2 Py), 168.6 (CO); *E* rotamer δ 17.7 (C-4), 18.4 (CH₃), 21.3 (COCH₃), 24.9 (C-3), 27.3 (C-7), 29.8 (C-8), 31.5 (C-6), 35.2 (C-5), 36.4 (C-2), 39.8 (C-4a), 42.0 (CH₂Py), 52.0 (C-8a), 121.1 (C-5 Py), 123.4 (C- 3 Py), 136.2

(C-4 Py), 149.4 (C-6 Py), 160.5 (C-2 Py), 169.0 (CO). HRMS calcd for $C_{18}H_{33}N_2O$ ($M+H$)⁺ 293.2587, found 293.2594.

For comparison of NMR data for natural serratezomine E (partially protonated) and compound **1**, see Tables S1 and S2.

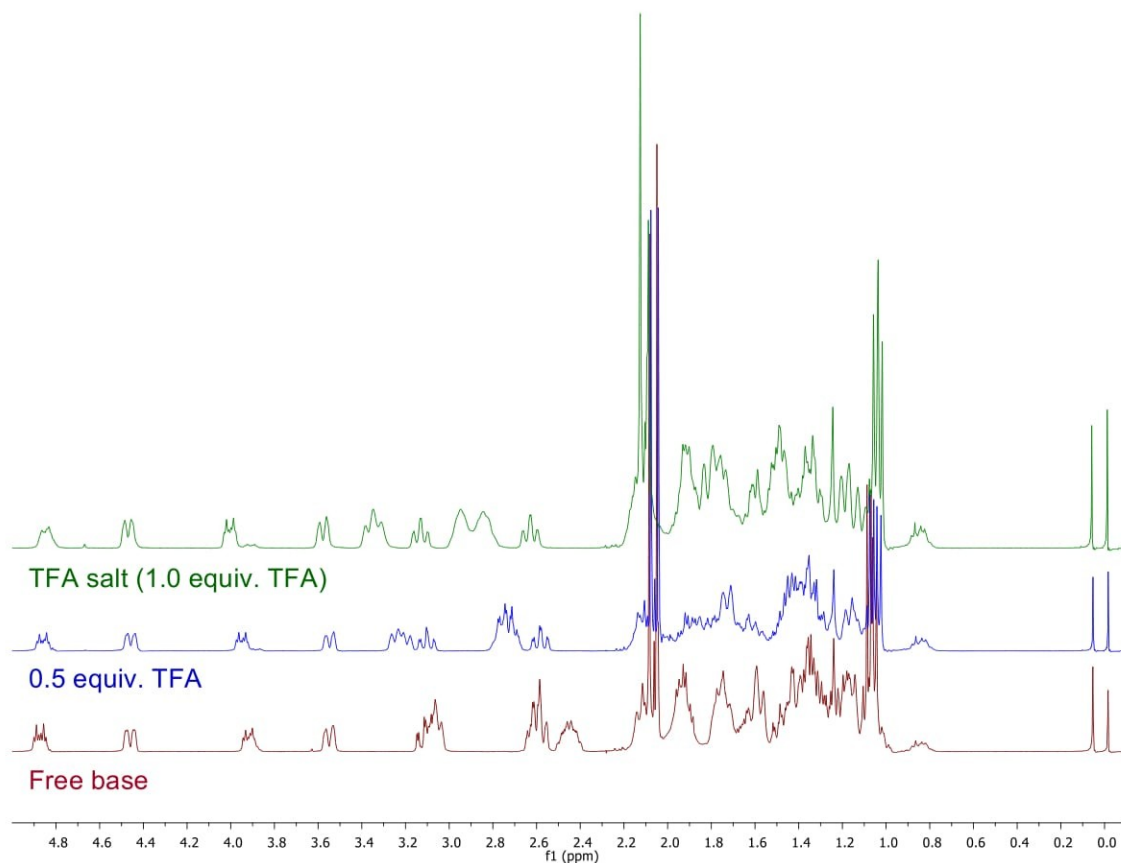
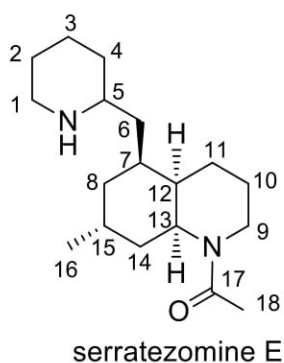
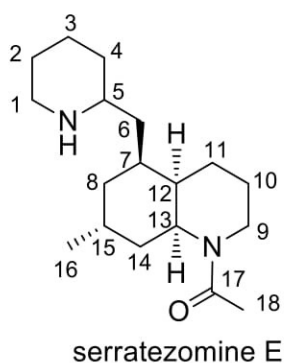


Figure 1: ¹H NMR spectra of synthetic serratezomine E (**1**) in CDCl₃ before and after addition of trifluoroacetic acid

Table S1. ^1H NMR data for (+) serratezomine E

	Rotamer <i>E</i>		Rotamer <i>Z</i>	
	δ ^1H	δ ^{13}C	δ ^1H	δ ^{13}C
1	3.25 (m) 2.59 (m)	45.3	3.25 (m) 2.59 (m)	45.3
2	1.75 (m) 1.67 (m)	23.4	1.75 (m) 1.67 (m)	23.4
3	1.94 (m) 1.28 (m)	28.4	1.83 (m) 1.39 (m)	30.2
4	1.87 (m) 1.41 (m)	23.0	1.87 (m) 1.41 (m)	23.0
5	2.76 (m)	54.0	2.76 (m)	54.0
6	1.61 (m) 1.29 (m)	37.6	1.61 (m) 1.29 (m)	37.6
7	1.94 (m)	29.6	1.94 (m)	29.6
8	1.38 (m) 1.10 (m)	33.1	1.38 (m) 1.18 (m)	32.5
9	3.56 (dd, 13.5, 4.3) 3.31 (dt, 13.5, 3.0)	41.8	4.47 (dd, 12.9, 3.7) 2.59 (dt, 13.8, 3.0)	36.4
10	1.75 (m) 1.38 (m)	25.9	1.75 (m) 1.32 (br d, 14)	24.9
11	1.48 (m)	17.1	1.47 (m)	16.9
12	1.57 (m)	37.4	1.70 (m)	39.7
13	4.85 (dt, 13.8, 4.6)	46.0	3.90 (dt, 12.6, 4.6)	52.0
14	1.93 (m) 1.18 (m)	27.6	2.13 (m) 1.18 (m)	29.6
15	2.13 (m)	27.2	2.13 (m)	27.2
16	1.09 (d, 7.8)	18.8	1.07 (d, 7.2)	18.4
17		169.0		168.8
18	2.04 (s)	22.1	2.06 (s)	21.3

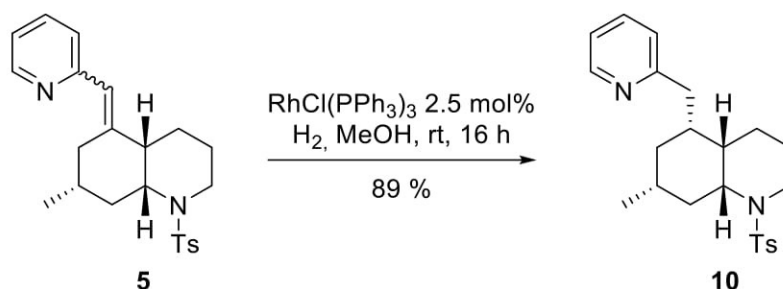
^1H NMR recorded at 600 MHz and ^{13}C NMR recorded at 150 MHz (*Bioorg. Med. Chem. Lett.*, **2009**, *19*, 3577-3580)

Table S2. ^1H NMR data for synthetic **1** (NH form)

	Rotamer <i>Z</i>		Rotamer <i>E</i>	
	δ ^1H	δ ^{13}C	δ ^1H	δ ^{13}C
1	3.08 (m)	47.1	3.08 (m)	47.1
	2.62 (m)		2.62 (m)	
2	1.72 (m)	26.6*	1.72 (m)	26.5*
	1.28 (m)		1.28 (m)	
3	1.87 (m)	23.0	1.87 (m)	23.0
	1.41 (m)		1.41 (m)	
4	1.94 (m)	28.4	1.83 (m)	30.2
	1.28 (m)		1.39 (m)	
5	2.46 (m)	53.4	2.46 (m)	53.4
6	1.23 (m)	40.9*	1.23 (m)	40.7*
7	1.94 (m)	29.5	1.94 (m)	29.5
8	1.35 (m)	32.8	1.35 (m)	32.5
	1.15 (m)		1.15 (m)	
9	3.56 (br d, 13.2)	41.8	4.47 (dd, 13.6, 2.8)	36.4
	3.12 (ddd, 13.2, 13.2, 3.2)		2.58 (m)	
10	1.75 (m)	26.0	1.75 (m)	25.0
	1.36 (m)		1.30 (m)	
11	1.44 (m)	17.5	1.44 (m)	17.5
12	1.65 (m)	38.5	1.78 (m)	39.7
13	4.89 (ddd, 13.2, 4.4, 4.4)	46.3	3.90 (ddd, 12.0, 4.4, 4.4)	52.1
14	1.90 (m)	27.6	2.13 (m)	29.6
	1.20 (m)		1.18 (m)	
15	2.12 (m)	27.3*	2.12 (m)	27.7*
16	1.09 (d, 7.3)	18.7	1.07 (d, 7.2)	18.5
17		169.1		168.7
18	2.06 (s)	22.1	2.10 (s)	21.3

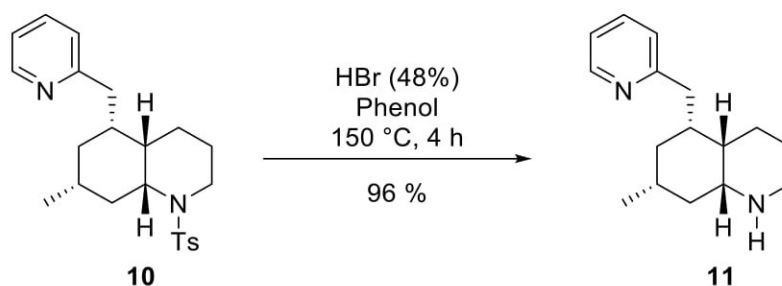
^1H NMR recorded at 400 MHz and ^{13}C NMR recorded at 100 MHz. Assignments were aided by gCOSY and gHSQCAD spectra.

(4a*S*,5*R*,7*R*,8a*R*)-7-Methyl-1-(4-methylphenylsulfonyl)-5-(pyridin-2-ylmethyl) decahydroquinoline (10**)**



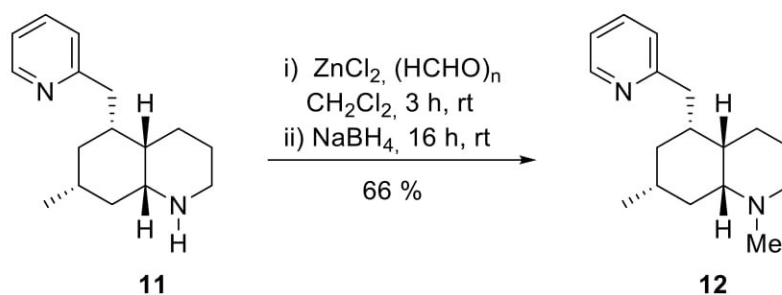
To a stirred solution of **5** (515 mg, 1.29 mmol) in MeOH (40 mL) was added Wilkinson's catalyst $\text{RhCl(PPh}_3)_3$ (30 mg, 0.033 mmol, 2.5 mol%) at room temperature. The resulting mixture was rapidly evacuated and backfilled with hydrogen 3 times and then stirred under an atmosphere of H_2 for 16 h. Evaporation of the solvent, and purification by chromatography (10→25→40% EtOAc in hexanes) gave **10** (460 mg, 89%) as a transparent oil. R_f 0.59 (50% EtOAc/hexanes); $[\alpha]_D - 45.8$ (c 1, CHCl_3); ^1H NMR (400 MHz, COSY) δ 0.83 (ddd, $J = 12.8, 12.8, 12.8$ Hz, 1H, H-6ax), 0.84 (d, $J = 5.6$ Hz, CH_3), 1.18-1.26 (m, 1H, H-3), 1.22-1.32 (m, 1H, H-6eq), 1.38-1.44 (m, 1H, H-4), 1.40-1.46 (m, 1H, H-7), 1.38-1.48 (m, 2H, H-8), 1.50-1.60 (m, 1H, H-4), 1.52-1.62 (m, 1H, H-4a), 1.54-1.66 (m, 1H, H-3), 2.10-2.32 (m, 1H, H-5ax), 2.40 (s, 3H, ArCH_3), 2.59 (dd, $J = 13.2, 8.4$ Hz, 1H, CH_2Py), 2.66 (dd, $J = 13.2, 7.2$ Hz, 1H, CH_2Py), 2.95 (ddd, $J = 13.6, 13.2, 2.4$ Hz, 1H, H-2ax), 3.66 (br dd, $J = 13.6, 4.0$ Hz, H-2eq), 3.96 (ddd, $J = 10.4, 5.2, 5.2$ Hz, 1H, H-8a), 7.05 (dd, $J = 8.4, 1.2$ Hz, 1H, H-3 Py), 7.11 (ddd, $J = 7.6, 4.8, 0.8$ Hz, 1H, H-5 Py), 7.21 (d, $J = 7.8$ Hz, 2H, m -Ts), 7.57 (ddd, $J = 7.6, 2.0$ Hz, 1H, H-4 Py), 7.65 (d, $J = 7.8$ Hz, 2H, o -Ts), 8.50 (dd, $J = 4.8, 0.8$ Hz, 1H, H-6 Py); ^{13}C NMR (400 MHz, HSQC) δ 18.0 (C-4), 21.5 (ArCH_3), 22.1 (CH_3), 24.9 (C-3), 31.5 (C-7), 32.3 (C-8), 34.5 (C-6), 38.0 (C-4a), 40.5 (C-2), 40.9 (C-5), 41.9 (CH_2Py), 55.5 (C-8a), 121.0 (C-5 Py), 123.3 (C-3 Py), 126.9 (o -Ts), 129.6 (m -Ts), 136.2 (C-4 Py), 138.7 (p -Ts), 142.6 ($ipso$ -Ts), 149.3 (C-6 Py), 160.6 (C-2 Py); HRMS calcd for $\text{C}_{23}\text{H}_{31}\text{N}_2\text{O}_2\text{S}$ ($\text{M}+\text{H}$) $^+$ 399.2101, found 399.2116.

(4a*S*,5*R*,7*R*,8a*R*)-7-Methyl-5-(pyridin-2-ylmethyl)decahydroquinoline (11)



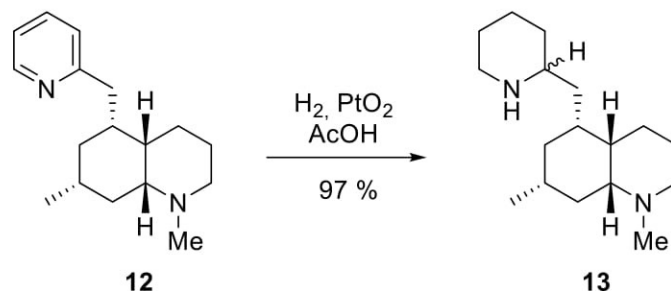
A solution of **10** (360 mg, 0.903 mmol) and phenol (298 mg, 3.16 mmol) in HBr 48% (6.5 mL) was stirred at reflux for 3 h. The reaction was quenched by addition of H₂O (10 mL) and diluted with EtOAc (10 mL). The organic layer was separated, and the aqueous layer was basified with sat. aq. NaOH and extracted with CH₂Cl₂ (5 × 20 mL). The combined organic extracts were dried over MgSO₄, concentrated and purified by chromatography on alumina (0→2.5→5→10% MeOH/CH₂Cl₂) to give the secondary amine **11** as a transparent oil: *R_f* 0.20 (10% MeOH/CH₂Cl₂ on alumina); [α]_D - 20.1 (*c* 1, CHCl₃); ¹H NMR (400 MHz, COSY) δ 0.86 (q, *J* = 12.8 Hz, 1H, H-6ax), 0.90 (d, *J* = 6.4 Hz, 3H, CH₃), 1.31 (bd, *J* = 12.8 Hz, 1H, H-6eq), 1.38-1.50 (m, 1H, H-7), 1.42-1.54 (m, 1H, H-4), 1.44-1.63 (m, 2H, H-8), 1.50-1.66 (m, 1H, H-3), 1.56-1.66 (m, 1H, H-4), 1.72-1.80 (m, 1H, H-3), 1.90-2.00 (m, 1H, H-4a), 2.00-2.10 (m, 1H, H-5), 2.61 (dd, *J* = 13.4, 8.4 Hz, 1H, CH₂Py), 2.73 (dd, *J* = 13.4, 6.4 Hz, 1H, CH₂Py), 2.86 (ddd, *J* = 12.8, 12.4, 2.4 Hz, 1H, H-2ax), 2.93 (br d, *J* = 12.8 Hz, 1H, H-2eq), 3.18 (ddd, *J* = 11.2, 4.4, 4.4 Hz, 1H, H-8a), 7.05-7.11 (m, 2H, H-3 Py and H-5 Py), 7.57 (ddd, *J* = 7.2, 7.2, 2.0 Hz, 1H, H-4 Py), 8.50 (dd, *J* = 5.2, 2.0 Hz, 1H, H-6 Py); ¹³C NMR (400 MHz, HSQC) δ 18.0 (C-4), 22.1 (CH₃), 24.8 (C-3), 31.5 (C-7), 32.3 (C-8), 34.5 (C-6), 37.9 (C-4a), 39.3 (C-2), 40.7 (C-5), 41.8 (CH₂Py), 54.6 (C-8a), 121.1 (C-5 Py), 123.3 (C-3 Py), 136.2 (C-4 Py), 149.3 (C-6 Py), 160.7 (C-2 Py); HRMS calcd for C₁₆H₂₅N₂ (M+H)⁺ 245.2012, found 245.2017.

(4a*S*,5*R*,7*R*,8a*R*)-1,7-Dimethyl-5-(pyridin-2-ylmethyl)decahydroquinoline (12)



A solution of **11** (200 mg, 0.82 mmol), zinc chloride (558 mg, 4.10 mmol) and paraformaldehyde (126 mg, 4.10 mmol) in CH₂Cl₂ (5 mL) was stirred at room temperature under argon. After 3 h, NaBH₄ (155 mg, 4.10 mmol) was added and the mixture was stirred overnight at room temperature. The reaction was quenched by addition of NH₄OH (2 N, 10 mL) and stirred for 30 min. The phases were separated and the aqueous layer was extracted with CH₂Cl₂ (3 x 15 mL). The combined organic extracts were dried, concentrated and purified by chromatography on silica (2.5→5→10% MeOH/CH₂Cl₂; then 90/10/1 MeOH/CH₂Cl₂/NH₃) providing **12** (140 mg, 66 %) as a yellowish oil. *R_f* 0.40 (90/10/1 MeOH/CH₂Cl₂/NH₃); [α]_D - 4.5 (*c* 1, CHCl₃); ¹H NMR (400 MHz, COSY) δ 0.89 (ddd, *J* = 12.4, 12.4, 12.4 Hz, 1H, H-6ax), 0.90 (d, *J* = 6.4 Hz, 3H, CH₃), 1.20 (ddd, *J* = 12.4, 12.4, 12.4 Hz, 1H, H-8ax), 1.28-1.36 (m, 1H, H-6eq), 1.28-1.38 (m, 1H, H-7), 1.30-1.41 (m, 1H, H-4), 1.46-1.52 (m, 1H, H-8eq), 1.44-1.55 (m, 1H, H-4), 1.42-1.57 (m, 1H, H-3), 1.62-1.70 (m, 1H, H-3), 1.80 (dddd, *J* = 12.4, 3.6, 3.6, 3.6 Hz 1H, H-4a), 2.00-2.12 (m, 1H, H-5), 2.33 (s, 3H, N-CH₃), 2.36-2.50 (m, 2H, H-2), 2.64 (dd, *J* = 13.2, 8.0 Hz, 1H, CH₂Py), 2.73 (dd, *J* = 13.2, 7.2 Hz, 1H, CH₂Py), 2.72-2.78 (m, 1H, H-8a), 7.07 (ddd, *J* = 7.6, 4.8, 1.8 Hz, 1H, H-5 Py), 7.09 (d, *J* = 7.6 Hz, 1H, H-3 Py), 7.55 (ddd, *J* = 7.6, 7.6, 1.8 Hz, 1H, H-4 Py), 8.50 (ddd, *J* = 4.8, 1.8, 0.9 Hz, 1H, H-6 Py); ¹³C NMR (400 MHz, HSQC) δ 17.7 (C-4), 22.5 (CH₃), 24.7 (C-8), 25.4 (C-3), 31.5 (C-7), 35.7 (C-6), 39.1 (C-4a), 41.3 (C-5), 42.1 (CH₂Py), 42.6 (N-CH₃), 48.0 (C-2), 61.8 (C-8a), 120.8 (C-5 Py), 123.4 (C-3 Py), 136.1 (C-4 Py), 149.3 (C-6 Py), 161.2 (C-2 Py); HRMS calcd for C₁₇H₂₇N₂ (M+H)⁺ 259.2169, found 259.2162.

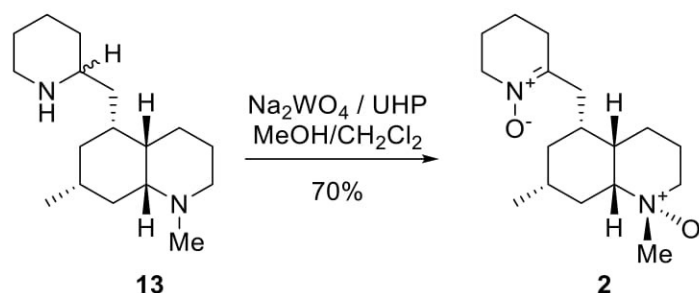
(4a*S*,5*R*,7*R*,8a*R*)-1,7-Dimethyl-5-(piperidin-2-ylmethyl)decahydroquinoline (13)



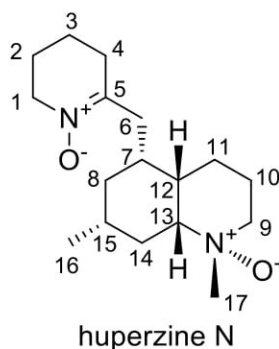
To a stirred solution of **12** (130 mg, 0.50 mmol) in AcOH (5 mL) was added PtO₂ (20% w/w, 30 mg) at room temperature. The resulting mixture was evacuated and backfilled with hydrogen 3 times and then stirred under an atmosphere of H₂ for 16 h. The mixture was diluted with CH₂Cl₂ (10 mL) before it was filtered through a pad of celite and washed through with CH₂Cl₂. The filtered solution was washed with 1 N NaOH, dried, concentrated, and purified by chromatography on alumina (2.5→10% MeOH/CH₂Cl₂; then 90/10/1 MeOH/CH₂Cl₂/NH₃) to give **13** (129 mg, 97 %; epimeric mixture) as a yellowish oil. *R_f* 0.10 (90/10/1 MeOH/CH₂Cl₂/NH₃); ¹H NMR (400 MHz, COSY) δ 0.92 (d, *J* = 6.2 Hz, 3H, CH₃), 1.12-1.18 (m, 1H, H-8), 1.16-1.22 (m, 1H, CH₂), 1.22-1.36 (m, 2H, H-4), 1.26-1.32 (m, 1H, H-4'), 1.27-1.31 (m, 1H, CH₂), 1.30-1.38 (m, 2H, H-7 and H-5'), 1.46-1.52 (m, 1H, H-8), 1.52-1.68 (m, 2H, H-3), 1.52-1.58 (m, 1H, H-5'), 1.54-1.60 (m, 1H, H-3'), 1.56-1.64 (m, 1H, H-5), 1.62-1.67 (m, 1H, H-3'), 1.72-1.77 (m, 1H, H-4'), 1.84 (dddd, *J* = 12.4, 3.6, 3.6, 3.6 Hz, 1H, H-4a), 2.35 (s, 3H, N-CH₃), 2.35-2.50 (m, 2H, H-2), 2.42-2.52 (m, 2H, H-2'), 2.52-2.60 (m, 1H, H-6'), 2.73 (ddd, *J* = 12.4, 4.0, 4.0 Hz, H-8a), 2.96-3.04 (m, 1H, H-6'); ¹³C NMR (400 MHz, HSQC) δ 17.5/17.6 (C-4), 22.6 (CH₃), 24.6 (C-8), 24.8/24.9 (C-4'), 25.6 (C-3), 26.6/26.7 (C-3'), 31.5/31.6 (C-7), 33.1/33.6 (C-3'), 36.0/36.1 (C-5), 36.5/37.0 (C-6), 38.8/39.4 (C-4a), 40.7/40.9 (CH₂), 42.7 (N-CH₃), 47.2 (C-6'), 48.1 (C-2), 53.5/53.8 (C-2'), 62.0 (C-8a).

HRMS calcd for C₁₇H₃₃N₂ (M+H)⁺ 265.2638, found 265.2644.

(4a*S*,5*R*,7*R*,8a*R*)-1,7-Dimethyl-5-(piperidin-2-ylmethyl)decahydroquinoline (2)



To a solution of mixture **13** (90 mg, 0.34 mmol) in $\text{MeOH}/\text{CH}_2\text{Cl}_2$ (1:1; 2 mL) were added in one portion UHP (325 mg, 3.40 mmol) and $\text{Na}_2\text{WO}_4 \cdot 2\text{H}_2\text{O}$ (21 mg, 0.06 mmol) and the mixture was stirred at room temperature for 72 h. The reaction mixture was quenched with NH_4OH solution (0.5 mL) and extracted with CHCl_3 until no more product was detected in the aqueous layer. The combined organic extracts were dried over Na_2SO_4 , concentrated and the resulting crude material was purified by flash chromatography on silica (85/15/1.5 $\text{CHCl}_3/\text{MeOH}/\text{NH}_3$) to give **2** (70 mg, 70 %) as a yellow oil. R_f 0.43 (80/20/2 $\text{CHCl}_3/\text{MeOH}/\text{NH}_3$); $[\alpha]_D$ -6.7 (c 1, CHCl_3); ^1H NMR (400 MHz, COSY) δ 0.99 (d, $J = 6.5$ Hz, 3H, CH_3), 1.05 (ddd, $J = 13.0, 13.0, 13.0$ Hz, 1H, H-6ax), 1.30 (m, 1H, H-8ax), 1.37 (m, 1H, H-4), 1.39 (m, 1H, H-6eq), 1.53 (m, 1H, H-7), 1.62 (m, 1H, H-3), 1.68 (m, 1H, H-4), 1.75 (m, 2H, H-3'), 1.81 (1H, ddd, $J = 11.5, 3.5, 3.5$ Hz, H-8eq), 1.92 (m, 2H, H-2'), 1.96 (m, 1H, H-5), 2.40 (dd, $J = 6.0, 6.0$ Hz, 2H, H-4'), 2.41 (m, 1H, H-3), 2.46 (dd, $J = 13.5, 6.5$ Hz, 1H, CH_2), 2.73 (dd, $J = 13.5, 8.0$ Hz, 1H, CH_2), 2.94 (dddd, $J = 12.4, 3.8, 3.8, 3.8$ Hz, H-4a), 3.05 (br dd, $J = 11.2, 3.5$ Hz, 1H, H-2), 3.11 (s, 3H, NCH_3), 3.16 (m, 1H, H-2), 3.17 (m, 1H, H-8a), 3.80 (dd, $J = 6.0, 6.0$ Hz, 2H, H-1'); ^{13}C NMR (400 MHz, HSQC) δ 16.2 (C-4), 18.8 (C-3'), 20.2 (C-3), 22.2 (CH_3), 23.1 (C-2'), 28.9 (C-4'), 31.8 (C-7), 31.8 (C-8), 33.4 (C-4a), 34.4 (CH_2), 34.8 (C-6), 36.8 (C-5), 58.2 (N- CH_3), 58.4 (C-1'), 61.0 (C-2), 76.8 (C-8a), 147.4 (C-5'); HRMS calcd for $\text{C}_{17}\text{H}_{33}\text{N}_2$ ($\text{M}+\text{H}$) $^+$ 265.2638, found 265.2644.

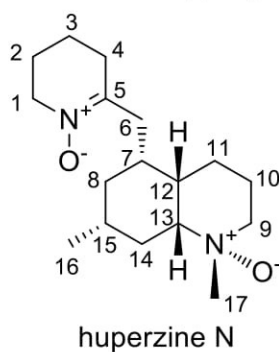
Table S3. Comparison of ^1H NMR data for (-) huperzine N and **2** in CDCl_3 

	Synthetic ¹ 2	Huperzine N ²
1	3.80 (t, 6.0)	3.75 (t, 6.0)
2	1.92 (m)	1.84-1.92 (m)
3	1.75 (m)	1.64-1.69 (m)
4	2.40 (dd, 6.0, 6.0)	2.34 (t, 6.0)
5		
6	2.73 (dd, 13.5, 8.0) 2.46 (dd, 13.5, 6.5)	2.96 (dd, 12, 3) 1.91 (d, 12)
7	1.96 (m)	2.10-2.17 (m)
8	1.39 (m) 1.05 (ddd, 13.0, 13.0, 13.0)	1.34 (ddd, 12, 8, 4) 1.29 (br d, 12)
9	3.16 (m) 3.05 (br dd, 11.2, 3.5)	3.35 (br d, 12) 3.14 (ddd, 12, 11, 3)
10	2.41 (m) 1.62 (m)	1.34-43 (m) 1.57 (br d, 14)
11	1.68 (m) 1.37 (m)	2.01-2.06 (m) 1.08-1.13 (m)
12	2.94(ddd, 12.4, 3.8, 3.8, 3.8)	1.78-1.83 (m)
13	3.17 (m)	2.89 (ddd, 11, 10, 3)
14	1.81 (m) 1.30 (m)	2.06-2.17 (m) 1.67-1.72 (m)
15	1.53 (m)	2.16-2.25 (m)
16	0.99 (d, 6.5)	0.93 (d, 7)
17	3.11 (s)	3.04 (s)

¹ Recorded at 400 MHz. Assignments were aided by gCOSY and gHSQCAD spectra.

² Recorded at 400 MHz (*Helv. Chim. Acta*, 2008, **91**, 1031-1035).

Table S4. Comparison of ^{13}C NMR data for (-) huperzine N and **2** in CDCl_3

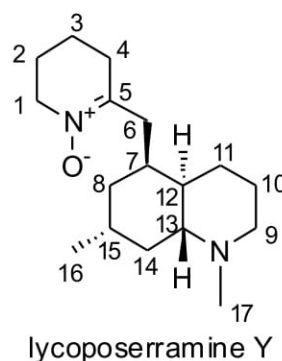
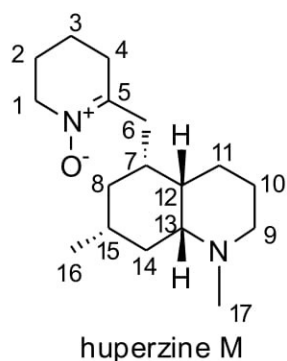


carbon	Synthetic ¹ 2	Huperzine N ²
1	58.4	58.2
2	23.1	23.1
3	18.8	18.8
4	28.9	30.0
5	147.4	148.0
6	34.4	36.4
7	36.8	32.3
8	34.8	36.6
9	61.0	69.0
10	20.2	20.1
11	16.2	27.0
12	33.4	40.8
13	76.8	73.4
14	31.8	30.0
15	31.8	26.8
16	22.2	19.0
17	58.2	57.6

¹ Recorded at 100 MHz. Assignments were aided by gCOSY and gHSQCAD spectra.

² Recorded at 100 MHz (*Helv. Chim. Acta*, 2008, **91**, 1031-1035).

Table S5. Comparison of ^1H NMR data for (-)-huperzine M and lycoposerramine Y in CDCl_3



huperzine M¹

lycoposerramine Y²

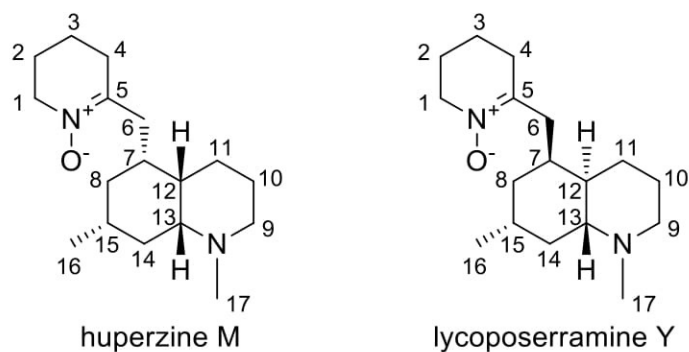
1	3.78 (t, 6.0)	3.73 (ddd, 6.2, 6.2, 1.2)
2	1.86-94 (m)	1.67 (m)
3	1.70-74 (m)	1.86 (m)
4	2.37 (t, 6.0, 6.0)	2.32 (dd, 6.1, 6.1)
5		
6	2.78 (dd, 13, 4) 2.26 (d, 13)	2.72 (dd, 13.4, 3.7) 2.23 (dd, 13.4, 10.1)
7	1.93-96 (m)	1.86 (m)
8	1.83-87 (m) 1.36-41 (m)	1.33 (m)* 1.25 (m)*
9	2.86 (br d, 12) 2.08-13 (m)	2.82 (br d, 11.0) 2.03 (m)
10	1.63-73 (m)	1.59 (m)
11	2.02 (br d, 14) 1.00-05 (m)	1.94 (m) 0.92 (m)
12	1.04-12(m)	0.99 (m)
13	1.82 (br d, 13)	1.73 (ddd, 12.5, 9.5, 3.1)
14	1.28-35 (m)	1.83 (m)* 1.31 (m)*
15	2.03-2.11 (m)	2.03 (m)
16	0.98 (d, 8)	0.93 (d, 7.3)
17	2.24 (s)	2.18 (s)

¹ Recorded at 400 MHz (*Helv. Chim. Acta*, 2008, **91**, 1031-1035).

² *Heterocycles*, 2006, **69**, 223-229

* Signals reversed in huperzine M

Table S6. Comparison of ^{13}C NMR data for (-) huperzine M and lycoposerramine Y in CDCl_3



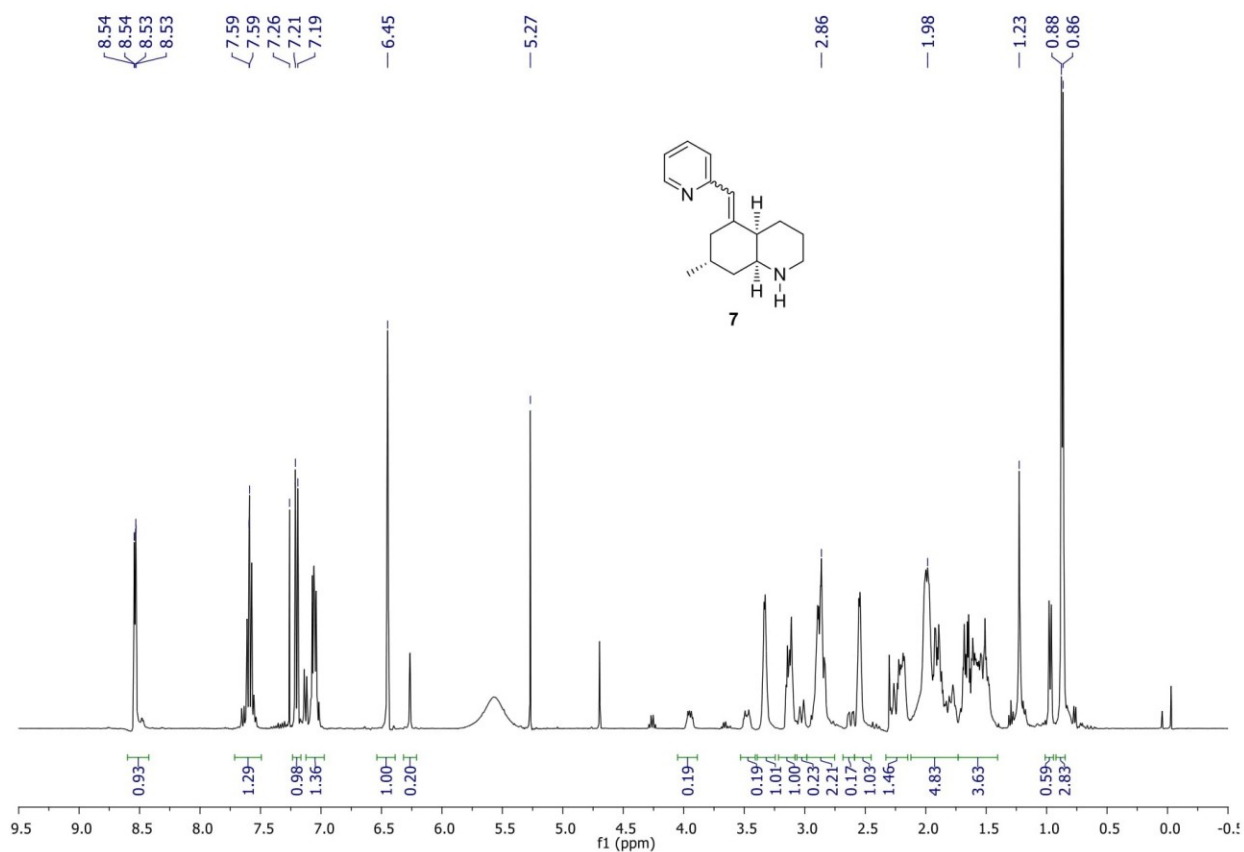
carbon	huperzine M ¹	Lycoposerramine Y ²
1	58.1	58.3
2	23.1	23.3
3	18.8	19.0
4	29.9	29.9
5	148.6	148.5
6	35.6	35.8
7	32.8	33.0
8	35.4	37.7*
9	57.5	57.7
10	25.1	25.4
11	28.3	28.5
12	46.7	47.0
13	63.3	63.4
14	37.5	35.7*
15	27.1	27.3
16	19.3	19.5
17	42.5	42.8

¹ Recorded at 100 MHz. Assignments were aided by gCOSY and gHSQCAD spectra.

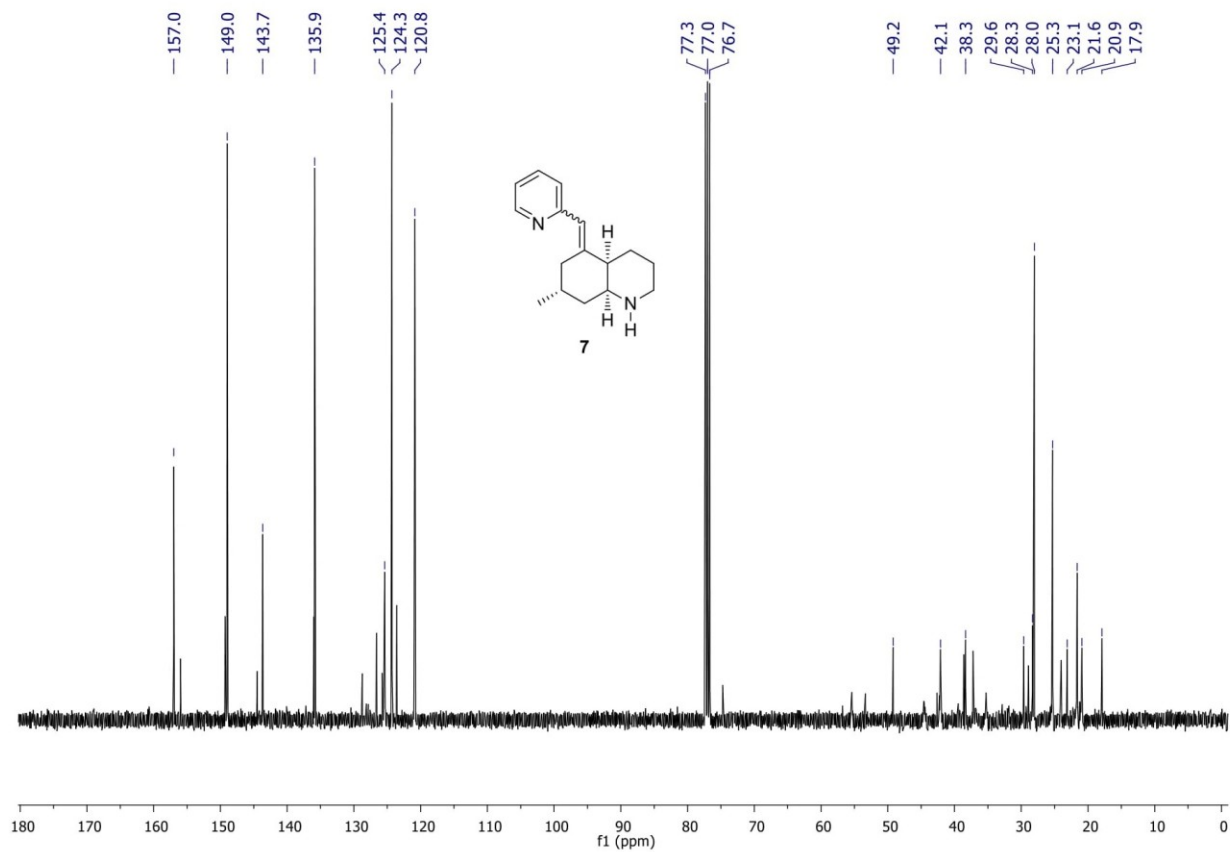
² Recorded at 100 MHz (*Helv. Chim. Acta*, 2008, **91**, 1031-1035).

* Signals reversed in huperzine M

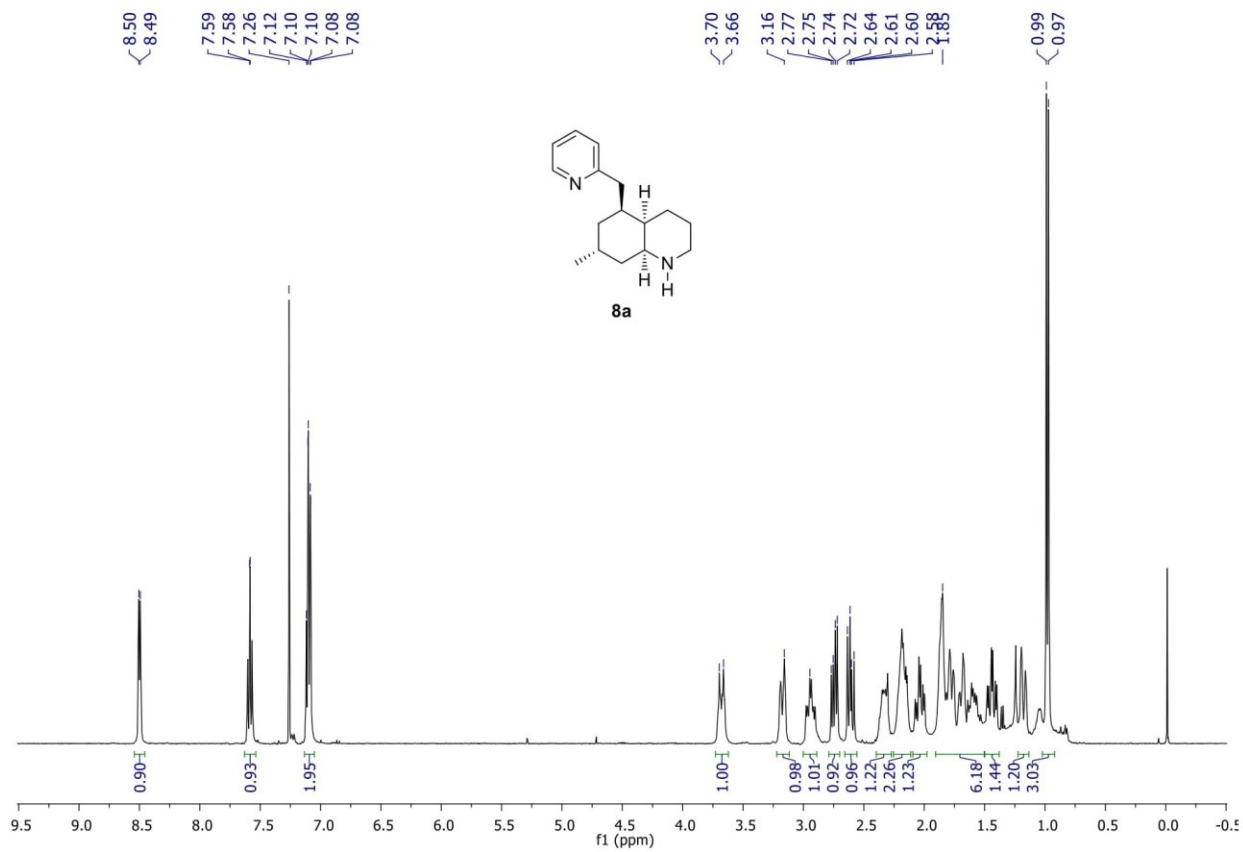
S22



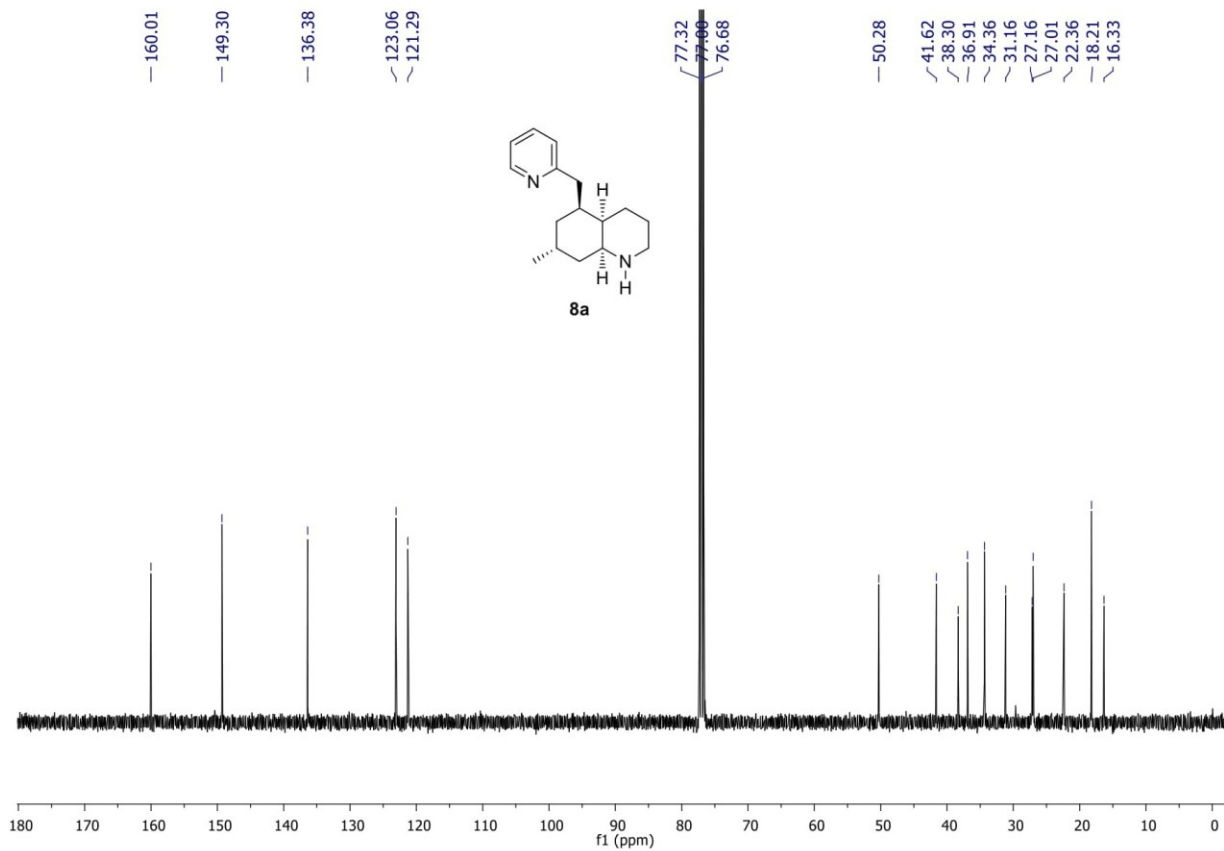
S23



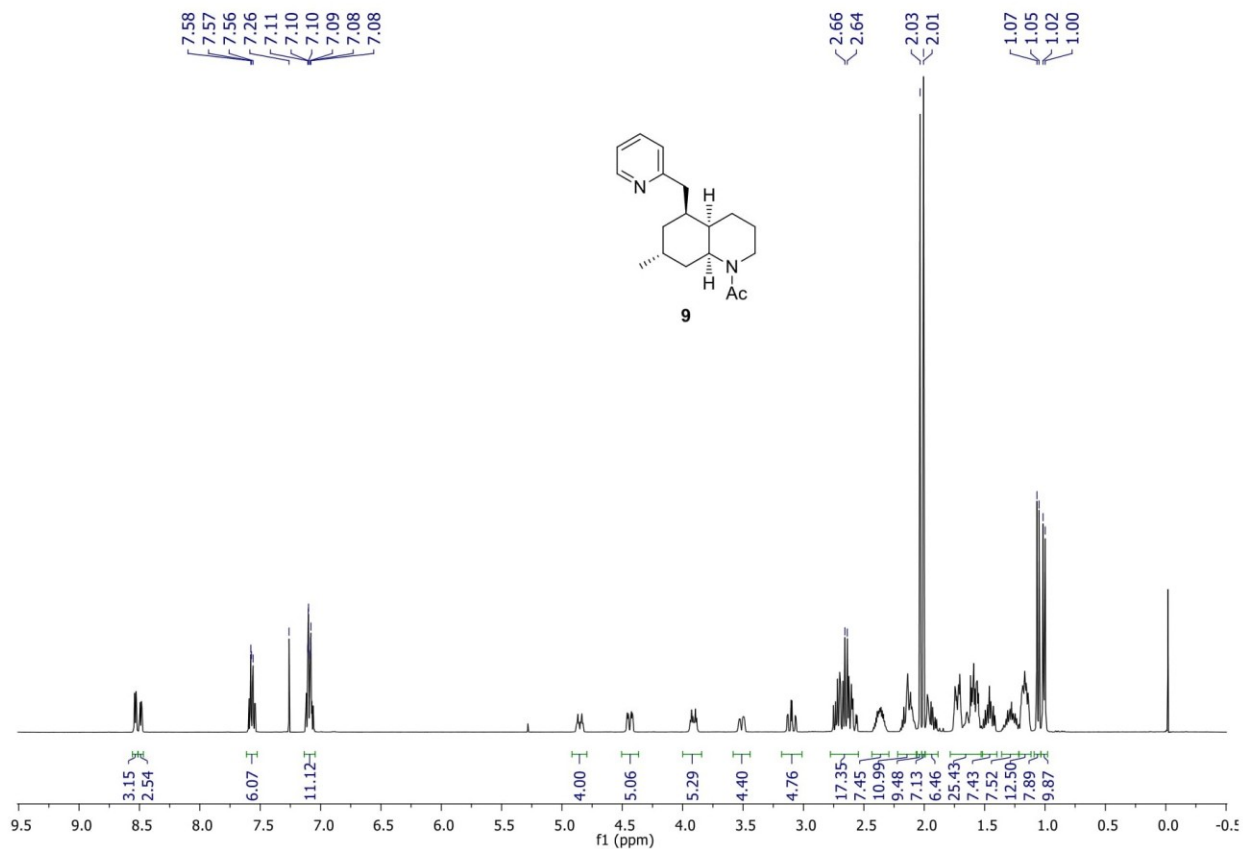
S24



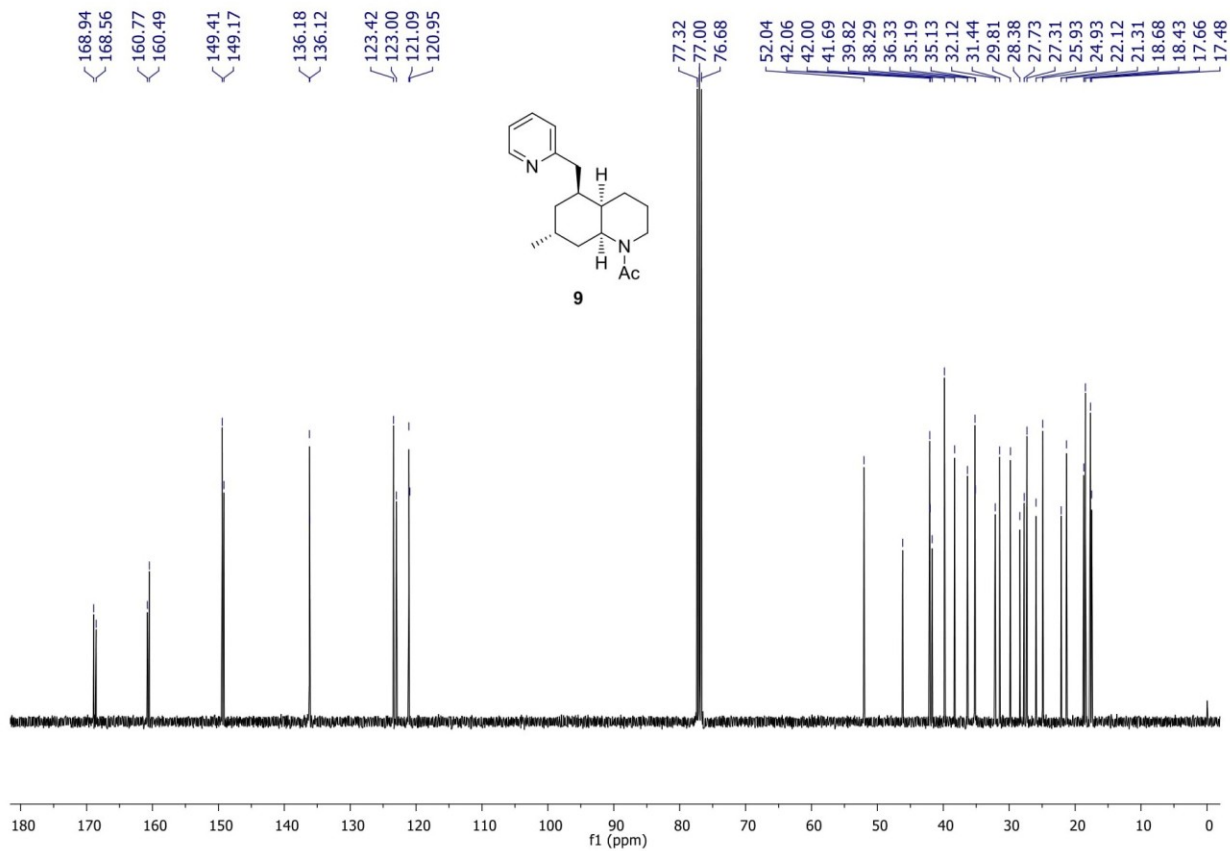
S25



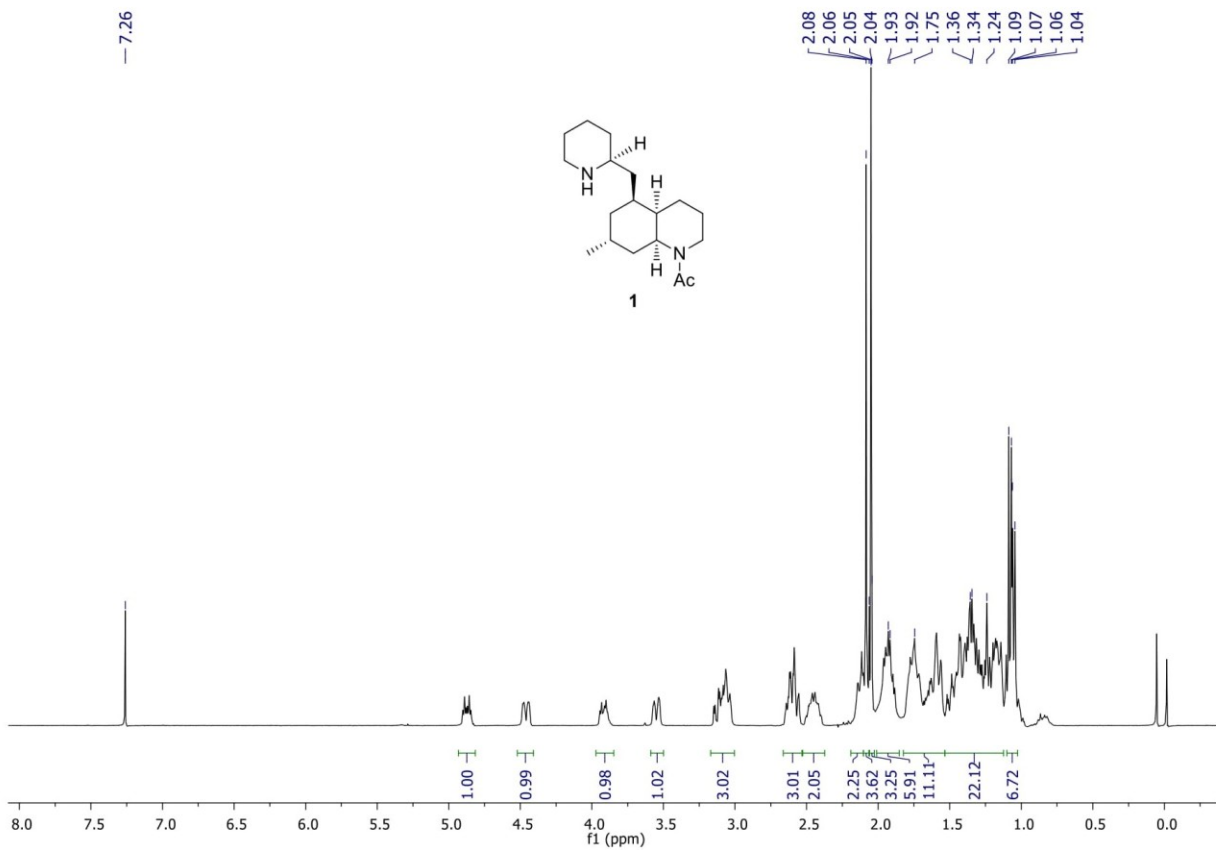
S26



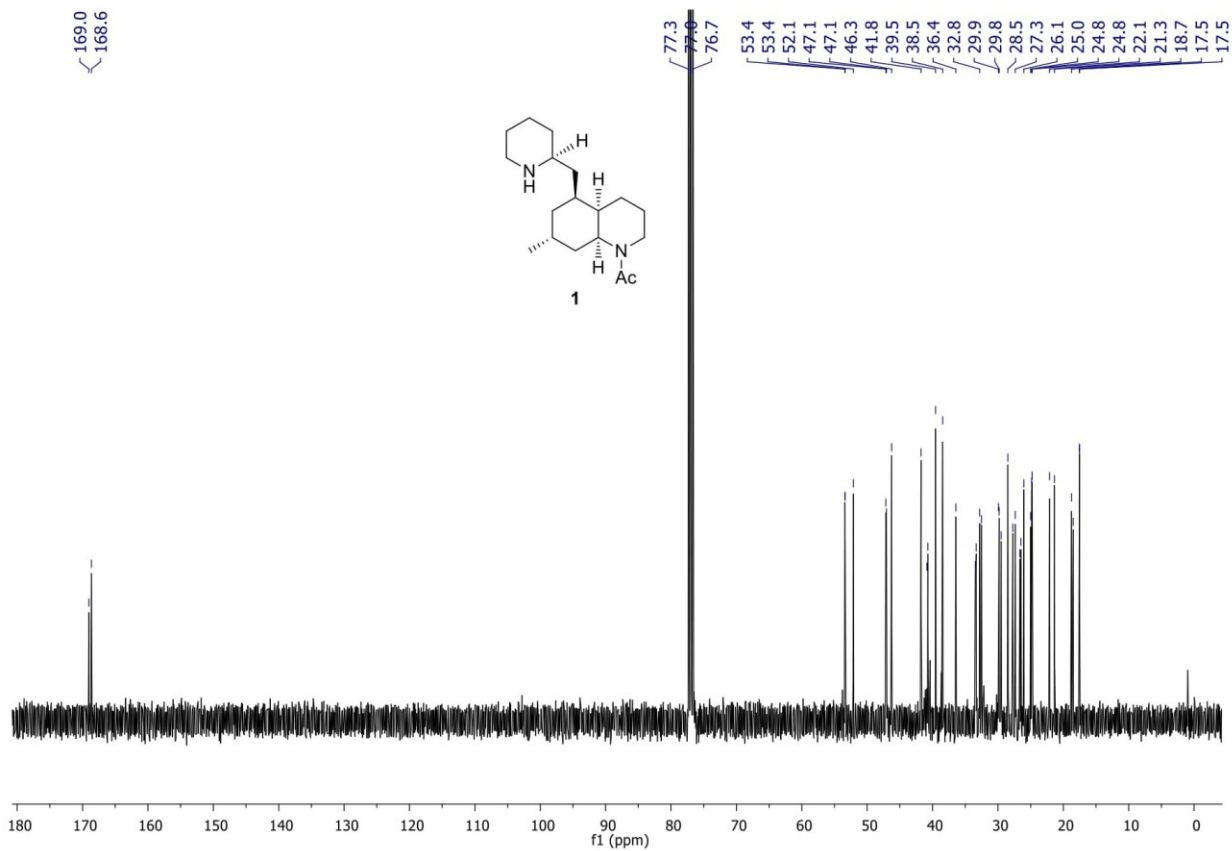
S27



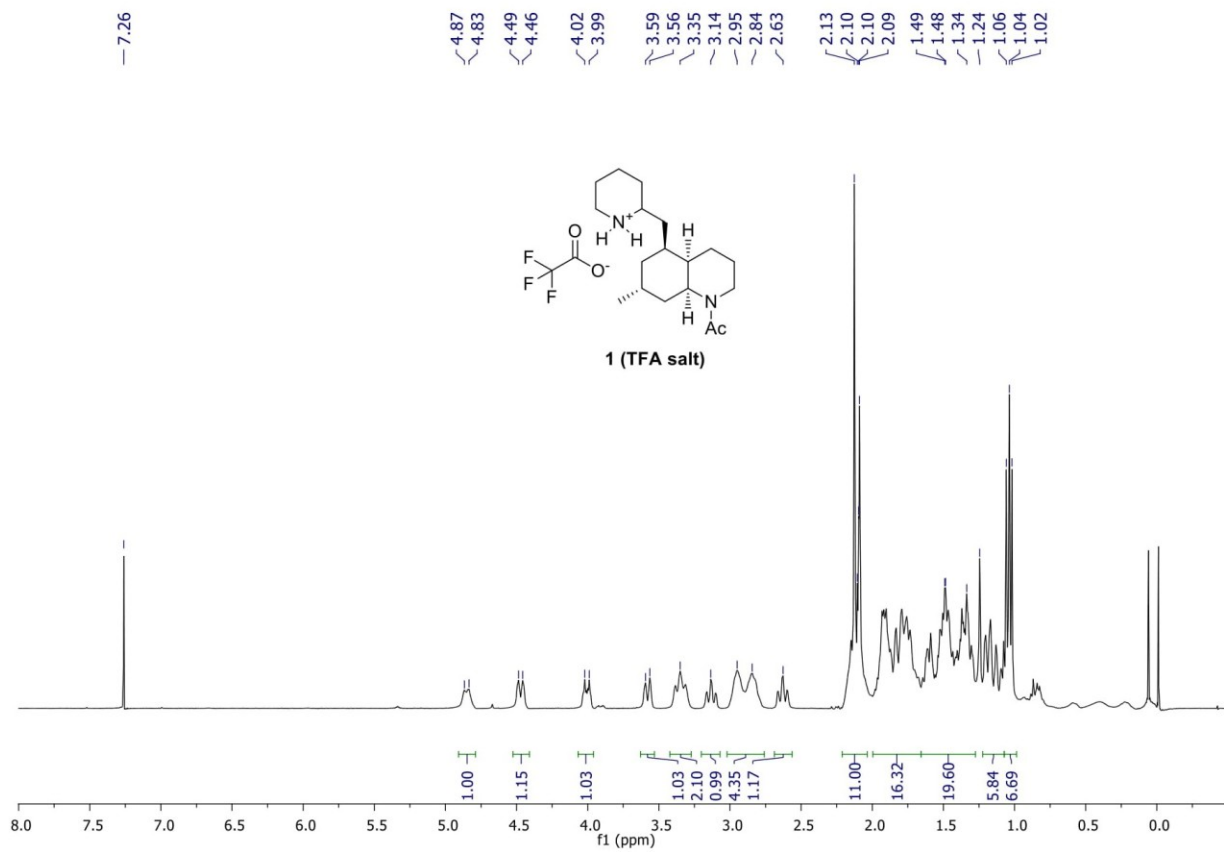
S28



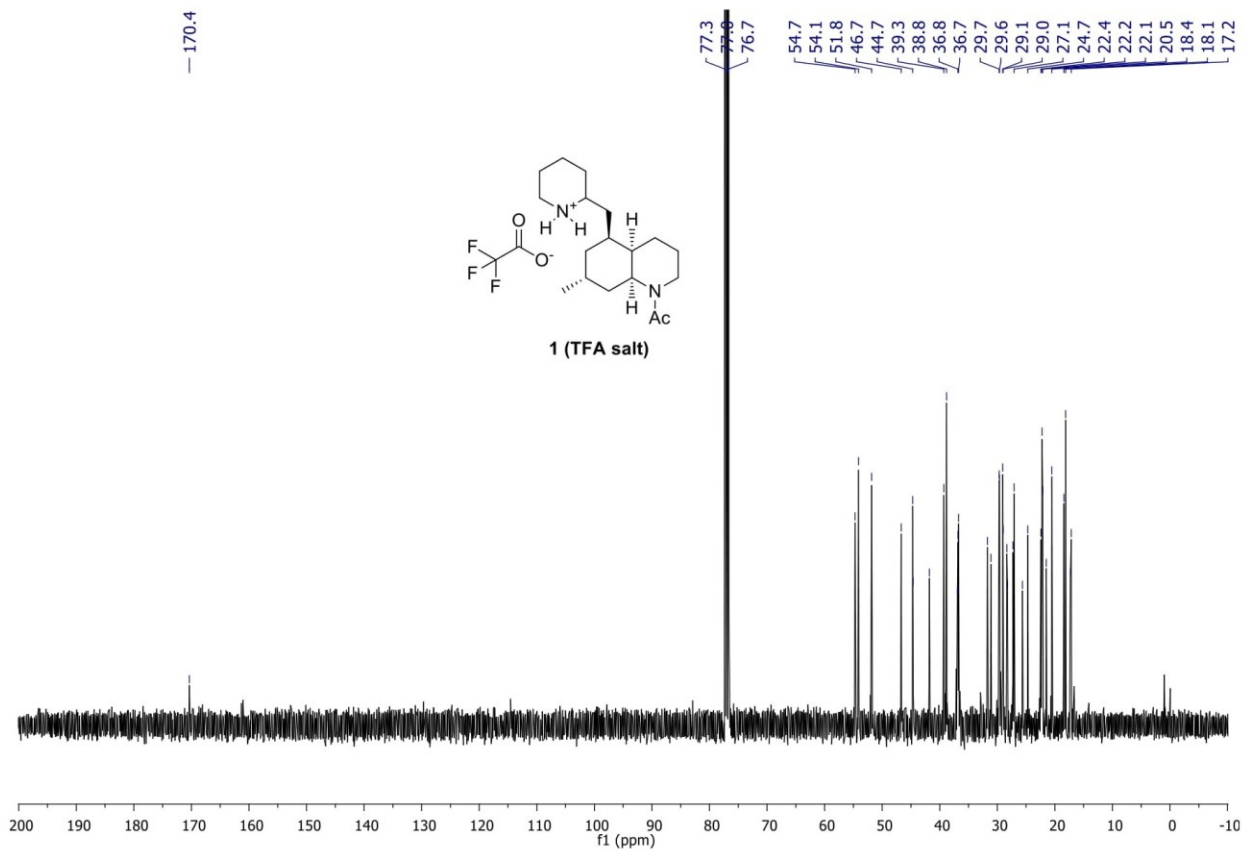
S29



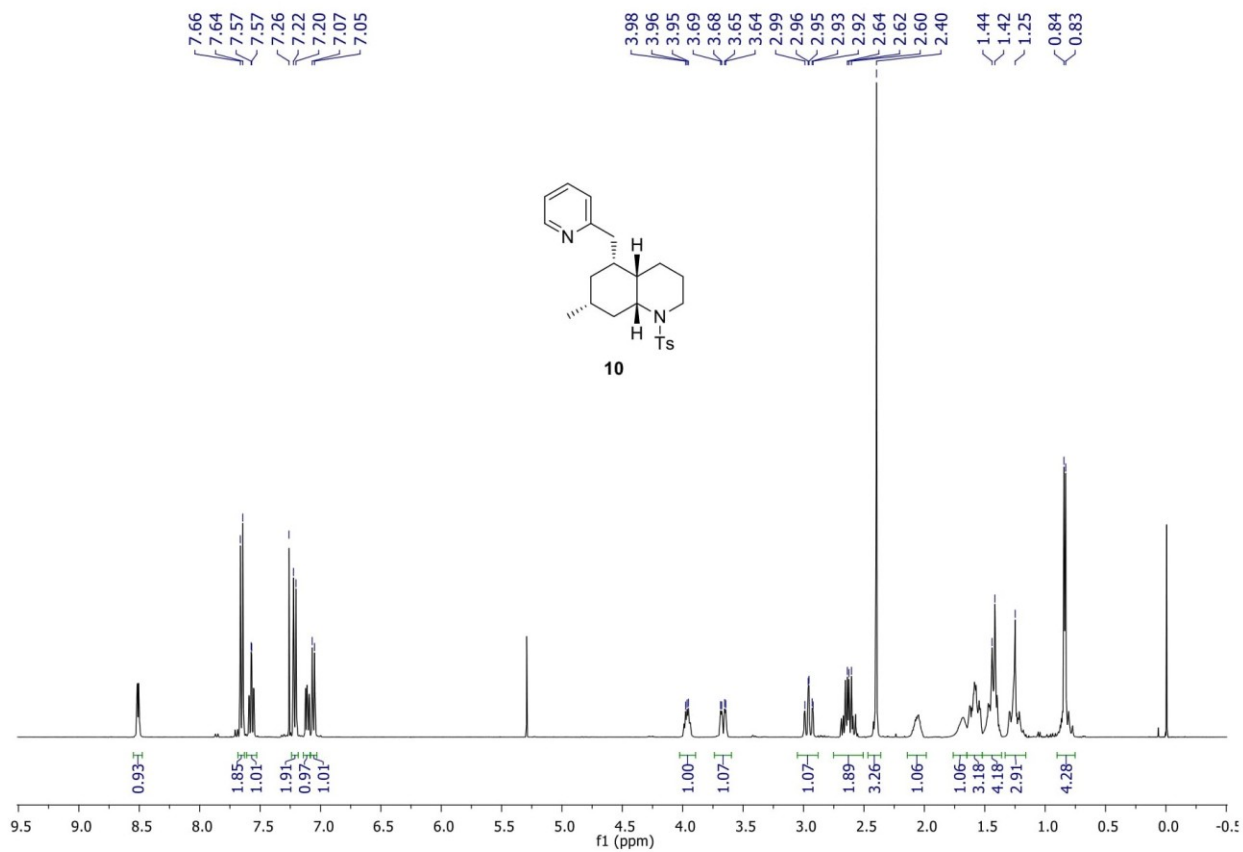
S30



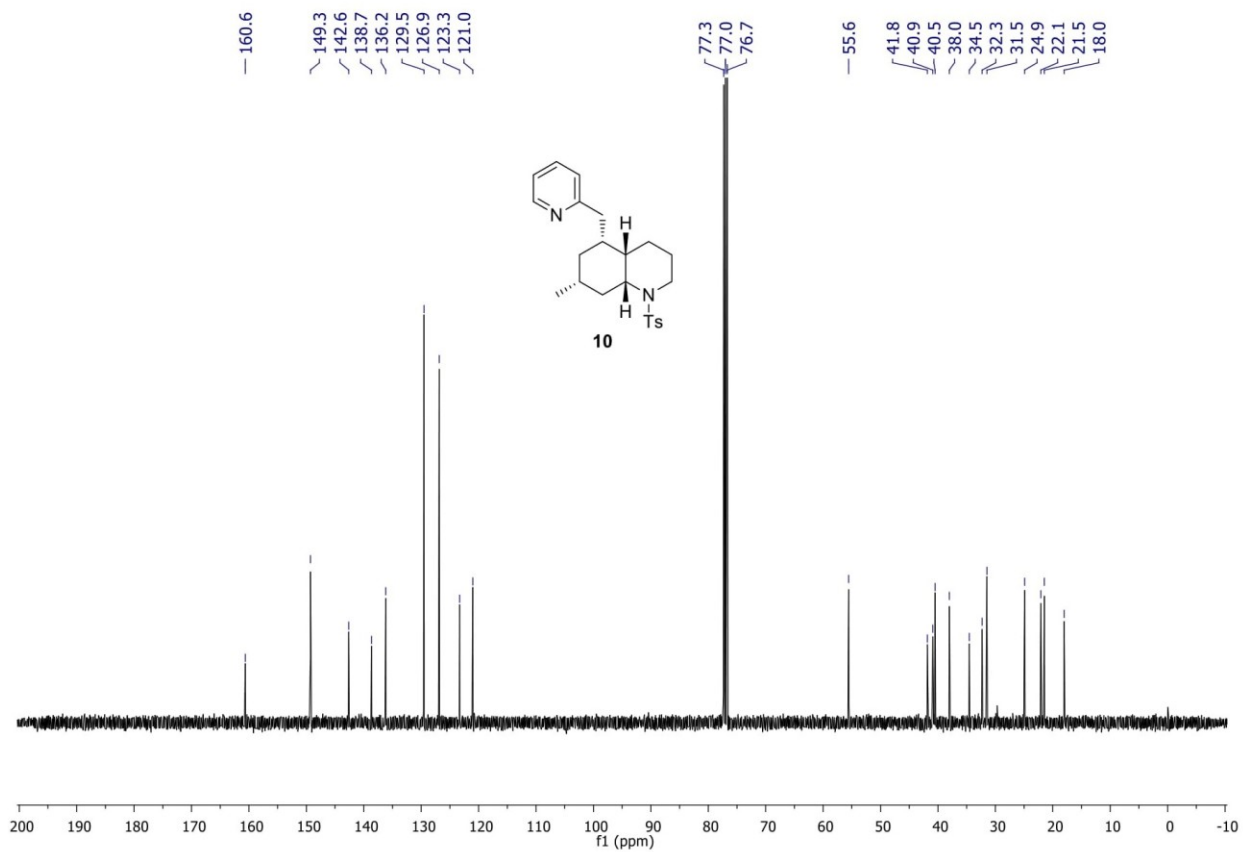
S31



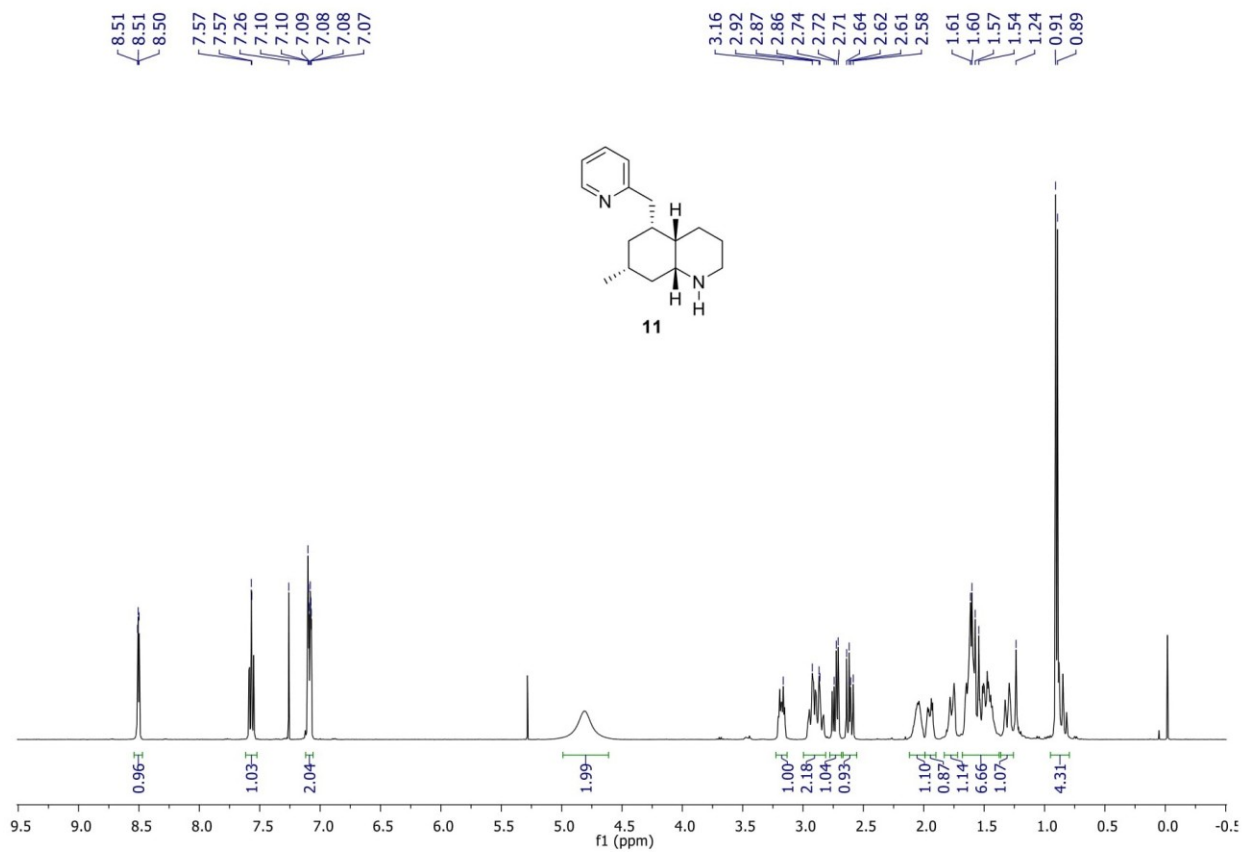
S32



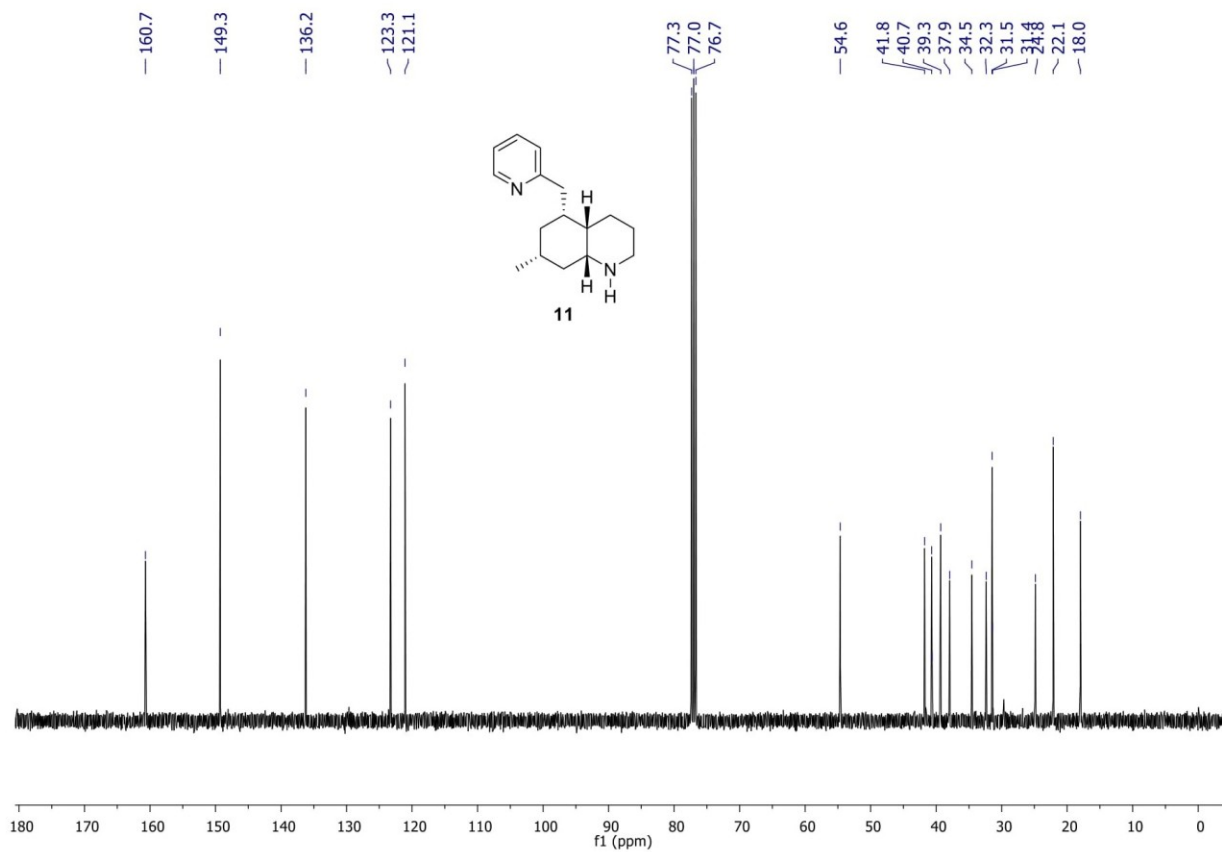
S33



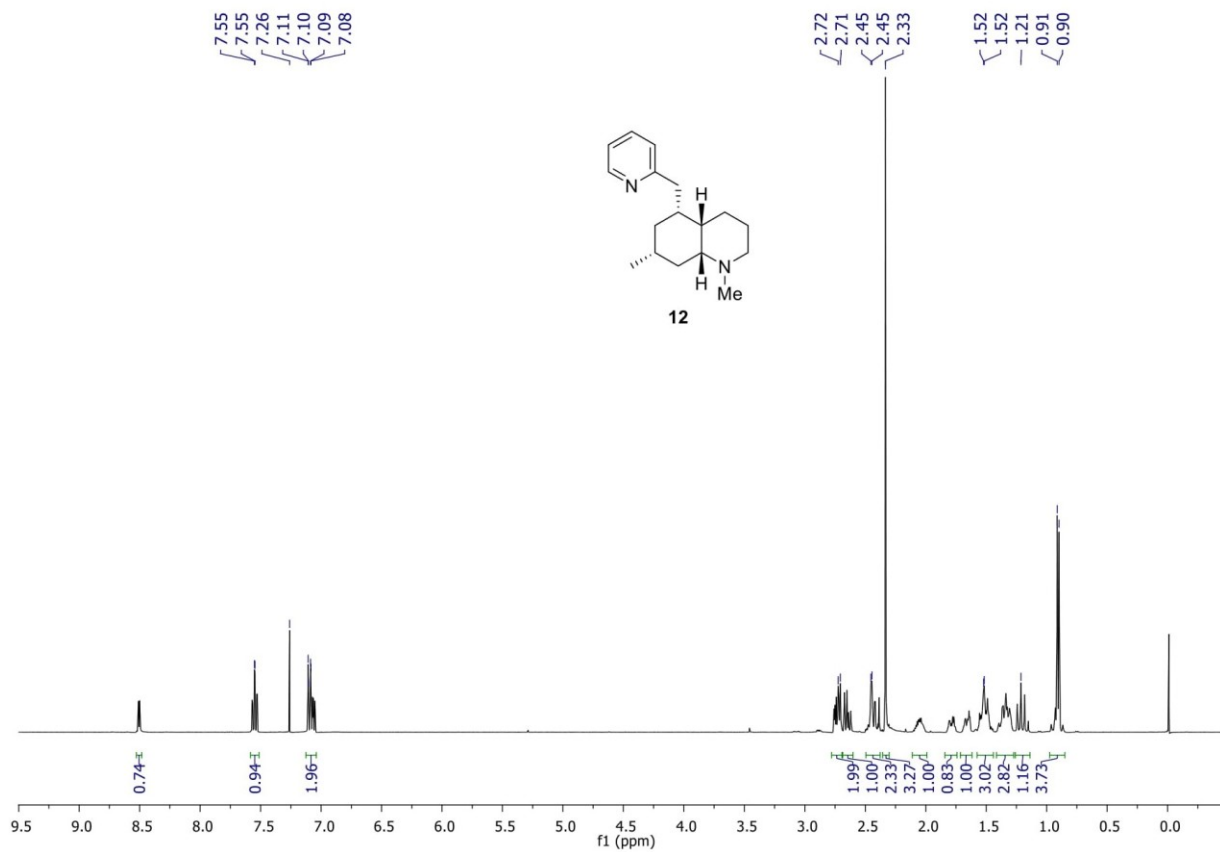
S34



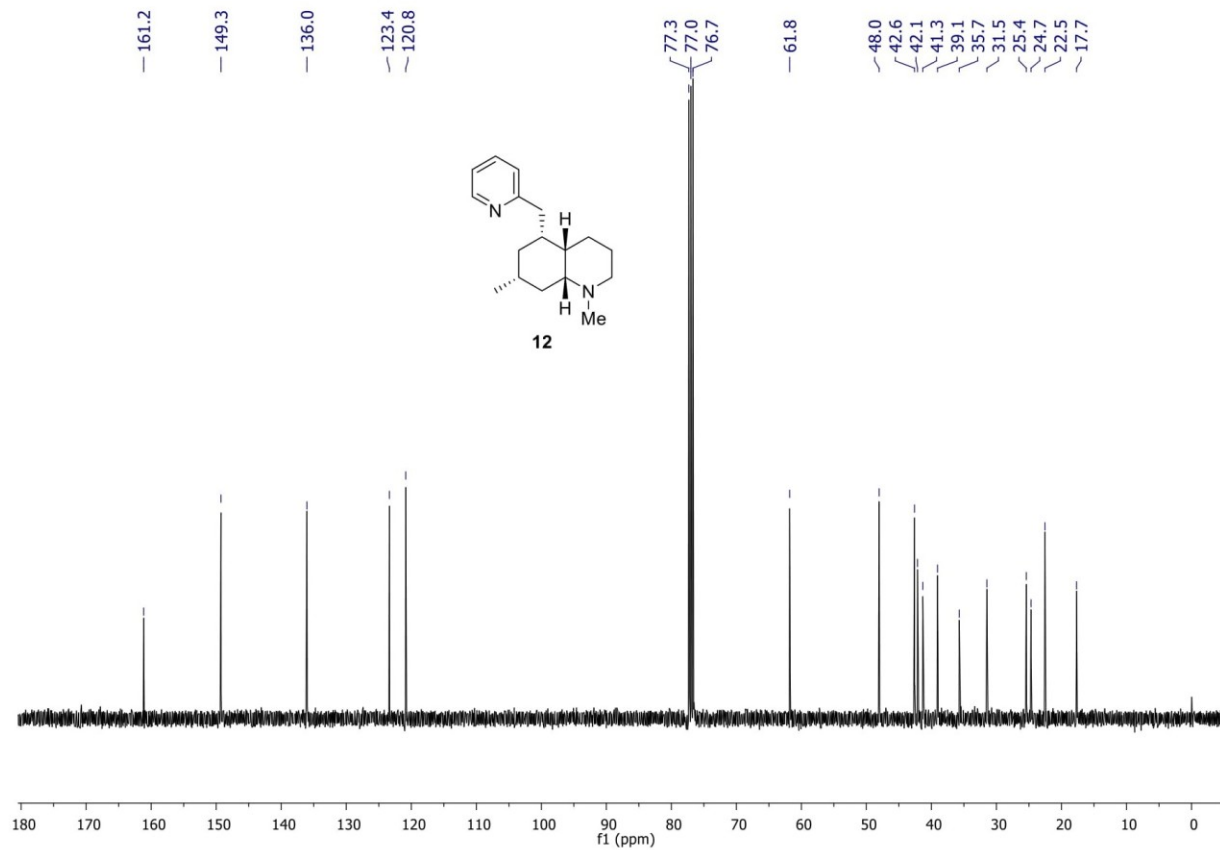
S35



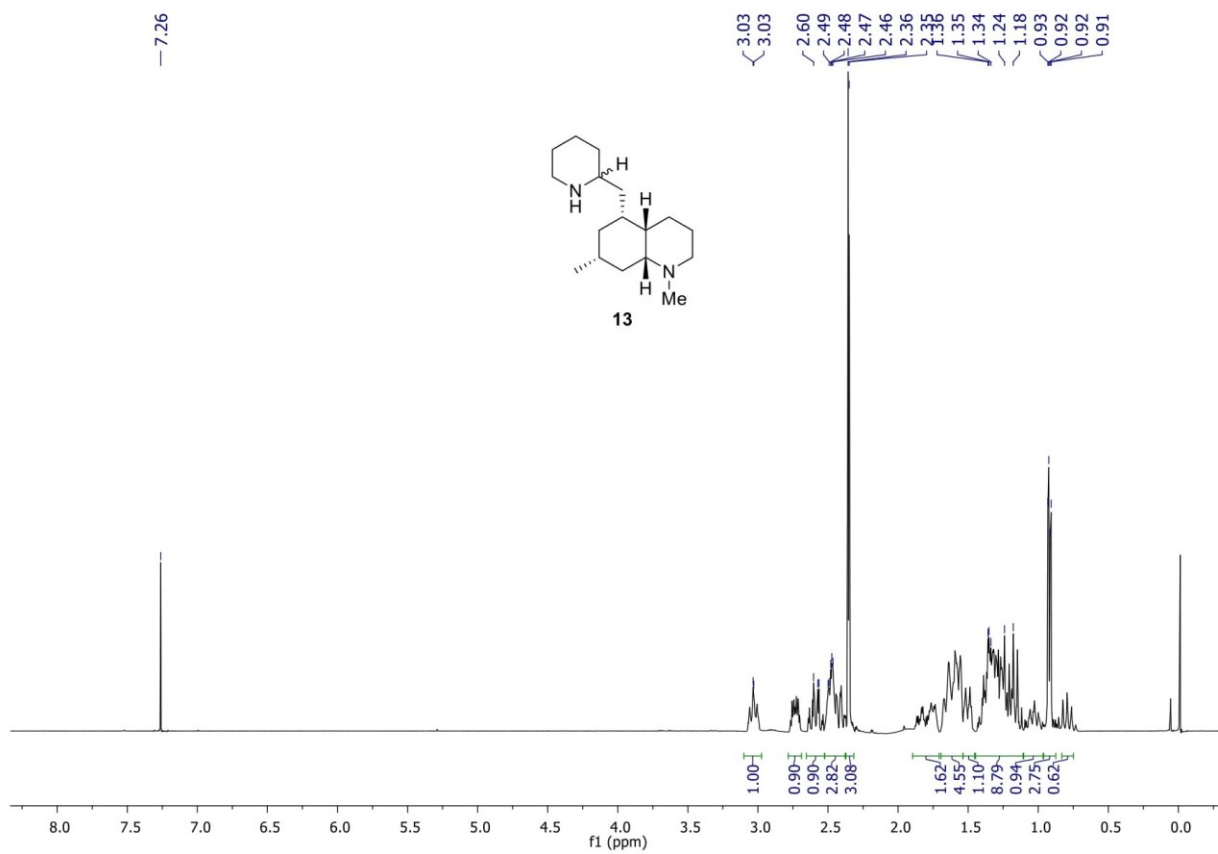
S36



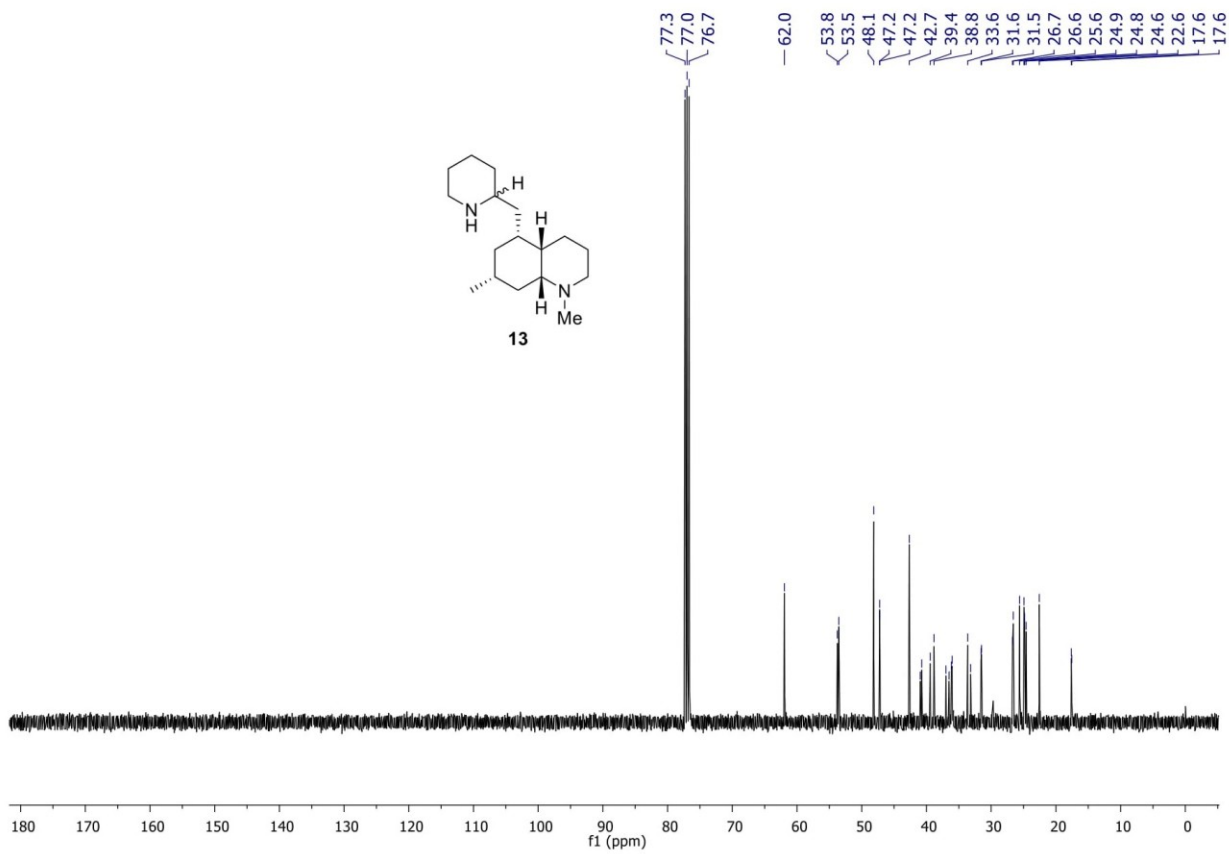
S37



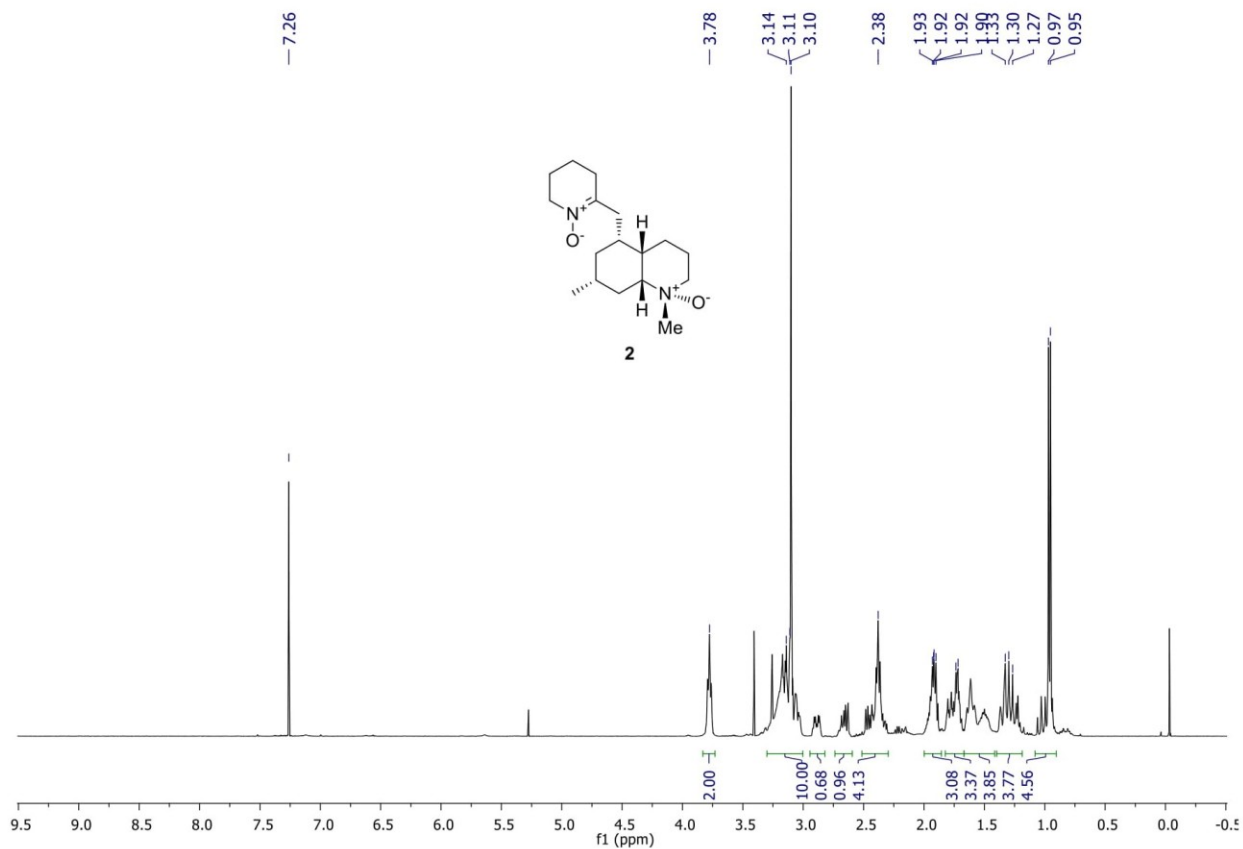
S38



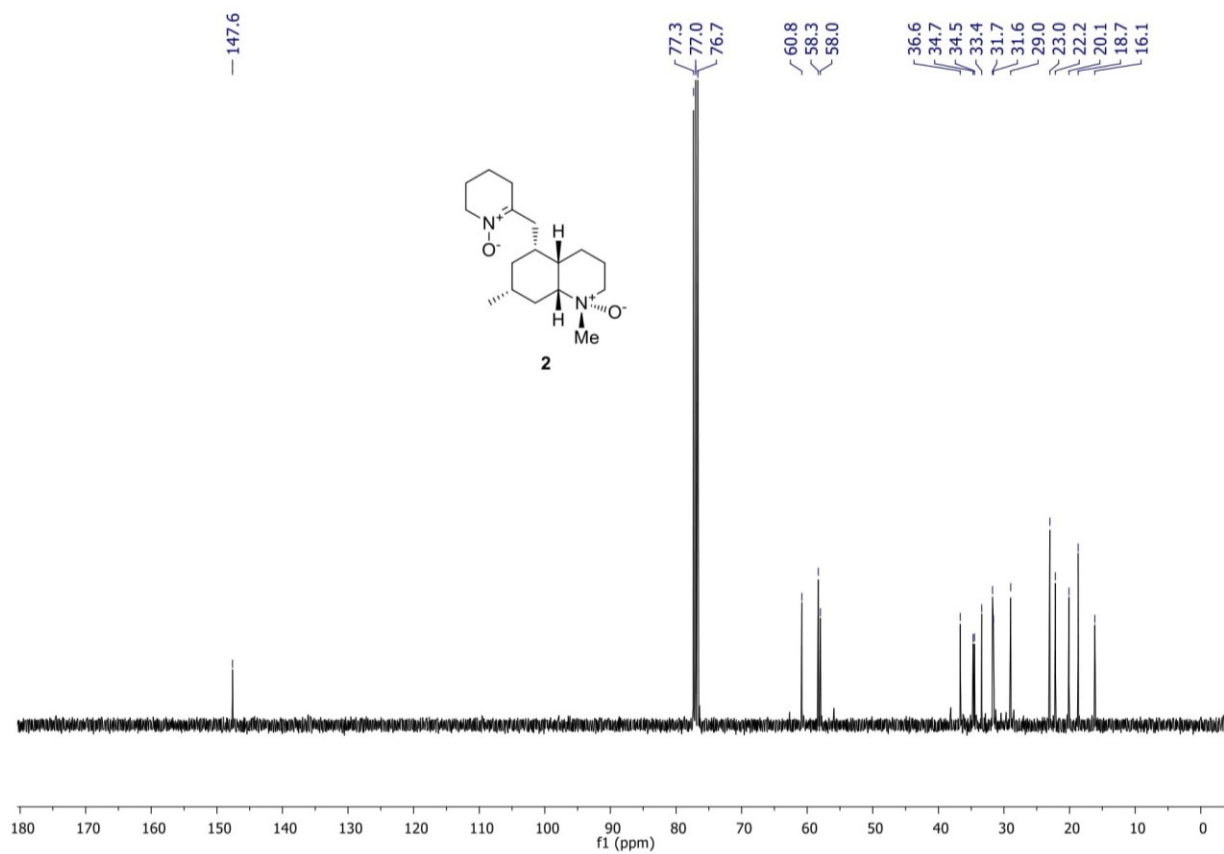
S39



S40



S41



X-Ray Crystallographic Data

X-Ray crystallographic Data for compound **1**

CCDC 1415240 contain the supplementary crystallographic data for this paper. These data can be obtained free of charge from the Cambridge Crystallographic Data Centre via

www.ccdc.cam.ac.uk/data_request/cif

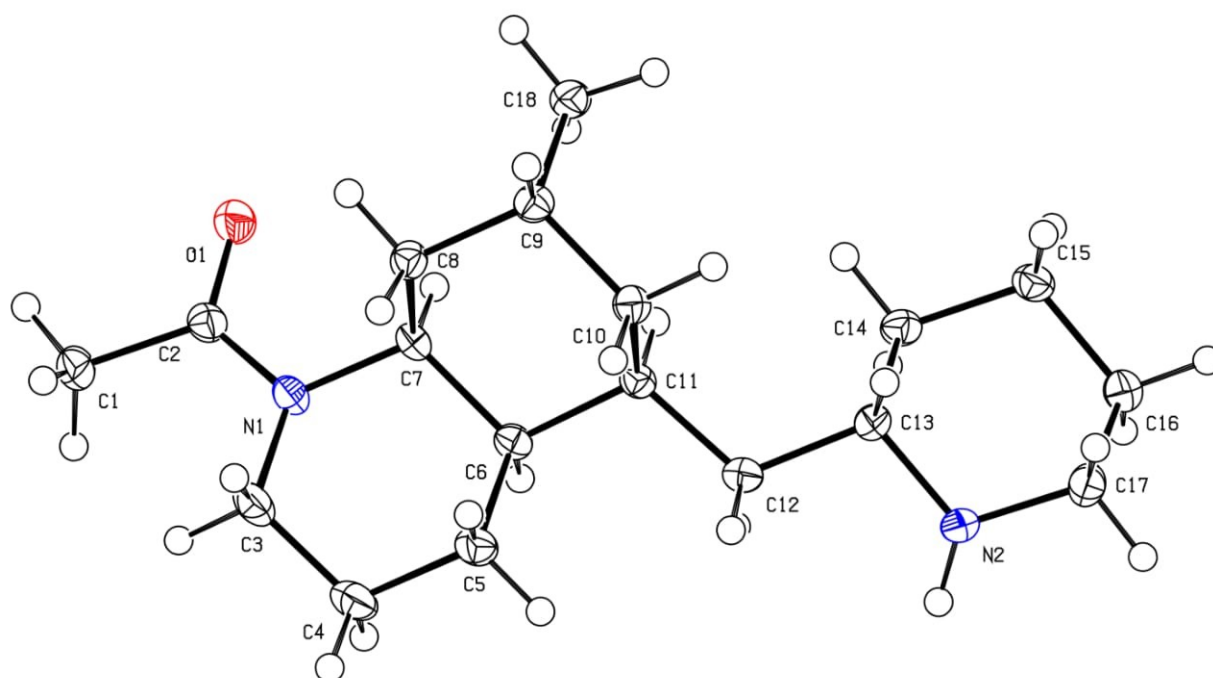


Table 1. Crystal data and structure refinement for **1**

Identification code	cu_d43tb109_0m
Empirical formula	C ₁₈ H ₃₂ N ₂ O
Formula weight	292.45
Temperature	100(2) K
Wavelength	1.54178 Å
Crystal system	Orthorhombic
Space group	P 21 21 21
Unit cell dimensions	a = 5.2870(2) Å α = 90°. b = 9.4826(3) Å β = 90°. c = 34.0330(12) Å γ = 90°.
Volume	1706.23(10) Å ³
Z	4
Density (calculated)	1.138 Mg/m ³
Absorption coefficient	0.537 mm ⁻¹

F(000)	648
Crystal size	0.417 x 0.229 x 0.141 mm ³
Theta range for data collection	2.597 to 72.146°.
Index ranges	-6<=h<=6, -11<=k<=11, -40<=l<=37
Reflections collected	12582
Independent reflections	3302 [R(int) = 0.0303]
Completeness to theta = 67.679°	99.2 %
Absorption correction	Semi-empirical from equivalents
Max. and min. transmission	0.7536 and 0.6564
Refinement method	Full-matrix least-squares on F ²
Data / restraints / parameters	3302 / 0 / 192
Goodness-of-fit on F ²	1.083
Final R indices [I>2sigma(I)]	R1 = 0.0360, wR2 = 0.0915
R indices (all data)	R1 = 0.0401, wR2 = 0.0943
Absolute structure parameter	-0.11(10)
Extinction coefficient	n/a
Largest diff. peak and hole	0.494 and -0.488 e.Å ⁻³

Table 2. Atomic coordinates ($\times 10^4$) and equivalent isotropic displacement parameters ($\text{\AA}^2 \times 10^3$) for **1**. $U(\text{eq})$ is defined as one third of the trace of the orthogonalized U^{ij} tensor.

	x	y	z	U(eq)
O(1)	4621(3)	10675(2)	2328(1)	24(1)
N(1)	7556(3)	9149(2)	2096(1)	19(1)
N(2)	8905(3)	8559(2)	-74(1)	19(1)
C(1)	6274(5)	9031(2)	2791(1)	26(1)
C(2)	6096(4)	9687(2)	2386(1)	19(1)
C(3)	9624(4)	8147(2)	2180(1)	25(1)
C(4)	10156(5)	7198(2)	1833(1)	29(1)
C(5)	10603(4)	8044(2)	1458(1)	23(1)
C(6)	8279(4)	8957(2)	1374(1)	17(1)
C(7)	7663(4)	9935(2)	1721(1)	16(1)
C(8)	9494(4)	11182(2)	1757(1)	18(1)
C(9)	9735(4)	12031(2)	1374(1)	18(1)
C(10)	10352(4)	11036(2)	1032(1)	18(1)
C(11)	8422(4)	9838(2)	994(1)	16(1)
C(12)	8895(4)	8914(2)	632(1)	18(1)
C(13)	8628(4)	9640(2)	234(1)	17(1)
C(14)	6103(4)	10390(2)	174(1)	19(1)
C(15)	5955(4)	11045(2)	-234(1)	21(1)
C(16)	6493(4)	9949(2)	-552(1)	22(1)
C(17)	8964(4)	9187(2)	-468(1)	21(1)
C(18)	7396(4)	12934(2)	1291(1)	23(1)

Total Synthesis of *cis*-Phlegmarines via stereodivergent reduction: (+)-Serratezomine E and Putative Structure of (-)-Huperzine N

Caroline Bosch,[†] Ben Bradshaw,^{*,†} and Josep Bonjoch^{*,†}

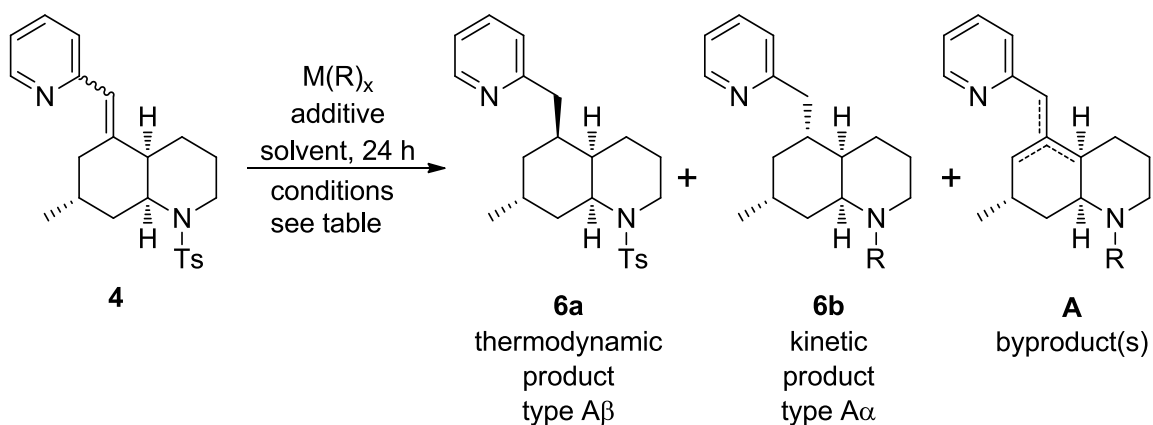
[†]Laboratori de Química Orgànica, Facultat de Farmàcia, IBUB,
Universitat de Barcelona, Av. Joan XXIII s/n, 08028-Barcelona, Spain
e-mail address: josep.bonjoch@ub.edu; benbradshaw@ub.edu

Unpublished results

General Procedure

To a flame dried vial equipped with a stirring bar was added Mn(dpm)₃ (23 mg, 0.038 mmol, 1.0 equiv), the starting material **4** (15 mg, 0.038 mmol, 1.0 equiv) and dichloroethane (0.5 mL). The resulting mixture was evacuated and backfilled with argon three times before degassing for 10 minutes with argon. PhSiH₃ (12 μL, 0.095 mmol, 2.5 equiv) was added and the reaction stirred for 24 h at 60 °C in an oil bath. Evaporation of the solvent followed by purification on column chromatography (5→50% EtOAc in hexanes) afford the product (epimer mixture) (13mg, 86%) as a pale oil. *R_f* 0.39 (50% EtOAc/hexanes). For NMR data see SI 4.

Table S4'-1 Radical Reduction of vinylpyridine 4 under Shenvi's protocol and related procedures

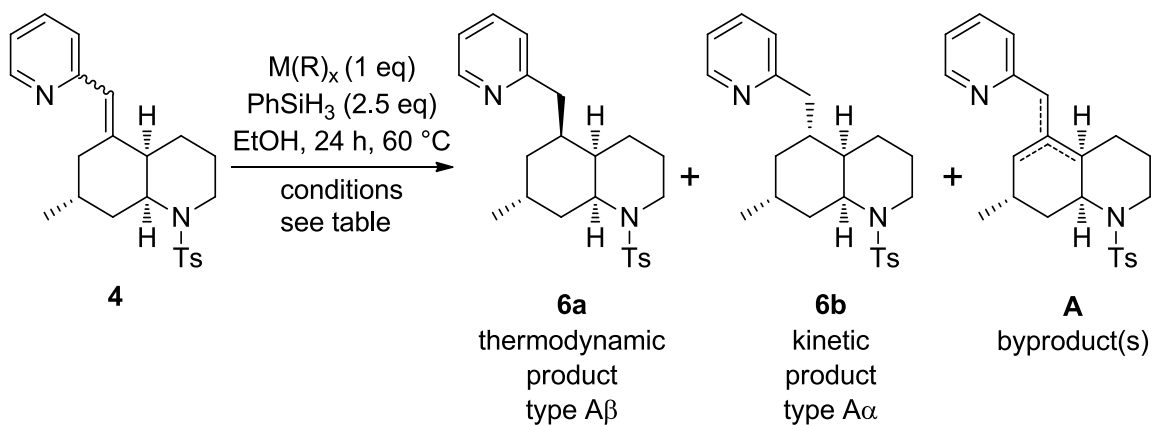


entry	R	catalyst (eq)	reducing agent (eq)	additive	temp (°C)	solvent	conv (%) ^a				ratio 6a:6b ^a
							4	6a	6b	A	
1	Ts	Mn(dpm) ₃ (0.1)	PhSiH ₃ (1)	TBHP (1)	24	<i>i</i> -PrOH	--	46	17	37	73:27
2	H	Mn(dpm) ₃ (0.1)	PhSiH ₃ (1)	TBHP (1)	24	<i>i</i> -PrOH	100	--	--	--	--
3	Ts	Fe(acac) ₃ (1)	PhSiH ₃ (2.5)	(CH ₂ OH) ₂ (50)	60	EtOH	51	33	16	--	67:33
4	Ts	Fe(acac) ₃ (2)	PhSiH ₃ (5)	(CH ₂ OH) ₂ (50)	60	EtOH	49	34	17	--	68:32
5	Ts	Fe(acac) ₃ (1)	PhSiH ₃ (2.5)	--	60	EtOH	50	35	15	--	70:30
7 ^b	Ts	Fe ₂ (ox) ₃ ·6H ₂ O (2)	NaBH ₄ (8)	--	0	EtOH/H ₂ O	68	8	2	22	-- ^{nr}
8 ^c	Ts	Co(acac) ₂ (1)	Et ₃ SiH (5)	TBHP (1) 1,4-CHD (5)	24	<i>n</i> -PrOH	70	5	2	23	-- ^{nr}
9 ^c	Ts	Co(acac) ₂ (1)	Et ₃ SiH (5)	1,4-CHD (5)	24	<i>n</i> -PrOH	83	6	1	10	-- ^{nr}

^a Conv and ratio determine by ¹H NMR ^b Boger procedure (*J. Am. Chem. Soc.* **2009**, *131*, 4904–4916). ^c Herzon procedure (*J. Am. Chem. Soc.* **2014**, *136*, 6884–6887).

^{nr} not representative due to the low conversion to hydrogenated products.

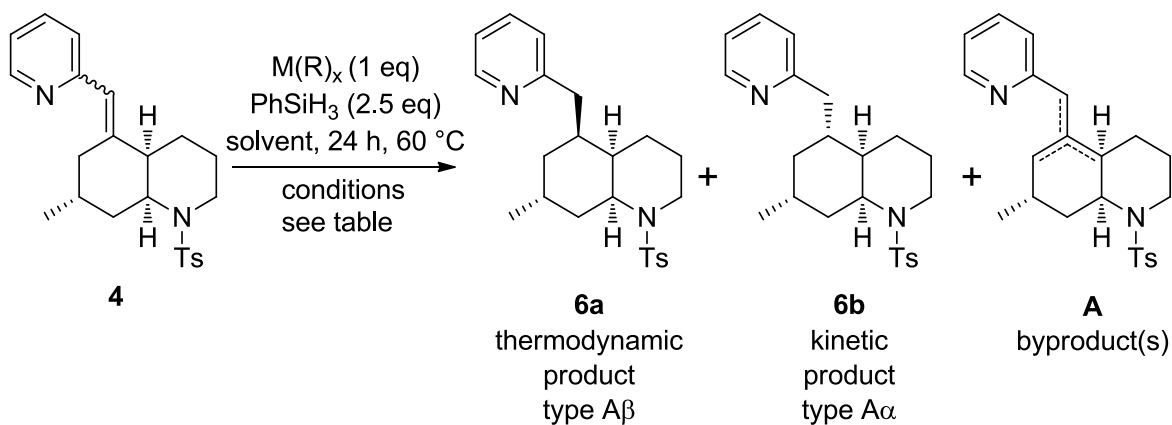
Table S4'-2 Radical reduction without additives of vinylpyridine 4



entry	catalyst	conv (%) ^a				ratio
		4	6a	6b	A	6a:6b^a
1	$Fe_2(ox)_3 \cdot 6H_2O$	100	--	--	--	----
2	$FeCl_3 \cdot 6H_2O$	--	--	--	--	Dec
3	$Co(dpm)_2$	100	--	--	--	--
4	$Co(acac)_3$	100	--	--	--	--
5	$Mn(OAc)_3$	50	20	10	20	65:35
7	$Mn(acac)_3$	--	50	26	24	65:35
8	$Ni(acac)_2$	--	29	71	--	29:71
9	$Fe(acac)_3$	50	35	15	--	70:30
10	$Mn(dpm)_3$	--	61	36	3	63:37

^a Conv and ratio determine by ¹H NMR

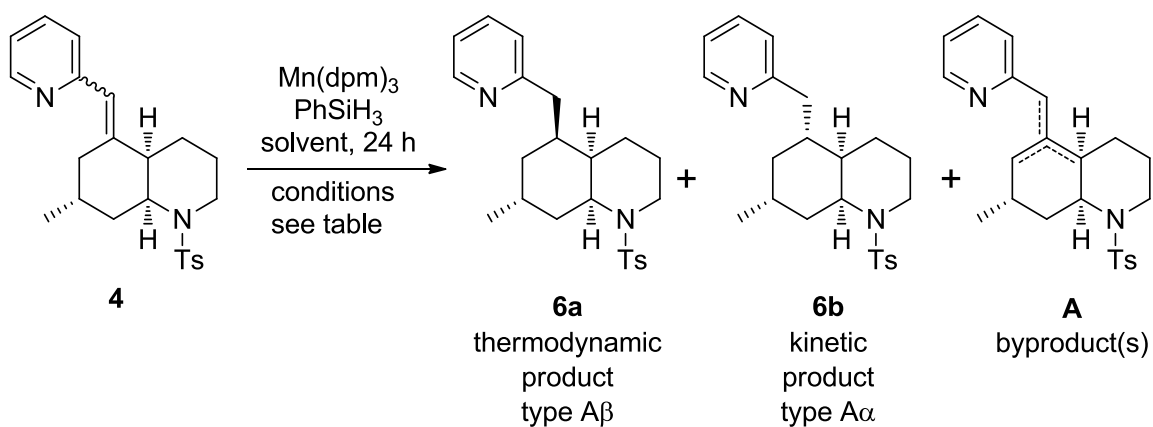
Table S4'-3 Screening of the solvent



entry	solvent	conv (%) ^a				ratio
		4	6a	6b	A	6a:6b^a
1	EtOH	--	61	36	3	63:37
2	<i>i</i> PrOH	8	59	25	8	70:30
3	1-heptanol	8	62	25	5	70:30
4	MeOH	28	41	14	17	75:25
5	$CHCl_3$	--	63	37	--	63:37
6	$CDCl_3$	--	55	19	26	75:25
7	DCE	--	69	31	--	69:31
8	THF	--	67	30	3	69:31
9	MeCN	--	72	22	6	76:26
10	TFE	5	54	22	19	70:30
11	EtOH/ DCE (50/50)	--	59	41	--	59:41

^a Conv and ratio determine by ¹H NMR

Table S4'-4 Optimization of the process



entry	Mn(dpm)_3 (eq.)	PhSiH_3 (eq)	temp. (°C)	solvent	conv (%) ^a				ratio
					4	6a	6b	A	6a:6b^a
1	1	2.5	60	DCE	--	69	31	--	69:31
2	1	2.5	rt	DCE	--	48	22	30	69:31
3	0.1	2.5	60	EtOH	82	9	5	4	62:38
4	0.1	2.5	60	DCE	62	24	5	9	62:38
5	0.5	2.5	60	DCE	--	43	20	37	62:38
6	2	2.5	60	DCE	--	67	33	--	67:33
7	1	5	60	DCE	--	70	30	--	70:30
8	1	100	60	solvent free	--	67	28	5	71:29

^a Conv and ratio determine by ¹H NMR

Synthesis of (\pm)-Serralongamine A and the Revised Structure of Huperzine N

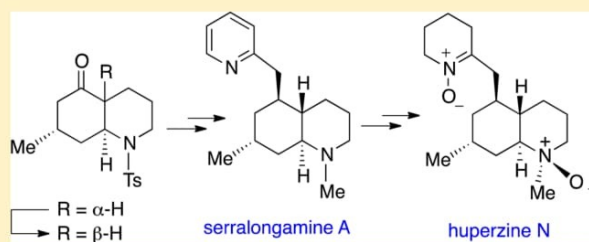
Gisela V. Saborit,[†] Caroline Bosch,[†] Teodor Parella,[‡] Ben Bradshaw,^{*,†} and Josep Bonjoch^{*,†}

[†]Laboratori de Química Orgànica, Facultat de Farmàcia, IBUB, Universitat de Barcelona, Av. Joan XXIII s/n, 08028-Barcelona, Spain

[‡]Servei de Ressonància Magnètica Nuclear, Universitat Autònoma de Barcelona, 08193-Bellaterra, Barcelona, Spain

Supporting Information

ABSTRACT: A revised structure for the *Lycopodium* alkaloid huperzine N is proposed and confirmed by synthesis. The key synthetic steps involve an epimerization of a *cis*-5-oxodecahydroquinoline to the corresponding *trans* isomer and a coupling, followed by a diastereoselective hydrogenation using Wilkinson's catalyst to incorporate the pyridylmethyl moiety. This route allowed the alkaloid serralongamine A to be synthesized for the first time, and two additional steps led to the revised structure of huperzine N, both products bearing an unusual decahydroquinoline stereostructure.



The phlegmarine alkaloids are structurally characterized by a 5,7-disubstituted decahydroquinoline ring and a $C_{16}N_2$ skeleton.¹ They can be classified in four types, designated here as A–D,² according to the relationship of the ring fusion hydrogens (H-4a and H-8a) with the H-7 in the decahydroquinoline ring (DHQ) (Figure 1).³ Moreover, the phlegmarine substitution pattern involves a (2-piperidyl)methyl side chain at

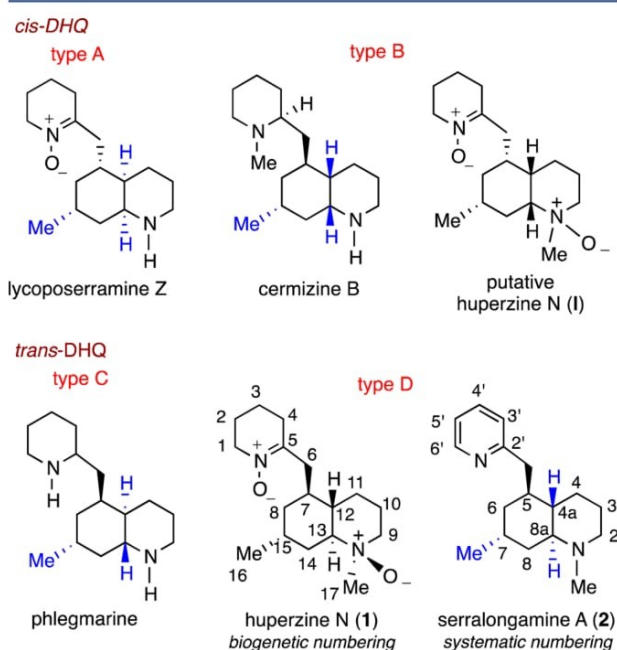


Figure 1. Phlegmarine alkaloids showing the four different stereo-parents.

C-5, which can be partially (as in nitron) or fully oxidized (as in pyridine), thus increasing the stereochemical variation.

After recently describing the total synthesis of **1**, the proposed structure of huperzine N,⁴ we revealed its misassignment. We here suggest an alternative structure for this natural product^{5,6} (i.e., **1**) and confirm it by a total synthesis. Moreover, the synthesis of serralongamine A (**2**),⁷ featuring a pyridine instead of the usual piperidine ring system, is also reported.

The putative (**I**) and natural huperzine (**1**) are clearly differentiated by their ¹³C NMR data: (i) The chemical shifts of C(2) and C(4) are more deshielded (8 and 11 ppm, respectively) in **1** (Figure 2). These data suggest that huperzine

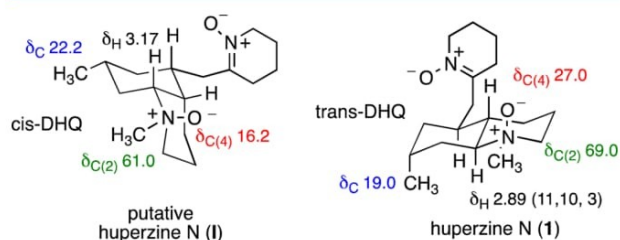
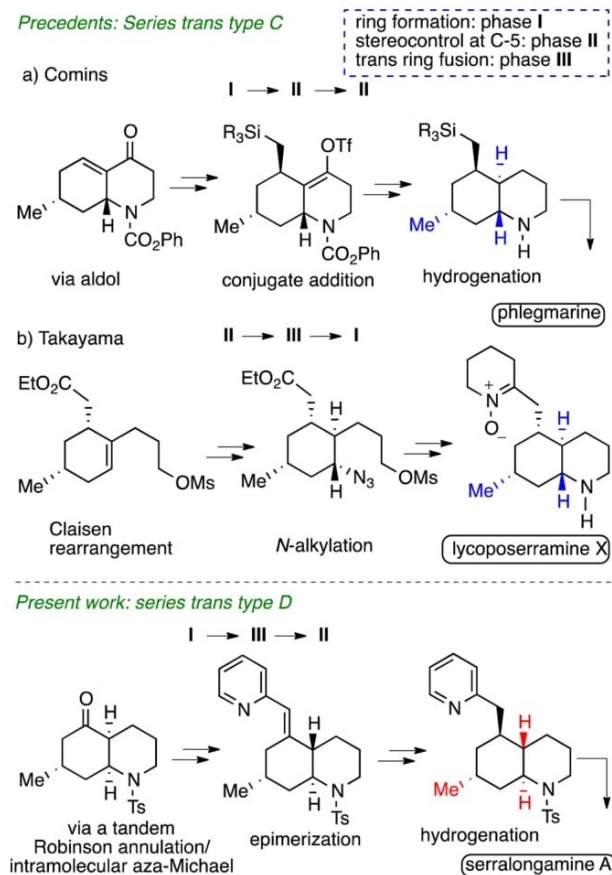


Figure 2. Differential NMR trends between putative and natural huperzine N.

N has a *trans*-decahydroquinoline ring core instead of the *cis*-ring fusion originally reported. (ii) The chemical shift of the methyl group at C(7), which resonates at δ 19.0 in huperzine N, but at δ 22.2 in **I**, indicates an axial disposition, which is only possible in a *trans*-decahydroquinoline with a stereoparent of type D (see Figures 1 and 2). Consequently, the NMR data reported for

Received: January 5, 2016

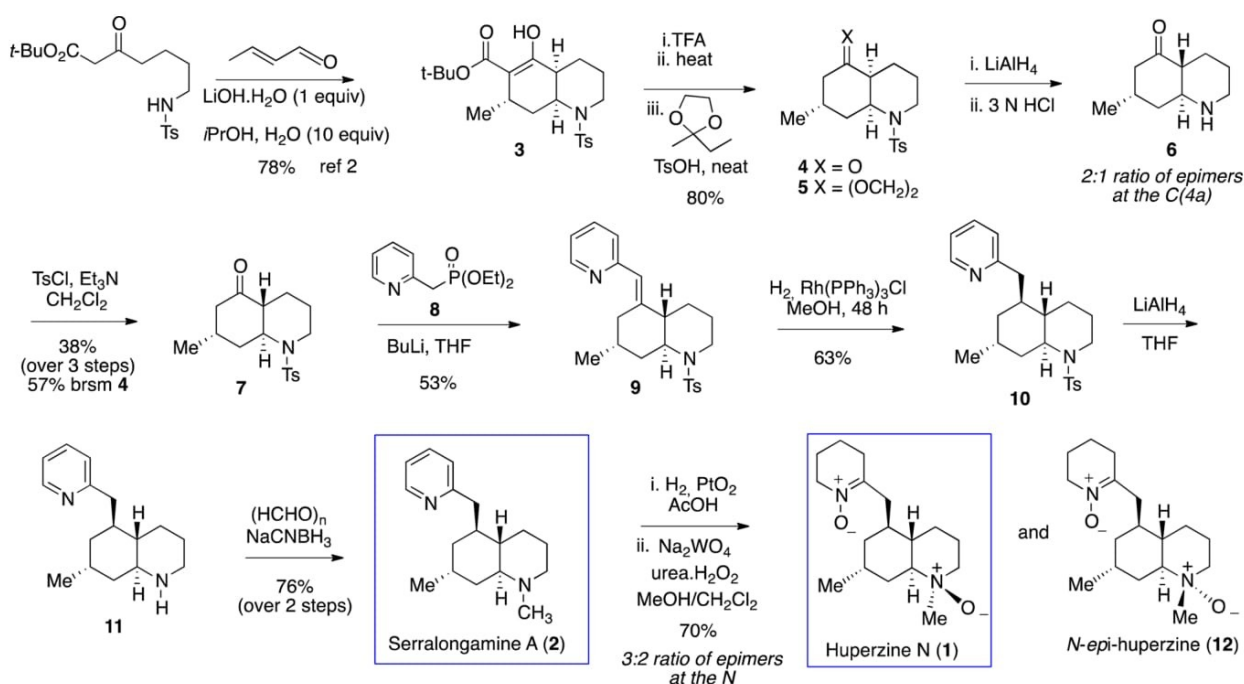
Published: March 1, 2016

Scheme 1. Synthesis of Phlegmarines with a *trans*-Decahydroquinoline Core

huperzine N can be explained by structure **1**. Building on this point of view, we synthesized **1** to confirm the new structural assignment.

Previous *trans*-phlegmarine syntheses have targeted alkaloids with the type C stereoparent. The synthesis of phlegmarine itself was completed by Comins,⁸ who also reported the synthesis of three related alkaloids bearing different substituents at the two nitrogen atoms, while Takayama⁹ achieved lycoserramine X. The key challenges in the synthesis of these alkaloids are the generation of the *trans*-decahydroquinoline core and the stereocontrol in the genesis of the stereocenter at C-5 where the pyridylmethyl backbone is attached (Scheme 1). The two different approaches to construct the *trans*-decahydroquinoline ring with the required stereochemistry in the four stereogenic centers are summarized in Scheme 1. Comins, applying his methodology based on pyridinium salts, prepared a polysubstituted piperidine that furnished the bicyclic ring by an aldol reaction. Stereoselective conjugated addition, followed by a hydrogenation process, allowed a stereochemical control at C-5 and in the ring fusion, respectively. In contrast, the Takayama approach involved the elaboration of a polyfunctionalized cyclohexane compound in which the four stereogenic centers were established before the cyclization, leading to the decahydroquinoline ring.

Our approach differs from the aforementioned in both its synthetic strategy and the targeted compounds, which have a decahydroquinoline core with a type D stereoparent.¹⁰ The synthetic plan involved the same building block used in our previous synthesis of *cis*-phlegmarines and the epimerization of the stereogenic center at C-4a to achieve a ketone with a *trans*-decahydroquinoline ring, which would allow access to phlegmarine alkaloids with a new stereochemical pattern. Control of the stereochemistry at C5 through a substrate-directable hydrogenation process would be crucial in this synthetic proposal (Scheme 2).

Scheme 2. Synthesis of (±)-Serralongamine A (**2**) and (±)-Huperzine N (**1**)

Commencing the synthesis from the easily available ketone **4**,¹¹ our original protocol² allowed the ring fusion to be changed from *cis* to *trans*, via the conversion of acetal **5** to the corresponding secondary amine and acid-induced epimerization at C(4a). Tosylation of the resulting 2:1 mixture of ketones **6** and its C4a-epimer furnished the required decahydroquinoline **7** with a *trans* ring fusion¹² as a single isomer after chromatographic separation. This ketone reacted with a solution of the lithium anion of phosphonate **8**¹³ to give vinylpyridine derivative **9** in 53% yield, diastereoselectively providing the *E* isomer.¹⁴ Hydrogenation of vinylpyridine **9** using Wilkinson's catalyst allowed the hydrogen to be delivered exclusively from the bottom face. Thus, a pyridine-directed hydrogenation provided access to the valuable intermediate **10** with a contrasteric selectivity (Figure 3).

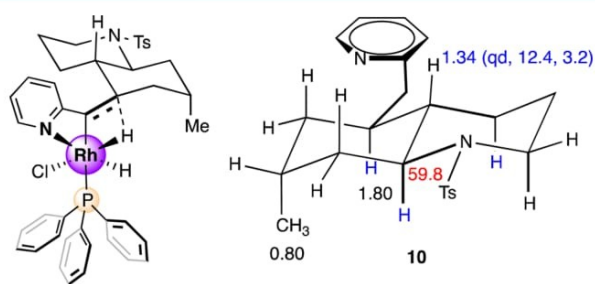


Figure 3. Transition state leading to **10** and its representative NMR data.

The stereoselectively formed decahydroquinoline **10** showed the same relative configuration in its four stereogenic centers as the target **1** and serralongamine A (**2**). The configuration at C-5 was ascertained considering the multiplicity of the signal corresponding to H-4a, which implies a *trans* relationship between H-4a and H-5, both in an axial disposition. Moreover, the chemical shift for C-8a (δ 59.8) did not differ from that observed in the precursors **7** (δ 60.3) and **9** (δ 60.6), indicating that the pyridylmethyl side chain is not axially located (Figure 3).¹⁵

Removal of the tosyl group in **10** using LiAlH_4 , followed by reductive *N*-methylation of **11**, gave serralongamine A (**2**) in 76% yield for the two steps, which constitutes the first synthetic entry to a phlegmarine alkaloid embodying its decahydroquinoline stereoparent. The *trans*-decahydroquinoline serralongamine A differs from phlegmarine itself in the stereochemical relationship between the configuration at C7 and the *trans* ring fusion carbons, C4a and C8a (Figure 1).

It is noteworthy that the NMR data of our synthetic **2** were clearly different from those reported for the isolated serralongamine A in CD_3OD . Since basic nitrogen atoms readily protonate, we were able to reproducibly obtain ^1H and ^{13}C NMR spectra of the free base forms of serralongamine A in CD_3OD containing NaOCD_3 .¹⁶ We surmised that the natural isolate corresponded to its ditrifluoroacetate salt. Thus, the NMR spectra of synthetic serralongamine A was examined by titrating a sample of the free base with TFA. For a comparison of NMR data for natural and synthetic serralongamine A (**2**) as the double TFA salt, see the Supporting Information. As reproduced in Figure S1, NMR spectra identical to those reported for the natural product were obtained.

Having achieved **2**, we were two steps from completing the new structure proposed for huperzine N (**1**). Toward this end,

reduction of the pyridine ring in **B** gave the corresponding piperidine, which, after oxidation with $\text{Na}_2\text{WO}_4/\text{urea}\cdot\text{H}_2\text{O}_2$ (UHP),³ led to **1** by formation of both the amine *N*-oxide and nitron functionalities, which were further confirmed by ^{15}N chemical shift NMR data. The spectroscopic data of the synthetic sample were identical in all respects to those reported for the natural product,⁵ although a side product purified together with huperzine N was also formed. Two-dimensional NMR spectroscopy of the mixture identified the minor product as the *N*-oxide epimer of huperzine N. Although the oxidation of cyclic tertiary amines normally takes place axially,¹⁷ the presence of an equatorial substituent increases the equatorial oxidation,¹⁸ as occurred in our substrate (C8–C8a bond). Thus, the reaction did not work diastereoselectively and epimeric *N*-oxide **12** was also formed. The stereostructure and the complete ^1H , ^{13}C , and ^{15}N chemical shifts assignment of both epimers **1** and **12** (Figure 4) and also their protonated forms¹⁹ (see the Supporting

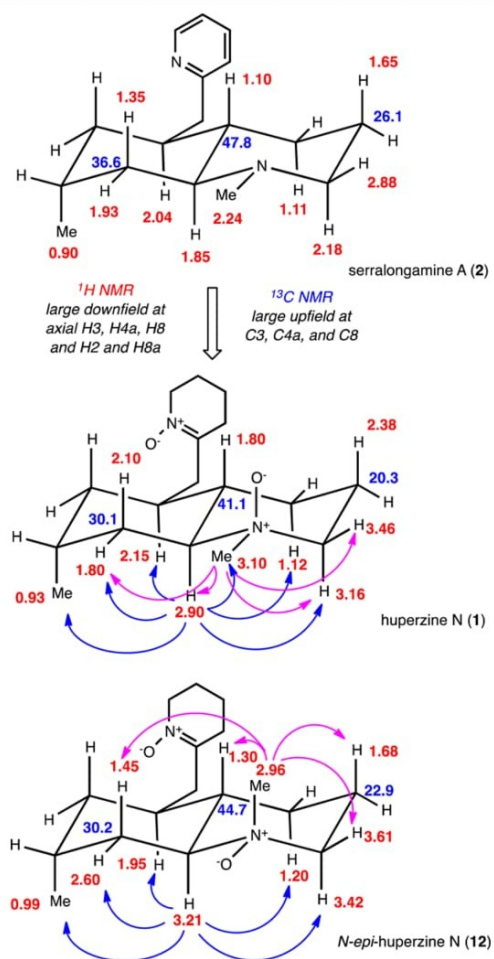


Figure 4. Characteristic NMR data and selected NOEs of huperzine N (**1**), *N*-epi-huperzine N (**12**), and serralongamine A (**2**).

Information for details) were performed from the analysis of COSY, ROESY,²⁰ HSQC, HMBC, and TOCSY correlation spectra of the mixture.

The configuration of the new stereogenic center at the nitrogen atom in huperzine N was corroborated as *R*, on the basis of ^1H and ^{13}C chemical shift NMR analysis of **1** and its *N*-epimer **12**. Thus, a clear upfield shift for C(3), C(4a), and C(8) was

observed, due to the 1,3-cis relationship between the N→O bond and the axial C–H bond of these carbon atoms (Figure 4), compared with either the free amine base nucleus (e.g., in **2**) or the *N*-epimeric *N*-oxide with the oxygen atom in an equatorial disposition (i.e., **12**).²¹ The NMR data of synthetic huperzine N matched those described for the natural product, thus establishing its configuration as 1*R*,4*aS*,5*S*,7*R*,8*aS*. Although we have reported the racemic form, the phlegmarine alkaloids have always shown an *R* absolute configuration in the carbon bonded to the methyl group in the decahydroquinoline ring. Thus, the relative configuration allowed the absolute configuration to be proposed.

In summary, in this work on the phlegmarine subset of *Lycopodium* alkaloids, the first total synthesis of serralongamine A and the revised structure of huperzine N have been accomplished. The absolute configuration of the huperzine N was established, and the NMR data of the serralongamine A in its free base form are reported for the first time.

EXPERIMENTAL SECTION

General. All reactions were carried out under an argon atmosphere with dry, freshly distilled solvents under anhydrous conditions. All product mixtures were analyzed by thin-layer chromatography using TLC silica gel plates with a fluorescent indicator ($\lambda = 254$ nm). Analytical thin-layer chromatography was performed on SiO₂ (Merck silica gel 60 F₂₅₄), and the spots were located by UV light and/or a 1% KMnO₄ aqueous solution or hexachloroplatinate reagent. Chromatography refers to flash chromatography and was carried out on SiO₂ (silica gel 60 ACC, 230–240 mesh). Drying of organic extracts during the reaction workup was performed over anhydrous Na₂SO₄. Chemical shifts of ¹H and ¹³C NMR spectra are reported in ppm downfield (δ) from Me₄Si. All NMR data assignments are supported by gCOSY and gHSQC experiments.

(4*aRS*,7*RS*,8*aRS*)-7-Methyl-1-(4-methylphenylsulfonyl)-5-oxodecahydroquinoline Ethylene Acetal (5**).** From crystallized keto ester **3** (536 mg, 1.27 mmol), following the procedure previously described,¹¹ ketone **4** was obtained and used in the next step without purification. After acetalization² of **4** and the purification step by chromatography (5% to 25% EtOAc in hexanes), **5** (373 g, 80%) was obtained as a white solid: *R*_f = 0.71 (1:1 EtOAc/hexanes); mp 100 °C. For NMR data, see ref 2.

(4*aRS*,7*SR*,8*aSR*)-7-Methyl-5-oxodecahydroquinoline (6**).** Operating as previously described,² starting from **5** (373 mg, 1.02 mmol), **6**, a 2:1 mixture of epimers at C(4*a*), was obtained (110 mg) as a colorless oil, which was used directly in the next step. For NMR data, see ref 2.

(4*aRS*,7*SR*,8*aSR*)-7-Methyl-5-oxo-1-(4-methylphenylsulfonyl)decahydroquinoline (7**).** To a cooled (0 °C) stirred solution of the above mixture of **6** and its epimer (110 mg) in CH₂Cl₂ (8 mL) was added a solution of TsCl (214 mg, 1.12 mmol, 1.1 equiv) in CH₂Cl₂ (4 mL), followed by Et₃N (0.17 mL, 1.23 mmol, 1.2 equiv). The mixture was stirred at rt for 6 h and diluted with CH₂Cl₂ (20 mL). The organics were washed with brine (2 × 5 mL), dried, concentrated, and purified by chromatography (5–25% EtOAc in hexanes) to yield successively **4** (59 mg) and **7** (121 mg, 38% in three steps, 57% brsm) as a white solid: *R*_f = 0.35 (25% EtOAc/hexanes); mp 108 °C; ¹H NMR (CDCl₃, 400 MHz) δ 0.81 (d, *J* = 7.2 Hz, 3H, CH₃), 1.32 (m, 1H, H-4ax), 1.64 (m, 1H, H-3ax), 1.76 (m, 1H, H-3eq), 2.00 (dd, *J* = 12.8, 3.6 Hz, 1H, H-4eq), 2.15 (dt, *J* = 13.6, 2.4 Hz, 1H, H-6ax), 2.23 (dm, *J* = 12.4 Hz, 1H, H-8eq), 2.33 (td, *J* = 13.6, 4.6 Hz, 1H, H-8ax), 2.40 (masked, H-7), 2.42 (s, 3H, CH₃Ar), 2.46 (qd, 1H, *J* = 11.4, 3.2 Hz, H-4a), 2.56 (dd, *J* = 11.6, 4.0 Hz, 1H, H-6eq), 2.66 (td, *J* = 11.2, 3.2, 1.6 Hz, 1H, H-2ax), 2.89 (td, *J* = 11.4, 4.0 Hz, 1H, H-8a), 4.13 (dtd, *J* = 12.8, 4.0, 1.2 Hz, 1H, H-2eq), 7.30 (d, *J* = 8.4 Hz, 2H, *o*-Ts), 7.68 (d, *J* = 8.4 Hz, 2H, *m*-Ts); ¹³C NMR (100 MHz, CDCl₃) δ 18.9 (CH₃), 21.6 (ArCH₃), 23.5 (C-4), 24.4 (C-3), 28.5 (C-7), 36.1 (C-8), 47.3 (C-6), 49.3 (C-2), 53.1 (C-4a), 60.3 (C-8a), 127.3 (*m*-Ts), 129.8 (*o*-Ts), 137.1 (*ipso*-Ts), 143.6 (*p*-Ts), 209.1 (C-5). HRMS (ESI-TOF) *m/z*: [M + H]⁺ calcd for C₁₇H₂₄NO₃S 322.1471, found 322.1464.

(E)-(4*aRS*,7*SR*,8*aRS*)-7-Methyl-1-(4-methylphenylsulfonyl)-5-(pyridin-2-ylmethylene)decahydroquinoline (9**).** Both the pyridine phosphonate **8** and decahydroquinoline **7** were previously dried by azeotropic with benzene. To a stirred solution of phosphonate **8** (227 mg, 1 mmol, 5 equiv) in THF (3 mL) at –78 °C was added *n*-BuLi (1.6 M in hexanes, 0.52 mL, 0.84 mmol, 4.5 equiv). The resulting dark red solution was stirred for 30 min at rt before a solution of the decahydroquinoline **7** (60 mg, 0.187 mmol) in THF (1.2 mL) was added dropwise via syringe at –78 °C. The reaction mixture was stirred for 30 min at –78 °C, 1 h at –30 °C, and 6 h at 0 °C, and quenched with sat. aq. NH₄Cl (1 mL) and water (1 mL). The mixture was extracted with EtOAc (2 × 3 mL), and the combined organic extracts were dried, concentrated, and purified by chromatography (5–40% EtOAc in hexanes) to give **9** (39 mg, 53%) as a white solid: *R*_f = 0.49 (50% hexane/EtOAc); mp 128 °C; ¹H NMR (400 MHz, CDCl₃) δ 0.77 (d, *J* = 7.2 Hz, 3H, CH₃), 1.31 (qd, 1H, *J* = 12.4, 2.0 Hz, H-4ax), 1.68 (m, 1H, H-3), 1.82 (m, 1H, H-3), 1.95 (dm, *J* = 13.2 Hz, 1H, H-4eq), 2.03 (dd, *J* = 12.6, 4.4 Hz, 1H, H-8eq), 2.12 (m, 1H, H-6ax), 2.15 (m, 1H, H-7), 2.19 (m, 1H, H-8ax), 2.24 (brt, *J* = 12.0 Hz, 1H, H-4a), 2.42 (s, 3H, ArCH₃), 2.91 (ddd, *J* = 13.2, 8.8, 4.4 Hz, 1H, H-8a), 2.94 (td, 1H, *J* = 12.8, 5.2 Hz, H-2ax), 3.07 (dt, *J* = 13.2, 2.0 Hz, 1H, H-6eq), 3.97 (dt, *J* = 12.8, 5.2 Hz, 1H, H-2eq), 6.31 (s, 1H, C=CH), 7.07 (dd, *J* = 7.6, 4.8 Hz, 1H, H-5 py), 7.13 (d, *J* = 8.0 Hz, 1H, H-3 py), 7.28 (d, *J* = 8.4 Hz, 2H, *o*-Ts), 7.59 (td, *J* = 7.6, 2.0 Hz, 1H, H-4 py), 7.69 (d, *J* = 8.4 Hz, 2H, *m*-Ts), 8.54 (dm, *J* = 4.8 Hz, 1H, H-6 py); ¹³C NMR (100 MHz, CDCl₃, HSQC) δ 18.2 (CH₃), 21.7 (CH₃Ar), 24.5 (C-3), 25.8 (C-4), 29.3 (C-7), 35.2 (C-6), 38.1 (C-8), 46.3 (C-4a), 46.8 (C-2), 60.6 (C-8a), 121.2 (C-5 py), 124.0 (C-3 Py), 124.1 (=CH), 127.3 (*o*-Ts), 129.7 (*m*-Ts), 136.0 (C-4 Py), 137.3 (*p*-Ts), 143.3 (*ipso*-Ts), 144.7 (C-5), 149.3 (C-6 Py), 157.3 (C-2 Py). HRMS (ESI-TOF) *m/z*: [M + H]⁺ calcd for C₂₃H₂₉N₂O₂S 397.1944, found 397.1953.

(4*aRS*,5*RS*,7*SR*,8*aRS*)-7-Methyl-5-(pyridin-2-ylmethyl)-1-(4-methylphenylsulfonyl)decahydroquinoline (10**).** To a stirred solution of **9** (27 mg, 0.068 mmol) in MeOH (7 mL) was added Wilkinson's catalyst RhCl(PPh₃)₃ (16 mg, 0.017 mmol, 25 mol %) at rt. The resulting mixture was rapidly evacuated and backfilled with H₂ three times and then stirred under an atmosphere of H₂ for 72 h. The mixture was concentrated, and purified by chromatography (5–25% EtOAc in cyclohexane) to give **10** (17 mg, 63%): *R*_f = 0.5 (1:1 EtOAc/cyclohexane); ¹H NMR (400 MHz, CDCl₃) δ 0.80 (d, *J* = 7.2 Hz, 3H, CH₃), 0.91 (qd, *J* = 12.4, 6.2 Hz, 1H, H-4ax), 1.20 (m, 2H, H-6), 1.34 (qd, *J* = 12.4, 3.2, 1H, H-4a), 1.65 (m, 2H, H-3), 1.80 (m, 1H, H-5), 1.86 (td, *J* = 12.4, 4.8 Hz, 1H, H-8ax), 1.94 (dm, *J* = 12.4 Hz, 1H, H-8eq), 2.00 (m, 1H, H-7), 2.12 (dm, *J* = 12.0 Hz, 1H, H-4eq), 2.30 (dd, *J* = 13.4, 8.8 Hz, 1H, CH₂Py), 2.42 (s, 3H, ArCH₃), 2.94–3.00 (m, 2H, H-2ax, H-8a), 3.11 (dd, *J* = 13.4, 4.0 Hz, 1H, CH₂Py), 3.97 (dt, *J* = 13.2, 5.6 Hz, 1H, H-2eq), 7.04 (d, *J* = 8.0 Hz, 1H, H-3 Py), 7.08 (m, 1H, H-5 Py), 7.28 (d, *J* = 8.4 Hz, 2H, *o*-Ts), 7.55 (td, *J* = 7.6, 1.6 Hz, 1H, H-4 Py), 7.68 (d, *J* = 8.0 Hz, 2H, *m*-Ts), 8.50 (dm, *J* = 4.0 Hz, 1H, H-6 Py); ¹³C NMR (100 MHz, CDCl₃, HSQC) δ 18.3 (CH₃), 21.6 (ArCH₃), 25.1 (C-3), 27.4 (C-4), 27.5 (C-7), 36.8 (C-6), 37.1 (C-8), 37.3 (C-5), 42.3 (CH₂Py), 45.6 (C-4a), 47.3 (C-2), 59.8 (C-8a), 121.1 (C-5 Py), 124.0 (C-3 Py), 127.2 (*o*-Ts), 129.7 (*m*-Ts), 136.2 (C-4 Py), 138.4 (*p*-Ts), 143.0 (*ipso*-Ts), 149.4 (C-6 Py), 161.1 (C-2 Py). HRMS (ESI-TOF) *m/z*: [M + H]⁺ calcd for C₂₃H₃₁N₂O₂S 399.2101, found 399.2116.

(4*aRS*,5*RS*,7*SR*,8*aRS*)-7-Methyl-5-(pyridin-2-ylmethyl)-decahydroquinoline (11**).** A solution of sulfonamide **10** (17 mg, 0.043 mmol) in anhydrous THF (1 mL) was added to a stirred suspension of LiAlH₄ (16 mg, 0.43 mmol) in THF (1 mL) at 0 °C. The reaction was stirred overnight at rt and quenched by addition of one drop of water, another of aqueous 15% NaOH, and three drops of water. The mixture was diluted with CH₂Cl₂, filtered through a pad of Celite, and washed thoroughly with CH₂Cl₂. Evaporation of the solvent gave **11**, which was pure enough to be used in the following step. An analytical sample of secondary amine **11** was obtained by chromatography on alumina (1–5% MeOH in CH₂Cl₂): *R*_f = 0.22 (5:95 MeOH:CH₂Cl₂); ¹H NMR (400 MHz, CDCl₃) δ 0.91 (d, *J* = 7.2 Hz, 3H, CH₃), 0.92 (qd, *J* = 12.0, 3.2 Hz, 1H, H-4a), 1.09 (qd, *J* = 12.0, 4.0 Hz, 1H, H-4ax), 1.20–1.25 (m, 2H, H-6), 1.44 (td, *J* = 12.0, 4.2 Hz, 1H, H-8ax), 1.52 (dt, *J* = 12.4, 2.0 Hz, 1H, H-8eq), 1.53 (m, 1H, H-3eq), 1.71 (tt, *J* = 13.2, 3.2 Hz,

1H, H-3ax), 1.82 (m, 1H, H-5), 2.01 (m, 1H, H-7eq), 2.14 (dd, $J = 13.0$, 3.0 Hz, 1H, H-4eq), 2.30 (dd, $J = 13.2$, 10.0 Hz, 1H, CH₂Py), 2.47 (ddd, 1H, $J = 11.2$, 10.0, 4.0 Hz, H-8a), 2.66 (td, 1H, $J = 12.2$, 3.0 Hz, H-2ax), 3.07 (dm, $J = 12.0$ Hz, 1H, H-2eq), 3.14 (dd, $J = 13.2$, 4.0 Hz, 1H, CH₂Py), 7.06–7.09 (m, 2H, H-3 Py, H-5 Py), 7.55 (td, $J = 8.0$, 1.6 Hz, 1H, H-4 Py), 8.52 (dd, $J = 5.2$, 2.0 Hz, 1H, H-6 Py); ¹³C NMR (100 MHz, CDCl₃) δ 19.2 (CH₃), 27.2 (C-3), 27.5 (C-7), 28.8 (C-4), 36.4 (C-5), 37.6 (C-6), 39.4 (C-8), 41.9 (CH₂Py), 47.0 (C-2), 48.4 (C-4a), 56.2 (H-8a), 120.9 (C-5 Py), 123.9 (C-3 Py), 136.1 (C-4 Py), 149.4 (C-6 Py), 161.8 (C-2 Py). HRMS (ESI-TOF) m/z : [M + H]⁺ calcd for C₁₆H₂₄N₂, 245.2012, found 245.2009.

(4aRS,5RS,7SR,8aRS)-1,7-Dimethyl-5-(pyridin-2-ylmethyl)-decahydroquinoline (rac-Serralongamine A, 2). To a solution of the above crude amine **11** (10 mg, 0.043 mmol) in MeOH (2.3 mL) was added 37% aqueous formaldehyde (24 mL, 0.328 mmol) and NaBH₃CN (18 mg, 0.287 mmol) at 0 °C, and the mixture was stirred at rt for 30 min. The volatiles were evaporated, and the crude was purified on neutral alumina (CH₂Cl₂ to 5% MeOH in CH₂Cl₂) to give **2** (8.4 mg, 76% over two steps from **10**): $R_f = 0.70$ (5% CH₃OH in CH₂Cl₂). This sample was dissolved in CD₃OD, and NaOCD₃ (0.1 M in CD₃OD) was added. ¹H and ¹³C NMR spectra of the free base were obtained: ¹H NMR (400 MHz, CD₃OD, NaOCD₃) δ 0.90 (d, $J = 7.6$ Hz, 3H, CH₃), 1.10–1.15 (masked, 1H, H-4a), 1.11 (br q, $J = 12.0$ Hz, 1H, H-4ax), 1.15 (br d, $J = 12$ Hz, 1H, H-6eq), 1.25 (td, $J = 12.4$, 4.4 Hz, 1H, H-6ax), 1.35 (td, $J = 12.4$, 4.8 Hz, 1H, H-8ax), 1.65–1.75 (m, 2H, 2H-3), 1.80–1.92 (m, 2H, H-5 and H-8a), 1.93 (dm, $J = 12.0$ Hz, 1H, H-8eq), 2.03 (m, 1H, H-7), 2.16 (dm, $J = 11.8$ Hz, 1H, H-4eq), 2.18 (td, $J = 12.8$, 3.2 Hz, 1H, H-2ax), 2.24 (s, 3H, CH₃), 2.30 (dd, $J = 13.2$, 10.4 Hz, 1H, CH₂py), 2.88 (dm, $J = 12.0$ Hz, 1H, H-2eq), 3.19 (dd, $J = 13.2$, 4.0 Hz, 1H, CH₂py), 7.24 (dd, $J = 7.6$, 4.8 Hz, 1H, H-5 py), 7.25 (t, $J = 7.4$ Hz, 1H, H-3 py), 7.73 (t, $J = 7.6$, 1.6 Hz, 1H, H-4 py), 8.42 (dm, $J = 4.8$, 1H, H-6 py). ¹³C NMR (100 MHz, CD₃OD, NaOCD₃) δ 19.5 (CH₃), 26.1 (C-3), 28.5 (C-7), 29.6 (C-4), 36.6 (C-8), 37.8 (C-5), 38.0 (C-6), 42.6 (CH₂py), 43.1 (NCH₃), 47.8 (C-4a), 58.5 (C-2), 64.8 (C-8a), 122.7 (C-3 py), 125.7 (C-5 py), 138.4 (C-4 py), 149.5 (C-6 py), 162.6 (C-2 py). HRMS (ESI-TOF) m/z : [M + H]⁺ calcd for C₁₇H₂₇N₂, 259.2168, found 259.2169.

Spectra matching the reported spectra of (–)-serralongamine A⁶ were obtained after the addition of TFA in CD₃OD to the above sample of **2**: ¹H (400 MHz, CD₃OD, TFA) δ 0.95 (d, $J = 7.6$ Hz, 3H, CH₃), 1.15 (br d, $J = 13.2$ Hz, 1H, H-6eq), 1.41 (td, $J = 12.8$, 4.8 Hz, 1H, H-6ax), 1.44 (td, $J = 12.4$, 4.4 Hz, 1H, H-4ax), 1.53 (qd, $J = 12.0$, 2.8 Hz, 1H, H-4a), 1.64 (td, $J = 12.4$, 4.8 Hz, 1H, H-8ax), 1.88 (qt, $J = 12.4$, 4.0 Hz, 1H, H-3ax), 2.00–2.09 (m, 2H, H-3eq, H-5ax), 2.15 (br d, $J = 12.4$ Hz, 1H, H-8eq), 2.22 (br d, $J = 12.0$ Hz, 1H, H-7eq), 2.24 (m, 1H, H-4eq), 2.72 (dd, $J = 14.4$, 10.4 Hz, 1H, CH₂py), 2.86 (s, 3H, NCH₃), 3.12 (td, $J = 13.0$, 3.2 Hz, 1H, H-2ax), 3.15 (td, $J = 12.2$, 4.0 Hz, 1H, H-8a), 3.52 (br, $J = 13.0$ Hz, 1H, H-2eq), 3.56 (dd, $J = 14.4$, 4.0 Hz, 1H, CH₂py), 7.85 (ddd, $J = 7.2$, 5.6, 0.8 Hz, 1H, H-5py), 7.88 (d, $J = 8.0$ Hz, 1H, H-3py), 8.54 (td, $J = 8.0$, 1.6 Hz, 1H, H-4py), 8.77 (d, $J = 5.6$ Hz, 1H, H-6py); ¹³C NMR (100 MHz, CD₃OD, TFA) δ 18.3 (CH₃), 24.0 (C-3), 27.1 (C-4), 28.1 (C-7), 33.8 (C-8), 36.8 (C-6), 37.5 (C-5), 37.9 (CH₂py), 41.4 (NCH₃), 46.3 (C-4a), 57.4 (C-2), 66.0 (C-8a), 126.3 (C-5py), 129.4 (C-3py), 142.8 (C-6py), 147.8 (C-4py), 157.7 (C-2py).

(1RS,4aSR,5SR,7RS,8aSR)-1,7-Dimethyl-5-(2,3,4,5-tetrahydropyridine 1-oxide)decahydroquinoline N-Oxide (Huperzine N, 1). To a stirred solution of **2** (8 mg, 0.031 mmol) in AcOH (0.25 mL) was added PtO₂ (20% w/w, 2 mg) at rt. The resulting mixture was evacuated and backfilled with hydrogen 3 times and then stirred under an atmosphere of H₂ for 16 h. The mixture was diluted with CH₂Cl₂ (2 mL) before it was filtered through a pad of Celite and washed through with CH₂Cl₂. The filtered solution was washed with 1 N NaOH, dried, and concentrated. To a solution of the above crude diamine in MeOH/CH₂Cl₂ (1:1; 0.2 mL) were added in one portion UHP (30 mg, 0.31 mmol) and Na₂WO₄·2H₂O (2 mg, 0.006 mmol), and the mixture was stirred at rt for 72 h. After concentration, CH₂Cl₂ was added and the reaction mixture was filtered, concentrated, and purified by chromatography (2.5–10% MeOH in CH₂Cl₂ and then 85/15/1.5 CHCl₃/MeOH/NH₃) to give **1** and its epimer **12** (6 mg, 66%, 3:2 ratio) as a

colorless oil, which solidified on standing: $R_f = 0.20$ (80/20/2 CHCl₃/MeOH/NH₃).

Data for Huperzine N (1). ¹H NMR (400 MHz, CDCl₃) δ 0.93 (d, $J = 7.2$ Hz, 3H, CH₃), 1.12 (qd, $J = 12.0$, 3.0 Hz, 1H, H-4ax), 1.28 (masked, 1H, H-6eq), 1.40 (td, $J = 12.0$, 4.0 Hz, 1H, H-6ax), 1.58 (br d, $J = 13.0$ Hz, 1H, H-3eq), 1.68 (m, 2H, H-4'), 1.80 (m, 2H, H-4a, H-8ax), 1.88 (m, 2H, H-5'), 1.88 (masked, 1H, CH₂py), 2.05 (m, 1H, H-4eq), 2.10 (1H, m, H-8eq), 2.21 (m, 1H, H-5), 2.38 (masked, 1H, H-3ax), 2.40 (t, $J = 6.0$ Hz, 2H, H-3'), 2.98 (dd, $J = 12.0$, 3.0 Hz, 1H, CH₂py), 2.90 (td, $J = 11.5$, 3.2 Hz, 1H, H-8a), 3.10 (s, 3H, NCH₃), 3.14 (ddd, $J = 12.0$, 11.0, 3.0 Hz, 1H, H-2ax), 3.46 (br d, $J = 12.0$ Hz, 1H, H-2eq), 3.75 (t, $J = 6.4$ Hz, 2H, H-6'); ¹³C NMR (100 MHz, HSQC) δ 18.9 (C-4'), 19.0 (CH₃), 20.3 (C-3), 23.3 (C-5'), 27.0 (C-4), 27.1 (C-7), 29.9 (C-3'), 30.1 (C-8), 32.4 (C-5), 36.7 (CH₂py), 36.8 (C-6), 41.1 (C-4a), 57.6 (NCH₃), 58.5 (C-6'), 69.1 (C-2), 73.8 (C-8a), 148.0 (C-2'); ¹⁵N (50 MHz, deduced from ¹H–¹⁵N HMBC correlations) δ 114.7 (N-oxide), 271.7 (nitron). HRMS (ESI-TOF) m/z : [M + H]⁺ calcd for C₁₇H₃₁N₂O₂, 295.2380; found 295.2374.

Data for N-epi-Huperzine N (12). ¹H NMR (400 MHz, CDCl₃) δ 0.99 (d, $J = 7.2$ Hz, 3H, CH₃), 1.20 (masked, 1H, H-4ax), 1.30 (m, 1H, H-4a), 1.35 (m, 1H, H-6), 1.40 (m, 1H, H-6), 1.45 (td, $J = 12.0$, 3.0 Hz, 1H, H-8ax), 1.68 (m, 1H, H-3eq), 1.68 (m, 2H, H-4'), 1.87 (m, 2H, H-5'), 1.87 (masked, 1H, H-3ax), 1.95 (m, 1H, H-5), 2.05 (m, 1H, H-4eq), 2.35 (masked, 1H, CH₂py), 2.40 (t, $J = 6.0$ Hz, 2H, H-2'), 2.60 (1H, m, H-8eq), 2.70 (m, 1H, CH₂py), 2.96 (s, 3H, NCH₃), 3.21 (br t, $J = 12.0$ Hz, 1H, H-8a), 3.42 (td, $J = 12.0$, 3.0 Hz, 1H, H-2ax), 3.61 (br d, $J = 12.0$ Hz, 1H, H-2eq), 3.72 (t, $J = 6.4$ Hz, 2H, H-6'); ¹³C NMR (100 MHz, HSQC) δ 18.2 (CH₃), 19.2 (C-4'), 22.9 (C-3), 23.3 (C-5'), 27.1 (C-4), 27.2 (C-7), 29.9 (C-3'), 30.2 (C-8), 34.6 (C-5), 35.5 (CH₂py), 37.5 (C-6), 44.7 (C-4a), 48.0 (NCH₃), 58.6 (C-6'), 71.1 (C-2), 75.9 (C-8a), 147.2 (C-2'); ¹⁵N (50 MHz, deduced from ¹H–¹⁵N HMBC correlations) δ 113.8 (N-oxide), 271.0 (nitron). HRMS (ESI-TOF) m/z : [M + H]⁺ calcd for C₁₇H₃₁N₂O₂, 295.2380; found 295.2374.

■ ASSOCIATED CONTENT

Supporting Information

The Supporting Information is available free of charge on the ACS Publications website at DOI: 10.1021/acs.joc.6b00025.

Tables for ¹H and ¹³C NMR data of synthetic serralongamine A (**2**, free base and diprotonated sample) and huperzine N (**1**) as well as NMR data of isolated alkaloids; copies of ¹H and ¹³C NMR spectra of new compounds; COSY, TOCSY, ROESY, HSQC, HMBC, and ¹H–¹⁵N HMBC spectra of huperzine N (**1**) and its epimer **12** (PDF)

■ AUTHOR INFORMATION

Corresponding Authors

*E-mail: josep.bonjoch@ub.edu (J.B.).

*E-mail: benbradshaw@ub.edu (B.B.).

Notes

The authors declare no competing financial interest.

■ ACKNOWLEDGMENTS

Financial support for this research was provided by the Projects CTQ2013-41338-P and CTQ2012-32436 from the Ministry of Economy and Competitiveness of Spain and the FP7Marie Curie Actions of the European Commission via the ITN ECHONET Network (MCITN-2012-316379).

■ REFERENCES

- (1) (a) Ma, X.; Gang, D. R. *Nat. Prod. Rep.* **2004**, *21*, 752–772. (b) Siengalewicz, P.; Mulzer, J.; Rinner, U. *Alkaloids* **2013**, *72*, 1–152.
- (2) Bradshaw, B.; Luque-Corredera, C.; Saborit, G.; Cativiela, C.; Dorel, R.; Bo, C.; Bonjoch, J. *Chem.—Eur. J.* **2013**, *19*, 13881–13892.

(3) Systematic numbering is used throughout this paper. In the Supporting Information, the biogenetic numbering is included in all tables to facilitate the comparison of the NMR data reported for phlegmarine alkaloids with those recorded from a synthetic source (compounds **1** and **2**).

(4) Bosch, C.; Fiser, B.; Gómez-Bengo, E.; Bradshaw, B.; Bonjoch, J. *Org. Lett.* **2015**, *17*, 5084–5087.

(5) For isolation of huperzine N, see: Gao, W. Y.; Li, Y. M.; Jiang, S. H.; Zhu, D. Y. *Helv. Chim. Acta* **2008**, *91*, 1031.

(6) Initially, after the synthesis of putative huperzine N, we indicated that the configuration of the natural product should be trans (ref 4), but we depicted a structure of type C instead of type D as proposed here.

(7) For isolation of serralongamine A: Jiang, W.-P.; Ishiuchi, K.; Wu, J.-B.; Kitanaka, S. *Heterocycles* **2014**, *89*, 747–752.

(8) Wolfe, B. H.; Libby, A. H.; Al-awar, R. S.; Foti, C. J.; Comins, D. L. *J. Org. Chem.* **2010**, *75*, 8564–8570.

(9) Tanaka, T.; Kogure, N.; Kitajima, M.; Takayama, H. *J. Org. Chem.* **2009**, *74*, 8675–8680.

(10) For a synthetic approach to 5-oxo-trans-decahydroquinoline used in the synthesis of the lycopodium alkaloid lycoperine, see: Nakamura, Y.; Burke, A. M.; Kotani, S.; Ziller, J. W.; Rychnovsky, S. D. *Org. Lett.* **2010**, *12*, 72–75.

(11) Bradshaw, B.; Luque-Corredera, C.; Bonjoch, J. *Org. Lett.* **2013**, *15*, 326–329.

(12) The coupling constants of H-4a (11.4, 11.4, 11.4, 3.2 Hz) and H-8a (11.4, 11.4, 4.0 Hz) would allow the trans-ring fusion in **7** to be clearly established.

(13) Gan, X.; Binyamin, I.; Rapko, B. M.; Fox, J.; Duesler, E. N.; Paine, R. T. *Inorg. Chem.* **2004**, *43*, 2443–2448.

(14) The downfield shift of the H-6eq (δ 3.07) and the upfield shift at C-6 (δ 35.2) agree with a steric crowding of the pyridyl ring upon H-6eq associated with the *E* configuration of the exocyclic double bond. For comparison of NMR data in a related system, see ref 11.

(15) For the influence of the steric compression effect on NMR chemical shifts, see: (a) Katakawa, K.; Kitajima, M.; Yamaguchi, K.; Takayama, H. *Heterocycles* **2006**, *69*, 223–229. (b) Kolocouris, A. *Tetrahedron Lett.* **2007**, *48*, 2117–2122.

(16) For a similar NMR protocol to measure the free base and its TFA salt spectra in alkaloid synthesis, see: (a) Altman, R. A.; Nilsson, B. L.; Overman, L. E.; Read de Alaniz, J.; Rohde, J. M.; Taupin, V. *J. Org. Chem.* **2010**, *75*, 7519–7534. (b) Lee, A. S.; Liau, B. B.; Shair, M. D. *J. Am. Chem. Soc.* **2014**, *136*, 13442–13452.

(17) Shvo, Y.; Kaufman, E. D. *J. Org. Chem.* **1981**, *46*, 2148–2152.

(18) Kawazoe, Y.; Tsuda, M. *Chem. Pharm. Bull.* **1967**, *15*, 1405–1410.

(19) In **1** and **12**, the protonation of the *N*-oxide function leads to a deshielding of the α -hydrogens (Table S3). It should be noted that the protons in a 1,3-diaxial relationship with the *N*-oxide function are not affected or even slightly shielded upon protonation (e.g., H-10, H-12, and H-14 in huperzine N). For NMR studies in this field, see: Lebrun, B.; Braekman, J. C.; Daloze, D. *Magn. Reson. Chem.* **1999**, *37*, 60–64.

(20) When huperzine N was originally isolated (ref 5), NOE correlations were established between the putative H-12 proton and signals at *N*-Me and H-13. However, according to our ROESY NMR spectrum of **1**, which allowed the revised trans configuration to be established, these cross-peaks were due to H-14eq. This error is attributed to the ^1H chemical shift degeneracy between H-12 and H-14eq in **1**. This observation is fully confirmed by the NOE contacts observed in the related epimer (**12**) (Figure 4) and protonated *N*-oxide (see Figure S2) derivatives, as well as of the characteristic multiplet *J* pattern of H-12 and H-13.

(21) For NMR studies in *N*-oxide piperidine compounds, see: (a) Potmischil, F.; Cimpeanu, V.; Herzog, H.; Buddrus, J.; Duddeck, H. *Magn. Reson. Chem.* **2003**, *41*, 554–556. (b) Budesinsky, M.; Vanek, V.; Dracinsky, M.; Pohl, R.; Postova-Slavetinska, L.; Sychrovsky, V.; Picha, J.; Cisarova, I. *Tetrahedron* **2014**, *70*, 3871–3886.

Synthesis of (\pm)-Serralongamine A and the Revised Structure of Huperzine N

Gisela V. Saborit,[†] Caroline Bosch,[†] Teodor Parella,[‡] Ben Bradshaw^{*†} and Josep Bonjoch^{*†}

[†] Laboratori de Química Orgànica, Facultat de Farmàcia, IBUB,
Universitat de Barcelona, Av. Joan XXIII s/n, 08028-Barcelona, Spain

[‡] Servei de RMN and Departament de Química, Universitat Autònoma de Barcelona,
08913-Bellaterra, Barcelona, Spain

josep.bonjoch@ub.edu; benbradshaw@ub.edu

Contents

	page
Figure S1. ¹ H NMR Spectra of synthetic serralongamine A (2) in CD ₃ OD/NaOCD ₃ before and after addition of trifluoroacetic acid	S2
Comparison of ¹ H- and ¹³ C-NMR data for serralongamine A and 2 (Tables S1 and S2)	S3
Comparison of ¹ H- and ¹³ C-NMR data for huperzine N, 1 , and 12 (Tables S3 and S4)	S5
Copies of ¹ H- and ¹³ C-NMR spectra of compounds 1 , 2 , 5-7 , 9-12	S7
Figure S2. ¹ H- and ¹³ C-NMR data of protonated <i>N</i> -oxides 1 and 12	S27
Figures S3-S9. Copies of COSY, TOCSY, ROESY, HSQC, HMBC, and ¹ H- ¹⁵ N HMBC spectra of Huperzine N (1) and its epimer 12	S28

For a comparison of NMR data for natural serralongamine A (protonated form) and compound **2**, see Tables S1 and S2.

Figure S1: ^1H NMR spectra of synthetic serralongamine A (2**) in $\text{CD}_3\text{OD}/\text{NaOCD}_3$ before and after addition of trifluoroacetic acid**

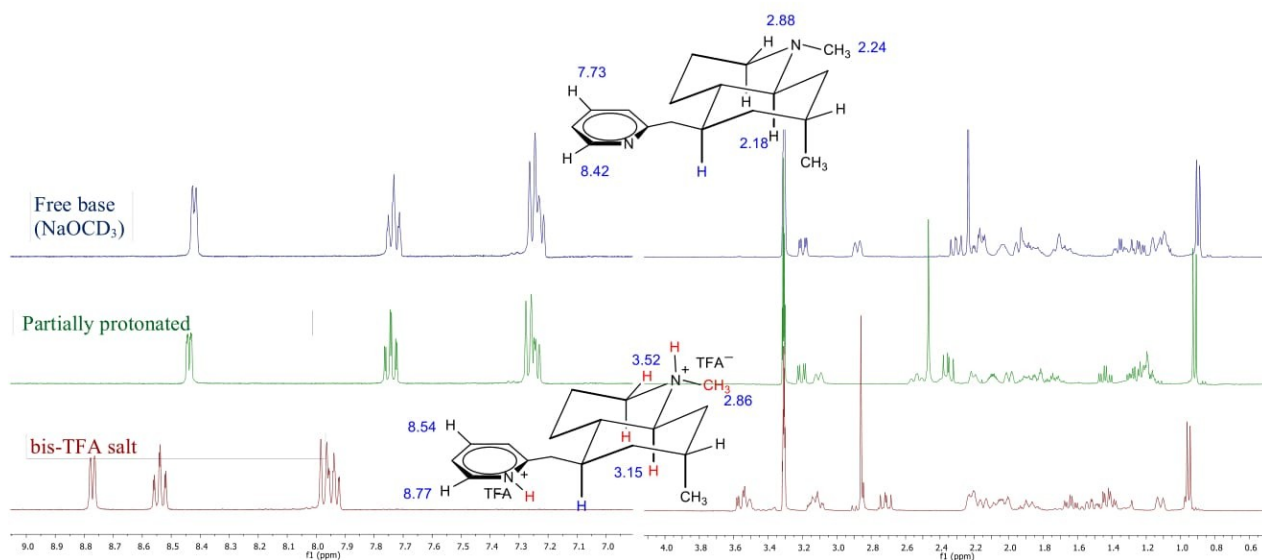
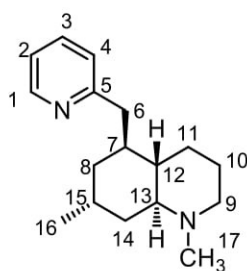
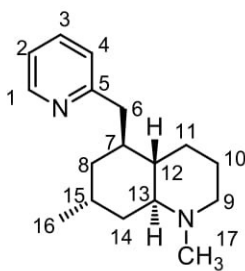


Table S1. ^1H NMR data for serralogamine A in CD_3OD **Serralongamine A (2)**

	Synthetic free base (2) ¹	2 bis-TFA salt ¹	Isolated serralongamine A ²
	δ ^1H	δ ^1H	δ ^1H
1	8.42 (dm, 4.8 Hz)	8.77 (d 5.6 Hz)	8.73 (d 5.7 Hz)
2	7.24 (dd, 7.6, 4.8 Hz)	7.94 (m)	7.85 (dd, 6.9, 5.7 Hz)
3	7.73 (tt, 7.6, 1.6 Hz)	8.54 (td, 8.0, 1.6 Hz)	8.44 (dd, 8.0, 6.9 Hz)
4	7.25 (t, 7.4 Hz)	7.97 (d, 8.0 Hz)	7.88 (d, 8.0 Hz)
6a	2.30 (dd, 13.2, 10.4 Hz)	3.51 (m)	3.51 (dd, 13.6, 4.2 Hz)
6b	3.19 (dd, 13.2, 4.0 Hz)	2.71 (dd 14.0, 10.4 Hz)	2.66 (dd, 13.6, 10.9 Hz)
7	1.80-1.92 (m)	2.04 (m)	2.04 (m)
8a	1.15 (br d, 12.0 Hz)	1.39 (m)	1.38 (m)
8b	1.25 (td, 12.4, 4.4 Hz)	1.14 (brd 14.8 Hz)	1.15 (brd 13.4 Hz)
9a	2.88 (dm, 12.0 Hz)	3.56 (m)	3.54 (m)
9b	2.18 (td, 12.8, 3.2 Hz)	3.09 (m)	3.12 (ddd, 13.4, 13.4, 2.4 Hz)
10a	1.65 (m)	2.04 (m)	2.04 (m)
10b	1.65 (m)	1.88 (m)	1.86 (m)
11a	2.16 (dm, 11.8 Hz)	2.23 (m)	2.24 (m)
11b	1.11 (br, 12.0 Hz)	1.45 (m)	1.41 (m)
12	1.10-1.15 (masked)	1.50 (m)	1.48 (m)
13	1.80-1.92 (m)	3.16 (m)	3.15 (m)
14a	1.93 (dm, 12.0 Hz)	2.15 (brd 12.4 Hz)	2.16 (brd 12.8 Hz)
14b	1.35 (td, 12.4, 4.8 Hz)	1.60 (td 12.4, 4.8 Hz)	1.60 (ddd 12.8, 12.8, 4.6 Hz)
15	2.03 (m)	2.20 (m)	2.22 (1H, m)
16	0.90 (d, 7.6 Hz)	0.96 (d 7.6 Hz)	0.96 (d 6.9 Hz)
17	2.24 (s)	2.86 (s)	2.87 (s)

¹ ^1H NMR recorded at 400 MHz. Assignments were aided by gCOSY and gHSQCAD spectra.

² Jiang, W.-P.; Ishiuchi, K.; Wu, J.-B.; Kitanaka, S. *Heterocycles*, **2014**, *89*, 747-752.

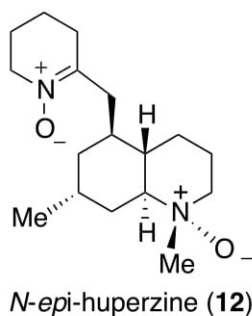
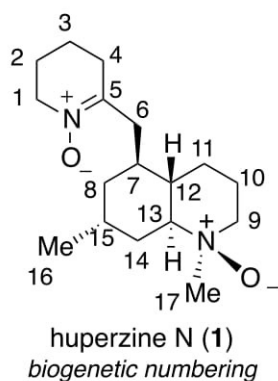
Table S2. ^{13}C NMR data for serralongamine A in CD_3OD **Serralongamine A (2)**

	Synthetic free base (2) ¹	2 bis-TFA salt ¹	Isolated serralongamine A ²
	$\delta^{13}\text{C}$	$\delta^{13}\text{C}$	$\delta^{13}\text{C}$
1	149.5	142.8	143.8
2	125.7	126.3	125.9
3	138.4	147.8	146.6
4	122.7	129.4	128.8
5	162.6	157.7	158.1
6	42.6	37.9	38.5
7	37.8	37.5	37.5
8	38.0	36.8	36.8
9	58.5	57.4	57.4
10	26.1	24.0	24.1
11	29.6	27.1	27.2
12	47.8	46.3	46.4
13	64.8	66.0	66.0
14	36.6	33.8	33.9
15	28.5	28.1	28.1
16	19.5	18.3	18.3
17	43.1	41.4	41.4

¹ ^{13}C NMR recorded at 100 MHz. Assignments were aided by gCOSY and gHSQCAD spectra.

² Jiang, W.-P.; Ishiuchi, K.; Wu, J.-B.; Kitanaka, S. *Heterocycles*, **2014**, *89*, 747-752.

Table S3. Comparison of ^1H NMR data for huperzine N, **1**, and **12** in CDCl_3

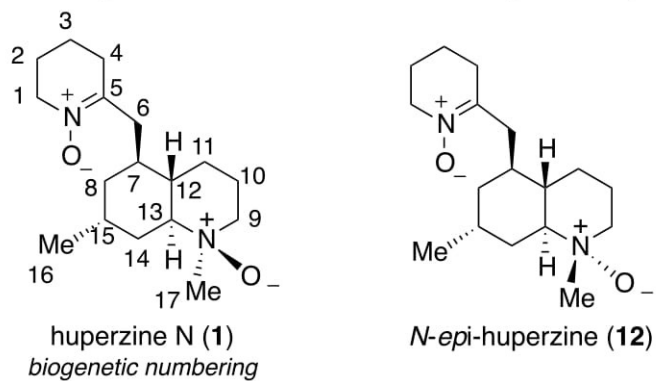


Synthetic ¹ 1	12 ¹	Huperzine N ²
δ ^1H	δ ^1H	δ ^1H
1 3.75 (t, 6.4)	3.72 (t, 6.4)	3.75 (t, 6.0)
2 1.87 (m)	1.87 (m)	1.84-1.92 (m)
3 1.68 (m)	1.68 (m)	1.64-1.69 (m)
4 2.40 (t, 6.0)	2.40	2.34 (t, 6.0)
6 2.98 (dd, 12.0, 3.0)	2.70	2.96 (dd, 12, 3)
1.88 (masked)	2.35	1.91 (d, 12)
7 2.15 (m)	1.95 (m)	2.10-2.17 (m)
8 1.40 (td, 12.0, 4.0)	1.40 (m)	1.34 (ddd, 12, 8, 4)
1.28 (masked)	1.35 (m)	1.29 (br d, 12)
9 3.46 (br d, 12.0)	3.61 (br d, 12.0)	3.35 (br d, 12)
3.16 (ddd, 12.0, 11.0, 3.0)	3.42 (td, 12.0, 3.0)	3.14 (ddd, 12, 11, 3)
10 1.58 (br d, 13.0)	1.68	1.57 (br d, 14)
2.38 (masked)	1.87	1.34-43 (m)
11 2.05 (m)	2.05 (m)	2.01-2.06 (m)
1.12 (qd, 12.0, 3.0)	1.20 (masked)	1.08-1.13 (m)
12 1.80 (m)	1.30 (m)	1.78-1.83 (m)
13 2.90 (td, 11.5, 3.2)	3.21 (br t, 12.0)	2.89 (ddd, 11, 10, 3)
14 2.10 (m)	2.60	2.06-2.17 (m)
1.80 (m)	1.45 (td, 12.0, 3.0)	1.67-1.72 (m)
15 2.21 (m)	2.23 (m)	2.16-2.25 (m)
16 0.93 (d, 7.2)	0.99 (d, 7.2)	0.93 (d, 7)
17 3.10 (s)	2.96 (s)	3.04 (s)

¹ Recorded at 400 MHz. Assignments were aided by gCOSY and gHSQCAD spectra.

² Recorded at 400 MHz (*Helv. Chim. Acta*, 2008, **91**, 1031-1035).

Table S4. Comparison of ^{13}C NMR data for huperzine N, **1**, and **12** in CDCl_3



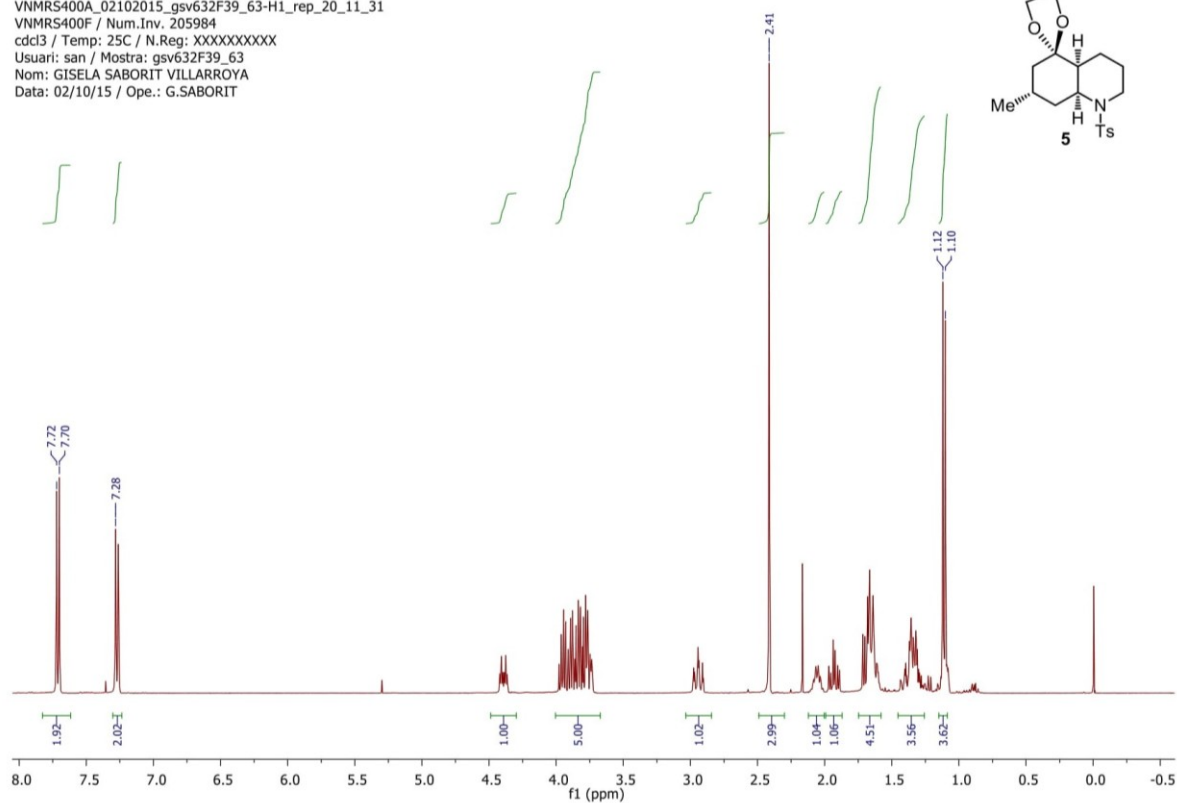
carbon	Synthetic 1 ¹	12 ¹	Huperzine N ²
	$\delta^{13}\text{C}$	$\delta^{13}\text{C}$	$\delta^{13}\text{C}$
1	58.5	58.6	58.2
2	23.3	23.3	23.1
3	18.9	19.2	18.8
4	29.9	29.9	30.0
5	147.9	147.2	148.0
6	36.7	35.5	36.4
7	32.4	34.6	32.3
8	36.8	37.5	36.6
9	69.1	71.1	69.0
10	20.3	22.9	20.1
11	27.0	27.1	27.0
12	41.1	44.7	40.8
13	73.8	75.9	73.4
14	30.1	30.2	30.0
15	27.1	27.2	26.8
16	19.0	18.2	19.0
17	57.6	48.0	57.6

¹ Recorded at 100 MHz. Assignments were aided by gCOSY and gHSQCAD spectra.

² Recorded at 100 MHz (*Helv. Chim. Acta*, 2008, **91**, 1031-1035).

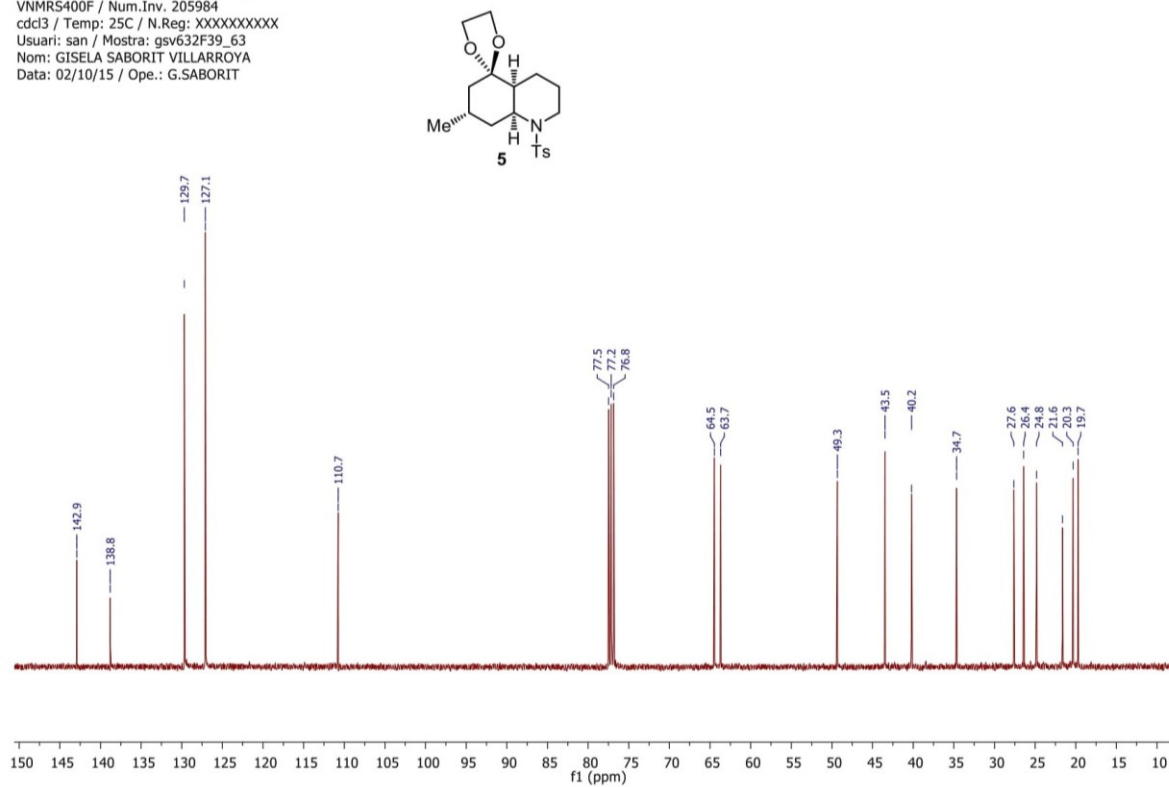
S7

VNMR5400A_02102015_gsv632F39_63-H1_rep_20_11_31
 VNMR5400F / Num.Inv. 205984
 cdc13 / Temp: 25C / N.Reg: XXXXXXXXXX
 Usuari: san / Mostra: gsv632F39_63
 Nom: GISELA SABORIT VILLARROYA
 Data: 02/10/15 / Ope.: G.SABORIT

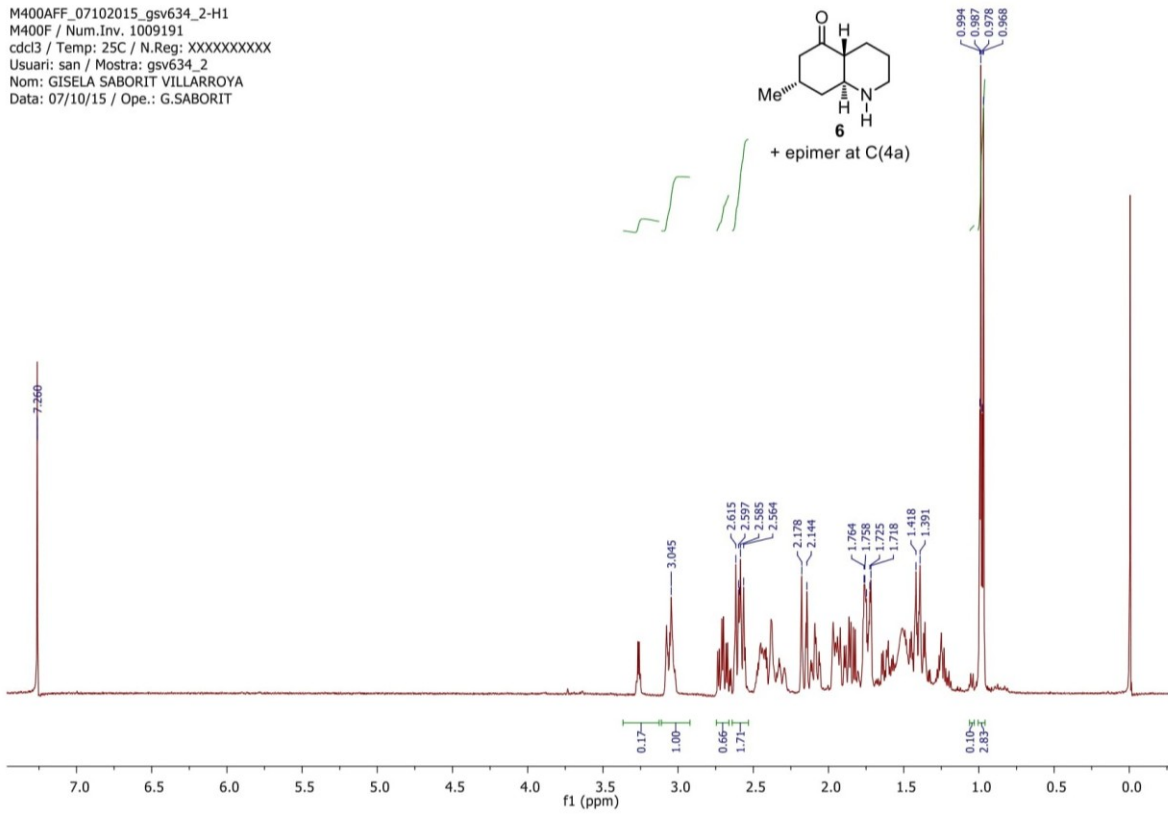
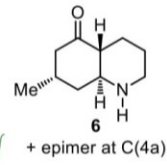


S8

VNMR5400A_02102015_gsv632F39_63-C13
 VNMR5400F / Num.Inv. 205984
 cdc13 / Temp: 25C / N.Reg: XXXXXXXXXX
 Usuari: san / Mostra: gsv632F39_63
 Nom: GISELA SABORIT VILLARROYA
 Data: 02/10/15 / Ope.: G.SABORIT

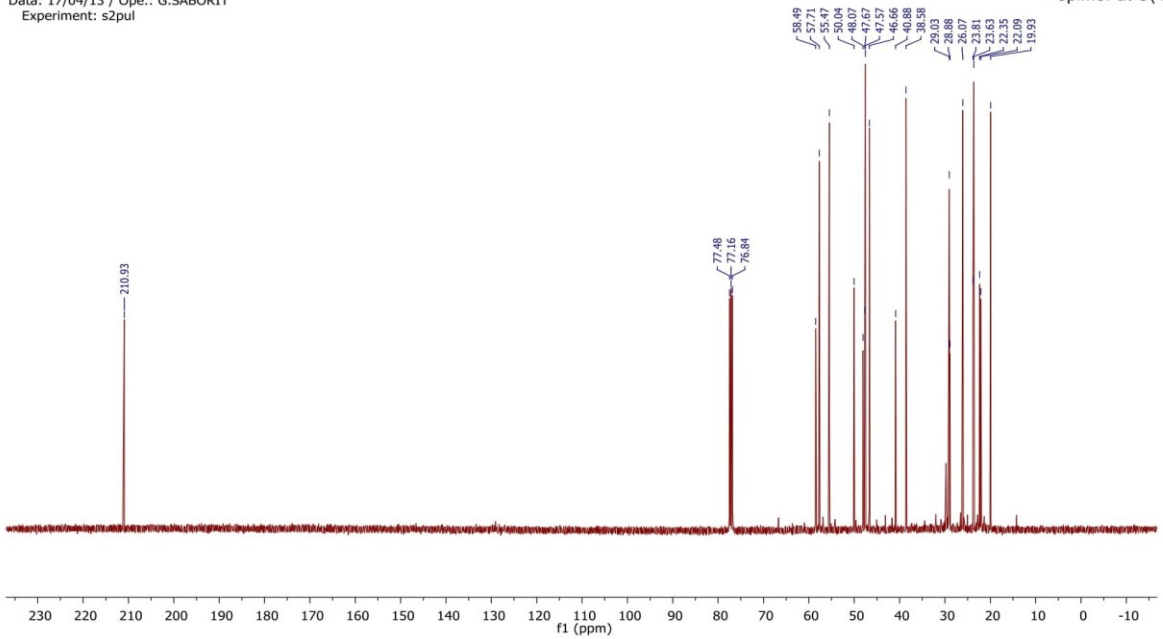
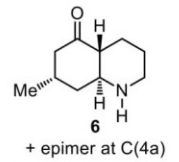


M400AFF_07102015_gsv634_2-H1
M400F / Num.Inv. 1009191
cdcl3 / Temp: 25C / N.Reg: XXXXXXXXXX
Usuari: san / Mostra: gsv634_2
Nom: GISELA SABORIT VILLARROYA
Data: 07/10/15 / Ope.: G.SABORIT



6S

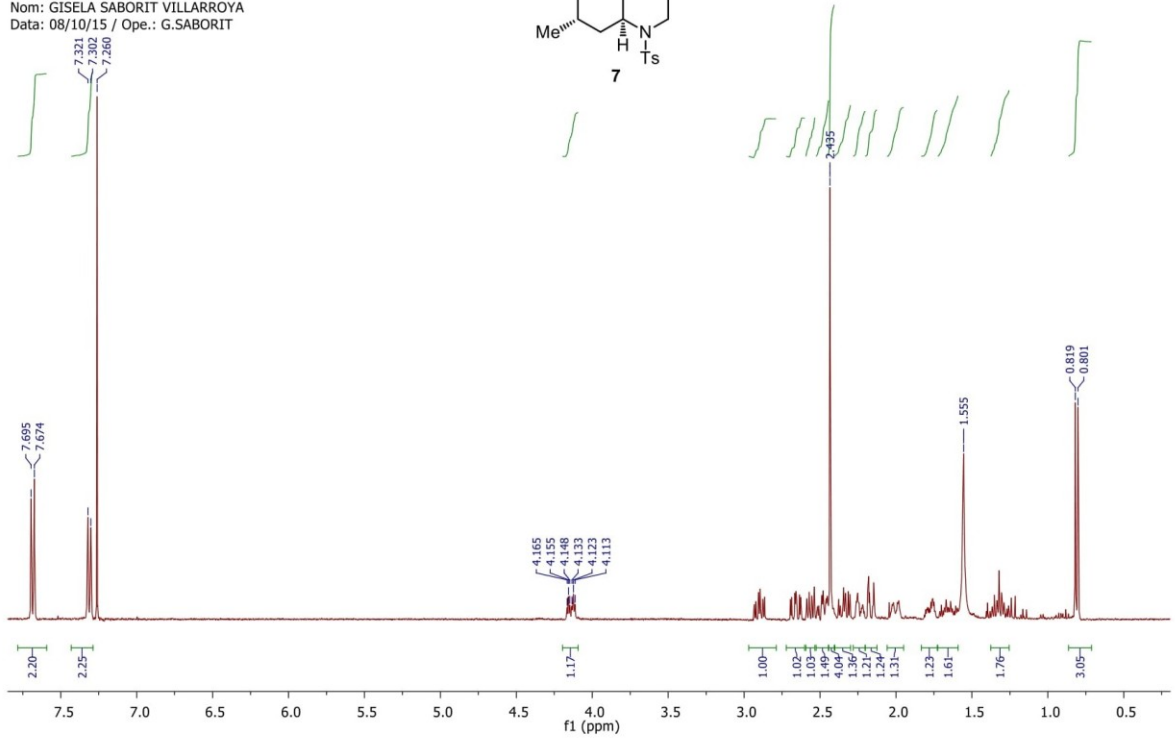
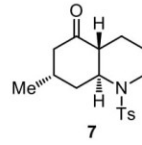
V400A_18042013_gsv265_typeD-C13
H1 / Mercury-400F
cdcl3 / Temp: Ambient / N.Reg: XXXXXXXXXX
Usuari: san / Mostra: gsv265_typeD
Nom: GISELA SABORIT VILLARROYA
Data: 17/04/13 / Ope.: G.SABORIT
Experiment: s2pul



01S

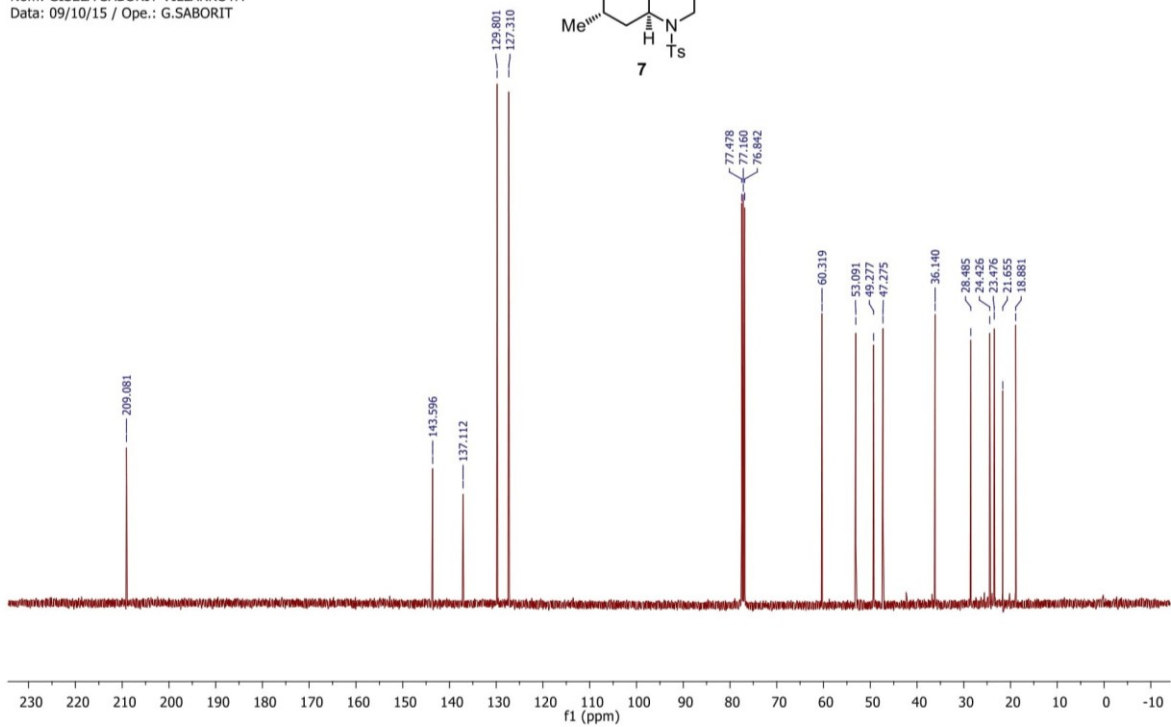
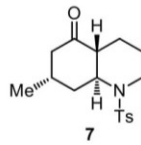
S11

M400AFF_08102015_gsv634F19_21-H1
 M400F / Num.Inv. 1009191
 cdcl3 / Temp: 25C / N.Reg: XXXXXXXXXX
 Usuari: san / Mostra: gsv634F19_21
 Nom: GISELA SABORIT VILLARROYA
 Data: 08/10/15 / Ope.: G.SABORIT

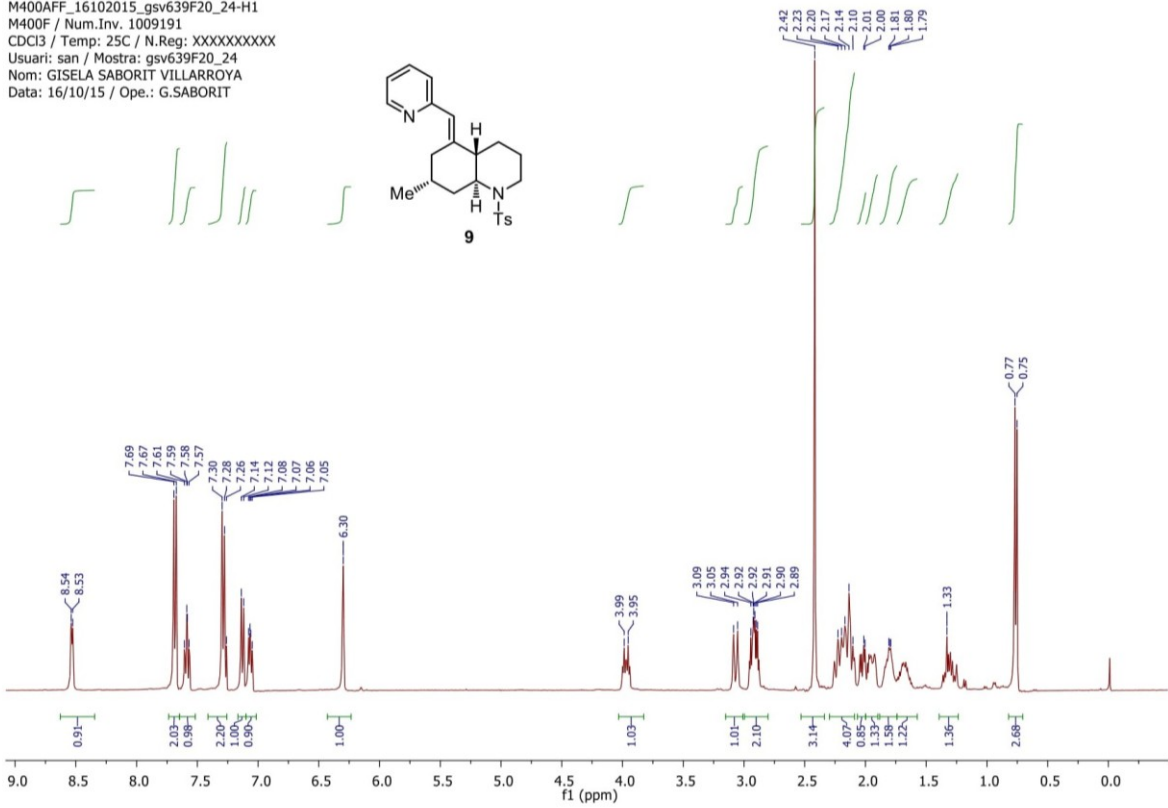


S12

VNMRS400A_09102015_gsv634F19_21-C13
 VNMRS400F / Num.Inv. 205984
 cdcl3 / Temp: 25C / N.Reg: XXXXXXXXXX
 Usuari: san / Mostra: gsv634F19_21
 Nom: GISELA SABORIT VILLARROYA
 Data: 09/10/15 / Ope.: G.SABORIT

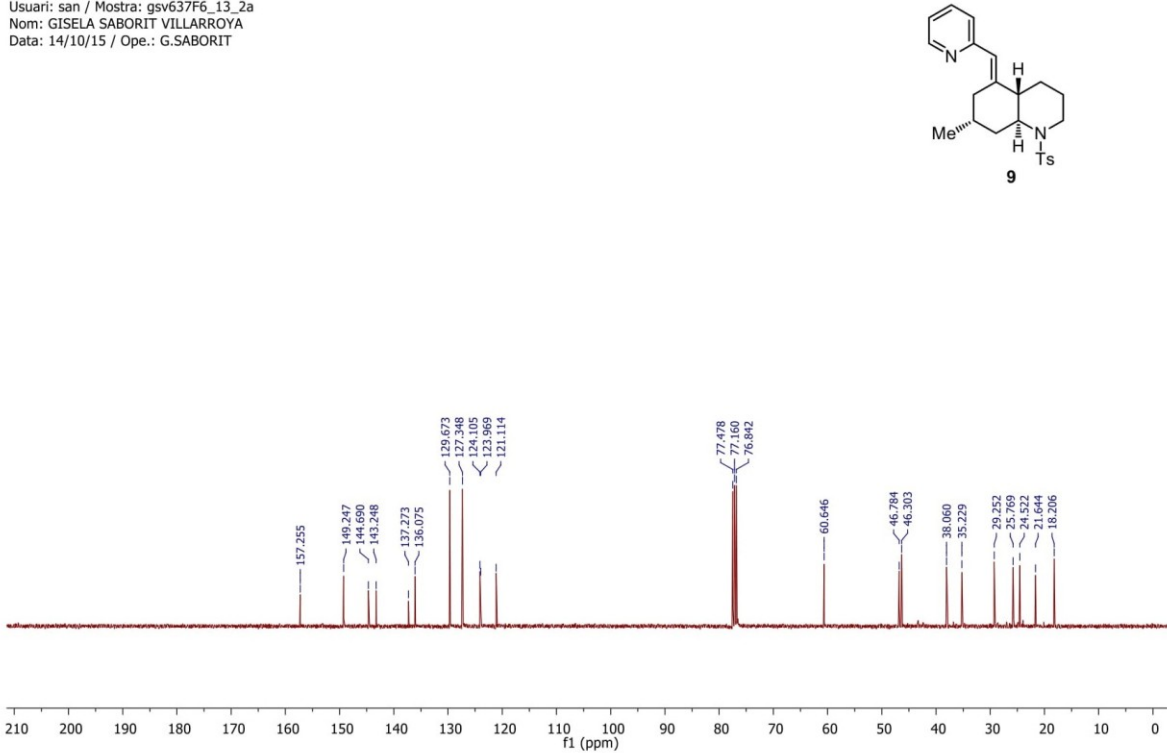


M400AFF_16102015_gsv639F20_24-H1
M400F / Num.Inv. 1009191
CDCl3 / Temp: 25C / N.Reg: XXXXXXXXXX
Usuari: san / Mostra: gsv639F20_24
Nom: GISELA SABORIT VILLARROYA
Data: 16/10/15 / Ope.: G.SABORIT



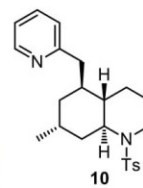
S13

VNMRS400A_14102015_gsv637F6_13_2a-C13
VNMRS400F / Num.Inv. 205984
cdCl3 / Temp: 25C / N.Reg: XXXXXXXXXX
Usuari: san / Mostra: gsv637F6_13_2a
Nom: GISELA SABORIT VILLARROYA
Data: 14/10/15 / Ope.: G.SABORIT

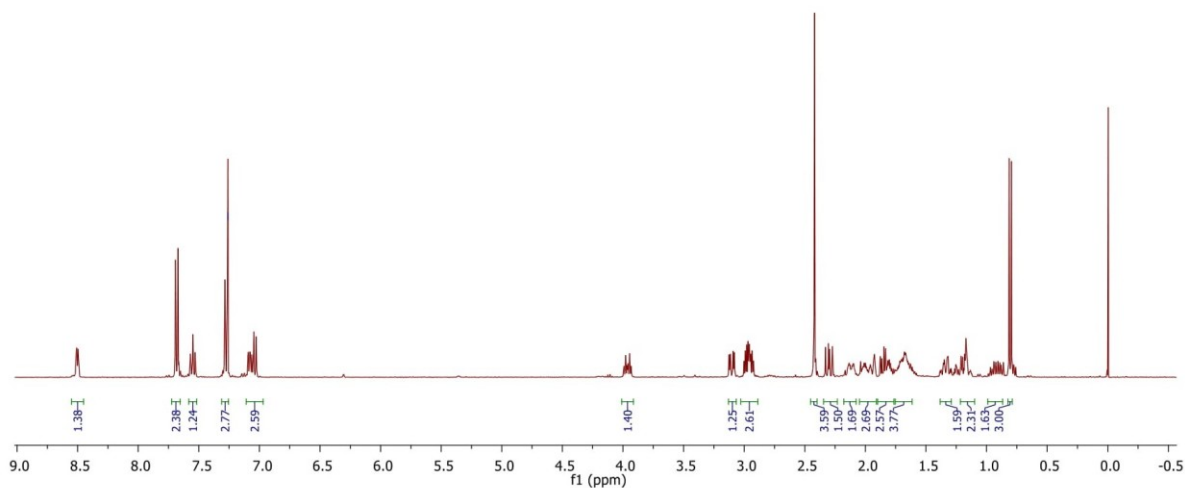


S14

VNMRS400A_19102015_gsv638F25_34-H1_rep_21_28_56
 VNMRS400F / Num.Inv. 205984
 CDCl3 / Temp: 25C / N.Reg: XXXXXXXXXX
 Usuari: san / Mostra: gsv638F25_34
 Nom: GISELA SABORIT VILLARROYA
 Data: 19/10/15 / Ope.: G.SABORIT

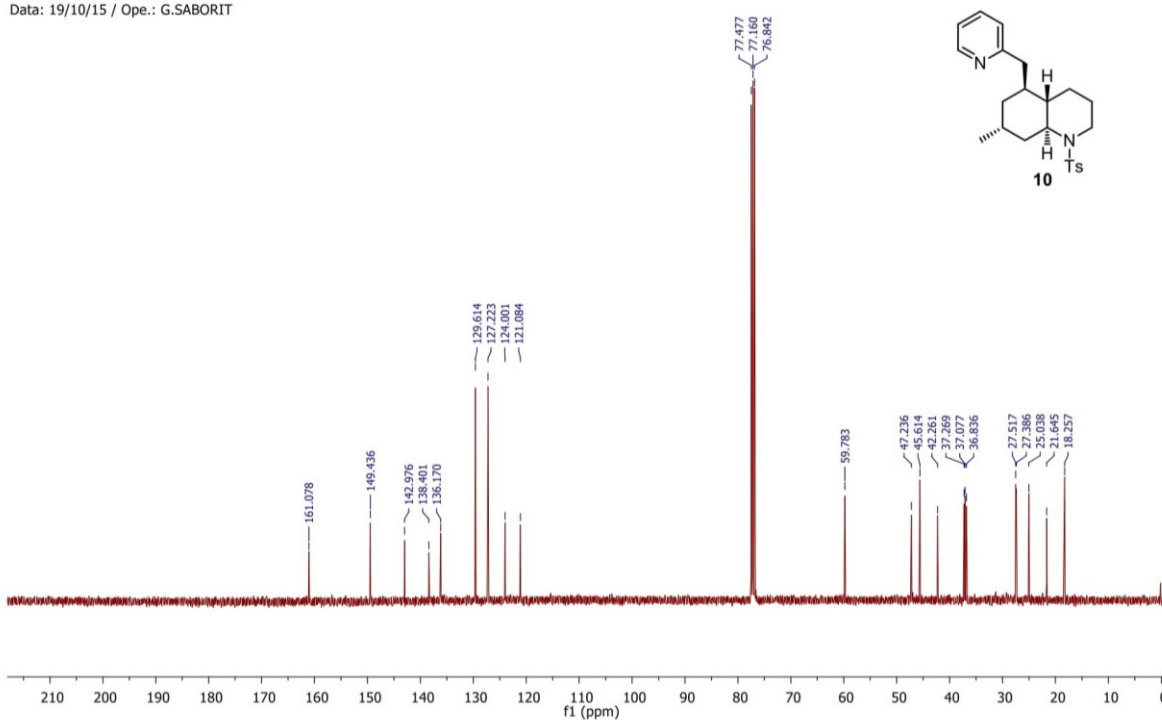
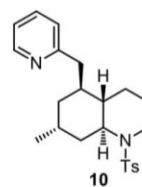


S15



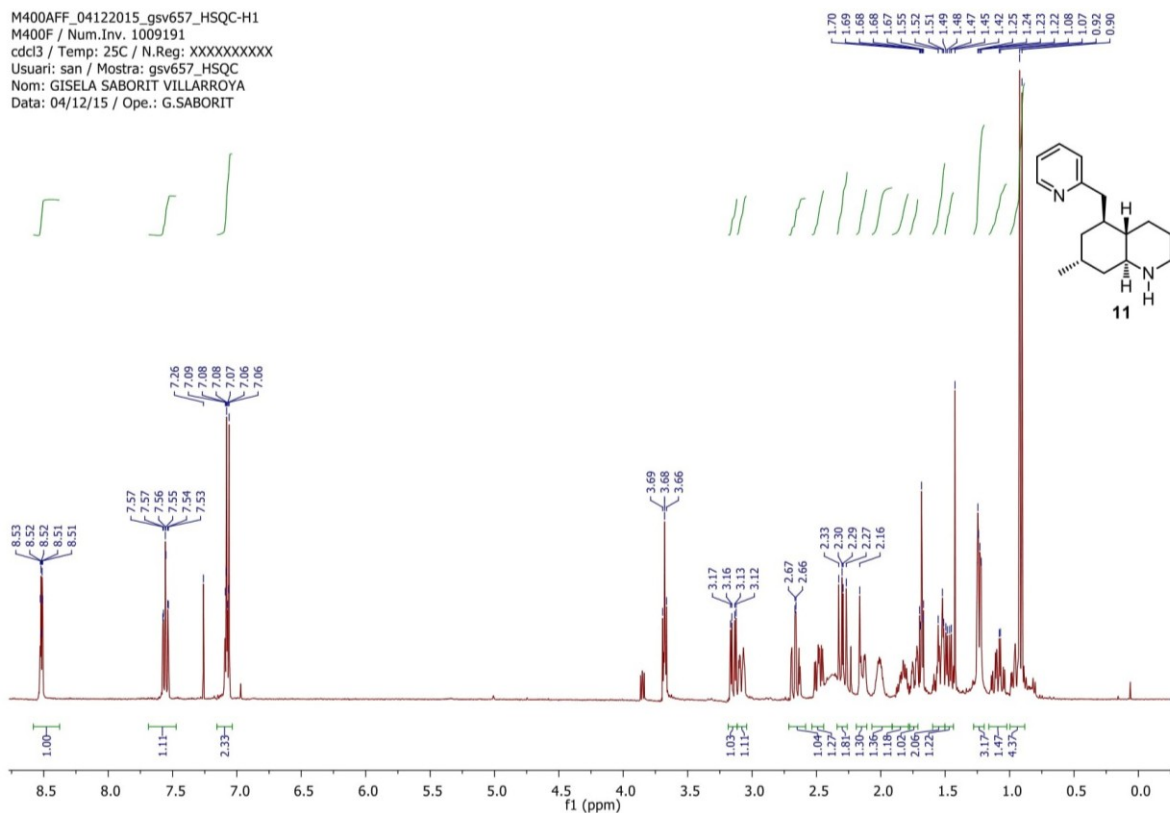
S16

VNMRS400A_19102015_gsv638F25_34-C13
 VNMRS400F / Num.Inv. 205984
 CDCl3 / Temp: 25C / N.Reg: XXXXXXXXXX
 Usuari: san / Mostra: gsv638F25_34
 Nom: GISELA SABORIT VILLARROYA
 Data: 19/10/15 / Ope.: G.SABORIT



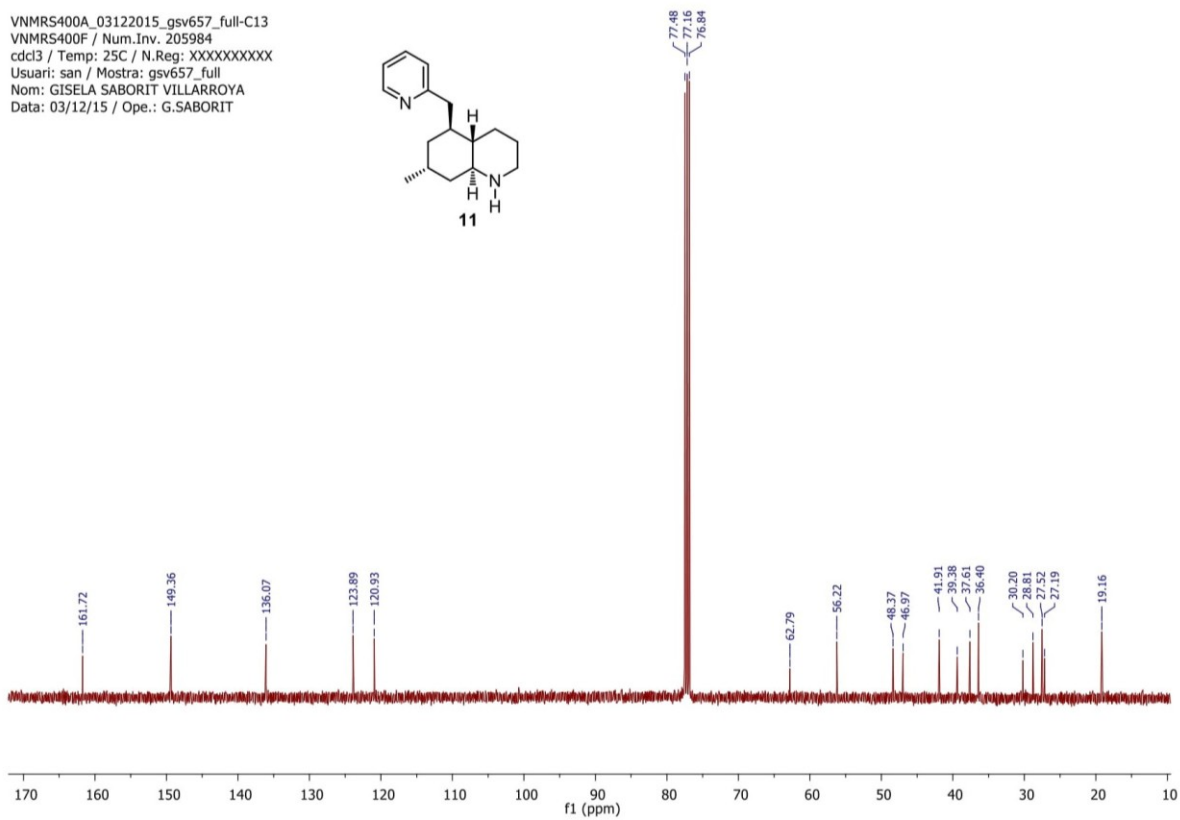
S17

M400AFF_04122015_gsv657_HSQC-H1
 M400F / Num.Inv. 1009191
 cdcl3 / Temp: 25C / N.Reg: XXXXXXXXXX
 Usuari: san / Mostra: gsv657_HSQC
 Nom: GISELA SABORIT VILLARROYA
 Data: 04/12/15 / Ope.: G.SABORIT

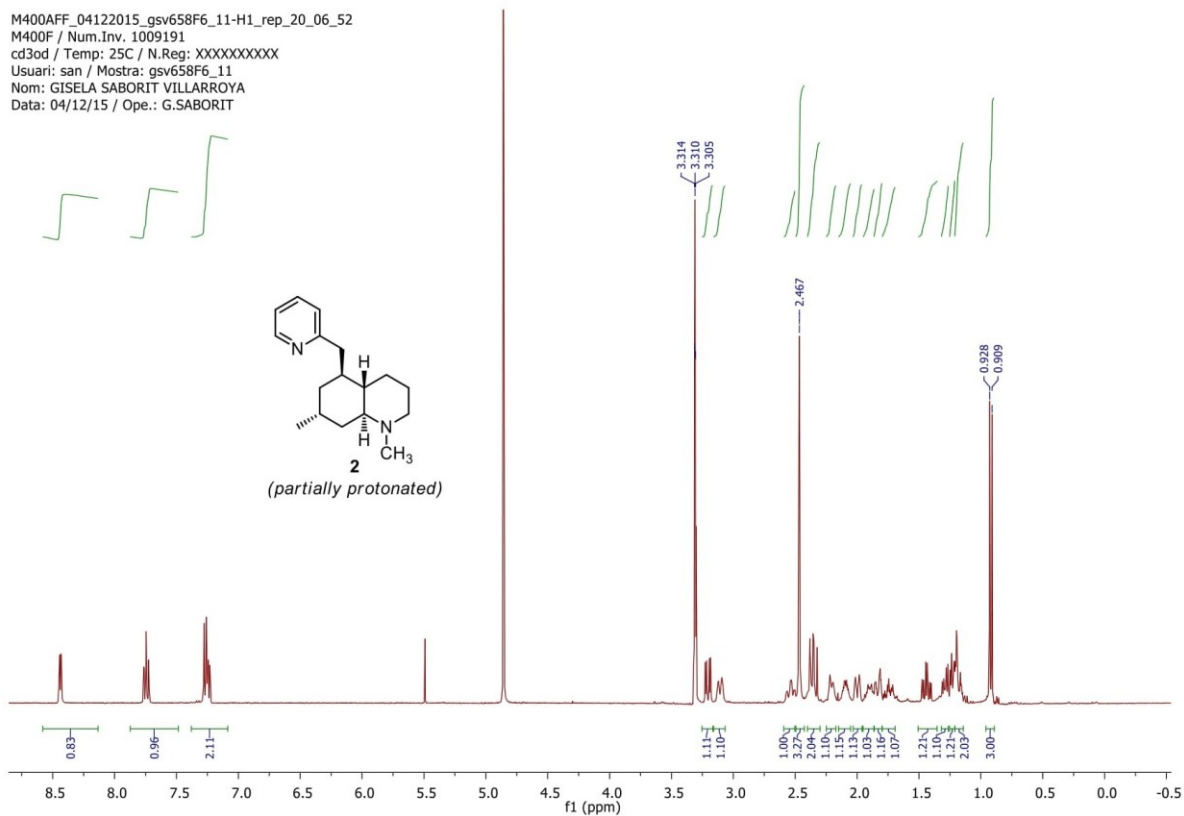


S18

VNMRS400A_03122015_gsv657_full-C13
 VNMRS400F / Num.Inv. 205984
 cdcl3 / Temp: 25C / N.Reg: XXXXXXXXXX
 Usuari: san / Mostra: gsv657_full
 Nom: GISELA SABORIT VILLARROYA
 Data: 03/12/15 / Ope.: G.SABORIT

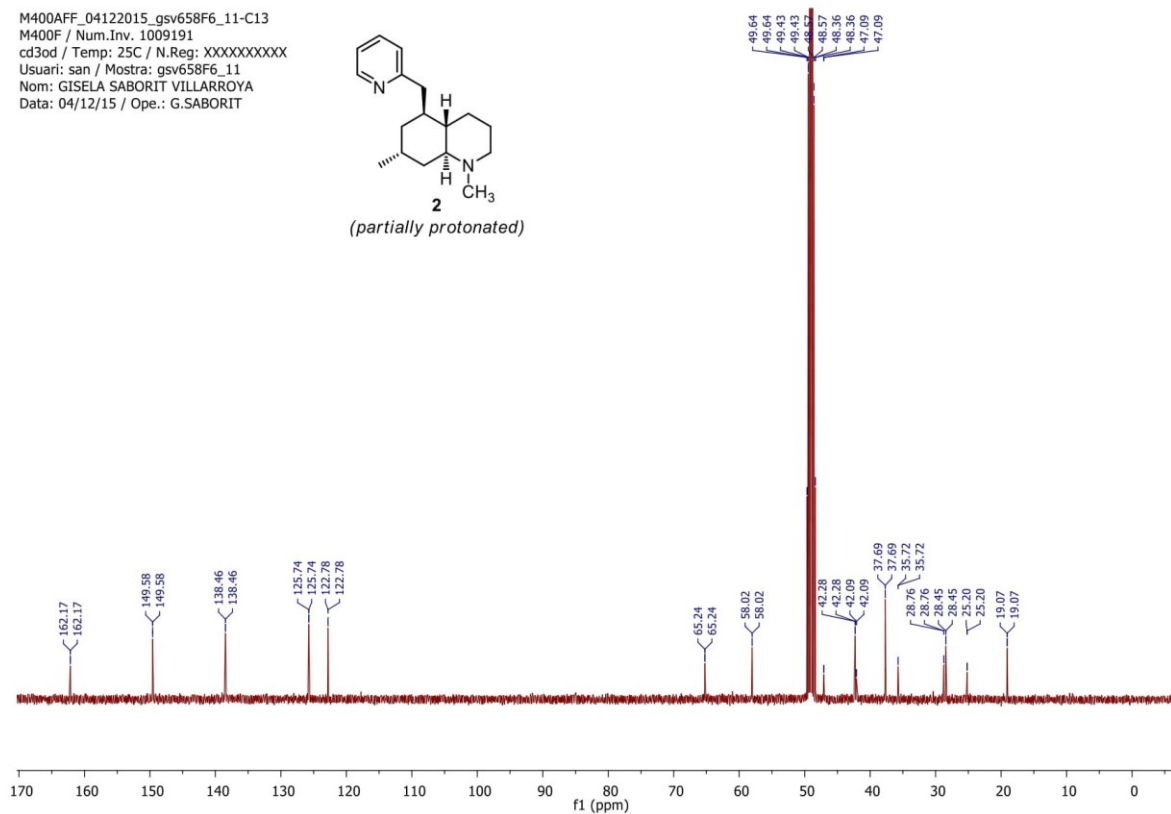


M400AFF_04122015_gsv658F6_11-H1_rep_20_06_S2
M400F / Num.Inv. 1009191
cd3od / Temp: 25C / N.Reg: XXXXXXXXXXXX
Usuari: san / Mostra: gsv658F6_11
Nom: GISELA SABORIT VILLARROYA
Data: 04/12/15 / Ope.: G.SABORIT



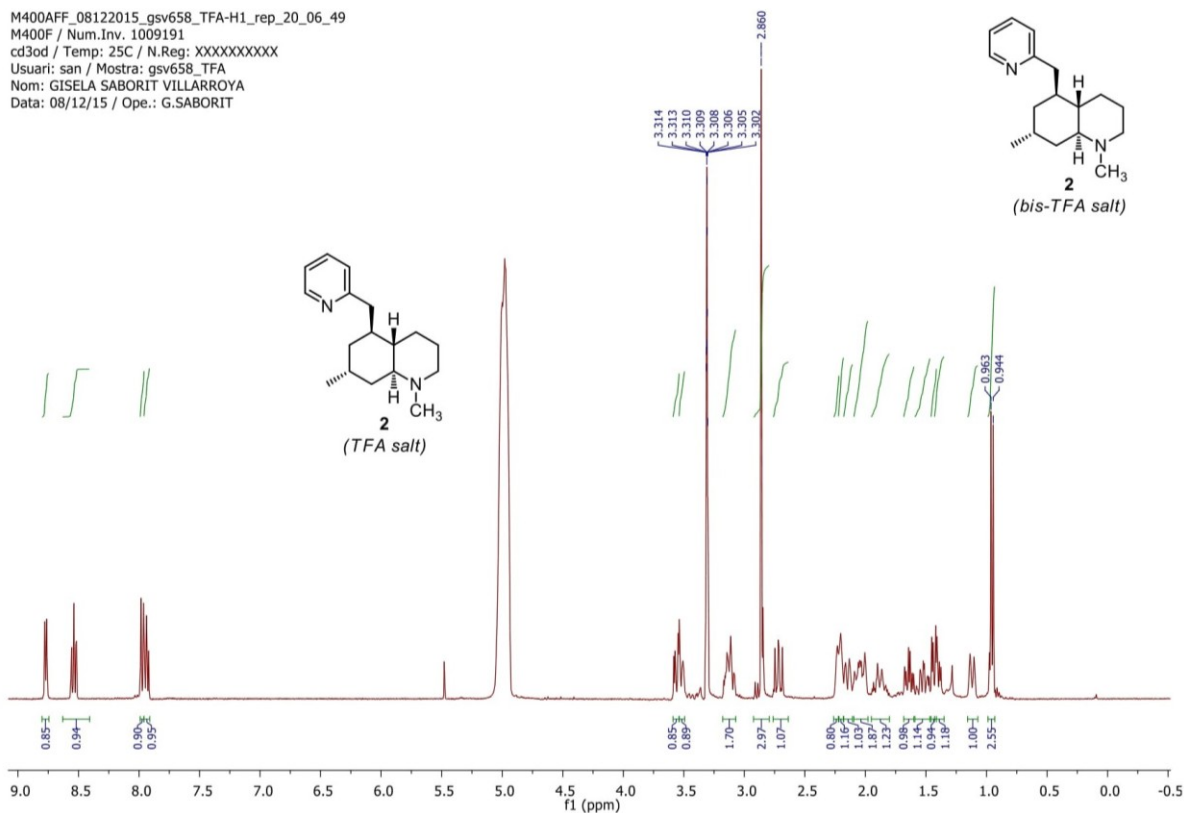
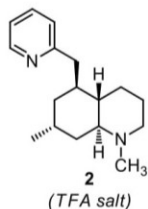
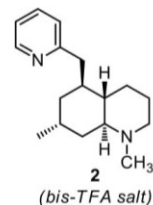
S21

M400AFF_04122015_gsv658F6_11-C13
M400F / Num.Inv. 1009191
cd3od / Temp: 25C / N.Reg: XXXXXXXXXXXX
Usuari: san / Mostra: gsv658F6_11
Nom: GISELA SABORIT VILLARROYA
Data: 04/12/15 / Ope.: G.SABORIT



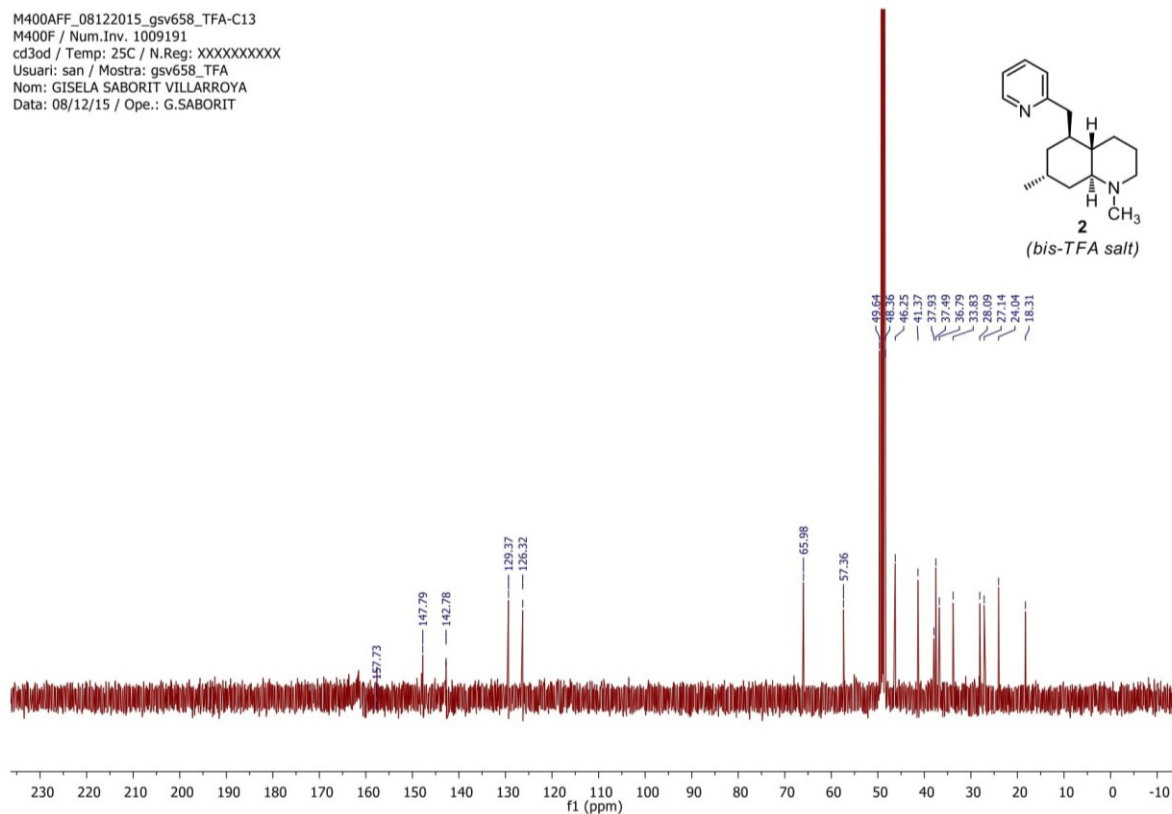
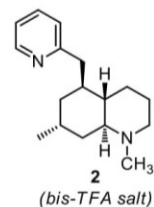
S22

M400AFF_08122015_gsv658_TFA-H1_rep_20_06_49
M400F / Num.Inv. 1009191
cd3od / Temp: 25C / N.Reg: XXXXXXXXXX
Usuari: san / Mostra: gsv658_TFA
Nom: GISELA SABORIT VILLARROYA
Data: 08/12/15 / Ope.: G.SABORIT



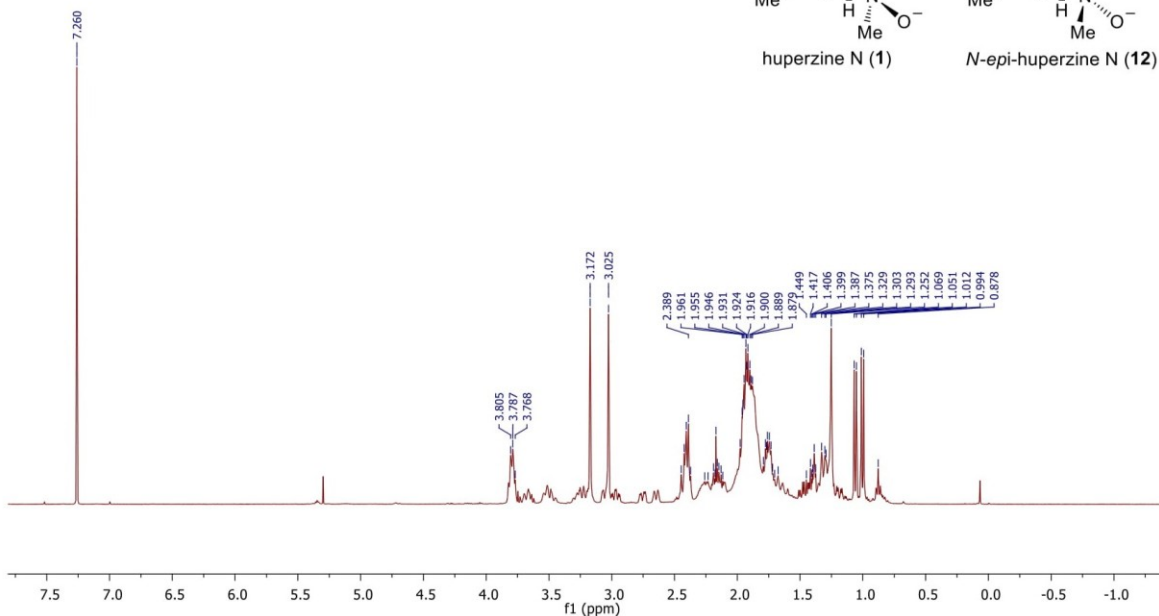
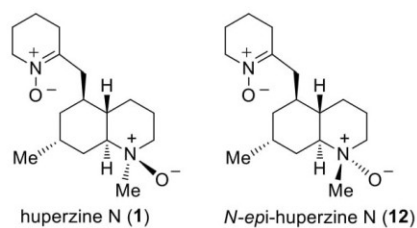
S23

M400AFF_08122015_gsv658_TFA-C13
M400F / Num.Inv. 1009191
cd3od / Temp: 25C / N.Reg: XXXXXXXXXX
Usuari: san / Mostra: gsv658_TFA
Nom: GISELA SABORIT VILLARROYA
Data: 08/12/15 / Ope.: G.SABORIT



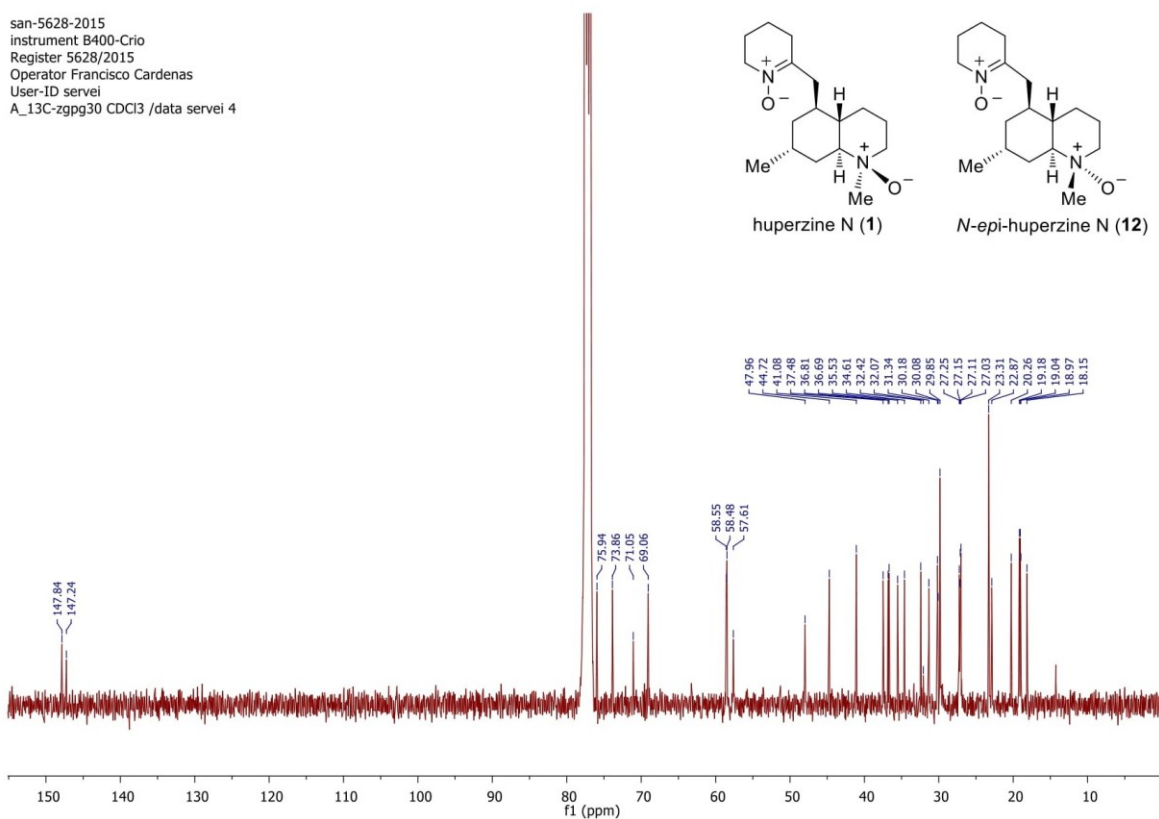
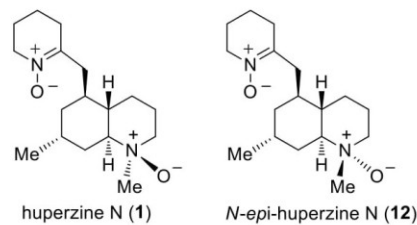
S24

san-5628-2015
 Equip: B400Q / N.Inv: 1009989
 N.Reg: 5628/2015
 Usuari: san / Mostra: gsv659F26_28
 Nom: GISELA SABORIT VILLARROYA
 Data: 18/12/2015 10:39:59 h./ Ope.: Francisco Cardenas
 EXP: A_1H-zg30 CDCl3



S25

san-5628-2015
 Instrument B400-Crio
 Register 5628/2015
 Operator Francisco Cardenas
 User-ID servei
 A_13C-zgpg30 CDCl3 /data servei 4



S26

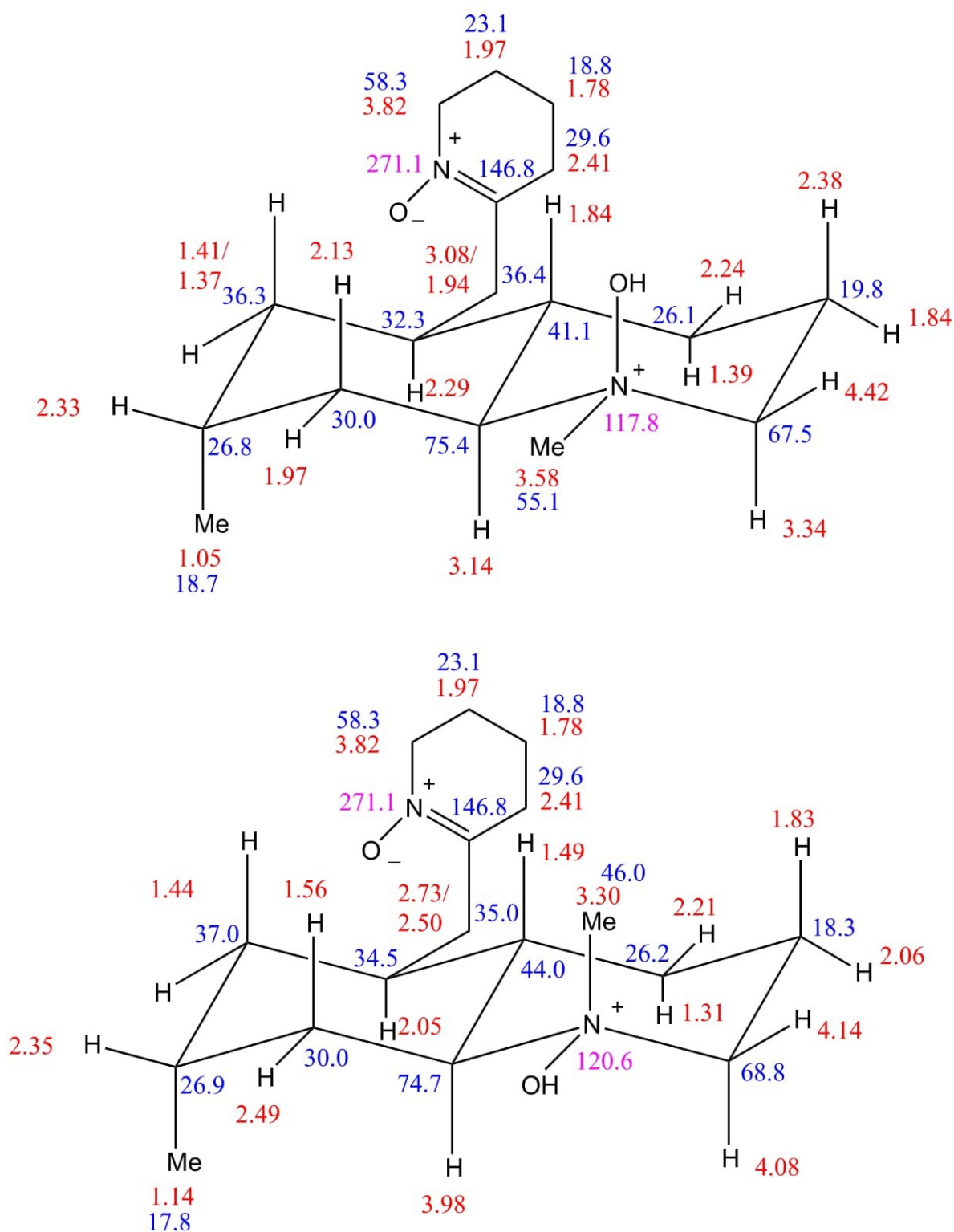


Figure S2.
NMR data (^1H , ^{13}C , and ^{15}N) of protonated samples of huperzine N (1) and its epimer 12.

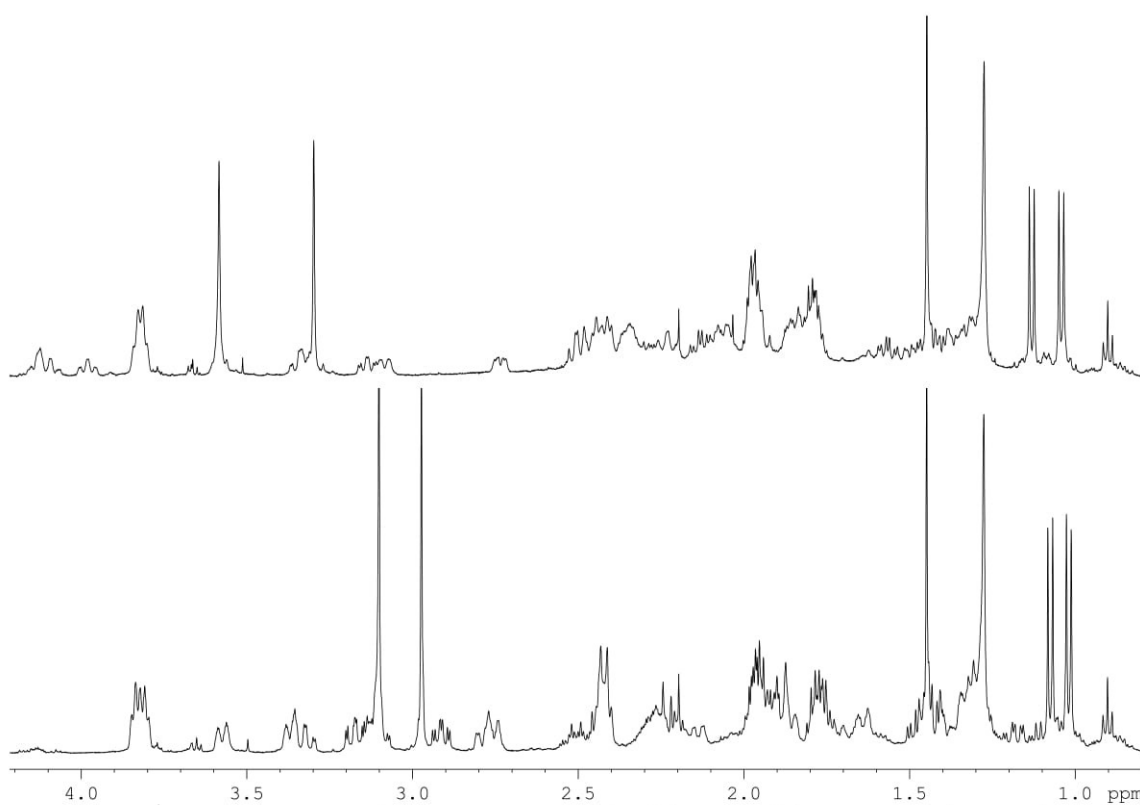


Figure S3. ^1H NMR spectra (500 MHz, CDCl_3) of the *N*-oxide compounds **1** and **12** (bottom) and their protonated derivatives (top). Note the strong downfield effect on all proton resonances near to the protonated *N*-oxide functionality.

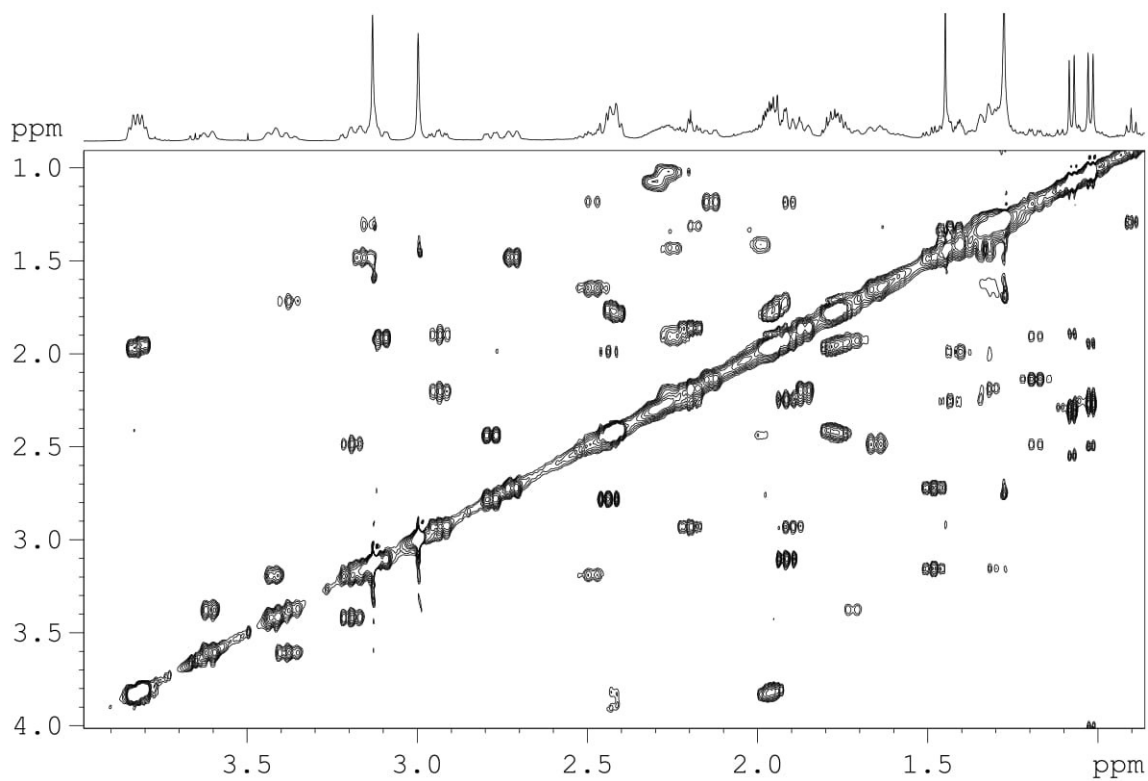


Figure S4. 2D ^1H - ^1H COSY spectrum of the mixture containing the two *N*-oxide derivatives.

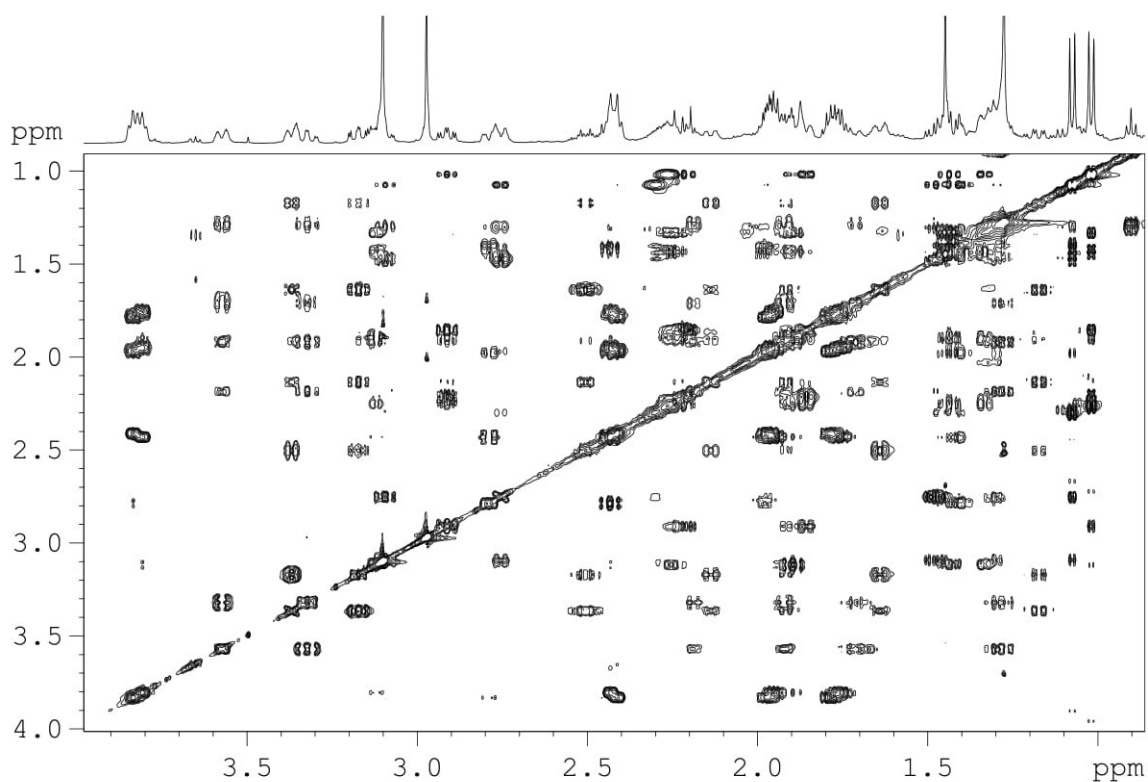


Figure S5. 2D ¹H-¹H TOCSY spectrum (mixing time of 60 ms) of the mixture containing the two N-oxide derivatives.

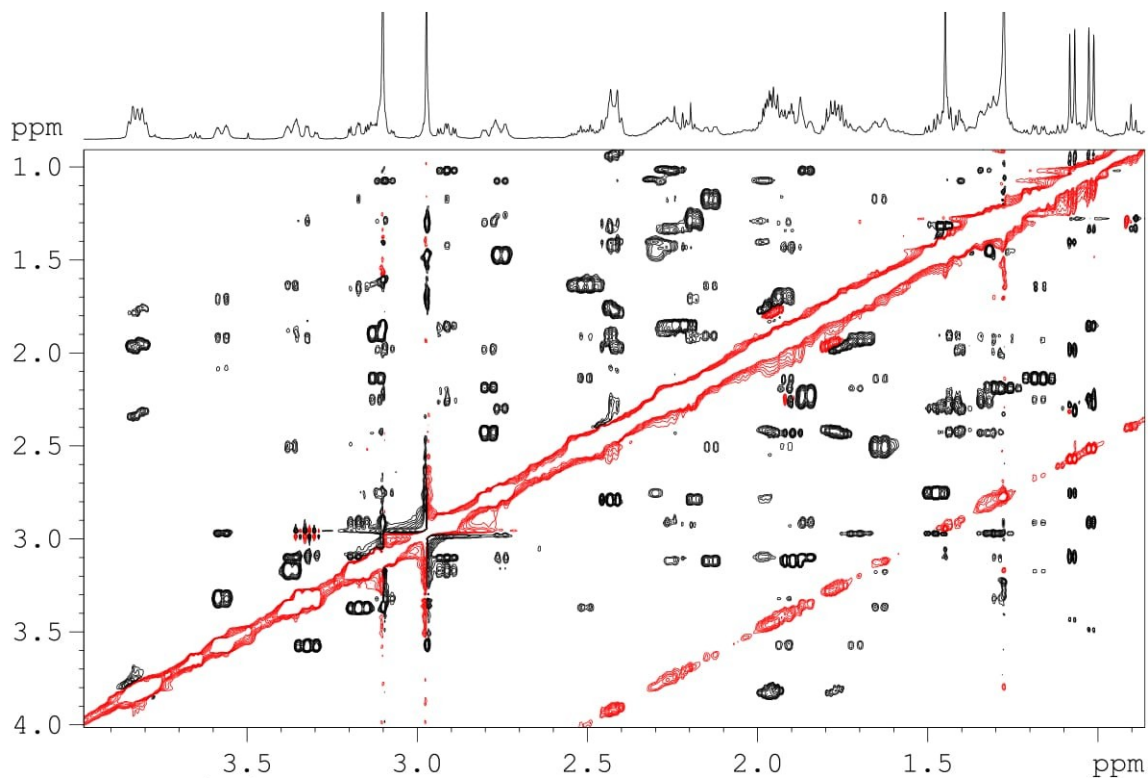


Figure S6. 2D ¹H-¹H ROESY spectrum (mixing time of 500ms) of the mixture containing the two N-oxide derivatives.

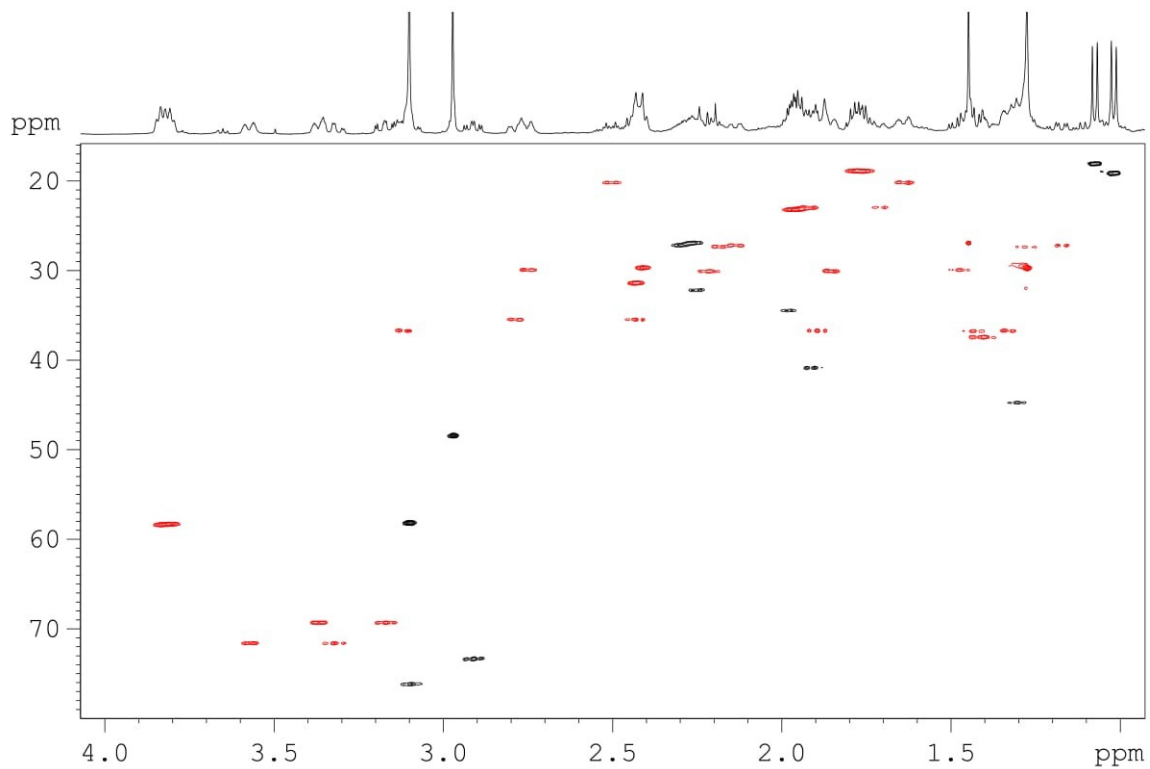
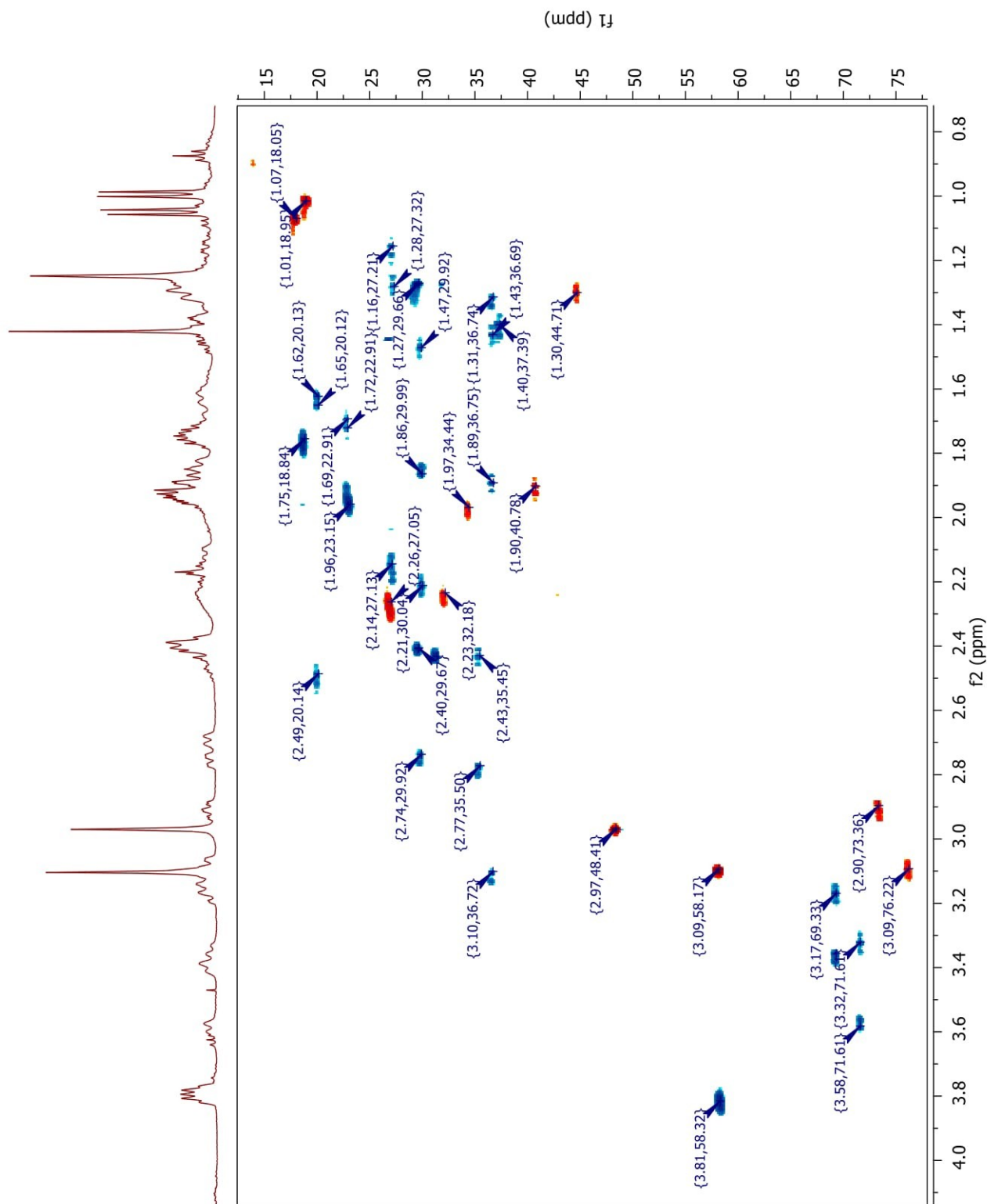


Figure S7. ^1H - ^{13}C multiplicity-edited HSQC

Figure S7. ^1H - ^{13}C multiplicity-edited HSQC



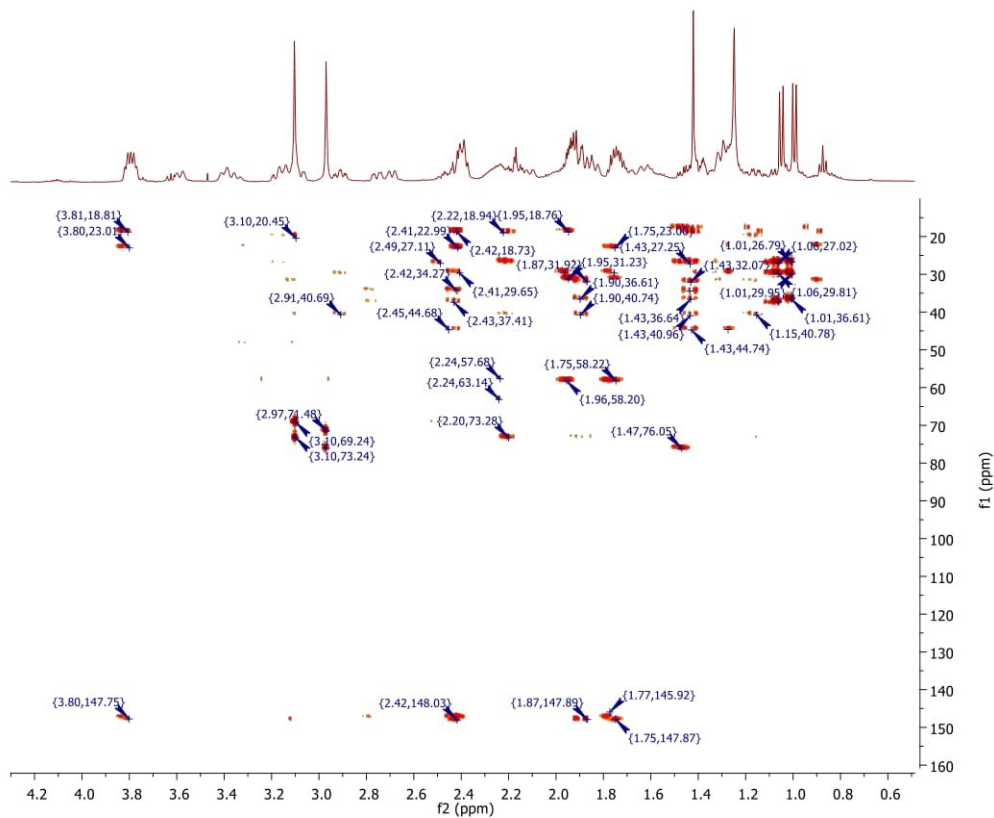


Figure S8. ^1H - ^{13}C HMBC spectrum (optimized to 8 Hz)

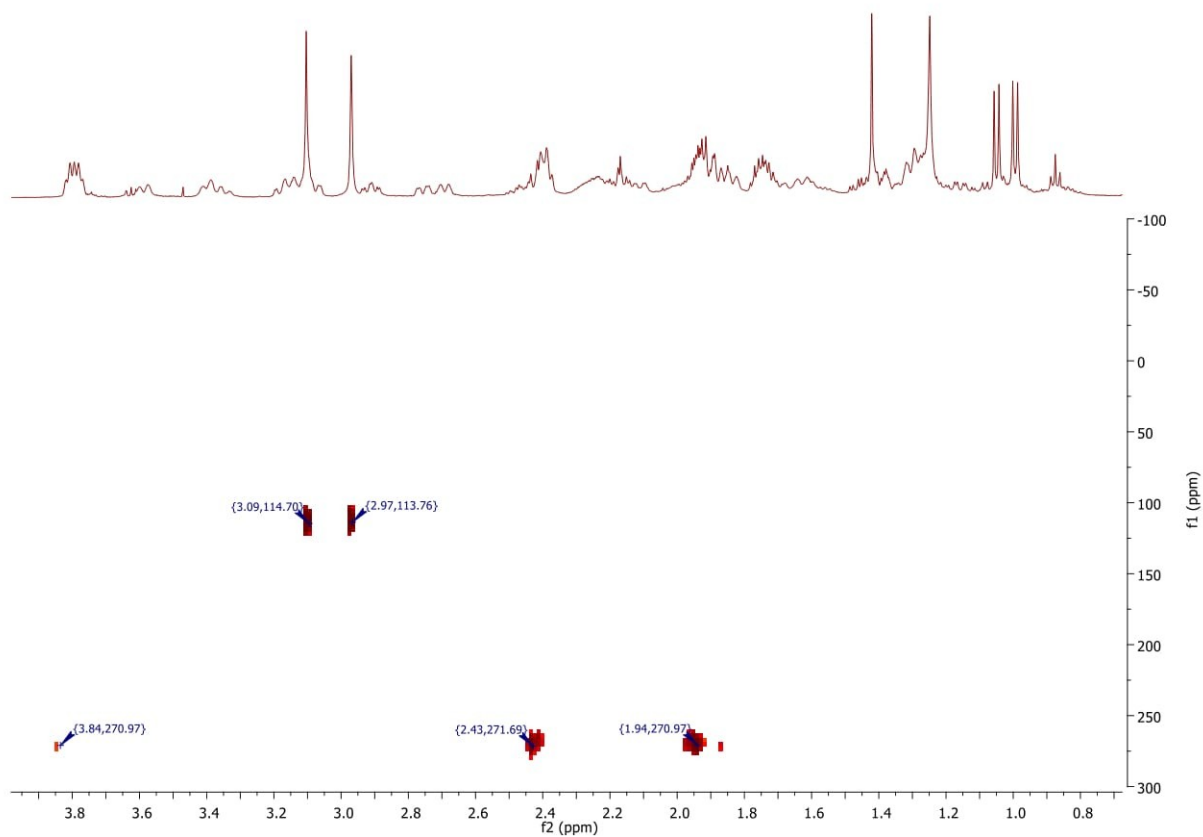


Figure S9. ^1H - ^{15}N HMBC (optimized to 8 Hz).

Decahydroquinoline Ring NMR Patterns for the Stereochemical Elucidation of Phlegmarine Alkaloids: Synthesis of (-)-Serralongamine A and the Revised Structures of (-)-Huperzine K and Huperzine M

Caroline Bosch,[†] Teodor Parella,[‡] Ben Bradshaw,^{*,†} and Josep Bonjoch^{*,†}

[†] Laboratori de Química Orgànica, Facultat de Farmàcia, IBUB, Universitat de Barcelona, Av. Joan XXIII s/n, 08028-Barcelona, Spain

[‡] Servei de Ressonància Magnètica Nuclear, Universitat Autònoma de Barcelona, 08193-Bellaterra, Barcelona, Spain

e-mail address: josep.bonjoch@ub.edu; benbradshaw@ub.edu

Unpublished results

EXPERIMENTAL SECTION

General Methods. All reactions were carried out under an argon atmosphere with dry, freshly distilled solvents under anhydrous conditions. All product mixtures were analyzed by thin-layer chromatography using TLC silica gel plates with a fluorescent indicator ($\lambda = 254$ nm). Analytical thin-layer chromatography was performed on SiO₂ (Merck silica gel 60 F₂₅₄), and the spots were located by UV light or/and a 1% KMnO₄ aqueous solution or hexachloroplatinate reagent. Chromatography refers to flash chromatography and was carried out on SiO₂ (silica gel 60 ACC, 230-240 mesh). Drying of organic extracts during the reaction workup was performed over anhydrous Na₂SO₄. Chemical shifts of ¹H and ¹³C NMR spectra are reported in ppm downfield (δ) from Me₄Si. All NMR data assignments are supported by gCOSY and gHSQC experiments.

(4aS,7S,8aS)-7-Methyl-1-(4-methylphenylsulfonyl)-5-oxodeca-hydroquinoline ethylene acetal ((+)-21). From crystallized enantiopure keto ester **(+)-19** (2.16 g, 5.12 mmol), following the procedure previously described,¹¹³ ketone **(+)-20** was obtained after treatment with TFA and used in the next step without purification. Acetalization¹¹⁴ of **(+)-20** gave **(+)-21** (1.76 g, 93%) as a white solid. Purification of an aliquot by chromatography (5% to 25% EtOAc in hexanes), gave the pure product as a white solid: $R_f = 0.71$ (1:1 EtOAc/hexanes); mp 100 °C, $\alpha_D = +12.3$ (c 1, CHCl₃). For NMR data, see ref 113

(4aR,7S,8aS)-7-Methyl-5-oxodecahydroquinoline ((+)-23). Operating as previously described,¹¹⁴ starting from **(+)-21** (1.75 g, 4.79 mmol), **(+)-23**, a 2:1 mixture of epimers at C-4a, was obtained (631 mg) as a colorless oil, which was used directly in the next step. For NMR data, see ref 114.

(4aR,7S,8aS)-7-Methyl-5-oxo-1-(4-methylphenylsulfonyl)decahydroquinoline ((+)-24). To a cooled (0 °C) stirred solution of the above mixture of **(+)-23** and its epimer (630 mg, 3.7 mmol) in CH₂Cl₂ (45 mL) was added a solution of TsCl (776 mg, 4.07 mmol, 1.1 equiv) in CH₂Cl₂ (20 mL) followed by Et₃N (0.60 mL, 4.44 mmol, 1.2 equiv). The mixture was stirred at rt for 6 h and diluted with CH₂Cl₂ (100 mL). The organics were washed with brine (2 x 20 mL), dried, concentrated, and purified by chromatography (5% to 25% EtOAc in hexanes) to yield successively **(+)-20** (305 mg) and **(+)-24** (340 mg, 37% in three steps, 56% brsm) as a white solid: $R_f = 0.35$ (25% EtOAc/ hexanes); mp 108 °C, $\alpha_D = +42.0$ (c 1, CHCl₃); ¹H NMR (CDCl₃, 400 MHz) δ 0.81 (d, $J = 7.2$ Hz, 3H, CH₃), 1.32 (m, 1H, H-4ax), 1.64 (m, 1H, H-3ax), 1.76 (m, 1H, H-3eq), 2.00 (dd,

¹¹³ Bradshaw, B.; Luque-Corredera, C.; Bonjoch, J. *Org. Lett.* **2013**, *15*, 326-329.

¹¹⁴ Bradshaw, B.; Luque-Corredera, C.; Saborit, G.; Cativiela, C.; Dorel, R.; Bo, C.; Bonjoch, J. *Chem. Eur. J.* **2013**, *19*, 13881-13892.

$J = 12.8, 3.6$ Hz, 1H, H-4eq), 2.15 (dt, $J = 13.6, 2.4$ Hz, 1H, H-6ax), 2.23 (dm, $J = 12.4$ Hz, 1H, H-8eq), 2.33 (td, $J = 13.6, 4.6$ Hz, 1H, H-8ax), 2.40 (masked, H-7), 2.42 (s, 3H, CH₃Ar), 2.46 (qd, 1H, $J = 11.4, 3.2$ Hz, H-4a), 2.56 (dd, $J = 11.6, 4.0$ Hz, 1H, H-6eq), 2.66 (td, $J = 11.2, 3.2, 1.6$ Hz, 1H, H-2ax), 2.89 (td, $J = 11.4, 4.0$ Hz, 1H, H-8a), 4.13 (dtd, $J = 12.8, 4.0, 1.2$ Hz, 1H, H-2eq), 7.30 (d, $J = 8.4$ Hz, 2H, *o*-Ts), 7.68 (d, $J = 8.4$ Hz, 2H, *m*-Ts); ¹³C NMR (100 MHz, CDCl₃) δ 18.9 (CH₃), 21.6 (ArCH₃), 23.5 (C-4), 24.4 (C-3), 28.5 (C-7), 36.1 (C-8), 47.3 (C-6), 49.3 (C-2), 53.1 (C-4a), 60.3 (C-8a), 127.3 (*m*-Ts), 129.8 (*o*-Ts), 137.1 (*ipso*-Ts), 143.6 (*p*-Ts), 209.1 (C-5). HRMS (ESI-TOF) m/z : [M+H]⁺ calcd for C₁₇H₂₄NO₃S 322.1471, found 322.1464.

(*E*)-(4a*S*,7*R*,8a*S*)-7-Methyl-1-(4-methylphenylsulfonyl)-5-(pyridin-2-yl-methylene)decahydroquinoline ((+)-25). Both the pyridine phosphonate and decahydroquinoline **(+)-23** were previously dried by azeotroping with benzene. To a stirred solution of phosphonate (1.18 g, 5.13 mmol, 5 equiv) in THF (15 mL) at -78 °C was added *n*-BuLi (1.6 M in hexanes, 2.88 mL, 4.62 mmol, 4.5 equiv). The resulting dark red solution was stirred for 30 min at rt before a solution of the decahydroquinoline **(+)-23** (330 mg, 1.03 mmol) in THF (6 mL) was added dropwise via syringe at -78 °C. The reaction mixture was stirred for 30 min at -78 °C, 1 h at -30 °C, and 6 h at 0 °C, and quenched with sat. aq. NH₄Cl (5 mL) and water (5 mL). The mixture was extracted with EtOAc (2 × 20 mL) and the combined organic extracts were dried, concentrated, and purified by chromatography (5% to 40% EtOAc in hexanes) to give **(+)-24** (52 mg, 16%) and **(+)-25** (286 mg, 70%, 82% brsm) as a white solid: $R_f = 0.49$ (50% hexane/EtOAc); mp 128 °C, $\alpha_D = +138.2$ (c 1, CHCl₃); ¹H NMR (400 MHz, CDCl₃) δ 0.77 (d, $J = 7.2$ Hz, 3H, CH₃), 1.31 (qd, 1H, $J = 12.4, 2.0$ Hz, H-4ax),

1.68 (m, 1H, H-3), 1.82 (m, 1H, H-3), 1.95 (dm, $J = 13.2$ Hz, 1H, H-4eq), 2.03 (dd, $J = 12.6, 4.4$ Hz, 1H, H-8eq), 2.12 (m, 1H, H-6ax), 2.15 (m, 1H, H-7), 2.19 (m, 1H, H-8ax), 2.24 (brt, $J = 12.0$ Hz, 1H, H-4a), 2.42 (s, 3H, ArCH₃), 2.91 (ddd, $J = 13.2, 8.8, 4.4$ Hz, 1H, H-8a), 2.94 (td, 1H, $J = 12.8, 5.2$ Hz, H-2ax), 3.07 (dt, $J = 13.2, 2.0$ Hz, 1H, H-6eq), 3.97 (dt, $J = 12.8, 5.2$ Hz, 1H, H-2eq), 6.31 (s, 1H, C=CH), 7.07 (dd, $J = 7.6, 4.8$ Hz, 1H, H-5 py), 7.13 (d, $J = 8.0$ Hz, 1H, H-3 py), 7.28 (d, $J = 8.4$ Hz, 2H, *o*-Ts), 7.59 (td, $J = 7.6, 2.0$ Hz, 1H, H-4 py), 7.69 (d, $J = 8.4$ Hz, 2H, *m*-Ts), 8.54 (dm, $J = 4.8$ Hz, 1H, H-6 py); ¹³C NMR (100 MHz, CDCl₃, HSQC) δ 18.2 (CH₃), 21.7 (CH₃Ar), 24.5 (C-3), 25.8 (C-4), 29.3 (C-7), 35.2 (C-6), 38.1 (C-8), 46.3 (C-4a), 46.8 (C-2), 60.6 (C-8a), 121.2 (C-5 py), 124.0 (C-3 Py), 124.1 (=CH), 127.3 (*o*-Ts), 129.7 (*m*-Ts), 136.0 (C-4 Py), 137.3 (*p*-Ts), 143.3 (*ipso*-Ts), 144.7 (C-5), 149.3 (C-6 Py), 157.3 (C-2 Py). HRMS (ESI-TOF) m/z : [M+H]⁺ calcd for C₂₃H₂₉N₂O₂S 397.1944, found 397.1953.

(4a*S*,5*S*,7*R*,8a*S*)-7-Methyl-5-(pyridin-2-ylmethyl)-1-(4-methylphenyl-sulfonyl)decahydroquinoline ((+)-26**)**. To a stirred solution of **(+)-25** (260 mg, 0.656 mmol) in MeOH (20 mL) was added Wilkinson's catalyst RhCl(PPh₃)₃ (14 mg, 0.013 mmol, 2 mol %) at rt. The resulting mixture was rapidly evacuated and backfilled with H₂ three times and then stirred under an atmosphere of H₂ for 20 h. The mixture was concentrated, and purified by chromatography (10% to 40% EtOAc in cyclohexane) to give **(+)-26** (248 mg, 95%): $R_f = 0.5$ (1:1 EtOAc/cyclohexane), mp 159 °C, $\alpha_D = +54.0$ (c 1, CHCl₃); ¹H NMR (400 MHz, CDCl₃) δ 0.80 (d, $J = 7.2$ Hz, 3H, CH₃), 0.91 (qd, $J = 12.4, 6.2$ Hz, 1H, H-4ax), 1.20 (m, 2H, H-6), 1.34 (qd, $J = 12.4, 3.2$, 1H, H-4a), 1.65 (m, 2H, H-3), 1.80 (m, 1H, H-5), 1.86 (td, $J = 12.4, 4.8$ Hz, 1H, H-8ax), 1.94 (dm, $J = 12.4$ Hz, 1H,

H-8eq), 2.00 (m, 1H, H-7), 2.12 (dm, $J = 12.0$ Hz, 1H, H-4eq), 2.30 (dd, $J = 13.4, 8.8$ Hz, 1H, CH₂Py), 2.42 (s, 3H, ArCH₃), 2.94-3.00 (m, 2H, H-2ax, H-8a), 3.11 (dd, $J = 13.4, 4.0$ Hz, 1H, CH₂Py), 3.97 (dt, $J = 13.2, 5.6$ Hz, 1H, H-2eq), 7.04 (d, $J = 8.0$ Hz, 1H, H-3 Py), 7.08 (m, 1H, H-5 Py), 7.28 (d, $J = 8.4$ Hz, 2H, *o*-Ts), 7.55 (td, $J = 7.6, 1.6$ Hz, 1H, H-4 Py), 7.68 (d, $J = 8.0$ Hz, 2H, *m*-Ts), 8.50 (dm, $J = 4.0$ Hz, 1H, H-6 Py); ¹³C NMR (100 MHz, CDCl₃, HSQC) δ 18.3 (CH₃), 21.6 (ArCH₃), 25.1 (C-3), 27.4 (C-4), 27.5 (C-7), 36.8 (C-6), 37.1 (C-8), 37.3 (C-5), 42.3 (CH₂Py), 45.6 (C-4a), 47.3 (C-2), 59.8 (C-8a), 121.1 (C-5 Py), 124.0 (C-3 Py), 127.2 (*o*-Ts), 129.7 (*m*-Ts), 136.2 (C-4 Py), 138.4 (*p*-Ts), 143.0 (*ipso*-Ts), 149.4 (C-6 Py), 161.1 (C-2 Py). HRMS (ESI-TOF) m/z : [M+H]⁺ calcd for C₂₃H₃₁N₂O₂S 399.2101, found 399.2116.

(4aS,5S,7R,8aS)-7-Methyl-5-(pyridin-2-ylmethyl)decahydroquinoline ((-)-27).

A solution of (+)-**26** (240 mg, 0.602 mmol) and phenol (200 mg, 2.1 mmol, 3.5 equiv) in HBr 48% (7.0 mL) was stirred at reflux for 4 h. The reaction was quenched by addition of H₂O (5 mL) and diluted with EtOAc (5 mL). The organic layer was separated, and the aqueous layer was basified with saturated aqueous NaOH and extracted with CH₂Cl₂ (3 × 10 mL). The combined organic extracts were dried over MgSO₄ and concentrated affording clean crude product (-)-**27** (140 mg, 95%) as a colorless oil which was used directly in the next step. An analytical sample was purified on alumina (1-5% MeOH/CH₂Cl₂): R_f 0.22 (5% MeOH/CH₂Cl₂), $\alpha_D = -42.4$ (c 1, CHCl₃); ¹H NMR (400 MHz, CDCl₃) δ 0.91 (d, $J = 7.2$ Hz, 3H, CH₃), 0.92 (qd, $J = 12.0, 3.2$ Hz, 1H, H-4a), 1.09 (qd, $J = 12.0, 4.0$ Hz, 1H, H-4ax), 1.20-1.25 (m, 2H, 2H-6), 1.44 (td, $J = 12.0, 4.2$ Hz, 1H, H-8ax), 1.52 (dt, $J = 12.4, 2.0$ Hz, 1H, H-8eq), 1.53 (m, 1H, H-3eq), 1.71 (tt, $J = 13.2, 3.2$ Hz, 1H, H-3ax), 1.82 (m, 1H, H-5), 2.01 (m, 1H, H-7eq), 2.14 (dd, J

= 13.0, 3.0 Hz, 1H, H-4eq), 2.30 (dd, $J = 13.2, 10.0$ Hz, 1H, CH₂Py), 2.47 (ddd, 1H, $J = 11.2, 10.0, 4.0$ Hz, H-8a), 2.66 (td, 1H, $J = 12.2, 3.0$ Hz, H-2ax), 3.07 (dm, $J = 12.0$ Hz, 1H, H-2eq), 3.14 (dd, $J = 13.2, 4.0$ Hz, 1H, CH₂Py), 7.06-7.09 (m, 2H, H-3 Py, H-5 Py), 7.55 (td, $J = 8.0, 1.6$ Hz, 1H, H-4 Py), 8.52 (dd, $J = 5.2, 2.0$ Hz, 1H, H-6 Py); ¹³C NMR (100 MHz, CDCl₃) δ 19.2 (CH₃), 27.2 (C-3), 27.5 (C-7), 28.8 (C-4), 36.4 (C-5), 37.6 (C-6), 39.4 (C-8), 41.9 (CH₂Py), 47.0 (C-2), 48.4 (C-4a), 56.2 (H-8a), 120.9 (C-5 Py), 123.9 (C-3 Py), 136.1 (C-4 Py), 149.4 (C-6 Py), 161.8 (C-2 Py). HRMS (ESI-TOF) m/z : [M+H]⁺ calcd for C₁₆H₂₄N₂ 245.2012, found 245.2009.

(4aS,5S,7R,8aS)-1,7-Dimethyl-5-(pyridin-2-ylmethyl)decahydro-quinoline

((-)-serralongamine A, (-)-14). To a solution of the above crude amine **(-)-27** (10 mg, 0.043 mmol) in MeOH (2.5 mL) was added 37% aqueous formaldehyde (24 mL, 0.328 mmol) and NaBH₃CN (18 mg, 0.287 mmol) at 0 °C, and the mixture was stirred at rt for 30 min. The volatiles were evaporated and the crude was purified on neutral alumina (CH₂Cl₂ to 5% MeOH in CH₂Cl₂) to give **(-)-11** (8.4 mg, 76% over two steps from **(+)-26**): $R_f = 0.70$ (5% CH₃OH in CH₂Cl₂), $\alpha_D^{25} = -15.1$ (c 0.6, MeOH) free base, Litt¹¹⁵ $\alpha_D^{18} = -9.1$ (c 0.6, MeOH). This sample was dissolved in CD₃OD and NaOCD₃ (0.1 M in CD₃OD) was added. ¹H and ¹³C NMR spectra of the free base consistent with the data obtained in chapter 5 for *rac*-serralongamine were obtained: ¹H NMR (400 MHz, CD₃OD, NaOCD₃) δ 0.90 (d, $J = 7.6$ Hz, 3H, CH₃), 1.10-1.15 (masked, 1H, H-4a), 1.11 (br q, $J = 12.0$ Hz, 1H, H-4ax), 1.15 (br d, $J = 12$ Hz, 1H, H-6eq), 1.25 (td, $J = 12.4, 4.4$ Hz, 1H, H-6ax), 1.35 (td, $J = 12.4, 4.8$ Hz, 1H, H-8ax), 1.65-1.75 (m, 2H, 2H-3), 1.80-1.92 (m, 2H, H-5 and H-8a), 1.93 (dm, $J = 12.0$ Hz, 1H, H-8eq),

¹¹⁵ Jiang, W.-P.; Ishiuchi, K.; Wu, J.-B.; Kitanaka, S. *Heterocycles*, **2014**, *89*, 747-752.

2.03 (m, 1H, H-7), 2.16 (dm, $J = 11.8$ Hz, 1H, H-4eq), 2.18 (td, $J = 12.8, 3.2$ Hz, 1H, H-2ax), 2.24 (s, 3H, CH₃), 2.30 (dd, $J = 13.2, 10.4$ Hz, 1H, CH₂py), 2.88 (dm, $J = 12.0$ Hz, 1H, H-2eq), 3.19 (dd, $J = 13.2, 4.0$ Hz, 1H, CH₂py), 7.24 (dd, $J = 7.6, 4.8$ Hz, 1H, H-5 py), 7.25 (t, $J = 7.4$ Hz, 1H, H-3 py), 7.73 (tt, $J = 7.6, 1.6$ Hz, 1H, H-4 py), 8.42 (dm, $J = 4.8$, 1H, H-6 py). ¹³C NMR (100 MHz, CD₃OD, NaOCD₃) δ 19.5 (CH₃), 26.1 (C-3), 28.5 (C-7), 29.6 (C-4), 36.6 (C-8), 37.8 (C-5), 38.0 (C-6), 42.6 (CH₂py), 43.1 (NCH₃), 47.8 (C-4a), 58.5 (C-2), 64.8 (C-8a), 122.7 (C-3 py), 125.7 (C-5 py), 138.4 (C-4 py), 149.5 (C-6 py), 162.6 (C-2 py). HRMS (ESI-TOF) m/z : [M+H]⁺ calcd for C₁₇H₂₇N₂ 259.2168, found 259.2169.

(4aS,5S,7R,8aS)-tert-butyl 7-methyl-5-(pyridin-2-ylmethyl)octahydroquinoline-1(2H)-carboxylate ((+)-28). A solution of crude (-)-**27** (120 mg, 0.499 mmol, 1equiv) and triethylamine (210 μ L, 1.497 mmol, 3 equiv) in CH₂Cl₂ (10mL) was cooled to 0 °C. To this solution was added (Boc)₂O (171 μ L, 0.750 mmol, 1.5 equiv). The reaction mixture was allowed to warm to room temperature and stirred for 7 h. The solvent and triethylamine in excess were removed under vacuum. Purification by chromatography.(5-50%EtOAc/Hexane) affords **(+)-28** (160 mg, 95% yield) as a colorless oil: R_f 0.36 (25% EtOAc/Hexane), $\alpha_D = +40.7$ (c 1, CHCl₃); ¹H NMR (400 MHz, CDCl₃) δ 0.96 (d, $J = 7.2$ Hz, 3H, CH₃), 1.05-1.15 (m, 1H, H-4), 1.23-1.33 (m, 3H, H4a & H-6), 1.45 (s, 9H, CH₃ tBu), 1.55-1.63 (m, 2H, H-8 & H-3), 1.80-1.95 (m, 3H, H-3, H-5 & H-8), 1.95-2.08 (m, 2H, H-7 & H-4), 2.35 (dd, $J = 13.2, 9.6$ Hz, 1H, CH₂Py), 3.03 (ddd, $J = 14.0, 11.2, 5.6$ Hz, 1H, H-2ax), 3.14 (dd, $J = 13.2, 4.4$ Hz, 1H, CH₂Py), 3.47 (td, $J = 11.4, 3.2$ Hz, 1H, H-8a), 3.73 (ddd, $J = 14.0, 7.0, 2.4$ Hz, 1H, H-2eq), 7.06-7.11 (m, 2H, H-3 Py, H-5 Py), 7.56 (td, $J = 7.6, 2.0$ Hz, 1H, H-

4 Py), 8.52 (dm, $J = 5.2, 2.0$ Hz, 1H, H-6 Py); ^{13}C NMR (100 MHz, CDCl_3) δ 18.7 (CH_3), 23.0 (C-3), 23.3 (C-4), 27.7 (C-7), 28.6 (CH_3 *t*Bu), 36.5 (C-8), 37.5 (C-5), 37.7 (C-2), 37.9 (C-6), 42.3 (CH_2 Py), 43.9 (C-4a), 55.9 (H-8a), 78.9 (C-*t*Bu), 120.9 (C-5 Py), 123.6 (C-3 Py), 136.0 (C-4 Py), 149.2 (C-6 Py), 155.4 (CO), 161.2 (C-2 Py). HRMS (ESI-TOF) m/z : $[\text{M}+\text{H}]^+$ calcd for $\text{C}_{21}\text{H}_{33}\text{N}_2\text{O}_2$ 345.2537, found 345.2538.

(4a*S*,5*S*,7*R*,8a*S*)-tert-butyl 7-methyl-5-(piperidin-2-ylmethyl)octahydroquinoline-1(2*H*)-carboxylate ((+)-29) A solution of (+)-28 (155 mg, 0.450 mmol) and $\text{PtO}_2 \cdot \text{H}_2\text{O}$ (30 mg, 20 % w/w) in AcOH was stirred under H_2 atmosphere at room temperature for 2 h. The reaction was diluted with DCM and filtered on Celite (rinse with DCM). The crude was concentrated and purified on alumina (0-10% MeOH/ CH_2Cl_2) affording first (+)-29a (51 mg) as a transparent oil, then a mixture of (+)-29a and (+)-29b (75 mg) as a transparent oil and finally (+)-29b (30 mg) as a white solid. Combined yield 98%.

(+)-29a: R_f 0.42 (2.5% MeOH/ CH_2Cl_2), $\alpha_D = +36.1$ (c 1, CHCl_3); ^1H NMR (400 MHz, CDCl_3) δ 0.92-1.00 (m, 2H, H-4ax & CH_2), 1.06 (d, $J = 7.2$ Hz, 3H, CH_3), 1.10-1.20 (m, 2H, H-4a, H-6 & H-5'), 1.30-1.40 (m, 1H, H-5), 1.46 (s, 9H, CH_3 *t*Bu), 1.50-1.70 (m, 7H, H-3, 2xH-3', H-5', H-8, H-6 & CH_2), 1.70-1.85 (m, 4H, H-3, 2xH-4' & H-8), 1.95 (br t, $J = 11.4$ Hz, 1H, H-4), 2.07-2.17 (m, 1H, H-7), 2.47-2.56 (m, 1H, H-6'), 2.61 (td, $J = 11.6, 2.4$ Hz, 1H, H-2'), 2.99 (ddd, $J = 13.6, 11.2, 5.6$ Hz, 1H, H-2ax), 3.08 (br d, $J = 11.6$ Hz, 1H, H-2'), 3.41 (td, $J = 11.6, 3.2$ Hz, 1H, H-8a), 3.71 (ddd, $J = 13.6, 7.2, 2.0$ Hz, 1H, H-2eq); ^{13}C NMR (100 MHz, CDCl_3) δ 18.9 (CH_3), 22.9 (C-3), 23.0 (C-4), 24.7 (C-4'), 26.0 (C-3'), 27.8 (C-7), 28.5 (CH_3 *t*Bu), 33.1 (C-5), 33.7 (C-5'), 36.3 (C-8), 37.6 (C-2), 38.4 (C-6), 40.8 (CH_2), 44.2 (C-4a), 46.9 (C-2'), 54.1 (C-6'), 55.9 (C-8a), 78.9 (C-*t*Bu),

155.3 (CO). HRMS (ESI-TOF) m/z : $[M+H]^+$ calcd for $C_{21}H_{39}N_2O_2$ 351.3006, found 351.3004

(+)-29b: R_f 0.21 (2.5% MeOH/ CH_2Cl_2), mp =194-196 °C, $\alpha_D = +21.0$ (c 1, $CHCl_3$); 1H NMR (400 MHz, $CDCl_3$) δ 0.90-1.00 (m, 1H, H-4ax), 1.06 (d, $J = 7.6$ Hz, 3H, CH_3), 1.10-1.20 (m, 1H, H-4a), 1.17-1.30 (m, 3H, H-5', H-6 & CH_2), 1.30-1.42 (m, 1H, H-5), 1.46 (s, 9H, CH_3 *t*Bu), 1.50-1.60 (m, 3H, H-6, H-8 & H-3), 1.60-1.70 (m, 2H, H-3'), 1.72-1.95 (m, 7H, H-3, H-4, 2xH-4', H-5', H-8 & CH_2), 2.07-2.15 (m, 1H, H-7), 2.67-2.75 (m, 2H, H-2' & H-6'), 2.99 (ddd, $J = 14.0$, 11.2, 5.6 Hz, 1H, H-2ax), 3.24 (br d, $J = 12.4$ Hz, 1H, H-2'), 3.41 (td, $J = 11.2$, 2.8 Hz, 1H, H-8a), 3.72 (ddd, $J = 14.0$, 7.2, 2.0 Hz, 1H, H-2eq); ^{13}C NMR (100 MHz, $CDCl_3$) δ 18.8 (CH_3), 22.8 (C-3), 23.0 (C-4), 23.5 (C-4'), 24.5 (C-3'), 27.7 (C-7), 28.5 (CH_3 *t*Bu), 29.8 (C-5'), 33.2 (C-5), 36.3 (C-8), 37.5 (C-2), 37.9 (C-6), 38.7 (CH_2), 43.8 (C-4a), 45.9 (C-2'), 54.8 (C-6'), 55.8 (C-8a), 79.0 (C-*t*Bu), 155.3 (CO). HRMS (ESI-TOF) m/z : $[M+H]^+$ calcd for $C_{21}H_{39}N_2O_2$ 351.3006, found 351.3004.

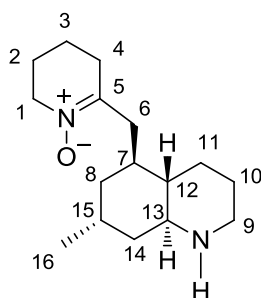
6-(((4a*S*,5*S*,7*R*,8a*S*)-1-(*tert*-butoxycarbonyl)-7-methyldecahydroquinolin-5-yl)methyl)-2,3,4,5-tetrahydropyridine 1-oxide ((+)-30) To a solution of a 1/1 mixture of **(+)-29a** and **(+)-29b** (75 mg, 0.214 mmol) in MeOH/ CH_2Cl_2 (1:1; 2 mL) were added in one portion UHP (205 mg, 2.14 mmol) and $Na_2WO_4 \cdot 2H_2O$ (15 mg, 0.043 mmol) and the mixture was stirred at rt for 72 h. After concentration, CH_2Cl_2 was added and the reaction mixture was filtered, concentrated and purified by chromatography (1 to 10% MeOH in CH_2Cl_2 and then 85/15/1.5 $CHCl_3$ /MeOH/ NH_3) to give **(+)-30** (48 mg, 62%) as a colorless oil, $R_f = 0.41$ (95/5 CH_2Cl_2 /MeOH); $\alpha_D^{25} = +37.1$ (c 1, $CHCl_3$); 1H NMR (400 MHz, $CDCl_3$) δ 1.06 (d, $J = 7.2$ Hz, 3H, CH_3), 1.03-1.15 (m, 1H, H-4), 1.26-1.33

(m, 1H, H4a), 1.35-1.43 (m, 2H, 2H-6), 1.45 (s, 9H, CH₃ tBu), 1.53-1.65 (m, 2H, H-8 & H-3), 1.72-1.78 (m, 2H, 2H-4'), 1.85-2.00 (m, 6H, H-3, H-4, 2H-3' H-5 & H-8), 2.05-2.15 (m, 1H, H-7), 2.38-2.45 (m, 3H, 2H-5' & CH₂Py), 2.73 (dd, *J* = 13.6, 4.4 Hz, 1H, CH₂Py), 3.01 (ddd, *J* = 13.6, 11.2, 5.6 Hz, 1H, H-2ax), 3.45 (td, *J* = 11.6, 3.2 Hz, 1H, H-8a), 3.72 (ddd, *J* = 13.6, 6.8, 2.0 Hz, 1H, H-2eq), 3.82 (br t, *J* = 6.0 Hz, 2H, 2H-2'); ¹³C NMR (100 MHz, CDCl₃) δ 18.7 (CH₃), 18.8 (C-4'), 22.9 (C-3 & C-4), 23.1 (C-3'), 27.7 (C-7), 28.5 (CH₃ tBu), 29.5 (C-5'), 34.1 (C-5), 35.4 (CH₂), 36.3 (C-8), 37.6 (C-2), 38.3 (C-6), 44.2 (C-4a), 55.6 (C-8a), 58.2 (C-2'), 79.0 (C-tBu), 148.8 (C-6'), 155.3 (CO); HRMS (ESI-TOF) *m/z*: [M+H]⁺ calcd for C₂₁H₃₇N₂O₃ 365.2799, found 365.2810.

6-(((4a*S*,5*S*,7*R*,8a*S*)-7-methyldecahydroquinolin-5-yl)methyl)-2,3,4,5-tetrahydropyridine 1-oxide ((-)-Huperzine K, (-)-11) To a stirred solution of **(+)-30** (18 mg, 0.049 mmol) in dry CH₂Cl₂ (5.0 mL), was added TFA (1.5 mL) and the reaction mixture was stirred for 3 h at room temperature before being concentrated to dryness under reduced pressure. To the crude mixture was added water (0.85 μL), MeOH (0.3 μL) and CH₂Cl₂ (10 mL) followed by solid NaHCO₃ (500 mg) and the resulting mixture was stirred for 15 min. Na₂SO₄ (1.5 g), was added, the mixture stirred for a further 20 min and then filtered, the filter cake was washed with 5% MeOH in CH₂Cl₂ and the filtrate concentrated under reduced pressure. The resulting crude material was purified by silica column chromatography (0→10% MeOH in CH₂Cl₂ followed by 1:2:0.1 MeOH/CH₂Cl₂/concd NH₄OH) to give huperzine K **(-)-11** (9.4 mg, 73%) as a colourless oil: *R_f* = 0.28 (90/10 CH₂Cl₂/MeOH), α_D²⁵ = - 19.1 (c 0.08, CHCl₃) as eluted from column (*i.e.* partially protonated). This sample was stirred for 1h30 in CDCl₃ and solid Na₂CO₃ and filtered. Analytical data obtained for the free

base matching the reported spectra of (-)-huperzine K are: $\alpha_D^{25} = -17.9$ (c 0.07, CHCl₃), Litt¹¹⁶ $\alpha_D^{20} = -16.8$ (c 0.06, CHCl₃); ¹H NMR (400 MHz, CDCl₃) δ 1.00 (d, $J = 7.2$ Hz, 3H, CH₃), 1.08-1.13 (m, 2H, H-4 & H-4a), 1.34-1.44 (m, 1H, H-8), 1.54-1.58 (m, 1H, H-6), 1.60-1.66 (m, 1H, H-3), 1.63-1.68 (m, 1H, H-6), 1.72-1.79 (m, 3H, H-3 & 2H-4'), 1.90-1.96 (m, 3H, 2H-3' & H-5), 2.05-2.12 (m, 2H, H-7 & H-4), 2.22 (dd, $J = 13.6, 10.0$ Hz, 1H, CH₂), 2.39 (t, $J = 6.0$ Hz, 2H, H-5'), 2.59-2.64 (m, 1H, H-8a), 2.70 (td, $J = 12.4, 3.2$ Hz, 1H, H-2), 2.80 (brd, $J = 13.6$ Hz, 1H, CH₂), 3.18 (brd, $J = 12.4$ Hz, 1H, H-2), 3.80 (t, $J = 6.0$ Hz, 2H, H-2'); ¹³C NMR (100 MHz, CDCl₃) δ 18.8 (CH₃ & C-4'), 23.1 (C-3'), 25.3 (C-3), 27.1 (C-7), 27.6 (C-4), 30.0 (C-5'), 32.6 (C-5), 35.2 (CH₂), 37.5 (C-6), 37.7 (C-8), 45.7 (C-2), 47.0 (C-4a), 55.9 (C-8a), 58.2 (C-2'), 148.4 (C-6'); HRMS (ESI-TOF) m/z : [M+H]⁺ calcd for C₁₆H₂₉N₂O 265.2274, found 265.2284.

¹¹⁶ Gao, W. Y.; Li, Y. M.; Jiang, S. H.; Zhu, D. Y. *Planta Medica*, **2000**, *66*, 664-667

Table S6.1 ^{13}C NMR data for huperzine K in CDCl_3 

huperzine K ((-)-11)

bio #	synthetic (-)-11 ¹ partially protonated	synthetic (-)-11 ¹ free base	isolated huperzine K ²
1	58.2	58.2	58.3
2	22.6	23.1	23.2
3	18.6	18.8	18.9
4	30.6	30.0	30.1
5		148.4	148.2
6	35.0	35.2	35.2
7	32.3	32.6	32.6
8	35.0	37.5	37.8
9	44.4	45.7	46.0
10	23.0	25.3	25.6
11	26.4	27.6	27.8
12	44.5	47.0	47.2
13	56.1	55.9	56.0
14	37.0	37.7	37.8
15	26.8	27.1	27.2
16	18.1	18.8	18.9

¹ ^{13}C NMR recorded at 100 MHz. Assignments were aided by COSY and HSQC spectra.

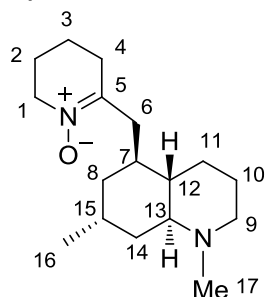
² Katakawa, K.; Kitajima, M.; Yamaguchi, K.; Takayama, H. *Heterocycles*, **2006**, *69*, 223-229

6-(((4a*S*,5*S*,7*R*,8a*S*)-1,7-dimethyldecahydroquinolin-5-yl)methyl)-2,3,4,5-tetrahydropyridine 1-oxide ((-)-huperzine M = (-)-lycoposerramine Y, (-)-12)

To a stirred solution of (-)-11 (9.2 mg, 0.0348 mmol) in MeOH (1 mL) was added K₂CO₃ (24 mg, 0.174 mmol) and MeI (2.3 μL, 0.0365 mmol) and the mix was stirred at 50 °C for 3 h. The crude mixture was evaporated and water (60 μL) and CH₂Cl₂ (5 mL) were added. Addition of Na₂SO₄ (1 g) and stirring for 15 min followed by filtration on Celite afforded the crude product. Purification by column chromatography (5 to 20% MeOH in CH₂Cl₂ and then 85/15/1.5 to 65/30/5 CHCl₃/MeOH/NH₃) give (-)-12 and unreacted (-)-11 (6.1 mg, 62%, ratio 3:2) as a colorless oil¹¹⁷. Similarly as for (-)-huperzine K, this sample was stirred for 1h30 in CDCl₃ and solid Na₂CO₃ and filtered. Analytical data reported were obtained for the free base *R*_f = 0.41 (80/20/0.2 CHCl₃/MeOH/NH₃); HRMS (ESI-TOF) *m/z*: [M+H]⁺ calcd for C₁₇H₃₁N₂O 279.2430, found 279.2437

Data for (-)-huperzine M (-)-12: ¹H NMR (400 MHz, CDCl₃) δ 0.99 (d, *J* = 6.0 Hz, 3H, CH₃), 1.03-1.20 (m, 2H, H-4 & H-4a), 1.30-1.40 (m, 1H, H-8) 1.42-1.52 (m, 1H, H-6), 1.68-1.82 (m, 4H, H₂-4' & H₂-3), 1.85-2.00 (m, 5H, H₂-3', H-5, H-6 & H-8a), 2.03-2.13 (m, 2H, H-4 & H-7), 2.18-2.30 (m, 2H, CH₂ & H-2), 2.34 (s, 3H, N-CH₃), 2.39 (t, *J* = 5.0 Hz, 2H, H₂-5'), 2.84 (brd, *J* = 11.0 Hz, 1H, CH₂), 3.04 (brd, *J* = 10.0 Hz, 1H, H-2), 3.80 (t, *J* = 5.0 Hz, 2H, H-2'); ¹³C NMR (100 MHz, CDCl₃) δ 18.7 (C-4'), 19.2 (CH₃), 23.1 (C-3'), 24.6 (C-3), 27.1 (C-7), 28.0 (C-4), 30.2 (C-5'), 32.7 (C-5), 35.3 (C-6), 35.7 (CH₂), 37.3 (C-8), 42.1 (N-CH₃), 46.2 (C-4a), 57.2 (C-2), 58.2 (C-2'), 63.8 (C-8a), 148.6 (C-6').

¹¹⁷ Product was also contaminated by phthalates from solvents used.

Table S6.2 ^{13}C NMR data for huperzine M in CDCl_3 

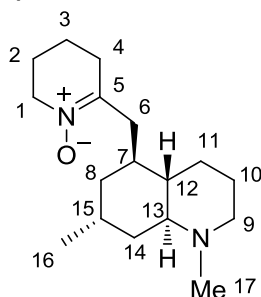
huperzine M ((-)-12)

bio #	synthetic (-)-12 ¹	huperzine M ²	lycoposerramine Y ³
1	58.2	58.1	58.3
2	23.1	23.1	23.3
3	18.7	18.8	19.0
4	30.2	29.9	29.9
5	148.6	148.6	148.5
6	35.7	35.6	35.8
7	32.7	32.8	33.0
8	35.3	35.4	37.7
9	57.2	57.5	57.7
10	24.6	25.1	25.4
11	28.0	28.3	28.5
12	46.2	46.7	47.0
13	63.6	63.3	63.4
14	37.3	37.5	35.7
15	27.1	27.1	27.3
16	19.2	19.3	19.5
17	42.1	42.5	42.8

¹ ^{13}C NMR recorded at 100 MHz. Assignments were aided by COSY and HSQC spectra.

² Gao, W. Y.; Li, Y. M.; Jiang, S. H.; Zhu, D. Y. *Helv. Chim. Acta* **2008**, *91*, 1031-1035.

³ Katakawa, K.; Kitajima, M.; Yamaguchi, K.; Takayama, H. *Heterocycles*, **2006**, *69*, 223-229.

Table S6.3 ^1H NMR data for huperzine M in CDCl_3 

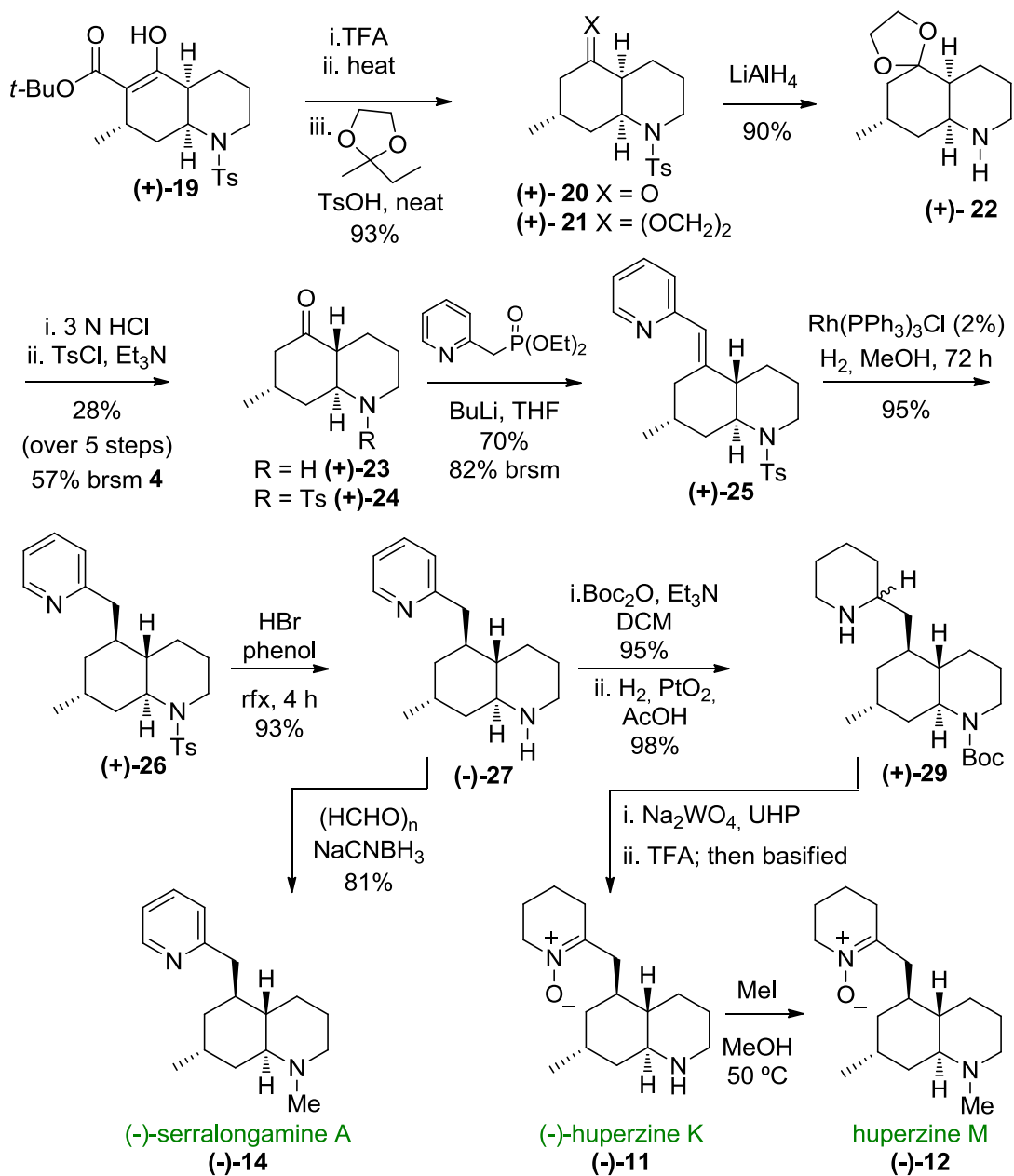
huperzine M ((-)-12)

bio #	synthetic (-)-1 ¹	huperzine M ²	lycoposerramine Y ³
1	3.80 (t, 5)	3.78 (t, 6)	3.73 (t, 6)
2	1.90	1.90*	1.67*
3	1.76	1.72*	1.86*
4	2.39 (t, 5)	2.37 (t, 6)	2.32
6	2.84 (br.d, 11)	2.78 (dd, 13,4)	2.72
	2.22	2.26 (d, 13)	2.23
7	1.98	1.95	1.86
8	1.87	1.85	1.33*
	1.48	1.38	1.25
9	3.04 (br.d, 10)	2.86 (br.d, 12)	2.82
	2.26	2.10	2.03
10	1.70	1.68	1.59
11	2.06	2.02 (br;d, 14)	1.94
	1.08	1.03	0.92
12	1.15	1.08	0.99
13	1.95	1.82 (br.d, 13)	1.73
14	1.40-1.30	1.30	1.83*
			1.31
15	2.10	2.06	2.03
16	0.99 (d, 6)	0.98 (d, 8)	0.93
17	2.34	2.24	2.18

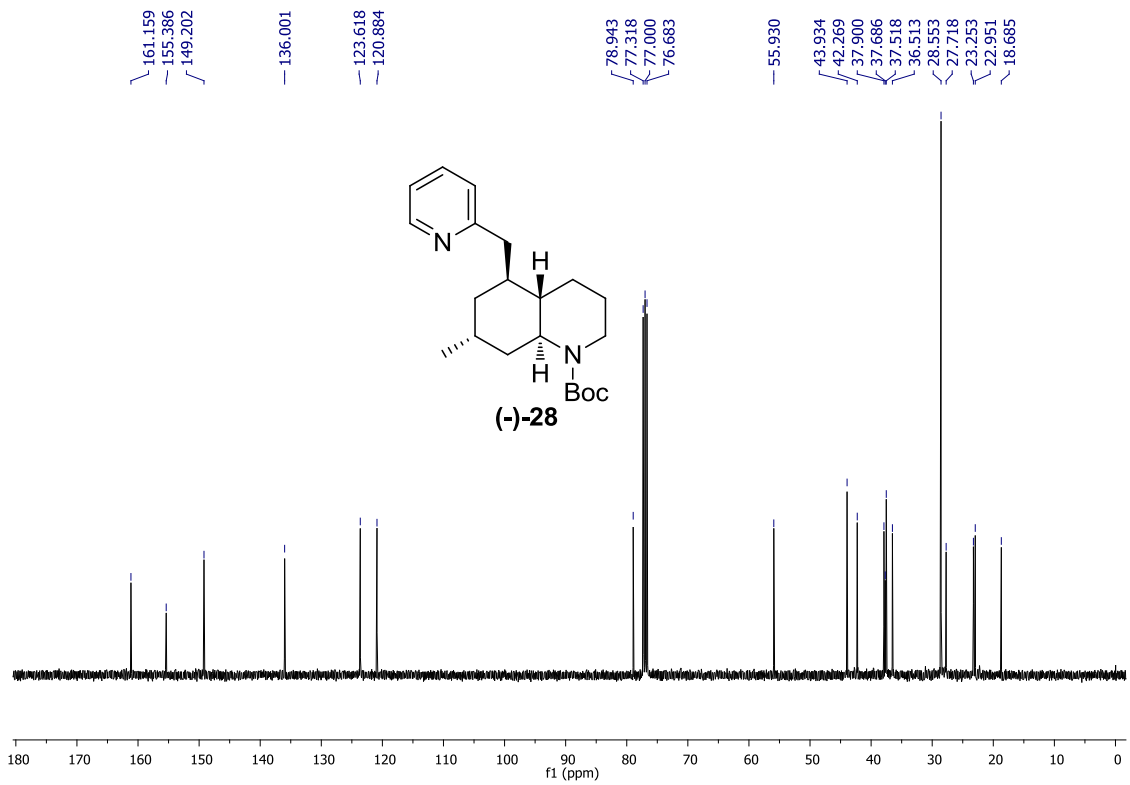
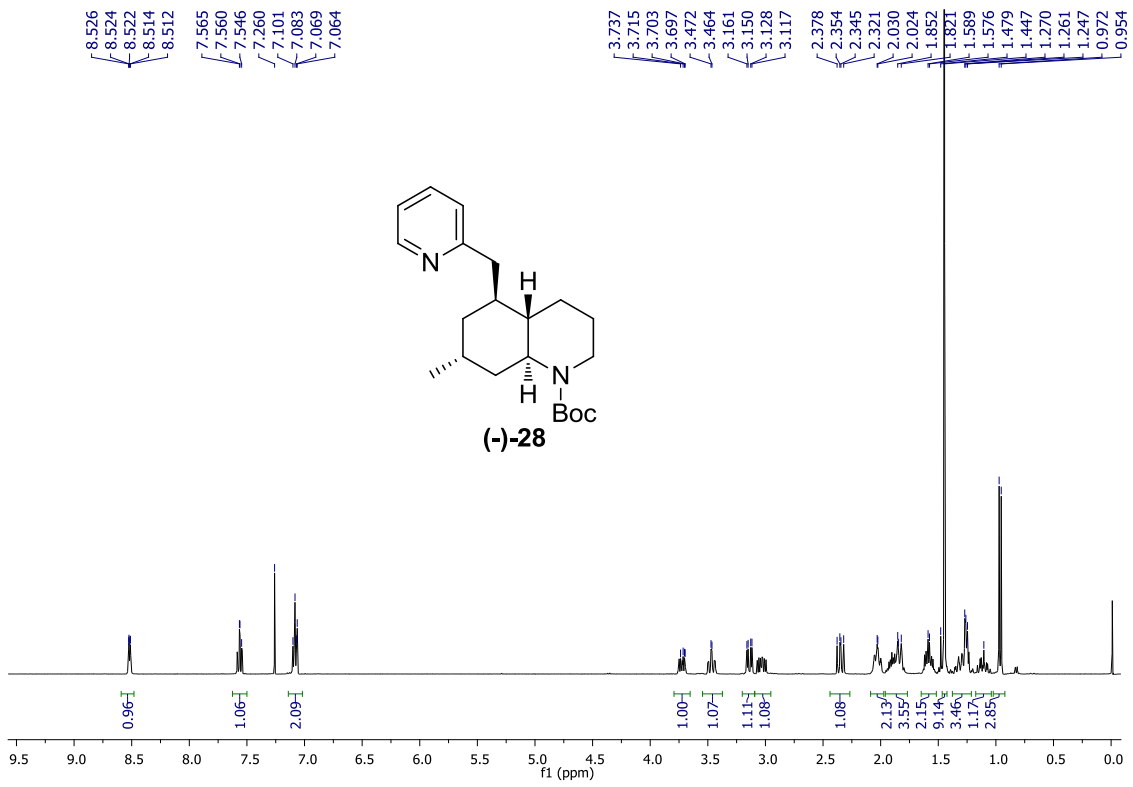
¹H NMR recorded at 400 MHz. Assignments were aided by COSY and HSQC spectra.

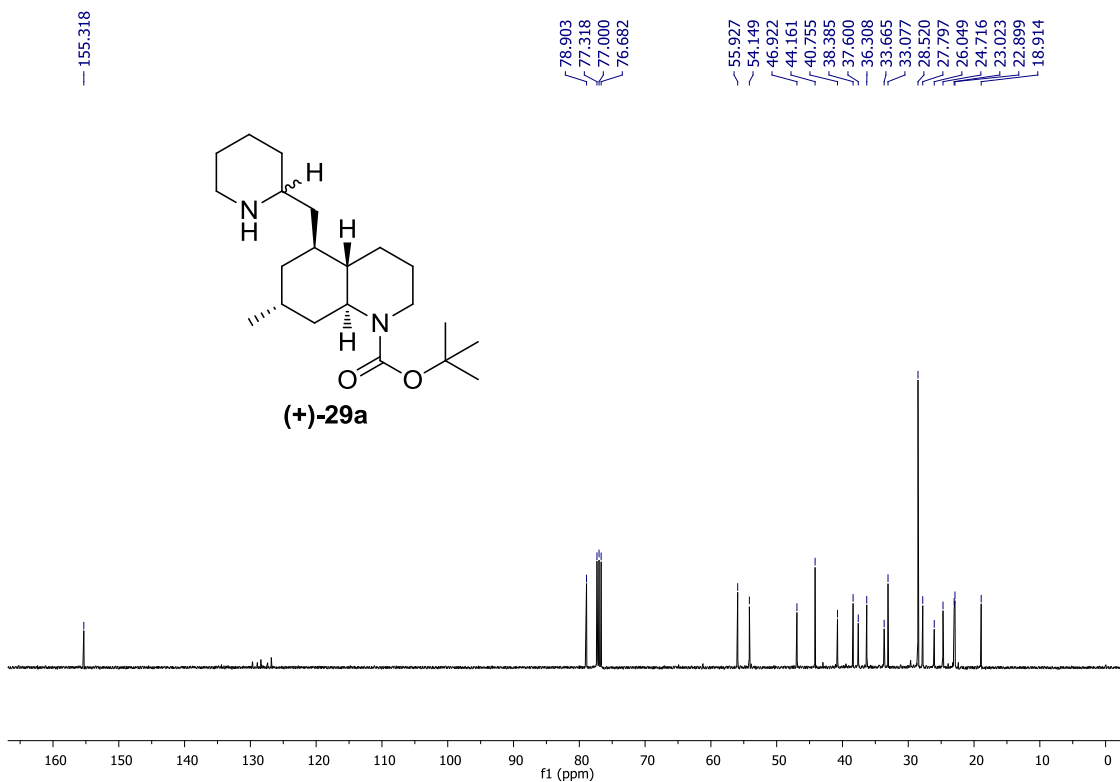
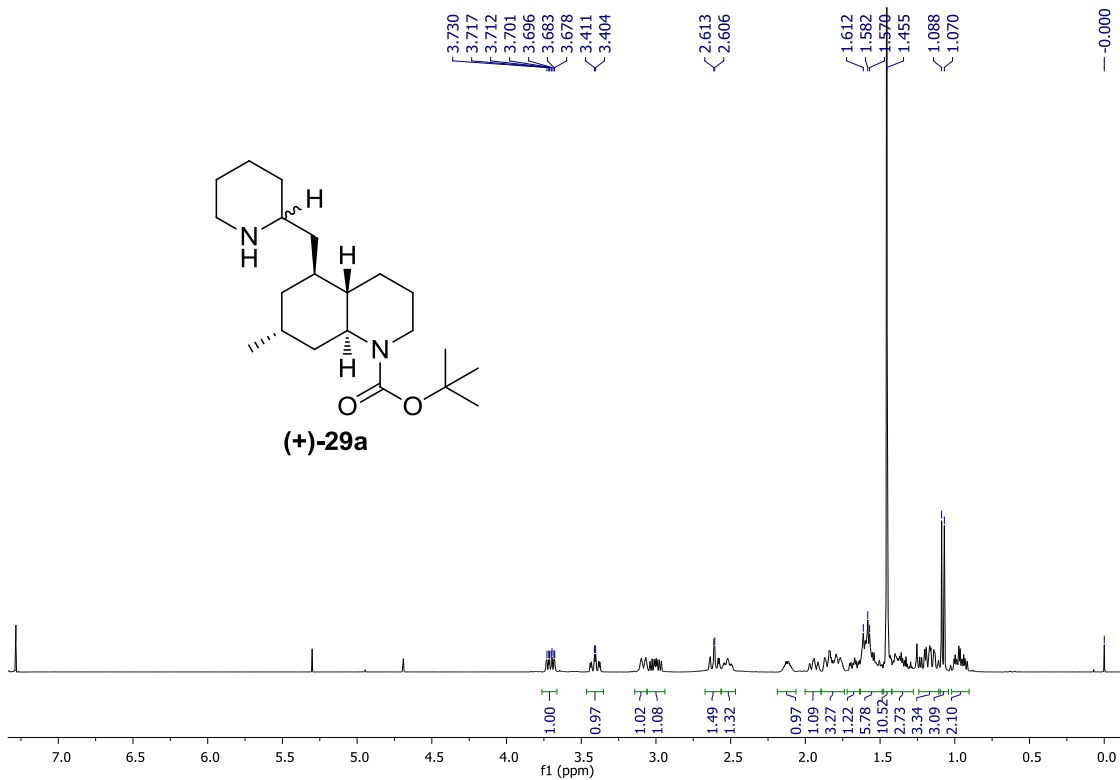
² Gao, W. Y.; Li, Y. M.; Jiang, S. H.; Zhu, D. Y. *Helv. Chim. Acta* **2008**, *91*, 1031-1035.

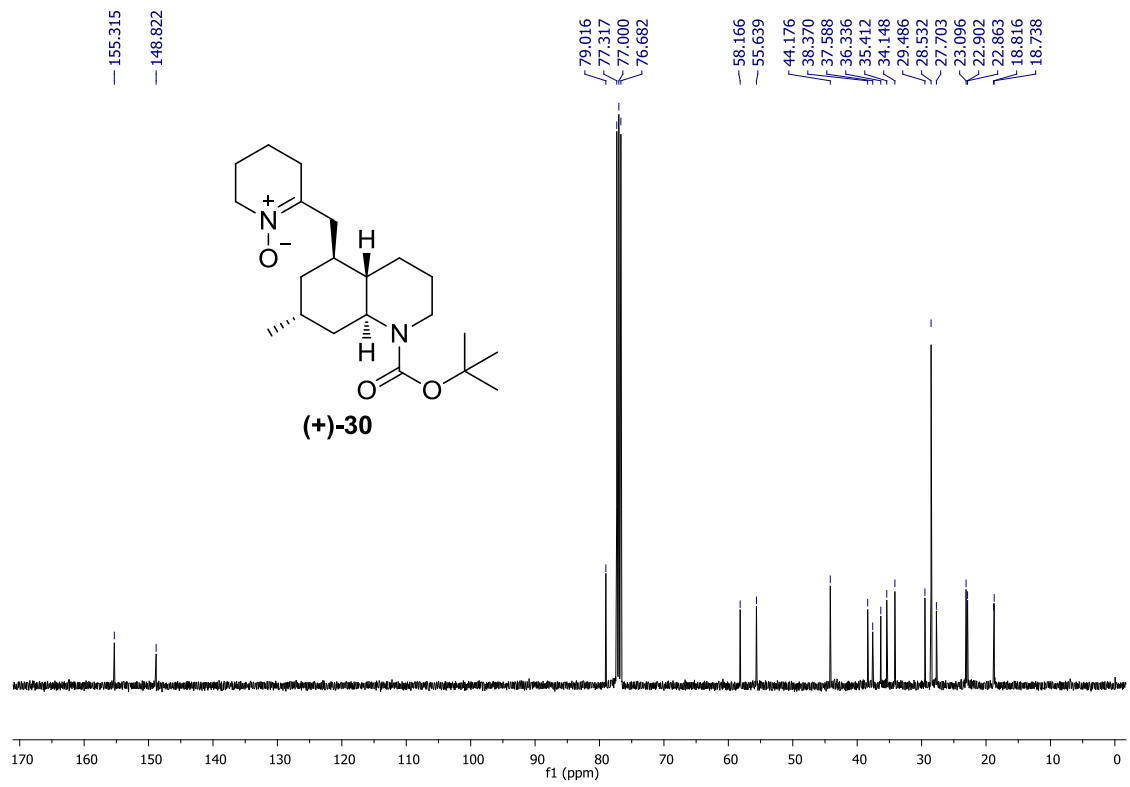
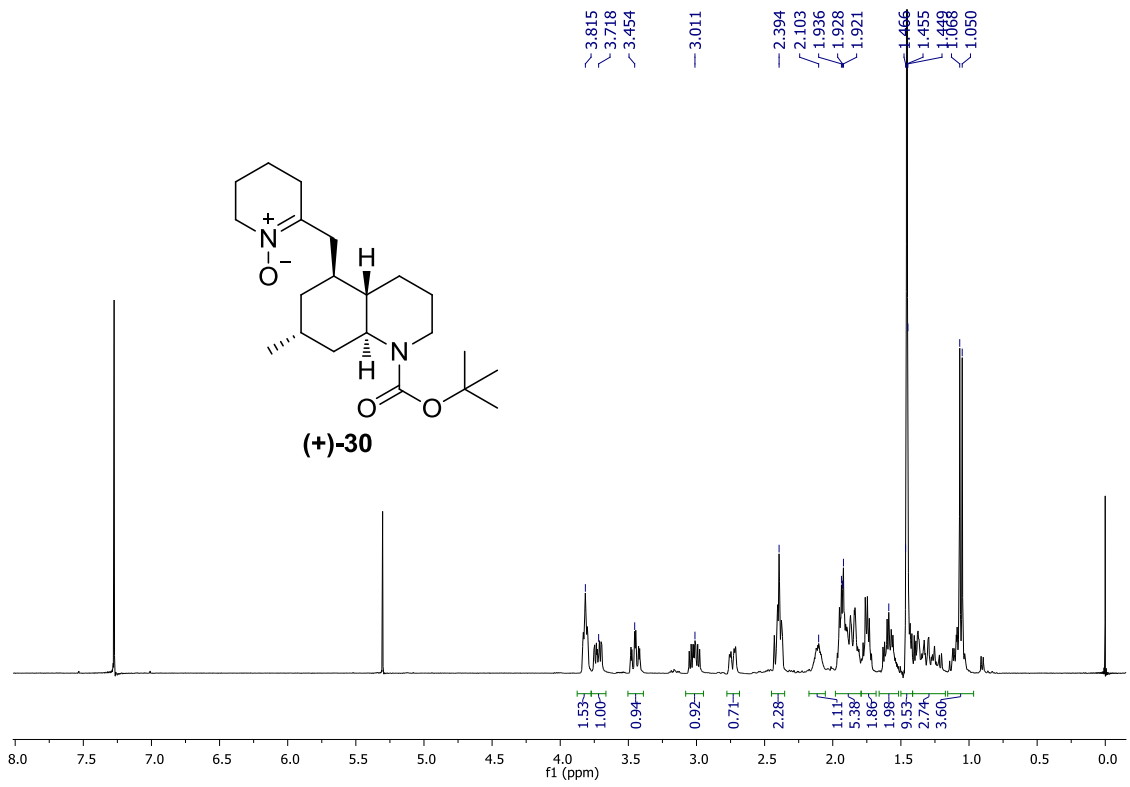
³ Katakawa, K.; Kitajima, M.; Yamaguchi, K.; Takayama, H. *Heterocycles*, **2006**, *69*, 223-229.

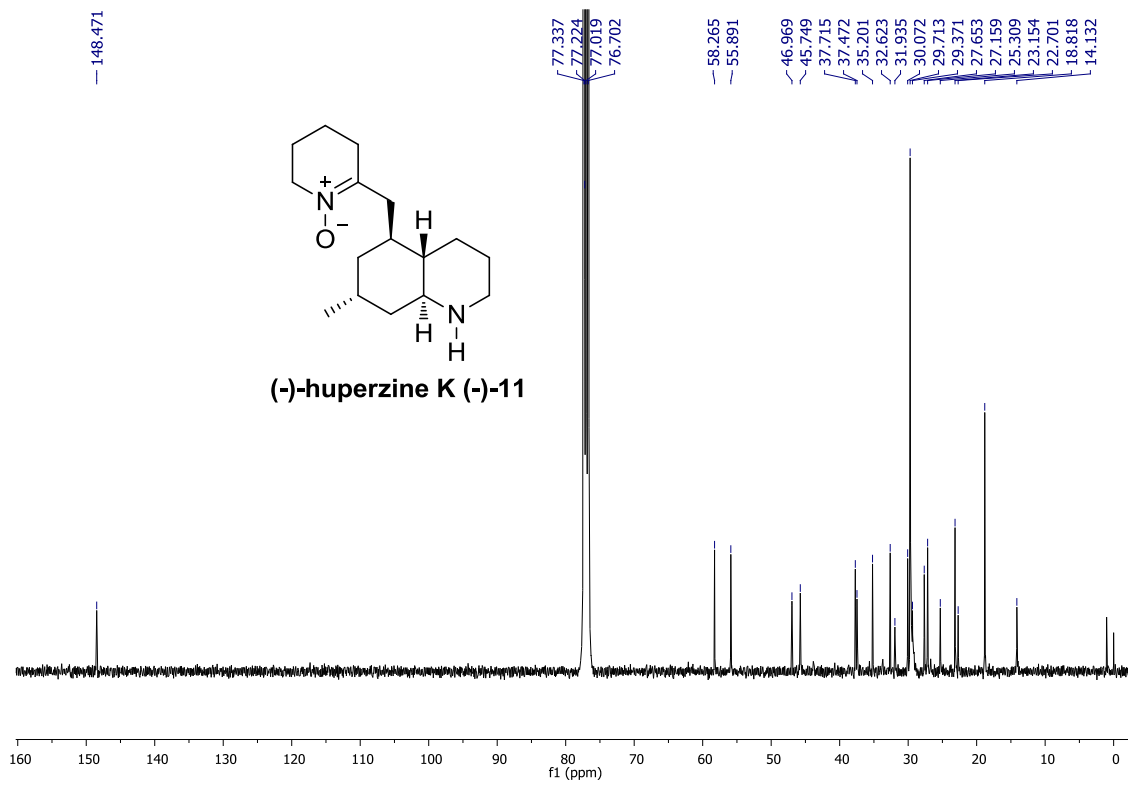
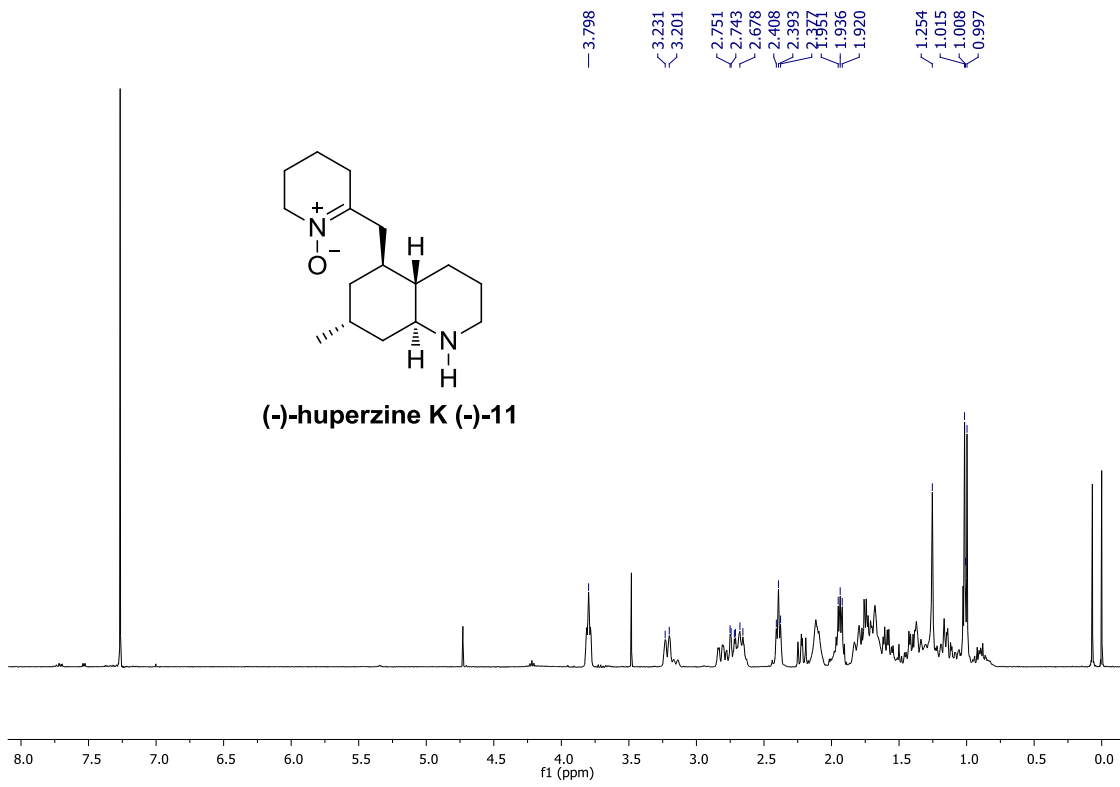


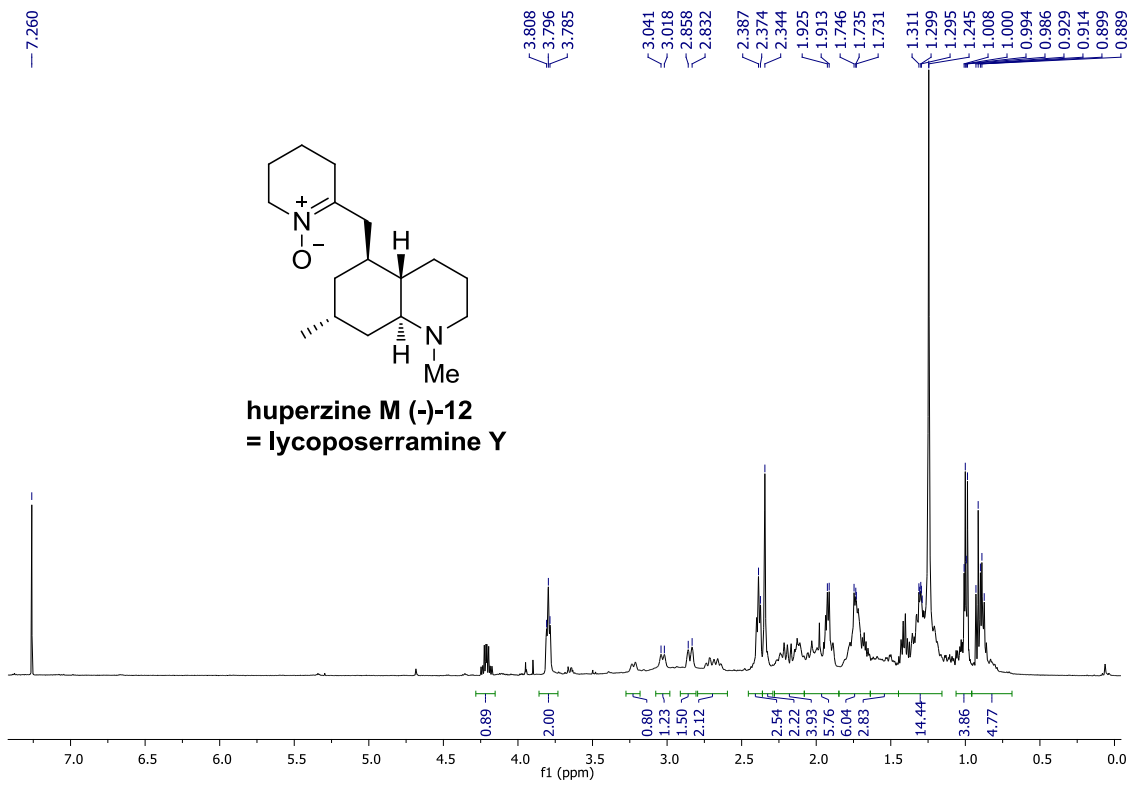
For copies of NMR spectras of compounds (+)-21 to (-)-27 and (-)-14 see SI chapter 5.



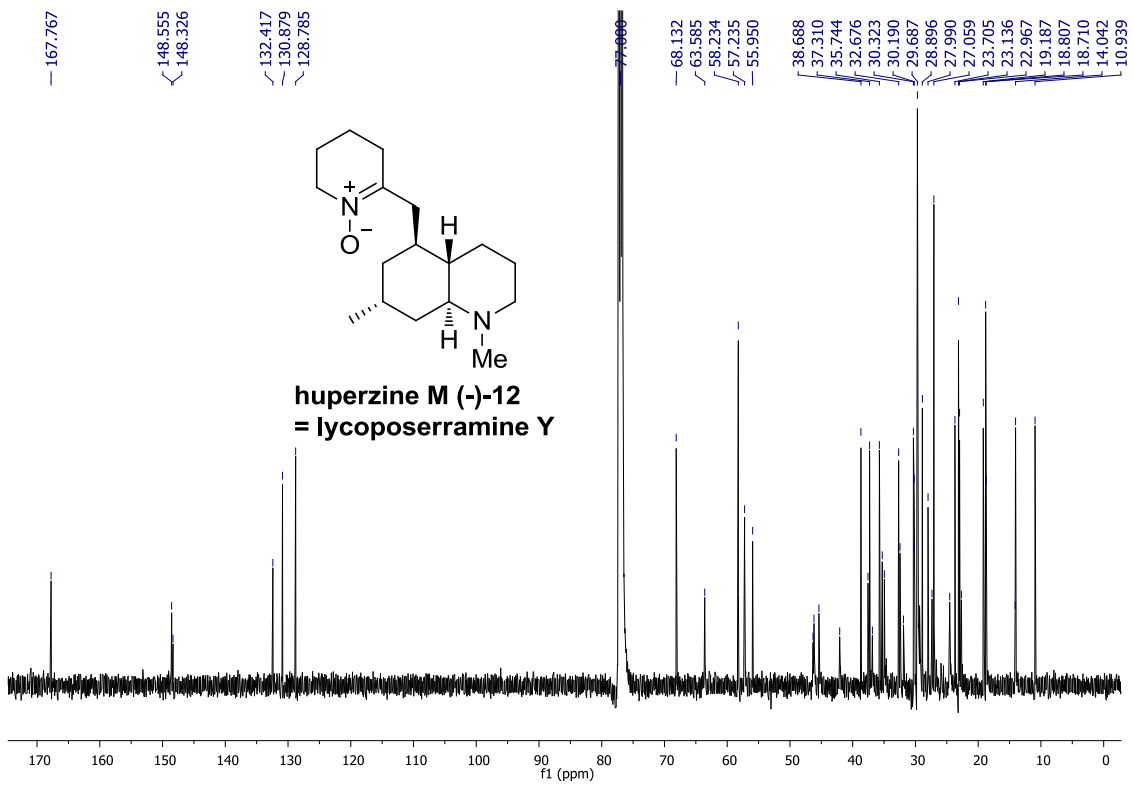








huperzine M (-)-12
= lycoserramine Y



huperzine M (-)-12
= lycoserramine Y